

OIL PALM FIBRES: A POTENTIAL REINFORCEMENT IN PHENOLIC RESINS

THESIS SUBMITTED TO
MAHATMA GANDHI UNIVERSITY
IN PARTIAL FULFILMENT OF THE REQUIREMENTS FOR
THE AWARD OF THE DEGREE OF
DOCTOR OF PHILOSOPHY
IN CHEMISTRY
UNDER THE FACULTY OF SCIENCE

M.S. SREEKALA M.Phil.

RUBBER RESEARCH INSTITUTE OF INDIA
KOTTAYAM, KERALA, INDIA 686 009

&

SCHOOL OF CHEMICAL SCIENCES
MAHATMA GANDHI UNIVERSITY
PRIYADARSHINI HILLS P.O., KOTTAYAM
KERALA, INDIA 686 560

NOVEMBER 1999

To My Family



रबड बोर्ड
(वाणिज्य मंत्रालय, भारत सरकार)
THE RUBBER BOARD
(Ministry of Commerce, Government of India)

रबड प्रसंस्करण विभाग

DEPARTMENT OF PROCESSING & PRODUCT DEVELOPMENT

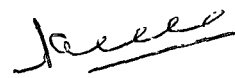
Reply to be addressed to
THE DIRECTOR (P & PD)

Ref No.....

कोट्टयम - ९, केरल
KOTTAYAM - 686 009,
KERALA STATE
Date Nov. 99

Certificate

This is to certify that the thesis entitled *Oil palm fibres : A potential reinforcement in phenolic resins* is an authentic record of the research work carried out by Ms. Sreekala M. S under the joint supervision and guidance of myself and Dr. Sabu Thomas, Reader, School of Chemical Sciences, Mahatma Gandhi University, in partial fulfilment of the requirements for the award of the degree of Doctor of Philosophy in chemistry under the Faculty of Science of the Mahatma Gandhi University, Kottayam. The work presented in this thesis has not been submitted for any other degree or diploma earlier. It is also certified that Ms. Sreekala M. S has fulfilled all the course requirements for the Ph. D. degree of the university.


Dr. M. G. Kumaran
Joint Director

Dr. SABU THOMAS B. Tech., Ph.D.

READER IN POLYMER SCIENCE & TECHNOLOGY

SCHOOL OF CHEMICAL SCIENCES

MAHATMA GANDHI UNIVERSITY

PRIYADARSHINI HILLS P. O.

KOTTAYAM 686 560

KERALA, INDIA

E-mail : mgu@md2.vsnl.net.in

Phone} Office : (0481) 598015

Res. : (0481) 597914

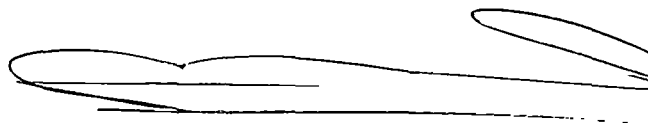
Fax : 91 - 481 - 561190

: 91 - 481 - 561800

November, 1999

Certificate

This is to certify that the thesis entitled *Oil palm fibres : A potential reinforcement in phenolic resins* is an authentic record of the research work carried out by Ms. Sreekala M. S under the joint supervision and guidance of myself and Dr. M. G. Kumaran, Joint Director, Rubber Board, in partial fulfilment of the requirements for the award of the degree of Doctor of Philosophy in chemistry under the Faculty of Science of the Mahatma Gandhi University, Kottayam. The work presented in this thesis has not been submitted for any other degree or diploma earlier. It is also certified that Ms. Sreekala M. S has fulfilled all the course requirements for the Ph. D. degree of the university.



(Sabu Thomas)

Declaration

I hereby declare that the thesis entitled *Oil palm fibres : A potential reinforcement in phenolic resins* is a record of the research work carried out by me under the joint supervision and guidance of Dr. M. G. Kumaran, Joint Director, Rubber Board, Kottayam, and Dr. Sabu Thomas, Reader, School of Chemical Sciences, Mahatma Gandhi University, Kottayam. No part of this thesis has been presented for any other degree or diploma earlier.

Kottayam
November 1999


Sreekala. M. S

Acknowledgements

I express my deep sense of gratitude and sincere thanks to my supervising teachers Dr. Sabu Thomas, Reader, School of Chemical Sciences, M. G. University and Dr. M. G. Kumaran, Jt. Director, Rubber Board for their inspiring guidance, encouragement and help throughout my research work.

I gratefully acknowledge the valuable help extended to me by Dr. M. R. Sethuraj, former Director and Dr. N. M. Mathew, Director, RRII, Kottayam for permitting me to utilise the library and laboratory facilities of the institute and for the help given to me at various stages of this work. I am extremely thankful to Prof. (Dr.) V. N. Rajasekharan Pillai, Vice-Chancellor, M. G. University and former Director, School of Chemical Sciences, M. G. University, for his continued support and encouragement throughout this work. I express my sincere gratitude to Dr. M. Padmanabhan, Reader-in-charge, School of Chemical Sciences, M. G. University, for his encouragement and help throughout this work.

May I express my sincere thanks to each and every member of Polymer Technology Laboratory, School of Chemical Sciences, M. G. University, for their help and constant encouragement throughout the course of this investigation. My special thanks to Mr. S. Shyam Kumar and Ms. Jaimol Jacob, Computer Assistants, School of Chemical Sciences, M. G. University, for their help during the preparation of this manuscript.

I gratefully acknowledge the help received from the staff, RCPT Division, RRII, Kottayam especially from Dr. K. T. Thomas, Ms. Reethamma Joseph, Ms. C. K. Premaletha and Dr. M. L. Geethakumariyamma and also from staff, Pathology Division, RRII, Kottayam especially from Dr. R. Kothandaraman and Dr. Jacob Mathew during the testing of my samples.

I take this opportunity to thank Dr. S. S. Bhagawan, Scientist, PED, VSSC, Thiruvanthapuram for his help during the course of this investigation.

My sincere thanks are also due to Dr. M. A. Ittyachen, Professor and Director, SPAP, M. G. University and Dr. Cyriac Joseph from the same department for their help during this work.

I remember the help and encouragement received from Ms. Laly. A. Pothen, Lecturer, Bishop Moore College, Mavelikara and Dr. R. Asaletha, Lecturer, STAS, M. G. University at different stages of this work.

I also express my gratitude to staff, Central Laboratory and Research Accounts Division, RRII, Kottayam and staff, School of Chemical Sciences, M. G. University for their help during the course of this work. My sincere thanks are due to staff, M. G. University Library and staff, RRII Library for their valuable helps during this investigation.

I gratefully remember the moral support received from my beloved family members for the successful completion of this work.

Glossary of Terms

ACN	-	Acrylonitrile
AFM	-	Atomic force microscopy
APDS	-	γ -aminopropyl dimethoxy methyl silane
APTS	-	γ -aminopropyl trimethoxy silane
ASTM	-	American standard for testing materials
C	-	Capacitance
DMTA	-	Dynamic mechanical thermal analysis
DTA	-	Differential thermal analysis
DTG	-	Differential thermogravimetry
E_i	-	Tensile modulus of the i^{th} component
E'	-	Storage modulus
E''	-	Loss modulus
E_D	-	Diffusion activation energy
E_H	-	Modulus of the hybrid laminate
E_P	-	Permeation activation energy
ESCA	-	Electron spectroscopy for chemical analysis
FRC	-	Fibre reinforced composites
FRP	-	Fibre reinforced plastics
g	-	Gravitational constant
HDPE	-	High density polyethylene
HP-PE	-	High performance polyethylene
IFSS	-	Interfacial shear stress
l_c	-	Critical fibre length
LDPE	-	Low density polyethylene
LLDPE	-	Linear low density poly ethylene
M_c	-	Young's modulus of the composite
M_f	-	Young's modulus of the fibre
M_m	-	Young's modulus of the matrix
NR	-	Natural rubber
NVH	-	Noise, vibration and harshness
OPEFB	-	Oil palm empty fruit bunch
PAN	-	Polyacrylonitrile
PF	-	Phenol formaldehyde
PMMA	-	Poly (methyl methacrylate)
PMPPIC	-	Polymethylene (polyphenyl isocyanate)
PP-g-MA	-	Maleic anhydride-grafted polypropylene
PS	-	Polystyrene
Q_∞	-	Mole percent uptake at infinite time
Q_t	-	Mole percent uptake at equilibrium
ROM	-	Rule of mixtures
SEBS-MA	-	Maleic anhydride-grafted styrene-ethylene-butylene styrene
SEM	-	Scanning electron microscopy

S-glass	-	Strength-glass
$\tan\delta$	-	Damping factor
$\tan\delta_c$	-	Damping values of the composite
$\tan\delta_f$	-	Damping values of the fibre
$\tan\delta_m$	-	Damping values of the matrix
T_c	-	Tensile strength of the composite
T_d	-	Theoretical density
TDI/ TDIC	-	Toluene 2,4-diisocyanate
TEM	-	Transmission electron microscopy
T_f	-	Tensile strength of the fibre
T_g	-	Glass transition temperature
TGA	-	Thermogravimetric analysis
T_m	-	Tensile strength of the matrix
UF	-	Urea formaldehyde
V. F	-	Volume fraction
V_f	-	Volume fraction of the fibre
V_{fe}	-	Effective fibre volume fraction
V_i	-	Volume fraction of the i^{th} component
V_m	-	Volume fraction of the matrix
WLF	-	William Landel and Ferry
σ_i^*	-	Ultimate stress for the i^{th} component
ε_i^*	-	Ultimate strain for the i^{th} component
λ	-	Compatibility parameter
γ_1	-	Surface free energy of the liquid
γ_2	-	Surface free energy of the solid
γ_{12}	-	Free energy of the liquid-solid interface
γ_{SV}	-	Surface free energies of solid vapour interface
γ_{SL}	-	Surface free energies of solid liquid interface
γ_{LV}	-	Surface free energies of liquid vapour interface
τ	-	Mean interfacial shear stress
ε_c	-	Strain in the composite
σ_f	-	Ultimate fibre strength
ε'	-	Dielectric constant
ε''	-	Dielectric loss
ε_0	-	Permittivity of air
ε	-	Percentage elongation
σ	-	Fibre strength
ϕ_f	-	Volume fraction of filler
ΔH_s	-	Enthalpy of the sorption
ΔS	-	Entropy of the sorption
ΔG	-	Free energy change
σ_{cu}	-	Ultimate strength of the composites
σ_m	-	Matrix strength at the failure strain of the fibre
σ_{fu}	-	Ultimate strength of the fibre

Contents

Preface

Chapter 1 Introduction

1.1	Fibre reinforced composites	3
1.2	Hybrid composites	4
1.2.1	Hybrid effect	4
1.3	Woven fabric (Textile) composites	12
1.4	Factors affecting the properties of a fibre reinforced composite	14
1.4.1	Fibre-matrix interface	14
1.4.2	Fibre length, loading and Orientation	30
1.4.3	Presence of voids	35
1.5	Natural fibres as a reinforcement in polymer matrix	35
1.6	Scope and objective of the present work	38

Chapter 2 Materials and experimental techniques

2.1	Materials	50
2.1.1	Oil palm fibres	50
2.1.2	Glass fibre mat	50
2.1.3	Phenol formaldehyde resin	50
2.1.4	Chemicals	51
2.2	Chemical composition of oil palm fibres	52
2.3	Resin modification	52
2.4	Fibre surface modifications	52
2.5	Composite preparation	54
2.6	Scanning electron microscopy and Optical microscopy	54
2.7	IR Spectroscopy	55
2.8	Thermogravimetric analysis	55
2.9	Mechanical tests	55
2.10	Stress relaxation	56
2.11	Dynamic mechanical analysis	56
2.12	Water sorption studies	56
2.13	Ageing studies	57
2.14	Electrical property measurements	58

Chapter 3 Oil palm fibres : Studies on chemical composition, surface modifications, morphology and mechanical properties

3.1	Properties of oil palm empty fruit bunch(OPEFB) fibre	62
3.1.1	Chemical analysis	62

3.1.2	Physical modifications : Scanning electron microscopic studies	63
3.1.3	Chemical modifications : IR Spectroscopy	67
3.1.4	Dimensional changes on treatments	74
3.1.5	Thermal studies	74
3.1.6	Effect of fibre surface modifications on the mechanical performance of oil palm fibre	78
3.1.7	Theoretical prediction of microfibrillar angle and strength of the OPEFB fibre	82
3.2	Properties of oil palm mesocarp fibre (Fruit fibre)	83
3.2.1	Chemical analysis	83
3.2.2	Chemical modifications	83
3.2.3	Physical modifications : Scanning electron microscopic studies	83
3.2.4	Chemical modifications : IR Spectroscopy	83
3.2.5	Thermal studies	86
3.2.6	Mechanical performance	86
3.2.7	Dimensional changes on treatments	89
3.2.8	Theoretical prediction of microfibrillar angle and strength of the oil palm mesocarp fibre	90

Chapter 4

Influence of fibre surface modifications on the mechanical performance of oil palm fibre reinforced phenol formaldehyde composites

4.1	Effect of fibre surface modifications on the mechanical performance of the composites	97
4.1.1	Tensile properties	97
4.1.2	Flexural properties	102
4.1.3	Impact properties	103

Chapter 5

Mechanical performance of oil palm/glass hybrid fibre reinforced phenol formaldehyde composites

5.1	Tensile properties	111
5.1.1	Tensile stress-strain behaviour	111
5.1.2	Tensile strength	112
5.1.3	Tensile modulus	116
5.1.4	Elongation at break	116
5.1.5	Tensile fracture mechanism	117
5.2	Flexural properties	120
5.2.1	Flexural stress-strain behaviour	120
5.2.2	Flexural strength	121
5.2.3	Flexural modulus	123
5.3	Impact properties	124
5.3.1	Impact fracture mechanism	126
5.4	Hardness, density and void formation	127

Chapter 6

Stress relaxation behaviour of oil palm fibres and composites based on short oil palm fibre and phenol formaldehyde resin

6.1	Stress relaxation behaviour in oil palm empty fruit bunch fibre	136
6.1.1	Effect of fibre treatments	136
6.1.2	Effect of physical ageing	140
6.1.3	Effect of strain level	142
6.2	Stress relaxation behaviour in oil palm empty fruit bunch fibre reinforced phenol formaldehyde composites	145
6.2.1	Effect of fibre loading	145
6.2.2	Effect of fibre treatment	147
6.2.3	Effect of hybridisation with glass	151
6.2.4	Effect of physical ageing	152
6.2.5	Effect of strain level	154

Chapter 7

Dynamic mechanical properties of oil palm fibre/phenol formaldehyde and oil palm-glass hybrid fibre/phenol formaldehyde composites

7.1	Dynamic mechanical properties of neat phenol formaldehyde	164
7.2	Dynamic mechanical properties of oil palm fibre/PF composites	167
7.2.1	Effect of fibre length	167
7.2.2	Effect of fibre content	173
7.2.3	Effect of fibre modification	180
7.3	Dynamic mechanical properties of oil palm fibre/glass hybrid PF composites	188
7.3.1	Effect of hybrid fibre ratio	188
7.4	Cole-Cole analysis	194
7.5	Time-Temperature superposition	194

Chapter 8

Water sorption studies in oil palm fibres and in oil palm fibre reinforced phenol formaldehyde composites

Part I Water sorption studies in oil palm fibres

8.1	Water sorption of oil palm fibres in distilled water, mineral water and salt water	202
8.2	Effect of OPEFB fibre treatment on the mechanism of sorption	209
8.3	Tensilemetry	216
8.4	Effect of fibre treatment on the tensile properties of the OPEFB fibre on sorption	219

Part II Water sorption in oil palm fibre reinforced phenol formaldehyde composites

8.5	Water uptake	227
-----	--------------	-----

8.6	Kinetics of water sorption	238
8.7	Thermodynamics of water sorption	243
8.8	Concentration dependence of diffusion coefficient	248
8.9	Effect of water sorption on the mechanical properties of the composites	254
8.9.1	Tensile properties	254
8.9.2	Flexural properties	255
8.9.3	Impact properties	257

Chapter 9

Environmental effects in oil palm fibre reinforced phenol formaldehyde composites : Studies on thermal, biological, moisture and high energy radiation effects

9.1	Ageing effects on tensile properties	261
9.1.1	Tensile fracture mechanism	269
9.2	Ageing effects on the flexural properties	271
9.3	Ageing effects on the impact properties	275
9.3.1	Impact fracture mechanism	277
9.4	Thermal stability of the composites	278

Chapter 10

Electrical properties of oil palm fibre/phenol formaldehyde composites : Effect of fibre loading, fibre surface modifications and hybridisation of oil palm fibre with glass

10.1	Volume resistivity	290
10.1.1	Effect of fibre loading	290
10.1.2	Effect of fibre treatment	292
10.1.3	Effect of hybridisation	294
10.2	Dielectric constant	296
10.2.1	Effect of fibre loading	296
10.2.2	Effect of treatments	297
10.2.3	Effect of hybridisation	300
10.3	Loss factor and dissipation factor	301
10.3.1	Effect of fibre loading	301
10.3.2	Effect of fibre treatment	302
10.3.3	Effect of hybridisation	305

Chapter 11

Theoretical modelling of tensile properties of oil palm fibre/PF and oil palm fibre/glass hybrid PF composites

11.1	Theoretical prediction of tensile properties of composites	315
------	--	-----

Conclusions and Future Outlook

Appendices

Preface

Effective and economic utilisation of organic waste materials as reinforcement in cheap thermosetting plastics was investigated in the present study. Oil palm fibres, a major waste material left unutilised in palm oil industry could be used to prepare high impact composite materials by reinforcing in phenol formaldehyde resin. These composite materials will have added advantages such as enhanced biodegradability, enhanced damping, cost effectiveness, light weight, good appearance, etc. Now-a-days the natural fibre reinforced plastic composites have emerged as a covetable substitute for other materials in automobile industry as well as in building industry.

Review on the recent developments in fibre reinforced composites along with the characterisation techniques of various composites is presented in Chapter 1. Chapter 2 describes the details of the materials used in this study along with the experimental techniques for sample preparation and characterisation methods. Important physical and chemical properties of oil palm fibres are investigated and discussed in Chapter 3. This chapter also deals with various modifications given to the fibres and their effect on their thermal and mechanical properties. The static mechanical properties of untreated and treated oil palm fibre reinforced phenol formaldehyde composites are given in Chapter 4. Chapter 5 gives the hybridisation effect of oil palm fibre with glass on the mechanical properties of the composites. Chapter 6 and Chapter 7 deal with stress relaxation and dynamic mechanical thermal analysis of the composites. Water sorption characteristics of the composites studied in detail and are given in Chapter 8. The composites were subjected to accelerated weathering studies and the changes in the properties are reported in Chapter 9. Electrical properties of the composites were determined and are illustrated in Chapter 10. The tensile properties of the composites were theoretically calculated and compared with the experimental results. This is presented in Chapter 11. Finally, the thesis concludes by giving the summary of the results obtained in the present work and an outline of the future prospects in this topic.

CHAPTER 1

Introduction

Composite material can be defined as a macroscopic combination of two or more distinct materials, having a recognisable interface between them. Composites are made up of continuous and discontinuous mediums. The discontinuous medium or particle phase that is stiffer and stronger than the continuous 'matrix' phase is called the 'reinforcement'. The properties of a composite are dependent on the properties of the constituent materials, and their distribution and interaction. Composite materials are developed because no single, homogeneous structural material can be found that has all of the desired attributes for a given application.¹ At present, composite materials play a key role in aerospace industry, automobile industry and in other engineering applications as they exhibit outstanding strength to weight and modulus to weight ratio.

Based on the matrix material which forms the continuous phase, the composites are broadly classified into metal matrix, ceramic matrix and polymer matrix composites. Of these, polymer matrix composites are much easier to fabricate than metal matrix and ceramic matrix composites. This is due to relatively low processing temperature required for fabricating polymer-matrix composites. The structure, properties and applications of various composites are being investigated world wide by several researchers.²⁻²⁵ New composites based on concrete are prepared with a view to improve properties such as strength, toughness, ductility and durability of the portland cement concrete.²⁶⁻²⁸ Polymer concretes are increasingly being used in buildings and other structures. They represent a new type of structural material capable of withstanding highly corrosive environments. However steel reinforced concretes, which are the conventional materials for construction will deteriorate due to corrosion of steel. Fibre reinforced plastics can eliminate this problem and open up new avenues, which has been recently explored. The high strength-to-weight ratio and non-corrosive characteristics of these materials can be utilised to build innovative structures which are durable and economical.²⁹

1.1 FIBRE REINFORCED COMPOSITES

Fibre reinforced composites (FRC) contain reinforcements having lengths much higher than their cross-sectional dimensions. Fibres are the load-carrying members, while the surrounding matrix keeps them in the desired location and orientation. Further the matrix acts as load transfer medium and protects the fibres from environmental damages due to elevated temperature and humidity. They have got low specific gravities and high strength-weight and modulus-weight ratio, which have tremendous potential advantages over conventional materials. Now-a-days fibre reinforced composites have emerged as a major class of structural material in many weight critical components in aerospace, marine, automotive and other industries. Fibre reinforced plastic (FRP) composites form a major class of composites. The versatility, strength and non-corrosive properties of plastics in combination with fibres offer them as good candidate for several applications.

A fibre reinforced composite is considered to be a discontinuous or short fibre composite if its properties vary with fibre length. On the otherhand, when the length of the fibre is such that any further increase in length does not, for example, further increase the elastic modulus of the composite, the composite is considered to be continuous fibre reinforced. Most continuous fibre composites, in fact, contain fibres that are comparable in length to the overall dimensions of the composite part.

The fibre reinforced composites exhibit anisotropy in properties. The high strength and moduli of these composites can be tailored to the high load directions. They exhibit better dimensional stability over a wide range of temperatures due to their lower coefficient of thermal expansion than those of metals. These differences in thermal expansion between metals and composite materials may create undue thermal stresses during processing. Fibre reinforced composites exhibit high internal damping. This leads to better vibration energy absorption within the material and results in reduced transmission of noise and vibrations to neighbouring structures. High damping capacity of composite materials can be beneficial in many automotive applications in which noise, vibration and harshness (NVH) is a critical issue for passenger comfort.³⁰ Composites absorb moisture from the

surrounding environment, which creates dimensional changes as well as adverse internal stresses within the material. This can be minimised by giving appropriate paints or coating on the composite surface.

Almost all high-strength/high modulus materials fail because of the propagation of flaws. The initiation and propagation of flaws are easier in bulk material than in a fibre. In a fibrous composite it is found that even if a flaw does produce failure in a fibre, it will not propagate to fail the entire assemblage of fibres thus withstanding the entire failure of the composite.

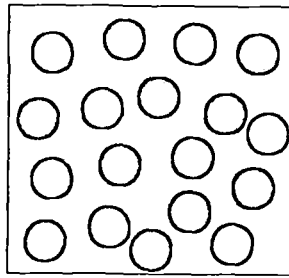
1.2 HYBRID COMPOSITES

They usually refer to composites containing more than one type of filler and/or more than one type of matrix. Hybrid fibre composites are more common than hybrid matrix.³¹ Short and Summerscales^{32, 33} have reviewed properties of the hybrid composites. Hybridisation is commonly used for improving the properties and/or lowering the cost of conventional composites. Various fibre arrangements are possible in hybrid composites, which is an important parameter in determining the strength of the composite. Possible arrangements are illustrated in Figure 1.1.^{34, 35}

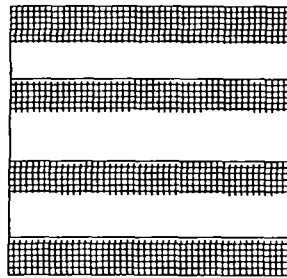
Additional possibilities are the use of woven fabrics with one fibre type in the warp and another in the weft, and further variations using interspersed tows in woven configurations. Plies containing different fibres or mixture of fibres may be stacked with the fibres aligned in different direction to form still another combination.

1.2.1 Hybrid Effect

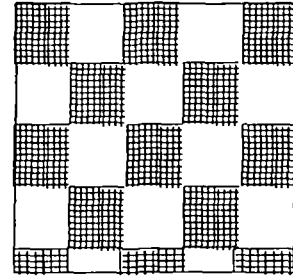
The hybrid effect refers to the apparent synergistic improvement in the properties of a composite containing two or more types of fibres. The stiffness of the hybrid composites may be accurately predicted from the relative proportions of the two types of fibre by using rule of mixtures as follows.



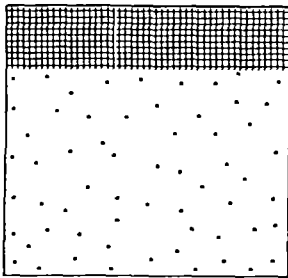
Intermingled fibres



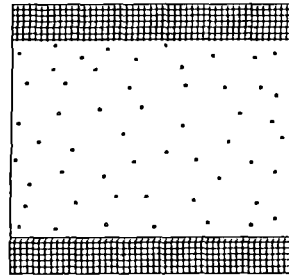
Alternating plies



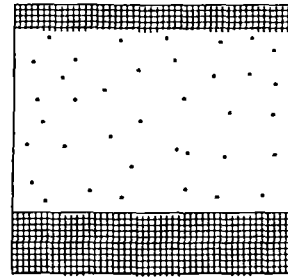
Interspersed fibre bundles



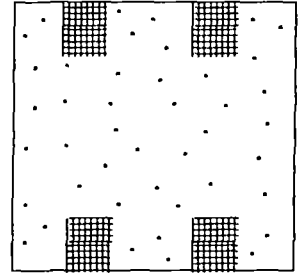
a



b

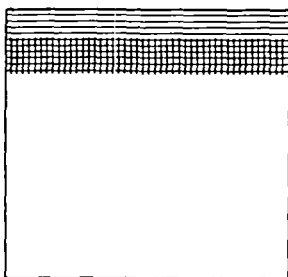


c

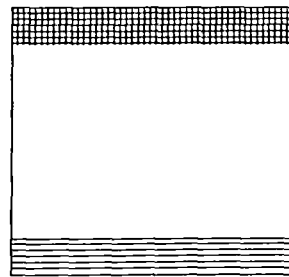


d

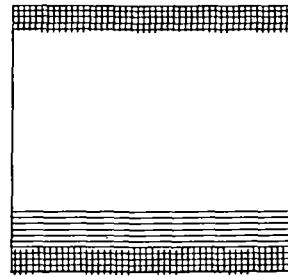
Fibre skin and fibre core



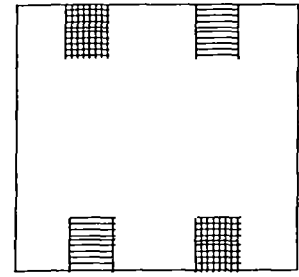
a



b



c



d

Fibre skin and non fibre core

Figure 1.1 Schematic diagram showing different hybrid configurations

[Ref.: N. L. Hancox (Ed.), *Fibre Composite Hybrid Materials*, Applied Science Publishers Ltd., London (1981)]

$$E_H = E_1V_1 + E_2V_2 \quad (1.1)$$

where E_H is the modulus of the hybrid laminate and E_1, V_1, E_2, V_2 are the respective moduli and volume fractions of the component laminae. However the tensile strength relationship is more complex in hybrid composites and cannot be predicted by simple rule of mixtures.

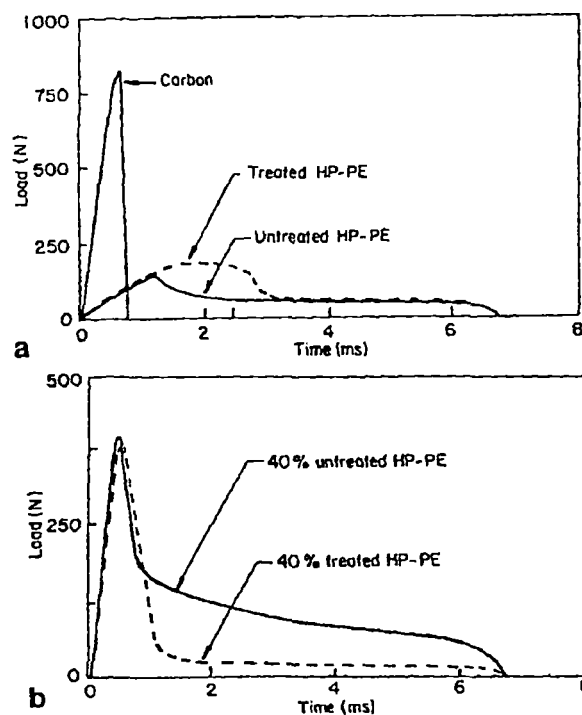
Positive and negative hybrid effects have been reported in various hybrid combinations. A negative synergistic effect was observed by Kirk et al.³⁶ in thin tape specimens containing regularly arranged carbon and glass fibre tows. Arrington and Harris observed a positive hybrid effect on hybridisation of two types of carbon fibre.³⁷ Recently hybrid effect in sisal/glass hybrid fibre reinforced polyethylene composites was reported.³⁸ A positive hybrid effect was observed in tensile strength, modulus, tear strength and hardness except for elongation at break which shows a negative deviation. It was found that the hybrid fibre configuration affects the hybrid effect. Intermingled combination in sisal/glass combination exhibited positive hybrid effect. Peijs et al.^{39, 40} worked on polyethylene/carbon fibre hybrid systems in epoxy matrix. They observed a positive hybrid effect in failure strain of the composite. Failure strain data observed in this system is given in Table 1.1. An apparent enhancement in first failure strain of the carbon component is observed. This enhancement of first failure strain is referred to as the 'hybrid effect'. The hybrids incorporating untreated HP-PE fibres exhibit positive hybrid effect whereas hybrids with chromic acid treated HP-PE fibres show an impact performance that varies linearly with composition. This is evident from Figure 1.2.

To illustrate the hybrid effect in tensile strength, a composite made up of E-glass and high modulus carbon fibres at similar fibre fractions in a common matrix resin is considered.³⁵ The tensile strength predicted by rule of proportionality is represented by broken line AD in Figure 1.3. But the actual behaviour deviates from this. This is because the strains to failure of the two types of fibre are different.

Table 1.1 Tensile Test Data for Unidirectional Hybrids

HP-PE fraction (%)	E modulus (GPa)	Tensile strength (MPa)	Failure strain (%)	Hybrid effect (%)
Untreated HP-PE				
0	113	1776	1.52	--
14	104	1623	1.66	9.2
40	90	1367	1.68	10.5
57	77	1222	1.67	9.9
80	62	928	1.60	5.3
100	52	1160	3.33	--
Treated HP-PE				
0	113	1776	1.52	--
14	103	1666	1.62	6.6
40	86	1384	1.60	5.3
57	75	1282	1.70	11.8
80	61	986	1.64	7.9
100	49	1273	3.42	--

[Ref.: A. A. J. M. Peijs, P. Catsman, L. E. Govaert and P. J. Lemstra, *Composites*, 21, 513 (1990)]

**Figure 1.2** Load/time response in impact of (a) plain HP-PE and carbon composites (b) hybrid HP-PE/carbon composites.

[Ref.: A. A. J. M. Peijs, P. Catsman, L. E. Govaert and P. J. Lemstra, *Composites*, 21, 513 (1990)]

The failure strain of the carbon fibre is lower (0.01) than that of E-glass (0.028). The stress at which the carbon and glass plies would fail was given by the lines BD and AE respectively, in Figure 1.3. Considering the relative proportions of the two fibres, if there is only a small proportion of carbon, the glass will be sufficiently strong to withstand the load after failure of carbon. Then the failure of the composites will be at the failure strain of the glass. However at high proportion of carbon, there will be insufficient glass to carry the load and the failure of the composite will take place at the stress corresponding to the failure of carbon. The point C in the graph marks the change in failure behaviour. Manders and Bader^{41, 42} (Experimental curve in Figure 1.3) observed a positive hybrid effect; ie. the stresses are well above the predicted strength curve, ACD. It is observed that the failure strain of the lowest strain component is enhanced by hybridisation.

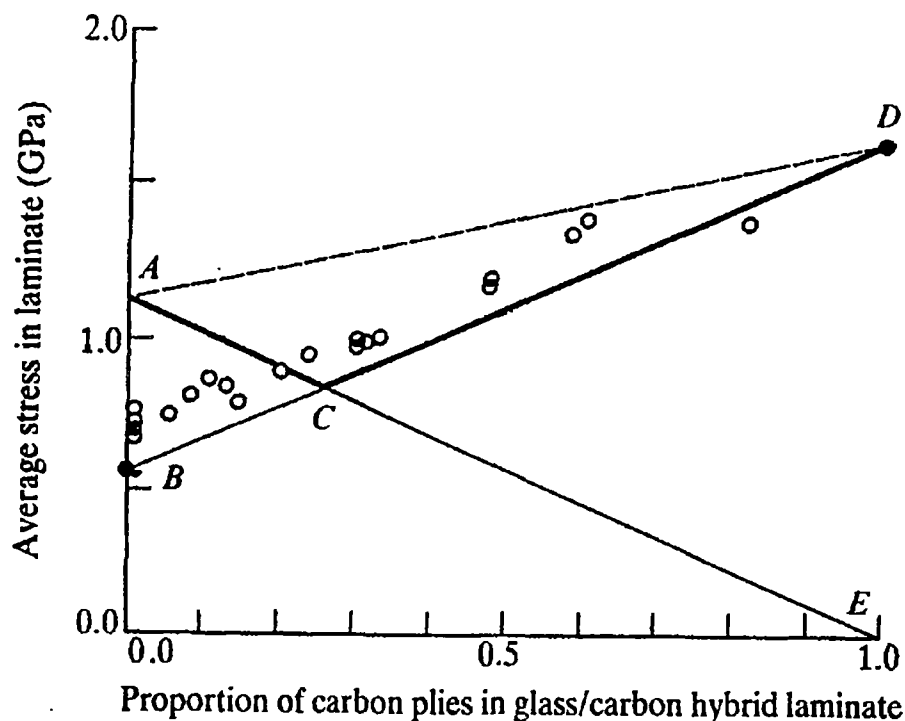


Figure 1.3 Illustration of the hybrid effect

[The line AD is simple rule-of-mixture prediction. ACD indicates the predicted strengths based on the failure strains of the two components. BD is the stress at which the least extendable plies are expected to fail.]

[Ref.: F. R. Jones (Ed.), *Handbook of Polymer-Fibre Composites*, Longman Scientific and Technical, England (1994)]

Thus the failure strain of the individual fibres will be an important criteria in determining the strength of the composites. Inorder to achieve better hybrid results, one must select fibres with higher strain compatibility. McCullough and Peterson⁴³ investigated the strain compatibility aspects in hybrid composites. According to them the strength of a collection of fibres is governed by the fibre component with the smallest elongation to break. As the tensile load is increased, the collection of the fibres is uniformly strained; eventually, a strain level is reached which corresponds to the smallest breaking strain of the fibre family within the collection. A subsequent infinitesimal increase in strain causes all those fibres characterised by the smallest breaking strain to fail. The sudden transfer of load to the remaining unbroken fibres lead to catastrophic failure.

From Hooke's law and rule of mixture relationship,

$$\sigma = \varepsilon E = \sum_{i=1}^n v_i E_i \quad (1.2)$$

where σ is current level of tensile stress, ε is the current level of strain, E_i is the tensile modulus of the i^{th} component and v_i is the volume fraction of the i^{th} component. The strength of the i^{th} component is given by

$$\sigma_i^* = \varepsilon_i^* E_i \quad (1.3)$$

where σ_i^* and ε_i^* are the ultimate stress and strain respectively for the i^{th} component. From this it can be concluded that the ultimate strength of a system is the stress level at which the elongation of the system has reached the ultimate elongation of the fibre family having the smallest strain to break. ie. $\min\{\varepsilon^*\}$. The ultimate strength of the system is given by,

$$\sigma^* = \varepsilon_j^* E = \varepsilon_j^* \sum_{i=1}^n v_i E_i \quad (1.4)$$

or:

$$\sigma^* = \sum_{i=1}^n v_i \lambda_i \sigma_i^* \quad (1.5)$$

where ε_j^* is the smallest strain to break of the collection $\{\varepsilon_i^*\}$; $\varepsilon_j^* = \min\{\varepsilon_i^*\}$

The strain compatibility parameter λ can be expressed as,

$$\lambda_i = \frac{\varepsilon_j^*}{\varepsilon_i^*} \quad (1.6)$$

The fibre combinations are strain compatible if the compatibility parameter $\lambda \sim 1$. The combinations, glass, boron ($\lambda = 0.2$) and glass, graphite ($\lambda = 0.1$) are strain incompatible while graphite, boron ($\lambda = 0.9$) combination is strain compatible.

Hybridisation of fibres with particulate fillers and whiskers improved the performance of the composites. Mechanical properties of carbon fibre reinforced epoxy composites were improved by incorporating micro-sized Al_2O_3 particles into the epoxy matrix.⁴⁴ Increase in fracture toughness of epoxy matrix was observed by hybridisation of glass fibre with beads.⁴⁵ The incorporation of various amounts of rubber and solid glass spheres into a ductile epoxy matrix improved the fatigue crack propagation resistance of the composite.⁴⁶ Hybridisation of the fibre reinforced glass matrix composites with particulate fillers results in substantial improvements in microcrack stress, transverse strength and interlaminar shear strength. However it is reported that the ultimate strengths and strain declined upon hybridisation.⁴⁷ This is illustrated in Figure 1.4. Gadkaree et al.⁴⁸ investigated the effect of an additional whisker phase such as silicon carbide in a fibre-reinforced ceramic matrix composite on the matrix micro cracking stress. Hybridisation with whiskers results in a doubling or tripling of the transverse strength and the interlaminar shear strength.

Studies on the synthetic/synthetic, synthetic/natural and natural/natural fibre hybrid composites were also reported. Addition of natural fibres to synthetic polymers results in lightweight and cost effective composites which has got comparatively low strength than the synthetic reinforcement. Effective hybridisation of natural fibres with stronger fibres could be a possible solution to

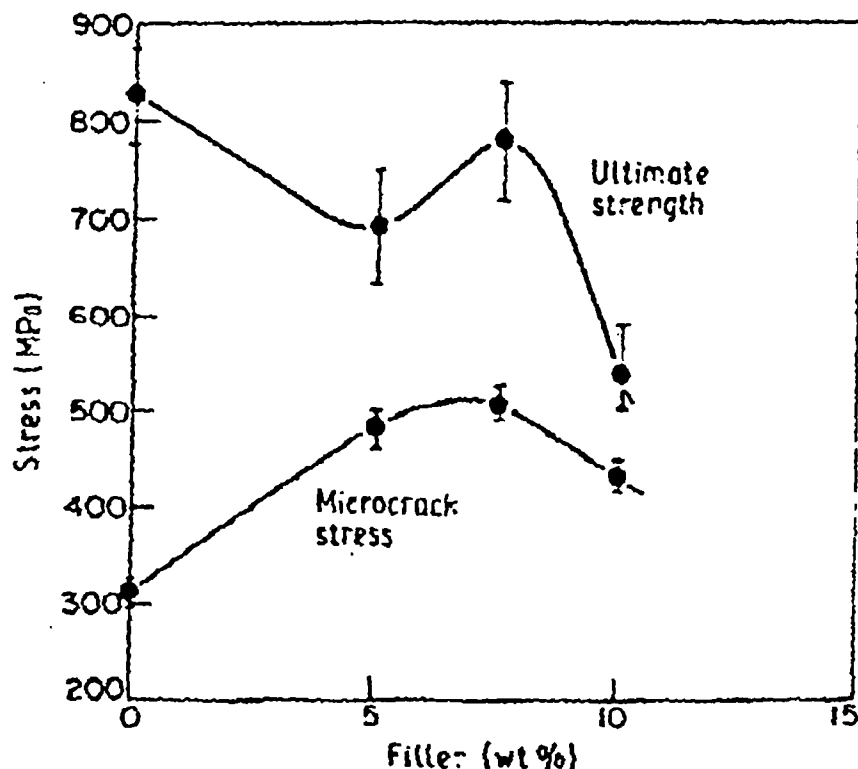


Figure 1.4 Variation of microcrack stress and ultimate strength as a function of filler loading level.

[Ref.: K. P. Gadkaree, *J. Mater. Sci.*, 27, 3827 (1992)]

overcome this limitation. Chand and Rohatgi⁴⁹ reported on the hybridising effects of sunhemp-carbon fibres in polyester resin on the tensile strength values of the composites. With the incorporation of small percent of carbon fibre, the strength of the sunhemp-polyester composites is considerably increased.

Banana/glass hybrid polyester composites were found to have better mechanical properties compared to composites with banana fibre alone.⁵⁰ Impact properties were found to increase upto a glass volume fraction 0.11 and then decreases slightly (Fig. 1.5). The slight lowering of impact strength was attributed to the change in energy dissipation mechanism. At high glass content, the fracture mechanism was mainly fibre fracture, due to the brittle nature of glass. However at lower glass volume fraction, the fracture mechanism was mainly by fibre pull out due to the presence of higher volume fraction of banana fibre. Different layering patterns were tried out and the mechanical properties were found to be affected by

the layering pattern. The banana-cotton fabric reinforced polyester composites were reported to have very good ageing resistance even though their strength properties were lower than the matrix resin.⁵¹

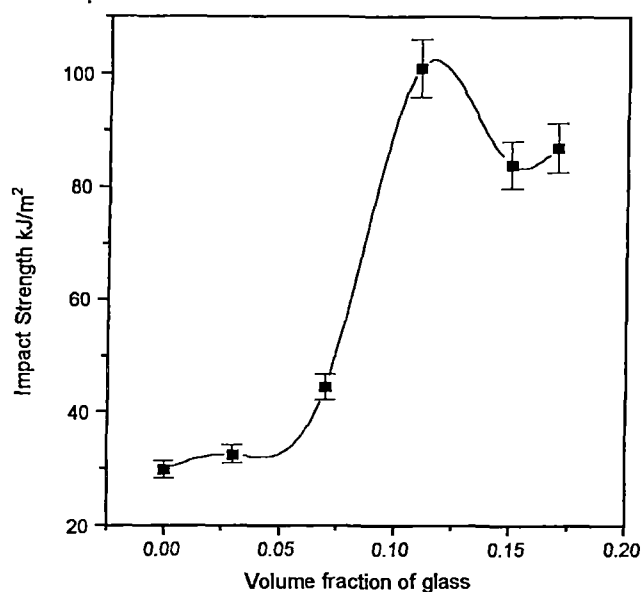


Figure 1.5 Effect of glass volume fraction on the impact strength of banana-glass hybrid composites

[Ref.: L. A. Pothen, S. Thomas, J. George and Z. Oommen, *Polimery*, **44**, nr11-12, 750 (1999)]

1.3 WOVEN FABRIC (TEXTILE) COMPOSITES

Woven fabric composites form another important class of composites, which are widely used as textile structural composites. They provide excellent integrity and conformability for advanced structural composite applications. Woven fabrics are considered as laminated bodies, each layer of which is a woven fabric formed by interlacing two sets of threads, the warp and the fill or weft. Warp and weft may be either identical or different threads and the various types of weaves can be identified by the patterns of repeats in the warp and weft directions. The woven fabric composites provide more balanced properties on the weave plane than unidirectional fibre composites. This is due to the fact that the two-directional reinforcement inside the lamina behaves like a quasi-isotropic substance. This can resist biaxial loading and especially in impact more efficiently.⁵² Woven fabric

composites provide more balanced properties in the fabric plane and higher impact resistance than unidirectional composites. The variety of manufacturing methods has made the textile composites cost-competitive with unidirectional composites. The 2D orthogonal fundamental weaves among woven fabrics are plain, twill and satin. The various types of fundamental weave pattern are shown in Figure 1.6.⁵³ A number of parameters are involved in determining the fabric structure; weave, density of yarns in the fabric, fabric count, characteristics of warp and fill (weft) yarns, characteristics of fibres and factors induced during weaving such as yarn crimp etc.

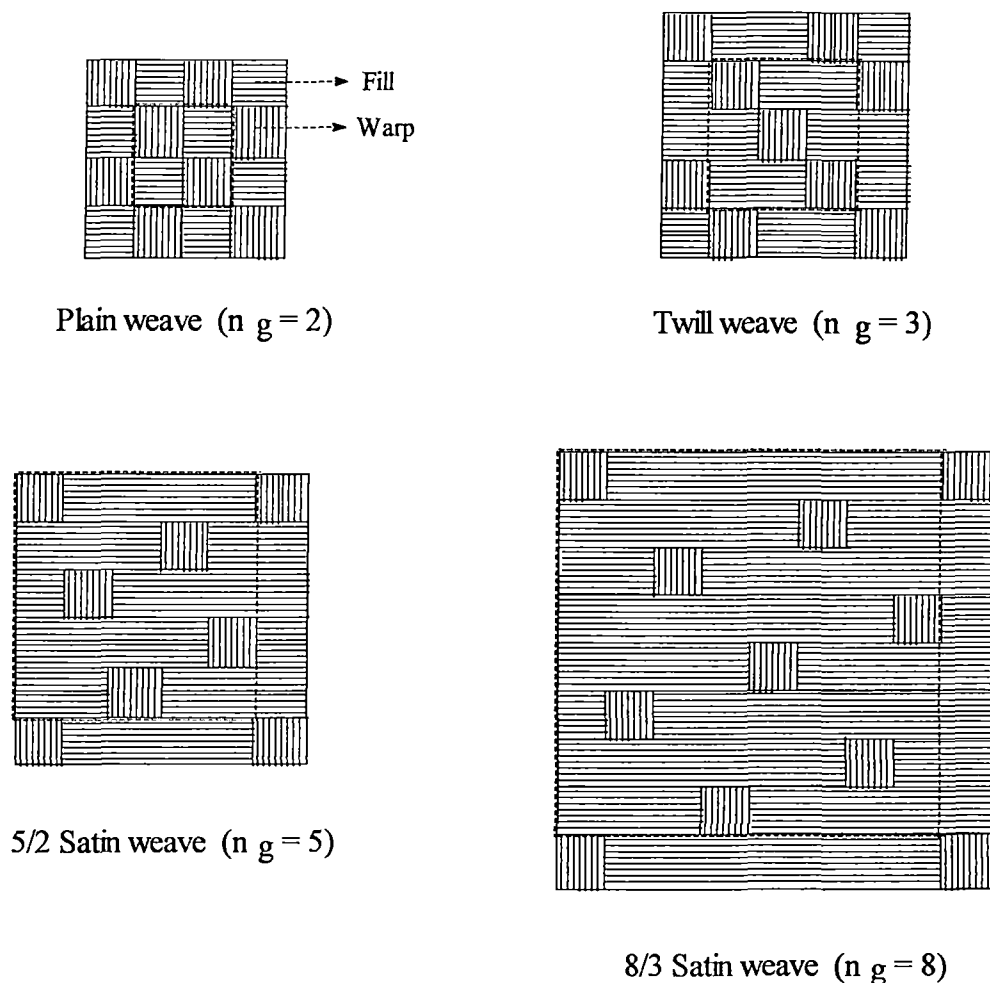


Figure 1.6 Fundamental weaves (n_g = number of repeats)

[Ref.: N. K. Naik (Ed.), *Woven fabric composites*, Technomic publishing Co. Inc., Lancaster, January (1994)]

Woven fabric composites show poor inter laminar properties. Delamination is the main failure form observed in these composites. Laroche and Vu-Khanh⁵⁴ predicted the complex rearrangement that occurs during moulding of complex components from woven carbon fabric in epoxy matrix. They found that the fabric yarn slippage is negligible for carbon/epoxy prepregs. Wang and Zhao⁵⁵ studied the mechanical behaviour of fibreglass and Kevlar woven fabric reinforced epoxy composite laminates with different weave patterns. They suggest that matrix toughening by microfibrils could be an effective way to improve the inter laminar toughness of composites. Gilchrist et al.⁵⁶ investigated the fracture and fatigue performance of textile comingled yarn composites from glass and polyethylene terephthalate. Kotaki et al.⁵⁷ reported interfacial interactions on the delamination and interlaminar fracture toughness of glass woven fabric composites. Studies are going on in banana woven polyester, banana/glass interwoven polyester and banana/cotton interwoven polyester composites.⁵⁸ It has been observed that the tensile and impact properties improve by about 100% when the same volume fraction of fibres are used in the woven form.

1.4 FACTORS AFFECTING THE PROPERTIES OF A FIBRE REINFORCED COMPOSITE

1.4.1 Fibre-Matrix Interface

The fibre-matrix interface plays a major role in the mechanical and physical properties of composite materials. The stresses acting on the matrix are transmitted to the fibre across the interface. For efficient stress-transfer, the fibres have to be strongly bonded to the matrix. Composite materials with weak interfaces have relatively low strength and stiffness but high resistance to fracture whereas materials with strong interfaces have high strength and stiffness but are very brittle. The effects are related to the ease of debonding and pull out of fibres from the matrix during crack propagation.

The interface/interphase concept in a fibrous composite is clear from the Figure 1.7.⁵⁹ Interface is defined as a two dimensional region between fibre and

matrix having zero thickness. The interphase in a composite is the matrix surrounding a fibre. There is a gradient in properties observed between matrix and interphase. Interface is an area whereas interphase is a volume.

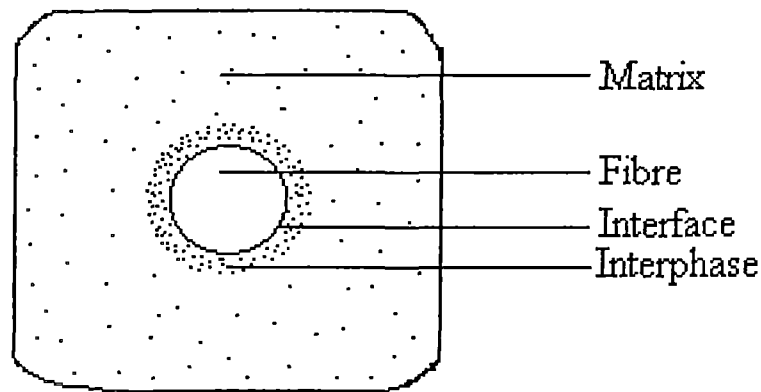


Figure 1.7 Interface/Interphase in a fibre reinforced composite
[Ref.: G. M. Newaz, Polym. Comp., 7, 421 (1986)]

Pagano and Tandon⁶⁰ carried out a systematic study to explore possible consequences an interphase could have on the stress field in composites. Cervenka⁶¹ has detailed a micromechanical model together with an account of modulation of the stress field due to an anisotropic interphase. Newaz⁵⁹ reported that fibre-matrix bond quality could be evaluated via an evaluation of the interphasial fracture toughness. They used a tensile test with single edge notched specimens. Piggott⁶² has investigated the effect of interface/interphase on the composite properties. The stress-transfer through the fibre-matrix interface and its effect on the strength of the composites were reported by Dilandro et al.⁶³ If the fibre-matrix adhesion is poor, the interface will fail at an early stage. Fibre slippage can also occur due to weak fibre-matrix adhesion.

1.4.1.1 Theories of Adhesion

The fibre-matrix interface adhesion can be attributed to five main mechanisms.

a) *Adsorption and Wetting*

This is due to the physical attraction between the surfaces, which is better understood by considering the wetting of solid surfaces by liquids. Between two solids, the surface roughness prevents the wetting except at isolated points. In a solid-liquid system, for effective wetting of a fibre surface, the liquid resin must cover all parts of the surface to displace all the air.

Wetting that can be explained by Dupre equation for the thermodynamic work of adhesion, W_A of a liquid to a solid states that,⁶⁴

$$W_A = \gamma_1 + \gamma_2 - \gamma_{12} \quad (1.7)$$

Where γ_1 and γ_2 are the surface free energies of the liquid and solid respectively and γ_{12} is the free energy of the liquid-solid interface. This can be related to the Young equation for the physical situation of a liquid drop on a solid surface (Fig. 1.8) which states that,

$$\gamma_{SV} = \gamma_{SL} + \gamma_{LV} \cos \theta \quad (1.8)$$

where γ_{SV} , γ_{SL} and γ_{LV} are the surface free energies or surface tensions of the solid-vapour, solid-liquid and liquid-vapour interfaces respectively and θ is the contact angle. For spontaneous wetting to occur the contact angle must be 0° .

Combining equations 1.7 and 1.8, and putting $\gamma_1 = \gamma_{SV}$, $\gamma_2 = \gamma_{LV}$ and $\gamma_{12} = \gamma_{SL}$;

$$W_A = \gamma_{SV} + \gamma_{LV} - \gamma_{SL} \quad (1.9)$$

where W_A represents the physical bond.

When the fibre surface is contaminated, the effective surface energy decreases. This hinders a strong physical bond between the fibre and matrix. Presence of entrapped air or large shrinkage stresses during curing process also affects the physical bonding at the fibre-matrix interface.

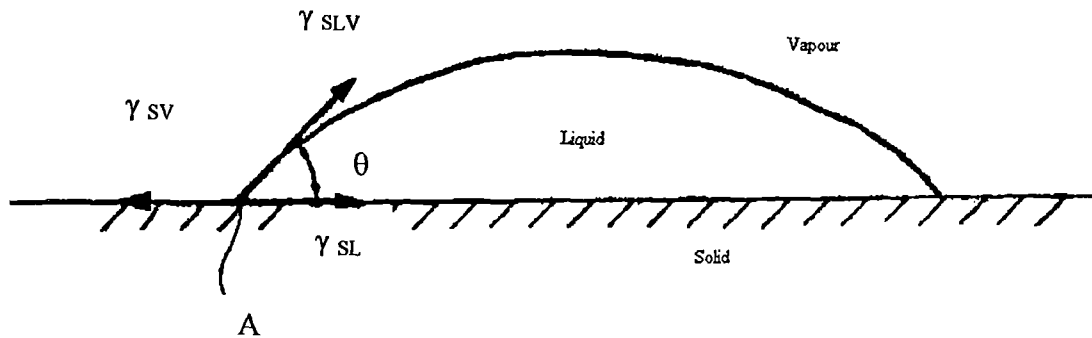


Figure 1.8 Contact angle (θ) and surface tensions (γ) for a liquid drop on a solid surface. SV, SL and LV stand for solid-vapour, solid-liquid and liquid-vapour interfaces respectively.

[Ref.: D. Hull (Ed.), *An Introduction to Composite Materials*, Cambridge University Press, London (1981)]

b) Interdiffusion

Polymer molecules can be diffused into the molecular network of the other surface, say fibre as shown schematically in Figure 1.9a. The bond strength will depend on the amount of molecular entanglement and the number of molecules involved. Presence of solvents and plasticising agents promote interdiffusion.⁶⁴ The amount of diffusion will depend on the molecular conformation, constituents involved and the ease of molecular motion.

c) Electrostatic Attraction

This type of linkage is possible when there is a charge difference at the interface. The strength of the interface will depend on the charge density. The electrostatic interaction at the interface can be represented as in Figure 1.9b. The anionic and cationic species present at the fibre and matrix phases will have an important role in the bonding of the fibre-matrix composites via electrostatic attraction (Fig. 1.9c). Introduction of suitable coupling agents at the interface can enhance the bonding through the attraction of cationic functional groups by anionic surface and vice versa. Introduction of silane coupling agent on the glass surface is an example of this type of interaction. In this case, the pH of the silane can be controlled to get optimum coupling effect.

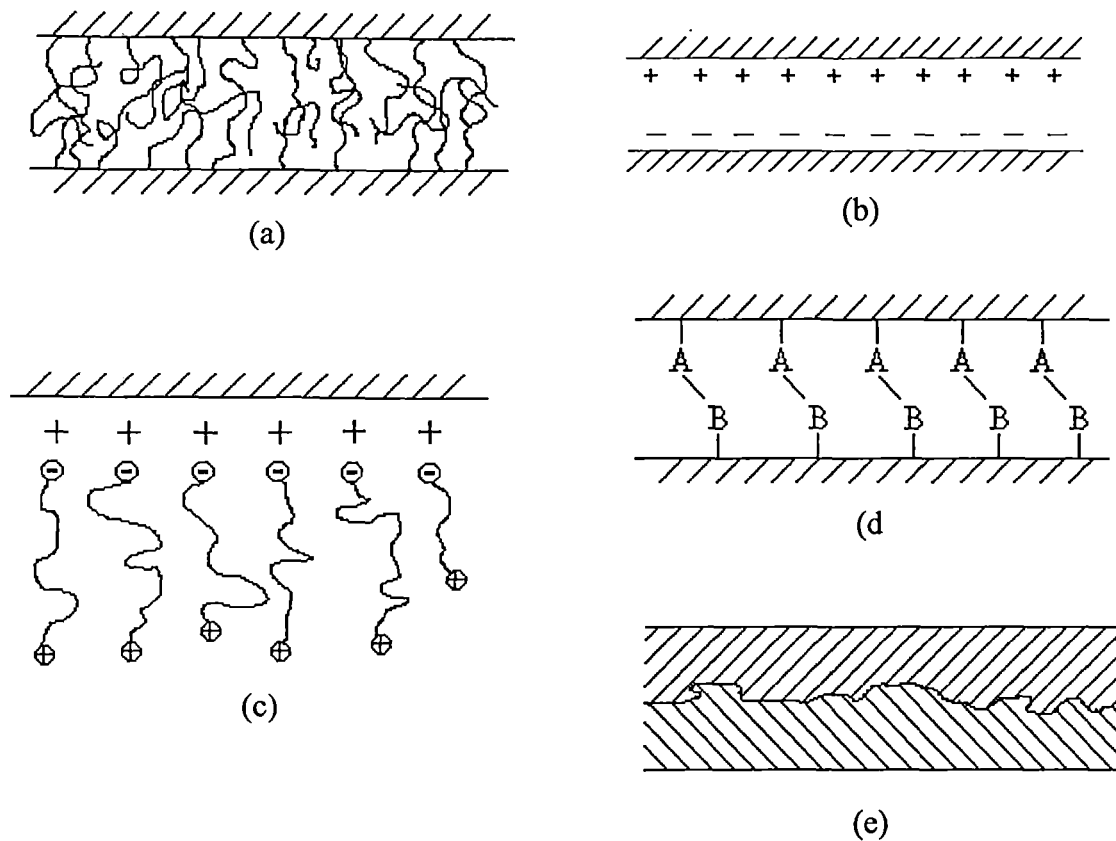


Figure 1.9 (a) Bond formed by molecular entanglement following interdiffusion. (b) Bond formed by electrostatic attraction (c) Cationic groups at the end of molecules attracted to an anionic surface resulting in polymer orientation at the surface. (d) Chemical bond formed between groups A on one surface and groups B on the other surface. (e) Mechanical bond formed when a liquid polymer wets a rough solid surface.

[Ref.: D. Hull (Ed.), *An Introduction to Composite Materials*, Cambridge University Press, London (1981)]

d) Chemical Bonding

Chemical bonds can be formed between chemical grouping on the fibre surface and a compatible chemical group in the matrix as shown in Figure 1.9d. The type of bond determines the strength. The interface breakage involves bond cleavage. Interfacial chemical bonding can increase the adhesive bond strength by preventing molecular slippage at a sharp interface during fracture and by increasing the fracture

energy by increasing the interfacial attraction. A sharp interface formed when little or no interfacial diffusion occurs unlike in a diffuse interface in which case sufficient interfacial diffusion occurs. Dispersion forces at the interface (1-5kcal/mole) are too weak to prevent molecular slippage at a sharp interface. But a chemical bond (50-250kcal/mole) can prevent the slippage.⁶⁵

e) Mechanical Adhesion

Mechanical interlocking at the fibre-matrix interface is possible as represented schematically in Figure 1.9e. The degree of roughness of the fibre surface is very significant in determining the mechanical and chemical bonding at the interface. This is due to the larger surface area available on a rough fibre. Surface roughness can increase the adhesive bond strength by promoting wetting or providing mechanical anchoring sites.

1.4.1.2 Interface Modifications

Intimate molecular contact at fibre-matrix interface is necessary to obtain strong interfacial attraction. Without intimate molecular contact, the interfacial adhesion will be very weak, and the applied stress that can be transmitted from one phase to the other through the interface will accordingly be very low. The interface can be classified into sharp and diffuse interface.

The adhesive behaviour can be visualised into three. 1. Sharp interface with weak molecular force as in the case of non-polar polymer with a polar polymer. In such a case the interface will be mechanically weak because of lack of molecular entanglement leading to interfacial slippage. 2. Sharp interface with strong molecular force such as the dispersion force between a non-polar polymer and a high energy material or molecular forces involving specific interactions. In this case interface slippage will not occur and the interface will be mechanically strong. 3. Diffuse interface with any molecular force; if there is sufficient molecular diffusion and entanglement, interfacial slippage will not occur. Therefore both primary (chemical bonds) and secondary (van der Waals attractions) bonds are

important in adhesion depending on interfacial structure. The energies associated with possible primary and secondary interactions at the interface are given in Table 1.2.

As discussed earlier, in a fibre reinforced polymer composite, the interfacial interaction depends on the physical and chemical structure, polarity etc. of the components. The interfacial properties can be improved by giving appropriate modifications to the components, which give rise to changes in physical and chemical interactions at the interface. Several classes of compounds are known to promote adhesion apparently by chemically coupling the adhesive to the adherends. Several processes have been developed to modify polymers and fibre surfaces including chemical treatments, photochemical treatments, plasma treatments, surface grafting etc. This causes physical and chemical changes on the surface layer without affecting the bulk properties.

Table 1.2 Comparison of Various Attractive Energies

Type of force	Typical energy range (kcal/mole)
van der Waals forces	
Dispersion force	5
Dipole-dipole	Up to 10
Dipole-induced dipole	Up to 0.5
Hydrogen bond	4 - 41
Chemical bonds	
Covalent bond	15 - 170
Ionic bond	140 - 250
Metallic bond	27 - 83

[Ref: S. Wu (Ed.), *Polymer Interface and Adhesion*, Marcel Dekker Inc., New York (1982)]

Coupling agents usually improve the degree of crosslinking in the interface region and a perfect bonding results. Various silanes are found to have effectively improved the interface properties of wood-polypropylene, mineral filled elastomers, fibre reinforced epoxies and phenolics etc.⁶⁶⁻⁶⁹ Silanes having reactive alkyl groups

can chemically couple the adhesive and the adherend by reacting with appropriate groups and thus promote adhesion. Silanes having non-reactive alkyl groups have no chemical coupling activity and in such cases adhesion appears to arise from improved interfacial compatibility. Silanes have been used to promote adhesion to hydrophilic adherends, such as glass, aluminium, clay, talc, calcium carbonate etc. Ulkem and Schreiber⁷⁰ observed enhanced interface adhesion in Nylon 6,6–glass fibre composites on aminosilane modification. Hamada et al.⁷¹ studied the effect of siloxane sequence of chemically bonded silane on the interfacial strength of silane treated glass fibre epoxy composites. The crosslinking of the silane reduces the interfacial strength. They determined interfacial stress transmissibility as an index of interfacial strength using a modified single-filament test. The interfacial transmissibility is increased with the wt.% of γ -aminopropyldimethoxymethylsilane (APDS) in the mixture with γ -aminopropyltrimethoxysilane (APTS) (Fig. 1.10). The greater the crosslink density of the network formed, the lower the permeability of resin in the interphase. The uncrosslinked dimethoxysilane interphase results in the highest interfacial strength.

The silane coupling agents were found to be effective in modifying natural fibre-polymer matrix interface. Gonzalez et al.^{72, 73} investigated the effect of silane coupling agent and alkaline treatment on the interface performance of henequen reinforced high-density polyethylene composites. The fibre-surface silanization results in a better interfacial load transfer efficiency but does not seem to improve the wetting of the fibre. The alkali treatment increases the surface roughness that results in better mechanical interlocking and it increases the amount of cellulose exposed on the fibre surface. This increases the number of possible reaction sites and allows better fibre wetting. The silane treatment enhances the tensile strength of the composite.

Many other compounds such as chromium complexes, titanates, isocyanates etc. can be used as coupling agents. Monte and Sugerman⁷⁴ reviewed processing of composites with titanate coupling agents. It was found that the deposition of

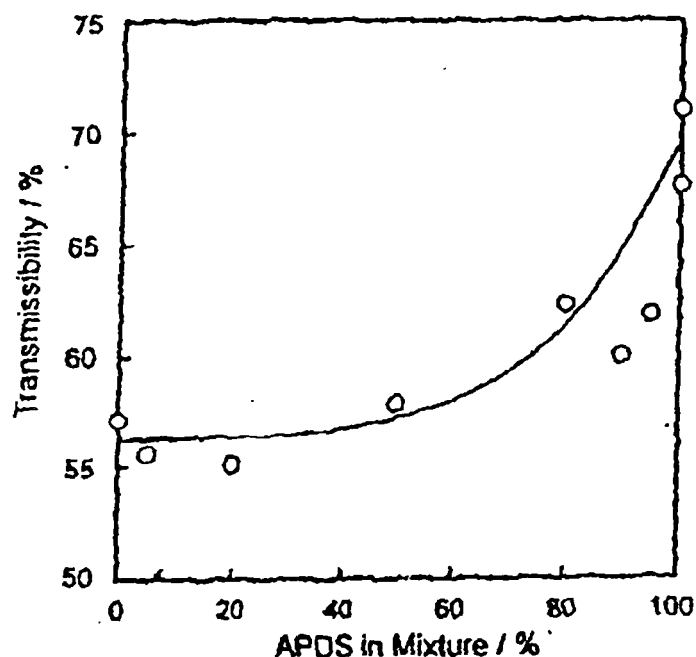


Figure 1.10 Change of interfacial transmissibility with weight percentage of APDS in silane mixture.

[Ref.: H. Hamada, N. Ikuta, N. Nishida and Z. Maekawa, *Composites*, 25, 512 (1994)]

a monolayer of organo functional titanate which eliminates the water of hydration leading to deagglomeration. This enhances the dispersion and compatibility at the interface. It is proposed that dispersion of an inorganic in an organic phase, in the presence of titanate coupling agents is enhanced by the replacement of the water of hydration at the inorganic surface with a monomolecular layer of organo functional titanate causing inorganic/organic phase compatibilization at the interface, thereby increasing the degree of displacement of air by the organic phase in the voids of the inorganic component. Figure 1.11 shows the proposed effect of coupling an agglomerated inorganic with a monoalkoxy titanate. The titanate coupling agents were found to be effective in natural fibre composites. Varma et al.⁷⁵ observed a 22% improvement in interlaminar shear strength in hybrid laminates of glass fabric and titanate treated bristle coir fibres.

Performance of isocyanate as a coupling agent has been reported by Kokta et al.^{76, 77} Isocyanates provide better interaction with thermoplastics resulting in

superior properties. It was found that isocyanates can act as promoters or as an inhibitor, depending on the concentration of isocyanate used. They observed an optimum concentration of isocyanates above which the strength does not increase significantly. Figure 1.12 shows the effect of polymethylene (polyphenyl isocyanate) (PMPPIC) concentration on the tensile strength of HDPE-Aspen composites. The stress increased steadily with the addition of fibre, but the increase was marginal at higher concentration of PMPPIC. The stress and modulus of the HDPE and LLDPE composites enhanced 60 and 90 percent respectively on isocyanate treatment.

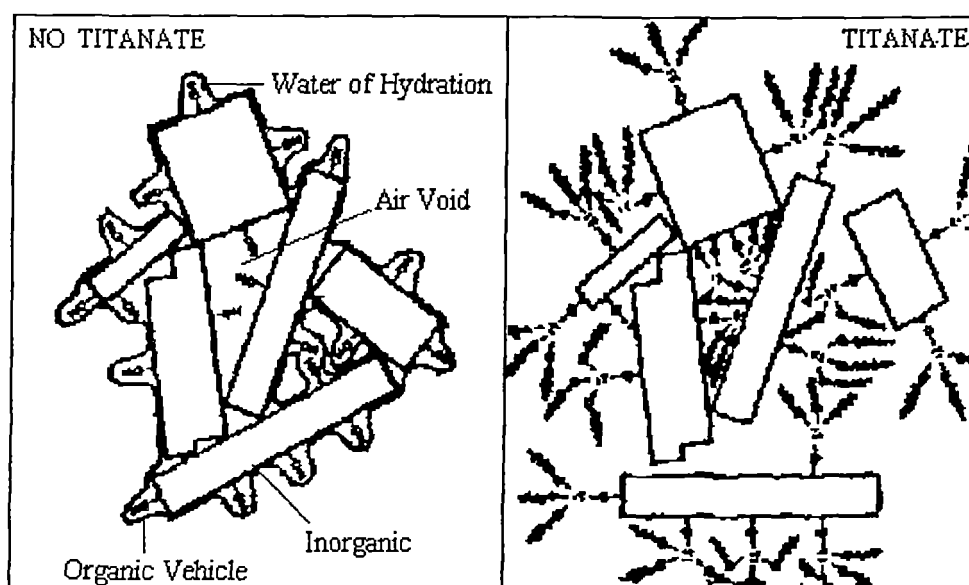


Figure 1.11 The proposed mechanism for deposition of a monolayer of triorganofunctional titanate to effect the elimination of inorganic water of hydration and air voids resulting in deagglomeration.

[Ref.: S. J. Monte and G. Sugerman, *Polym. Eng. Sci.*, 24, 1369 (1984)]

Remarkable improvements in strength properties in jute/polypropylene⁷⁸ and wood flour/polyethylene⁷⁹ composites were observed by the action of compatibilizers. A maleic-anhydride-grafted styrene-ethylene-butylene-styrene (SEBS-MA) triblock copolymers has been used as a compatibiliser in low-density polyethylene-wood flour composite. The MA reacts with wood through

esterification and hydrogen bonding and also possibly through interaction between the styrene and wood. Joly et al.⁸⁰ studied the effect of PP-g-MA grafting and alkyl chain grafting of cellulosic fibres on the physico-mechanical behaviour of PP/ramie fibre composites. The grafting leads to an optimised interface of high modulus. The chemical modification of the cellulosic fibres and interactions with polypropylene matrix are schematically shown in Figure 1.13.⁸⁰

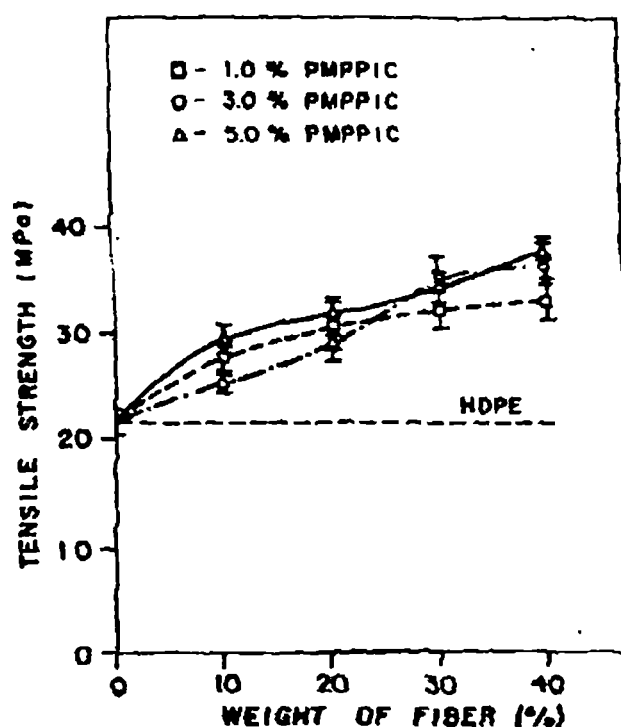


Figure 1.12 Effect of PMPPIC concentration on tensile strength of HDPE-aspen composites.

[Ref.: R. G. Raj, B. V. Kokta, D. Maldas and C. Daneault, *Polym. Comp.*, **9**, 404 (1988)]

Several interface modification methods were reported in literature. Studies on the acrylonitrile grafting of coir fibre were reported by Mohanty et al.⁸¹ The treatment affects the moisture uptake capacity of the fibre and therefore modify the electrical, mechanical, thermal and tensile properties of the fibre. Reddy et al.⁸² studied cyanoethylation of jute fibres at different conditions on the moisture regain. Moisture regain decreased significantly on cyanoethylation. Corona treatment was found to enhance the wettability of wood surface.⁸³ Negligible chemical effects of

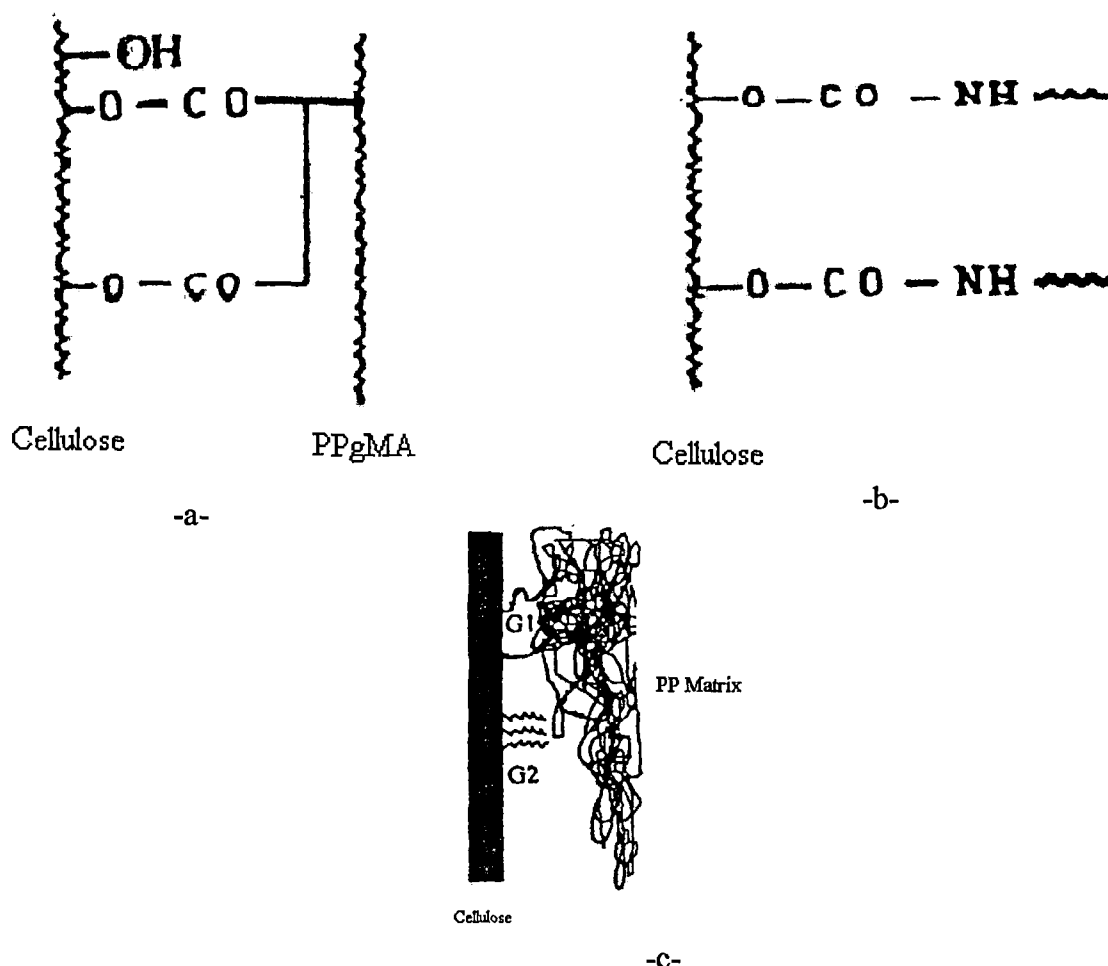


Figure 1.13 Chemical modifications of cellulosic fibres (a) Grafting of a PP chain from a solution of toluene containing 10% PP-g-MA (G₁) (b) Grafting of an alkyl chain from a solution of isocyanate in pyridine (G₂) (c) Schematic representation of both the treatments. [Ref.: C. Joly, R. Gauthier and B. Chabert, *Comp. Sci. Technol.*, **56**, 761 (1996)]

the corona treatment on the cellulose, hemicellulose and lignin were reported. The corona treatment affected the neutral fraction in the alcohol-benzene extractives and oxidised them to aldehyde groups. The neutral fraction originally contains benzene ring and double-bond structures and the treatment reduces the hydrophobicity. Plasma treatment is found to effectively enhance the interface sensitive mechanical properties in aramid/epoxy composites.⁸⁴ The interlaminar shear and T-peel strength between the fibre and epoxy resin markedly improved by plasma treatment. Carlotti and Mars⁸⁵ observed improvement in adhesion of polyethylene terephthalate fibres to rubber matrix. Various other modifications such as

acetylation, benzylation, acrylation, permanganate treatment, peroxide treatment etc. were found to increase the compatibility of natural fibres with polymers such as polyethylene, polypropylene and natural rubber.^{86–97}

1.4.1.3 Fibre Surface and Interface Characterisation

The modified and virgin fibre surfaces and interface can be characterised by spectral and microscopic methods. The characterisation gives evidence of chemical composition of the surface region as well as information on interactions between fibre and matrix. Electron spectroscopy for chemical analysis (ESCA) is one of the important tools to study solid surfaces. Zadorecki and Ronnhult⁹⁸ conducted ESCA studies of cellulose fibres. This technique has an information depth of 1-5 nm and is capable of examining only the outer layers of fibres. They used ESCA for the ‘finger print’ analysis of diallyl triazine treated cellulose fibres. Computerised peak separation and peak area measurements were applied to determine the chemical composition of the modified surfaces. The spectra of diallylamino-s-triazine treated fibres are given in Figure 1.14.⁹⁸ Other than this, many other spectroscopic methods such as Mass spectroscopy, X-ray diffraction study, electron induced vibration spectroscopy, photoacoustic spectroscopy were shown to be successful in polymer surface and interfacial interaction characterization.^{99–101} Infrared spectroscopy was found to be effective in determining interactions at the modified interfaces.^{102, 103} Yamaoka et al.¹⁰⁴ utilised neutron activation analysis technique to identify the radioactive nuclides produced in inorganic fillers for polymer composites.

Frequently used thermodynamic methods for the characterisation in reinforced polymers are wettability study, inverse gas chromatography measurement, zeta potential measurement etc. Contact angle measurements have been used to characterise the thermodynamic work of adhesion between solids and liquids as well as surface of solids. It is reported that the contact angle between a single fibre in a fibre reinforced polymer melt is given by the following relationship.¹⁰⁵

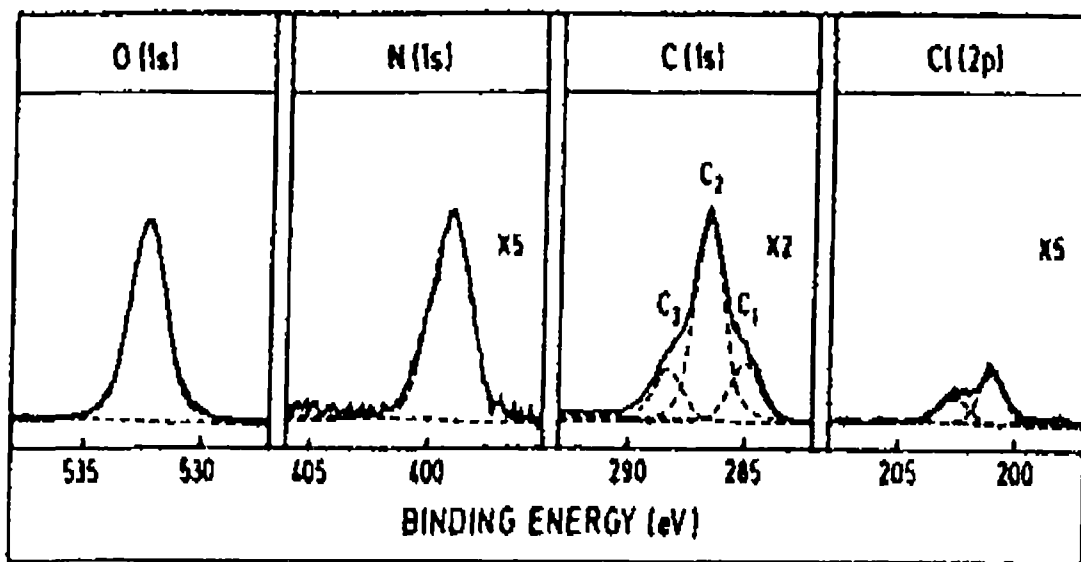


Figure 1.14 ESCA spectra of cellulose fibres treated with diallyl triazine.

[Ref.: P. Zadorecki and T. Ronnhult, *J. Polym. Sci.: Part A: Polym. Chem.*, **24**, 737 (1986)]

$$\cos \theta = \frac{F}{P} = \frac{g \cdot \Delta m}{P} \quad (1.10)$$

where θ is the contact angle, F is force per unit length, P is fibre perimeter, g is gravitational constant and Δm is the change in mass before and after immersion of the fibre in the polymer melt.

Microscopic studies such as optical microscopy, scanning electron microscopy (SEM), transmission electron microscopy (TEM), and atomic force microscopy can be used to study the morphological changes on the surface and can predict the extent of mechanical bonding at the interface. The adhesive strength of fibre to various matrices can be determined by AFM studies. Many studies were reported on the microscopical evidence of fibre dispersion, fibre-matrix adhesion, interface failure mechanisms etc.¹⁰⁶⁻¹⁰⁹

The extent of fibre-matrix interface bonding can be tested by different mechanical tests such as fibre pullout, fibre fragmentation test, fibre push-out test etc. Various models were suggested to explain the failure of fibre in a composite.¹¹⁰⁻¹¹² The single fibre failure is associated with many factors within the

composite such as fibre length, fibre-matrix adhesion etc. Desaegeer and Verpoest¹¹³ suggested the use of micro-indentation test technique to measure interfacial shear strength in fibre reinforced composites. The study revealed that the test could be used for real composite parts. It has been shown that parameter such as fibre splitting, fibre diameter etc. influence the strength. Kim et al.¹¹⁴ studied the influence of interface layer on the stress transfer during fibre pull-out process and the effects of interfacial coating on the debonding process. They found that a discrete coating layer between fibre and matrix significantly reduces the stress concentration occurring particularly near the fibre entry. Pitkethly and Doble¹¹⁵ characterized the fibre-matrix interface of carbon fibres embedded in epoxy matrix using a single fibre pull out technique. They presented a non-graphical technique to evaluate the maximum interfacial shear stress. The experimental set up for a single fibre pull out testing is given in Figure 1.15. A typical load-extension curve for a single fibre pull out process is as shown in Figure 1.16.¹¹⁵

Li and Grubb¹¹⁶ investigated the interfacial shear strength and stress distribution in the fibre pull-out test. The stress distribution along the fibre after debonding can be used to evaluate the interfacial normal stress and the frictional coefficient. The failure paths in carbon fibre reinforced thermoplastics were analysed from fibre pull-out tests.¹¹⁷ Debonding at the fibre-matrix interface and cohesive failure of the matrix close to the fibre surface were found to be the failure pattern in this case. Piggott¹¹⁸ reported a study on the role of friction in tests to measure strength of the fibre-matrix interface. Friction plays an important role in fibre-matrix debonding. Figure 1.17 shows partially debonded fibre with friction in a pull out test. As the debond proceeds along the interphase, frictional shears will be exerted in the part that is already debonded. The reactions between surface interphase and final composite properties of glass reinforced epoxy systems were studied by Mader et al.¹¹⁹ They utilised pull-out test, zeta potential measurements and contact angle measurements for interface characterisation. Single fibre push-out test was also utilised to predict the interfacial properties.^{120, 121} The limitation of

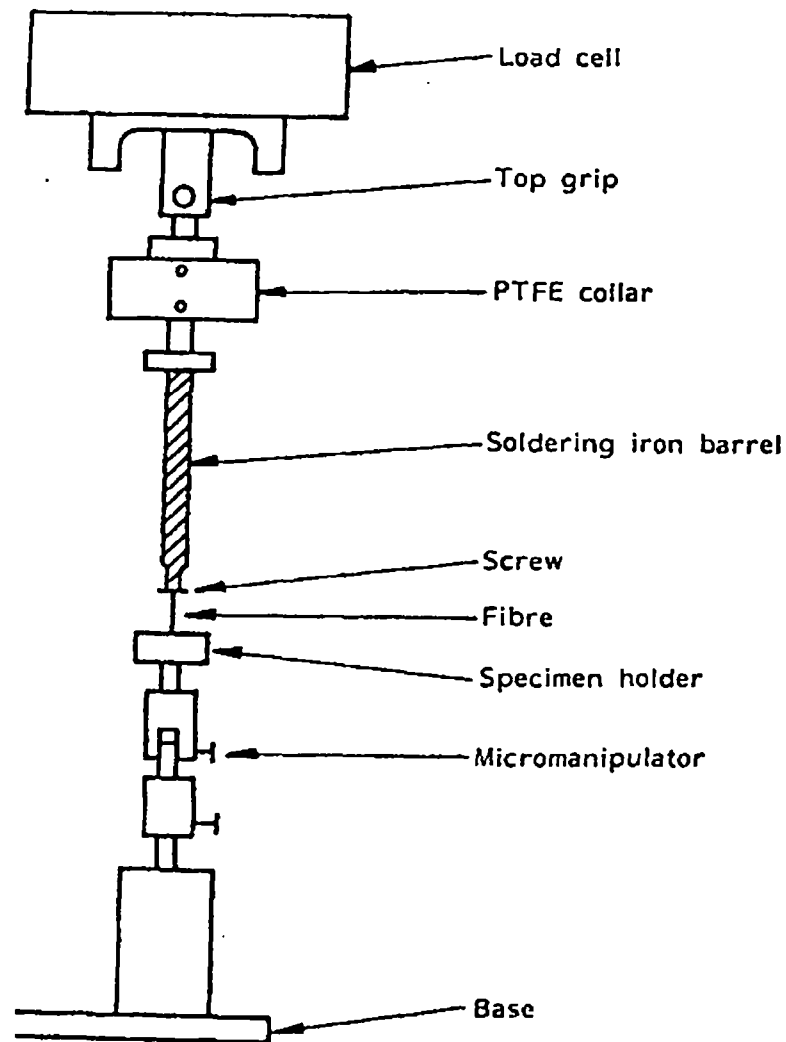


Figure 1.15 Adaptations made to the top grip of a tensile testing machine for single fibre pull-out testing

[Ref.: M. J. Pitkethly and J. B. Doble, *Composites*, 21, 389 (1990)]

the push-out test is that the interface is axially compressed during loading and large loads are required. Joly et al.⁸⁰ characterised the adhesion of polypropylene onto cellulosic fibre by micro-bond test. The study involved extraction of a polymer droplet formed around a single fibre. By means of a high precision sight, the fibre diameter, d , and droplet length or debonding length, l , are measured *in situ* (Figure 1.18). From the record of debonding force, F , and by knowing the fitted surface, the mean interfacial shear stress (IFSS), τ , between fibre and matrix can be calculated by the following expression:⁸⁰

$$\tau = \frac{F}{\pi dl} \quad (1.11)$$

A schematic representation of the microbond test is shown in Figure 1.18.

1.4.2 Fibre Length, Loading and Orientation

The composite properties depend strongly on fibre content, fibre length distribution, fibre orientation and to some extent on fibre dispersion. The distribution of fibre length may be influenced by processing parameters. Considerable fibre damage occurred reducing the number average fibre length from starting value of 4.5mm to 1mm in poly(butylene terephthalate/polyethylene alloys reinforced with short glass fibres processed by injection moulding.¹²² In order to understand the effect of fibre length, consider a composite reinforced with continuous fibres.

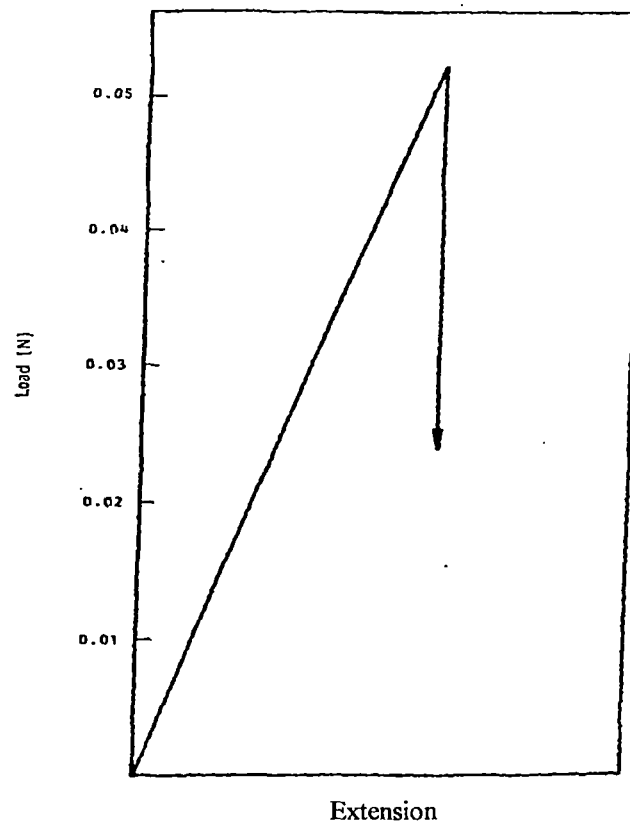


Figure 1.16 Typical load/extension curve for a pull-out test.

[Ref.: M. J. Pitkethly and J. B. Doble, *Composites*, 21, 389 (1990)]

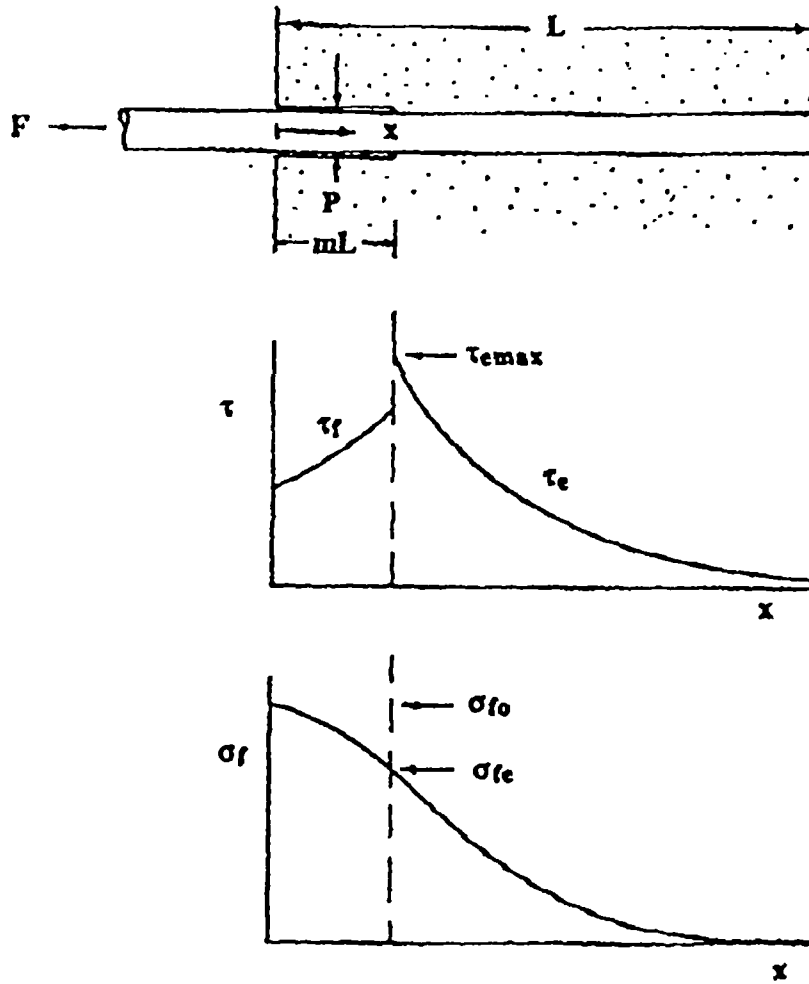


Figure 1.17 Partly debonded fibre with friction in the debonded region in a pull-out test. Debonding crack is suppose to be closed and crack faces pressed together with pressure P .

[Ref.: M. R. Piggott, *Comp. Sci. Technol.*, 42, 57 (1991)]

The tensile stress (σ_c) applied to the composite along the fibre direction will be distributed between the fibre and matrix and can be explained by simple rule of mixtures behaviour.

$$\sigma_c = E_m V_m \epsilon_c + E_f V_f \epsilon_c \quad (1.12)$$

where ϵ_c is the strain in the composite, E_m and E_f are the Young's modulus of the matrix and fibre, V_m and V_f are the volume fraction of the matrix and fibre respectively.

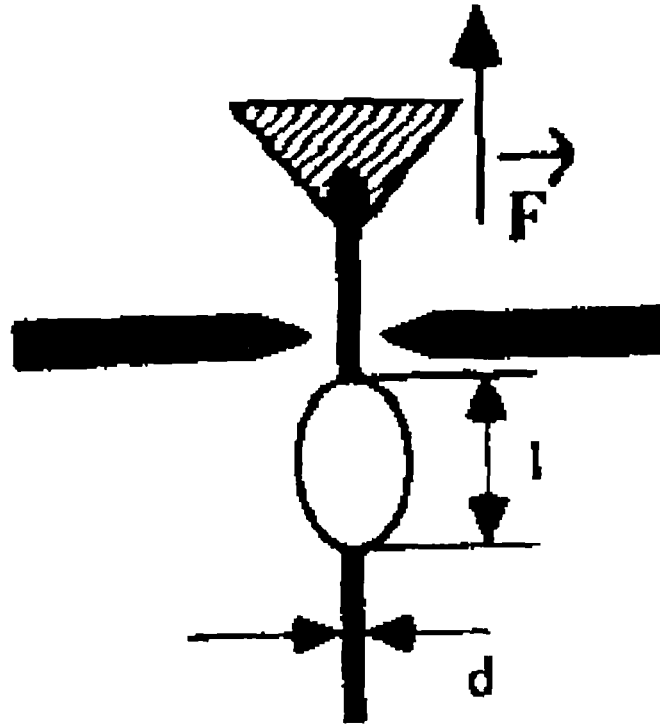


Figure 1.18 Schematic diagram of the microbond test.

[Ref.: C. Joly, R. Gauthier and B. Chabert, *Comp. Sci. Technol.*, **56**, 761 (1996)]

However in a composite reinforced with unidirectional long discrete fibres, the tensile stress applied along the fibre direction will be unevenly distributed along each fibre and cannot be explained by equation 1.11. It can be shown that¹²³

$$\sigma_x \pi r^2 = \int_0^x \tau(x) 2\pi R dx + \sigma_m \pi r^2 \quad (1.13)$$

where $\sigma_x \pi r^2$ is the tensile load transmitted to the end segment of length x by the rest of the fibre, $\int_0^x \tau(x) 2\pi R dx$ is the portion of the tensile load transmitted by the tangential stress developed at the interface to the side face of the fibre and $\sigma_m \pi r^2$ is the portion of the tensile stress transmitted by normal stress from the matrix to the fibre end face. This value can be ignored for large x . As the fibre length increases, the stress increases until it becomes equal to that on a continuous fibre.

Then

$$\sigma_x S_f = E_f \varepsilon_f S_f = \int_0^{x=l_c} \tau(x) 2\pi r dx \quad (1.14)$$

The ultimate fibre strength σ_f is given by

$$(E_f \varepsilon_f)_{\max} = \sigma_f \quad (1.15)$$

From this we get an equation for l_c ,

$$l_c = \frac{\sigma_f r}{2\tau_m} \quad (1.16)$$

Since fibre length is a function of fibre diameter d ,

$$\frac{l_c}{d} = \frac{\sigma_f}{4\tau} \quad (1.17)$$

Taking into account both ends of the fibres, the critical fibre is given as

$$\frac{l_c}{d} = \frac{\sigma_f}{2\tau} \quad (1.18)$$

During flow moulding processes like injection moulding, transfer moulding and compression moulding, orientation occurs inevitably. Fibre orientation leads to isotropic effects in micro structural properties and geometrical stability. The degree of fibre orientation determines the anisotropy in composite properties. Anisotropy can be utilised to make the composite part lighter, stiffer and stronger. Optimum fibre orientation and dispersion occur at a critical fibre loading, which offers maximum performance to the composite. Image analysis instrumentation can be used to study the spatial orientation in a composite.¹²⁴ Ko and Yoon¹²⁵ predicted the fibre orientation in the thickness plane during flow moulding of short fibre composites. Recently the effect of discontinuous fibre orientation on the wear properties of composites was reported by Chen et al.¹²⁶ Tai¹²⁷ investigated the dependence of the transverse thermal conductivity of unidirectional composites on

fibre shape. It was found that fibre loading in a composite has a greater role in stress transfer and in failure process. Okoli and Smith¹²⁸ studied various failure modes of fibre reinforced composites as a function of fibre content.

Various others techniques such as x-ray diffraction, birefringence, infrared dichroism, small angle light scattering and electron microscopy can be used to characterise matrix orientation, fibre orientation and fibre length distribution. Kamal et al.¹²⁹ used these techniques to study the orientation factors in glass fibre reinforced polypropylene composites. Mallick¹³⁰ studied the effect of fibre misorientation on the strength of compression moulded continuous fibre composites. Resin cross flow during compression moulding may cause severe misorientation of the continuous fibres in the outer layers. During the preparation of sheet moulding composites, as the mould surface coverage was reduced the cross-flow increases. The tracer fibres in the outer layers buckled (bowed-out) in a concave fashion in the direction of flow. This is evident from Figure 1.19.¹³⁰ Fu and Lanke¹³¹ found that the strength of composites increases with the increase of fibre orientation coefficient and the decrease of mean fibre orientation angle.

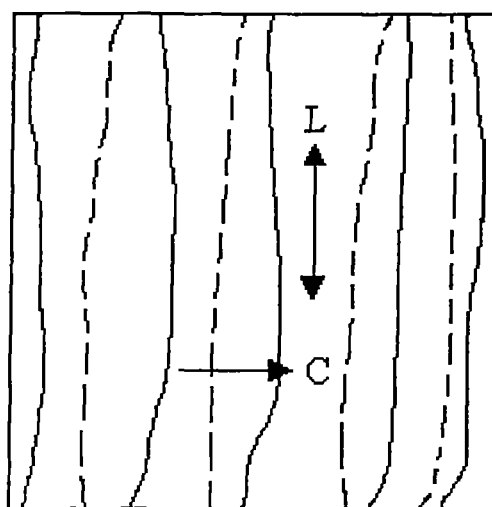


Figure 1.19 Buckling misorientation of fibres due to cross flow in the mould during compression moulding. (L: longitudinal direction of the mold; C: direction of cross flow)

[Ref.: P. K. Mallick, *Polym. Comp.*, 7, 14, (1986)]

1.4.3 Presence of Voids

Voids or bubbles are formed in short fibre composites because of entrapment of air in processing steps and as a result of uneven shrinkage due to temperature gradients involved in the solidification step by cooling. There are two types of voids in composite materials: (1) voids formed along individual fibres, which is related to the fibre spacing and (2) voids formed between laminae and in resin rich regions.

Entrapment of air results from the incomplete wetting out of the fibres by the resin. The volatiles produced during the curing cycle in thermosetting resins and during melt processing operation in thermoplastic polymers may result in creation of voids in composite materials. Quantitative analysis of voids in a composite can be done by point counting techniques on microphotographs or by an ultrasonic scanning technique. Many studies have been reported on the generation of voids and its effect on composite properties.^{132, 133}

1.5 NATURAL FIBRES AS A REINFORCEMENT IN POLYMER MATRIX

Now-a-days natural fibre reinforced polymer composites come prior to synthetic fibre reinforced composites in properties such as enhanced biodegradability, combustibility, light weight, non toxicity, decreased environmental pollution, low cost, ease of recyclability etc. These advantages place the natural fibre composites among the high performance composites having economical and environmental advantages. The physico mechanical properties of important vegetable fibres are given in Table 1.3. Chemical composition of some of the important natural fibre are given in Table 1.4.^{134, 135} The versatile high performance applications of natural fibre composites, which can replace glass and carbon fibres, were listed in an article by Hill.¹³⁶ The vegetable fibre have density of about half that of glass fibre. During the processing of natural fibre composites there will be no abrasion of the processing machines. These fibres can withstand processing temperatures up to 250°C. Reinforcement of polymers with vegetable fibres gives good opportunities for the effective utilisation of agricultural by-products.

Table 1.3 Physical and Mechanical Properties of Some Important Vegetable Fibres

Fibre	Diameter (μm)	Density (kg/m^3)	Tensile strength (MPa)	Elongation at break (%)
Oil palm	50-500	700-1550	150-500	10-18
Banana	80-250	1350	529-754	1-3.5
Coir	100-460	1150	131-175	15-40
Cotton	15-25	1500	500-880	6-7
Jute	12-25	1450	460-533	1.2
Pineapple	20-80	1440	413-1627	0.8-1.6
Sisal	100-300	1450	400-700	5-14
Flax	----	----	780	2-4
Sunhemp	----	----	760	2-4
Palmyrah	----	----	180-215	7-15

[Ref.: J. G. Cook, *Handbook of Textile Fibre and Natural Fibres*, 4th Edn., Morrow Publishing, England (1968) & K. G. Satyanarayana, B. C. Pai, K. Sukumaran and S. G. K. Pillai, *Handbook of Ceramics and Composites*, N. P. Cheremisinoff (Ed.), Marcel Dekkar, New York, Vol. 1 (1990)]

They are cent percent combustible without the production of either noxious gases or solid residues. Wright and Mathias succeeded in preparing lightweight materials from balsa wood and polymer.¹³⁷ Investigation has been carried out by Hedenberg and Gatenholm in recycling the plastic and cellulose waste into composite.¹³⁸ Maldas and Kokta have carried out systematic investigations on wood flour reinforced polystyrene composites.¹³⁹⁻¹⁴¹ The effects of hybridisation of sawdust with glass and mica and of the surface treatment of the reinforcing filler on the mechanical properties were studied by them.

Natural fibres like sisal and coir have been proved to be a better reinforcement in rubber matrix.¹⁴²⁻¹⁴³ Incorporation of natural fibres resulted in better long term mechanical performance of elastomers. The poor reinforcing effect of these cellulosic fibres in elastomers were overcome by giving specific modifications. Recently value added composite materials were developed from used neisan jute fabric and polypropylene having enhanced mechanical properties and reduced hydrophilicity.¹⁴⁴

Table 1.4 Chemical Composition of Some Vegetable Fibres

Fibre	Cellulose (%)	Hemicellulose (%)	Lignin (%)	Moisture content (65% RH)
Oil palm	65	----	19	9-13
Banana	63-64	19	5	10-12
Coir	32-43	15-25	40-45	10-12
Cotton	89	2.5	0.5	8
Jute	71.5	13.4	5-13	12.5
Pineapple	81.5	----	12.7	13.5
Sisal	66-72	12	10-14	11
Flax	70-72	----	5.5	7
Ramie	83-87	----	0.5	6.5
Sunhemp	71-78	----	4	10.5
Palmyrah	40-52	----	42-43	10-12

[Ref.: J. G. Cook, *Handbook of Textile Fibre and Natural Fibres*, 4th Edn., Morrow Publishing, England (1968) & K. G. Satyanarayana, B. C. Pai, K. Sukumaran and S. G. K. Pillai, *Handbook of Ceramics and Composites*, N. P. Cheremisinoff (Ed.), Marcel Dekkar, New York, Vol. 1 (1990)]

To alleviate problems resulting from the incorporation of synthetic fibres such as high abrasiveness, health hazards, machine wearing, disposal problems etc., incorporation of natural fibres in polymers is proposed. They are abundant, renewable, cheap and are having low density. They are biodegradable also. Studies are going on in developing high performance regenerated fibres from wood pulp.¹⁴⁵,¹⁴⁶ Flax, kenaf, hemp and wood flour are reported to be highly suitable for the preparation of load bearing and impact absorbing components of vehicles.¹⁴⁷, ¹⁴⁸ Peijs et al.¹⁴⁹ reported that flax fibre reinforced thermoplastics were of interest in low-cost engineering applications and can compete with the commercial glass mat reinforced thermoplastics. Hybridisation with synthetic fibres results in materials, which combine high strength with flexibility and resistance to impacts along with an added advantage of biodegradability. Investigations are going on in cellulose fibre reinforced polymer matrices with a view to attain cost effectiveness, enhanced biodegradability and high performance to composites.¹⁵⁰⁻¹⁵³ Studies have been so

far reported on the successful incorporation of natural fibres in brittle matrices such as polystyrene, polyester, epoxies etc.¹⁵⁴⁻¹⁶¹ These fillers not only improve the impact, tensile and flexural properties of the composites, but they also reduce the final cost. The studies on the enhancement of properties of brittle polystyrene by saw dust reinforcement was reported by Maldas and Kokta.¹⁶² Oil palm fibres are highly cellulosic and can reinforce polymeric matrices. As they are organic waste materials in palm oil industry, which can cause great environmental problems when left unutilised, their utilisation will eliminate the waste disposal problem. Recently studies are reported on the preparation of composites based on oil palm wood flour and oil palm fruit bunch fibre in plastic and rubber matrices.¹⁶³⁻¹⁶⁸ Ismail et al.¹⁶⁶ reported that mechanical properties of oil palm fibre reinforced natural rubber composites are enhanced with modification on fibre surface and use of various bonding agents. Rozman and coworkers^{167, 168} studied the compounding techniques and properties of composites based on oil palm fruit bunch fibre and polyethylene and polypropylene matrices. Effect of coupling agents and compatibilizers on the mechanical properties of the composites were investigated. Yamini et al.¹⁶⁹ investigated the effect of board density on the properties of particle board from oil palm fruit bunch fibre and urea formaldehyde resin. The strength properties and screw withdrawal increased with increase in board density. The physical properties such as thickness swelling and water absorption generally improved with increase in board density. Major results of this study are given in Table 1.5. The studies so far reported proved that the utilisation of natural fibres especially oil palm fibres as reinforcement in polymer composites offer economical, environmental and qualitative advantages. We can prepare composites having high performance qualities by the incorporation of natural fibre along with synthetic fibre. They may find application in automotive industry as well as in building industry.

1.6 SCOPE AND OBJECTIVE OF THE PRESENT WORK

Incorporation of oil palm fibres in phenolic resin can considerably reduce the shrinkage of the resin during curing. The composite buckling can be completely

eliminated by incorporating higher percentage of fibres. The oil palm fibre reinforcement can increase the mechanical damping of the composite. The weight of the composite can be considerably reduced by reinforcing with a low-density fibre like oil palm fibre. It can act as a toughness modifier in phenolic resin. Owing to the polar nature of lignocellulosic oil palm fibre and phenolic resin, better interfacial properties in composite are expected. Hybridisation of these fibres with synthetic fibres will be effective in improving the properties of the composite. The biodegradable oil palm fibres can make the composites more environment friendly. Oil palm fibres form a major agricultural waste material and their processing is comparatively easy. Hence their utilisation in composites can eliminate waste disposal problems and can reduce the cost of the composite material.

Table 1.5 The Effect of Board Density on Strength Properties of Oil Palm Empty Fruit Bunch Fibre/UF Resin.

Board density (kg/m ³)	Screw withdrawal (N)	Modulus of rupture (NPa)	Internal bond (MPa)	Thickness swelling (%)	Water absorption (%)
561	534.58	14.478	0.2768	18.497	92.297
641	650.41	19.406	0.4799	17.210	71.393
721	946.10	25.385	0.5925	13.323	32.283

[Ref.: S. A. K. Yamini, A. J. Ahmad, J. Kasim, N. M. Nasir and J. Harun, *Proc. of the Int. Symposium on Biocomposites and Blends based on Jute and Allied Fibers*, p. 135 (1994)]

The important objective of this work is the utilisation of oil palm fibres as reinforcement in phenolic resin to produce cost effective and environment friendly composite materials. In order to achieve this major objective several fundamental investigations has been undertaken. The effect of fibrous reinforcement on the properties of the composites as a function of fibre length, fibre loading and fibre surface modifications has been systematically studied. Oil palm fibres were hybridised with glass fibre to prepare high performance composites with several added advantages. The present work focuses on following aspects:

Processing, characterisation and modifications of oil palm fibres:-

Processing of oil palm fibres and characterisation of physical and chemical properties of oil palm empty fruit bunch fibre and oil palm mesocarp fibre were studied in detail. Chemical composition, surface morphology and thermal stability of the fibres were analysed. Several modifications onto the fibre were tried, in order to enhance the reinforcing ability of the fibres. Infrared spectroscopy and scanning electron microscopy were used to characterise the modified fibre surfaces. Changes in the mechanical performance of the fibres on various modifications were studied.

Static mechanical properties:- Both the untreated and treated oil palm empty fruit bunch fibres have been used as reinforcement in phenol formaldehyde resin. The tensile, flexural and impact performance of the composites were analysed. The failure mechanisms were studied using scanning electron microscope.

Hybrid composites:- Oil palm fibres were hybridised with glass to improve the properties and to decrease the water absorption of the resultant composite. Mechanical properties of the hybrid composites were analysed giving special reference to the relative volume fraction ratio of the fibres. Hardness of the composites and presence of voids were determined. Hybrid effect of glass and oil palm fibres was also analysed.

Stress relaxation studies:- Tensile stress relaxation behaviour of individual oil palm empty fruit bunch fibre and oil palm fibre reinforced PF composites was investigated. The effects of fibre modifications, physical ageing and strain level on the stress relaxation behaviour of the fibre and the composites were investigated. Effect of fibre loading on the relaxation mechanism of the composites was also analysed. In order to predict the long-term behaviour of the fibres and composites, master stress relaxation curves of the fibres and composites were computed.

Dynamic mechanical properties:- The dynamic mechanical properties of the composites were analysed giving special reference to parameters such as fibre length, fibre loading, fibre treatment and hybrid fibre ratio. The storage modulus,

loss modulus and mechanical damping of the composites were analysed. Variation in the glass transition temperature of the composites upon incorporation of fibres was determined. Activation energy of the relaxation processes in various composites was calculated. Master curves for the dynamic properties of the composites were constructed to explain the long-term dynamic properties of the composites. The phase behaviour and modulus variations were studied from cole-cole analysis.

Water sorption studies:- Water sorption characteristics of oil palm fibres in distilled water, mineral water and water containing salt at different temperatures were studied. The kinetics of sorption in oil palm fibre reinforced PF composites and oil palm/glass hybrid fibre reinforced PF composites were also analysed. The concentration dependency of the diffusion coefficient was analysed.

Accelerated weathering studies:- Environmental effects such as thermal, moisture, biological and gamma irradiation on the composite properties were investigated. Mechanical properties such as tensile, flexural and izod impact performance of the unaged and aged composites were compared. Thermal stability of the composites was determined from corresponding TGA and DTG curves. Changes in the fibre-matrix adhesion on ageing and the tensile and impact fracture mechanism of the aged composites were studied using scanning electron microscopy.

Electrical properties:- The electrical properties of the composites were studied giving special reference to the effect of fibre loading, fibre modifications and hybridisation effect of oil palm fibre with glass. Volume resistivity, dielectric constant, loss factor and dissipation factor of the composites have been evaluated.

Theoretical modelling:- The experimental strength values of the composites were compared with theoretical predictions. Theoretical models such as parallel, series, Hirsch's, modified Bowyer and Bader's and modified rule of mixtures were applied to predict the tensile strength and Young's modulus of the composites. Law of additive rule of mixtures was applied to calculate the theoretical strength of hybrid composites.

REFERENCES

1. Encyclopedia of Polymer Science and Engineering, H. F. Mark (Ed.), *John Wiley and Sons*, New York (1985)
2. S. C. Tjong and Y. Z. Meng, *J. Appl. Polym. Sci.*, **72**, 501 (1999)
3. P. I. Gonzalez and R. J. Yong, *J. Mater. Sci.*, **33**, 5715 (1998)
4. M. P. Thomas and M. R. Winstone, *J. Mater. Sci.*, **33**, 5499 (1998)
5. A. Kelly, *Phil. Trans. R. Soc. Lond.*, **A 354**, 1841 (1996)
6. I. C. Visconti, *Polym.-Plast. Technol. Eng.*, 31(1&2), 1 (1992)
7. N. Jagannathan, *Polym.-Plast. Technol. Eng.*, 5 (1), 107 (1975)
8. M. Daoud, A. Chateauminois and L. Vincent, *J. Mater. Sci.*, **34**, 191 (1999)
9. Q. Zheng, Y. H. Song and X. S. Yi, *J. Mater. Sci. Lett.*, **18**, 35 (1999)
10. Y. J. Sun and R. N. Singh, *Acta Materialia*, **46**, 1657 (1998)
11. I. Hudec, E. Spirk, J. Grom, A. Gruskova and J. Slama, *J. macro. Sci.-Phys.*, **B37**, 171 (1998)
12. A. Amash and P. Zugenmaier, *Polymer Bulletin*, **40**, 251 (1998)
13. S. V. Ranade, X. Q. Xie and A. T. Dibeneditto, *J. Adhesion*, **64**, 7 (1997)
14. V. K. Srivastava and P. J. Hogg, *J. Mater. Sci.*, **33**, 1119 (1998)
15. Kishore and S. Venkatraman, *J. Appl. Polym. Sci.*, **67**, 1565 (1998)
16. D. M. Dean, L. Rebenfeld, R. A. Register and B. S. Hsiao, *J. Mater. Sci.*, **33**, 4797 (1998)
17. T. Mang and F. Iaulena, *Macromolecular Symposia*, **135**, 147 (1998)
18. J. Jancer (Ed.), Mineral Fillers in Thermoplastics I (Series: Advances in polymer science), *Springer-Verlag Berlin, Germany*, **139**, 1 (1999)
19. O. Siron, J. Lamon, *Acta Materialia*, **46**, 6631 (1998)
20. S. J. Martin, J. E. OBrien, J. Dowling and V. J. McBrierty, *Eur. Polym. J.*, **34**, 1817 (1998)
21. J. Raghavan and R. P. Wool, *J. Appl. Polym. Sci.*, **71**, 775 (1999)
22. N. Oya, H. Hamada, *J. Mater. Sci.*, **33**, 3407 (1998)
23. N. Takeda, S. Ogihara, K. Nakata and A. Kobayasi, *Composite Interfaces*, **5**, 305 (1998)
24. R. Paar, J. L. Valles and R. Danzer, *Mater. Sci. Eng. A- Structural mater. Props.*, 250, 209 (1998)
25. R. Hussein, *Polym.-Plast. Technol. Eng.*, 28(1), 55 (1989)
26. D. Raghavan, H. Huynh and C. F. Ferraris, *J. Mater. Sci.*, **33**, 1745 (1998)
27. M. Kakemi, D. J. Hannant and M. Mulheron, *J. Mater. Sci.*, **33**, 5375 (1998)

28. A. Bouguerra, M. B. Diop, J. P. Laurent, M. L. Benmalek and M. Queneudec, *J. Phys. D-Appl. Phys.*, **31**, 3457 (1998)
29. S. H. Rizkalla and A. A. Abdelrahman, *Proceedings of the International Conference on Fibre Reinforced Structural Plastics in Civil Engineering*, Madras, p.3 (1995)
30. P. K. Mallick (Ed.), *Fibre-Reinforced Composites, Materials, Manufacturing and Design*, Marcel dekker Inc., New york (1988)
31. M. A. Leaity, P. A. Smith, M. G. Bader and P. T. Curtis, *Composites*, **23**, 387 (1992)
32. D. Short and J. Summerscales, *Composites*, **10**, 215 (1979)
33. Ibid, **11**, 33 (1980)
34. N. L. Hancox (Ed.), *Fibre Composite Hybrid Materials*, *Applied Science Publishers Ltd.*, London (1981)
35. F. R. Jones (Ed.), *Handbook of Polymer-Fibre Composites*, *Longman Scientific and Technical*, England (1994)
36. J. N. Kirk, M. Munro and P. W. R. Beaumont, *J. Mater. Sci.*, **13**, 2197 (1978)
37. M. Arrington and B. Harris, *Composites*, **9**, 149 (1978)
38. G. Kalaprasad, Ph. D. Thesis, Mahatma Gandhi University, Kottayam, Kerala, India, May (1999)
39. A. A. J. M. Peijs, P. Catsman, L. E. Govaert and P. J. Lemstra, *Composites*, **21**, 513 (1990)
40. A. A. J. M. Peijs, R. W. Venderbosch and P. J. Lemstra, *Composites*, **21**, 522 (1990)
41. P. W. Manders and M. G. Bader, *J. Mater. Sci.*, **16**, 2233 (1981)
42. Ibid, **16**, 2246 (1981)
43. R. L. McCullough and J. M. Peterson in *Developments in Composite Materials*, G. S. Holister (Ed.), *Applied Science Publishers*, London, p.85 (1977)
44. M. Hussain, A. Nakahira and K. Niihara, *Mater. Lett.*, **26(3)**, 185 (1996)
45. J. J. Lee and C. M. Suh, *J. Mater. Sci.*, **30(24)**, 6179 (1995)
46. H. R. Azimi, R. A. Pearson and R. W. Hertzberg, *J. Appl. Polym. Sci.*, **58**, 449 (1995)
47. K. P. Gadkaree, *J. Mater. Sci.*, **27**, 3827 (1992)
48. K. P. Gadkaree, K. C. Chyung and M. P. Taylor, *J. Mater. Sci.*, **23**, 3711 (1988)
49. N. Chand and P. K. Rohatgi, *J. Mater. Sci. lett.*, **5**, 1181 (1986)
50. L. A. Pothen, S. Thomas, J. George and Z. Oommen, *Polimery*, **44**, nr11-12, 750 (1999)
51. K. G. Satyanarayana, K. Sukumaran, A. G. Kulkarni, S. G. K. Pillai and P. K. Rohatgi, *Proceedings of the Second International Conference on Composite*

- Structures, I. H. Marshall (Ed.), *Applied Science Publishers, London*, P.35, (1983)
52. P. S. Theocaris, *Acta Mechanica*, **95**, 69 (1992)
 53. N. K. Naik (Ed.), Woven fabric composites, *Technomic publishing Co. Inc.*, Lancaster, January (1994)
 54. D. Larocche and T. Vu-Khanh, *J. Comp. Mater.*, **28**, 1825 (1994)
 55. Y. Wang, J. Li and D. Zhao, *Composites Engineering*, **5**, 1159 (1995)
 56. M. D. Gilchrist, N. Svensson and R. Shishoo, *J. Mater. Sci.*, **33**, 4049 (1998)
 57. M. Kotaki, M. Hojo, H. Hamada and Z. Maekawa, *J. Mater. Sci. Lett.*, **17**, 515 (1998)
 58. L. A. Pothen, Z. Oommen and S. Thomas (Unpublished work)
 59. G. M. Newaz, *Polym. Comp.*, **7**, 421 (1986)
 60. N. J. Pagano and G. P. Tandon, *J. Mater. Sci.*, **38**, 247 (1990)
 61. A. Cervenka, *Composite Interfaces*, **3**, 135 (1995)
 62. M. R. Piggott, *Polym. Comp.*, **8**, 291 (1987)
 63. L. Dilandro, A. T. Dibenedetto and J. Groeger, *Polym. Comp.*, **9**, 209 (1988)
 64. D. Hull (Ed.), *An Introduction to Composite Materials*, Cambridge University Press, London (1981)
 65. S. Wu (Ed.), *polymer Interface and Adhesion*, Marcel Dekker Inc., New york (1982)
 66. F. M. B. Coutinho, T. H. S. Costa and D. L. Carvalho, *J. Appl. Polym. Sci.*, **65**, 1227 (1997)
 67. L. Gonzalez, A. Rodriguez, J. L. DeBenito and A. Marcos-Fernandez, *J. Appl. Polym. Sci.*, **63**, 1353 (1997)
 68. S. R. Culler, H. Ishida and J. L. Koenig, *Polym. Comp.*, **7**, 231 (1986)
 69. N. D. Ghatge and R. S. Khisti, *J. Polym. Mater.*, **6**, 145 (1989)
 70. I. Ulkem and H. P. Schreiber, *Composite Interfaces*, **2**, 253 (1994)
 71. H. Hamada, N. Ikuta, N. Nishida and Z. Maekawa, *Composites*, **25**, 512 (1994)
 72. A. Valadez-Gonzalez, J. M. Cervantes-Uc, R. Olayo and P. J. Herrera-Franco, *Composites Part B*, **30**, 309 (1999)
 73. Ibid, *Composites Part B*, **30**, 321 (1999)
 74. S. J. Monte and G. Sugerman, *Polym. Eng. Sci.*, **24**, 1369 (1984)
 75. D. S. Varma, M. Varma and I. K. Varma, *J. Polym. Mater.*, **3**, 101 (1986)
 76. B. V. Kokta, D. Maldas, C. Daneault and P. Beland, *Polym.-Plast. Technol. Eng.*, **29(1&2)**, 87 (1990)
 77. R. G. Raj, B. V. Kokta, D. Maldas and C. Daneault, *Polym. Comp.*, **9**, 404 (1988)

78. A. K. Rana, A. Mandal, B. C. Mitra, R. Jacobson, R. Rowell and A. N. Banerjee, *J. Appl. Polym. Sci.*, **69**, 329 (1998)
79. K. Oksman, H. Lindberg and A. Holmgren, *J. Appl. Polym. Sci.*, **69**, 201 (1998)
80. C. Joly, R. Gauthier and B. Chabert, *Comp. Sci. Technol.*, **56**, 761 (1996)
81. N. Mohanty, S. N. Torasia, B. Pradhan, D. K. Rout and H. K. Das, *J. Macromol. Sci.-Chem.*, **A21(2)**, 193 (1984)
82. S. S. Reddy, S. K. Bhaduri and S. N. Pandey, *J. Appl. Polym. Sci.*, **47**, 73 (1993)
83. I. Sakata, M. Morita, N. Tsuruta and K. Morita, *J. Appl. Polym. Sci.*, **49**, 1251 (1993)
84. S. R. Wu, G. S. Sheu and S. S. Shyu, *J. Appl. Polym. Sci.*, **62**, 1347 (1996)
85. S. Carlotti and A. Mas, *J. Appl. Polym. Sci.*, **69**, 2321 (1998)
86. G. Samaranayake and W. G. Glasser, *Carbohydrate Polymers*, **22**, 1 (1993)
87. K. Joseph, Ph. D. Thesis, Mahatma Gandhi University, Kottayam, Kerala, India (1992)
88. R. Prasantha Kumar and S. Thomas, *Polym. Internat.*, **38**, 173 (1995)
89. K. C. Manikandan Nair, S. M. Diwan and S. Thomas, *J. Appl. Polym. Sci.*, **60**, 1483 (1996)
90. J. George, Ph. D. Thesis, Mahatma Gandhi University, Kottayam, Kerala, India (1997)
91. S. I. Moon, J. Jang, *J. Mater. Sci.*, **33**, 3419 (1998)
92. C. Plessier, B. Gupta and A. Chapiro, *J. Appl. Polym. Sci.*, **69**, 1343 (1998)
93. A. Bezeredi, Z. Demjen and B. Pukanszky, *Angewandte Makromolekulare Chemie*, **256**, 61 (1998)
94. J. A. Trejo, O. Reilly, J. Y. Cavaille, N. M. Belgacem and A. Gandini, *J. Adhesion*, **67**, 359 (1998)
95. K. Veluraja, S. Ayyalnarayanassubburaj and A. J. Paulraj, *Carbohydrate Polymers*, **34**, 377 (1997)
96. B. Singh, A. Verma and M. Gupta, *J. Appl. Polym. Sci.*, **70**, 1847 (1998)
97. X. L. Fu, W. M. Lu and D. D. L. Chung, *Carbon*, **36**, 1337 (1998)
98. P. Zadorecki and T. Ronnhult, *J. Polym. Sci.: Part A: Polym. Chem.*, **24**, 737 (1986)
99. A. Garton (Ed.), *Infrared Spectroscopy of Polymer Blends, Composites and Surfaces*, Hanser, Munich (1992)
100. X. M. Cherian, P. Sayamoorthy, J. J. Andrew and S. K. Bhattacharya, *Macromolecular reports*, **A 31 (Suppls. 3&4)**, 261 (1994)
101. Kh. M. Mannan, *Polymer*, **34**, 2485 (1993)
102. M. Nitschke and J. Meichsner, *J. Appl. Polym. Sci.*, **65**, 381 (1997)
103. M. A. Khan, K. M. I. Ali and S. C. Basu, *J. Appl. Polym. Sci.*, **49**, 1547 (1993)

104. H. Yamaoka, R. Matsushita, K. Miyath and Y. Nakayama, *Radiat. Phys. Chem.*, **48**, 243 (1996)
105. K. Grundke, P. Uhlmann, T. Gietzelt, B. Redlich and H. J. Jacobasch, *Colloids and Surfaces A: Physicochemical and Engineering Aspects*, **116**, 93 (1996)
106. M. Guigon and E. Klinklin, *Composites*, **25**, 534 (1994)
107. S. Suto and M. Inoue, *Reports on progress in Polymer Physics in Japan*, **38**, 259 (1995)
108. L. S. Penn, G. C. Tesoro and H. X. Zhou, *Polym. Comp.*, **9**, 184 (1988)
109. Q. Aikens, O. O. Ochoa and J. J. Engblom, *Comp. Sci. Technol.*, **47**, 193 (1993)
110. J. Andersons and V. Tamuzs, *Comp. Sci. Technol.*, **48**, 57 (1993)
111. M. R. Nedeke and M. R. Wisnom, *Comp. Sci. Technol.*, **51**, 517 (1994)
112. C. Marotzke, *Comp. Sci. Technol.*, **50**, 393 (1994)
113. M. Desaegeer and I. Verpoest, *Comp. Sci. Technol.*, **48**, 215 (1993)
114. J. Kim, S. Lu and Y. Mai, *J. Mater. Sci.*, **29**, 554 (1994)
115. M. J. Pitkethly and J. B. Doble, *Composites*, **21**, 389 (1990)
116. Z. Li and D. T. Grubb, *J. Mater. Sci.*, **29**, 189 (1994)
117. L. Ye, T. Scheuring and K. Friedrich, *J. Mater. Sci.*, **30**, 4761 (1995)
118. M. R. Piggott, *Comp. Sci. Technol.*, **42**, 57 (1991)
119. E. Mader, K. Grundke, H. J. Jacobasch and G. Wachinger, *Composites*, **25**, 739 (1994)
120. C. Y. Yue, N. L. Loh and L. L. Lee, *J. Mater. Sci.*, **31**, 3271 (1996)
121. T. W. Clyne and M. C. Watson, *Comp. Sci. Technol.*, **42**, 25 (1991)
122. M. Joshi, S. N. Maiti, A. Misra and R. K. Mittal, *Polym. Comp.*, **15**, 349 (1994)
123. H. Cantow (Ed.), *Polymers, Properties and Applications*, Springer-Verlag, Berlin Heidelberg, **10** (1986)
124. G. Fischer and P. Eyerer, *Polym. Comp.*, **9**, 297 (1988)
125. J. Ko and J. R. Youn, *Polym. Comp.*, **16**, 114 (1995)
126. J. Chen, B. L. Shen, S. J. Gao, J. M. Xiao and M. J. Tu, *J. Mater. Sci. Lett.*, **17**, 253 (1998)
127. H. Tai, *International J. of Thermophysics*, **19**, 1485 (1998)
128. O. I. Okoli and G. F. Smith, *J. Mater. Sci.*, **33**, 5415 (1998)
129. M. R. Kamal, L. Song and P. Singh, *Polym. Comp.*, **7**, 323 (1986)
130. P. K. Mallick, *Polym. Comp.*, **7**, 14, (1986)
131. S. Y. Fu and B. Lanke, *Comp. Sci. Technol.*, **56**, 1179 (1996)
132. K. J. Bowles and S. Frimpong, *J. Comp. Mater.*, **26**, 1487 (1992)
133. M. Akey and D. F. O'Regan, *Plast. Rubb. Comp. Process. Appl.*, **24**, 97 (1995)
134. J. G. Cook, *Handbook of Textile Fibre and Natural Fibres*, 4th Edn., Morrow Publishing, England (1968)

135. K. G. Satyanarayana, B. C. Pai, K. Sukumaran and S. G. K. Pillai, Handbook of Ceramics and Composites, N. P. Cheremisinoff (Ed.), *Marcel Dekkar*, New York, Vol. 1 (1990)
136. S. Hill, *New Scientist*, 1 Feb. 1997, p. 36
137. J. R. Wright and L. J. Mathias, *J. Appl. Polym. Sci.*, **48**, 2241 (1993)
138. P. Hedenberg and P. Gatenholm, *J. Appl. Polym. Sci.*, **56**, 641 (1995).
139. D. Maldas and B. V. Kokta, *J. Comp. Mater.*, **25**, 375 (1991).
140. D. Maldas and B. V. Kokta, *Polym. Plast. Technol. Eng.*, **29**, 419 (1990)
141. D. Maldas, B. V. Kokta, R. G. Raj and C. Daneault, *Polymer*, **29**, 1255 (1988)
142. S. Varghese, Ph.D. Thesis, Mahatma Gandhi University, Kottayam, Kerala, India (1992)
143. V. G. Geethamma, K.T. Mathew, R. Lakshminarayanan and S. Thomas, *Polymer.*, **39**, 1483 (1998)
144. K. R. Harikumar, K. Joseph and S. Thomas, *J. Rein. Plast. Comp.*, **18**, 346 (1999)
145. R. S. P. Coutts, Y. Ni and B. C. Tobias, *J. Mater. Sci. Lett.*, **13**, 283 (1994)
146. J. Jang, H. Chung, M. Kim and Y. Kim, *J. Appl. Polym. Sci.*, **69**, 2043 (1998)
147. X. H. Yuan, Y. X. Zhang and X. F. Zhang, *J. Appl. Polym. Sci.*, **71**, 333 (1999)
148. K. Oksman and H. Lindberg, *J. Appl. Polym. Sci.*, **68**, 1845 (1998)
149. T. Peijis, S. Garkhail, R. Heijenrath, M. Vanden Oever and H. Bos, *Macro. Symp.*, **127**, 193 (1998)
150. S. L. Bai, R. K. Y. Li, L. C. M. Wu, H. M. Zeng and Y. W. Mai, *J. Mater. Sci. Lett.*, **17**, 1805 (1998)
151. J. J. Balatineez and M. M. Sain, *Macro. Symp.*, **135**, 167 (1998)
152. B. C. Mitra, R. K. Basak and M. Sarkar, *J. Appl. Polym. Sci.*, **67**, 1093 (1998)
153. T. G. Rials and M. P. Wolcott, *J. Mater. Sci. Lett.*, **17**, 317 (1998)
154. I. M. Low, P. Schmidt and J. Lane, *J. Mater. Sci. Lett.*, **14**, 170 (1995)
155. M. A. Semsarzadeh, *Polym. Plast. Technol. Eng.*, **24**, 323 (1985)
156. N. E. Marcovich, M. M. Reboredo and M. I. Aranguren, *J. Appl. Polym. Sci.*, **70**, 2121 (1998)
157. P. Zadorecki and P. Flodin, *Polym. Comp.*, **7**, 170 (1986)
158. P. V. Alston, *Textile Res. J.*, **64**(10), 592 (1994)
159. W. H. Zhu, B. C. Tobias and R. S. P. Coutts, *J. Mater. Sci. Lett.*, **14**, 508 (1995)
160. L. Umadevi, S. S. Bhagawan and S. Thomas, *J. Appl. Polym. Sci.*, **64**, 1739 (1997)
161. L. A. Pothan, N. R. Neelakantan and S. Thomas, *J. Reinf. Plast. Comp.*, **16**, 8 (1997)

162. D. Maldas and B. V. Kokta, *J. Rein. Plast. Comp.*, **10**, 42 (1991)
163. J. Tay and K. Show, *Resources, Conservation and Recycling*, **13**, 27 (1995)
164. M. J. Zaini, M. Y. A. Fuad, Z. Ismail, M. S. Mansor and J. Mustafah, *Polym. Inter.*, **40**, 51 (1996)
165. H. D. Rozman, R. N. Kumar, H. P. S. A. Khalil, A. Abusamah, P. P. Lim and H. Ismail, *Eur. Polym. J.*, **33**, 225 (1997)
166. H. Ismail, N. Rosnah, and H. D. Rozman, *Polymer*, **38**, 4059 (1997)
167. H. D. Rozman, G. B. Peng and Z. A. M. Ishak, *J. Appl. Polym. Sci.*, **70**, 2647 (1998)
168. Z. A. M. Ishak, A. Aminullah, H. Ismail and H. D. Rozman, *J. Appl. Polym. Sci.*, **68**, 2189 (1998)
169. S. A. K. Yamini, A. J. Ahmad, J. Kasim, N. M. Nasir and J. Harun, Proc. of the Int. Symposium on Biocomposites and Blends based on Jute and Allied Fibers, p. 135 (1994)

CHAPTER 2

Materials and Experimental Techniques

2.1 MATERIALS

2.1.1 Oil Palm Fibres

Oil palm empty fruit bunches were collected from Oil Palm India Ltd., Kottayam, Kerala, India and fibres were processed by retting technique. The oil palm empty fruit bunch (OPEFB) fibres were separated, cleaned off pithy materials and dried. The average length of a fibre is approximately 15cms. Oil palm mesocarp fibres were collected from palm oil mill after the extraction of oil from fruits. These fibres were cleaned off from oily matter and pithy materials. The physical and chemical characteristics of oil palm fibres are discussed in chapter 3 and are already reported elsewhere.¹

2.1.2 Glass Fibre Mat

M/s Ceat Ltd, Hyderabad, India, supplied multidirectional short E-glass strand mat. The fibre length was 50mm. They are high silicate materials having high strength to weight ratio. The important physical and mechanical properties of glass fibre are given Table 2.1.²

Table 2.1 Physical and Mechanical Properties of Glass

Diameter (μm)	5 - 25
Density (g/cc)	2.54
Tensile strength (GPa)	1.7 - 3.5
Young's modulus (GPa)	66 - 72
Elongation at break (%)	3

2.1.3 Phenol Formaldehyde Resin

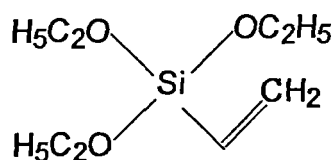
Phenol formaldehyde (PF) resole type resin is used and is procured from M/s West Coast Polymers Pvt. Ltd., Kannur, Kerala, India. The physical, chemical and mechanical characteristics of the PF resin are given in Table 2.2.

Table 2.2 Typical Properties of Phenol Formaldehyde Resole Resin

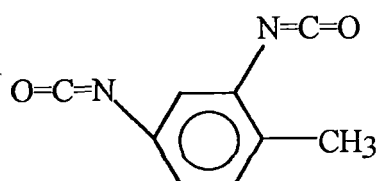
Liquid resin	
Appearance	Deep brown colour
Viscosity (cps)	18 – 22 s. on Ford cup B4
Water tolerance	1 : 8
Solid content (%)	50 ± 1
Cured resin	
Density (g/cc)	1.3
Tensile strength (MPa)	10
Young's modulus (MPa)	375
Elongation at break (%)	2
Flexural strength (MPa)	10
Flexural modulus (MPa)	1875
Izod impact strength (kJ/m ²)	20

2.1.4 Chemicals

Acrylic acid, acrylonitrile monomer, NaOH, KMnO₄, acetic anhydride and benzoyl peroxide were used for fibre surface modifications. These chemicals were of reagent grades. The structures of the coupling agents, triethoxy vinyl silane and toluene 2,4-diisocyanate used are given below.



Tri ethoxy vinyl silane (A 151)



Toluene 2,4-diisocyanate

These chemicals were procured from M/s Union Carbide Co., Montreal, Canada and Poly Sciences, USA respectively.

2.2 CHEMICAL COMPOSITION OF OIL PALM FIBRES

Chemical composition of fibres was estimated according to ASTM procedures. Lignin-ASTM D1106; Holocellulose-ASTM D1104; Ash content-ASTM D1102; Alcohol-benzene solubility-ASTM D1107; Ether solubility-ASTM D1108; One per cent caustic soda solubility-ASTM D1109; Water solubility-ASTM D1110

2.3 RESIN MODIFICATION

The PF resin was treated with benzoyl peroxide. Different quantities (0.1, 0.5 and 1% of the resin) of the peroxide were added into the resin and stirred for one hour for intimate mixing. The peroxide can act as a free radical initiator and can take part in the crosslinking reactions.

2.4 FIBRE SURFACE MODIFICATIONS

Mercerisation: Fibres were immersed in 5% solution of sodium hydroxide for different time intervals such as 72, 48 and 24 hrs. at room temp. Fibres were then washed many times in distilled water and finally washed with water containing a little acetic acid and dried.

Acetylation: Fibres were pre-treated with 2% sodium hydroxide for about half an hour in order to activate the hydroxyl groups on the cellulose and lignin. Fibres were subjected to acetylation with acetic anhydride in acetic acid medium. Conc. H_2SO_4 acts as a catalyst in this reaction. Fibres were washed in distilled water and then dried.

Peroxide treatment: Fibres were coated with benzoyl peroxide in acetone solution after alkali pre-treatment. Saturated solution of the peroxide in acetone was used. Finally, the treated fibres were then dried

Permanganate treatment: Fibres were pre-treated with sodium hydroxide and then dipped in permanganate solution in acetone for about 2-3 minutes. The permanganate solutions of concentrations 0.01, 0.05 and 0.1% were used. Fibres were washed in distilled water and finally dried.

⁶⁰Co γ -ray irradiation: Oil palm fibres were exposed to γ -ray irradiation from a ⁶⁰Co source at a dose rate of 0.1 Mrad per hour for about 30hrs.

Isocyanate treatment: The alkali treated fibres were taken in a round-bottomed flask and soaked in chloroform containing dibutyl tin dilaurate catalyst. Toluene diisocyanate was added dropwise into the flask using a pressure equalising funnel. The reaction was allowed to take place for two hours with continuous stirring. Fibres were purified by refluxing with acetone and then washed with distilled water and dried in oven.

Silane treatment: The pre-treated fibres were dipped in alcohol water mixture (60:40) containing tri ethoxy vinyl silane coupling agent. The pH of the solution was maintained between 3.5 and 4. Fibres were washed in distilled water and dried.

Acrylation: Fibres were mixed with 10% NaOH for about 30minutes at room temperature. The solution was decanted and the wet product treated with solution containing different concentrations of acrylic acid. The reaction was allowed to be carried out for about one hour at 50°C. Fibres were washed with water/alcohol mixture and dried.

Acrylonitrile grafting: Fibres were bleached with 2% alkali for 30 minutes and then oxidised with 0.02mL⁻¹ KMnO₄ (liquor ratio, 1:150) for 10 minutes. The fibres were further washed with water and then soaked in 1% H₂SO₄ containing acrylonitrile in the ratio 30:1. The sample was then placed in a thermostatic water bath, and the temperature was kept at 50°C for 2 hours without any disturbance. The sample was then washed with water thoroughly and dried. The grafted fibre was isolated from any homopolymer formed (PAN) by soxhlet extraction using dimethyl formamide.

Latex modification: Fibres were given a latex coating by dipping in natural rubber latex having 10% dry rubber content after pre-treatment with NaOH.

2.5 COMPOSITE PREPARATION

Oil palm empty fruit bunch fibre having higher cellulose content and mechanical properties than mesocarp fibre was selected for reinforcing PF resin. Prepreg route was followed for the preparation of composites. Hand lay up method followed by compression moulding was adopted for composite fabrication. Fibres were chopped into desired lengths (10, 20, 30 and 40mm) and dried in oven at 60-70°C for about 2 hrs. These chopped fibres were uniformly spread in a mould cavity. Mould was then closed and pressure applied to form a single mat. The mat was then impregnated in the resin and the prepreg was kept at room temperature up to a semicured stage. It was then pressed at 100°C to get a three dimensionally crosslinked network. Composites with different fibre loading (20, 30, 40 and 50wt.%) were prepared and properties evaluated. It has already been reported that composite containing oil palm fibre with 40mm length and a loading of 40 wt.% resulted in better reinforcement and provided optimum properties.³

The glass fibre mats were sized. Glass mat reinforced PF resin composites with various fibre loading (10, 23, 27, 40 and 45 wt.%) were prepared as described above. Effect of fibre loading on the mechanical properties was analysed. Hybrid composite was prepared by arranging randomly oriented short glass and oil palm fibre mats as alternate layers. It was then soaked in PF resin and cured under hot pressing. By keeping the total fibre loading of the hybrid composite constant ie.40wt.%, the relative volume fractions of the individual fibres were changed. Composites having different volume ratio of glass/oil palm fibre such as 1:0, 0.7:0.3, 0.5:0.5, 0.3:0.7, 0.1:0.9, 0.08:0.92, 0.04:0.96 & 0:1 were prepared.

2.6 SCANNING ELECTRON MICROSCOPY AND OPTICAL MICROSCOPY

The SEM photographs of fibre surfaces and cross sections of untreated and treated fibres were taken using scanning electron microscope Philips model PSEM-500. The tensile and impact fractograph of the composites were taken to study the

fracture mechanisms and interface adhesion of the composites. The crack propagation and fibre dispersion in composites were analysed by using an optical microscope of Leitz Metallux 3, Germany.

2.7 IR SPECTROSCOPY

The modified fibre surfaces were characterised by IR spectroscopy. KBr disk method is followed in taking IR spectra. The instrument used was Shimadzu infrared spectrophotometer IR-470.

2.8 THERMOGRAVIMETRIC ANALYSIS

Thermogram of untreated and treated fibres and composites were taken in an inert atmosphere at a heating rate of 10°C/min. Shimadzu thermal analyser DT-40 was used for the study.

2.9 MECHANICAL TESTS

Strength of the oil palm fibres was determined using FIE electronic tensile testing machine TNE-500. The fibres were mounted in a fixture made of paperboard with a central window and pulled at a strain rate of 20 mm/min. The gauge length was 50 mm and 20 mm in the case of OPEFB fibre and oil palm mesocarp fibre, respectively. Strength, Young's modulus and elongation at break were evaluated.

Test specimens were cut from the composite sheets. Tensile testing was carried using FIE electronic tensile testing machine TNE-500 according to ASTM D 638-76 at a strain rate of 50mm/min. Three point flexure properties were also tested using the same machine according to ASTM D 790. Impact tester of Ceast Torino, Italy was used to test the unnotched izod impact strength of the composites. It was tested according to ASTM D 256. Hardness of the composites was checked on a shore D Hardness Durometer on ASTM D 2240. Density of the samples was determined by displacement method according to ASTM D 792.

2.10 STRESS RELAXATION

The stress relaxation experiments in oil palm fibre and the composite samples were carried out at ambient temperature on a Zwick Universal testing machine, model 1474 in uniaxial tension according to ASTM D638. The gauge lengths were fixed at 30 and 50mm for the fibre and composite samples respectively and tested at a speed of 5mm/min. The strain was held constant after the required level was reached and the decay in stress was recorded as a function of time for about 3hrs. The samples were tested at three different strain levels, 3, 10 & 17% for fibre and 1, 2 & 3% for composites to study the effect of strain level on the relaxation mechanism.

2.11 DYNAMIC MECHANICAL ANALYSIS

A dynamic mechanical thermal analyser of Polymer laboratories (Model PL-Mk II) was employed for dynamic mechanical property evaluation of the composites. Samples of dimension $5 \times 1 \times 0.25 \text{ cm}^3$ were used for testing. The testing temperature ranged from 25 to 150°C and the experiment was carried out at frequencies 0.1, 1, 10, 50 and 100Hz. The experiment was performed under tensile mode at a strain amplitude of 0.1%.

2.12 WATER SORPTION STUDIES

Oil palm fibres: About 0.5 gms of dried oil palm empty fruit bunch fibre having an appropriate length of 5cm and oil palm mesocarp fibres were taken for the water sorption study. The diameter of the fibres was noted. The samples were immersed in distilled water, mineral water and water containing salt at different temperature 30, 50, 70 and 90°C in a thermostatically controlled air oven. Increase in weight of the samples was noted at specific time intervals. This process was continued till equilibrium was reached.

Composites: For water sorption experiments rectangular samples of 10x10mm size were cut from the composite sheets. Corners of the samples were curved to avoid non-uniform water diffusion. The thickness of the samples was

measured. Samples were immersed in distilled water and the experiment was carried out as described above. The values obtained were found to be perfectly reproducible. The mole percent uptake Q_t for water by 100g. of the polymer was plotted against the square root of time. The Q_t value can be expressed as

$$Q_t = \frac{Me(w) / Mr(w)}{Mi(s)} \times 100 \quad (2.1)$$

where $Me(w)$ is the mass of water at equilibrium, $Mr(w)$ is the relative molecular mass of water ie.18 and $Mi(s)$ is the initial mass of the sample. At equilibrium, Q_t was taken as the mole percent uptake at infinite time. ie. Q_∞ . The water sorption of polymers was calculated as number of moles of water absorbed by 100g of the polymer.

2.13 AGEING STUDIES

Thermal ageing: Composite samples were cut into specified dimension according to ASTM standards for mechanical testing. It was then placed in an air oven at 100°C for about three days. Samples were then allowed to cool to room temperature.

Water ageing: Composite samples were kept in distilled water at room temperature for two weeks to attain a saturation level. Samples were taken out and air dried.

Boiling water ageing: Samples were kept in boiling water for 2hrs. and then air dried.

Radiation ageing: Composite samples were irradiated from a ^{60}Co γ ray source. The samples were given 0.1, 1, 10, 50, and 100 Mrad dose.

Biodegradation: The composite samples were inoculated with two fungi Tricoderma and Aspergillus. Inoculation was done at the cut portions of the composites and the samples were kept in a moist environment. Samples were kept for several months under the same condition.

2.14 ELECTRICAL PROPERTY MEASUREMENTS

Rectangular pieces of the composites having an approximate dimension, 1x1x0.25 cm³ were used for the measurement. The samples were coated with conductive silver paint on both sides. Copper wires were fixed as electrodes on either side. The measurement was carried out at room temperature using a 4192 LF Impedance Analyser (Hewlett-Packard Co., Palo Alto, CA, USA) at a frequency range of 10KHz – 10MHz. The resistance, capacitance and dissipation factors (tan δ) were measured directly. The volume resistivity (ρ_v), dielectric constant (ϵ') and dielectric loss (ϵ'') were calculated from the following relationships.

Volume resistivity of the composites is given by the following eqn.

$$\rho_v = \frac{R \cdot A}{t} \quad \Omega \text{ cm} \quad (2.2)$$

where R is the volume resistance, A is the area and t is the thickness of the sample.

The dielectric constant of the composites is given by,

$$\epsilon' = \frac{C \cdot t}{\epsilon_0 \cdot A} \quad (2.3)$$

where C is the capacitance, ϵ_0 is the permittivity of air ($8.85 \times 10^{-12} \text{ Fm}^{-1}$).

The dielectric loss factor is given by,

$$\epsilon'' = \epsilon' \cdot \tan \delta \quad (2.4)$$

REFERENCES

- 1 M. S. Sreekala, M. G. Kumaran, S. Thomas, *J. Appl. Polym. Sci.*, **66**, 821 (1997)
- 2 D. Hull, *An Introduction to Composite Materials*, Cambridge University press, Great Britain, 1981
- 3 M. S. Sreekala, S. Thomas, N. R. Neelakantan, *J. Polym. Eng.*, **16**, 265 (1997)

CHAPTER 3

Oil Palm Fibres : Studies on Chemical Composition, Surface Modifications, Morphology and Mechanical Properties

Results of this study have been published in Journal of Applied Polymer Science, 66, 821 (1997)

Abstract

The morphology and properties of oil palm fibres have been analysed. The properties of two important types of fibre, the oil palm empty fruit bunch (OPEFB) fibre and the oil palm mesocarp fibre (fruit fibre) have been described. The surface topology of the fibres has been studied by scanning electron microscopy. Thermogravimetry (TGA), differential thermogravimetry (DTG) and differential thermal analysis (DTA) were used to determine the thermal stability of the fibres. Various fibre surface modifications were made on the fibre. The physically and chemically modified surfaces were characterised by IR spectroscopy and scanning electron microscopy. The chemical constituents of the fibres were estimated according to ASTM standards. Mechanical performance of the fibres was also investigated. The effect of water sorption on the mechanical performance of the fibres was studied. Microfibrillar angle of the fibres was theoretically predicted. The theoretical strength of the fibres was also calculated and compared with the experimental results.

Oil palm is one of the most economical and very high potential perennial oil crops. It belongs to the species *Elaeis Guineensis* under the family *Palmacea*. It originated in the tropical forests of West Africa. Major industrial cultivation of oil palm is in South East Asian Countries like Malaysia and Indonesia. Large scale cultivation has come up in Latin America. In India oil palm cultivation is coming up on a large scale basis with a view to attain self sufficiency in oil production. Oil palm empty fruit bunch (OPEFB) fibre and oil palm mesocarp fibre are the two important types of fibrous materials left in the palm oil mill.

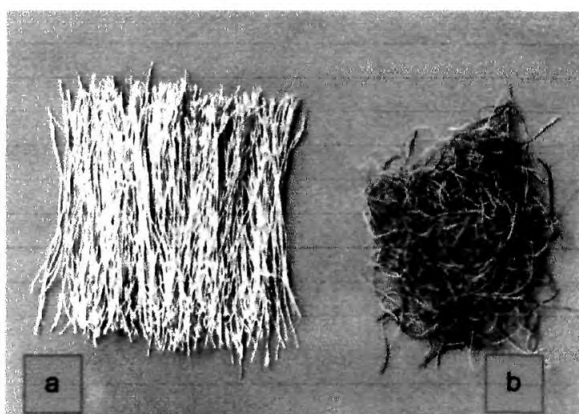


Figure 3.1 Photograph of (a) oil palm empty fruit bunch fibre, and (b) oil palm mesocarp fibre



Figure 3.2 Photograph of an oil palm empty fruit bunch

Figures 3.1(a & b) show the photographs of fruit bunch fibre and oil palm mesocarp fibre, respectively. Oil palm empty fruit bunch is obtained after the removal of oil seeds from fruit bunch for oil extraction. Photograph of an empty fruit bunch is shown in Figure 3.2. OPEFB fibre is extracted by the retting process of the empty fruit bunch. Average yield of OPEFB fibre is about 400 g per bunch. Mesocarp fibres are left as a waste material after the oil extraction. These fibres must be cleaned off from oily and dirty materials. The only current utilisation of this highly cellulosic material is as boiler fuel and in the preparation of potassium fertilisers. These waste materials when left on the plantation floor creates great environmental problems. Therefore, economic utilisation of these fibres will be beneficial. This requires extensive study on the chemical and physical

characteristics of these fibres. Many of the natural fibres like coir, banana, sisal, talipot, palmyrah, jute, pineapple leaf fibre, etc. find applications as a resource for industrial materials.^{1,2} Properties of the natural fibres depend mainly on the nature of the plant, locality in which it is grown, age of the plant and the extraction method used. For example, coir is a hard and tough fibre. It is multicellular with a central portion called lacuna. On the other hand, banana fibre is weak and cylindrical in shape. Sisal is an important leaf fibre and is strong. Pineapple leaf fibre is soft and has high cellulose content. The investigations based on these fibres are still going on. Many studies have been reported on the natural fibre based composite products.³⁻⁵ Oil palm fibres are hard and tough. These fibres show similarity to coir fibres in its cellular structure. To date, no systematic work has been undertaken to evaluate the morphology and physical properties of oil palm fibres.

The physical properties of other natural fibres have already been reported.⁶⁻¹⁴ Barkakaty⁶ reported on the structural aspects of sisal fibres. Martinez et al.⁷ studied the physical and mechanical properties of the lignocellulosic henequen fibres. Thermal stability and moisture regain of wood fibres were studied by Rao et al.⁸ They utilised scanning electron microscope to study the morphological characteristics.

Chemical treatments of cellulosic materials usually changes the physical and chemical structure of the fibre surface.⁹ Mukherjee et al.¹⁰ reported the effect of ethylene diamine on the physico-chemical properties of jute fibres. X-ray and IR studies can be used to investigate the changes in the fine structure of fibre surface.¹¹ Effects of alkali, silane coupling agent and acetylation have been tried on the oil palm fibres. It is reported that the alkali treatment on coir fibre enhanced the thermal stability and maximum moisture retention.¹² Prasad et al.¹³ reported that the use of alkali treated coir fibres greatly improves the mechanical properties of coir-polyester composites. Chemical analysis of the oil palm fibres shows that the principal component is cellulose. The cellulose content plays an important role

in the performance of the fibre. The properties of the particle boards prepared from oil palm empty fruit bunch fibre and urea formaldehyde resin have been reported earlier.¹⁴ Many studies have been reported on the determination of fibre strength using various techniques.¹⁵⁻¹⁷

In this chapter, the chemical, physical and morphological characteristics of the oil palm fibres have been investigated. Surface modifications of the fibres have been tried. Morphological analysis has been carried out with the help of IR and scanning electron microscopy studies. The chemical constituents of the fibres were determined. Mechanical properties such as tensile strength, Young's modulus and elongation at break were evaluated. The deformation characteristics of the fibres were studied with the help of stress-strain curves. Effect of water sorption on these properties was investigated. TGA, DTG and DTA were carried out to study the thermal stability of the fibres. Microfibrillar angle and strength of the fibres were theoretically calculated.

3.1 PROPERTIES OF OIL PALM EMPTY FRUIT BUNCH (OPEFB) FIBRE

3.1.1 Chemical Analysis

Table 3.1 shows the various chemical components present in the OPEFB fibre. The fibre contains higher percentage of cellulose. Lignin content is comparatively low. The total cellulose content (holocellulose) of the fibre is found to be 65%. The fibre is found to have very low ash content.

Table 3.1 Chemical Composition of Oil Palm Fibres and Some Important Natural Fibres

Fibre	Lignin (%)	Cellulose (%)	Hemicellulose (%)	Ash Content (%)
OPEFB fibre	19	65	---	2
Oil palm mesocarp fibre	11	60	---	3
Coir	40-45	32-43	0.15-0.25	----
Banana	5	63-64	19	----
Sisal	10-14	66-72	12	----
Pineapple leaf fibre	13	82	----	----

Source: ref. 1.

All these factors result in the better performance of the fibre. The fibre is hygroscopic and its moisture content is found to be 12%. The results are compared with that of some other important natural fibres (Table 3.1). Compared to coir fibres, OPEFB fibre is highly cellulosic. Coir has high percentage of lignin than OPEFB fibre. However, the cellulose content of OPEFB fibre is slightly less than that of banana and sisal. It is much less than that of pineapple leaf fibre. The lignin content of banana, sisal and pineapple leaf fibre is less than that of OPEFB fibre.

Solubility of the fibre in different solvents is given in Table 3.2. Caustic soda solubility is higher than other solvent solubility. The fibre contains 10% water soluble matter.

Table 3.2 Solubility of Oil Palm Fibres in Different Solvents

Solvent	Oil Palm Empty Fruit Bunch Fibre (%)	Oil Palm Mesocarp Fibre (Fruit Fibre) (%)
Alcohol-Benzene	12	12
Ether	12	20
1% caustic soda	20	27
Cold-water	8	12
Hot-water	10	12

3.1.2 Physical Modifications: Scanning Electron Microscopic Studies

Figures 3.3a and 3.3b are the SEM photographs of the untreated fibre surface and its cross section respectively. Porous structure is observed for untreated fibre. The pores are found to have an average diameter of $0.07\mu\text{m}$. The cross section of the fibre shows lacuna like portion in the middle. The porous surface morphology is useful to have better mechanical interlocking with the matrix resin for composite fabrication. SEM gives strong evidence for the physical microstructural changes occurred to the fibre surface on modifications. The alkali treated fibre surface is presented in Figure 3.4. Upon mercerisation, the pores became clear and this may

be due to the leaching out of the waxy cuticle layer. This renders roughness to the fibre thereby enhancing the mechanical interlocking at the interface. The fibre became curly and soft upon alkali treatment. Average diameter of the pores is found to be $0.15\mu\text{m}$. The distribution of the pores of different size before and after alkali treatment can be understood from the distribution curve (Figure 3.5).

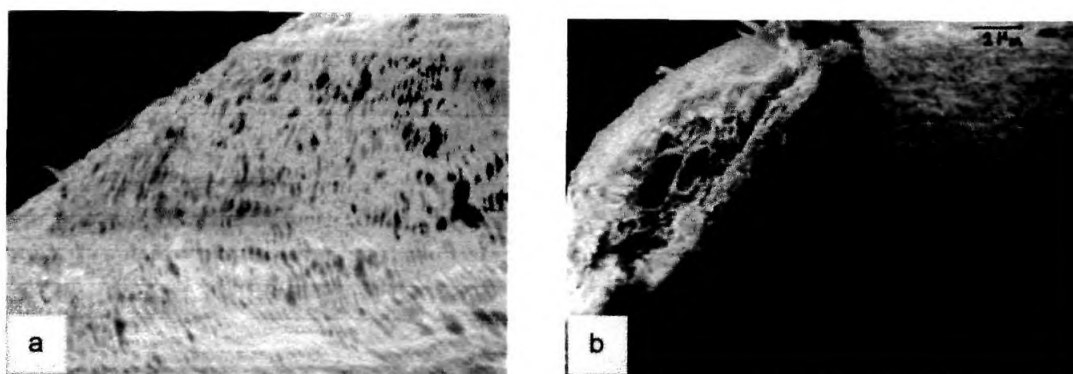


Figure 3.3 SEM's of untreated OPEFB fibre (a) fibre surface (x 400) and (b) cross section (x 200)

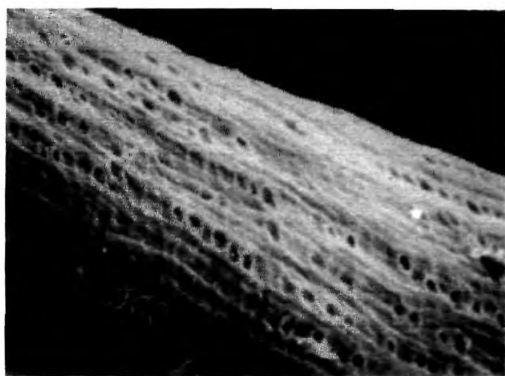


Figure 3.4 SEM of alkali treated OPEFB fibre fibre surface (x 400)

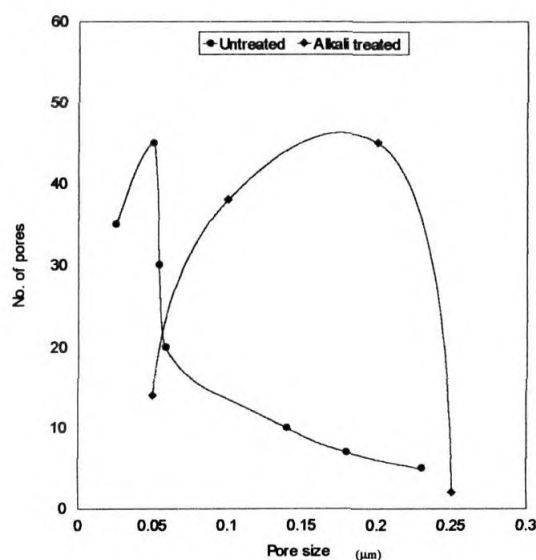


Figure 3.5 Distribution curve of pore size of the untreated and alkali treated OPEFB fibre surface

Figures 3.6 give the micrographs of acetylated fibre surface. Acetylation clearly eliminates the waxy cuticle layer on the surface. This is evident from the micrograph. Here also physical changes are clearly observed; the waxy layer is completely removed. Acetylated fibres are more stiff compared to untreated fibres. The surface topography is entirely modified upon benzoyl peroxide treatment (Fig. 3.7). The fibrillar structure of the individual ultimate fibres is revealed from the photograph and may be due to the leaching out of waxes, gums and pectic substances. Micropores, particles adhering to the surface, groove like portions and protruding structures make the fibre surface very rough. The colour of the fibre is



Figure 3.6 SEM of acetylated OPEFB fibre surface (x200)

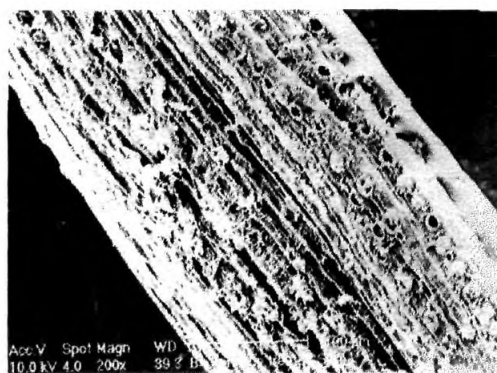


Figure 3.7 SEM of peroxide treated OPEFB fibre surface (x200)



Figure 3.8 SEM of permanganate treated OPEFB fibre surface (x100)

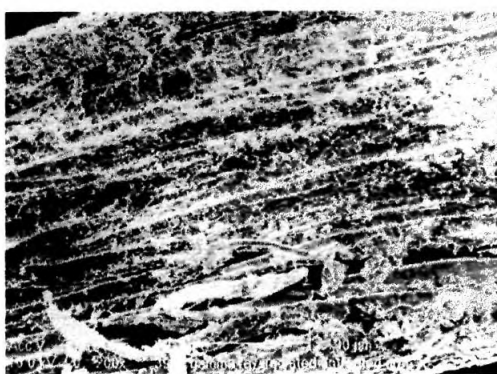


Figure 3.9 SEM of γ irradiated OPEFB fibre surface (x200)

changed and became soft upon permanganate treatment. In fact a porous structure is observed upon treatment with permanganate (Fig. 3.8). Gamma ray irradiation eliminates the porous structure and microlevel disintegration of the fibre is observed (Fig. 3.9). Major cracks are developed upon radiation treatment. It is important to mention that the changes on the fibre surface topography affect the interfacial adhesion. The toluene diisocyanate treatment leads to major changes on the fibre surface. Irregular fibre surface is seen due to the mass like substances deposited on the surface of the fibres (Fig. 3.10). Silane treatment and acrylation give surface coatings to the fibres. Surface features of the fibre are not clearly visible (Fig. 3.11 & 3.12).



Figure 3.10 SEM of isocyanate treated OPEFB fibre surface (x100)

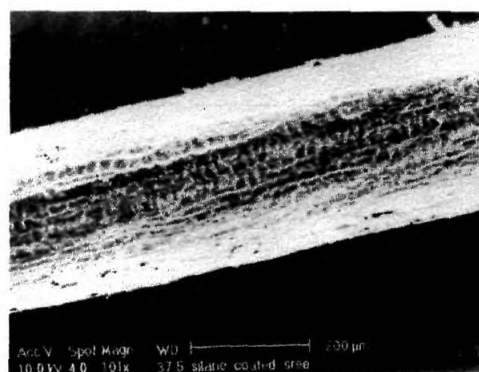


Figure 3.11 SEM of silane treated OPEFB fibre surface (x101)

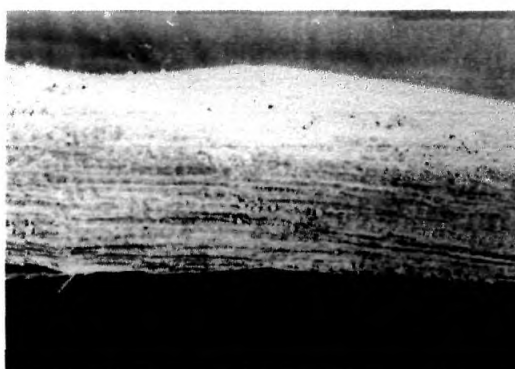


Figure 3.12 SEM of acrylated OPEFB fibre surface (x100)

Similar changes were reported on grafted natural fibres like cotton and jute.^{18, 19} Slight fibrillation is observed in acrylated fibre (Fig. 3.12). Acrylonitrile grafted fibre shows fibrillated and porous structure (Fig. 3.13). Initiation of longitudinal cracks seen on the grafted surface, may be due to the presence of the grafting materials. The deposition of the polymer onto the fibre makes a film and it fills the gap between the fibrils. The fibre became smooth and fibrillation is minimised upon latex coating (Fig. 3.14). The pores are filled with rubber making it more hydrophobic.

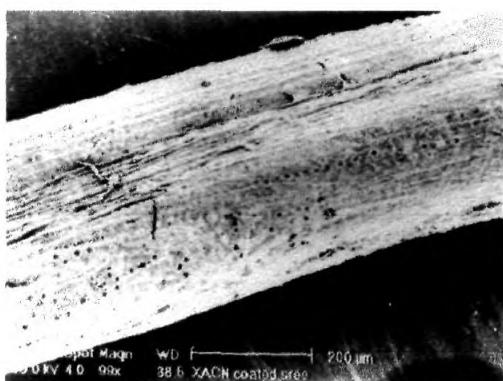


Figure 3.13 SEM of acrylonitrile grafted OPEFB fibre surface (x99)

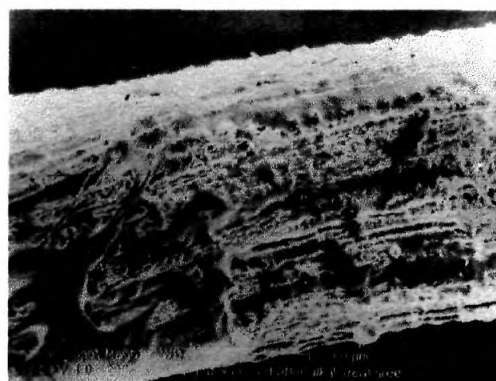


Figure 3.14 SEM of latex coated OPEFB fibre surface (x200)

3.1.3 Chemical Modifications – IR Spectroscopy

Untreated fibre: Figure 3.15a is the IR spectra of the untreated fibre. The untreated fibre shows peaks corresponding C–O stretching and C–H stretching at 770 and 2850 cm^{-1} respectively. The parent fibre shows bands at 3450 cm^{-1} due to the –O–H stretching. The peak observed at 1735 cm^{-1} may be due to C=O stretching of hemicellulose and that at 1606 cm^{-1} is due to the stretching of the aromatic ring in lignin components. A peak at 895 cm^{-1} observed arises from β -glucosidic linkage (Fig. 3.15a).

Mercerisation (Alkali treatment): Mercerisation leads to an increase in the amount of amorphous cellulose at the expense of crystalline cellulose. The important modification expected here is the removal of hydrogen bonding in the network.

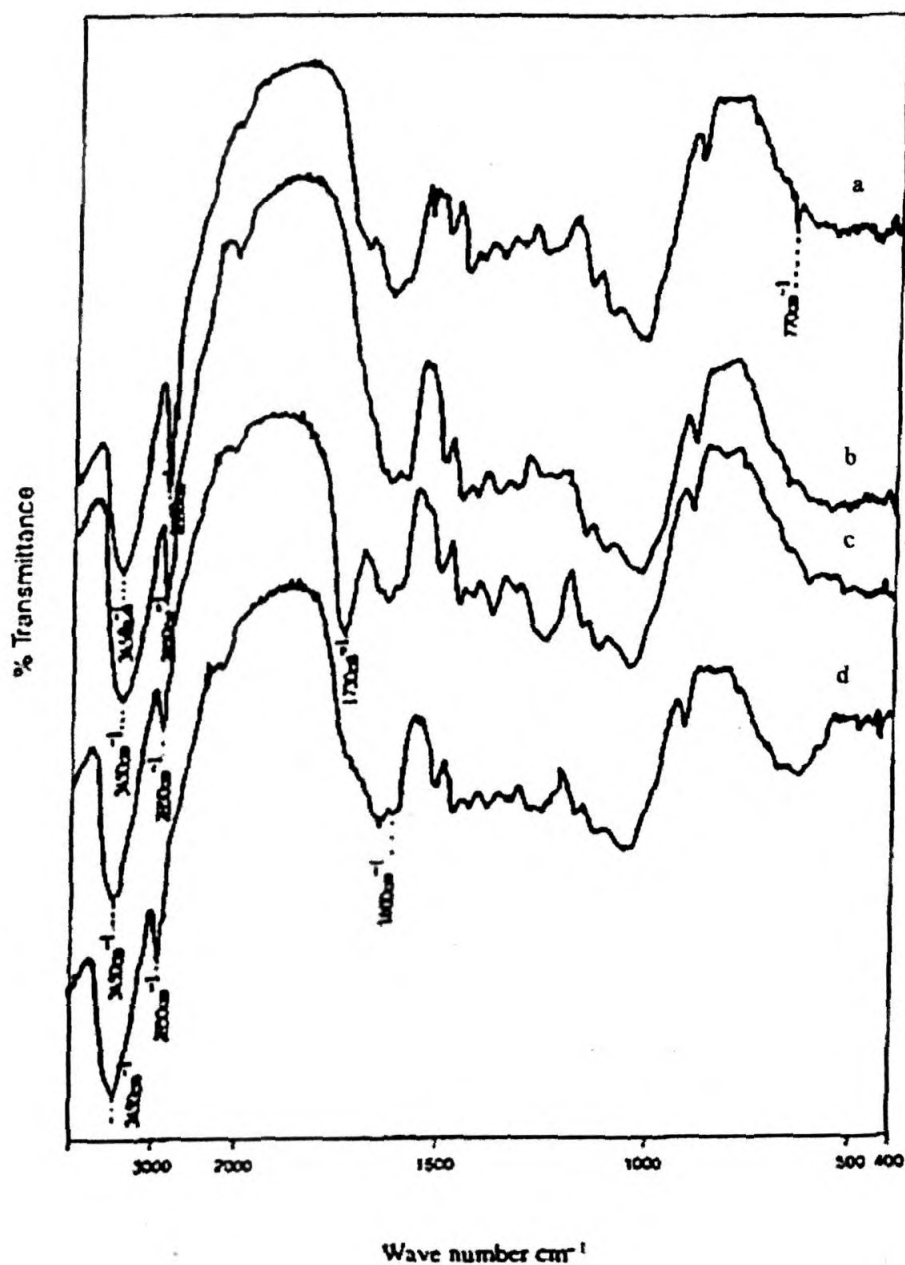
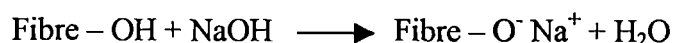
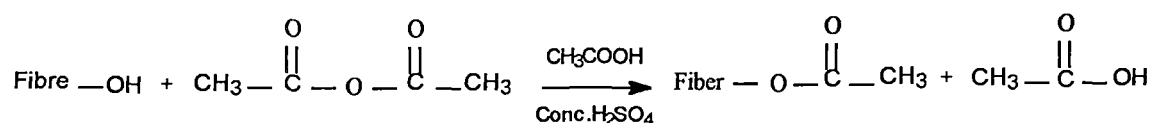


Figure 3.15 IR spectra of OPEFB fibres (a) Untreated (b) Mercerised (c) Acetylated (d) Silane treated

This is evident from the increased intensity of the OH peaks at 3450cm^{-1} in the IR spectrum (Fig. 3.15b). The following reaction takes place as a result of alkali treatment:



Acetylation: Acetylation at the -OH groups from cellulose and lignin are shown below

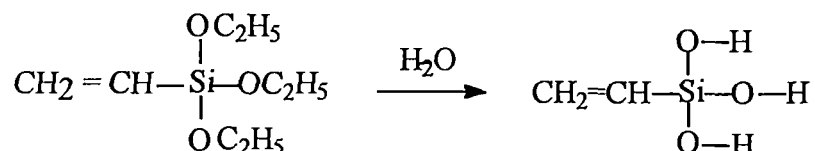


A strong peak at 1730cm^{-1} in the IR spectrum (Fig. 3.15c) indicates the presence of acetyl group in the fibre. This peak arises from combined C=O stretching of hemicellulose and C=O stretching of the $-\text{O}-\text{CO}-\text{CH}_3$ resulting from acetylation. The band at 1255cm^{-1} arises from the acetate $\text{C}-\text{C}(=\text{O})-\text{O}$ stretching. The extent of acetylation is estimated by the titrimetric method. The number of O-acetyl groups in a certain amount of acetylated fibre is estimated by hydrolysing with excess normal caustic soda. The unreacted alkali is then determined by titrating against normal oxalic acid. The number of O-acetyl groups in 0.5g of acetylated fibre was found to be 0.006.

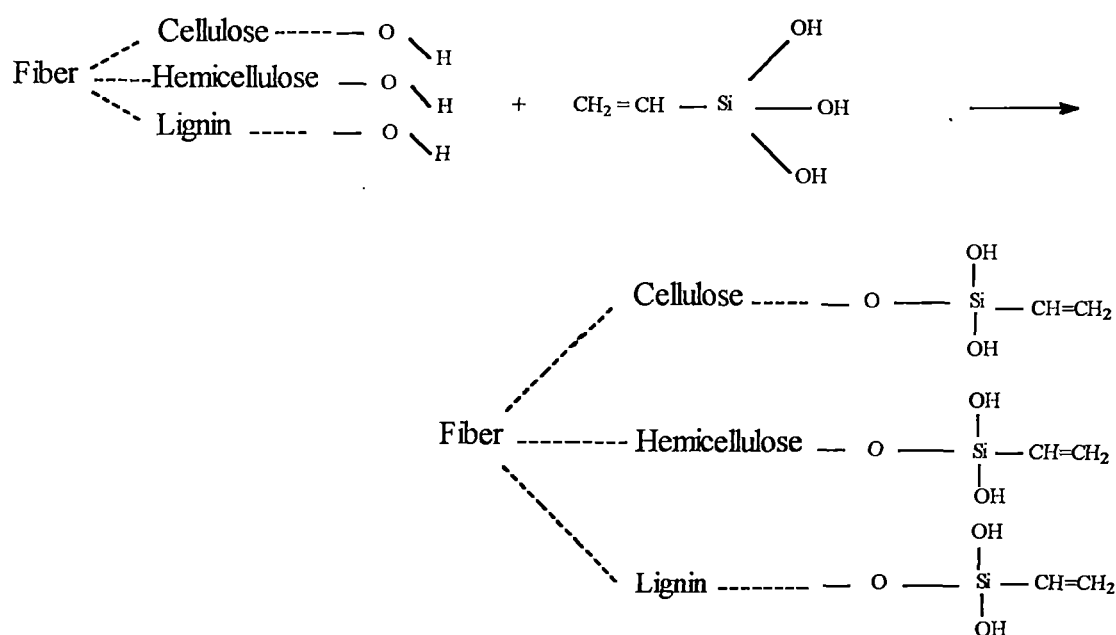
Silane treatment: Alkoxy silanes are able to form bonds with hydroxyl groups. Silanes undergo hydrolysis, condensation and the bond formation stage. Silanols can form polysiloxane structures by the reaction with hydroxyl group of the fibres.²⁰ The peak at 1525cm^{-1} in the IR spectrum of the untreated fibres is shifted to 1600cm^{-1} in the IR spectrum of the silane treated fibres (Fig. 3.15d). This may be due to the C=C stretching. The reaction scheme given below explains this.

Hydrolysis of silane: -

In presence of moisture, the hydrolyzable alkoxy group leads to the formation of silanols.



Hypothetical reaction of fibre and silane:



Acrylonitrile grafting: The lignin content in the fibre is a governing factor on the extent of acrylonitrile grafting. Presence of lignin generally retards the polymerisation rate and acts as an inhibitor at higher lignin levels.^{21, 22} Oil palm fibre contains low level of lignin (19wt.%). The accessibility of the monomer molecules to the active centres of the cellulose is easier in water than in an organic solvent.²³ The IR spectrum after extraction shows a peak at 2240cm^{-1} which is characteristic for the nitrile group corresponding to acrylonitrile grafted onto the fibre (Fig. 3.16a). The peak at 1460cm^{-1} is due to the CH_2 deformation intensified

upon grafting. Extensive studies on the acrylonitrile grafting onto the lignocellulosic materials have been reported.^{24, 25} It was found that without the presence of lignin, the grafting reaction could favourably proceed between cellulose and acrylonitrile.

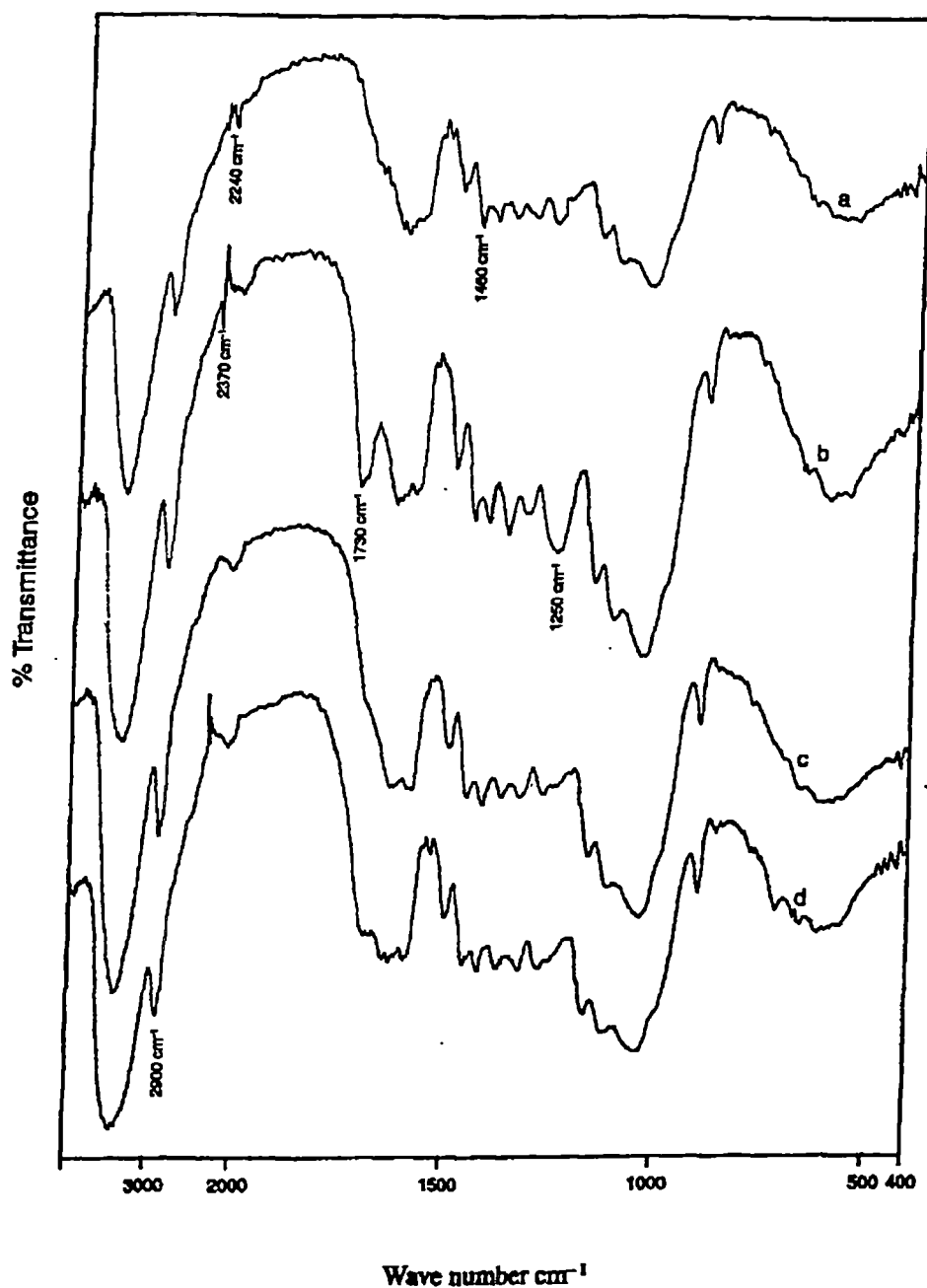
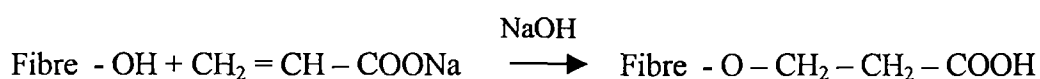


Figure 3.16 IR spectra of OPEFB fibres (a) Acrylonitrile grafted (b) Latex coated (c) Acrylated (d) Peroxide treated

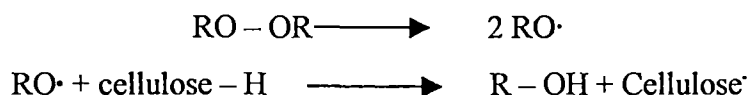
Latex Coating: Latex coating imparts physical and chemical modifications to the fibre. The fibre became more elastic. Strong peaks are observed in the IR spectrum at 2370, 1730 and at 1250 cm^{-1} when compared with the untreated fibre (Fig. 3.16b). Peaks observed at 1452 and 1375 cm^{-1} correspond to the characteristic peaks reported for natural rubber which are due to the aliphatic C–H stretching.

Acrylation: Acrylation reaction is expected to occur at the hydroxyl groups of the fibre.²⁶



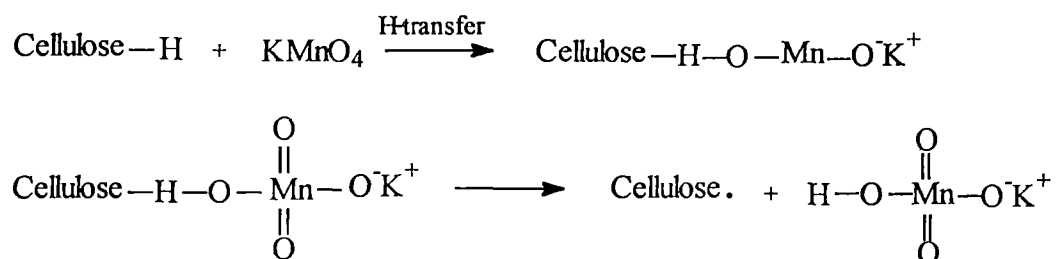
More intense peak corresponding to –O–H stretching is observed in the IR spectra (Fig. 3.16c).

Peroxide treatment: The decomposition of the peroxide and the subsequent reaction at the interface is expected at the time of curing of composites. Higher temperature is favoured for decomposition of the peroxides. This can be shown as



There is no significant change in the IR spectra upon peroxide treatment. However, the C–H stretching peak at 2850 cm^{-1} is shifted to 2900 cm^{-1} . This may be due to the slight decomposition of the peroxide (Fig. 3.16d).

Permanganate treatment: This treatment leads to the formation of cellulose radical through MnO_3^- ion formation.²⁶ The reaction scheme is as shown below



The radical enhances the chemical interlocking at the interface. Figure 3.17a shows the IR spectrum of permanganate treated fibre. The C=O stretching peak at 1735cm^{-1} in the parent fibre disappeared upon treatment.

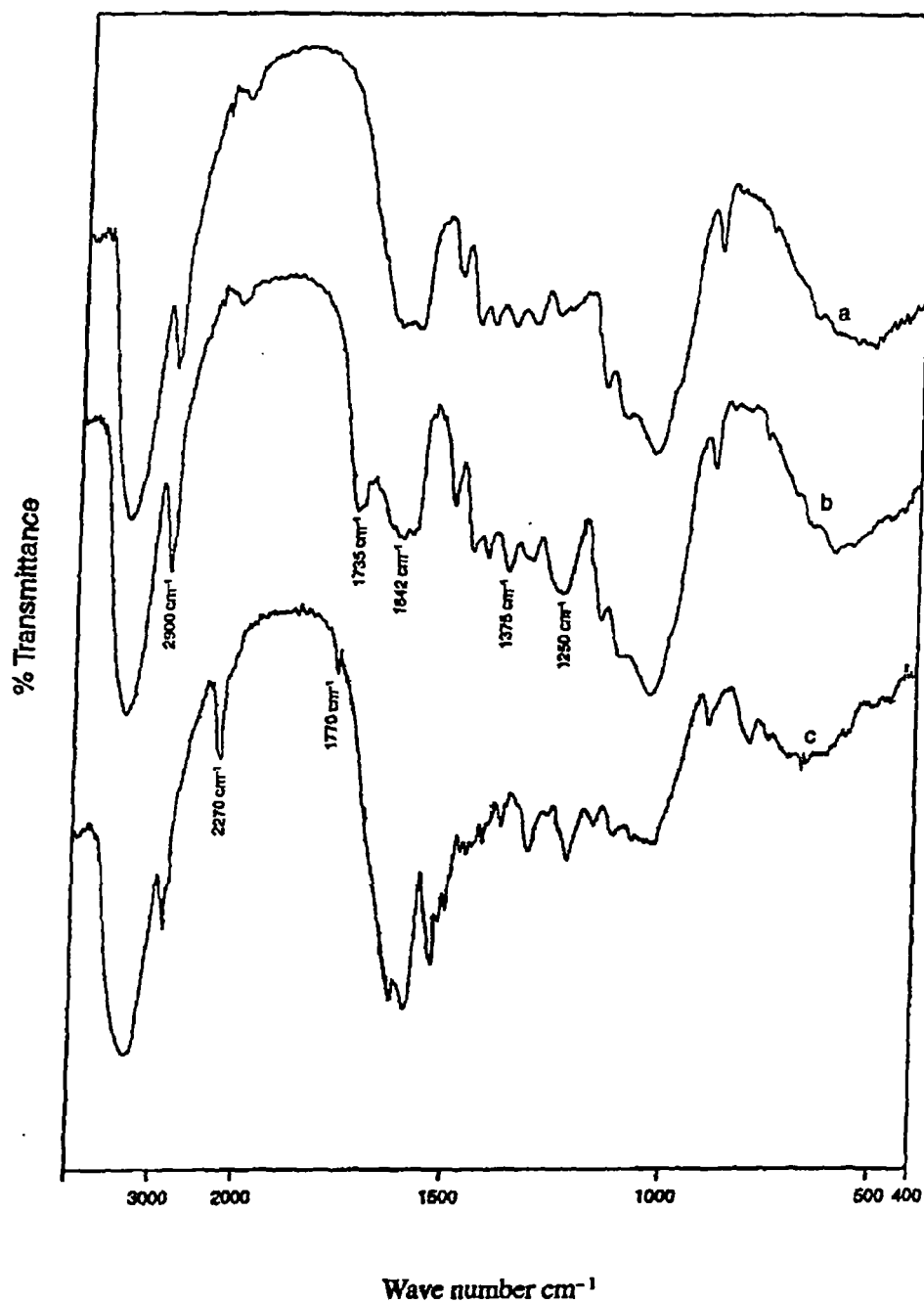
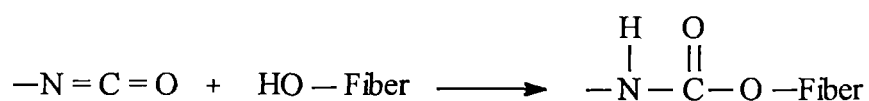


Figure 3.17 IR spectra of OPEFB fibres
(a) Permanganate treated (b) γ -irradiated (c) TDIC treated

Gamma ray irradiation: Radiation onto the fibre surface leads to major changes in the fibre. Peak at 1735cm^{-1} intensified upon γ irradiation (Fig. 3.17b). The C–H stretching peak at 2850cm^{-1} is shifted to 2900cm^{-1} . Prominent peaks are observed at 1642 , 1375 and 1250cm^{-1} . This may arise from the changes in the crystalline region, C–H bending vibration and interaction between O–H bending and C–O stretching.

Isocyanate treatment: Isocyanates have functional groups $-\text{N}=\text{C}=\text{O}$ which are very susceptible to reaction with the hydroxyl group of cellulose and lignin in fibres.



IR spectrum (Fig. 3.17c) indicates the formation of urethane linkages. A small peak at 2270cm^{-1} is observed due to the $-\text{NCO}$ stretching of the unreacted isocyanate present in the fibre. Emergence of the peak at 1770cm^{-1} may be due to the presence of $-\text{C}=\text{O}$ stretching of the urethane linkage.

3.1.4 Dimensional Changes on Treatments

The dimensional changes of the fibres after treatments can be seen from the distribution curves (Fig. 3.18). The diameters of about 100 fibres before and after treatments were measured and distribution curves were plotted. Chemical treatments significantly reduce the diameter of the fibres.

3.1.5 Thermal Studies

Figures 3.19a, b, c and d show thermal degradation pattern of untreated, alkali treated, silane treated and acetylated OPEFB fibres, respectively. Figure 3.20a, b and c show thermograms of latex treated, isocyanate treated and permanganate treated fibres respectively. Below 100°C , 5-8% weight loss was observed. This may be due to the dehydration of the fibres. Initial degradation temperature is higher for the alkali treated fibre.

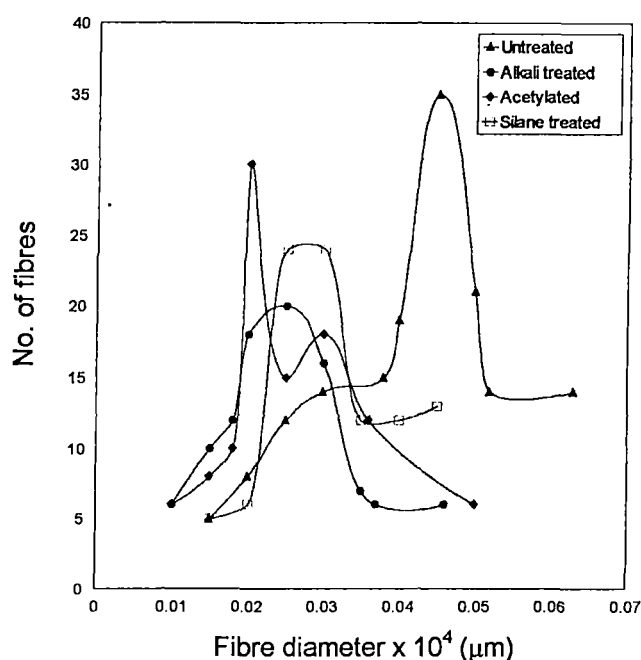


Figure 3.18 Distribution curve of fibre diameter of untreated and treated OPEFB fibres

This is evident from the DTA and TG curves (Figure 3.19b). Major weight losses of the untreated and acetylated fibres take place at about 325°C. Alkali treatment raises this temperature to 350°C while silane treatment raises to 365°C (Figure 3.19c). DTA curve shows major peak in this region. This peak that may be due to the thermal depolymerisation of hemicellulose and the cleavage of the glucosidic linkages of cellulose.²⁷ This is an exothermic process. At the first stage of degradation DTA curve shows an endothermic peak in all cases (Figures 3.19a,b,c,d). This peak may be due to the volatilisation effect. Breakage of the decomposition products of the second stage (second peak) leads to the formation of charred residue. The third exothermic peak present in the DTA curve is due to this oxidation and burning of the high molecular weight residues. In acetylated fibre the second peak is not prominent. In permanganate and isocyanate treated fibres, major weight change occurs at 330°C. However in latex coated fibre, the DTG curve shows a small peak at 325°C and a prominent peak at 375°C (Fig. 3.20a). The initial peak will be due to the degradation of the rubber phase. Complete

decomposition of all the samples takes place around 500°C in alkali, acetylated and silane treated fibres. In permanganate and isocyanate treated fibres, the decomposition come to an end at 635 and 580°C respectively. In latex coated fibre the complete degradation occurs at 700°C. The percentage weight losses of untreated and treated fibres at various temperatures are given in Table 3.3. From the table it can be understood that both alkali and silane treatment improve the thermal stability of the fibres.

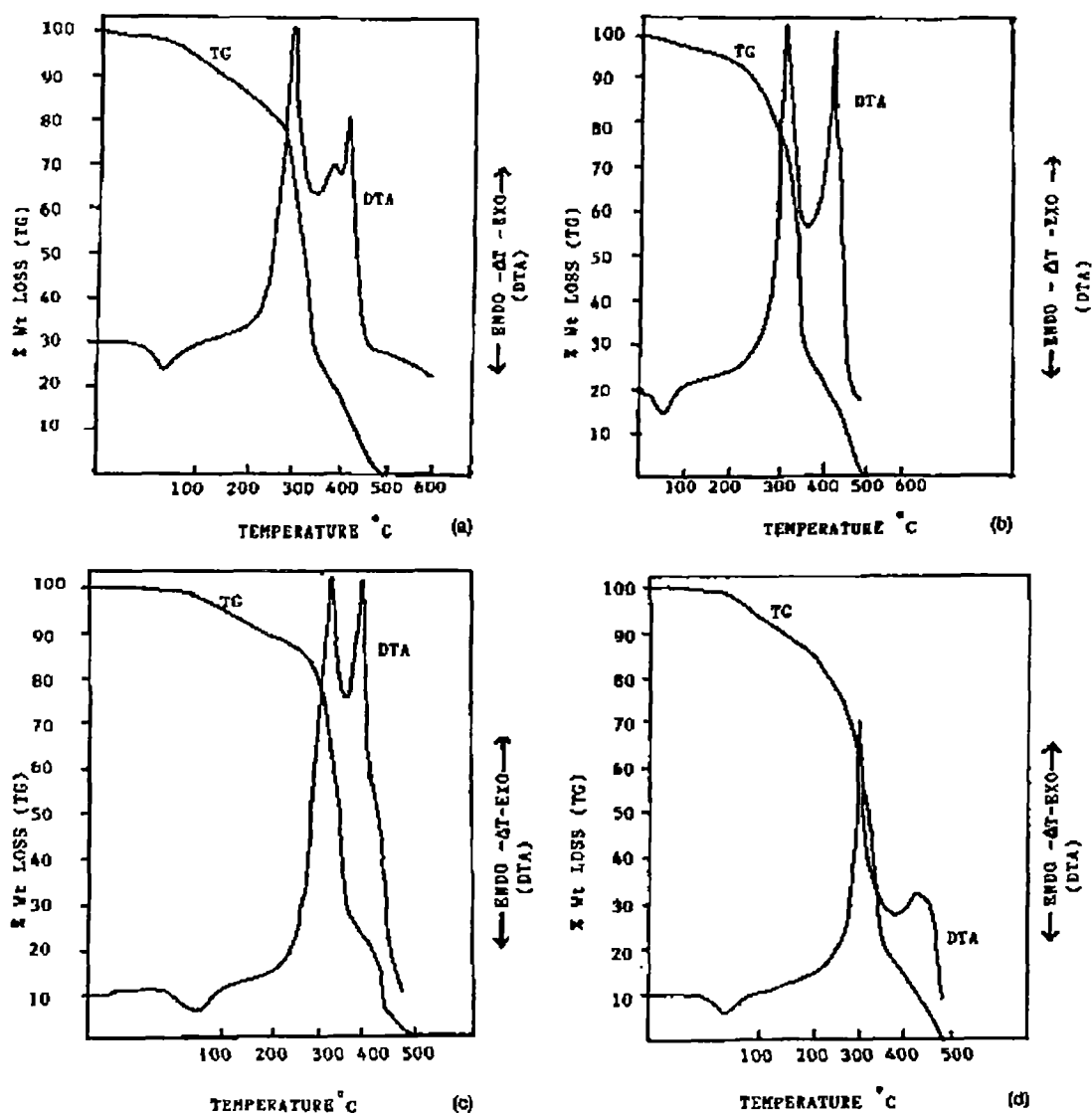


Figure 3.19 TG and DTA curves of OPEFB fibres: (a) untreated, (b) alkali treated, (c) silane treated, and (d) acetylated.

It was reported by Mahato et al.¹² that 5-15% alkali treated coir fibres showed maximum thermal stability. Varma et al.²⁸ also investigated the effect of alkali treatment of natural fibres on thermal stability. Shah et al.²⁹ reported that sodium hydroxide treatment of lignocellulosic fibres lead to the formation of a lignin-cellulose complex which gives more stability to the fibre.

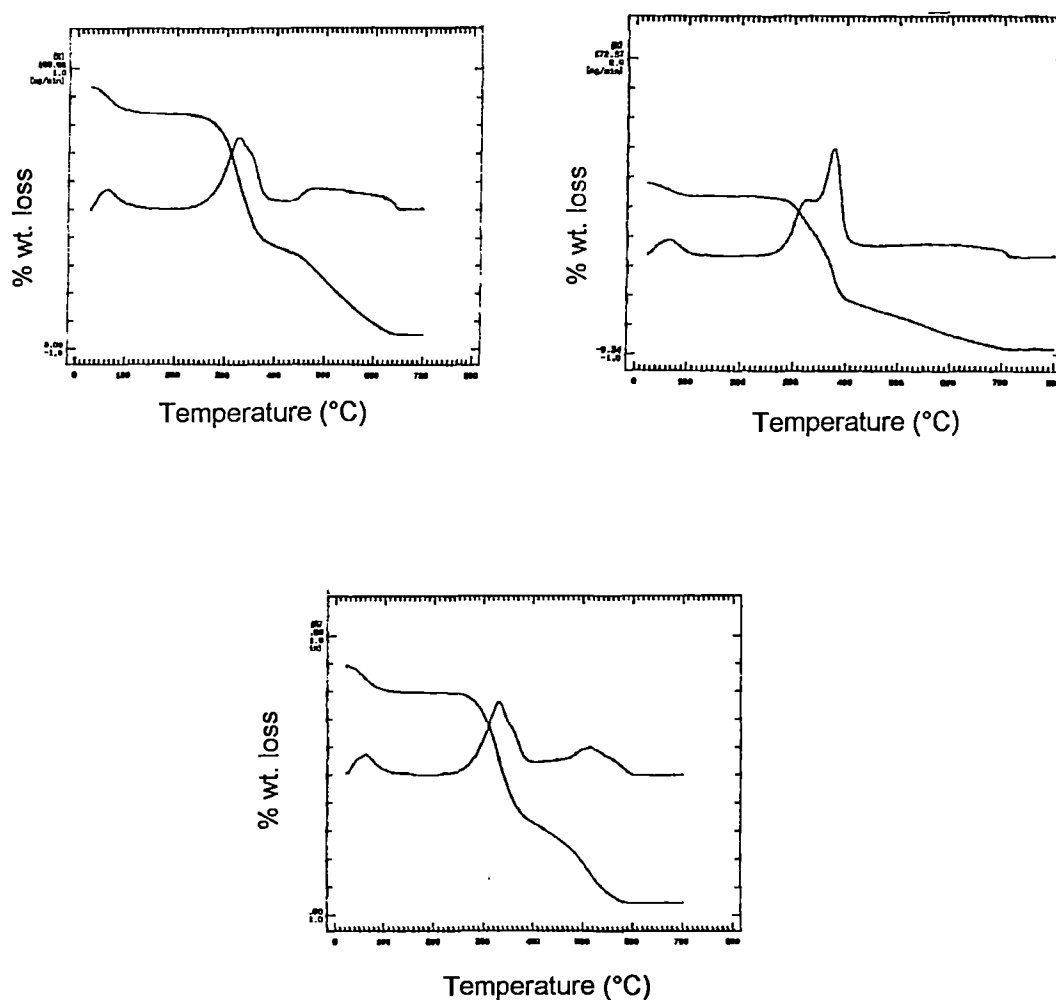


Figure 3.20 TG and DTA curves of OPEFB fibres: (a) latex treated, (b) isocyanate treated and (c) permanganate treated.

3.1.6 Effect of Fibre Surface Modifications on the Mechanical Performance of Oil Palm Fibre

The effects of various chemical treatments on the mechanical properties of the fibre have been studied. The nature and texture of the fibres obtained from different plants may not be the same. The diameter of the fibres varies in the range $0.015 \times 10^4 - 0.05 \times 10^4 \mu\text{m}$. Average density of these fibres were found to be 0.8 kg/m^3 . All these factors affect the properties of the fibre. Therefore there is large variation in the observed properties. The average value of the properties are reported.

Table 3.3 Weight Losses of Untreated and Treated OPEFB Fibres at Various Temperatures

Untreated (°C)	Alkali (°C)	Acetylated (°C)	Silane (°C)	Latex (°C)	Isocyanate (°C)	KMnO ₄ (°C)	Weight loss (%)
150	235	145	180	270	270	121	10
260	290	240	300	320	310	305	20
300	325	285	328	340	330	320	30
315	350	308	360	360	340	335	40
340	352	325	370	370	360	350	50
340	352	338	370	385	410	375	60
345	360	340	370	416	466	475	70
395	415	370	420	516	510	525	80
440	460	435	440	616	560	618	90
480	510	495	520	>740	>665	>678	100

Stress-strain behaviour: The mechanical performance of the fibre is dependent upon the chemical composition, chemical structure and cellular arrangement. Oil palm fibre contains 19% lignin and 65% cellulose. The tensile stress-strain curves for the parent and modified fibres are given in Figure 3.21. Each individual fibre is composed of fibrils held together by non-cellulosic substances like lignin, pectin etc. Failure of the fibre is gradual upon the application of tensile stress. It shows intermediate behaviour between brittle and

amorphous materials. At the very beginning ($< 1\%$ elongation) there is linearity and thereafter curvature is observed. As the applied stress increases, the weak primary cell wall collapses and decohesion of cells occurs resulting in the mechanical failure of the fibre. As stress gradually increases some of the fibrils may slip out. Total of the stress is then shared by fewer cells. Further increase of the stress leads to the rupture of cell walls and decohesion of cells. This results in a catastrophic failure of the fibre. This could be understood from the slope changes in the stress-strain curve. Modifications lead to major changes on the fibrillar structure of the fibre. These modifications remove the amorphous components leading to changes in the deformation behaviour of the fibres. Stress-strain behaviour of the treated fibres clearly shows this. The brittleness of the fibre is substantially reduced upon treatments.

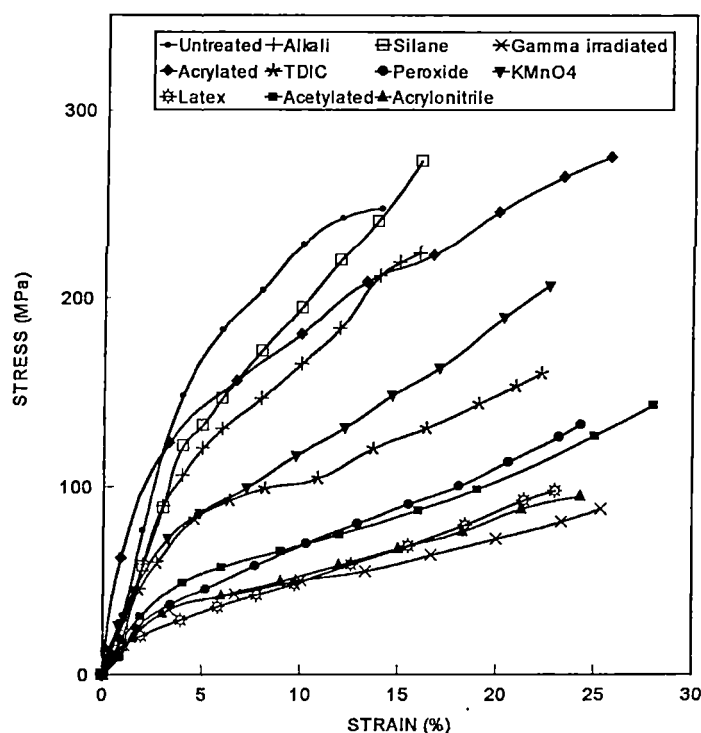


Figure 3.21 Stress-strain curves of untreated and treated OPEFB fibres

Tensile properties: Important tensile properties of the fibre, tensile strength, Young's modulus and elongation at break are given in Table 3.4.

Optimum mechanical performances are observed for silane treated and acrylated fibre. Large fibre to fibre variations in properties were observed. Hence an average value obtained from the total of ten samples for each case is reported. Many of the modifications decrease the strength properties due to the breakage of the bound structure and also due to the disintegration of the non-cellulosic materials. Major degradation occurred as a result of γ radiation. Some of the treatments like silane and acrylation lead to strong covalent bond formation and thereby the strength is enhanced. Latex modification enhances the elasticity of the fibres. Since the oil palm fibres exhibit micropores on its surface, the latex can penetrate into the pores and can form a mechanically interlocked coating on its surface. This can contribute to its tensile properties by withstanding the fibre failure even after the major internal failure. The reinforcing ability of the fibres does not just depend upon the mechanical strength of the fibres but on many other features like polarity of the fibre, surface characteristics and presence of reactive centres like functional groups. These factors control the interfacial interaction.

Table 3.4 Mechanical Performance of Parent and Modified OPEFB Fibres

OPEFB fibre	Tensile strength (MPa)	Young's modulus (MPa)	Elongation at break (%)
Untreated	248	6700	14
Mercerised	224	5000	16
Acetylated	143	2000	28
Peroxide treated	133	1100	24
KMnO ₄ treated	207	4000	23
γ radiated	88	16 00	25
TDIC treated	160	2000	22
Silane treated	273	5250	16
Acrylated	275	11100	26
Acrylonitrile grafted	95	1700	24
Latex coated	98	1850	23

The Young's modulus of the fibres is improved upon acrylation reaction. Untreated, alkali and silane treated fibres show very good modulus properties. The improved stiffness of the fibre is attributed to the crystalline region (cellulosic) of the fibre. The fibre shows very good elongation properties. The untreated fibre shows 14% elongation. This may be due to the firmly bound chemical structure of the fibre. Lignin binds the three dimensional cellulose network as well as the fibrils. The value shows sharp increase upon modifications. Lower elongation of the untreated fibre may be due to the three dimensionally crosslinked network of cellulose and lignin. Treatment breaks this network structure giving the fibre higher elongation and lower strength properties.

Figure 3.22 is the scanning electron micrograph of the tensile fracture of the untreated oil palm empty fruit bunch fibre. The fracture surface morphology of the broken end shows marked irregularities.

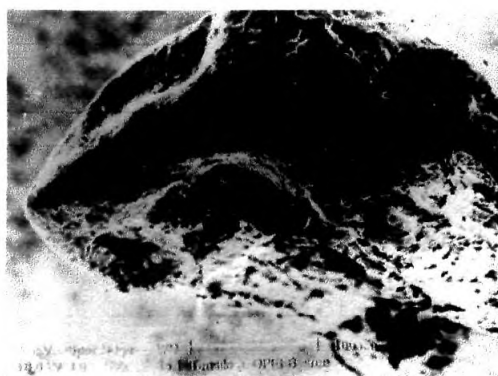


Figure 3.22 Scanning electron micrograph of tensile fracture of OPEFB fibre

The properties of the fibre were compared with that of some important natural fibres. Table 3.5 gives the mechanical property values of these natural fibres.³⁰ The strength and stiffness of the OPEFB fibre is much higher than that of coir. Coir shows highest elongation among commonly used natural fibres. OPEFB fibre shows higher elongation than sisal, pineapple and banana. The fibre is highly

tough. However, the tensile strength of the fibre is less than that of sisal, pineapple and banana fibres.

Table 3.5 Mechanical Properties of Some Important Natural Fibres

Fibre	Tensile strength (MPa)	Elongation (%)	Toughness (MPa)
Sisal	580	4.3	1250
Pineapple	640	2.4	970
Banana	540	3	816
Coir	140	25	3200
OPEFB fibre	248	14	6700
Oil palm mesocarp fibre	80	17	500

Source Ref. (30)

3.1.7 Theoretical Prediction of Microfibrillar Angle and Strength of the OPEFB Fibre

Strength properties of the fibres are dependent mainly on the fibrillar structure, microfibrillar angle and cellulose content. There is a correlation between percentage elongation, ϵ and the microfibrillar angle, θ as³¹

$$\epsilon = 2.78 + 7.28 \times 10^{-2}\theta + 7.7 \times 10^{-3}\theta^2 \quad (3.1)$$

Using this equation, the microfibrillar angle of OPEFB fibre is found to be 42°. There exists a relationship between the strength properties with microfibrillar angle and cellulose content.³¹ This is given by

$$\sigma = 334.005 - 2.830\theta + 12.22W \quad (3.2)$$

where σ = fibre strength, θ = microfibrillar angle, W = cellulose content

The strength of the fibre is calculated as 341 MPa. However, the experimental value was found to be 248 MPa.

3.2 PROPERTIES OF OIL PALM MESOCARP FIBRE (FRUIT FIBRE)

3.2.1 Chemical Analysis

Chemical composition of the fibre is given in Table 3.1. Cellulose and lignin content are less than that of OPEFB fibre. It is comparable with other natural fibres (Table 3.1). Fibre surface contains traces of oil. It dissolves on treatment with NaOH solution. Solubility of the fibre in different solvents is given in Table 3.2. This fibre shows higher percentage solubility in ether, caustic soda, cold water and hot water than OPEFB fibre. Moisture content of the fibre is found to be 11%.

3.2.2 Chemical Modifications

Fibre surface modifications have been done by alkali treatment and silane treatment. Mechanisms suggested for OPEFB fibre modifications are applicable here also.

3.2.3 Physical Modifications : Scanning Electron Microscopic Studies

Surface characteristics of the untreated fibre are clear from Figure 3.23a. The fibre surface is rough. It exhibits protruding portions and grooves like portions on its surface. The cross-section of the fibre is not uniform (Figure 3.23b). The morphological changes of fibre on alkali treatment and silane treatment are evident from the respective SEM photographs given in Figures 3.24 and 3.25. Alkali treated fibre surface shows some protrusions on its surface. This may be associated with the removal of the cuticle layer from the fibre surface. The fibre surface became clear on silane treatment (Figure 3.25). Large number of micropores could be seen on the surface. They have an average diameter 0.2 μm .

3.2.4 Chemical Modifications – IR Spectroscopy

On comparing the IR spectra of untreated OPEFB fibre and oil palm mesocarp fibre (Figs. 3.15 and 3.26), it is seen that there is structural similarity between

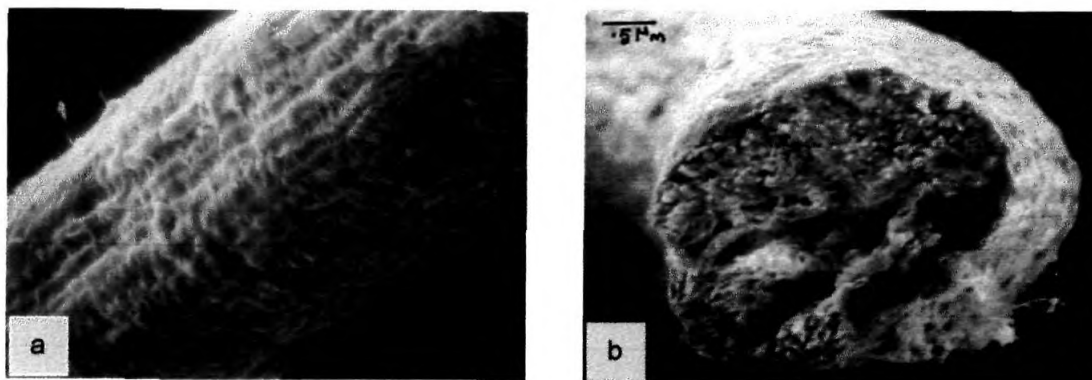


Figure 3.23 SEM's of untreated oil palm mesocarp fibre (a) fibre surface (x 400) and (b) cross section (x 800)

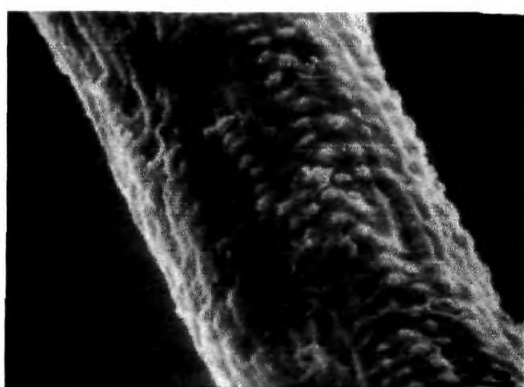


Figure 3.24 SEM of alkali treated oil palm mesocarp fibre surface (x400)

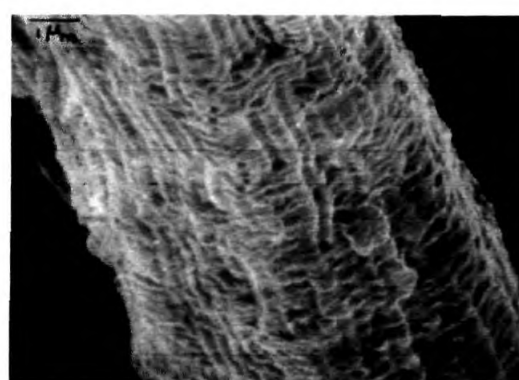


Figure 3.25 SEM of silane treated oil palm mesocarp fibre surface (x400)

these fibres. Both the spectra show intense peaks at 3450cm^{-1} and 2850cm^{-1} (O-H stretching and C-H stretching, respectively).

The fine structural changes of oil palm mesocarp fibres upon chemical modification can be understood from IR spectra. This is given in Figure 3.26. Major changes in the absorbance occur in the case of alkali treatment. The C=O stretching frequency of carboxylic group (1730cm^{-1}) disappears on alkali treatment. This may be due to the removal of carboxylic group by alkali. Carboxylic group may be present on the fibre surface from traces of fatty acids present. The intensity of the peak at 2125cm^{-1} increases upon alkali and silane treatments. This may be due to the CH stretching. The intensity of the hydroxyl

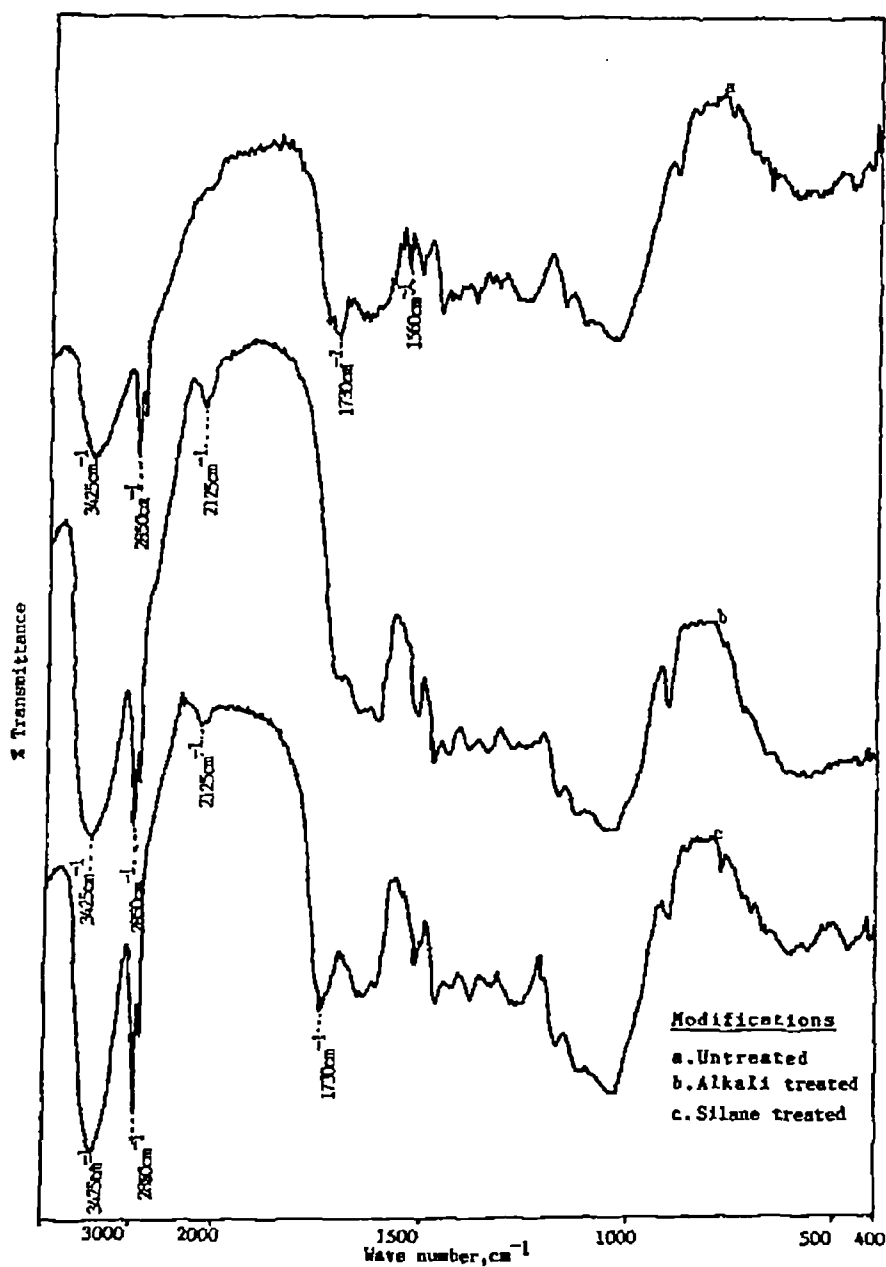


Figure 3.26 Infrared spectra of treated and untreated oil palm mesocarp fibres.

vibration absorption (3425cm^{-1}) increased considerably upon alkali and silane treatments as in the case of OPEFB fibre. Cellulosic hydroxyl groups may be involved in hydrogen bonding. There are chances for bonding with carboxylic groups of the fatty acids present on the fibre. Presence of a peak at 1730cm^{-1} in

untreated fibre gives evidence for this. On treatments, these bonds may break. The peak at 1560cm^{-1} (C=C str.) disappeared on alkali and silane treatments. This may be due to the removal of unsaturation present in the traces of oils by the treatments. From these studies it is clear that several chemical reactions took place during treatments.

3.2.5 Thermal Studies

Thermal stability of OPEFB fibre is higher than that of oil palm mesocarp fibre. Silane treated OPEFB fibre is stable up to 365°C whereas stability of the alkali treated oil palm mesocarp fibre is only up to 340°C .

TG and DTA scans of the untreated and treated fibres are presented in Figure 3.27. The untreated fibre is stable up to 310°C . Alkali and silane treatment raises the stability of fibre up to 340°C . Alkali treatment raises the initial degradation temperature (weight loss of 10%) to 180°C from 138°C . The initial weight loss may be due to the vaporisation of water present in the sample. DTA curve shows a corresponding endothermic peak in this region. Major degradation of untreated fibres occurs at about 310°C . Treatment raises this temperature to 340°C . Decomposition of cellulose may occur at this stage. A corresponding exothermic peak is observed in DTA curve. The third exothermic peak in the DTA curve may be due to the formation of charred residue from the first degradation products. Broadening of the DTA peak is observed for silane treated sample. The gradual degradation and percentage weight losses of untreated and treated fibres can be understood from Table 3.6. From these results, it can be concluded that alkali treatment is found to be more effective in improving the thermal stability.

3.2.6 Mechanical Performance

The strength and Young's modulus of the OPEFB fibre is greater than that of oil palm mesocarp fibre. But the mesocarp fibre shows higher percentage of elongation. The mechanical performance of the mesocarp fibre is comparatively

low with respect to other natural fibres (Table 3.5). Properties of lignocellulosic fibres depend mainly on the cellulose content and microfibrillar angle. Various mechanical properties of oil palm mesocarp fibres are given in Table 3.7. The average density of this fibre is found to be 0.9 kg/m^3 . An average diameter of $0.02 \times 10^4 \mu\text{m}$ is observed for these fibres. The stress-strain characteristics of treated and untreated fibres are given in Figure 3.28. The modulus of the fibre is increased upon modification by alkali and silane coupling agent.

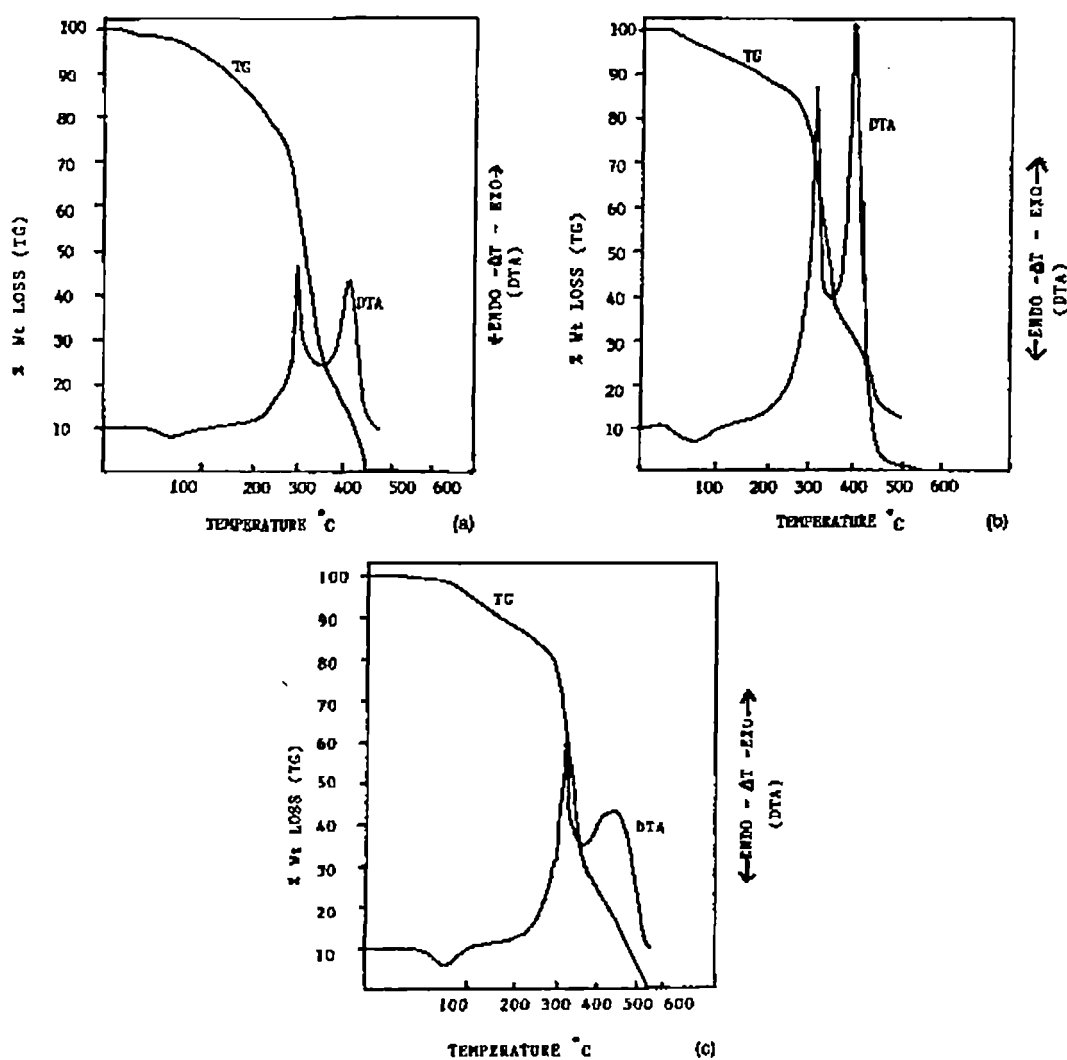


Figure 3.27 TG and DTA curves of oil palm mesocarp fibres: (a) untreated, (b) alkali treated, and (c) silane treated.

Silane treatment is found to be more effective. Silane treated fibre shows maximum tensile strength. However, alkali treatment slightly decreases the tensile strength. The elongation at break is maximum for untreated fibres. The value shows decrease upon treatment. The firmly bound three dimensional network of cellular arrangement may be partly destroyed upon treatment. Alkali treatment reduces the tensile strength of the mesocarp fibre. This may be due to the bleaching of the oily and waxy materials from the fibre surface. Mesocarp fibres may contain traces of oil even after processing since the oil is present in the flesh of the fruit. Silane treatment is found to be more effective in improving mechanical properties.

Table 3.6 Weight Losses of Untreated and Treated Oil Palm Mesocarp Fibres at Various Temperatures

Untreated (°C)	Alkali (°C)	Silane (°C)	Weight loss (%)
138	180	165	10
218	285	285	20
275	310	315	30
290	340	330	40
315	350	350	50
328	355	360	60
340	410	370	70
373	450	425	80
430	470	480	90
455	540	520	100

Figure 3.29 is the scanning electron micrograph of tensile fracture surface of mesocarp fibre. The structural failure of the fibres on application of stress is clear from the micrograph. The fractured surface shows irregularities in its morphology. As the applied stress increased the weak primary cell wall collapses and decohesion of cells occurs which leads to the failure of the fibre.

Table 3.7 Mechanical Performance of Parent and Modified Oil Palm Mesocarp Fibres

Oil palm mesocarp fibre	Tensile strength (MPa)	Young's modulus (MPa)	Elongation at break (%)
Untreated	80	500	17
Alkali treated	64	740	6.5
Silane treated	111	1120	13.5

3.2.7 Dimensional Changes on Treatments

The dimensional changes of the mesocarp fibres after treatments are given by the distribution curves in Figure 3.30. The measurements were done as in the case of OPEFB fibre. Here too chemical treatment reduces the diameter of the fibres.

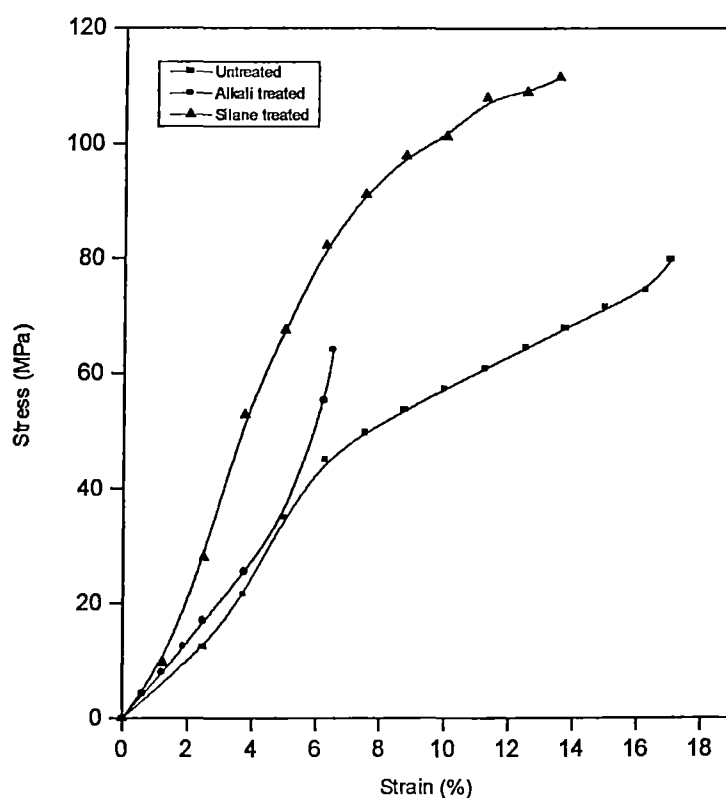


Figure 3.28 Stress-strain characteristics of untreated and treated oil palm mesocarp fibres

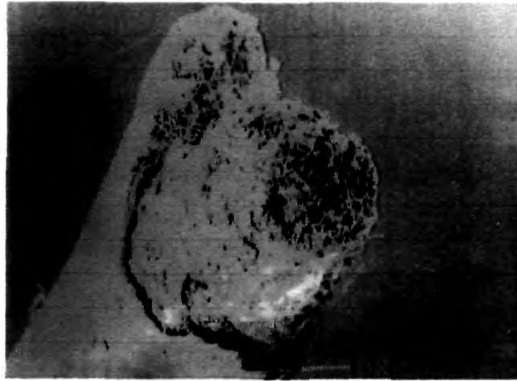


Figure 3.29 Scanning electron micrograph of tensile fracture of oil palm mesocarp fibre

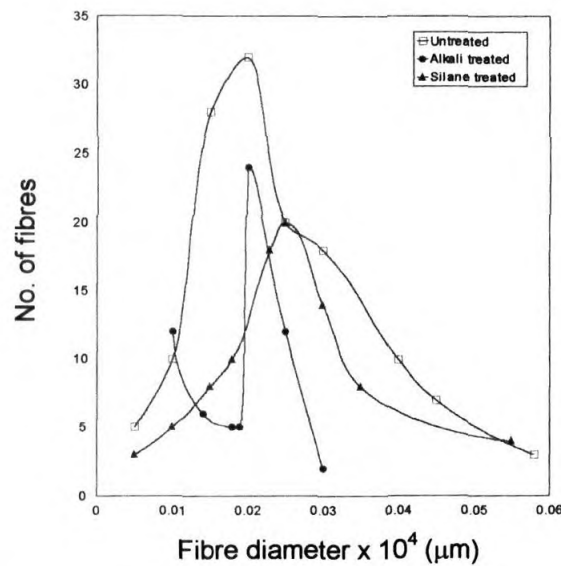


Figure 3.30 Distribution curve of fibre diameter of untreated and treated oil palm mesocarp fibres

3.2.8 Theoretical Prediction of Microfibrillar Angle and Strength of the Oil Palm Mesocarp Fibre

The fibre shows about 17% elongation at break. Using Equation 3.1, the microfibrillar angle of the fibre is calculated. It is found to be 46° . Using Equation 3.2, the strength of the fibre is predicted. The calculated strength of the fibre is 269 MPa. But the experimental value is very much lower than this. This may be due to the nature of cellular arrangement of the fibre and the effect of traces of oil present on the fibre surface.

REFERENCES

1. K. G. Satyanarayana, A. G. Kulkarni and P. K. Rohatgi, *J. Sci. Ind. Res.*, **40**, 222 (1981)
2. K. G. Satyanarayana, A. G. Kulkarni and P. K. Rohatgi, *J. Sci. Ind. Res.*, **42**, 425 (1983)
3. A. N. Shah and S. C. Lakkad, *Fibre Sci. Technol.*, **15**, 41 (1981)
4. C. Pavithran, P. S. Mukherjee, M. Brahmakumar and A. D. Damodaran, *J. Mater. Sci. Lett.*, **6**, 882 (1987)
5. D. Maldas and B. V. Kokta, *Polym. Plast. Technol. Eng.*, **29**, 419 (1990)
6. B. C. Barkakaty, *J. Appl. Polym. Sci.*, **20**, 2921 (1976)
7. M. N. C. Martinez, P. J. Herrera-franco, P. I. Gonzalez-Chi and M. Aguilar-vega, *J. Appl. Polym. Sci.*, **43**, 749 (1991)
8. D. R. Rao and V. B. Gupta, *Ind. J. Fibre Tex. Res.*, **17**, 1 (1992)
9. C. David, R. Fornasier, W. Lejong and N. Vanlautem, *J. Appl. Polym. Sci.*, **36**, 29 (1988)
10. A. C. Mukherjee, S. K. Bandyopadhyay, A. K. Mukhopadhyay and U. Mukhopadhyay, *Ind. J. Fibre Tex. Res.*, **17**, 80 (1992)
11. D. M. Brewis, J. Comyn, J. R. Fowler, D. Briggs and V. A. Gibson, *Fibre Sci. Technol.*, **12**, 41 (1979)
12. D. N. Mahato, B. K. Mathur and S. Bhattacharjee, *Ind. J. Fibre Tex. Res.*, **20**, 202 (1995)
13. S. V. Prasad, C. Pavithran and P. K. Rohatgi, *J. Mater. Sci.*, **18**, 1443 (1983).
14. S. A. K. Yamini, A. J. Ahmad, J. Kasim, N. M. Nasir and J. Harun, *Proc. of the Int. Symposium on Biocomposites and Blends based on Jute and Allied Fibres*, p. 135 (1994)
15. W. A. Curtin, *Polym. Comp.*, **15**, 474 (1994)
16. M. R. Nedele and M. R. Wisnom, *Comp. Sci. Technol.*, **51**, 517 (1994)
17. P. K. Jarvela, *Fibre Sci. Technol.*, **20**, 83 (1984)
18. N. Thejappa and S. N. Pandey, *J. Appl. Polym. Sci.*, **27**, 2307 (1982)
19. S. K. Kundu, P. K. Ray, S. K. Sen & S. K. Bhaduri, *J. Appl. Polym. Sci.*, **49**, 25 (1993)
20. A. K. Bledzki, S. Reihmane and J. Gassan, *J. Appl. Polym. Sci.*, **59**, 1329 (1996)
21. B. Sikdar, R. K. Basak and B. C. Mitra, *J. Appl. Polym. Sci.*, **55**, 1673 (1995)
22. V. Hornof, B. V. Kokta and J. L. Valade, *J. Appl. Polym. Sci.*, **20**, 1543 (1976)
23. L. Kessira and A. Ricard, *J. Appl. Polym. Sci.*, **49**, 1603 (1993)

24. David N. S. Hon (Ed.), *Graft copolymerization of lignocellulosic fibres*, ACS Symposium series 187, Washington D. C (1982)
25. A. K. Mohanty, S. Parija and M. Misra, *J. Appl. Polym. Sci.*, **60**, 931 (1996)
26. G. Demma, D. Acierno, P. Russo and J. M. Kenny, *J. Polym. Eng.*, **14**, 283 (1995)
27. J. George, S. S. Bhagawan and S. Thomas, *Composite Interfaces*, **5**, 201 (1998)
28. D. S. Varma, M. Varma and I. K. Varma, *Thermochimica Acta*, **108**, 199 (1986)
29. S. C. Shah, P. K. Ray, S. N. Pandey and K. Goswami, *J. Polym. Sci.*, **42**, 2767 (1991)
30. P. S. Mukherjee and K. G. Satyanarayana, *J. Mater. Sci.*, **21**, 4162 (1986)
31. K. G. Satyanarayana, C. K. S. Pillai, K. Sukumaran, S. G. K. Pillai, P. K. Rohatgi and K. Vijayan, *J. Mater. Sci.*, **17**, 2453 (1982)

CHAPTER 4

Influence of Fibre Surface Modifications on the Mechanical Performance of Oil Palm Fibre Reinforced Phenol Formaldehyde Composites

*Results of this study have been accepted for publication in the journal
Applied Composite Materials (In press)*

Abstract

OPEFB fibres have been used as reinforcement in phenol formaldehyde resin. In order to improve the interfacial properties, the fibres for reinforcement were subjected to different chemical modifications such as mercerisation, acrylonitrile grafting, acrylation, latex coating, permanganate treatment, acetylation, and peroxide treatment. The effect of fibre coating on the interface properties has also been investigated. The incorporation of the modified fibres in PF resulted in composites having excellent impact resistance. Fibre coating enhanced the impact strength of untreated composite by a factor of four. Tensile and flexural performances of the composites were also investigated. Finally, in order to have an insight into the failure behaviour, the tensile and impact fracture surfaces of the composites were analysed using scanning electron microscope.

Mechanical performance of a fibrous composite is mainly determined by the fibre properties. Extent of interfacial interaction between the fibre and matrix determines the stress transfer ability of a fibrous composite. Possibility of forming mechanical and chemical bonding at the interface is mainly dependent on the surface morphology and chemical composition of the fibres, polarity of the matrix or presence of reactive probes in the matrix resin etc. Hydrophilicity of the fibre and resin is an important factor determining the extent of fibre-matrix adhesion. Therefore, microscopic analysis of fibre surface topology and fracture surface morphology deserves utmost importance in fibrous composites.

Natural fibres are amenable to modifications as they bear hydroxyl groups from cellulose and lignin. The hydroxyl groups may be involved in the hydrogen bonding within the cellulose molecules thereby reducing the activity towards the matrix. Chemical modifications may activate these groups or can introduce new moieties that can effectively interlock with the matrix. Surface characteristics such as wetting, adhesion, surface tension, porosity etc. can be improved upon modifications. Chemical bleaching of the fibres may lead to major changes in fibre surface roughness. The irregularities of the fibre surface play an important role in the mechanical interlocking at the interface. Parameters such as van der Waals force, dipole-dipole interactions, hydrogen bonds etc. determine the extent of physical bonding. Enhancement in the physical and chemical adhesion can be understood from the schematic model (Fig. 4.1). The model represents increase in adhesion of the resin onto the fibres due to the physical and chemical changes occurred on the fibre upon chemical treatments. Physical changes may include removal of the waxy cuticle layer, changes in the surface roughness, physical appearance of the fibre and density. This may lead to changes in the adhesive strength of the fibre onto the matrix. As a result, the interface properties of the composite will be improved. Chemical bond formation at the interface is possible by some treatments that lead to a higher compatibilized system. Extensive studies on the important modification methods for vegetable fibres and their effect on the mechanical performance of the natural fibre composites were reported.¹⁻¹²

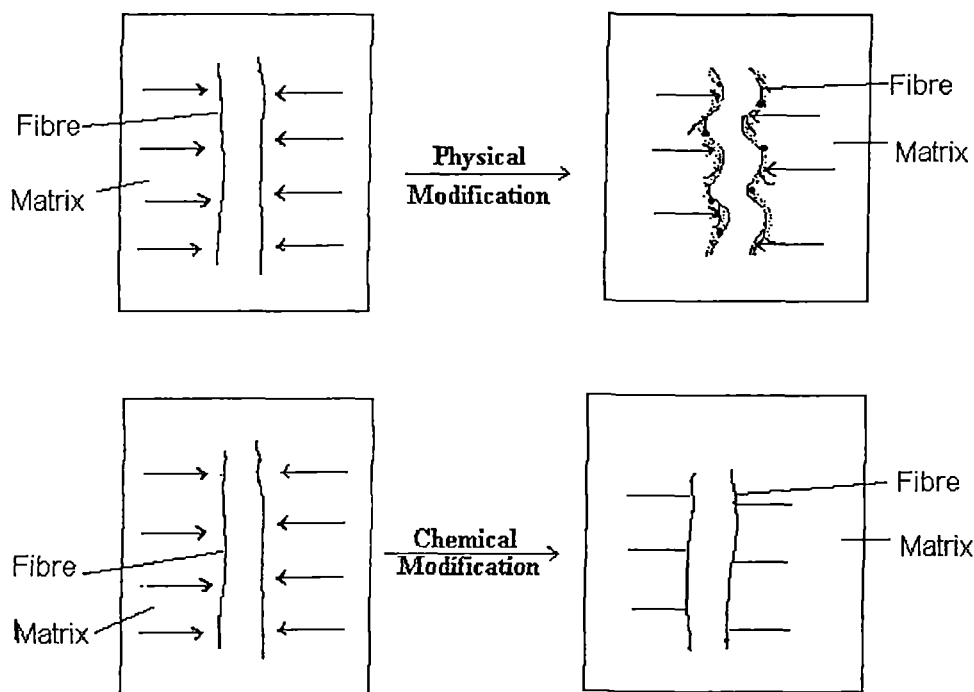


Figure 4.1 Schematic model showing fibre modifications

Corona discharge treatment on cellulosic fibre and hydrophobic matrix was found to be effective in improving compatibilization between hydrophilic fibre and hydrophobic matrix.¹³ King and co-workers introduced electrochemical polymeric coatings for improving fibre-matrix adhesion in liquid crystalline polymer composites.¹⁴ Plasma treatment is another important method to achieve better interfacial bonding between fibre and matrix.^{15, 16} Modification effects by plasma treatment depend on the nature, flux and energy distribution of the incident species. Improved fibre-matrix interactions upon chemical modifications of natural fibres such as pineapple leaf fibre, sisal, banana etc. have already been reported by Thomas et al.¹⁷⁻²⁰ Chemical modifications such as introduction of coupling agents, peroxide treatment, alkali and permanganate treatments make the pineapple leaf fibre more compatible with the hydrophobic polyethylene matrix thereby improving

the mechanical performance of the composites.¹⁷ Benzoylation of the sisal fibre was found to enhance the tensile properties of the sisal reinforced polystyrene composites.¹⁸ Tensile properties of sisal fibre reinforced LDPE composites were enhanced upon chemical treatment.¹⁹ Silane treatment onto the banana fibre improves interfacial adhesion with polyester matrix, which increases the mechanical strength of the composite²⁰.

In this chapter the role of fibre surface modifications on the static mechanical properties of the composites is presented. Fibres were subjected to acetylation and mercerisation. Effects of benzoyl peroxide, permanganate treatment and γ radiation of the fibre on the mechanical performance were tested. Coupling agents such as toluene diisocyanate and triethoxy vinyl silane were tried on the fibre surface in order to improve the interface properties. Acrylation reaction and acrylonitrile grafting were also performed on the fibre surface. In order to reduce the surface cracking and to improve impact strength, latex modification of the fibres were tried. The physical and chemical modifications occurred to OPEFB fibres on various treatments were discussed in Chapter 3. Mechanical properties of the oil palm fibre reinforced phenol-formaldehyde composites were investigated. The oil palm fibre is strongly polar due to hydroxyl groups and C-O-C links in its structure. This renders it more compatible with polar polymers. The phenol formaldehyde resole type resin is highly polar owing to its phenolic hydroxyl groups and methylol groups. Since both the fibre and the matrix are hydrophilic they are highly compatible. Chemical modifications may decrease the hydrophilicity of the fibre thereby reducing the interfacial adhesion. The influence of modifications such as mercerisation, peroxide treatment, permanganate treatment, acrylonitrile grafting on the mechanical properties of the composites has been studied in detail. The most characteristic property of the thermoset composites, the impact performance is highlighted in this study. More specifically, the influence of hydrophobic-hydrophilic balance on the impact properties has been analysed in detail. Finally the tensile and impact fractography of the modified and unmodified composites were analysed using scanning electron micrographs.

4.1 EFFECT OF FIBRE SURFACE MODIFICATIONS ON THE MECHANICAL PERFORMANCE OF THE COMPOSITES

4.1.1 Tensile Properties

Figure 4.2 gives tensile stress-strain behaviour of the parent and treated composites having 40wt.% fibre loading. Treatments such as mercerisation, permanganate and peroxide treatment on resin lead to brittle failure of the composites. The γ irradiated, acrylonitrile grafted as well as untreated composites show behaviour in between brittle and ductile failure. Isocyanate, silane, acrylated, latex coated and peroxide treated fibre composites can withstand the tensile stress to higher strain level. Necking followed by catastrophic failure is observed in untreated, mercerised, permanganate treated, acrylonitrile treated, γ irradiated and peroxide treated composites. Comparatively lower elongation is observed in these composites. Isocyanate treated, silane treated, acrylated, acetylated and latex coated composites show yielding and high extensibility. Latex modified composite exhibits maximum elongation and shows a rubbery nature.

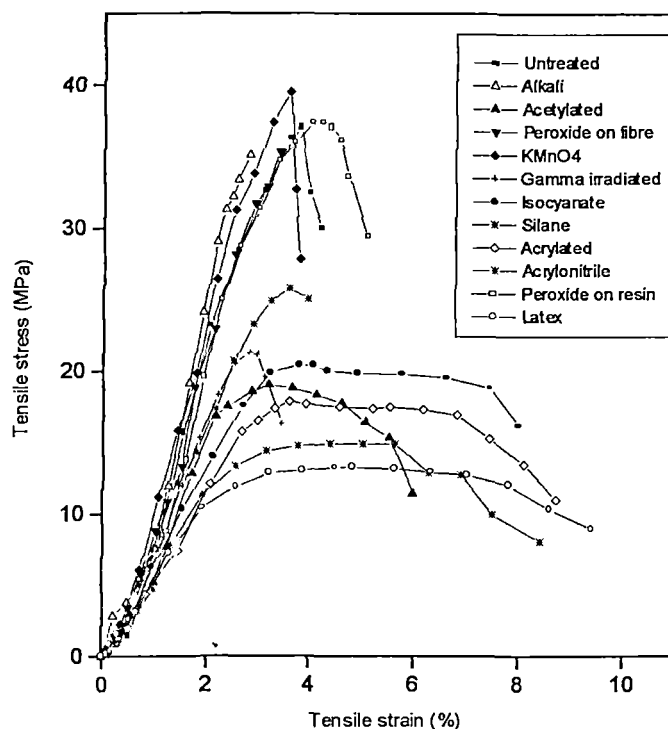


Figure 4.2 Tensile stress-strain behaviour of the parent and treated oil palm fibre/PF composites having 40 wt.% fibre loading

Mechanical performance of unmodified oil palm fibre reinforced PF composites as a function of fibre length and fibre loading were analysed and are reported elsewhere.²¹ Tensile strength values of the composite show a marginal increase on permanganate treatment. The values are given in Table 3.4 (refer Chapter 3). Permanganate treatment of fibre leads to composites having better tensile properties. However on fibre modifications by other chemical agents, the tensile strength is found to be decreased. Natural fibre reinforced plastic composites often show enhancement in tensile properties upon different modifications owing to the increased fibre-matrix adhesion.^{22 - 24, 17 & 19} Treatments like mercerisation, peroxide, γ irradiation and permanganate treatment do not make any major changes to the hydrophilicity of the lignocellulosic fibre. The interfacial bond remains intact even after these modifications. Generally, the interaction of cellulose fibre with PF resin is excellent due to the hydrophilic nature of cellulose and PF resin. This is shown schematically in Figure 4.3. Hydrophilicity of the fibre arises from the cellulosic hydroxyl groups and lignin hydroxyl groups, which are the major components of the fibre. These can easily form hydrogen bonds with the methylol and phenolic hydroxyl groups of the resole in the prepreg stage. On curing at 100°C, these groups can undergo condensation reaction leading to a three-dimensional network between the fibre and matrix. However upon acetylation, silane treatment, isocyanate treatment, acrylation, acrylonitrile grafting and on latex modification the hydrophilic fibre -OH groups are replaced by hydrophobic moieties. This decreases the strength of the chemical interlocking at the hydrophilic centres of the phenol formaldehyde resin. Thus, effective stress transfer does not take place at the interface leading to easy debonding of the fibres under tension.

Tensile modulus of the composites at 2% elongation (Table 4.1) shows slight enhancement upon mercerisation and permanganate treatment. The composite properties are mainly dependent on the interfacial strength. The interfacial strength in fact depends on the fibre and matrix properties. Modifications of the fibre play an important role on the interface properties. Increased adhesion upon mercerisation and permanganate treatment leads to better interfacial strength which

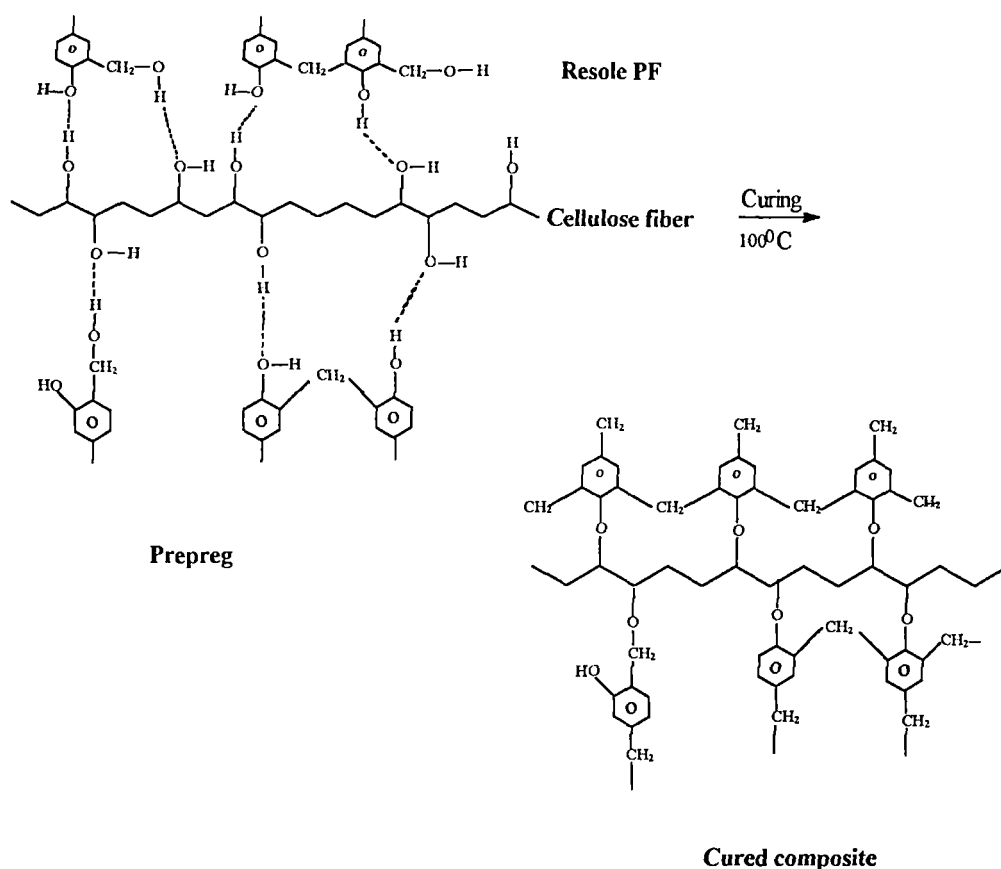


Figure 4.3 Schematic model showing the interface of oil palm fibre and phenol Formaldehyde

enhances the modulus of the composite. However, all other treatments show a decrease in tensile modulus due to the increased hydrophobicity of the fibre.

Elongation at break of the composites shows considerable change upon different modifications. Maximum elongation is observed for latex coated samples. The higher extensibility is attributed to the better stress transfer ability of the fibre due to the improvement in flexibility imparted as a result of latex coating. The variations in the elongation at break on different modifications are attributed to the changes in the chemical structure and bondability of the fibre.

Scanning electron micrographs of the tensile fracture of the untreated and treated composites reveal the failure mechanisms. Figure 4.4 shows the tensile fracture of untreated composite. Fibre breakage is the main failure criteria observed. Alkali treated composite shows better fibre matrix adhesion (Fig. 4.5).

Table 4.1 Tensile and Flexural Properties of Untreated and Treated Oil Palm Fibre Reinforced PF Composites

Oil palm fibre/ PF composite	Tensile strength (MPa)	Tensile modulus at 2% elongation (MPa)	Elongation at break (%)	Flexural strength (MPa)	Flexural Strain at break (%)	Flexural modulus at 1% strain (MPa)
Untreated	37	1150	4	49	6	3050
Mercerised	35	1300	3	75	6	2950
Acetylated	19	800	6	36	7	1900
Peroxide on fibre	35	1125	3	71	3	3950
KMnO ₄	40	1200	4	55	3	3750
γ irradiated	21	825	3	30	2	2200
Isocyanate	20	700	8	32	9	1800
Silane	15	700	8	23	8	1200
Acrylated	18	600	9	29	8	1800
Acrylonitrile	26	800	4	52	5	2500
Peroxide on resin	37	1050	5	54	7	3050
Latex coated	13	550	9	16	8	700



Figure 4.4 SEM of tensile fracture of untreated oil palm fibre/PF composite(x50)



Figure 4.5 SEM of tensile fracture of alkali treated oil palm fibre/PF composite (x100)

T35
28/6/2000
RS

Fibre-matrix debonding is clear from the fracture surface of acetylated composite (Fig. 4.6). Matrix cracking and fibre breakage were observed in peroxide treated fibre composite (Fig. 4.7). Permanganate treatment leads to very good fibre-matrix adhesion, as is evident from the highly fibrillated structure of the fibre (Fig. 4.8). Fracture surface of the silane treated composite shows crowded fibres and several broken ends (Fig. 4.9). This indicates decreased fibre-matrix interfacial adhesion. Fibre-matrix debonding is the main failure process observed in peroxide treated composites (Fig. 4.10). Fibrillation is observed here also.



Figure 4.6 SEM of tensile fracture of acetylated oil palm fibre/PF composite(x98)

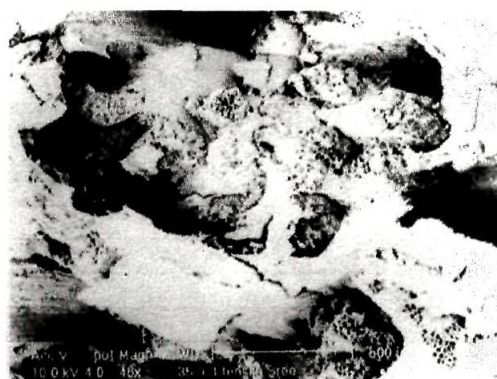


Figure 4.7 SEM of tensile fracture of peroxide treated oil palm fibre/PF composite (x46)



Figure 4.8 SEM of tensile fracture of KMnO₄ oil palm fibre/PF composite(x200)



Figure 4.9 SEM of tensile fracture of silane treated oil palm fibre/PF composite (x34)



Figure 4.10 SEM of tensile fracture of oil palm fibre/PF composite having peroxide treatment on resin (x34)

4.1.2 Flexural Properties

The deformation behaviour of the untreated and treated composites having 40wt.% fibre loading under flexural stress is seen from Figure 4.11. In the case of γ irradiated fibrous composites, the flexural stress abruptly decreases to a very small value at the break point. In all other treated composites, crack initiation and its gradual propagation is observed. The increasing deflection brings on matrix rupture progressively, resulting in fracture and pulling out of fibres, leading to a more or less regular decrease of strength. There is considerable energy absorption after partial failure of the sample. The regular decrease in the strength after partial rupture denotes composite's sensitivity towards fibre distribution. The behaviour is similar to that obtained on application of tensile stress. Permanganate treated, peroxide treated, acrylonitrile grafted and γ irradiated composites show necking effect. All others show yielding and high strain values. Composite's ability to withstand the applied flexural stress can be manifested by the strain values (Table 4.1). Higher strain values indicate the increased elastic nature of the composite.

Resistance to the compressive failure of the composites is manifested in flexural tests. The flexural properties of the composites are given in Table 4.1.

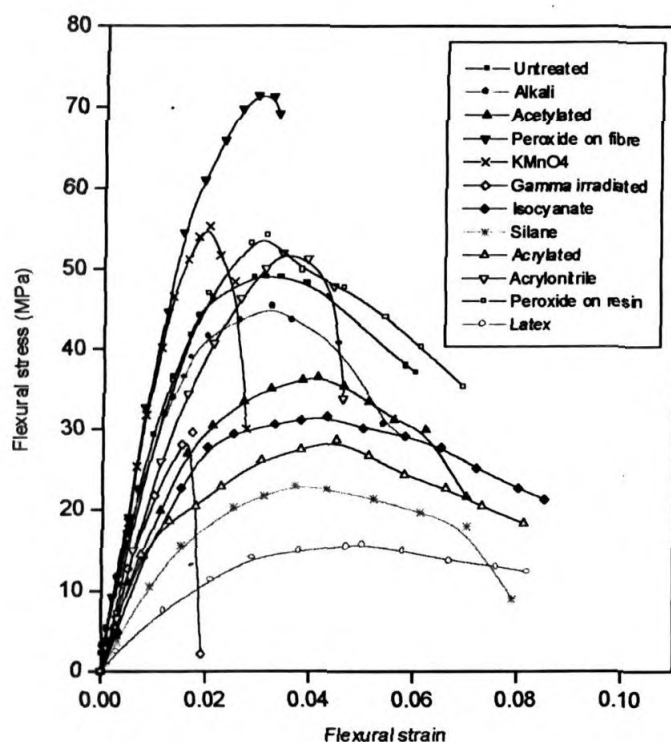


Figure 4.11 Flexural stress-strain behaviour of the parent and treated oil palm fibre/PF composites having 40 wt.% fibre loading

Mercerisation and peroxide treatment on the fibre increase the flexural strength of the composites. Permanganate treatment and acrylonitrile grafting give moderate stiffness to the composite. Peroxide treatment on resin also enhances the stiffness. The variation in these properties can be explained on the basis of the changes in chemical interactions at fibre-matrix interface on various treatments as explained under tensile properties.

Flexural modulus at 1% strain is given in Table 4.1. Improvement in flexural modulus is observed upon peroxide and permanganate treatments. Flexural modulus is a measure of strength and stiffness of the composite. Decrease in the values upon other modifications is attributed to the weaker interfacial bond formed.

4.1.3 Impact Properties

The main disadvantages of the thermoset mouldings are high shrinkage during curing, high brittle behaviour and surface cracking. Phenol formaldehyde

mouldings exhibit all these drawbacks. Incorporation of the oil palm fibres in phenol formaldehyde almost eliminates these drawbacks. Impact performance of the resin largely improved upon fibrous reinforcement. In order to use as a structural material, the phenolic composite should have good resistance to impact. Figure 4.12 shows the izod impact strength of the unmodified and modified composites having 40 wt.% fibre loading. Much promising results are obtained on modifications. Latex coating, acetylation, silane and TDIC treatment leads to impact resistant composites. Increased hydrophobicity of the fibres upon these treatments leads to weak interfacial linkage thereby facilitating the debonding process on stressed condition. This leads to the fibre pull out.

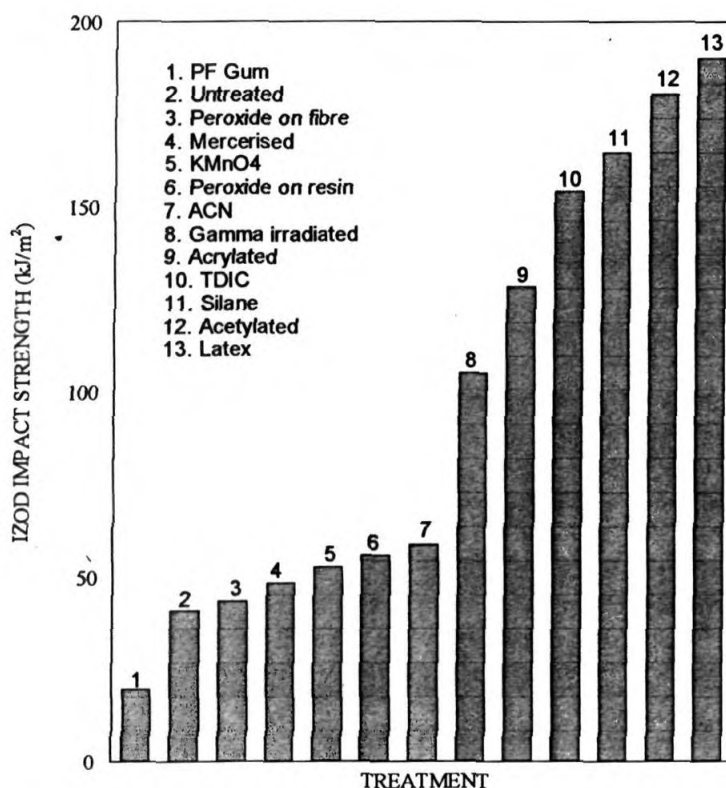


Figure 4.12 Unnotched izod impact strength of the untreated and treated oil palm fibre fibre/PF composites having 40wt.% fibre loading

Detailed studies have already been reported on the impact resistance of short fibre reinforced polymer composites.²⁵⁻²⁷ Fibres may have a significant effect on the impact resistance probably through the principle of stress transfer. When an impact

load is applied perpendicular to the fibres, good fibre-matrix adhesion is required for even moderate impact strength. When it acts parallel to the reinforcing fibres the better impact strength are obtained if the adhesion is relatively poor and the fibres are short, so that maximum energy can be dissipated by mechanical friction during the pullout process and by debonding of the fibres.²⁸ The strength of the matrix, the weakest part of the material should be related to the failure process. The total energy dissipated in the composite before final failure occurs is a measure of its impact resistance. The total energy absorbed by the composite is the sum of the energy consumed during plastic deformation and the energy needed for creating new surfaces. Major microfailure mechanisms operating during impact loading of the composite include initiation and propagation of matrix cracking, fibre-matrix debonding, fibre breakage and fibre pullout. The involvement of fibres in failure process is related to their interaction with the crack formation in the matrix and their stress transferring capability. The range of impact resistance provided by the fibres depend on several factors such as fibre rigidity, interfacial stress resistance, fibre aspect ratio etc.

Impact fracture morphology and failure mechanisms are clear from the respective scanning electron micrographs of impact fracture surface of untreated and treated composites. The failure process with respect to fibres is a combination of fibre pullout and fibre breakage and is evident from the respective scanning electron micrographs. Brittle fracture of the phenol formaldehyde matrix and fibre can be understood from the scanning electron micrograph of the untreated composite (Fig. 4.13). Alkali treated composite shows severe fibre breakage (Fig. 4.14). Fibre pullout occurs as a result of the impact failure in acetylated composites (Fig. 4.15). Impact strength shows lower value for permanganate treated composite. This may be due to enhanced fibre-matrix interlocking (Fig. 4.16). The silane treatment leads to easy debonding at the interface. The introduction of silane onto the fibre was found to make it more hydrophobic resulting in a decreased fibre-matrix interaction than in untreated composites.

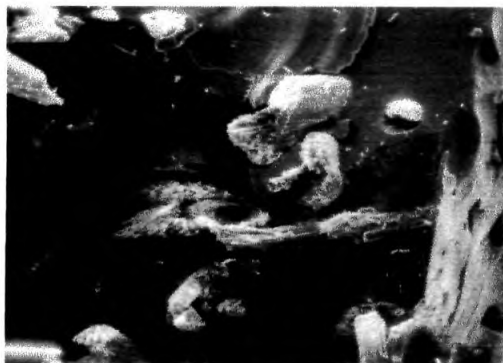


Figure 4.13 SEM of impact fracture of untreated oil palm fibre/PF composite(x50)



Figure 4.14 SEM of impact fracture of alkali treated oil palm fibre/PF composite (x100)



Figure 4.15 SEM of impact fracture of acetylated oil palm fibre/PF composite(x50)



Figure 4.16 SEM of impact fracture of KMnO₄ treated oil palm fibre/PF composite (x25)

This will lead to easy debonding of the fibres. Extra energy is needed to do the work of debonding which enhances the impact strength. Crack propagation is easier in this composite (Fig. 4.17). Liu and Kagawa investigated the basic problems involved in debonding and frictional sliding in fibre reinforced brittle matrix composites.²⁹



Figure 4.17 SEM of impact fracture of silane treated oil palm fibre/PF composite (x100)

REFERENCES

1. R. R. Warner and E. Rezai, *J. Appl. Polym. Sci.*, **65**, 1487 (1997)
2. A. K. Bledzki, S. Reihmane and J. Gassan, *J. Appl. Polym. Sci.*, **59**, 1329 (1996)
3. P. Gatenholm, H. Bertilsson and A. Mathiasson, *J. Appl. Polym. Sci.*, **49**, 197 (1993)
4. D. N. S. Hon and N. H. Ou, *J. Polym. Sci. Part A: Polym. Chem.*, **27**, 2457 (1989)
5. D. M. Blackketter, D. Upadhyaya, T. R. King and J. A. King, *Polym. Comps.*, **14**, 430 (1993)
6. C. Joly, M. Kofman and R. Gauthier, *J. M. S – Pure. Appl. Chem.*, A **33**(12), 1981 (1996)
7. P. Ghosh, D. Das and A. K. Samanta, *J. Polym. Mater.*, **12**, 297 (1995)
8. C. David, R. Fornasier, W. Lejong and N. Vanlautem, *J. Appl. Polym. Sci.*, **36**, 29 (1988)
9. D. M. Brewis, J. Comyn, J. R. Fowler, D. Briggs and V. A. Gibson, *Fib. Sci. Technol.*, **12**, 41 (1979)
10. J. A. King, D. A. Buttry and D. F. Adams, *Polym. Comps*, **14**, 292 (1993)
11. R. M. Rowell and D. I. Gutzmer, *Wood Sci.*, **7**, 240 (1975)
12. A. Hebeish, M. H. El-Rafie, M. I. Khalil and A. Bendak, *J. Appl. Polym. Sci.*, **21**, 1901 (1977)
13. M. N. Belgacem, P. Bataille and S. Sapieha, *J. Appl. Polym. Sci.*, **53**, 379 (1994)
14. J. A. King, D. A. Buttry and D. F. Adams, *Polym. Comps.*, **14**, 301 (1993)
15. M. Nitschke and J. Meichsner, *J. Appl. Polym. Sci.*, **65**, 381 (1997)

16. S. R. Wu, G. S. Sheu and S. S. Shyu, *J. Appl. Polym. Sci.*, **62**, 1347 (1996)
17. J. George, S. S. Bhagawan and S. Thomas, *Composite Interfaces*, **5**, 201 (1998)
18. K. C. M. Nair, S. M. Diwan and S. Thomas, *J. Appl. Polym. Sci.*, **60**, 1483 (1996)
19. K. Joseph, S. Thomas and C. Pavithran, *Polymer*, **37**, 5139 (1996)
20. L. A. Pothen, N. R. Neelakantan and S. Thomas, *J. Reinf. Plast. Comp.*, **16**, 744 (1997)
21. M. S. Sreekala, S. Thomas and N. R. Neelakantan, *J. Polym. Eng.*, **16**, 265 (1997)
22. D. L. Carvalho, *J. Appl. Polym. Sci.*, **65**, 1227 (1997)
23. P. Ghosh and P. K. Ganguly, *J. Appl. Polym. Sci.*, **52**, 77 (1994)
24. R. G. Raj, B. V. Kokta, G. Grouleau and C. Daneault, *Polym. Plast. Technol. Eng.*, **29**, 339 (1990)
25. H. T. Kau, *Polymer Composites*, **11**, 253 (1990)
26. B. Z. Jang, L. C. Chen, L. R. Hwang, J. E. Hawkes and R. H. Zee, *Polym. Comp.*, **11**, 144 (1990)
27. P. E. Reed and L. Bevan, *Polym. Comp.*, **14**, 286 (1993)
28. L. E. Nielsen, *Mechanical Properties of Polymers and Composites*, Vol.2, Marcel Dekker, New York (1974)
29. Yu-Fu Liu and Y. Kagawa, *Mater. Sci. Eng.*, A **212**, 75 (1996)

CHAPTER 5

Mechanical Performance of Oil Palm/Glass Hybrid Fibre Reinforced Phenol Formaldehyde Composites

*Results of this study have been submitted for publication in the journal **Composites Science and Technology***

Abstract

The effects of glass fibre loading on the performance of glass mat reinforced phenol formaldehyde resin composites were studied. Tensile strength, tensile modulus and flexural strength increase with increase in fibre loading. However elongation at break and flexural modulus are found to decrease beyond 40 wt.% fibre loading. Impact strength and the density of the composites showed similar trend. Compared to the gum sample, hardness of the composites decreased by glass fibre reinforcement. Hybrid composites were prepared from glass and oil palm empty fruit bunch (OPEFB) fibres. Hybrid effect of glass fibre and oil palm empty fruit bunch fibre on the tensile, flexural and impact response of the composites was investigated. Randomly oriented glass and OPEFB fibre mats were arranged as interlayers to enhance the hybrid effect. The overall performance of the composites improved by the glass fibre addition. Impact strength shows great enhancement by the introduction of slight amount of glass fibre. Density of the hybrid composite decreases as the volume fraction of the OPEFB fibre increases. Hardness of the composites also showed slight decrease on increased volume fraction of OPEFB fibre. Scanning electron micrographs of the fractured surfaces were taken to study the failure mechanism and fibre-matrix adhesion. The experimental results were compared with theoretical predictions. Hybrid effect of glass and OPEFB fibre was also calculated.

Hybrid composites are materials made by combining two or more different types of fibres in a common matrix. They offer a range of properties that can not be obtained with a single kind of reinforcement. By careful selection of reinforcing fibres, the material costs can be substantially reduced. Mechanical performance of composites is mainly dependent upon the properties of matrix and reinforcement and the interaction between matrix and reinforcement. Now-a-days FRP composites are used in thousands of structural applications such as aerospace, automotive parts, sports and recreation equipment, boats and office products, machineries etc. Glass fibre represents an excellent performance reinforcement for fibre reinforced plastic composites. High strength, light weight, dimensional stability, resistance to corrosion and electricity etc are major advantages of the glass reinforced composites. Glass has proven its major contributions in marine, transportation, communication, housing, chemical processing, construction industry etc. Glass fibres effectively reinforce thermoplastics as well as in thermosets. Mechanical strength of the composite is dependent upon the amount, type and arrangement of fibre within the composite. On the application basis glass is used as continuous strand mat, chopped strand mat, milled fibres and as glass flakes. Karger-Kocsis and co-workers^{1, 2} have worked on the failure behaviour of short and long glass fibres and glass mats reinforced polypropylene composites.

Addition of glass fibre to oil palm empty fruit bunch fibre reinforced PF composites will lead to improved performance qualities. Hybridisation of oil palm fibres with glass minimises water sorption and improves thermal stability of the oil palm/PF composites. Hybrid effect of the glass and oil palm fibre will improve the strength properties. The properties of the hybrid composite mainly depend upon the fibre content, length of the individual fibres, orientation, arrangement of both the fibres, extent of intermingling of the fibres and fibre to resin adhesion. Miwa et al.³ investigated the effect of fibre lengths on the mechanical performance of

hybrid composites. They found that there is optimum fibre length beyond that properties are decreased.

Now-a-days natural fibres play an important role in FRP systems since they provide good reinforcements in plastics and enhance the biodegradation of plastic systems thereby eliminating the great disposal problem of synthetic FRP's. It has been reported that glass has got good reinforcement effect along with natural fibres like sisal, jute etc.^{4,5} Oil palm empty fruit bunch fibre showed good reinforcement effects in phenolics. Mechanical property analysis of the composites based on OPEFB fibre and phenol formaldehyde resin has been reported earlier by our research group.⁶ The physical and chemical structure and properties of the OPEFB fibre have also been reported.⁷

This work establishes the mechanical performance of the glass/PF composite and glass/OPEFB fibre hybrid PF composite. Tensile properties such as tensile stress-strain behaviour, tensile strength, tensile modulus and elongation at break of the composites as a function of fibre composition were analysed. Tensile fracture mechanism of the composites were studied by scanning electron microscopy. Three point flexure properties of the composites such as flexural strength and flexural modulus were also investigated. The work of fracture of the composites was analysed as a function of relative volume fraction of fibres. Impact fracture mechanisms were studied using scanning electron microscopy. Variations in hardness and density of the composites with various fibre volume fractions were also checked. The density and void content of the composites were calculated to understand the variations in strength parameters. Finally the hybrid effects of the glass and OPEFB fibres were calculated.

5.1 TENSILE PROPERTIES

5.1.1 Tensile Stress- Strain Behaviour

Figures 5.1 and 5.2 show respectively the stress-strain behaviour of glass/PF composites and glass/OPEFB hybrid PF composites. The behaviour of neat PF

resin is also presented in Figure 5.1. The brittle nature of the resin is clear from the curves. The modulus and tensile strength of glass/PF composites become higher and larger as the glass fibre content is increased while a reverse trend is observed as the OPEFB fibre volume fraction increased in hybrid composites. Eventhough glass fibre is brittle its incorporation in PF resin reduces the composite's brittleness. The stress-strain curves of the composites show a linear behaviour at low strains followed by a significant change in slope showing a non-linear behaviour which is maintained up to complete failure of the composite. Composites with 45wt.% glass shows maximum tensile strength. Fibres and matrix behave linearly at lower strains (Fig. 5.1). The second stage of the curves leading to decrease in slope corresponds to the plastic deformation of matrix and to micro-crack initiation in matrix.

Randomly oriented fibres inhibits the crack propagation. Gradual debonding of the fibres from the matrix occurs during plastic deformation. Unstable propagation of the initiated cracks through matrix occurs and the strength decreases abruptly to an almost zero value. As the volume fraction of OPEFB fibre increased, the slope change of the stress -strain curve occurs at an early stage of deformation (Fig. 5.2). Toughness of the composite increased upon increasing the oil palm fibre reinforcement. Slight irregularities were observed due to the variations in wetting of the fibre layers. The toughness of the hybrid composites lies in between the unhybridised glass/PF and OPEFB/PF composites. This can be understood from the stress-strain curves.

5.1.2 Tensile Strength

Important tensile properties of glass and OPEFB fibre are shown in Table 2.1 (refer Chapter 2) and in Table 3.4 (refer Chapter 3) respectively. Figure 5.3 shows the variation of tensile strength with glass fibre loading in glass/PF composites. The strength linearly increases with fibre loading. Mechanical

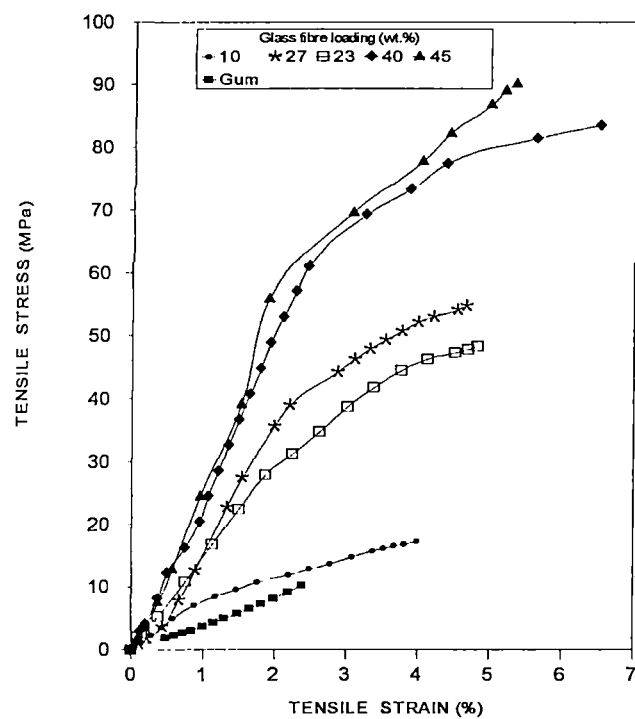


Figure 5.1 Tensile stress-strain behaviour of glass/PF composites having different glass fibre loading.

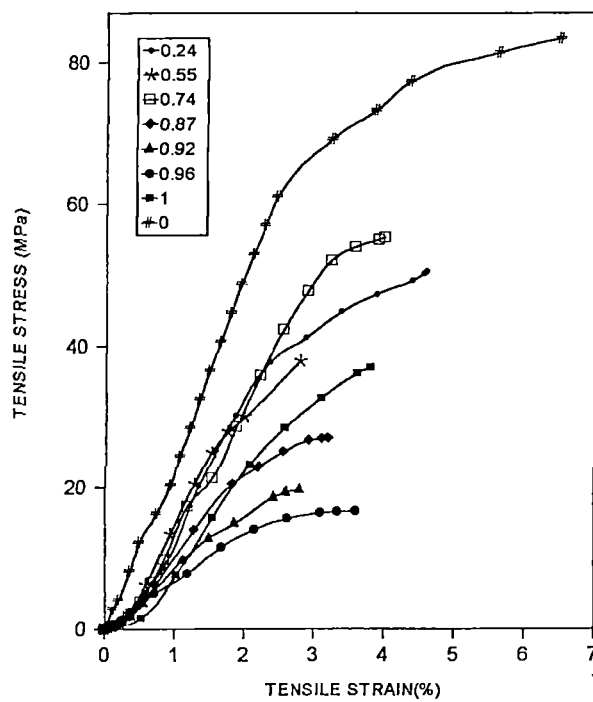


Figure 5.2 Tensile stress-strain behaviour of glass/OPEFB hybrid PF composites having different volume fractions of OPEFB fibre.

characteristics of the interfacial bond strength of glass-epoxy resin composites were reported by Koenig et al.⁸ The hybrid effect of OPEFB fibre and glass on the tensile strength of the composite having 40wt.% fibre loading is depicted in Figure 5.4. Comparatively less volume fraction of glass along with OPEFB fibre reinforcement results in composites of enhanced performance than 100% OPEFB fibre reinforced composites. Thus we can produce economically viable composites having high performance. It has been reported that glass fibre addition to sisal, jute and coir fibre filled thermoplastic as well as in thermosets improves the mechanical properties of the composites.⁹⁻¹¹ It is found that at very high OPEFB fibre loading the processing is difficult and the dispersion becomes very poor and this may be the reason for the decrease in properties at higher volume fraction of OPEFB fibre. Fibres layered out at higher loadings due to decreased interlaminar bonding. Packing defects may occur at higher loading which may reduce effective stress transfer from the matrix to the fibres. Possibility of fibre entanglement increases and uniformity in fibre dispersion decreases at higher loading. However rapid crack propagation is hindered by the interlining fibres.

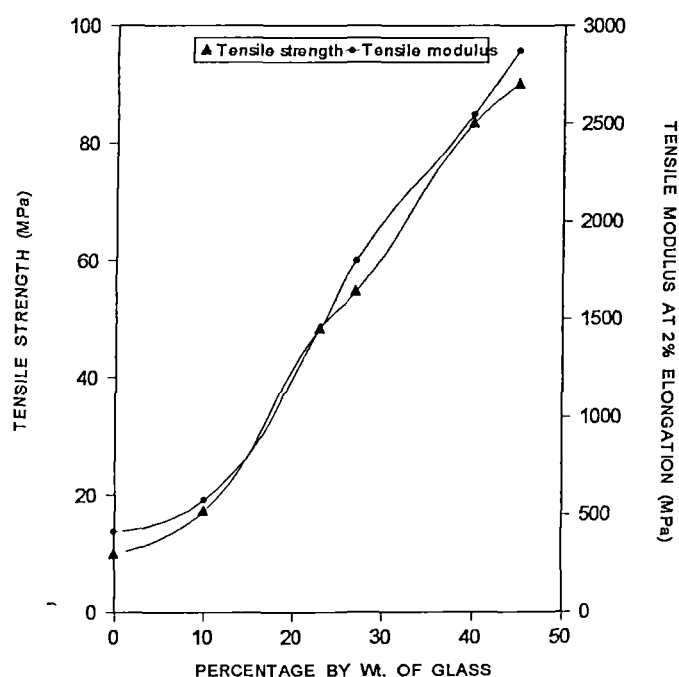


Figure 5.3 Effect of glass fibre loading on the tensile properties of glass/PF composites

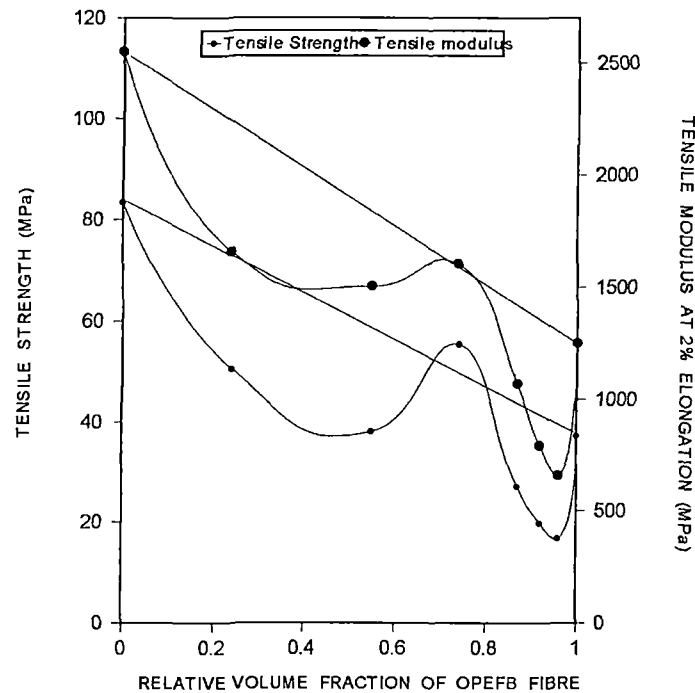


Figure 5.4 Variations in tensile properties of glass/OPEFB hybrid PF composites with relative volume fractions of glass and OPEFB fibre. (Total fibre loading of the composite = 40wt.%)

A schematic model showing the general fibre alignment in hybrid composites is given in Figure 5.5. In compression moulding the squeezing flow causes some transverse fibre orientation in the surface area which is a decisive factor in the mechanical performance of the composite. Possibility for this type of fibre orientation is decreased at higher fibre loading. Composite tensile strength slightly increases with increasing interlaminar shear strength and can be predicted by the rule of mixtures formulation. Marom et al.¹² discussed about the conditions of positive or negative deviations in hybrid effects on the mechanical properties of the composites from the rule of mixtures behaviour. The failure of the composite under tensile load is a complex, statistical process involving fibre strength characteristics, matrix and interfacial properties that determine the failure process. Zweben¹³ predicted that the introduction of high elongation fibres in a low elongation fibre composite raises the strain level required to propagate fibre breaks because the high elongation fibres behave like crack arrestors on a micromechanical level.

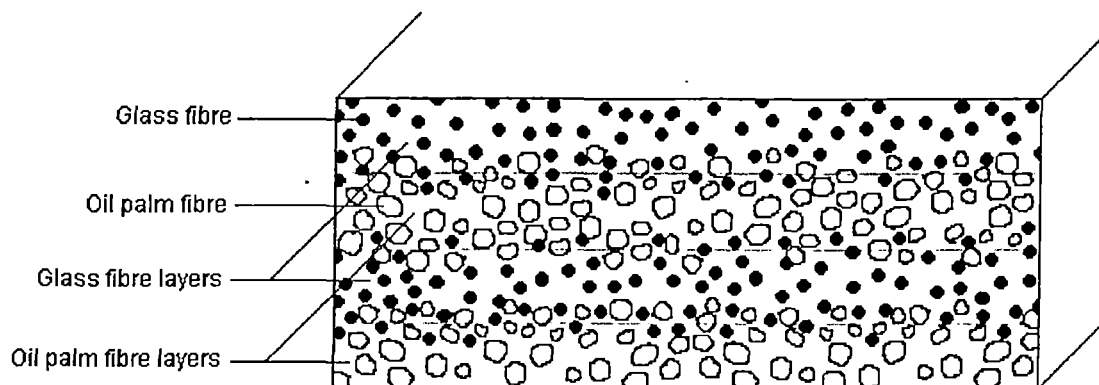


Figure 5.5 Schematic model showing the arrangement of fibre layers in hybrid composites.

5.1.3 Tensile Modulus

Tensile modulus of glass/PF composites and glass/OPEFB hybrid PF composites at 2% elongation are shown in Figure 5.3 and 5.4 respectively. Modulus values show similar trend as tensile strength in both the composites. Incorporation of 0.74 volume fraction of OPEFB fibre leads to composites having superior performance. Maximum intermingling of the fibres and higher compatibility are achieved at this volume fraction of fibres. The adhesion efficiency between the fibres and matrix determines the strength property of the composites. This is dependent upon the nature, shape and surface roughness of the reinforcing material.

5.1.4 Elongation at Break

The OPEFB fibre is highly cellulosic and shows high elongation while glass fibre has got low elongation properties. The percentage elongation at break of glass/PF composites declines after 40wt.% glass fibre loading (Fig. 5.6); upto 40wt.% fibre loading the elongation at break increases linearly. At very high fibre loading fibre agglomeration results which leads to decrease in adhesion between fibre and matrix. Easy debonding and fibre failure occur at lower strain. High elongation materials arrest the propagation of cracks in a composite on a macroscopic level.

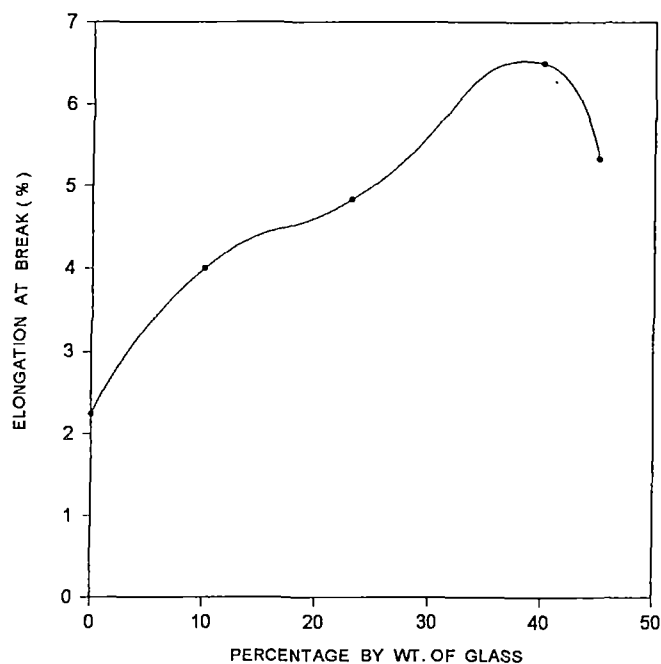


Figure 5.6 Variations in percentage elongation at break of glass/PF composites with different glass fibre loadings.

The elongation at break of the hybrid composite decreases by the presence of OPEFB fibre even though it is a high elongation fibre. This is evident from the Figure 5.7. This is due to the decreased strength of oil palm fibre compared to glass fibre. Glass being low elongating fails first and the oil palm fibre withstand the applied stress. As it is a low strength fibre catastrophic failure occurs very early than its actual extensible strain. However at 0.74 V. F. of oil palm fibre, the hybrid composite exhibits higher elongation due to the increased fibre-matrix adhesion. The hybrid composite exhibits medium elongation compared to the individual fibre reinforced composites. Brittle fracture due to glass fibre and PF resin happens preferably to oil palm fibres on tensile loading. This will lead to negative hybrid elongation effect of the composites.

5.1.5 Tensile Fracture Mechanism

Scanning electron micrographs of the tensile fractured surfaces of the composites were taken to understand the fracture mechanism. Figure 5.8(a & b) shows the

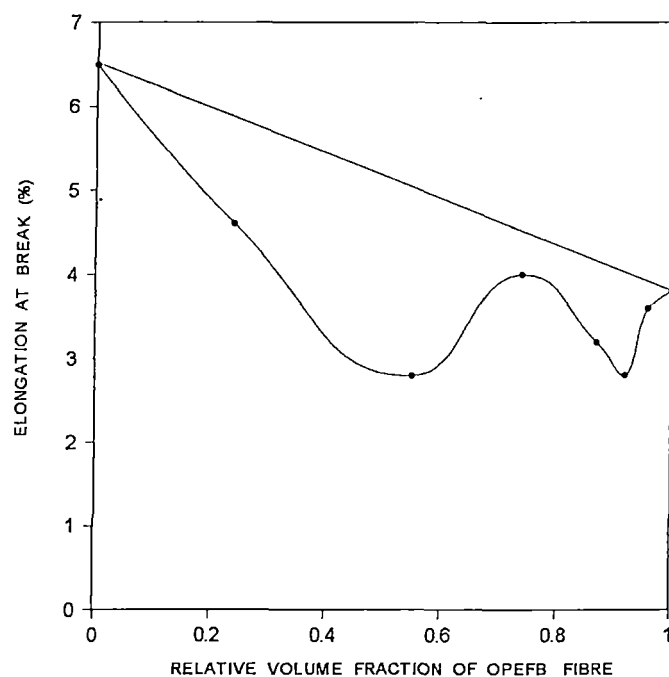


Figure 5.7 Variations in percentage elongation at break of glass/OPEFB hybrid PF composites with relative volume fractions of glass and OPEFB fibre.

fractographs of the glass/PF composites having 10 and 40wt.% fibre loadings respectively. Mainly the fibre breakage is observed. This implies the strong adhesion between the fibre and matrix. Figure 5.9 shows optical photograph of the tensile fracture surface of the composite. Crack propagation is clear from the photograph. The non uniformity in fibre dispersion is observed in the photograph. The strength of the composites is governed by the control of flow initiation characteristics. When a microcrack is initiated it propagates through the matrix and when it arrives at an interface it continues along the interface upto fracture of the fibre. After the fibre fracture, the crack propagates again into the matrix, then follows the next interface and so on upto complete fracture. The growth of microcracks which produces sharp stress gradients are influenced by the shape and orientation of reinforcements. Randomly oriented short fibres account for the better resistance to fracture. Figure 5.10 (a and b) show the fracture surfaces of hybrid composites under different magnifications. Layering out of the fibres can be seen from Figure 5.10a. Fibre breakage and short fibre pullout are also observed. This is responsible for the decline of their fracture resistance.

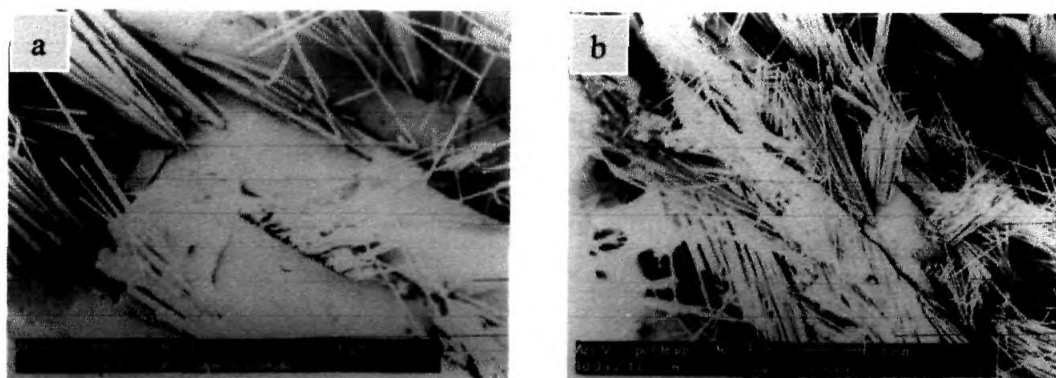


Figure 5.8 Scanning electron micrographs of tensile fractured surfaces of glass/PF composites (a) Fibre loading 10 wt.% (b) Fibre loading 40wt.%

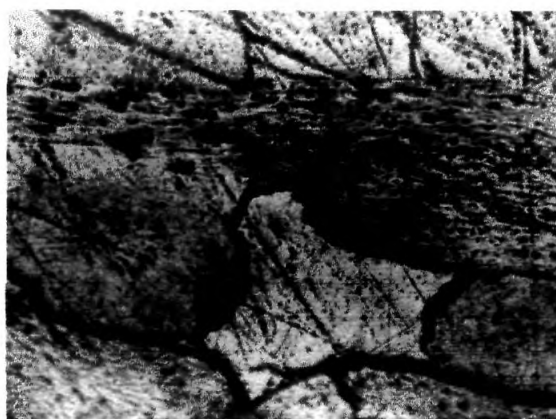


Figure 5.9 Optical photograph of tensile failed portion of oil palm fibre/PF composite (x50).

Fracture mechanisms like matrix cracking and fibre-matrix debonding are clear from Figure 5.10b. The photograph of tensile failure surfaces of the glass/PF and glass/OPEFB hybrid PF composites having 40wt.% fibre loadings are shown in Figure 5.11. The brittle nature of the glass is understood from the breakage mode. In hybrid composites, glass fibre show large extent of pullouts resulting from the low interaction with the oil palm fibre and PF matrix. Many scientists have investigated the fibre fracture behaviour in hybrid composite systems.¹⁴⁻¹⁷ Fracture is of elastic-plastic nature in hybrid composites.

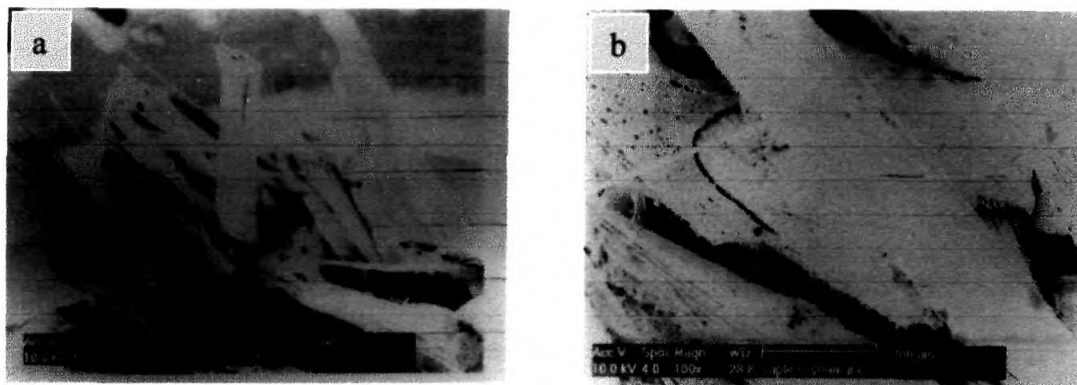


Figure 5.10 Scanning electron micrographs of tensile fractured surfaces of glass/OPEFB hybrid PF composite under different magnifications (a) x 20 (b) x 100.

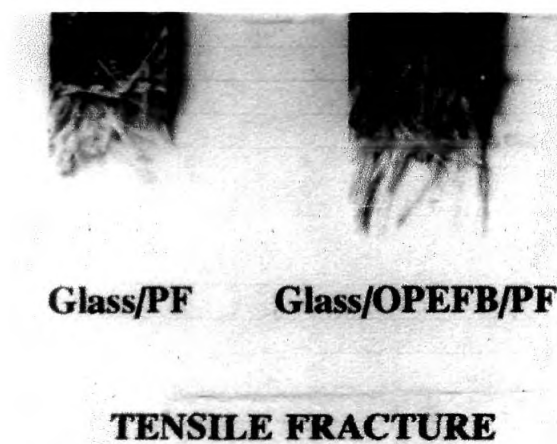


Figure 5.11 Photograph of tensile fracture of glass/PF and glass/Oil palm hybrid PF composites (x 5)

5.2 FLEXURAL PROPERTIES

5.2.1 Flexural Stress-Strain Behaviour

Figures 5.12 and 5.13 show flexural stress-strain characteristics of glass/PF composites and glass/OPEFB hybrid PF composites respectively. Almost linear deformation is observed for glass/PF composites (Fig. 5.12) except for 10wt.% glass fibre loading in which case a slope change is seen. The increasing deflection brings on matrix rupture progressively, resulting in fracture and pull out of fibres leading to a more or less regular decrease of strength.

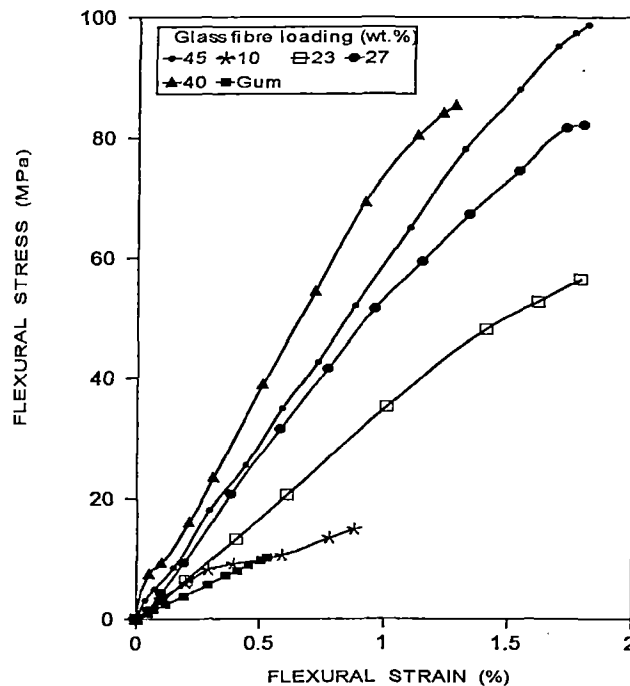


Figure 5.12 Flexural stress-strain behaviour of glass/PF composites having different glass fibre loading

The hybrid composites show linear deformation followed by a domain with decreasing slope characterised by crack initiation. The stiffness of the composite shows its highest value in composite having highest glass fibre reinforcement and is readily understood from the stress-strain curves (Fig. 5.13). The crack propagates through the matrix. The non-cracked matrix and fibres with stand the total fracture of the test specimen. Fibre distribution and orientation greatly influence the crack propagation. The flexural strain increases as the oil palm fibre volume fraction in the composite increases.

5.2.2 Flexural Strength

Flexural strength of the glass/PF composites and glass/OPEFB hybrid PF composites are given in Figure 5.14 and 5.15. The flexural strength increases as the fibre loading increases in glass/PF composites. Flexural strength is a combination of the tensile and compressive strengths which directly varies with the interlaminar shear strength.

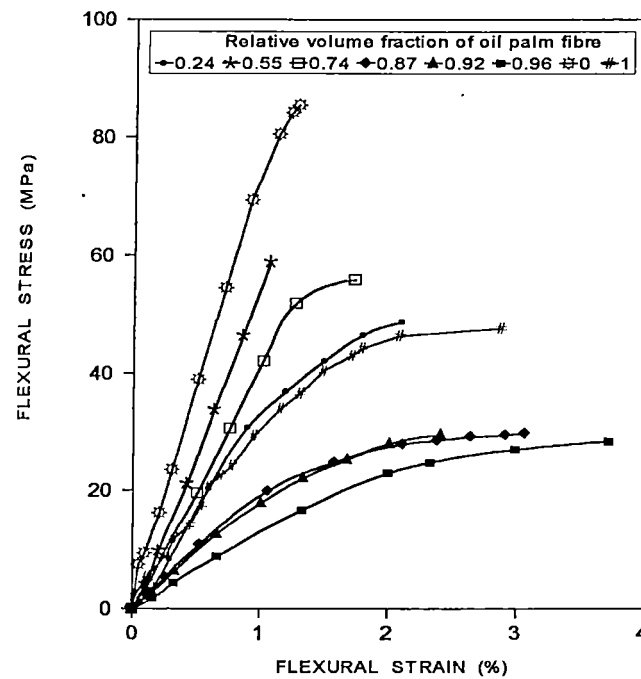


Figure 5.13 Flexural stress-strain behaviour of glass/OPEFB hybrid PF composites having different relative volume fractions of OPEFB fibre.

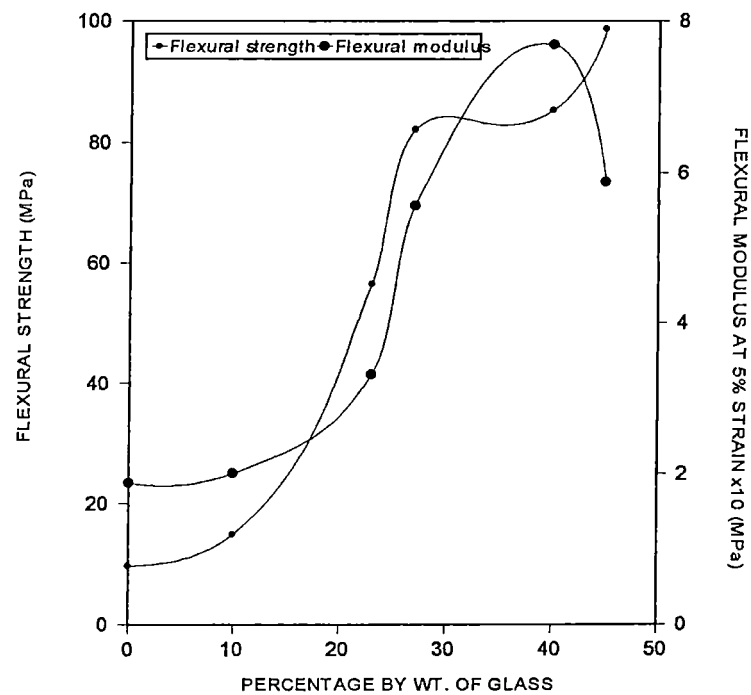


Figure 5.14 Effect of glass fibre loading on the flexural properties of glass/PF composites

Variation of flexural strength upon hybridisation of glass and OPEFB fibre is shown in Figure 5.15. The incorporation of 0.53 volume fraction of OPEFB fibre leads to hybrid composites having good flexural performance.

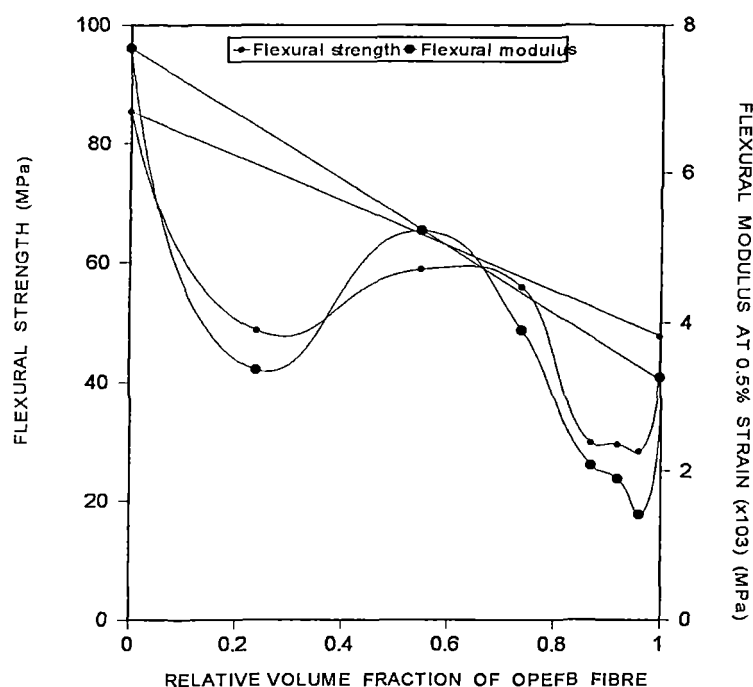


Figure 5.15 Variations in flexural properties of glass/OPEFB hybrid PF composites with relative volume fractions of glass and OPEFB fibre.

5.2.3 Flexural Modulus

Flexural modulus at 0.5% strain shows a decrease above 40wt.% glass fibre loading in glass/PF composites (Fig. 5.14). Flexural modulus of the hybrid composites shows similar trend as flexural strength. Hybridisation of lower quantities of glass fibre and OPEFB fibre (0.24 : 0.76) gives rise to composites having sufficient modulus (Fig. 5.15). Kretsis¹⁸ have made a review on the flexural properties of hybrid fibre reinforced plastics and according to the author, the flexural properties not only depend on the hybrid composition but also on the placing of the material layers. Peijs et al.¹⁹ investigated the influence of composition and adhesion level of fibre on the mechanical properties of hybrid

composites. They have reported linear variation of compressive properties with fibre composition.

5.3 IMPACT PROPERTIES

Impact resistance of a composite is the measure of total energy dissipated in the material before final failure occurs. Composite fracture toughness is affected by interlaminar and interfacial strength parameters. The interlaminar splitting and interfacial debonding act to relieve the stress concentrations at the crack tip. Thus high composite fracture toughness and high composite interlaminar properties are incompatible. The local volume fraction of the fibres and the local fibre spacing have a major role in the fracture toughness of the composites.

Figure 5.16 shows the variation of work of fracture of glass/PF composites with fibre loading. Impact strength shows its highest value at 40wt.% loading. The neat PF sample shows very low impact strength. A linear enhancement in impact strength is observed by the glass fibre addition upto 40wt.% fibre loading. At lower loading, (<40wt.%) fibres are found embedded in the matrix and hence fibre breakage and fibre pull-out occur on application of a sudden force. But at higher loadings fibre to fibre contact increases and fibre breakage will be the predominant failure mechanism. The inter fibre interaction decreases the effective stress transfer between the fibre and matrix. This contributes to a decrease in impact properties at higher fibre loadings.

When glass fibre is combined with OPEFB fibre, the work of fracture is considerably improved. This can be seen from Figure 5.17. By the addition of small amount of glass fibre, the impact performance of the OPEFB/PF composite has increased by above 100%. The maximum impact strength is observed for hybrid composites having 0.74 volume fraction of OPEFB fibre. The value is higher than glass/PF composites. Peijs and co-workers²⁰ have found that hybridisation of polyethylene fibres with carbon fibres resulted in composites

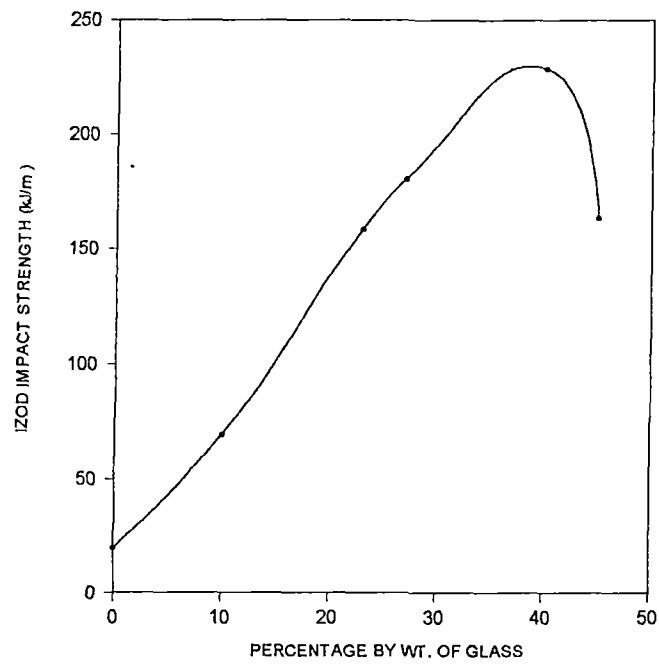


Figure 5.16 Izod impact strength versus glass fibre loading for glass/PF composites.

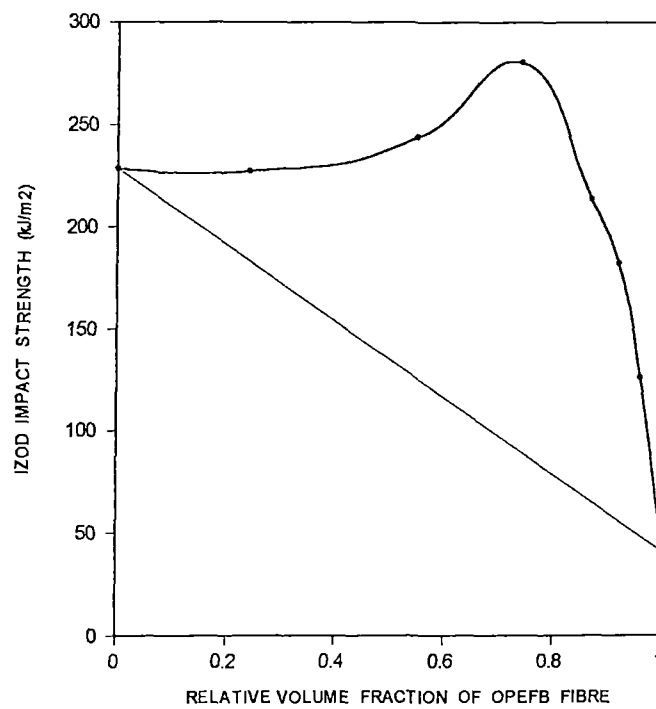


Figure 5.17 Izod impact strength versus OPEFB fibre volume fractions for glass/OPEFB hybrid PF composites.

having higher impact resistance than thicker and heavier laminates constructed entirely of carbon/epoxy. The fibres play an important role in the impact resistance of the composites as they interact with the crack formation in the matrix and acts as stress transferring medium. Many works have reported on the impact behaviour and factors affecting the impact strength of laminated composite materials.²¹⁻²³

5.3.1 Impact Fracture Mechanism

Impact fracture of composites could be a combination of fibre pull out and fibre breakage. The impact fractured portions of the composites were viewed under the scanning electron microscope. Figure 5.18(a & b) is the scanning electron micrograph of the impact failure surfaces of glass/PF composites having 10 and 40wt.% fibre loading.

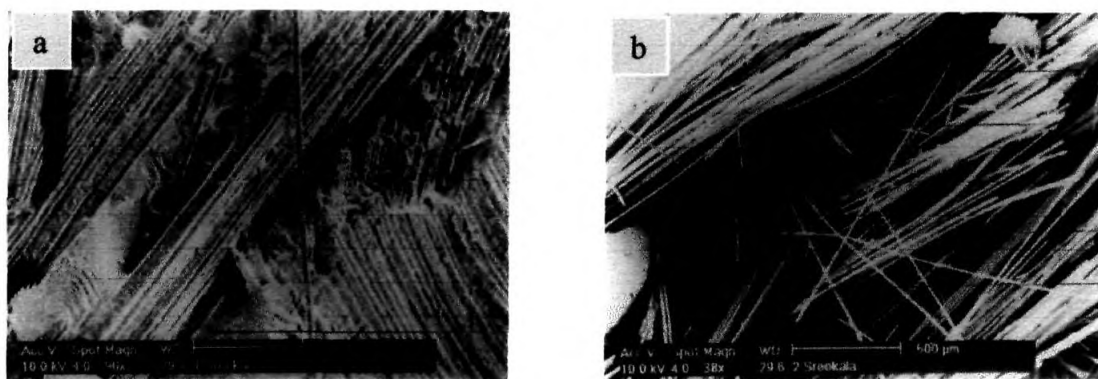


Figure 5.18 Scanning electron micrographs of impact fractured surfaces of glass/ PF composites (a) fibre loading 10wt.% (b) fibre loading 40wt.%

At low fibre loading fibre pullout paths are visible. Fibre-matrix interfacial failure is evident from the Figure 5.18a. Pulled out fibres are visible in Figure 5.18b. The fibre crowding leads to easy debonding at higher loading which increase the impact resistance. The difference in the impact failure of glass and OPEFB fibre can be seen from the impact fractography of the hybrid composite (Fig. 5.19). Oil palm fibre debonding and pull out occur as seen from the photograph.



Figure 5.19 Scanning electron micrograph of impact fractured surface of glass/OPEFB hybrid PF composite.

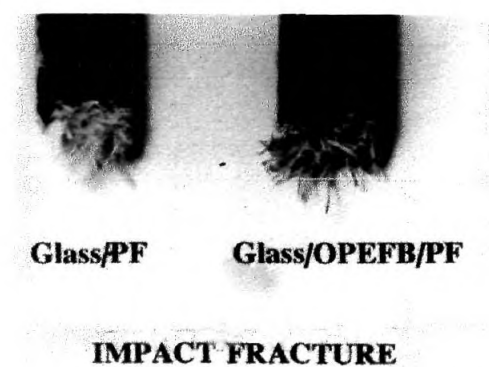


Figure 5.20 Photograph of impact fracture of glass/PF and glass/OPEFB hybrid PF composites (Magnifications x 5)

Decreased adhesion between the glass fibre and the matrix is evident from the surface morphology of the pulled out glass fibres. Oil palm fibre is more compatible to PF resin than glass fibre. Oil palm fibre breakage is also observed. Figure 5.20 is a photograph of fractured portions showing failure mode of impact tested composite samples. Brittle failure of glass fibres on the surface layers is observed. Compared to oil palm fibres, glass fibres show high pull out showing the decreased interaction with the matrix.

5.4 HARDNESS, DENSITY AND VOID FORMATION

Hardness and density of the composites are interrelated. The values are given in Table 5.1. Phenol formaldehyde itself is very hard and brittle. Reinforcement decreases its hardness. The oil palm fibre reinforcement decreases the value by 15 units. Density of glass is much higher than oil palm fibre (Table 2.1). Density of composites also shows the same trend. In the case of glass reinforced PF composites, as the glass fibre loading increases the density of the composites increases and reaches a maximum at 40wt.% fibre loading. At much higher fibre loadings (>40wt.%) the processing may be difficult due to fibre agglomeration leading to void formation inside the composite. That will affect the composite performance and decreases the density. Bowles and Colleagues²⁴ investigated the effect of voids on the interlaminar properties of graphite fibre reinforced

composites. The density of the hybrid composite decreases as the quantity of OPEFB fibre increases. By 100% OPEFB fibre reinforcement, the density became the lowest. Thus the weight of the composite can be considerably reduced by oil palm fibre reinforcement.

Theoretical density of the composites was calculated according to the following ASTM equation

$$Td = \frac{100}{\left[\frac{R}{D} + \frac{r1}{d1} + \frac{r2}{d2} \right]} \quad (5.1)$$

where T is the theoretical density R, r₁ and r₂ represent resin, glass fibre and oil palm fibre wt.% respectively. D, d₁ and d₂ denote densities of resin, glass and oil palm fibre. The values are given in Table 5.1.

Table 5.1 Hardness and Density Values of Glass/PF and Glass/OPEFB Hybrid PF Composites (Total Fibre Loading = 40wt.%)

Composite	Composition	Hardness ShoreD- units	Density Experimental (g/cc)	Density Theoretical (g/cc)	Void Content Theoretical (vol. %)
Glass/PF	Glass wt. %				
	10	90	1.34	1.27	0
	23	94	1.36	1.37	0.73
	27	92	1.37	1.40	2.14
	40	92	1.48	1.52	2.63
	45	80	1.35	1.57	14.01
	Gum	>95	1.33	1.20	0
Glass/OPEFB/PF	OPEFB(V.F)				
	0	92	1.48	1.52	2.63
	0.24	90	1.45	1.50	3.33
	0.55	85	1.37	1.37	0
	0.74	86	1.27	1.25	0
	0.87	82	1.30	1.16	0
	0.92	83	1.19	1.12	0
	0.96	82	1.20	1.08	0
	1	80	1.03	1.06	2.83

Except for 10wt.% of glass fibre loadings, the experimental density values of glass/PF composites are lower than the theoretically predicated values. This points out the possibility of having voids in the composites. Efficient packing and high extent of interfacial adhesion may be the reason for higher density value of 10wt.% glass/PF composites. In the case of gum samples, the density is greatly affected by the moulding temperature, moulding time and thereby the extent of crosslinking. Thus the density may vary according to these parameters. Theoretical void content of the composites are given in Table 5.1.

The void content is calculated using the equation

$$V = 100 (T_d - M_d)/T_d \quad (5.2)$$

where T_d is given by theoretical composite density, M_d measured composite density and V the void content in volume percent. Composites at higher fibre loadings exhibit voids. Voids in polymer composites is largely attributed to the processing effect which may arise from various sources such as volatiles arising during cure of the resin, residual solvents or from entrapped air. Shrinkage during curing of the resin and the cooling rate play important role in void formation. Presence of void is detrimental to the mechanical properties of the composites. Glass/PF composites at higher loadings exhibit voids (Table 5.1). The effects of fibre content and fibre length on void formation in short fibre thermoplastic composites were investigated by Vaxman et al.²⁵ Processing of the composite becomes difficult at higher fibre loadings. The fracture surfaces of the composite (Figs. 5.8, 5.10 and 5.19) show microvoids in the matrix and at the fibre ends. A decrease in density is observed with increase in fibre volume fraction of OPEFB fibre in hybrid composites and may be due to the decreased density of the fibres. Scanning electron micrograph of tensile fracture of the hybrid composites (Fig. 5.10b) shows cavities around the fibres. This is due to the poor fibre-matrix adhesion. Such cavities at the fibre-matrix interfaces contribute slightly to the void level in the composites. This will adversely affect the composite properties.

Akay and Regan²⁶ investigated the generation of voids in fibre reinforced composites. Hybridisation decreases the void content considerably.

REFERENCES

1. J. Karger-Kocsis, T. Harmia and T. Czigany, *Comp. Sci. Technol.*, **54**, 287 (1995)
2. J. Karger-Kocsis, *Comp. Sci. Technol.*, **48**, 273 (1993)
3. M. Miwa and N. Horiba., *J. Mat. Sci.*, **29**, 973 (1994)
4. C. Pavithran, P. S. Mukherjee, M. Brahmakumar and A. D. Domodaran., *J. Mat. Sci.*, **26**, 455 (1991)
5. R. Mohan, Kishore, M. K. Shridhar and R. M. V. G. K. Rao, *J. Mat. Sci. Lett.*, **2**, 99 (1983)
6. M. S. Sreekala, S. Thomas and N. R. Neelakantan, *J. Polym. Eng.*, **16**, 265 (1997)
7. M. S. Sreekala, M. G. Kumaran and S. Thomas., *J. Appl. Polym. Sci.*, **66**, 821 (1997)
8. J. L. Koenig and H. Emadipour, *Polym. comp.*, **6**, 142 (1985)
9. G. Kalaprasad, K. Joseph and S. Thomas., *J. Comp. Mat.*, **31**, 509 (1997)
10. C. Pavithran, P. S. Mukherjee and M. Brahmakumar., *J. Rein. Plast. comp.*, **10**, 91 (1991)
11. I. K. Varma, S. R. Anatha Krishnan and S. Krishnamoorthy., *Composites.*, **20**, 383 (1989)
12. G. Marom, S. Fischer, F. R. Tuler and H. D. Wagner., *J. Mat. Sci.*, **13**, 1419 (1978)
13. C. Zweben, *J. Mat. Sci.*, **12**, 1325 (1977)
14. K. D. Jones and A. T. DiBboendetto, *Comp. Sci. Techn.*, **51**, 53 (1994)
15. J. Karger-Kocsis, *J. Polym. Eng.*, **11**, 153 (1992)
16. M. A. French and G. Pritchard, *Comp. Sci. Techn.*, **47**, 217 (1993)
17. N. L. Hancox (Ed), Fibre Composite hybrid materials, *Applied Science Publishers Ltd.*, London (1981)
18. G. Kretsis, *Composites*, **18**, 13 (1987)
19. A. A. J. M. Peijs, P. Catsman, L. E. Govaert and P. J. Lemstra, *Composites*, **21**, 513 (1990).
20. A. A. J. M. Peijs, R. W. Venderbosch and P. J. Lemstra, *Composites*, **21**, 522 (1990)
21. J. Jang and Sung-In Moon, *Polym. Comp.*, **16**, 325 (1995)

22. P. E. Reed and L. Bevan, *Polym. comp.*, **14**, 286 (1993)
23. N. Sela and O. Ishai, *Composites*, **20**, 423 (1989)
24. K. J. Bowles and S. Frimpong, *J. Comp. Mater.*, **26**, 1487 (1992).
25. A. Vaxman, M. Narkis, A. Siegmann and S. Kenig, *Polym. Comp.*, **10**, 449 (1989)
26. M. A. Kay and D. F. O. Regan, *Plast. Rubb. Comp. Proc. Appl.*, **24**, 97 (1995)

CHAPTER 6

Stress Relaxation Behaviour of Oil Palm Fibres and Composites Based on Short Oil Palm Fibre and Phenol Formaldehyde Resin

*Results of this study have been submitted for publication in the journals **Composites Science and Technology** & **Journal of Applied Polymer Science***

Abstract

Tensile stress relaxation behaviour of individual oil palm empty fruit bunch fibre was investigated. The effects due to fibre surface modifications, physical ageing and strain level on the relaxation behaviour of the fibre were analysed. Stress relaxation of the fibres was reduced considerably with surface treatments like latex modification due to the physical interaction between the fibre surface and latex particles. Water ageing and thermal ageing reduced the relaxation rate of the oil palm fibre. It was found that the rate of relaxation of the fibre was maximum at 10% strain level. The relaxation in short oil palm empty fruit bunch fibre reinforced phenol formaldehyde composites as a function of fibre loading, fibre treatment, physical ageing and strain level was studied. Maximum stress relaxation was observed for 30wt.% fibre loading. Treated composites showed higher relaxation except in alkali and toluene 2, 4-diisocyanate treated composites. Water ageing increased the rate of relaxation. Effect of hybridisation of oil palm fibres with glass fibres on the relaxation behaviour was examined. The stress relaxation rate of the composite was lowered upon hybridisation. Rate of relaxation for different time intervals and crossover time was calculated in order to explain the relaxation mode of the fibres and composites. Master stress relaxation curves were drawn to explain the long-term behaviour of fibres and composites by superimposing the stress values at different strains by a horizontal shift along the logarithmic time axis. The relaxation modulus values for the fibre and composite show similar trend as in the case of relaxation of stress in composites.

Demand for fibre reinforced plastic composites in static and dynamic applications as structural materials particularly in automobile industry has increased as they demonstrate increased mechanical performance along with structural reduction. The long term mechanical behaviour of the composites receives much importance. This necessitates a kind of accelerated mechanical testing of the materials. Stress relaxation and creep are the two widely accepted test methods for predicting the long term mechanical performance of the composites. Knowledge of the stress relaxation behaviour of composites enables us to predict the dimensional stability of load bearing structures and the retention of clamping force for bolts fastened to composites.

Sullivan and co-workers¹ reported the various aspects of viscoelastic behaviour of a series of resin/composite systems. They demonstrated that the viscoelastic behaviour of composites and corresponding resins have a number of important characteristics in common to reveal the universal aspects of composite viscoelastic behaviour. Various aspects of polymer viscoelasticity were explained using different models by Ferry.² The influence of carbon black on stress relaxation behaviour of the black filled rubber vulcanizates at moderate strains was reported by MacKenzie et al.³ The effect of thermoplastic modifiers on the viscoelastic behaviour of the composites was studied by Tsotsis.⁴ Stress relaxation behaviour of polypropylene at elevated temperatures at different strain rates was investigated.⁵ The strain rate and temperature change the tension loading behaviour as well as the stress relaxation properties of the polypropylene specimens. The relaxation behaviour of isotactic polypropylene was strongly influenced by crystallinity and morphology of the system.⁶ The effects of volume changes on tension and compression on the corresponding stress relaxation behaviour of polycarbonate were reported.⁷ Both the relaxation modulus and volume changes are found to be time dependent.

Studies have been reported on the stress relaxation behaviour of short cellulose fibre reinforced natural rubber composites and the properties were found to be dependent on the rubber-fibre adhesion in the composite.⁸ Recently Thomas

et al.⁹⁻¹¹ reported stress relaxation studies on NR/PS blends, short sisal fibre reinforced natural rubber composites and short pineapple leaf fibre reinforced polyethylene composites. It was found that orientation of the fibres, fibre-matrix interaction and fibre loading influence the relaxation mechanism.

The tensile stress relaxation mechanism of short fibre reinforced plastic composites are much complicated owing to its physico-chemical variations within the systems at long durations. The long term and short-term mechanical performance of the composite depend on the interface properties. The stress transferring ability of a short fibre composite is dependent on the fibre length distribution, complicated non-uniform bulk distribution of the fibres and on complicated orientation of the fibres. As stress is applied to the composite there is possibility for matrix-fibre delamination, fibre breakage and destruction of matrix interlayers between the fibres. At fixed strain level, relaxation in stress may occur due to the molecular level rearrangements, fibre alignments, decreased fibre-matrix bonding etc. The stress transfer ability of the fibre is dependent on the texture and structure of the fibre. The relaxation processes that may occur in a fibre reinforced polymer composite is represented in a schematic model which is given in Figure 6.1. Bond breakage or rearrangement can occur which will lead to a stress relaxation in the composite. Moreover the chain segments can be more orderly arranged during relaxation which increases the crystallinity of the system. The major relaxation in a fibrous composite arises from the changes in the alignment of fibres within the matrix. In a randomly oriented composite the fibres become more oriented in the stretching direction during relaxation. This leads to changes in the fibre-matrix interaction that affects the stress relaxation in the composite. The percentage of amorphous and crystalline components of natural fibre is a determining factor in the mechanical behaviour of natural fibre reinforced plastic composites. Fibre surface modifications lead to changes in the physical and chemical structure of the fibres. This will affect the performance of the fibre and interface properties of the composite. The intrinsic relaxation behaviour of the natural fibre plays a major role in the stress relaxation of these composites.

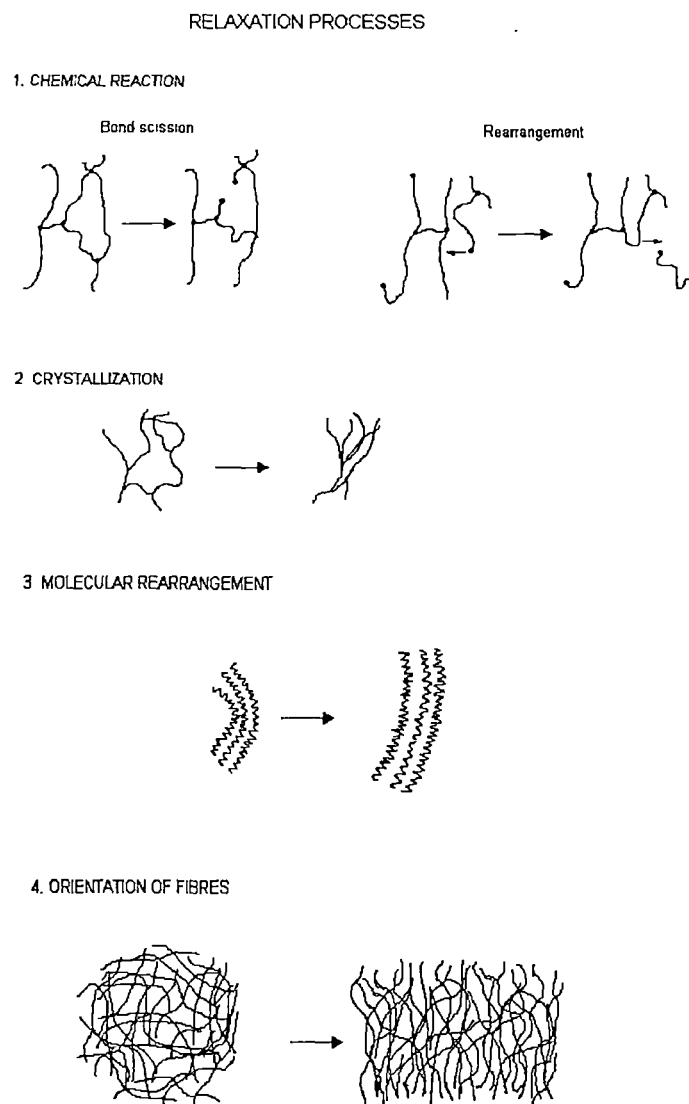


Figure 6.1 Various relaxation processes occurring in a fibrous composite.

Therefore a detailed study on the tensile stress relaxation of the oil palm empty fruit bunch fibre is presented. Changes in relaxation of the fibre upon various fibre modifications and on physical ageing were investigated. Relaxation of the fibre as a function of strain level was also investigated. The stress relaxation behaviour of oil palm empty fruit bunch fibre reinforced phenol formaldehyde composites has been studied in detail. Changes in the relaxation mechanism with fibre content were

analysed. Variations in relaxation of treated composites were also examined. Studies on the influence of environmental effects on composite relaxation mechanism were carried out. Hybrid composites were prepared by incorporating glass fibres along with oil palm fibres. Studies on stress relaxation in these hybrid composites have been made. Relaxation mechanism as a function of strain level was analysed. The rate of relaxation at different time intervals was calculated in order to explain the gradual changes in the relaxation mechanisms. At a given strain level the complete viscoelastic properties is certainly not covered. Therefore the stress relaxation data obtained at different strain levels have been superimposed by a horizontal translation along the logarithmic time axis.

6.1 STRESS RELAXATION BEHAVIOUR IN OIL PALM EMPTY FRUIT BUNCH FIBRE

6.1.1 Effect of Fibre Treatments

The physical and chemical modifications that occurred on the oil palm fibre surface on various treatments were discussed in chapter 4. In order to understand the behaviour of the fibres on static loading, stress relaxation studies of the fibres become necessary. Influence of fibre structure on the stress relaxation behaviour of polyethylene fibres was studied by Grubb et al.¹² Stress relaxation of polyethylene fibre occurs above room temperature and is associated with the crystalline α relaxation. Treated and untreated oil palm empty fruit bunch fibres were subjected to uniaxial tension up to 50% strain level. The variations in relaxation mechanism were clear from the σ_t/σ_0 Vs log time plot (Figure 6.2). The changes in the relaxation directly dependent on the modifications happened to the fibres. The oil palm fibre is lignocellulosic having 65% cellulose, 19% lignin and 2% ash content (Table 3.1, refer Chapter 3). The structure and properties of these fibres were extensively studied and reported elsewhere.¹³ Oil palm fibre has a firmly bound structure by three-dimensional linkage of crystalline cellulose in lignin bound together by waxy materials. Fibres are composed of fibrils held together by non-cellulosic substances. Application of stress may lead to failure processes such

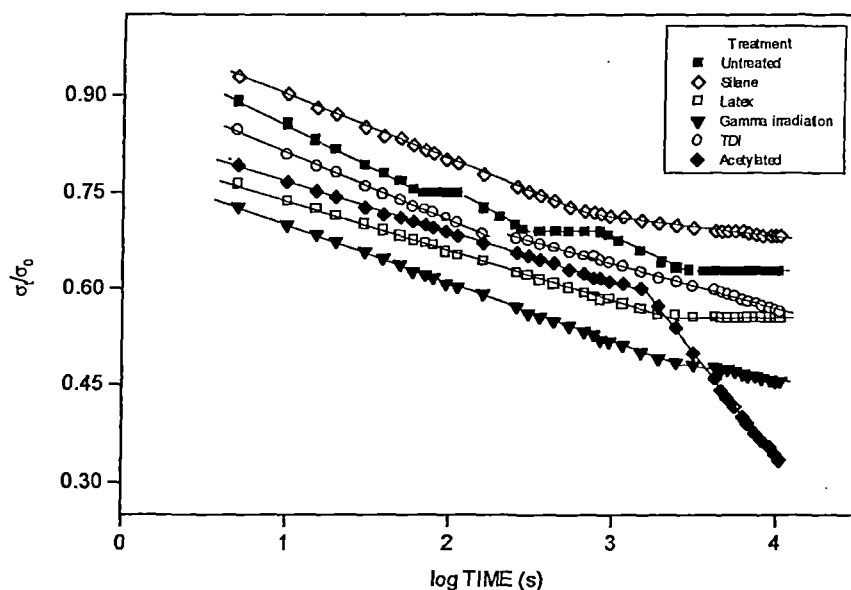


Figure 6.2 Stress relaxation curves of untreated and treated oil palm empty fruit bunch fibres at 10% strain.

as slipping out of fibrils, disruption of the chemical structure, decohesion of cells, rupture of cell walls etc. Propagation of these failures at constant strain determines the relaxation pattern. It is reported that radiation crosslinking restricts the molecular motion thereby reducing the relaxation time of ultra high molecular weight linear polyethylene.¹⁴ Slight irregularities are observed in the stress decay for the fibres (Fig.6.2). The fibre undergoes different relaxation mechanism during stress relaxation.

The crossover from one mechanism to another is evident from the changes in the slope of the relaxation curves and from crossover times (Table 6.1). Except silane treated fibres, all other treated fibres exhibit three steps in relaxation curves. Silane treatment shows a two step mechanism. The change over from first slope to second slope in treated fibres may be due to sudden failure of the cellular skeleton. At this time a change over takes place. Further changes in slope observed may be due to gradual rupture of the bound structure of the fibres. Silane and latex treated fibre shows almost constant stress values at longer duration. This may be due to the reorganised structure of the fibre after the initial stress decay. But in all other cases

Table 6.1 Crossover Time of Oil Palm Fibres during Stress Relaxation

Oil palm fibre	Cross-over time : log Time (s)				
	1 st	2 nd	3 rd	4 th	5 th
Untreated (Strain level 10%)	1.80	2.05	2.45	2.94	3.45
Silane (Strain level 10%)	2.88	----	----	----	----
Latex (Strain level 10%)	3.42	----	----	----	----
γ ray irradiation (Strain level 10%)	3.42	----	----	----	----
TDI (Strain level 10%)	2.3	----	----	----	----
Acetylated (Strain level 10%)	3.14	----	----	----	----
Thermal aged (Strain level 10%)	2.22	3.66	----	----	----
Water aged (Strain level 10%)	2.13	3.27	----	----	----
Untreated (Strain level 3%)	3.27	----	----	----	----
Untreated (Strain level 17%)	3.60	----	----	----	----

the stress goes on decreasing. The physical and structural failure of the fibre may advance for longer duration. Untreated fibre shows a six-step relaxation curve. The failure of the fibre is taking place at different stages. It is mainly due to the rearrangements and breakage of the crystalline cellular network. The cellular network is joined together by amorphous waxy and gummy materials. These amorphous components restrict the deformation of network. However, the stress decreases slightly at stretched condition and sometimes the value remains constant due to very slow relaxation process. At longer durations the stress decay will be too rapid to hinder it by the binding materials. These processes lead to different steps in stress relaxation.

The crossover time at each change in mechanism is given in Table 6.1. Compared to treated fibres the mechanism changes at shorter times in untreated

fibre; comparatively higher crossover time is observed in treated fibres. The relaxation of untreated fibre is much complex due to the presence of impurities, waxy materials etc. These will be eliminated upon fibre treatments. Amorphous component of the fibre gives major contribution to the relaxation. This is evident from the higher initial crossover time in treated fibres. The changes in mechanism of the treated fibre at higher times are attributed to the changes in the chemical structure of the fibres. Figure 6.3 shows the relaxation modulus of the fibres. A similar trend as the stress relaxation is observed in this case.

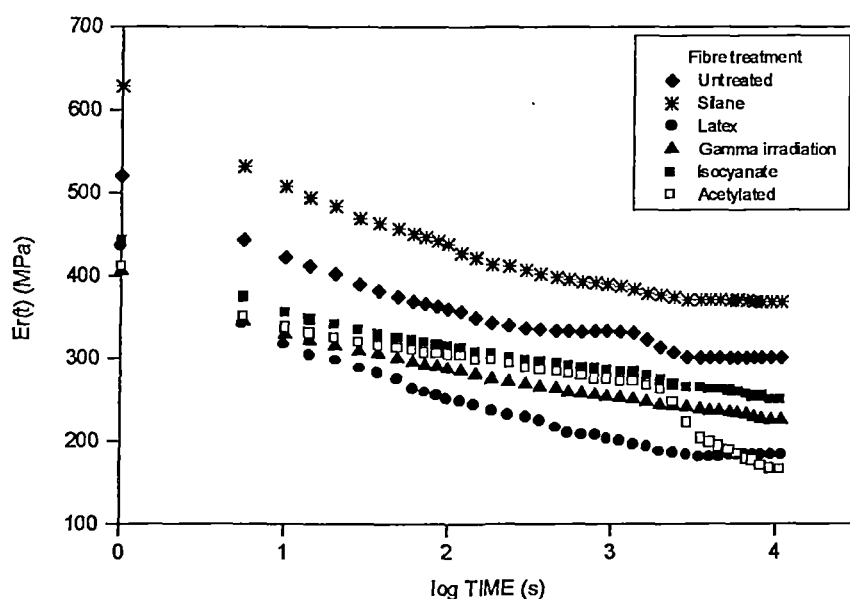


Figure 6.3 Modulus relaxation curves of untreated and treated oil palm empty fruit bunch fibres at 10% strain.

The rate of relaxation of the fibres at successive time spans are calculated and recorded in Table 6.2. The untreated, silane modified, latex coated and γ ray irradiated fibres show a gradual increase followed by decline in the rate of relaxation. Initially, the rate will be low due to the slight rearrangement in the crystalline region. As the time proceeds the weak primary cell wall will break and the regular ordered structure will be perturbed. This increases the rate of relaxation. The alignment of this disrupted structure again takes place at longer duration. This will be at slow rate. The irregular rate is observed for TDI treated and acetylated

fibres. Exceptionally high relaxation is observed for acetylated fibre at longer time. Chemical treatments especially acetylation removes the amorphous component of the fibre by bleaching. On acetylation the fibre became hard and brittle. At a stretched condition possibility of catastrophic brittle failure within the cellular network of the fibre is possible which relaxes the stress considerably at a particular time. An unexpected sudden failure within the cellular network can lead to very high relaxation rate.

Table 6.2 Rate of Stress Relaxation (%) in Untreated and Treated Oil Palm Empty Fruit Bunch Fibres at 10% Strain

Range(s)	Untreated	Silane	Latex	γ irradiation	TDI	Acetylated
1-10 ¹	3.79	3.35	3.01	4.14	4.84	3.74
10 ¹ -10 ²	13.18	13.61	10.25	12.82	11.79	10.57
10 ² -10 ³	11.77	11.75	9.16	12.73	9.85	10.19
10 ³ -10 ⁴	7.07	5.03	4.09	10.21	11.39	39.03

6.1.2 Effect of Physical Ageing

Thermal and moisture effects on the relaxation mechanism of the fibre were given in Figure 6.4. A three stage mechanism is observed in water aged and oven aged fibre. The initial crossover time is increased upon ageing (Table 6.1). But the relaxation is found to be decreased upon ageing. The oven aged fibre shows the lowest rate of relaxation. On thermal ageing water entrapped at the interstices of the cells may be eliminated and hence the probability dislocation decreases. Moreover the nature of the amorphous materials changes on ageing and that will not help in the fibrillation of the fibre on application of stress. This will reduce the relaxation of the fibre. In contrast on water immersion, water enters the interstices of the cells. This entrapped water affects the relaxation mechanism. The water

molecules will have a plasticizing effect. Water aged sample shows relaxation in between the unaged and oven aged samples. On ageing, the change in slope in

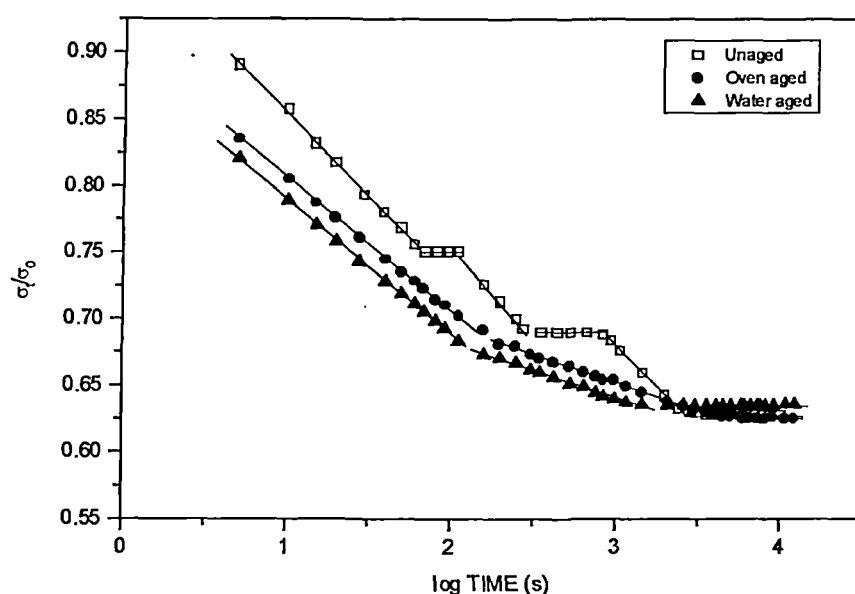


Figure 6.4 Stress relaxation curves of unaged and physically aged oil palm empty fruit bunch fibres at 10% strain.

the stress relaxation curve becomes less prominent than in unaged sample. From the rate of relaxation values we can see the decreased rates for aged fibres (Table 6.3). Initially gradual increase in rate was observed and thereafter decreases to an almost constant value.

Table 6.3 Rate of Stress Relaxation (%) in Unaged and Aged Oil Palm Empty Fruit Bunch Fibre at 10% Strain.

Range (s)	Unaged	Thermal aged	Water aged
1-10 ¹	3.79	4.67	4.26
10 ¹ -10 ²	13.18	11.18	13.09
10 ² -10 ³	11.77	8.77	6.43
10 ³ -10 ⁴	7.07	5.58	1.41

6.1.3 Effect of Strain Level

The test speed and the deformation rate will affect the failure pattern of the fibres and thereby the relaxation mechanism. The stress relaxation curves at 3, 10, and 17% strain was given in Figure 6.5. The extent of fibre failure occurred would be different at different strains. The crossover times are found to be increased at lower and higher strain levels. However, the number of steps is decreased at lower and higher strain levels than at 10% strain (Table 6.1). The major change in slope is observed for sample at 10% strain level. On application of stress, physical and chemical rearrangements may occur but on relaxation, the mechanism is purely physical. It is observed that the end relaxation is lower for 3% strain. At higher strain levels the highly fractured portions of the fibre leads to higher relaxation owing to its physical rearrangement.

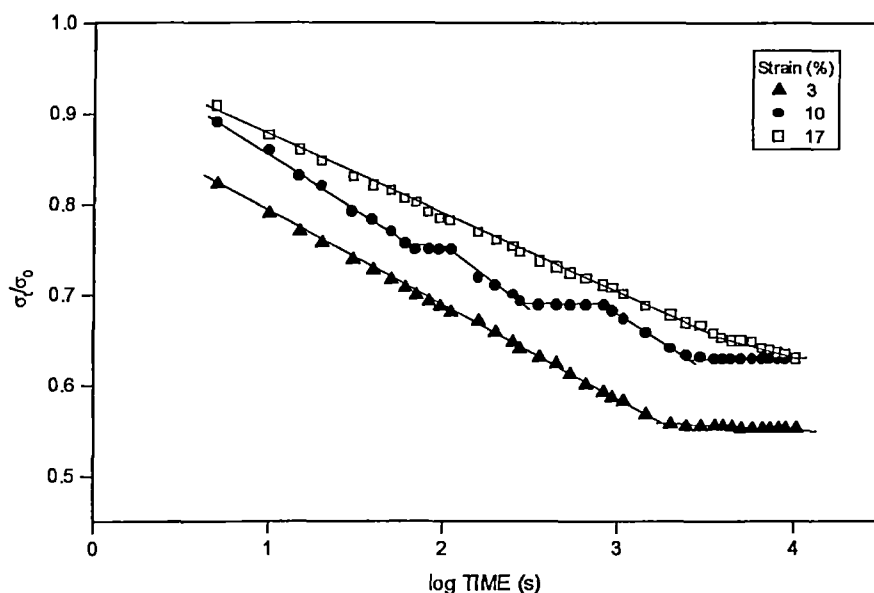


Figure 6.5 Stress relaxation curves of oil palm empty fruit bunch fibre at different strain levels.

The rate of relaxation shows the highest value for high strain levels particularly at longer durations (Table 6.4). Initial rearrangements at the lower strain level may be easy as evident from the rate of relaxation. At very low strain levels, commendable failure of fibre does not happen. In such a system, the relaxation rate will be very

low. At very high strain level also, there is possibility for a slow relaxation as the failure is already occurred. However, for the fibres which are not fully strained, ie. at a strain level of 10%, the fibres pass through a complicated failure mechanism. Hence the fibres, which are strained to 10% exhibit higher relaxation rate.

Table 6.4 Rate of Stress Relaxation (%) in Oil Palm Empty Fruit Bunch Fibre at Different Strain Levels.

Range (s)	Strain level (%)		
	3	10	17
1-10 ¹	4.24	3.79	3.82
10 ¹ -10 ²	11.74	13.18	11.81
10 ² -10 ³	13.98	11.77	11.48
10 ³ -10 ⁴	5.52	7.07	10.92

A master curve is constructed for all the strain levels with respect to 10% strain level and is given in Figure 6.6. The method of superposition was first suggested by Leaderman who observed that creep recovery data of polymers obtained at different temperatures can be superimposed by horizontal translation along the logarithmic time axis.¹⁵ Later Tobolsky and co-workers modified the superposition principle to account for proportionality of modulus to absolute temperature and applied to experimental data.^{16, 17} William, Landel and Ferry [WLF] proposed a shift factor at different strain levels to construct a master curve in order to explain the validity of the superposition principle.¹⁸

The horizontal shift factors were calculated by giving an empirical horizontal shift along the logarithmic axis of the stress relaxation curves.^{19, 20} It is found that the points at different strain levels merge into a single line on shifting. From this curve we can predict the relaxation behaviour of the fibre at a required strain level. The computed shift factors, $\log aT$ were plotted against corresponding

strain levels to understand the strain dependence of the shift factors (Figure 6.7). A curve parabolic to the axis is obtained.

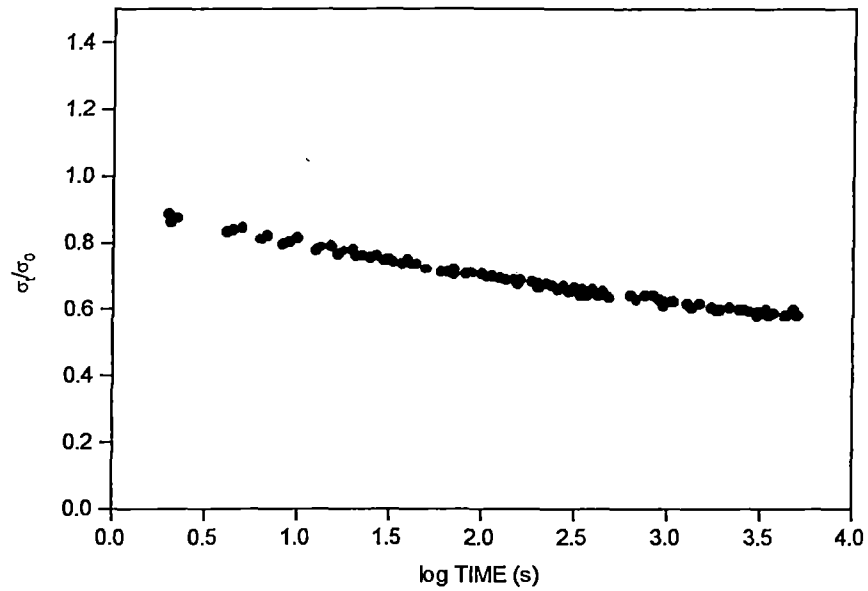


Figure 6.6 Master stress relaxation curves for oil palm empty fruit bunch fibre with respect to 10% strain.

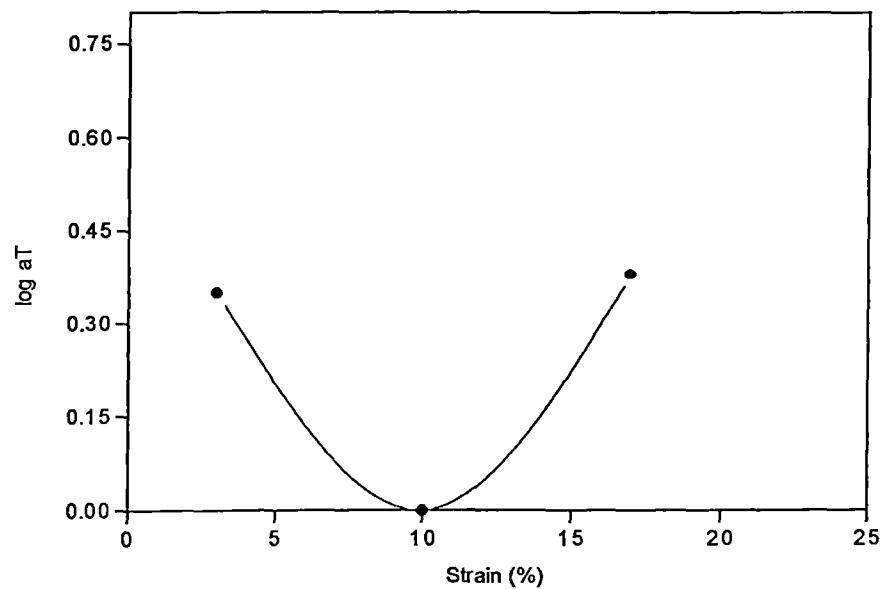


Figure 6.7 Semilogarithmic plot of strain dependence of the horizontal shift factors for oil palm empty fruit bunch fibre.

6.2 STRESS RELAXATION BEHAVIOUR IN OIL PALM EMPTY FRUIT BUNCH FIBRE REINFORCED PHENOL FORMALDEHYDE COMPOSITES

6.2.1 Effect of Fibre Loading

Figure 6.8 shows the stress relaxation behaviour of the composites having different fibre loading. Incorporation of the fibre results in a two step relaxation process. The relaxation mechanism is complicated due to the presence of fibre in between the matrix layers.

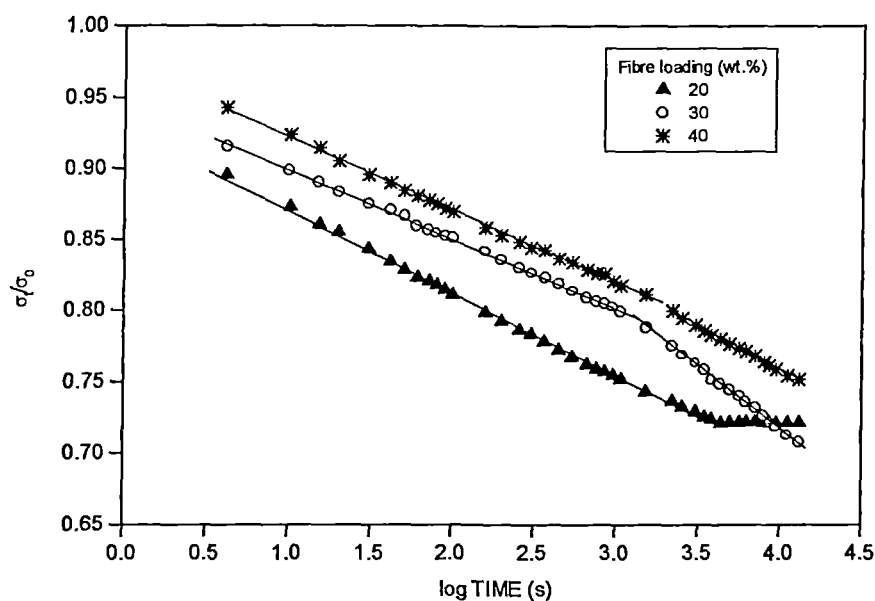


Figure 6.8 Stress relaxation curves of oil palm fibre/PF composites having different fibre loading at 2% strain.

Irregular trend is observed with fibre loading. The neat phenol formaldehyde resin has three dimensionally crosslinked network structure. It has got poor impact performance and is highly brittle. The examination of stress relaxation in gum sample became impractical as they undergo catastrophic failure at the initial stage of the experiment itself. High brittle failure of the matrix is observed in tensile tests. Therefore relaxation owing to the matrix resin could not be monitored. The relaxation mechanism of the fibre reinforced composite depends upon the uniformity of the fibre dispersion, extent of fibre to fibre contact, extent of fibre-matrix

interaction etc. Fibre-matrix bond failure contributes to the first step relaxation. This is illustrated in the schematic model (Figure 6.9). Therefore the extent of fibre-matrix interaction determines the initial relaxation. The second step relaxation is due to the matrix phase relaxation.

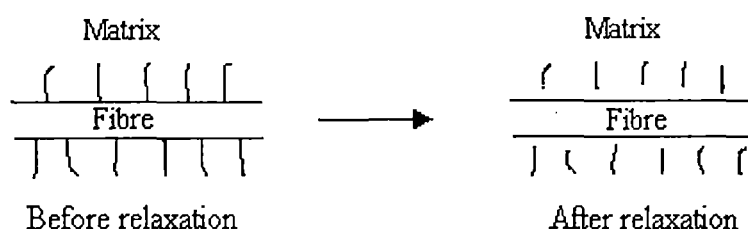


Figure 6.9 Schematic representation of debonding at the fibre matrix interface

Initially higher rate of relaxation is observed for 20wt.% loading (Table 6.5). Relatively rapid decay of stress is associated with a change of microcrystalline structure or texture of the sample, ie. an orientation of crystalline material arising from fibres (Figure 6.1). Tobolsky reported that birefringence study is an important

Table 6.5 Rate of Stress Relaxation (%) in Oil Palm Fibre/PF Composites having Different Fibre Loading at 2% Strain.

Range (s)	Fibre loading (wt.%)		
	20	30	40
1-10 ¹	2.67	2.04	2.03
10 ¹ -10 ²	7.65	5.09	5.86
10 ² -10 ³	7.42	6.33	6.35
10 ³ -10 ⁴	3.74	10.40	6.52

tool to analyse the stress relaxation arising from the growth of oriented crystalline material.²¹ But at very long times the relaxation rate becomes too high for composites having higher loading. The initial relaxation process may be due to the propagation of fibre-matrix debonding process. Thereafter relaxation in lower fibre

loading is retarded and is noted by the slope change. The number of steps involved in the relaxation process of composites having different fibre loading is evident from Figure 6.8. The initial crossover time decreased upon higher loading (Table 6.6). At lower fibre loading, fibre-matrix failure has got major contribution on relaxation due to the fine dispersion of fibres. As the initial relaxation is due to the debonding process, the relaxation rate becomes high at this stage at low fibre loading. In composites having 30 and 40 wt.% fibre loading, fibre alignment or gradual displacement of the fibres may happen, which facilitates the relaxation process and is denoted by the slope change in the stress relaxation curve (Figure 6.8). A notable change in fibre alignment will be observed at higher loading only. At higher loading, fibre to fibre contact increases which facilitates fibre alignment. At lower fibre loading, fibres are well impregnated in the matrix. The fibre-fibre interaction will be comparatively low at lower loading. This is evident from the higher crossover time for the lowest fibre loaded composite (Table 6.6). Fibre entanglement acts as temporary physical cross links that may break and remake. Breaking of bonds relaxes the stress. It is reported that the stress relaxation rate increases with increase in particulate reinforcement loading.²² The relaxation modulus curves of the composites having various fibre loading are given in Figure 6.10. The modulus relaxation behaviour of the composites can be explained in a similar manner as in the case of stress relaxation.

6.2.2 Effect of Fibre Treatment

Fibre surface modifications bring out major changes in the physical and chemical bonding at the interface. It has already been reported that alkali treatment to the oil palm fibre improves the tensile properties.²³ It is also reported that latex coating and introduction of coupling agents decrease the hydrophilicity of the fibres, which reduces the compatibility with the hydrophilic matrix resin. These composites have an advantage of superior impact resistance at the expense of decreased compatibilisation.

Table 6.6 Crossover Time of Treated and Untreated Oil Palm Fibre/PF Composites and Oil Palm Fibre/Glass Hybrid PF Composites during Stress Relaxation.

Composite	Cross-over time : log Time (s)	
	1 st	2 nd
Oil palm/PF (Fibre loading 20wt.%; Strain level 2%)	3.60	----
Oil palm/PF (Fibre loading 30wt.%; Strain level 2%)	3.14	----
Oil palm/PF (Fibre loading 40wt.%; Strain level 2%)	3.33	----
Oil palm/PF (Fibre loading 30wt.%; Strain level 1%)	3.55	----
Alkali treated Oil palm/PF (Fibre loading 40wt.%; Strain level 2%)	3.75	----
Latex treated Oil palm/PF (Fibre loading 40wt.%; Strain level 2%)	3.11	----
Silane treated Oil palm/PF (Fibre loading 40wt.%; Strain level 2%)	3.20	----
Isocyanate treated Oil palm/PF (Fibre loading 40wt.%; Strain level 2%)	3.13	3.88
Oil palm/glass hybrid PF (Fibre loading 40wt.%; Strain level 2%)	3.50	----
Glass/PF (Fibre loading 40wt.%; Strain level 2%)	3.13	----
Oil palm/PF, Oven aged (Fibre loading 30wt.%; Strain level 2%)	3.72	----
Oil palm/PF, Water aged (Fibre loading 40wt.%; Strain level 2%)	3.73	----

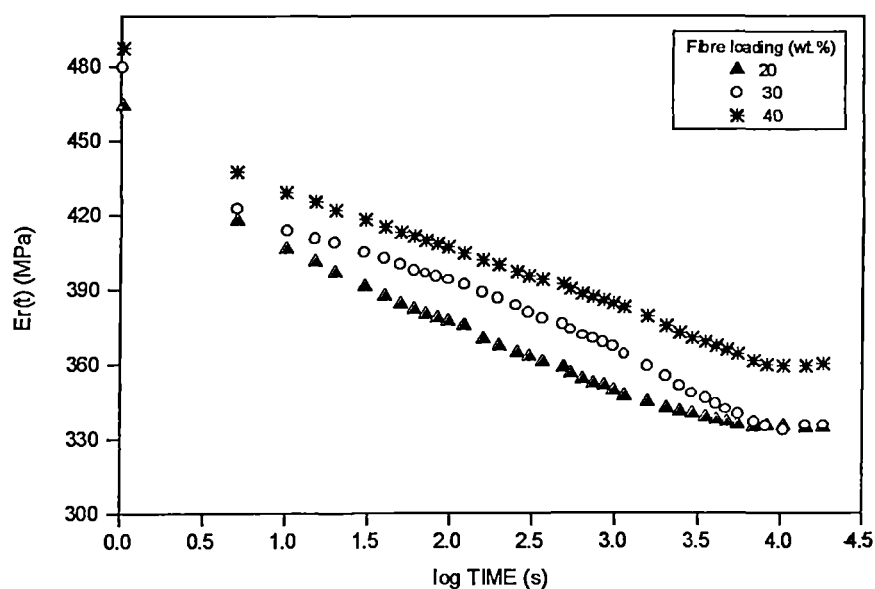


Figure 6.10 Modulus relaxation curves of oil palm fibre/PF composites having different fibre loading at 2% strain.

The variations on relaxation mechanisms are clear from the Figure 6.11. The decreased relaxation rate in the alkali treated fibre composite may be due to the strong interfacial interlocking between the fibre and matrix. A two-step relaxation process is observed for this composite. The crossover time is higher than that of the untreated composite (Table 6.6). The net relaxation in isocyanate treated composite is lower than untreated composite. Here, changes in slope give evidence to a three-step process. The silane treated composite also involves a two step relaxation process. Successive progress in the physical rearrangement of the fibres and chemical debonding may be responsible for the process. Latex treated composite exhibits maximum stress relaxation. A small change in slope is observed at long duration. Molecular rearrangements at the rubber phase may lead to higher relaxation. Latex coating and silane treatments impart hydrophobicity to the fibres, which reduces the fibre-matrix compatibility within the composite. The extent of fibre-matrix bonding in the untreated and treated composites is evident from the respective scanning electron micrographs of the tensile fracture surfaces (Figs. 4.4, 4.5 & 4.9; refer Chapter 4). This decreased bonding at the interface decreases the strength and stiffness of the composite and facilitates faster relaxation processes. The crossover time is considerably decreased in these composites (Table 6.6).

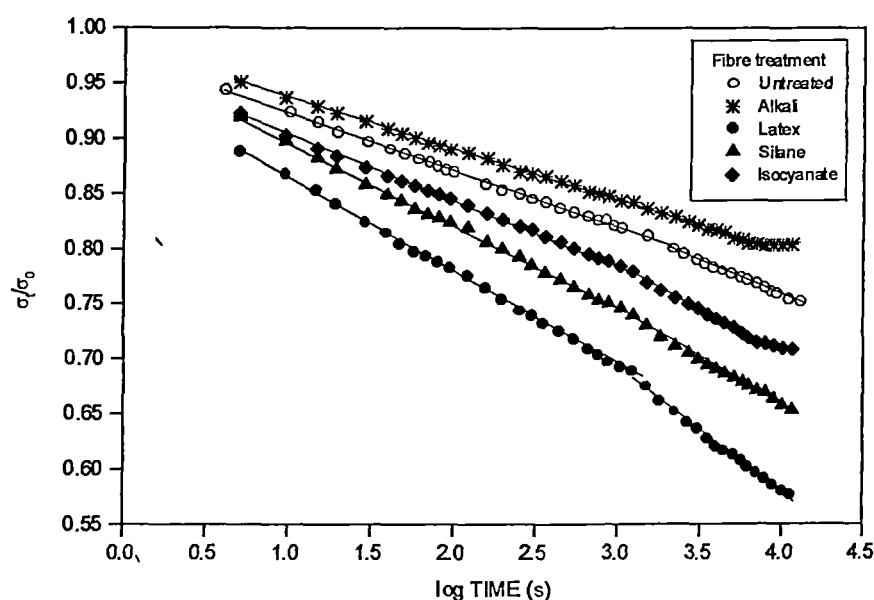


Figure 6.11 Stress relaxation curves of treated and untreated oil palm fibre/PF composites having 40wt.% fibre loading at 2% strain.

The rate of relaxation values shows gradual increase for all the composites (Table 6.7). The relaxation modulus of the untreated and treated composites was plotted against log time in Figure 6.12. Same trend as in the case of stress relaxation is observed here. All treated composites exhibit a steady relaxation in modulus values.

Table 6.7 Rate of Stress Relaxation (%) in Treated and Untreated Oil Palm Fibre/PF Composite having 40wt.% Fibre Loading at 2% Strain.

Range (s)	Untreated	Mercerised	Latex	Silane	TDI
1-10 ¹	2.03	2.20	2.14	2.39	2.17
10 ¹ -10 ²	5.86	4.75	10.13	8.47	6.53
10 ² -10 ³	6.35	4.86	11.91	9.62	7.35
10 ³ -10 ⁴	6.52	5.99	15.55	11.73	9.21

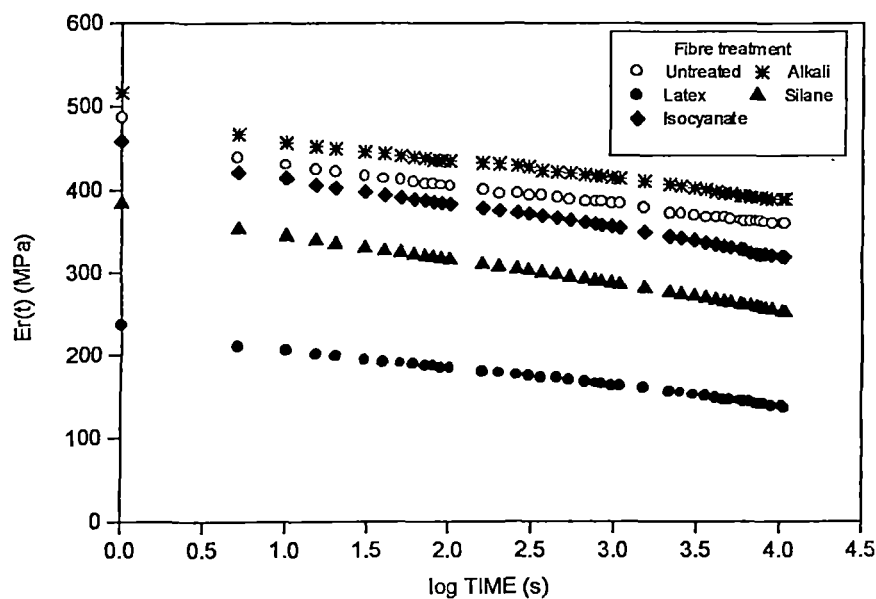


Figure 6.12 Modulus relaxation curves of treated and untreated oil palm fibre/PF composites having 40wt.% fibre loading at 2% strain.

6.2.3 Effect of Hybridisation with Glass

Relaxation behaviour of oil palm fibre/PF composite, oil palm fibre/glass hybrid PF composite and glass/PF composite were compared in Figure 6.13. Nonlinear stress relaxation behaviour was reported in thermosets such as polyester and phenolics.^{24, 25} Stress relaxation behaviour of polyethylene-carbon fibre reinforced PMMA hybrid composites was recently reported.²⁶ In this study the relaxation properties are dominated mainly by polyethylene fibres. The rate of stress relaxation decreases with time at all strain levels. The hybrid composite shows very low relaxation than glass/PF composite. The oil palm fibre/PF composite shows maximum relaxation. The intrinsic stress relaxation behaviour of the reinforcing fibre plays an important role in the relaxation process. The glass fibre is highly brittle and oil palm fibre is more elastic in nature. The hybridisation of these fibres may disrupt the relaxation process. Major change in slope in glass/ PF composite may be due to the uniaxial orientation of glass fibre.

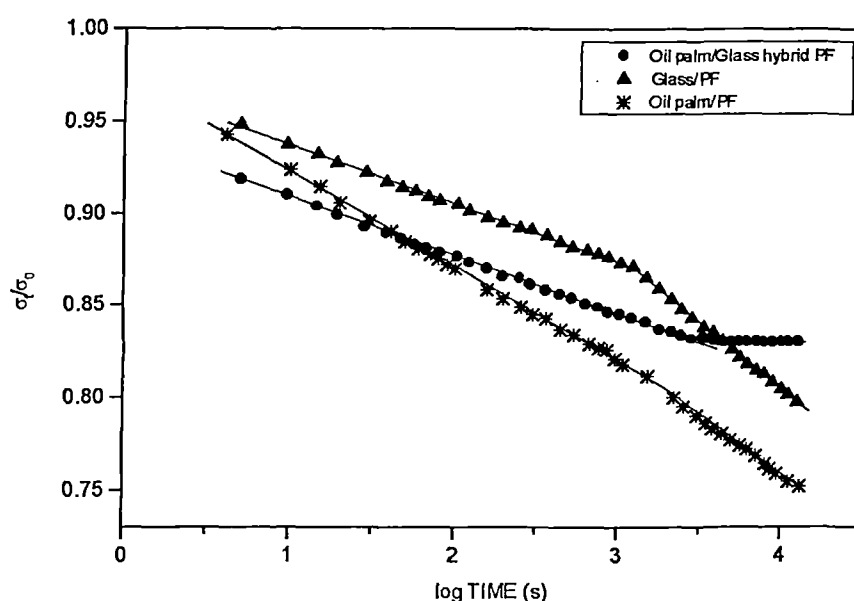


Figure 6.13 Stress relaxation curves of oil palm fibre/PF, oil palm fibre/glass hybrid PF and glass/PF composites having 40wt.% fibre loading at 2% strain.

The crossover time for the hybrid composites is higher than that of unhybridised composites (Table 6.6). Rate of relaxation of each composite is given in Table 6.8. Hybrid composite exhibit very low rate of relaxation. This is due to the inherent lower relaxation behaviour of the glass in hybrid composites. Very high rate of relaxation is observed at long duration for glass/PF composites. Thus hybridisation of oil palm fibre with glass fibre results in composites having superior long-term mechanical performance.

Table 6.8 Rate of Stress Relaxation (%) in Oil Palm Fibre/PF, Oil Palm Fibre/Glass Hybrid PF and Glass/PF Composites at 2% Strain.

Range (s)	Oil palm fibre/PF	Oil palm/glass /PF	Glass/PF
1-10 ¹	2.03	1.41	1.46
10 ¹ -10 ²	5.86	3.95	4.09
10 ² -10 ³	6.35	3.54	3.91
10 ³ -10 ⁴	6.52	1.66	9.01

6.2.4 Effect of Physical Ageing

The environmental effects especially the influence of moisture and temperature on composite mechanical properties has been extensively investigated. The information on the effect of environment on long term mechanical performance is rather limited.²⁷⁻²⁹ The effect of environmental cycling on the tensile performance of reinforced plastics for various fibre orientations, time of exposure, temperature etc. were investigated by Lendemo et al.³⁰ Khan and Ali studied the effect of accelerated weathering on the mechanical properties of wood-plastic composites.³¹

The stress relaxation behaviour of the water aged and thermal aged oil palm fibre/PF composites are given in Figure 6.14. The water aged samples show increased relaxation. This may be due to the changes in the interface properties attained on ageing. At long duration both water and thermal ageing leads to a major slope change. The crossover time of the water aged and thermal aged composites is higher than unaged composite (Table 6.6). Thermal and water ageing may change

the behaviour of fibres within the matrix. The physical and chemical interactions at the fibre-matrix interface are disrupted on thermal and water ageing. Hence the initial relaxation will be higher for aged samples. This is due to the weak interface in aged composites. The crack propagation pattern in the aged sample may change from that of unaged samples. It may be noted that the intrinsic stress relaxation rate of the fibre decreased upon ageing. The stress decay is faster at the initial stages for the aged samples. At higher durations the relaxation process gets retarded upon ageing [Table 6.9]. Struik studied the volume changes associated with physical ageing and found that the stress relaxation shifts to longer time span.³²

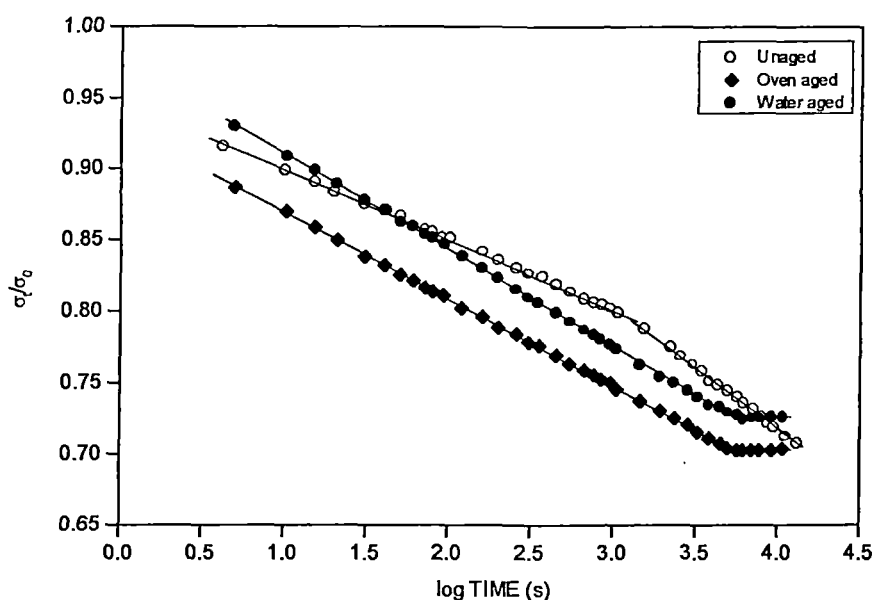


Figure 6.14 Stress relaxation curves of unaged and aged oil palm fibre/PF composites having 30wt.% fibre loading at 2% strain.

Table 6.9 Rate of Stress Relaxation (%) of Unaged and Aged Oil Palm Fibre/PF Composites having 30wt.% Fibre Loading at 2% Strain.

Range (s)	Unaged	Thermal aged	Water aged
1-10 ¹	2.04	1.88	2.33
10 ¹ -10 ²	5.09	6.87	7.39
10 ² -10 ³	6.33	7.26	9.09
10 ³ -10 ⁴	10.40	4.43	5.81

6.2.5 Effect of Strain Level

Figure 6.15 gives the stress relaxation behaviour of the oil palm fibre reinforced phenol formaldehyde composite at various strain levels. The relaxation mechanism varies according to the applied initial strain. Usually in composites, strain rate and the extent of strain applied to the composite affect the interfacial stress transfer and thereby their mechanical properties.^{33, 34} Effect of strain rate and strain level on the stress relaxation behaviour of the short fibre composites and blends were studied by many researchers.³⁵⁻³⁸ It has been reported that no substantial change in the shape of the decay curve occurs over the range of strains and times investigated for iPP. It is merely needed to multiply the stress decay curve by a strain dependent factor.³⁹

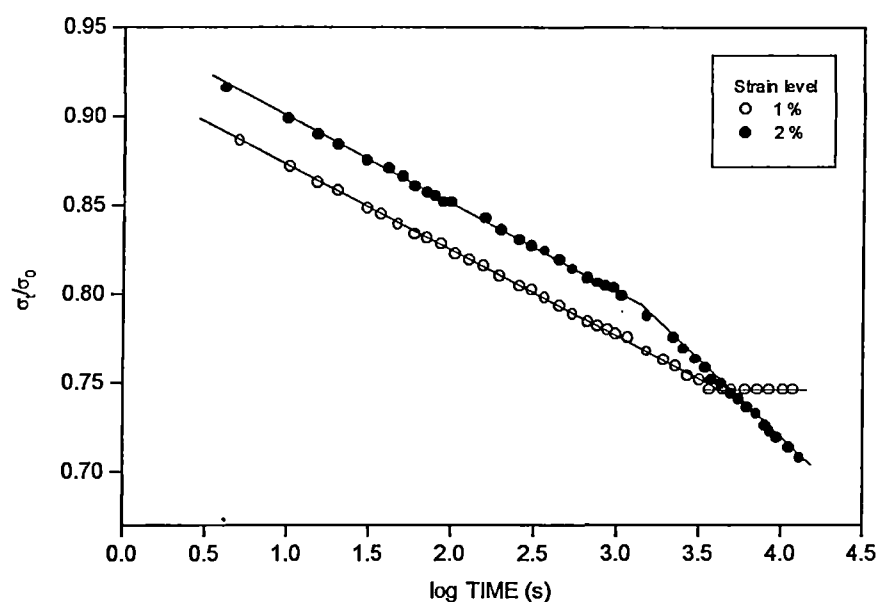


Figure 6.15 Stress relaxation curves of oil palm fibre/PF composites having 30wt.% fibre loading at different strain levels.

Increase of strain level from 1 to 2% increases the rate of relaxation of oil palm fibre/PF composites and further increase in strain level decreases the stress relaxation (Fig. 6.15). Beyond a certain strain level the fibre rearrangement during the application of stress will lead to partial internal failure of the composite. This process is irreversible and possibility for further physical or chemical rearrangement leading to relaxation is decreased. A two-stage process is observed

at 2% strain level. The relaxation process at 1% strain level can be explained on the basis of the extent of deformation occurred to the specimen. Upto 1% strain the specimen undergoes initiation of the failure mechanisms like crack formation, debonding etc. Small amount of fibre is involved in the deformation. Thus the stress relaxation in this case will be considerably low. At this strain level the relaxation undergoes different mechanisms. The crossover times for change in mechanism is given in Table 6.6. But at 2% strain, maximum fibres are involved in the failure process and the sample undergoes the crack propagation stage. The crossover time becomes higher at higher strain levels. A complicated mechanism involving the rearrangements of the partially failed fibres and the gradual scission of the interfacial bonds may occur at this stage. This will lead to a higher stress relaxation rate. At longer time the relaxation is found to be very fast owing to the increased failure of the fibres and can be understood from the relaxation rate at this stage (Table 6.10). Irregular relaxation rate is observed at 1% strain level [Table 6.10]. The relaxation rate gradually increased with time at 2% strain.

Table 6.10 Rate of Stress Relaxation (%) of Oil Palm Fibre/PF Composites having 30wt.% Fibre Loading at Different Strain Levels

Range (s)	Strain level (%)	
	1	2
1-10 ¹	1.60	2.04
10 ¹ -10 ²	5.97	5.09
10 ² -10 ³	3.69	6.33
10 ³ -10 ⁴	4.55	10.40

The stress relaxation values at different strain levels were superimposed by a horizontal shift along the log Time axis. Figure 6.16 is the master stress relaxation curve with respect to 2% strain. We can predict the long-term behaviour of the composite using this curve. The corresponding shift factors were calculated by

horizontal shift of the respective curves along the time axis. Figure 6.17 shows the shift factors plotted against corresponding strain levels.

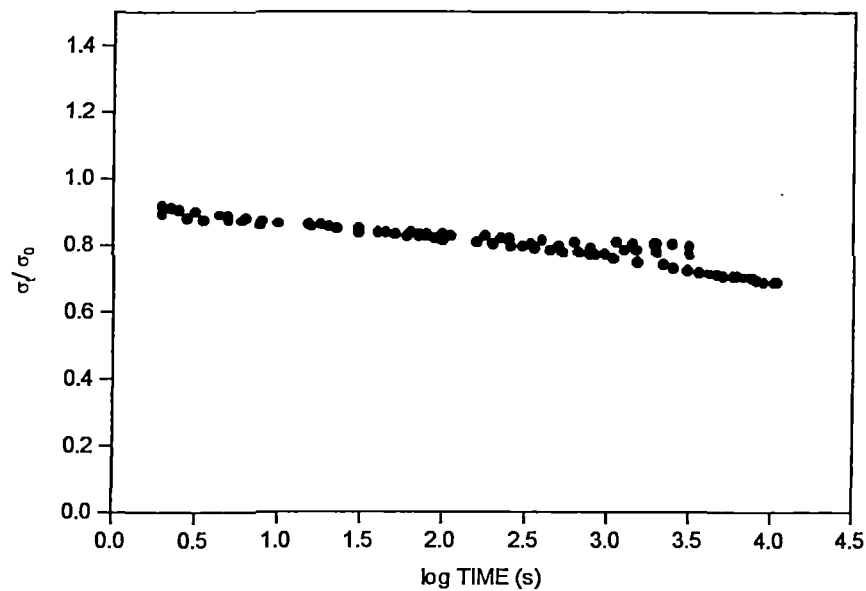


Figure 6.16 Master stress relaxation curve for oil palm fibre/PF composites with respect to 2% strain

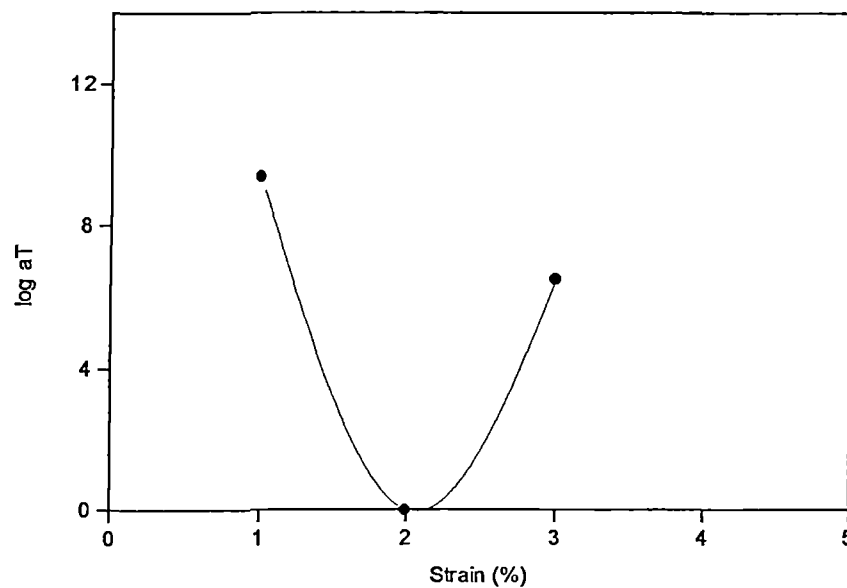


Figure 6.17 Semilogarithmic plot of strain dependence of the horizontal shift factors for oil palm fibre/PF composites.

REFERENCES

1. J. L. Sullivan, Y. F. Wen and R. F. Gibson, *Polym. Comp.*, **16**,3 (1995)
2. J. D. Ferry, Viscoelastic Properties of Polymers, *Wiley*, New York (1980)
3. C. I. MacKenzie and J. Scanlan, *Polymer*, **25**, 559 (1984)
4. T. K. Tsotsis, *Polym. Comp.*, **17**, 362 (1996)
5. T. Ariyama, Y. Mori and K. Kaneko, *Polym. Eng. Sci.*, **37**, 81 (1997)
6. G. Attalla, I. B. Guanella and R. E. Cohen, *Polym. Eng. Sci.*, **23**, 883 (1983)
7. D. M. Colucci, P. A. O'Connell and G. B. McKenna, *Polym. Eng. Sci.*, **37**, 1469 (1997)
8. P. Flink and B. Stenberg, *Brit. Polym. J.*, **22**, 193 (1990)
9. R. Asaletha, S. Thomas and M. G. Kumaran, *J. Appl. Polym. Sci.*, (Submitted)
10. S. Varghese, B. Kuriakose and S. Thomas, *J. Appl. Polym. Sci.*, **53**, 1051 (1994)
11. J. George, M. S. Sreekala, S. Thomas, S. S. Bhagawan and N. R. Neelakantan, *J. Rein. Plast. Comp.*, **17**, 651 (1998)
12. D. T. Grubb and Zong-Fu Li, *Polymer*, **33**, 2587 (1992)
13. M. S. Sreekala, M. G. Kumaran and S. Thomas, *J. Appl. Polym. Sci.*, **66**, 821 (1997)
14. S. K. Bhateja and E. H. Andrews, *J. Appl. Polym. Sci.*, **34**, 2809 (1987)
15. H. Leaderman, *Textile Research J.*, **11**, 171 (1941)
16. A. V. Tobolsky and J. R. McLoughlin, *J. Polym. Sci.*, **8**, 543 (1952)
17. R. D. Andrews and A. V. Tobolsky, *J. Polym. Sci.*, **7**, 221 (1951)
18. J. J. Aklonis, W. J. MacKnight and M. Shen, Introduction to Polymer Viscoelasticity, *Wiley-Interscience*, New York (1972)
19. P. M. Ogibalov, N. J. Malinin, V. P. Netrebko and B. P. Kishkin, Structural Polymers, *Wiley*, Vol.2, New York, p.284 (1974)
20. G. Kumar, Arindam, N. R. Neelakantan and N. Subramanian, *J. Appl. Polym. Sci.*, **50**, 2209 (1993)
21. A. V. Tobolsky, Properties and Structure of Polymers, *John Wiley and Sons, Inc.*, New York (1962)
22. C. J. Derham, *J. Mater. Sci.*, **8**, 1023 (1973)
23. M. S. Sreekala, M. G. Kumaran and S. Thomas, *Appl. Comp. Mater.*, (In press)
24. G. Tieghi, M. Levi, A. Fallini and F. Danusso, *Polymer*, **32**, 39 (1991)
25. R. A. Schapery, *Polym. Eng. Sci.*, **9**, 295 (1969)
26. N. Saha, A. N. Banerjee, *J. Appl. Polym. Sci.*, **67**, 1925 (1998)
27. G. S. Springer, Environmental effects on composite materials, *Technomic Publishing Co. Inc.*, Lancaster, Vol.3 (1988)

28. K. Ogi and N. Takeda, *J. Comp. Mater.*, **31**, 530 (1997)
29. R. Selzer and K. Friedrich, *Composites, Part A* **28A**, 595 (1997)
30. C. Y. Lendemo and S. E. Thor, *J. Comp. Mater.*, **11**, 276 (1977)
31. M. A. Khan and K. M. I. Ali, *Polym-Plast. Technol. Eng.*, **32(1&2)**, 5 (1993)
32. L. C. E. Struik, *Physical Ageing in Amorphous Polymers and Other Materials*, Elsevier, Amsterdam (1978)
33. M. Detassis, A. Pegoretti and C. Migliaresi, *Comp. Sci. Technol.*, **53**, 39 (1995)
34. I. Harismendy, R. Miner, A. Valea, R. Llano-Ponte, F. Mujika and I. Mondragon, *Polymer*, **38**, 5573 (1997)
35. S. S. Bhagawan, D. K. Tripathy and S. K. De, *J. Appl. Polym. Sci.*, **33**, 1623 (1987)
36. T. S. Creasy, S. G. Advani and R. K. Okine, *Rheol. Acta*, **35**, 347 (1996)
37. S. K. N. Kutty and G. B. Nando, *J. Appl. Polym. Sci.*, **42**, 1835 (1991)
38. L. Ibarra, A. Macias and E. Palma, *J. Appl. Polym. Sci.*, **61**, 2447 (1996)
39. N. K. Dutta and G. H. Edward, *J. Appl. Polym. Sci.*, **66**, 1101 (1997)

CHAPTER 7

Dynamic Mechanical Properties of Oil Palm Fibre/Phenol Formaldehyde and Oil Palm-Glass Hybrid Fibre/Phenol Formaldehyde Composites

*Results of this study have been submitted for publication in the journal **Polymer Engineering Science***

Abstract

The dynamic mechanical properties of oil palm fibre reinforced phenol formaldehyde composites and oil palm/glass hybrid fibre reinforced phenol formaldehyde composites were investigated as a function of fibre length, fibre content, fibre treatment and hybrid fibre ratio. Scanning electron microscopy was used to study the morphology of the fibre surfaces and interface adhesion in composites. The samples were subjected to dynamic mechanical thermal analysis at different frequencies over a range of temperatures (25 to 160°C). Variations in storage modulus E' , loss modulus E'' and mechanical damping parameter, $\tan\delta$, of the polymer upon the addition of fibres were investigated. The dynamic modulus of the neat PF sample decreases with decrease in frequency. Glass transition attributed with the α relaxation of the gum sample was observed around 140°C. The $\tan\delta$ values and storage moduli show great enhancement upon fibre addition. The values increase with increase in fibre content. The loss modulus shows a reverse trend with increase in fibre loading. Incorporation of oil palm fibre shifts the glass transition towards lower temperature value. Mercerisation of the fibre leads to an increase in the modulus and damping characteristics of the composite. The latex treated composite exhibits highest damping. The dynamic modulus of the composite is found to be increased on oil palm fibre surface modifications. The glass transition temperature of the hybrid composites is lower than that of the unhybridised composites. Highest value of mechanical damping is observed in hybrid composites. Storage modulus of the hybrid composites is lower than unhybridised oil palm fibre/PF composite. Similar trend is observed for loss modulus also. Activation energies for the relaxation processes in different composites were calculated. Activation energy increases with fibrous reinforcement. Complex modulus variations and phase behaviour of the composites were studied from cole-cole plots. Finally, master curves for the viscoelastic properties of the composites were constructed on the basis of time-temperature superposition principle.

Dynamic behaviour of composite materials receives considerable attention as most of the composite components on engineering applications are subjected to dynamic stress and strain. Knowledge of dynamic moduli and properties of composite materials is indispensable to intelligent design with these materials. Dynamic mechanical analysis has been used to determine the glass transition region, relaxation spectra, degree of crystallinity, molecular orientation, crosslinking, phase separation, structural changes resulting from processing and chemical composition of polymer composites. Time and temperature are extremely important factors in the study of dynamic properties of polymeric materials. The investigation of the dynamic modulus and loss factors over a wide range of temperatures has been used to evaluate the miscibility, interface, damping characteristics and morphological variation of polymer blends and composites¹⁻³. The dynamic modulus and internal friction are the most basic of all the viscoelastic properties. They are sensitive not only to many kinds of molecular motion but also to various transitions, relaxation processes, structural heterogeneities and the morphology of multiphase systems. The dynamic mechanical response of the multicomponent systems like composites is highly complex which requires the concepts of micromechanics and constitutive equations. It is dependent not only on the nature of constituents but also on the physical or structural arrangement of phases such as morphology and interface. Dynamic modulus gives a measure of the hardness or stiffness of the polymeric material and is temperature dependent.

The mechanical damping or internal friction of composite materials is important not only as a property index but also for environmental and industrial applications. High damping is essential in decreasing the effect of undesirable vibration, by reducing the amplitude of resonance vibrations to safe limits⁴. Incorporation of reinforcements brings out major changes in the damping characteristics of the matrix. Composite damping property results from the inherent damping of the constituents. This can be represented as⁵

$$\tan \delta_c = V_f \tan \delta_f + (1 - V_f) \tan \delta_m \quad (7.1)$$

where $\tan\delta_c$, $\tan\delta_f$ and $\tan\delta_m$ are the damping values of the composite, the fibre and the polymer respectively and V_f and V_m are the volume fraction of the fibre and the matrix respectively. The $\tan\delta$ value of the composite is dependent upon the fibre agglomeration in the composite and interactions at the polymer–filler interface. In the transition region the damping is high owing to the initiation of micro-Brownian motion in molecular chains. Some of the molecular chain segments are free to move, while others are not. For every time a stressed frozen-in segment becomes free to move, its excess energy is dissipated as heat. If the segments are either completely frozen in (below T_g) or free to move (above T_g), the damping is low. Neilsen,⁶ Manson and Sperling⁷ briefly reviewed studies on dynamic mechanical properties of composites. According to Nielsen,⁸ the composite to be ideal, agglomerate free and excluding interactions at the interface, the damping of a composite, $\tan\delta_c$ can be estimated by using the rule of mixtures. He explained that for reinforcement of low damping, $\tan\delta_c$ is given by the proportional contribution of the matrix according to its relative content.

$$\tan\delta_c = \tan\delta_m (1 - \phi_f) \quad (7.2)$$

where $\tan\delta_m$ is the damping value of the matrix and ϕ_f is the volume fraction of filler.

Around T_g , the matrix phase will not in general deform the filler particles. Damping therefore is due primarily to the polymer phase and the relative damping should be related simply to the polymer volume fraction as above. If there is significant physico-chemical or specific interaction between polymer and filler, this will tend to immobilise a layer of polymer around each solid particle. As a result of such matrix-fibre interaction eqn. (7.2) is rewritten as

$$\tan\delta_c = \tan\delta_m (1 - B\phi_f) \quad (7.3)$$

Where B is a correction parameter related to the effective thickness of the fibre-matrix interphase which was first introduced by Ziegel et al.⁹ The stronger the interfacial interactions, the thicker the immobilised layer and higher the value of parameter B . The damping parameter is dependent on the orientation of fibres with

the direction of oscillation. Thomason¹⁰ studied the influence of varying the fibre direction in glass fibre reinforced composite between 0 and 90 degrees. It was found that the presence of a second peak is dependent on the fibre orientation with respect to the damping direction. The crystallinity of the composite has a great effect on the primary relaxation corresponding to glass transition. Effect of the fibre volume fraction, interphase material and fibre diameter on the $\tan\delta$ values of glass fibre reinforced polyester composites has been investigated by Chua¹¹. According to him, the relationship between $\tan\delta$ and volume fraction cannot be predicted by simple rule of mixtures. He suggested that

$$\tan\delta = V_f \tan\delta_f + V_m \tan\delta_m + V_i \tan\delta_i \quad (7.4)$$

where V_i and $\tan\delta_i$ represent the values for the interphase of the material, a region surrounding the fibre where properties differ from those of the bulk matrix.¹² The interface is deliberately built into the composite by coating the fibres with a layer of material before the inclusion in the composite. Interface is dependent on the nature of the constituent materials of the composite and may be unexpectedly formed from a rigid polymer layer next to the fibre surface caused by the restricted molecular motion due to the fibre-matrix interaction.¹³ $\tan\delta$ value changes with fibre diameter because bonding surface area changes with fibre diameter.

Dynamic properties of short carbon fibre reinforced butadiene-styrene thermoplastic composites were investigated by Ibarra et al.^{14, 15} It was found that the dynamic properties depend upon the reinforcing fibre stiffness. Several studies have been reported on the dynamic mechanical analysis of polymer composites and blends.¹⁶⁻¹⁹ It was found that natural fibre reinforcement in polymer changes its dynamic properties to a considerable extent. Studies on dynamic properties of pineapple fibre reinforced LDPE and sisal fibre reinforced NR and low-density polyethylene systems were recently reported from this laboratory.^{20, 21, 22} It was found that incorporation of treated pineapple fibre reinforcement in LDPE leads to significant improvement in modulus owing to the increase in interfacial stiffness achieved through more intense fibre-matrix interaction. Addition of short sisal fibre

to natural rubber increased the storage modulus, loss modulus and $\tan\delta$ of rubber vulcanizates. It was found that the viscoelastic properties of sisal fibre filled low-density polyethylene composites were influenced by fibre length and fibre orientation.²² In natural fibre reinforced plastic composites the adsorbed water on fibre surface will affect the dynamic properties of the composites. The effects of adsorbed water on dynamic mechanical properties of wood were investigated by Obataya et al.²³ They have discussed the effects of adsorbed water on the matrix and the moisture dependence of E' and $\tan\delta$. The cure conditions and the extent of curing of the final product will be a determining factor of the dynamic properties of the composites. Valea et al.²⁴ discussed the variation of the dynamic properties of several vinyl ester and unsaturated polyester resins upon various cure conditions. Effect of temperature and frequency on dynamic thermomechanical properties of poly(ethylene terephthalate) was studied in detail by Bikiaris et al.²⁵ It is reported that in a compatibilized thermoplastic/thermoset blend the viscoelastic behaviour of the interphase relaxation is associated with the conditions of confinement of the components in the interphase zone.²⁶

The dynamic mechanical analysis of phenolic composites receives utmost importance as the crosslinking of the phenolics during cure is accompanied by increase in glass transition temperature which in turn have profound effect on the high temperature usefulness of these materials. This chapter discusses the effect of fibre length, fibre loading, fibre modification by mercerisation and hybrid fibre ratio of oil palm fibre/glass hybrid composites on storage modulus, loss modulus and mechanical damping parameter of the composites over a range of temperatures (25 to 150°C). The effect of frequency on the dynamic properties of the composites was evaluated. Glass transition temperature of the composites was determined from the relaxation spectra of the respective composites. Apparent activation energy of the relaxation process of the composites was analysed. Cole-cole plots were drawn to understand the heterogeneous nature of the composites. Master curve was constructed based on time-temperature superposition principle to explain long term dynamic behaviour of the composites.

7.1 DYNAMIC MECHANICAL PROPERTIES OF NEAT PHENOL FORMALDEHYDE

Dynamic mechanical behaviour of neat PF sample is shown in Figures 7.1 and 7.2. The variation of storage modulus, mechanical damping factor and loss modulus at different frequencies was plotted. At a frequency 0.1Hz, the sample shows two relaxation peaks in the $\tan\delta$ curve.

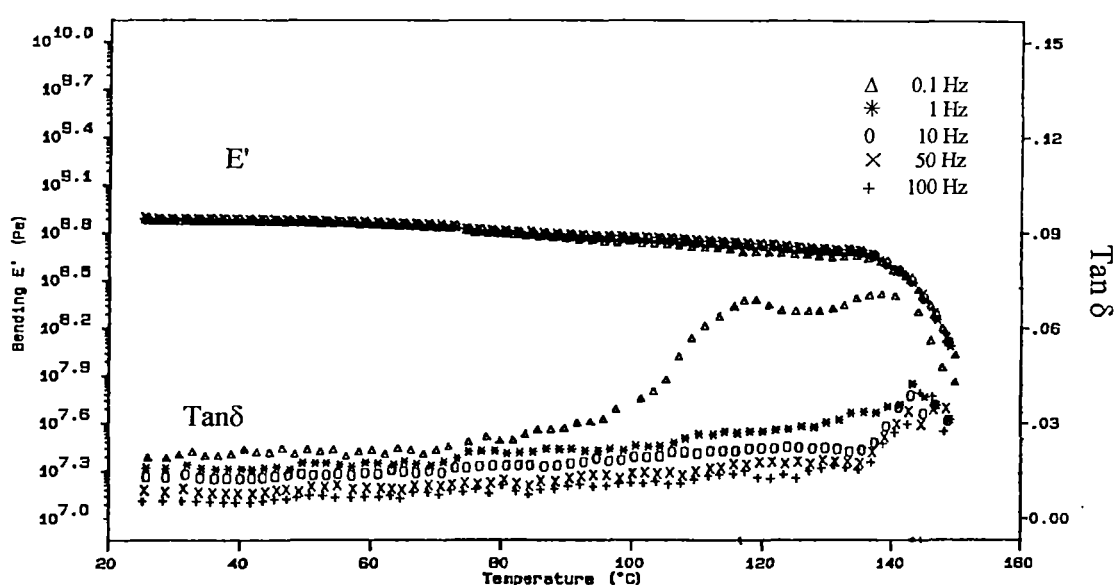


Figure 7.1 Temperature dependence of $\tan\delta$ and storage modulus of neat PF sample at different frequencies

The primary relaxation due to glass transition region is shown at a temperature of 139°C. This is due to the initiation of the molecular motions. The secondary relaxation observed at lower temperature is due to the restricted motion of the molecular chains in the crosslinked network.²⁵ The secondary transitions are caused by the same type of motion occurred at the main Tg but for some reasons become active at much lower temperatures.⁶ As expected, the transition temperatures are shifted to higher temperatures as the frequency is increased. The width of the relaxation spectrum expresses the diversity of chain segments and is expected to be higher in three-dimensional polymers than in linear polymers.²⁷ The damping shows its highest value at 0.1Hz frequency. The damping decreases beyond Tg.

The $\tan\delta$ maximum and T_g from the $\tan\delta$ curve for the PF gum sample at different frequencies are given in Table 7.1. The glass transition temperature increases with increase in frequency. The dynamic modulus of the neat PF resin decreases with decrease in frequency. Above T_g , the modulus decreases sharply showing the highly crosslinked nature of neat PF sample. This is due to the fact that the chain motions will be perturbed in the immediate vicinity of crosslinks.

Table 7.1 Values of $\tan\delta$ Maximum, E'' Maximum and T_g Values of Neat PF and Oil Palm Fibre Reinforced PF Composites having 40wt.% Fibre Loading

Fibre length (mm)	$\tan\delta_{max}$					T_g from $\tan\delta_{max}$ ($^{\circ}\text{C}$)				
	Frequency (Hz)					Frequency (Hz)				
	0.1	1	10	50	100	0.1	1	10	50	100
Neat PF	0.07	0.04	0.04	0.03	0.03	139	143	143	145	145
20	0.11	0.09	0.09	0.08	0.08	115	115	115	117	116
30	0.09	0.07	0.07	0.07	0.07	126	126	126	125	125
40	0.08	0.06	0.05	0.05	0.05	133	138	138	137	137
50	0.08	0.06	0.06	0.06	0.06	139	137	139	139	138
E'' Max. $\times 10^{-7}$ (Pa)						T_g from E'' ($^{\circ}\text{C}$)				
Neat PF	3.4	1.6	1.4	1.2	1.1	134	134	141	142	140
20	6.5	5.8	5.8	5.3	5.2	111	111	112	114	114
30	5	4.5	4	3.5	3.4	106	105	105	105	103
40	5	3.8	3.5	3.4	3	132	138	137	137	136
50	3.8	2.9	2.5	2.4	2.3	108	107	107	106	105

The loss modulus of the gum sample at different frequencies is given in Figure 7.2. The curves for 0.1 and 1Hz frequencies show sharp peaks at 134°C . The glass transition temperatures from the E'' curves at different frequencies are

given in Table 7.1. The E'' maximum shows its highest value at the lowest frequency. The T_g value is always lower than that obtained from the $\tan\delta$ curve.

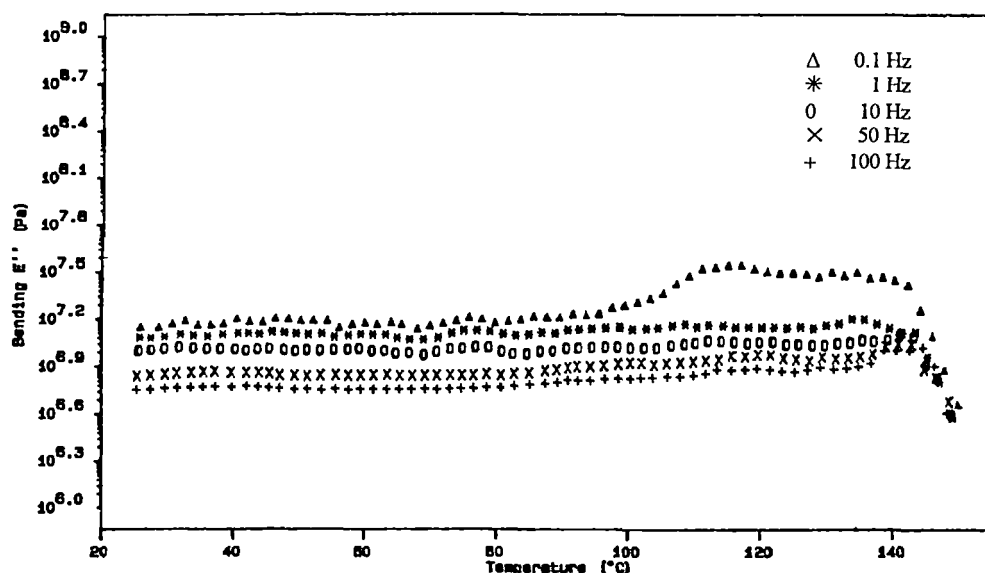


Figure 7.2 Temperature dependence of loss modulus of neat PF sample at different frequencies.

The influence of moulding time and temperature conditions on the modulus-temperature behaviour of phenolic resins has been reported by Landi et al.²⁸ He studied the effect of moulding time and temperature on the modulus and glass transition of phenolics. It was found that T_g of the phenolics increases with post baking. They also found that at low degrees of cure either through short cure time or by low mould temperatures, there were frequently more complex curves, with more than one large stepwise change in modulus and more than one $\tan\delta$ peak. They have reported that for cure time 30s at mould temperature 154°C sharp drop in modulus occurred at 120°C and $\tan\delta$ peaks were observed at 160 and 240°C. But when the cure time was increased to 1800s; sharp changes in storage modulus and $\tan\delta$ at glass transition observed around 180°C. Increase in crosslink density causes an increase in modulus. They also report that modulus of the phenolic resin increases as moulding temperature decreases. The activation energy of the PF

sample for the relaxation at glass transition region was calculated from the Arrhenius plot, which shows a lower value than the filled samples (Table 7.2).

Table 7.2 Activation Energy Values of Neat PF and Oil Palm Fibre/PF Composites having 40wt.% Fibre Loading for Relaxation at Glass Transition Temperature.

Fibre Length (mm)	Activation energy (kJ/mol)
Neat PF	14
20	151
30	264
40	63
50	93

7.2 DYNAMIC MECHANICAL PROPERTIES OF OIL PALM FIBRE/PF COMPOSITES

7.2.1 Effect of Fibre Length

Incorporation of lignocellulosic oil palm fibre in PF resin leads to major changes in the dynamic mechanical properties. Variations in mechanical damping factor and dynamic modulus of the composite as a function of fibre length and temperature at a frequency of 10Hz are drawn in Figure 7.3. It is seen that mechanical damping parameter $\tan\delta$ increases upon fibre addition. Maximum damping is observed for composites having 20mm fibre length at lower frequency and for 40mm fibre length at higher frequency (Table 7.1). At 40mm fibre length, uniform dispersion of the fibres result which leads to better fibre-matrix adhesion and will exhibit comparatively high modulus. However at 20mm fibre loading there will not be sufficient fibre length to withstand the full stress applied at higher frequencies. Irregular trend is observed with fibre length. Broadening of the $\tan\delta$ peak is observed upon fibre addition. The α transition is dependent upon the morphological changes of the components in the composite. Theoretically it is

predicted that the intensity of $\tan\delta$ peak decreases with increasing degree of crystallinity.²⁹ Incorporation of oil palm fibre in PF resin has got a marked impact on the damping characteristics of the composite. A systematic decrease in the intensity of the relaxation with crystallinity is reported for poly (ether ether ketone) by Krishnaswamy et.al.³⁰ Viscoelastic response of the matrix may be perturbed by the presence of fibres. The fibre has got crystalline cellulose region and amorphous waxy materials. This will make changes in the damping characteristics of the composites when incorporated with these fibres. Guo and Ashida³¹ reported that the relative damping of main relaxation of short fibre thermoplastic elastomer composites decreased with increasing fibre length. This is attributed to the unevenness of the strain distribution in the matrix phase, which depends on the fibre length and the modulus of matrix. The molecular and structural characteristics of oil palm fibre reinforced PF composite are more complex owing to its heterogeneous phases and interactions between them.

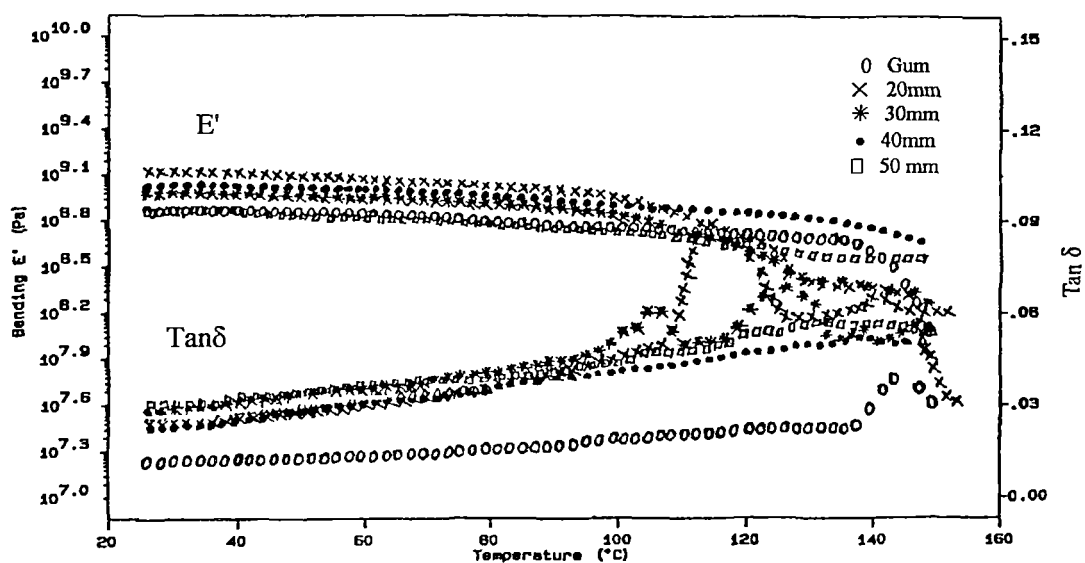


Figure 7.3 Variations in $\tan\delta$ and storage modulus of oil palm fibre/PF composites with fibre lengths having 40wt.% fibre loading at a frequency of 10Hz

The fibre is hydrophilic due to its cellulose and lignin hydroxyl groups. This can form strong chemical adhesion with the hydrophilic resole PF resin. This can be explained using the schematic model of the interface interaction which is given in Figure 4.3 (refer Chapter 4). The morphology and interactions at the interface influence the relaxation. Scanning electron micrograph of tensile fracture of oil palm fibre/PF composites give evidence for the fibre-matrix interactions (Fig. 4.4; refer Chapter 4). Fibre breakage and fibrillation were found to be the major failure criteria, which results from the better fibre-matrix adhesion. Ibarra and Panos³² interpreted dynamic properties of SBS/carbon fibre composites based on T_g measured in terms of maximum damping temperature as well as the apparent activation energy of the relaxation process to explain the fibre-matrix interactions. Viscoelastic phenomena in the fracture of thermosetting resins were reported recently by McKilliam et al.³³ The thermosetting resins have shown viscoelastic non-linearity to be compatible with the complex fracture behaviour of thermosets. In the case of composites having 20 and 30mm fibre lengths, a secondary relaxation peak is observed at a temperature of 115 and 105°C respectively (Fig. 7.3). The secondary transition may be due to the vibrational motion of the entrapped chain segments or chemical groups within the crosslinked network.⁶ The α -transition parameters (T_g) exhibit significant sensitivity to the morphological differences, chemical changes such as rupture of hydrogen bonds etc. occurring in the system. Presence of fibres restricts the segmental mobility. It is reported that the effect of fibre will depend on the fibre-matrix bond strength because strong bonding is essential for the activation of the fibre constraint during the stress transfer mechanism at the interface, whereas poor bonding results in energy dissipation at the interface.³⁴

Fibre length has got a determining role at the interfacial phenomena. Effective stress transfer takes place only at uniform dispersion of the fibres at critical fibre length. Figure 7.4 shows the variation of $\tan\delta$ at 100°C with fibre length. Upto 30mm fibre length gradual increase in damping is observed at all frequencies. At 40mm fibre length the value at 100°C decreases and further

increase in fibre length increases the $\tan\delta$ value. This can be attributed to the better fibre-matrix adhesion at 40mm fibre length. At very low fibre length, fibre agglomeration and at very high fibre length, fibre entanglement results which leads to increased fibre to fibre contact. These aspects change the effective aspect ratio. As a result fibre-matrix interaction is decreased. It has already been reported that at 40mm fibre length oil palm fibre exhibits better mechanical properties with PF due to the increased fibre-matrix interaction.³⁵ This is considered as its critical fibre length. In order to understand the effect of frequency on the dynamic mechanical properties of the composites, the $\tan\delta$ and storage modulus were plotted as a function of temperature at different frequencies (Fig. 7.5). The $\tan\delta$ value shows regular increase with decrease in frequency of vibration while E' shows a reverse trend.

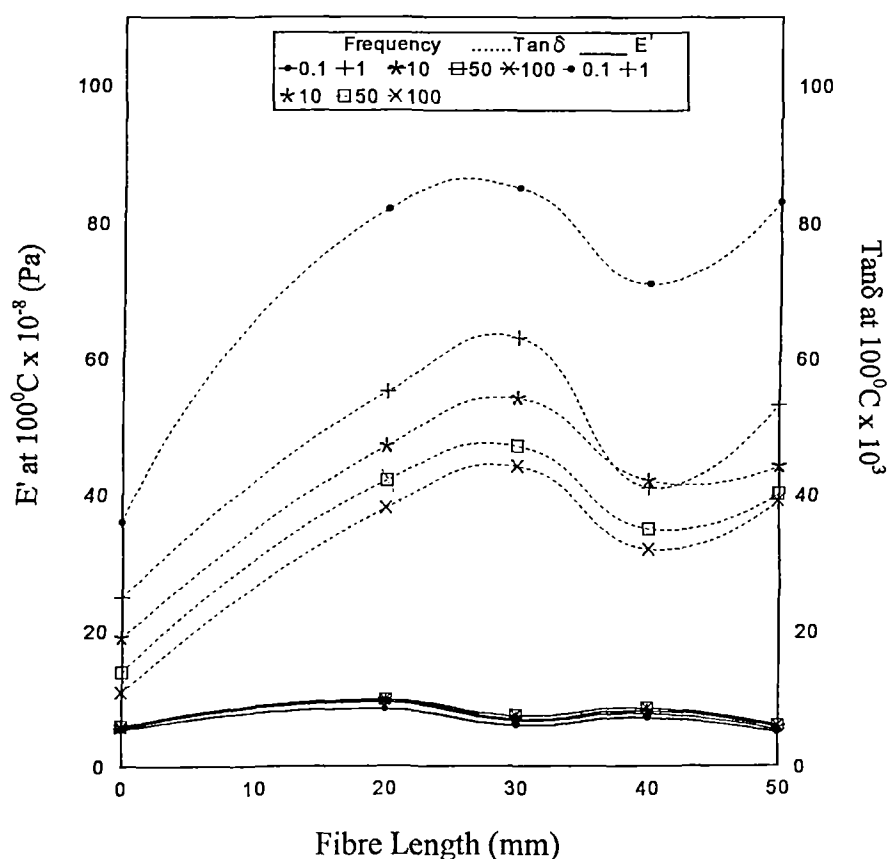


Figure 7.4 Effect of fibre length on the $\tan\delta$ and storage modulus of the oil palm fibre/PF composites at 100°C.

Higher relaxation is expected at low fibre length due to its inefficient packing than at higher fibre length. The increase in damping in a composite can be attributed to the matrix material. In a discontinuous fibre composite, the distance between two abutting fibre ends is called the fibre end gap size. The increased amount of matrix material leads to increased damping.³⁶ However, when the fibre length is increased the fibre end gap size decreases thereby decreasing the damping peak. Further increase of fibre length decreases the glass transition temperature of the system (Table 7.1). This can be interpreted as a result of variation in the properties of the interface between fibre and matrix of the composites having different fibre lengths. Composites having 20 and 30mm fibre lengths show high relaxation peak heights, which are closely related to glass transition phenomenon.

Fibre incorporation increases the storage modulus due to the stiffness conferred upon the material by the fibre within the matrix. For 20 and 30mm fibre length sharp drop in modulus is observed around 120°C (Fig. 7.3). Above this region these composites have lower modulus than PF gum sample. Variation in

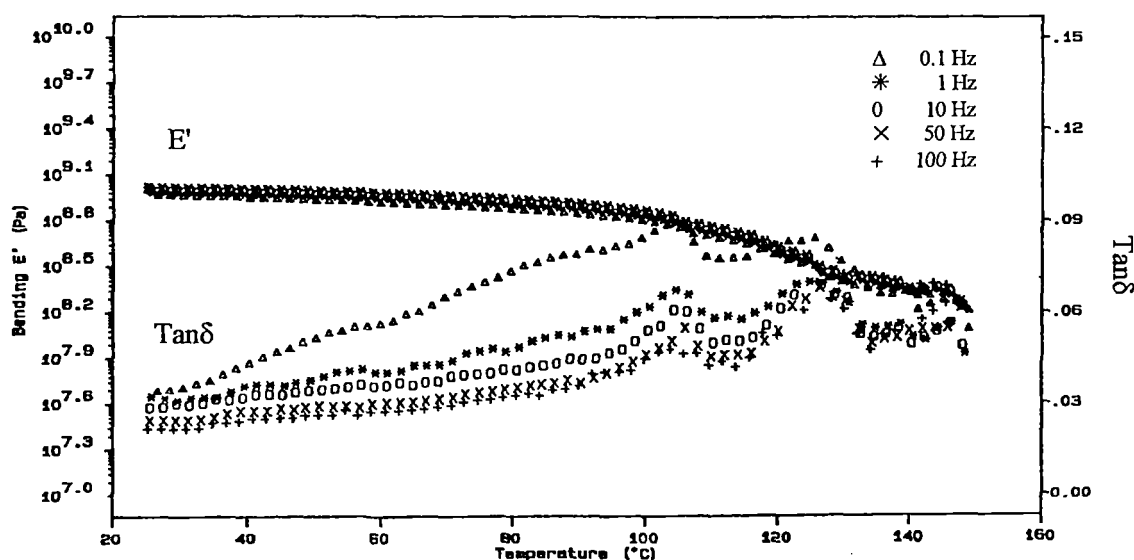


Figure 7.5 Effect of frequency on the variations in $\tan\delta$ and storage modulus of oil palm fibre/PF composites having 40wt.% fibre loading and 30mm fibre length.

dynamic modulus at 100°C with fibre length at different frequencies is plotted in Figure 7.4. The dynamic modulus and loss factors in fibre reinforced plastic composites are influenced by fibre orientations. At higher fibre lengths, fibre entanglement may occur which reduces the fibre orientation in composites. Randomly oriented fibres restrict the segmental motion of the polymer chains to a higher extent than aligned fibrous composite. The irregular variations in modulus with fibre length can be attributed to these changes in the orientation factor. Composites having the fibre with 20 and 40mm length exhibit comparatively higher loss modulus (Fig. 7.6). The E'' maximum observed for different fibre lengths is given in Table 7.1. Changes in loss modulus with frequency as a function of temperature for composite having 30mm fibre length is evident from Figure 7.7. The loss factor decreases with increasing the frequency. The glass transition temperatures from E'' curve are determined.

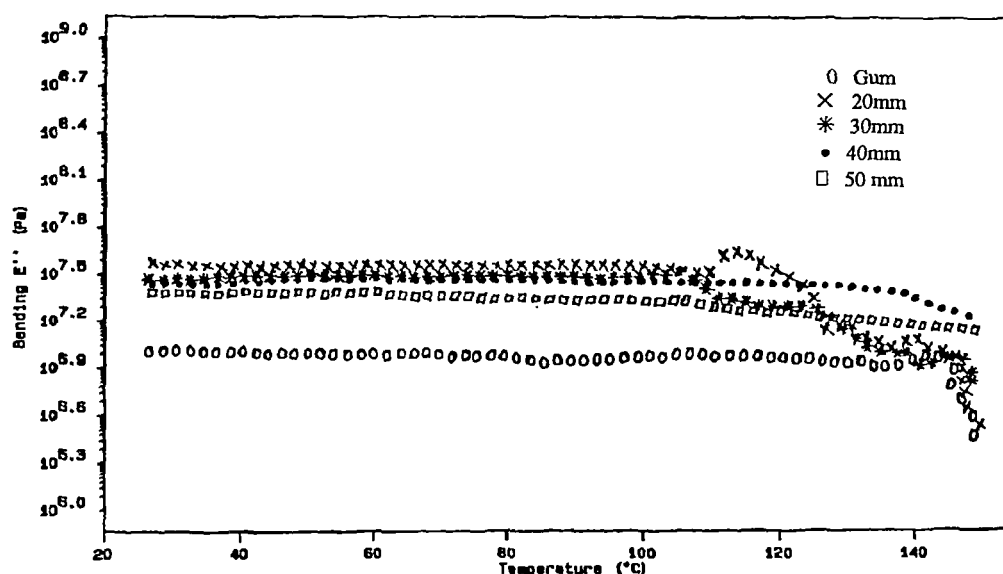


Figure 7.6 Variations in loss modulus of oil palm fibre/PF composites with fibre lengths having 40wt.% fibre loading at a frequency of 10Hz.

The relationship between glass transition temperature and frequency for the composites are well explained by the Arrhenius relationship. The apparent

activation energy (H) for the relaxation process at the glass transition region were calculated by means of the following equation.¹⁷

$$\log f = \log f_0 - H/2.303 RT \quad (7.5)$$

Where f_0 is an experimental constant, f and T are the measuring frequency and the glass transition temperature respectively and R is gas constant. The activation energy for the relaxation process is much increased upon fibrous reinforcement. Maximum activation energy is observed for 30mm fibre length (Table 7.2). Presence of fibre restricts the motion of the molecular chains and segments, which increases the apparent activation energy. Fibre length is a determining factor, which affects the relaxation process thereby the activation energy of the process. At higher fibre lengths, due to the lack of effective fibre-matrix adhesion, activation energy required for the relaxation is decreased.

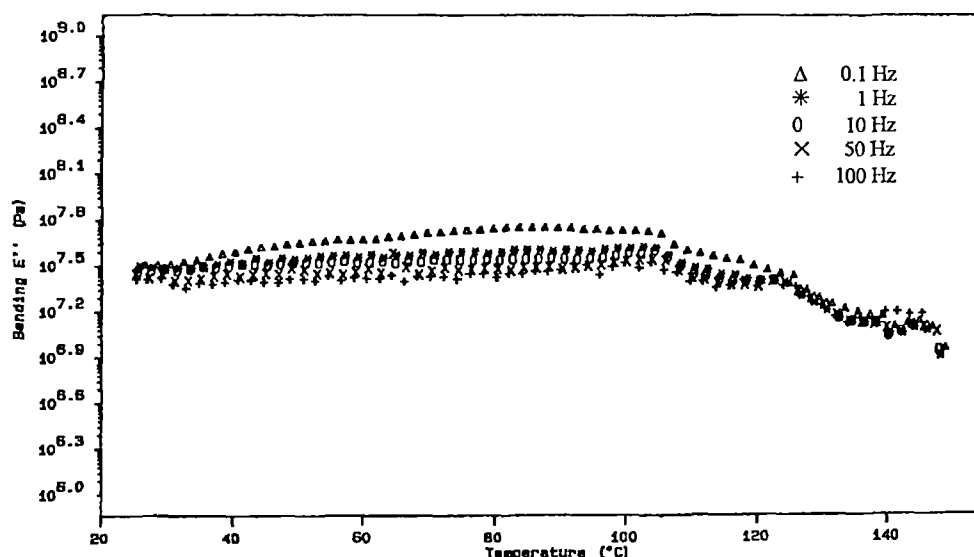


Figure 7.7 Effect of frequency on the variation of loss modulus of oil palm fibre/PF composites having 40wt.% fibre loading and 30mm fibre length.

7.2.2 Effect of Fibre Content

It is seen from Figure 7.8 that as the fibre content increases, the mechanical damping increases at a frequency of 10 Hz. The fibre-matrix interfacial area is proportional to the fibre content. The increase in the mechanical damping can be explained by

the fact that the larger the interface area, the more energy loss at the interfaces. Dong and Gauvin³⁷ observed a linear increase of the damping at the interfaces with fibre volume fraction in carbon fibre/epoxy composites. The composites having 50mm fibre length show two damping peaks. This may be due to the decreased fibre-matrix adhesion and agglomerate formation of the fibres within the matrix. The presence of single peak in damping curve of the composites suggests better interaction between the fibre and matrix. This is due to decreased heterogeneity in the composite. Hon and Chao³⁸ have carried out DMTA investigations on benzylated wood/polystyrene composites. They used dynamic properties as a tool to determine the compatibility and dispersion of wood and polystyrene.

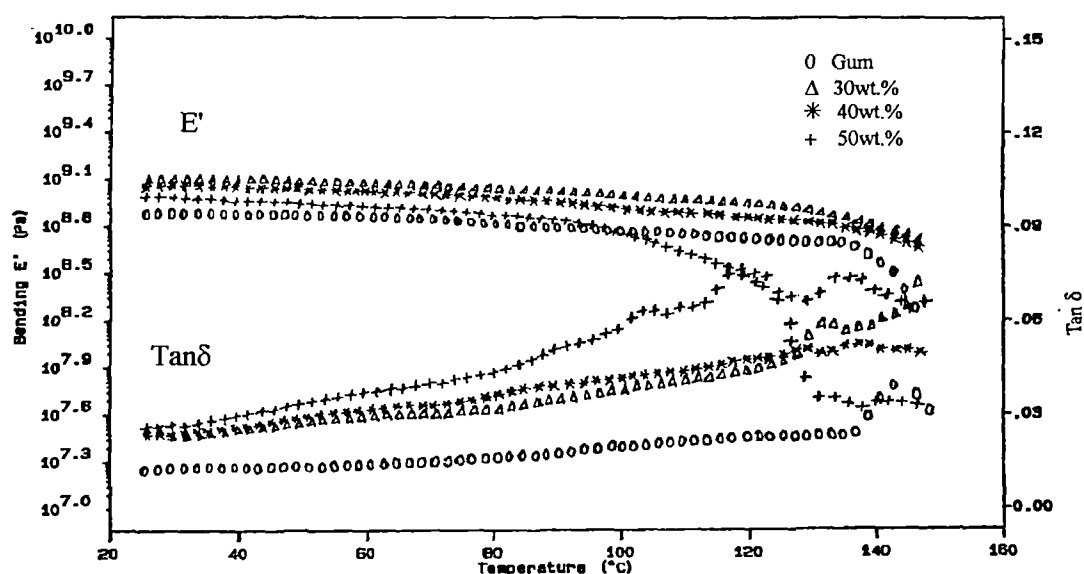


Figure 7.8 Variations in $\tan\delta$ and storage modulus of oil palm fibre/PF composites with fibre loading having 40mm fibre length at a frequency of 10Hz.

The $\tan\delta$ maximum observed at different frequencies is given in Table 7.3. Highest $\tan\delta$ value is observed for 50wt.% fibre loading at all the frequencies. Figure 7.9 gives the variation of $\tan\delta$ at 100°C with fibre content at different frequencies. A gradual increase in damping is observed with fibre content for all

frequencies. The effect of frequency on the mechanical damping of the composites is similar to that discussed earlier. Damping increases as frequency decreases. This can be understood from the three dimensional damping peak of 50wt.% composite from Figure 7.10. The glass transition temperature of the composite obtained from damping curve decreases beyond 30wt.% fibre loading at all frequencies (Table 7.3). Since the Tg of the natural fibre is expected to be very much lower than PF, fibre incorporation normally results in a decrease of the glass transition temperature. Flexibility of groups, molecular polarity of components and presence of voids in composites affect the Tg of a composite. The chances for void formation are higher with increasing fibre loading. At very high loading this effect becomes prominent and facilitates the chain mobility at lower temperatures resulting in the decrease of Tg value.

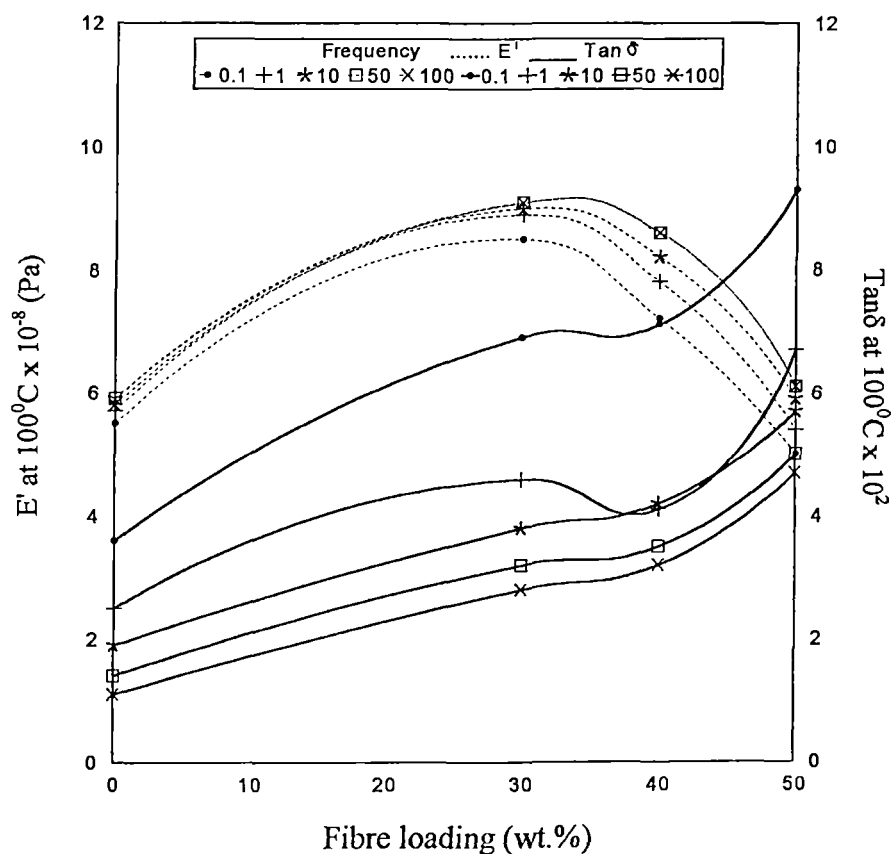


Figure 7.9 Effect of fibre loading on the $\tan\delta$ and storage modulus of oil palm fibre/PF composites at 100°C.

Table 7.3 Values of Tan δ Maximum, E" Maximum and Tg Values of Neat PF and Oil Palm Fibre/PF Composites having 40mm Fibre Length

Fibre loading (wt.%)	tan δ_{\max}					Tg from tan δ_{\max} ($^{\circ}\text{C}$)				
	Frequency (Hz)					Frequency (Hz)				
	0.1	1	10	50	100	0.1	1	10	50	100
Neat PF	0.07	0.04	0.04	0.03	0.03	139	143	143	145	145
30	0.08	0.07	0.07	0.07	0.07	148	148	148	147	147
40	0.08	0.06	0.05	0.05	0.05	133	138	138	137	137
50	0.10	0.08	0.08	0.15	0.15	119	119	119	136	142
	E" Max. $\times 10^{-7}$ (Pa)					Tg from E" ($^{\circ}\text{C}$)				
Neat PF	3.4	1.6	1.4	1.2	1.1	115	134	141	142	140
30	6	4.6	4.4	4.3	4.1	129	130	130	130	130
40	5	3.8	3.5	3.4	3	132	138	137	137	136
50	4.8	4	3.7	3.1	2.8	118	117	119	119	119

Changes in dynamic modulus, a measure of the stiffness of the composites with fibre loading at 10Hz frequency is given in Figure 7.8. Maximum modulus is observed for 30wt.% loading. Noticeable decrease in modulus value is observed for 50wt.% loaded composite beyond 95°C . This value is less than the neat PF sample. The E' value at 100°C is plotted as a function of fibre loading at different frequencies (Fig. 7.9). The decrease in the modulus values for 50wt.% may be due to the decreased interfacial bonding. At higher fibre loading processing becomes difficult resulting in the uneven distribution of the fibres in the matrix which leads to agglomeration, increased fibre to fibre contact and presence of voids in the composite. These factors will reduce the modulus of the composite. As the temperature increases the modulus decreases which may be due to the changes in the properties of the oil palm fibre and interfacial debonding during vibrational

motion. In the case of carbon fibre reinforced nylon 66 composites, an increase in relative storage modulus at all temperatures was observed with increase in volume fraction of fibre.³⁹ This is explained by the fact that the modulus of the carbon fibres is not affected by changes in temperatures. As frequency of vibration increases, the E' value of the composites increases. A regular trend is observed for all the composites. A sharp drop in modulus is observed at the glass transition region.

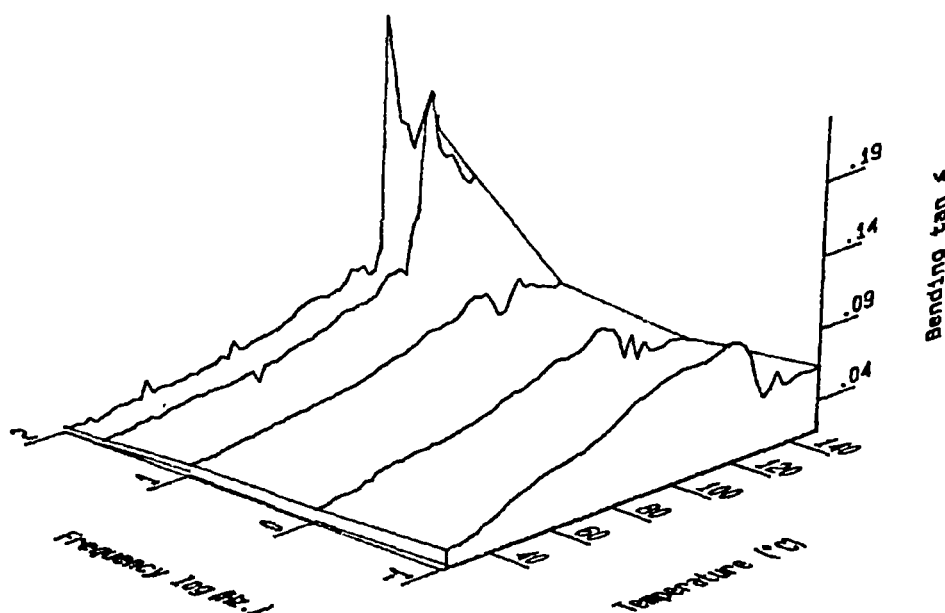


Figure 7.10 Mechanical damping parameter of oil palm fibre/PF composite having 50wt.% fibre loading and 40mm fibre length.

Figure 7.11 shows the variations in E'' value with fibre loading. The value decreases marginally with fibre loading. However it is greater than the gum sample. The loss factor of 50wt.% composite decreases to a very low value that is lower than that of PF sample beyond 120°C. Highest value of E'' maximum is observed for 30wt.% loading (Table 7.3). The T_g values obtained from E'' curves were lower than that obtained from $\tan\delta$ curves. This is due to the fact that the relaxation peak in loss modulus is always slightly shifted to lower temperature compared to the

damping peak. The variation of T_g with fibre loading of the composites is plotted in Figure 7.12. The T_g value shifts to a higher value at 30wt.% fibre loading, but a negative shift observed from loss modulus measurement. The loss modulus increases with decreasing frequency as described earlier. The large drop in modulus is observed at a temperature around 120°C for 0.1 and 1Hz frequencies.

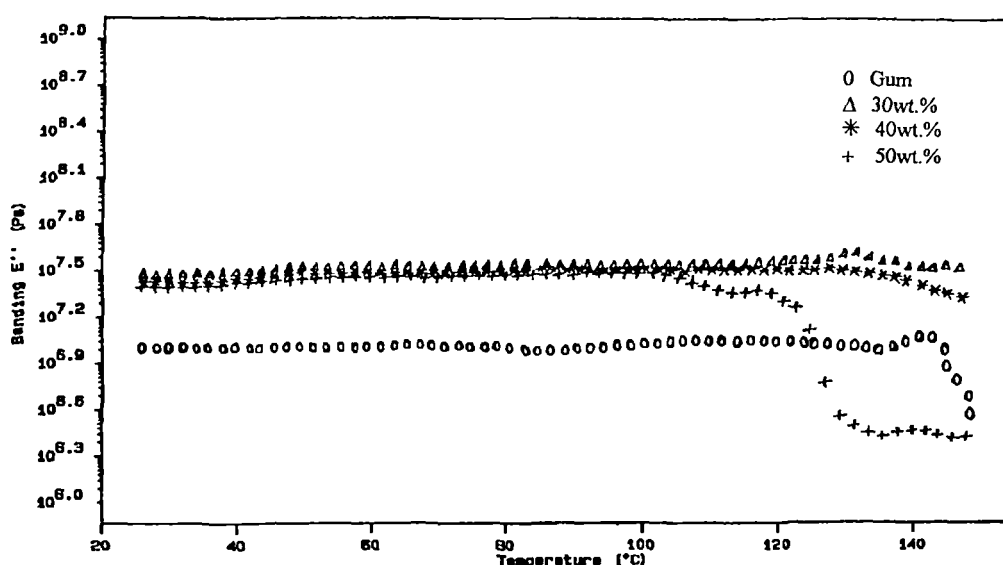


Figure 7.11 Variations in loss modulus of oil palm fibre/PF composites with fibre loading having 40mm fibre length at a frequency of 10Hz.

Activation energy for the relaxation process at glass transition region is calculated from the Arrhenius relationships. The activation energy values are given in Table 7.4. As the fibre loading increases, the activation energy decreases. At higher fibre loading the fibre-matrix adhesion decreases due to the increased fibre-fibre contact and phase separation, which decreases the activation energy for the relaxation process.

Composites having 30wt.% fibre loading exhibits highest energy as explained by its highest dynamic modulus. At a high fibre loading, fibre to fibre contact is more. Application of a vibrational stress therefore brings about interfacial failure.

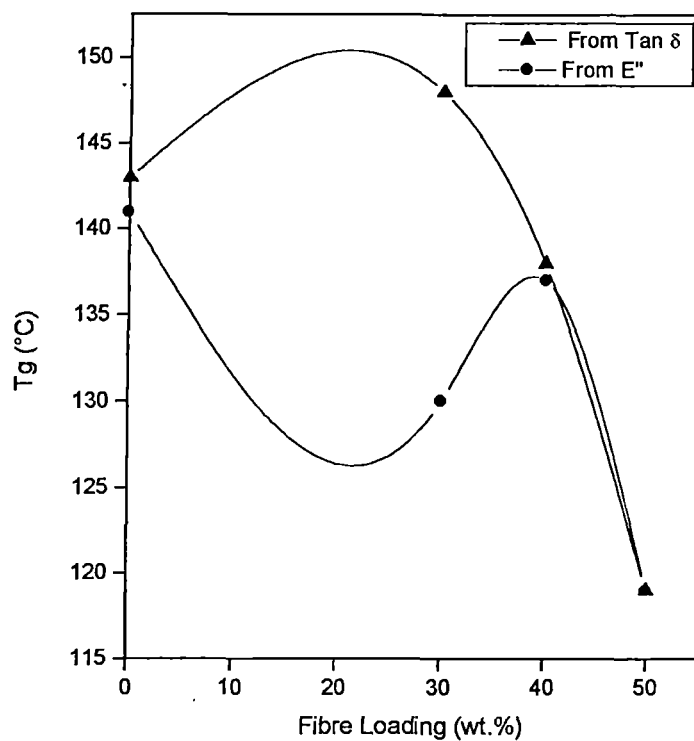


Figure 7.12 Variation of glass transition temperature of the oil palm fibre/PF composites with fibre loading at a frequency of 10Hz.

Table 7.4 Activation energy values of neat PF and oil palm fibre/PF composites having 40mm fibre length for relaxation at glass transition temperature

Fibre loading (wt.%)	Activation energy (kJ/mol)
Neat PF	14
30	308
40	63
50	15

7.2.3 Effect of Fibre Modification

The dynamic mechanical properties of the treated composites were analysed. Detailed discussion on the physical and chemical modifications occurred on the fibre surface on various treatments such as alkali treatment, acetylation, silane treatment, acrylonitrile grafting, latex coating, peroxide treatment, permanganate treatment and isocyanate treatment were given in Chapter 3. Damping and modulus characteristics of the treated composites are given in Figure 7.13. Composite mercerised for 24hrs. shows a jump at the glass transition with prominent secondary relaxation peak in the damping curve. A gradual increase in peak height is observed with frequency (Fig. 7.14).

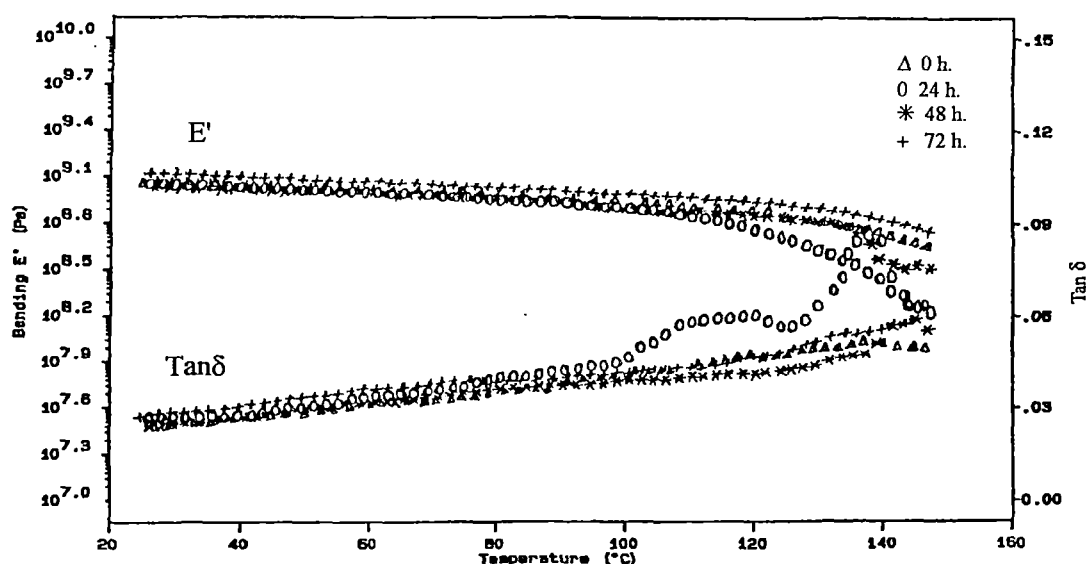


Figure 7.13 Variations in $\tan\delta$ and storage modulus of treated oil palm fibre/PF composites having 40wt.% fibre loading and 40mm fibre length at a frequency of 10Hz.

Increasing the treatment time to 48hrs. decreases the value, which is lower than for the untreated sample. However composite treated for 72hrs. shows higher value than untreated sample. It has already been observed that the higher the damping at the interfaces, the poorer the interface adhesion.³⁷ A decrease in damping associated with the improvement of interface bonding is observed by Cinquin et.al.⁴⁰ Ko et al.⁴¹

also observed a decrease in the damping that was related to the changes of interfaces in carbon fibre epoxy systems. This is due to the fact that a composite with poor interface bonding tends to dissipate more energy than that with good interface bonding. The highest value of $\tan\delta$ maximum is observed for 24hrs. treated composite (Table 7.5).

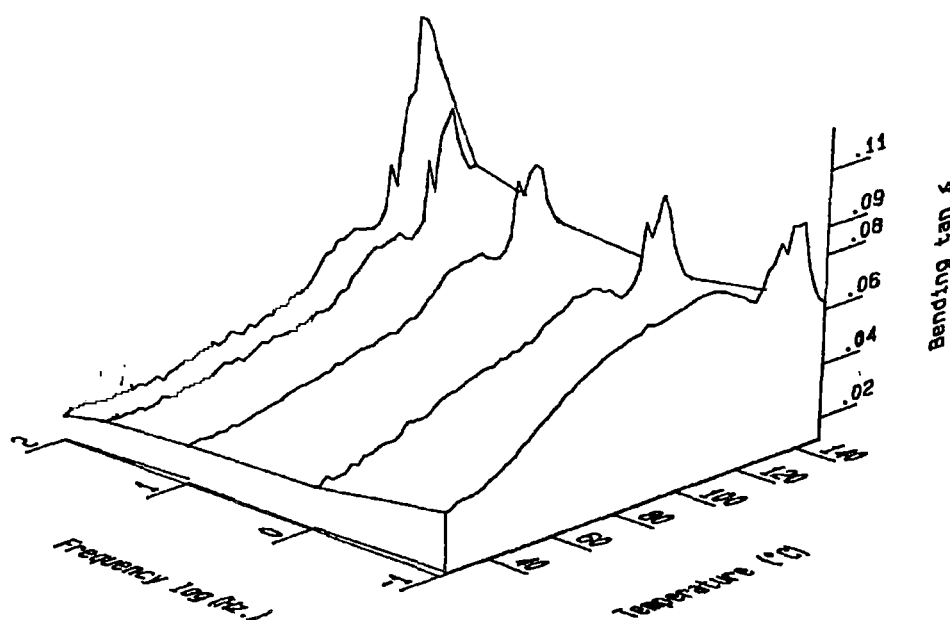


Figure 7.14 Mechanical damping parameter of alkali treated (24hrs) oil palm fibre/PF composite having 40wt.%fibre loading and 40mm fibre length.

Variation of $\tan\delta$ at 100°C with treatment at different frequencies is given in Figure 7.15. Effect of frequency on $\tan\delta$ shows similar trend as earlier. The highest jumping at T_g is observed at highest frequency. The variation of $\tan\delta$ with temperature shows similar trend at all frequencies for 24hrs. treated composite. The damping characteristics of other treated composites are shown in Figure 7.16. At all temperatures the latex treated composites exhibit highest $\tan\delta$ value among the untreated and treated composites. The fibre became most hydrophobic on latex coating, which leads to less fibre-matrix interaction resulting increase in damping properties. Other treatment leads to slight enhancement in damping values

(Table 7.5). Damping values of the treated composite generally decreased on increase of frequency. The $\tan\delta$ values at 100 °C for the untreated and treated composites are given in Table 7.6. Compared to the untreated composites all treated composites exhibit higher damping.

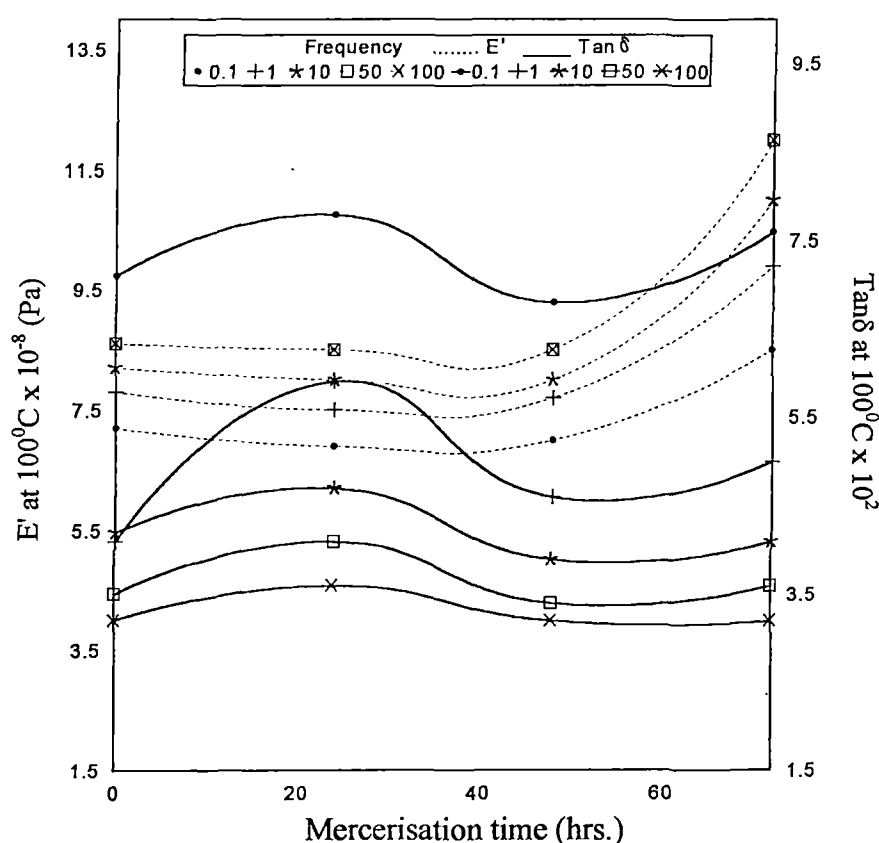


Figure 7.15 Effect of mercerisation time on the $\tan\delta$ and storage modulus of alkali treated oil palm fibre/PF composites having 40wt.% fibre loading at 100°C.

The glass transition temperature shows a shift towards higher temperature region on increasing the time of treatment. On silane, acrylation, acrylonitrile and latex treatments, a considerable decrease in T_g values is observed especially at lower frequencies. Lowest value is observed for latex coated composite (Table 7.5). This is also attributed to the weak interfacial interaction, which facilitates the relaxation process. The dynamic modulus of the composite increases with treatment time (Fig. 7.13). Maximum stiffness is exhibited by composite treated for 72hrs.

Table 7.5 Values of Tan δ Maximum, E" Maximum and Tg Values of Untreated and Treated Oil Palm Fibre/PF Composites having 40mm Fibre Length and 40 wt.% Fibre Loading.

Fibre treatment	tan δ_{\max} Frequency (Hz)					Tg from tan δ_{\max} ($^{\circ}$ C) Frequency (Hz)				
	0.1	1	10	50	100	0.1	1	10	50	100
Untreated	0.08	0.06	0.05	0.05	0.05	133	138	138	137	137
Mercerised (24hrs)	0.09	0.09	0.08	0.09	0.10	139	138	138	138	139
Mercerised (48hrs)	0.07	0.06	0.06	0.06	0.07	146	145	145	144	144
Mercerised (72hrs)	0.08	0.07	0.07	0.06	0.06	148	147	147	147	146
Acetylation	0.14	0.09	0.08	0.08	0.07	118	122	139	138	138
Peroxide	0.11	0.08	0.07	0.06	0.06	147	148	156	156	153
Permanganate	0.11	0.08	0.06	0.05	0.05	151	151	155	155	154
Isocyanate	0.14	0.10	0.10	0.09	0.09	133	136	135	134	134
Silane	0.14	0.08	0.07	0.06	0.06	110	118	118	120	121
Acrylation	0.13	0.09	0.08	0.07	0.07	120	138	137	137	137
Acrlonitrile	0.14	0.10	0.08	---	---	114	122	120	---	---
Latex	0.18	0.15	0.15	---	---	107	119	122	---	---
	E" Max. $\times 10^{-7}$ (Pa)					Tg from E" ($^{\circ}$ C)				
Untreated	5	3.8	3.5	3.4	3	132	138	137	137	136
Mercerised (24hrs)	5.8	4.8	4.5	4	3.8	133	133	131	131	130
Mercerised (48hrs)	5	3.9	3.5	3	3.4	138	137	137	137	137
Mercerised (72hrs)	7	4.5	4	3.8	3.9	135	134	134	135	135
Acetylation	7.88	7.70	7.65	7.60	7.57	97	120	119	122	121
Peroxide	7.97	7.87	7.84	7.81	7.77	130	142	145	149	151
Permanganate	7.91	7.78	7.72	7.66	7.63	144	151	155	155	155
Isocyanate	7.99	7.77	7.70	7.71	7.70	102	129	131	132	132
Silane	7.93	7.73	7.65	7.61	7.58	101	103	106	106	106
Acrylation	7.83	7.61	7.52	7.48	7.42	113	124	126	126	129
Acrylonitrile	8.05	7.85	7.79	---	---	99	113	114	---	---
Latex	7.49	7.44	7.44	---	---	101	102	102	---	---

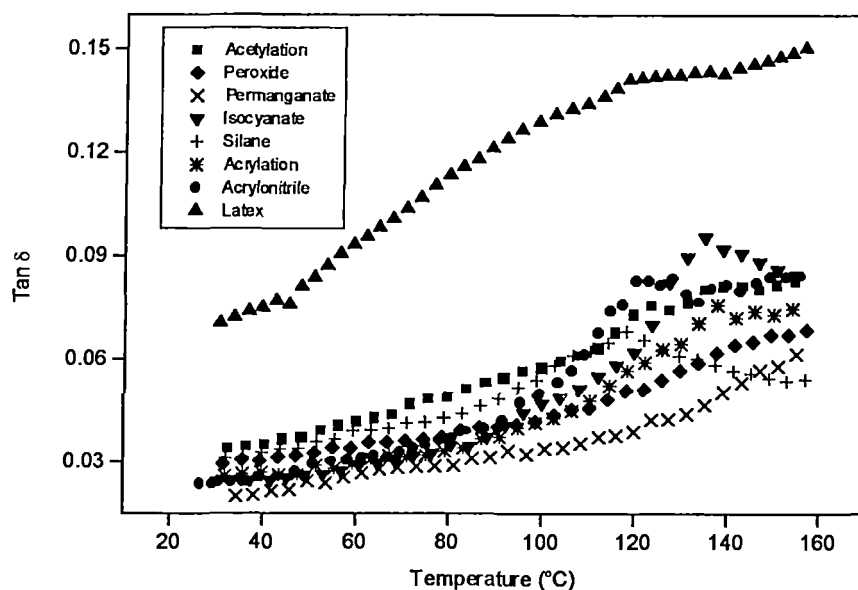


Figure 7.16 Effect of fibre surface modifications on the $\tan\delta$ of oil palm fibre/PF composites at a frequency of 10Hz.

Table 7.6 Values of E' at 100°C and $\tan\delta$ at 100°C of Treated Oil Palm Fibre/PF Composites having 40wt.% Fibre Loading

Fibre Treatment	E' at 100°C (Pa) Frequency (Hz)					$\tan\delta$ at 100°C ($^{\circ}\text{C}$) Frequency (Hz)				
	0.1	1	10	50	100	0.1	1	10	50	100
Untreated	7.20	7.80	8.20	8.60	8.60	0.07	0.04	0.04	0.04	0.03
Acetylation	8.81	8.85	8.88	8.89	8.9	0.12	0.07	0.06	0.05	0.05
Peroxide	9.04	9.07	9.09	9.1	9.11	0.07	0.05	0.04	0.04	0.03
Permanganate	8.99	9.02	9.04	9.05	9.05	0.06	0.04	0.03	0.03	0.03
Isocyanate	8.94	8.98	9.00	9.00	9.02	0.11	0.06	0.05	0.04	0.04
Silane	8.81	8.86	8.89	8.90	8.91	0.13	0.07	0.06	0.05	0.04
Acrylation	8.78	8.82	8.83	8.85	8.86	0.10	0.06	0.04	0.03	0.03
Acrylonitrile	8.95	8.99	9.02	---	---	0.13	0.07	0.05	---	---
Latex	8.18	8.23	8.27	---	---	0.18	0.14	0.13	---	---

This can be attributed to the increased fibre-matrix adhesion. Composite treated for 24hrs. shows a sharp drop in dynamic modulus beyond 110°C. Modulus of the treated composites at 100°C is plotted in Figure 7.15. Modulus increases with frequency. The storage modulus of the treated composites is given in Figure 7.17. Highest modulus is observed for peroxide and permanganate treated composites. In acetylated, silane treated, acrylonitrile, isocyanate and acrylated composites a sharp decrease in modulus is observed around 120°C. Latex treated composite has got the lowest storage modulus. The E' value at 100°C for treated composites is given in Table 7.6. Compared to the untreated composite, the dynamic modulus of the composites made out of treated fibre is high. The variation of loss factor for different treated composites is given in Figure 7.18 and 7.19. Irregular trend is observed with treatment time. But there is not much difference. Whenever there exists a strong interface, the material resists high strain and the loss factor does not show much increment. For 24hrs. treated composite two relaxations are observed. Acrylated and latex treated composites show very low loss modulus values. The E'' maximum for each treated composites at different frequencies are given in Table 7.5.

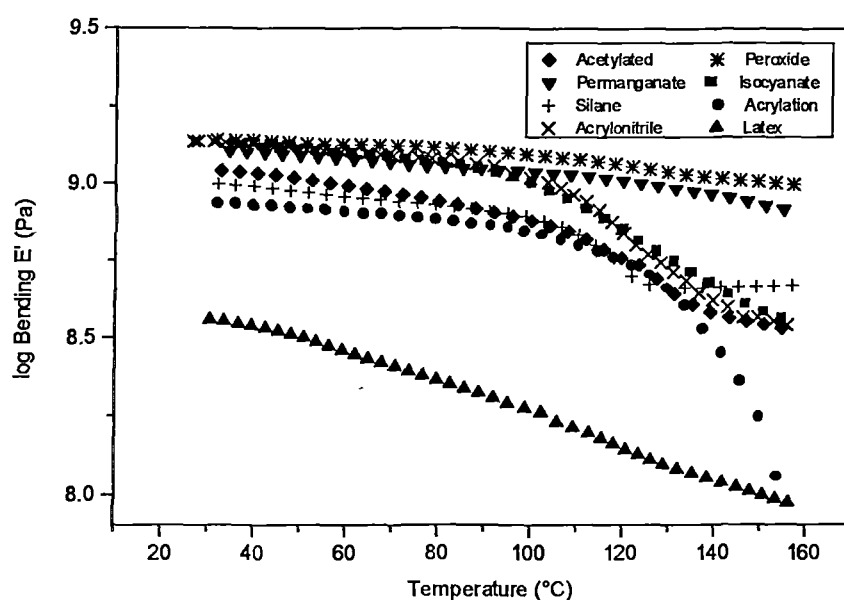


Figure 7.17 Effect of fibre surface modifications on the storage modulus of oil palm fibre/PF composites at a frequency of 10Hz.

The T_g value obtained from E'' curve are always lower than that obtained from $\tan\delta$ curve. Treated composites such as acrylonitrile, acetylated, isocyanate, silane and acrylated composites show sharp relaxation at the glass transition region. The loss modulus values increase with decrease in frequency. But after relaxation trend is reversed.

Activation energies of relaxation processes in treated composites were given in Table 7.7. The value of untreated composite is almost same for 24 hrs. alkali treated composite. On increasing the mercerisation time to 48 and 72hrs. the activation energy enhanced by four times. This supports the assumption that the interfacial adhesion became strong upon alkali treatment for higher durations. The relaxation process takes more energy for the tightly crosslinked fibre network system of the composites. This raises the activation energy. Permanganate treatment increases the activation energy. All other treatments decrease the activation energy for relaxation.

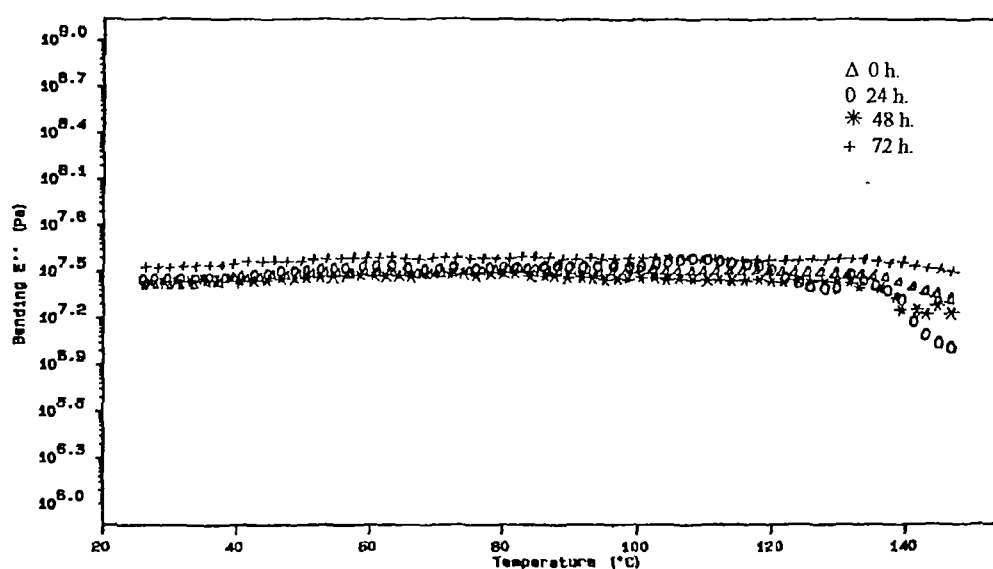


Figure 7.18 Variations in loss modulus of alkali treated oil palm fibre/PF composites having 40wt. % fibre loading and 40mm fibre length at a frequency of 10Hz.

Table 7.7 Activation Energy Values of Untreated and Treated Oil Palm Fibre/PF Composites having 40mm Fibre Length and 40wt.% Fibreloading for Relaxation at Glass Transition Temperature.

Fibre treatment	Activation energy (kJ/mol)
Untreated	63
Mercerised (24hrs)	67
Mercerised (48hrs)	253
Mercerised (72hrs)	250
Acetylation	16
Peroxide	44
Permanganate	93
Isocyanate	17
Silane	40
Acrylation	20
Acrylonitrile	27
Latex	18

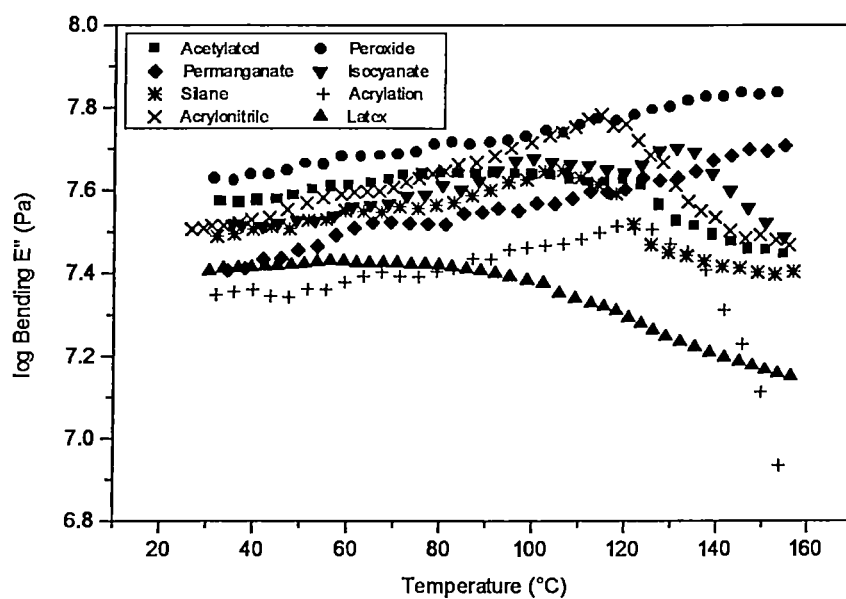


Figure 7.19 Effect of fibre surface modifications on the loss modulus of oil palm fibre/PF composites at a frequency of 10Hz.

7.3 DYNAMIC MECHANICAL PROPERTIES OF OIL PALM FIBRE/GLASS HYBRID PF COMPOSITES

7.3.1 Effect of Hybrid Fibre Ratio

A schematic representation of alignment of fibre in hybrid composites is given in Figure 5. . In hybrid composites intermingling of oil palm fibre and glass is possible on impregnation of fibre mats into PF resin. The variation of the mechanical damping parameter with temperature for the hybrid composites having different combinations of relative volume fractions of glass and oil palm fibres are shown in Figure 7.20. Unhybridised oil palm fibre/PF and glass/PF composites exhibit relatively lower damping compared to hybrid composites. Highest value of damping is observed for hybrid composite having maximum oil palm fibre volume fraction. However an irregular trend is observed with change in the oil palm fibre fraction. Large relaxation jump at glass transition is observed for the hybrid composites having 0, 0.3 and 0.7 relative volume fractions of oil palm fibre.

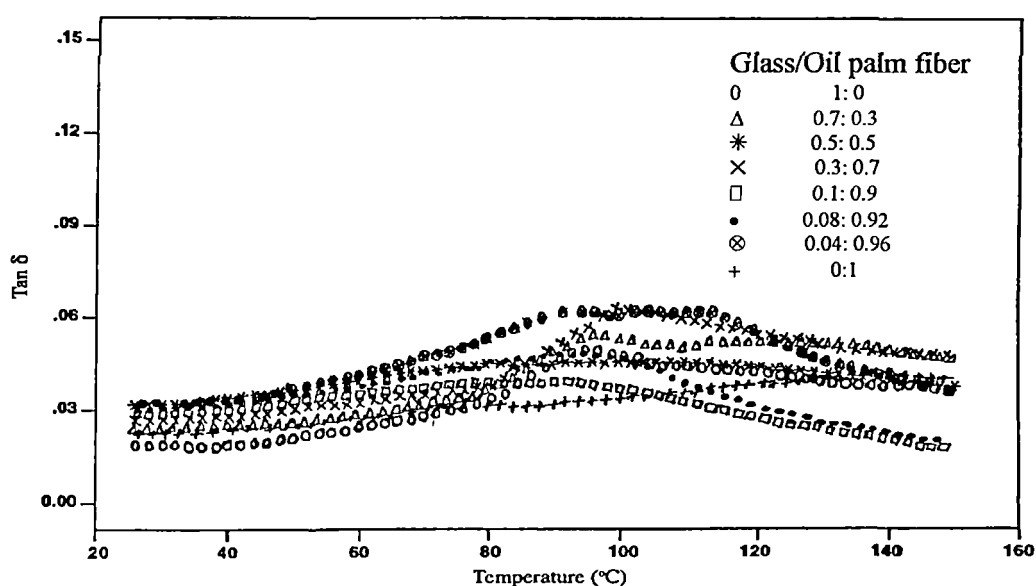


Figure 7.20 Variations in $\tan\delta$ of oil palm fibre/glass hybrid PF composites having 40wt.%fibre loading at a frequency of 10Hz.

Broad peaks are observed for the hybrid composites. The broadening of the transition region is due to the initiation of the relaxation process within the composites upon the incorporation of the fibres. Similar effect has been observed for glass-polyethylene/PMMA hybrid composites.⁴² Upto 80°C the damping decreases with increasing glass fibre content. At the glass transition region intense damping observed. Thus the incorporation of small amount of glass fibre to oil palm fibre/PF composite enhances the damping characteristics of the composite. Ghosh et al.⁴³ studied the damping effect of jute fibre/glass hybrid epoxy composite. They have found that use of jute fibre contributes to a lowering in the damping character of the composite. The $\tan\delta$ maximum observed at different frequencies is given in Table 7.8. The effect of relative volume fraction oil palm fibre on the $\tan\delta$ value is clear from Figure 7.21.

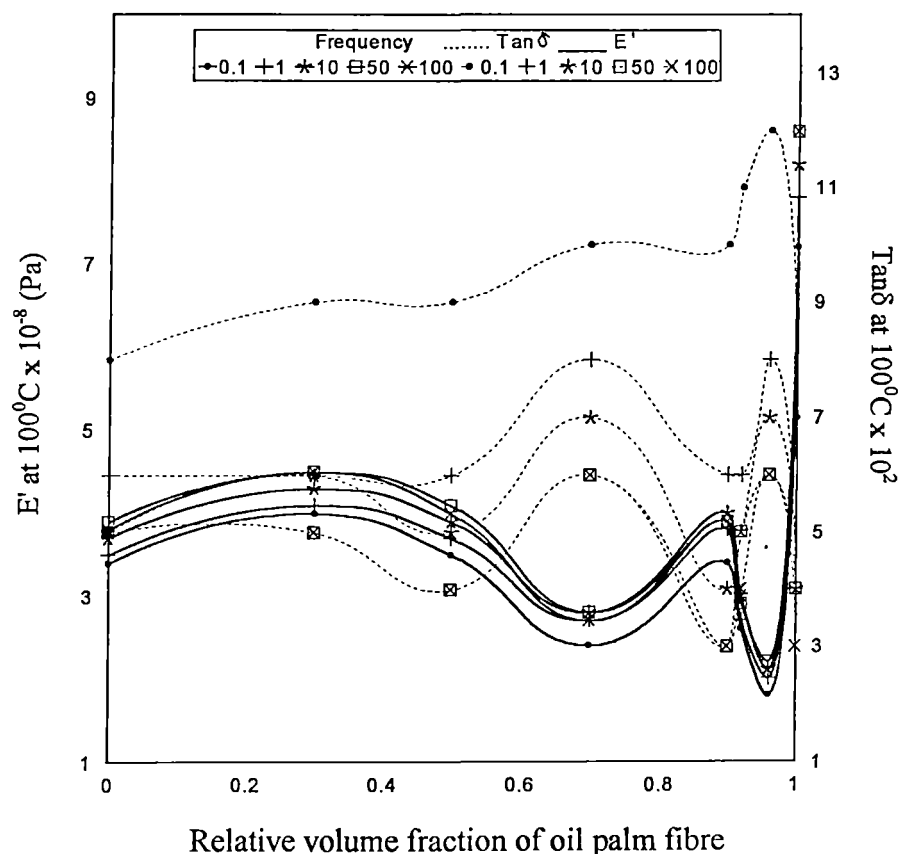


Figure 7.21 Effect of relative volume fraction of oil palm fibre on the $\tan\delta$ and storage modulus of oil palm fibre/glass hybrid PF composites at 100°C.

At lower frequencies the value shows gradual increase with increasing relative volume fraction of oil palm fibre. But at higher frequencies value decreases upon increasing the relative volume fraction of oil palm fibre. Mechanical damping of the composite decreased with increase in frequency. Prominent relaxation is observed at the glass transition region. The variation in $\tan\delta$ value as a function of temperature at different frequencies can be understood from the three-dimensional figure (Fig. 7.22). Glass transition temperature of the hybrid composites from the $\tan\delta$ curve is given in Table 7.8. The T_g value of the hybrid composites is lower than that of the unhybridised composites. Glass fibre is less hydrophilic compared to oil palm fibre and hence its reinforcement in hydrophilic PF resin leads to decreased fibre-matrix interaction. The possibility of the fibre layering out was observed at higher fibre loading. This lowers the temperature of relaxation due to glass transition.

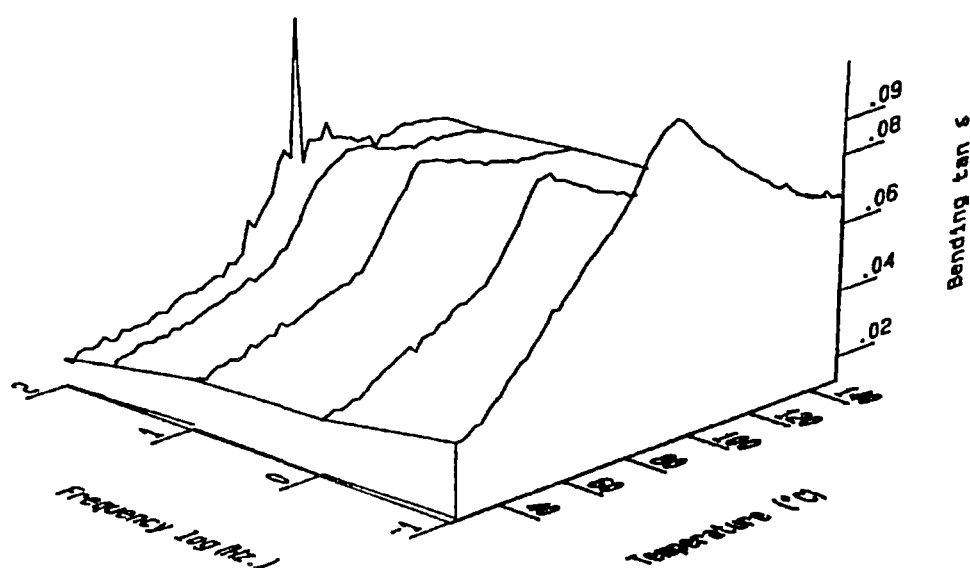


Figure 7.22 Mechanical damping parameter of oil palm fibre/glass hybrid PF composite having 0.3:0.7 glass/oil palm fibre relative volume fraction ratio.

Changes in the storage modulus of the hybrid composites with temperature at a frequency of 10Hz are given in Figure 7.23. Oil palm fibre/PF composite shows almost constant modulus throughout the temperature range. But for the glass/PF composite and hybrid composite having glass/oil palm fibre ratio 0.3:0.7, considerable decrease in modulus was observed after relaxation. With increase in oil palm fibre content in hybrid composites, the storage modulus decreases. However the values are much less than the unhybridised composites. The stiffness of the composite is dependent on the inherent stiffness imparted by the fibres that allows efficient stress transfer.

Table 7.8 Values of $\tan \delta$ Maximum, E'' Maximum and T_g Values of Oil Palm Fibre/Glass Hybrid PF Composites having Various Relative Volume Fractions of Oil Palm Fibre and Glass.

Glass/oil palm fibre V.F ratio	$\tan \delta_{\max}$					T_g from $\tan \delta_{\max}$ ($^{\circ}\text{C}$)				
	Frequency (Hz)					Frequency (Hz)				
	0.1	1	10	50	100	0.1	1	10	50	100
1:0	0.09	0.06	0.06	0.05	0.05	91	94	95	96	96
0.7:0.3	0.10	0.07	0.06	0.06	0.06	93	95	95	96	97
0.5:0.5	0.10	0.06	0.05	0.05	0.05	92	89	104	104	105
0.3:0.7	0.11	0.08	0.07	0.06	0.06	94	97	97	102	99
0.1:0.9	0.10	0.06	0.05	0.04	0.04	89	94	91	89	94
0.08:0.92	0.12	0.07	0.06	0.05	0.05	86	90	94	95	94
0.04:0.96	0.13	0.08	0.07	0.06	0.06	86	91	102	103	104
0:1	0.08	0.06	0.05	0.05	0.05	133	138	138	137	137
	E'' Max. $\times 10^{-7}$ (Pa)					T_g from E'' ($^{\circ}\text{C}$)				
	0.1	1	10	50	100	0.1	1	10	50	100
1:0	5.8	3.9	3	2.8	2.7	87	90	92	90	92
0.7:0.3	6	3.8	3.5	3.1	2.9	93	92	94	95	95
0.5:0.5	4	2.7	2.5	2.2	2	97	96	102	102	103
0.3:0.7	3.5	2.6	2.2	2	2	98	96	99	96	95
0.1:0.9	3.8	2.5	1.9	1.6	1.5	90	93	91	90	92
0.08:0.92	3.5	2.2	1.8	1.5	1.4	85	88	92	93	93
0.04:0.96	2.8	1.8	1.5	1.4	1.3	85	91	98	98	99
0:1	5	3.8	3.5	3.4	3	132	138	137	137	136

Efficient packing is possible in the unhybridised composites. This leads to an ideal composite having higher stiffness. In hybrid composites, decreased compatibility between synthetic glass and natural fibre decreases the wetting of the matrix, which decreases the stiffness of the composite. This is most pronounced in composites containing highest volume fraction of oil palm fibre. The fibre dispersion in hybrid composites at lower and higher oil palm fibre loading is evident from the optical micrograph of the tensile stressed portions of the composites (Fig. 5.9; refer Chapter 5). Better fibre dispersion is observed in composites having low fibre loading. The crack propagation upon the application of tensile load is clear from the photograph. Fibre layering out is clear from the scanning electron micrographs of the tensile failure surfaces (Fig. 5.10; refer Chapter 5). Better fibre-matrix adhesion is observed in oil palm fibre/PF part of the hybrid composite. The trend in the variation of E' with relative volume fractions of oil palm fibre at different frequencies is evident from Figure 7.21. Among hybrid composites maximum modulus is obtained for composite having 0.3 relative volume fraction of oil palm fibre. As the frequency increases the modulus also increases.

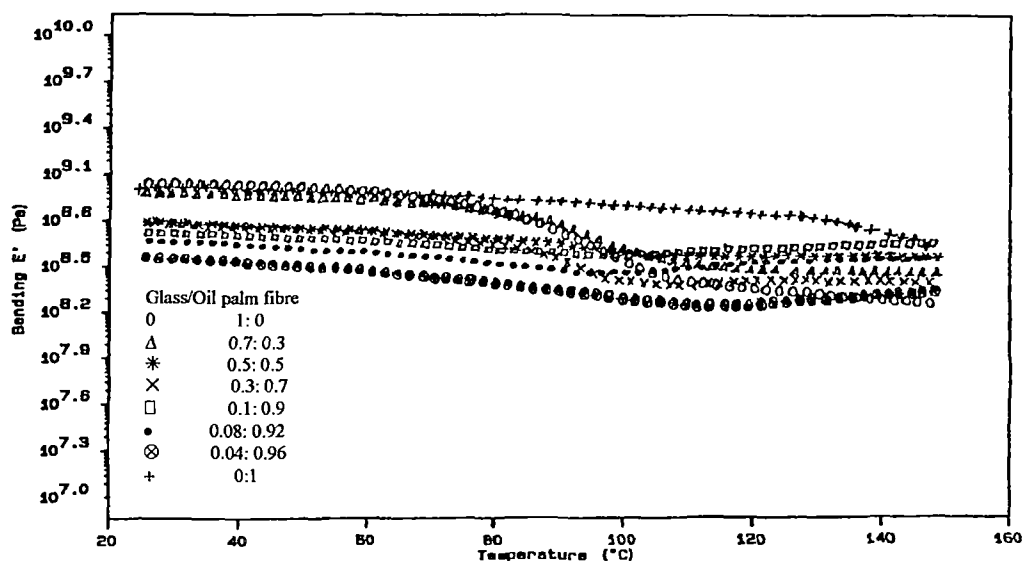


Figure 7.23 Variations in storage modulus of oil palm fibre/glass hybrid PF composites having 40wt.% fibre loading at a frequency of 10Hz.

Loss modulus also shows a similar trend as in the case of storage modulus with variation of relative volume fraction of oil palm fibres (Fig. 7.24). The E'' maximum for the hybrid composites is given in Table 7.8. Highest value of E'' maximum is observed for hybrid composite having lowest relative volume fraction of oil palm fibre. Gradual decrease in loss modulus is observed with increase in frequency (Fig. 7.39). Glass transition obtained from E'' curve is shown in Table 7.8.

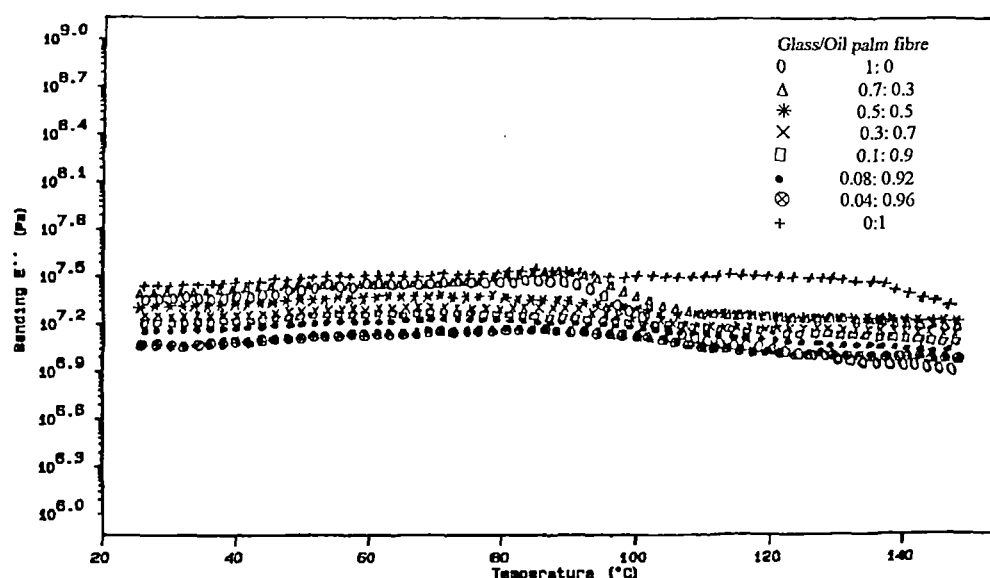


Figure 7.24 Variations in loss modulus of oil palm fibre/glass hybrid PF composites having 40wt.% fibre loading at a frequency of 10Hz.

The activation energies for the relaxation process of the hybrid composites are given in Table 7.9. Incorporation of oil palm fibre decreases the activation energy for relaxation in hybrid composites than that required for cent percent oil palm fibre reinforced composites. This is evident from the lower T_g values of the hybrid composites than that of the oil palm fibre/PF composites. This shows the inefficient compatibility between the matrix and reinforcement upon the incorporation of glass fibre.

Table 7.9 Activation Energy Values of Oil Palm Fibre/Glass Hybrid PF Composites having Various Relative Volume Fractions of Oil Palm Fibre and Glass for Relaxation at Glass Transition Temperature

Glass/oil palm fibre relative V.F.ratio	Activation energy (kJ/mol)
1:0	78
0.7:0.3	108
0.5:0.5	20
0.3:0.7	50
0.1:0.9	17
0.08:0.92	41
0.04:0.96	20
0:1	63

7.4 COLE - COLE ANALYSIS

The viscoelastic properties of the composites were demonstrated by means of Cole-Cole plot. Representative plots are given in Figure 7.25. All the curves show an imperfect semicircular shape. Purely homogeneous system shows a perfect semicircular curve. Incorporation of oil palm fibre gives a broad curve while hybrid composite shows a narrow one. This shows that these composites are not perfectly homogenous. It is seen that the amount and dimension of the dispersed fibres, surface characteristics of the fibres and type of the fibres will affect the shape of the Cole-Cole plot thereby influencing the viscoelastic response.

7.5 TIME - TEMPERATURE SUPERPOSITION

The dynamic modulus of the composite is a function of time (frequency) as well as temperature. The long-term effects of frequency on the dynamic modulus can be illustrated by time-temperature superposition principle. Time and temperature have same effect on the viscoelastic behaviour while a reverse effect with frequency occurs.

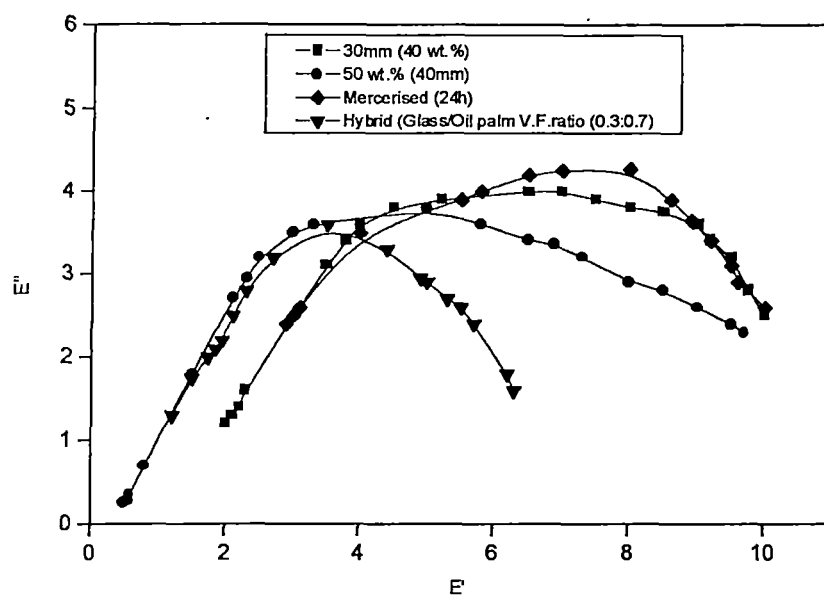


Figure 7.25 Cole-cole plots of the composites

Figure 7.26 is a plot of the storage modulus as a function of time at five different temperatures.

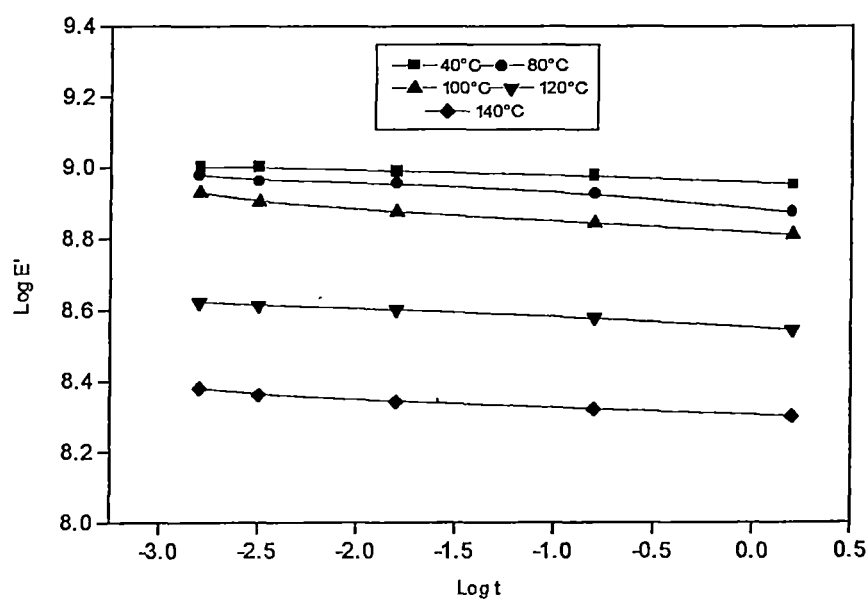


Figure 7.26 E' Vs $\log t$ curves of oil palm fibre/PF composites having 30mm fibre length and 40wt.% fibre loading at different temperatures.

Time is related to frequency by the following equation.

$$t = 1/2\pi f \quad (7.6)$$

Master curve is drawn by plotting $\log (t/aT)$ Vs $\log (E'T_0/T)$ to explain the long-term behaviour of the composite. In developing the master curve, the reference temperature was randomly chosen as 100°C and aT values were found out. The WLF fit of the shift factors of the composite at different temperatures is given in Figure 7.27. Figure 7.28 shows the master curve of the oil palm fibre/PF composite. Shift factors were calculated by displacing the $\log E'$ Vs $\log t$ curves vertically and horizontally.

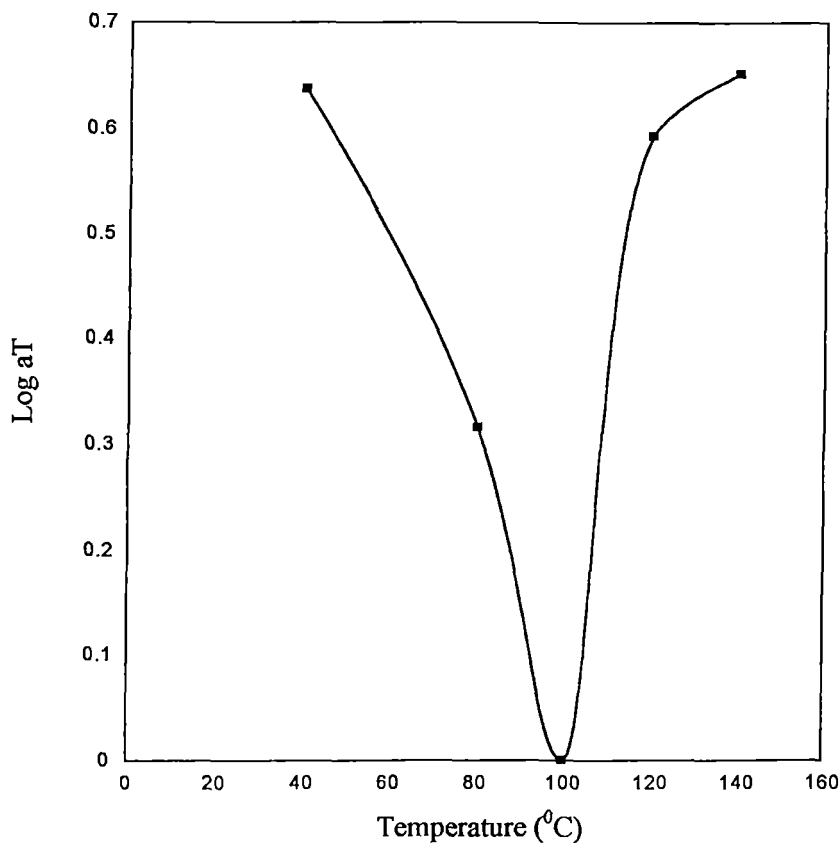


Figure 7.27 Plot of shift factor of oil palm fibre/PF composite at different temperature with 100°C as the reference temperature

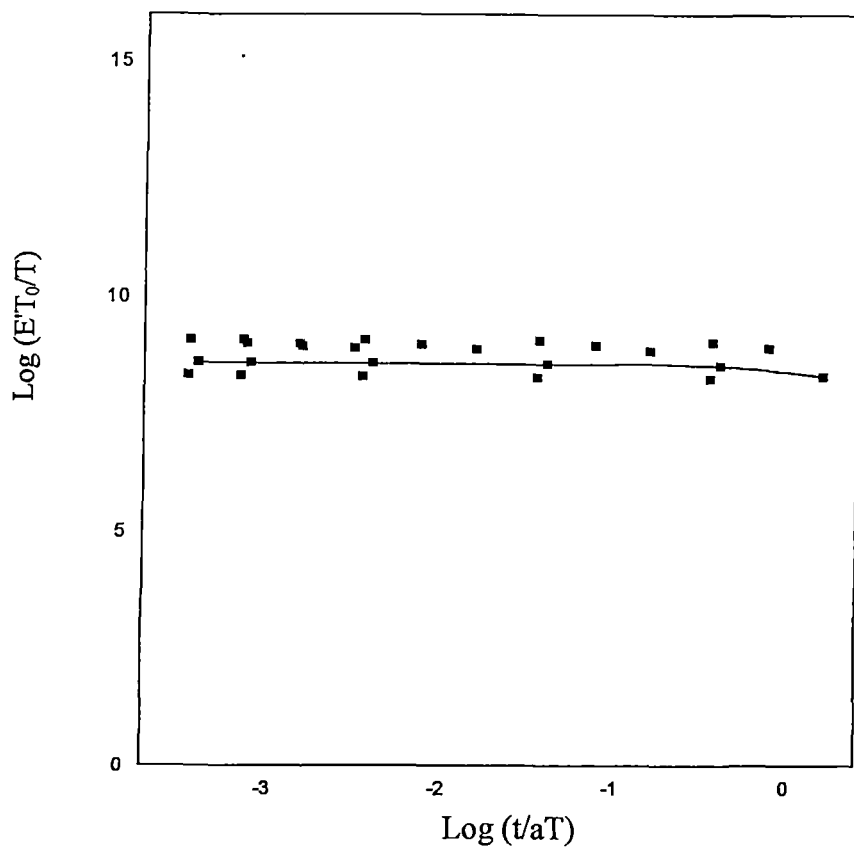


Figure 7.28 Storage modulus master curve for oil palm fibre/PF composite having 30mm fibre length and 40wt.% fibre loading

REFERENCES

1. R. D. Corsaro and L. H. Sperling (Eds.), Sound and vibration damping with polymers, ACS Symposium series, **424**, ACS, Washington D.C (1990)
2. K. R. Kim, J. H. An, K. W. Cho and C. E. Park, *J. Appl. Polym. Sci.*, **47**, 305 (1993)
3. D. Klempner, C. L. Wang, M. Ashitiani and K. C. Frisch, *J. Appl. Polym. Sci.*, **32**, 4197 (1986)
4. Takayuki Murayama (Ed.), Dynamic mechanical analysis of polymeric material, *Elsevier Scientific Publishing Company*, New York (1978)

5. M. O. W. Richardson, Polymer engineering composites, *Applied Science*, London (1977)
6. L. E. Nielsen, Mechanical properties of polymers and composites, Vol.2, *Dekker*, New York (1974)
7. J. A. Manson and L. H. Sperling, Polymer blends and composites, *Plenum*, New York (1976)
8. L. E. Nielsen, *J. Polym. Sci. Part B Polym. Phys.*, **17**, 1897 (1979)
9. K. D. Ziegel and A. Romanov, *J. Appl. Polym. Sci.*, **17**, 1119 (1973)
10. J. L. Thomason, *Polym. Comp.*, **11**, 105 (1990)
11. P. S. Chua, *Polym. Comp.*, **8**, 308 (1987)
12. P. S. Theocaris, *Colloid Polym. Sci.*, **262**, 929 (1984)
13. H. Ishida and J. L. Koenig, *Polym. Eng. Sci.*, **18**, 128 (1978)
14. L. Ibarra, A. Macias and E. Palma, *Polym. Inter.*, **40**, 169 (1996)
15. L. Ibarra, A. Macias and E. Palma, *J. Appl. Polym. Sci.*, **57**, 831 (1995)
16. M. Akay, *Comp. Sci. Technol.*, **47**, 419 (1993)
17. M. Ashida, T. Noguchi and S. Mashimo, *J. Appl. Polym. Sci.*, **30**, 1011 (1985)
18. A. Takahara, T. Magome and T. Kajiyama, *J. Polym. Sci. Part B Polym. Phys.*, **32**, 839 (1994)
19. G. J. Osanaiye, *J. Appl. Polym. Sci.*, **59**, 567 (1996)
20. J. George, S. S. Bhagawan and S. Thomas, *J. Therm. Anal.*, **47**, 1121 (1996)
21. S. Varghese, B. Kuriakose and S. Thomas, *J. Adhn. Sci. Technol.*, **8**, 234 (1994)
22. K. Joseph, S. Thomas and C. Pavithran, *Mater. Letts.*, **15**, 224 (1992)
23. E. Obataya, M. Norimoto and J. Gril, *Polymer*, **39**, 3059 (1998)
24. A. Valea, M. L. Gonzalez and I. Mondragon, *J. Appl. Polym. Sci.*, **71**, 21 (1999)
25. D. N. Bikiaris and G. P. Karayannidis, *J. Appl. Polym. Sci.*, **70**, 797 (1998)
26. D. Colombini, G. Merle, J. J. M. Vega, E. G. Reydet, J. P. Pascault and J. F. Gerard, *Polymer*, **40**, 935 (1999)
27. A. Tcharkhtchi, A. S. Lucas, J. P. Trotignon and J. Verdu, *Polymer*, **39**, 1233 (1998)
28. V. R. Landi, J. M. Mersereau and S. E. Dorman, *Polym. Comp.*, **7**, 152 (1986)
29. H. F. Mark (Ed.), Encyclopaedia of polymer science and engineering, Vol.5, Sec.Edn., *John Wiley and Sons*, New York (1985)
30. R. K. Krishnaswamy and D. S. Kalika, *Polymer*, **35**, 1157 (1994)
31. W. Guo and M. Ashida, *J. Appl. Polym. Sci.*, **50**, 1435 (1993)
32. L. Ibarra and D. Panos, *J. Appl. Polym. Sci.*, **67**, 1819 (1998)
33. G. McKilliam, G. Moltschaniwskyj and D. P. W. Horrigan, *J. Mater. Sci.*, **33**, 103 (1998)
34. N. Klein, G. Marom, A. Pegoretti and C. Migliaresi, *Composites*, **26**, 707 (1995)

35. M. S. Sreekala, S. Thomas and N. R. Neelakantan, *J. Polym. Eng.*, **16**, 265 (1997)
36. I. C. Finegan and R. F. Gibson, *Comp. Str.*, **44**, 89 (1999)
37. S. Dong and R. Gauvin, *Polym. Comp.*, **14**, 414 (1993)
38. D. N. S. Hon and W. Y. Chao, *J. Appl. Polym. Sci.*, **50**, 7 (1993)
39. Z. A. M. Ishak and J. P. Berry, *Polym. Comp.*, **15**, 223 (1994)
40. J. Cinquin, B. Chabert, J. Chauchard, E. Morel and J. P. Trotignon, *Composites*, **21**, 141 (1990)
41. Y. S. Ko, W. C. Forsman and T. S. Dziemianowicz, *Polym. Eng. Sci.*, **22**, 805 (1982)
42. N. Saha and A. N. Banerjee, *J. Appl. Polym. Sci.*, **62**, 1199 (1996)
43. P. Ghosh, N. R. Bose, B. C. Mitra and S. Das, *J. Appl. Polym. Sci.*, **64**, 2467 (1997)

CHAPTER 8

Water Sorption Studies in Oil Palm Fibres and in Oil Palm Fibre Reinforced Phenol Formaldehyde Composites

*Results of this study have been submitted for publication in **European Polymer Journal***

Abstract

Sorption characteristics of two types of oil palm fibres, oil palm empty fruit bunch (OPEFB) fibre and oil palm mesocarp fibre in distilled water, mineral water and water containing salt at four different temperatures were investigated. The uptake of water decreased with increase in temperature. The OPEFB fibre showed higher sorption than the mesocarp fibre. The effects of OPEFB fibre treatment on the sorption behaviour in distilled water were investigated at different temperatures. Treatment reduced the overall water uptake at all temperatures. Changes in physical and chemical modifications of fibres upon different treatments changed the water sorption behaviour. Isocyanate treated composite showed least water sorption. Sorption at the capillary region is also reduced on treatments. The effect of sorption on the mechanical performance of the treated and untreated fibres were also investigated

Water sorption kinetics in oil palm fibre reinforced phenol formaldehyde composites and oil palm/glass hybrid fibre reinforced PF composites were investigated with special reference to fibre loading, relative volume fractions of fibres in hybrid composites and fibre surface modifications. Hybridisation of the oil palm fibre with glass considerably decreased the water sorption by the composite. The concentration dependency of the diffusion coefficient is analysed and discussed. The changes in the mechanical properties of the composites on water sorption were studied.

PART 1 WATER SORPTION STUDIES IN OIL PALM FIBRES

Being lignocellulosic and organic in origin, oil palm fibres are hydrophilic in nature. To achieve the full potential of polymer composites, they must have good environmental stability particularly that of moisture combined with high temperature. Various aspects of the phenomenon of moisture absorption in polymer composites and its effect on their mechanical properties have been reported by many scientists.¹⁻⁴ Detailed study on the kinetics of water sorption and influence of water on the interphases in plastics and rubber composites has been reported.⁵⁻⁷ Sapieha et al.⁸ investigated the swelling of cellulosic fibres in composites and showed that water sorption is a complex phenomenon that requires detailed study. Mechanical changes of dry keratin fibres by water sorption was studied in detail by Feughelman.⁹ As a raw material for polymer composites, the water sorption behaviour of these fibres have to be studied in detail.

The present study pertains to the water diffusion characteristics of oil palm fibres in distilled water, mineral water and salt water. The influence of temperature on the sorption was investigated. Distilled water contains no impurities. They contain mainly calcium, magnesium and carbonate ions. But mineral water contains large number of ions such as Na^+ , K^+ , Mg^{2+} , Ca^{2+} , HCO_3^- , Cl^- , SO_4^{2-} , F^- etc. The salt water used in this investigation contains mainly Na^+ and Cl^- ions. The presence of these ions may affect the sorption and diffusion mechanisms. Effect of chemical modifications of fibre on the sorption behaviour was also investigated. Mercerization, introduction of coupling agents like isocyanate and silane, γ irradiation effects, latex coating, acetylation and peroxide treatment on fibre were done to reduce the water sorption. Tensile properties of both the fibres in swollen stage and in the desorbed stage were analysed. Tensile strength, percentage elongation at break and tensile modulus at 5% elongation were evaluated. Effects of fibre treatment on the tensile properties in the swollen and in desorbed stages were also analysed. Tensile fracture mechanism of the

fibres were analysed using scanning electron microscopic examination of the fracture surfaces.

8.1 WATER SORPTION OF OIL PALM FIBRES IN DISTILLED WATER, MINERAL WATER AND SALT WATER

The major factors that control the interaction between fibres and water are diffusion, permeability and sorption. Swelling behaviour of natural fibres is greatly affected by its morphology, physical and chemical structure. Oil palm fibres are lignocellulosic. In addition to lignin and cellulose they contain waxy materials. Feughelman explained the mechanism of water penetration by Keratin fibres.¹⁰ They made use of the basic concepts of structure for keratin fibres, consisting of a water impenetrable phase embedded in a water penetrable matrix phase. The water penetration through the natural fibre can be explained using a schematic model given in Figure 8.1. Water penetration by capillary action through the micropores of the fibre surface is evident from the model. The fibre has a porous internal structure. The cross section of the fibres become the main access to the penetrating water. The waxy materials present on the fibre surface helps to retain the water molecules onto the fibre. The porous nature of the oil palm fibres accounts for the large initial uptake at the capillary region.

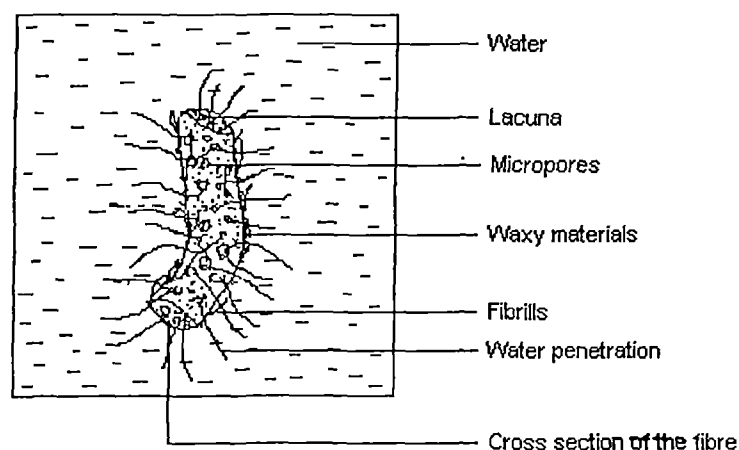
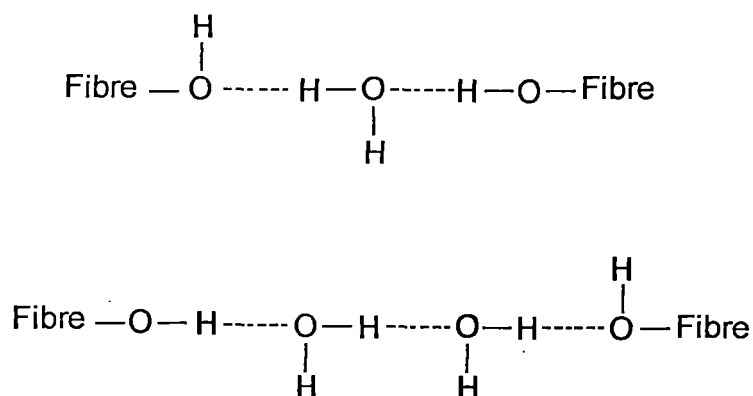


Figure 8.1 A schematic representation of water sorption in oil palm fibres.

The water entering into the fibre may produce an advancing front of water. The portion behind the advancing front is swollen relative to the portion ahead of the front. As the water uptake proceeds, the outer layer of the fibre continuously changes to accommodate the further sorption. The process stops when the sorption reaches the equilibrium. Unlike other organic penetrants, water molecule is small and is strongly associated through hydrogen bond formation. They can form strong localized interactions with hydroxyl groups available on cellulose and lignin. The possible hydrogen bond associations are as follows:¹¹



General features of water absorption by cellulosic materials are reported earlier.¹²⁻¹⁴

Oil palm fibres have micropores on its surface. The surface topography of OPEFB fibre and the mesocarp fibre is evident from the scanning electron micrographs given in Chapter 3 (Figs. 3.3 & 3.23, refer Chapter 3). The number and size of the pores is higher for OPEFB fibre than mesocarp fibre. Water sorption is mainly dependent on the penetrativity of water and radii of the capillaries. The length and radii of the capillaries determine the capillary action. Average micropore diameter of the OPEFB fibre is found to be 0.07 μm . Untreated oil palm mesocarp fibre exhibits very little pores on its surface. Protruding portions and groove like structures are seen on its surface (Fig. 3.23). Both the fibres show initially higher uptake values. Water can easily penetrate through the micropores. This accounts for the initial higher uptake at the capillary region. Among the two fibres, OPEFB fibre has got higher sorption.

Figures 8.2, 8.3 and 8.4 shows the mole% uptake of distilled water, mineral water and salt water, respectively by OPEFB fibre at different temperatures. Upon distilled water and mineral water sorption, the fibre shows single step behaviour at 90 and 70°C. At 30 and 50°C a two step behaviour is observed in both cases. After the initial capillary uptake of water, a levelling off is observed. At the water sorbed stage, structural rearrangements or creation of voids in the cellular network of fibres may occur. This will lead to a case II sorption behaviour. Enhanced hydrogen bonding at this stage facilitates the case II sorption. The sigmoidal shape of the sorption curve also support this.

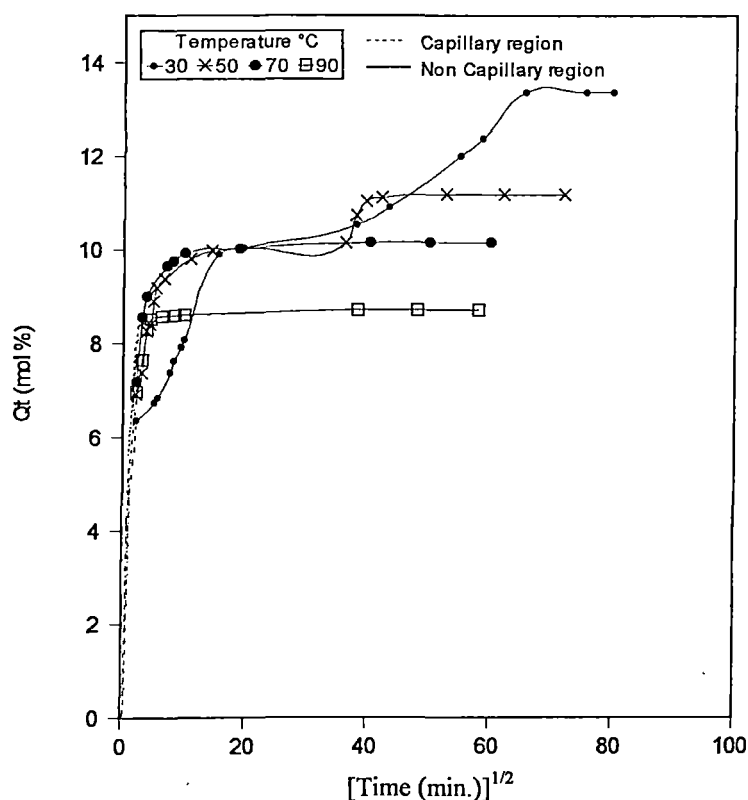


Figure 8.2 Sorption curves for distilled water/OPEFB fibre at different temperatures.

The OPEFB fibre contains 8% cold water soluble matter and 10% hot water soluble matter in it. The capillary region uptake is similar at all temperatures. But in the advanced stage of absorption, at lower temperature the the sorption process

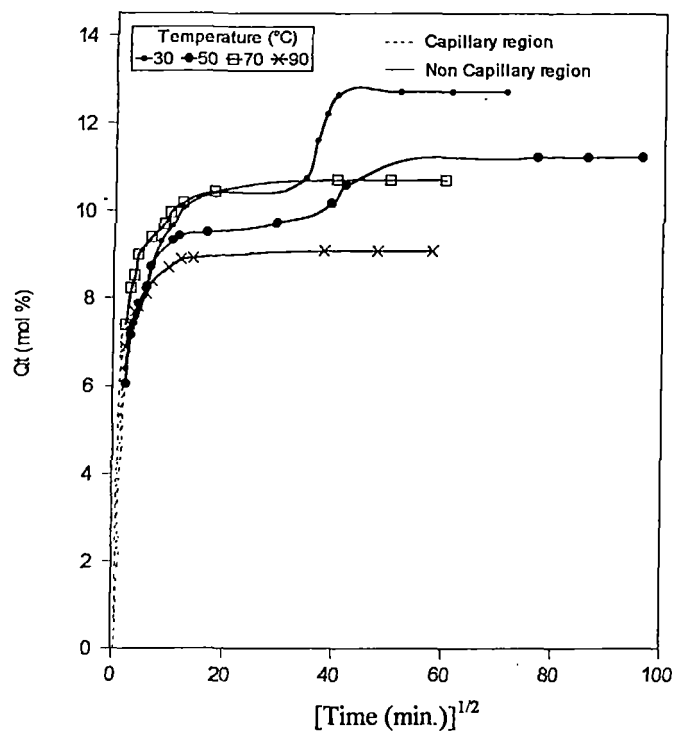


Figure 8.3 Sorption curves for mineral water/OPEFB fibre at different temperatures.

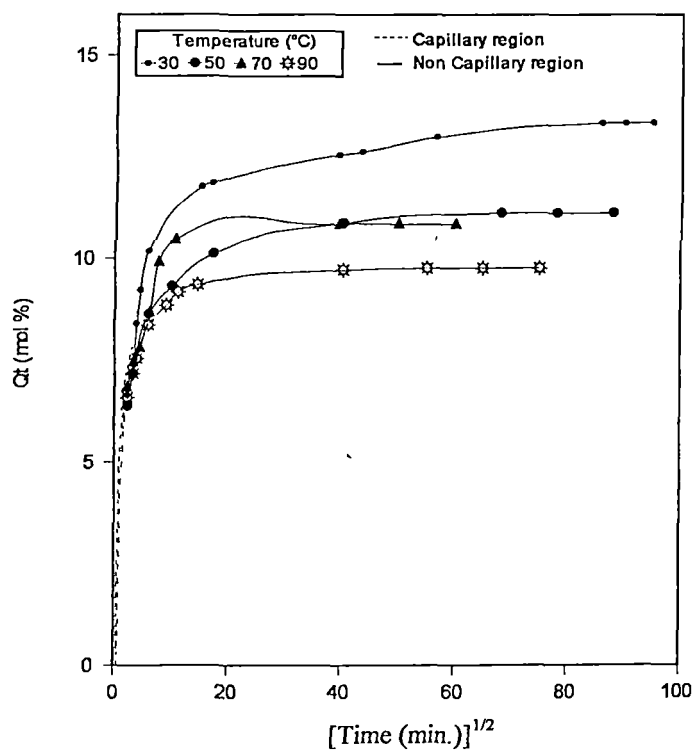


Figure 8.4 Sorption curves for salt water/OPEFB fibre at different temperatures.

will be slow due to the presence of waxy cuticle layer. At higher temperature the degradation of this waxy layer is possible and enables the sorption at a single stretch. Sorption curves for salt water in OPEFB fibre is different from those of distilled water and mineral water. A single step absorption is observed in this case. The ionic solution can dissolve the amorphous matter present on the fibre surface and can directly penetrate into the fibre. Similar sorption curves as observed for OPEFB fibre is shown for oil palm mesocarp fibre also and is given in Figs. 8.5, 8.6, & 8.7. Sorption behaviour at the capillary and non capillary region is evident from the curves. In mesocarp/salt water system also a single stage sorption behaviour is observed.

At 50°C the equilibrium reaches after at long duration. In this case after the initial capillary uptake a slope change occurs and a linear increase in absorption takes place. The initial stage of water penetration by capillary action followed by a non-linear stage of water absorption could be easily understood from the curves. Similar non-linear behaviour was reported for the absorption of moisture by jute fibres and for the absorption of moisture by charcoal.^{15, 16} The non-linear portion for water absorption may arise from the late filling of the micropores and the slow filling of the enlarged pores. The equilibrium mol% uptake Q_{∞} for all the systems are given in Table 8.1. The equilibrium sorption is higher for distilled water at lower temperature in OPEFB fibre. But at higher temperature the sorption is highest for salt water. A gradual decrease in the uptake with temperature is observed for all the systems except for mesocarp fibre in salt water. The Q_{∞} values are lower for mesocarp fibre. The mesocarp fibre is (60%) is less cellulosic than OPEFB fibre (65%). Fibre surface morphological difference and difference in cellulose content explains for the lower Q_{∞} values in mesocarp fibre. Also, presence of oily layer on the surface of the mesocarp fibre reduces the sorption. The fibre surface have a waxy cuticle layer which on immersion in water gives slimy appearance to the fibre surface at room temperature. This may enhance the slow water sorption. But as the temperature increases the slimy nature disappears

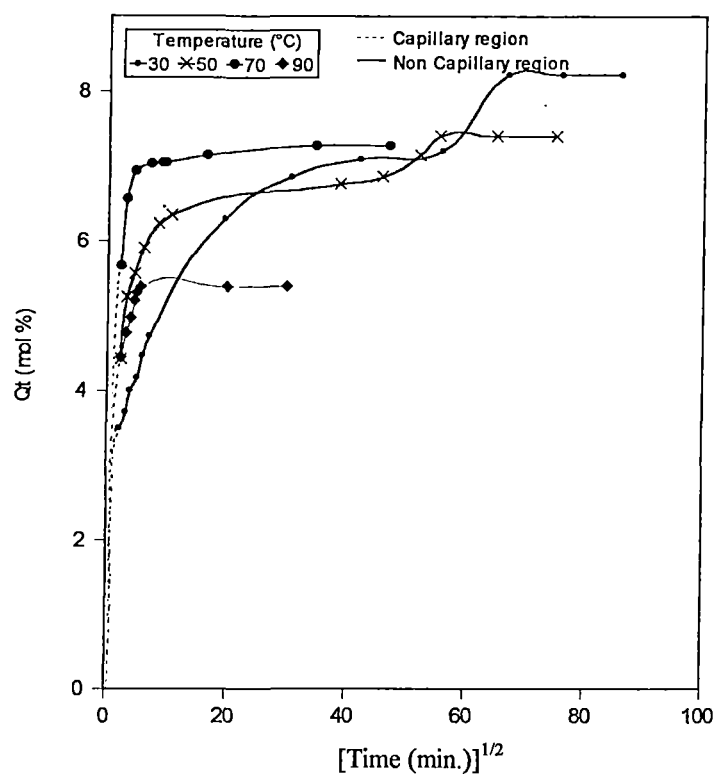


Figure 8.5 Sorption curves for distilled water/oil palm mesocarp fibre at different temperatures.

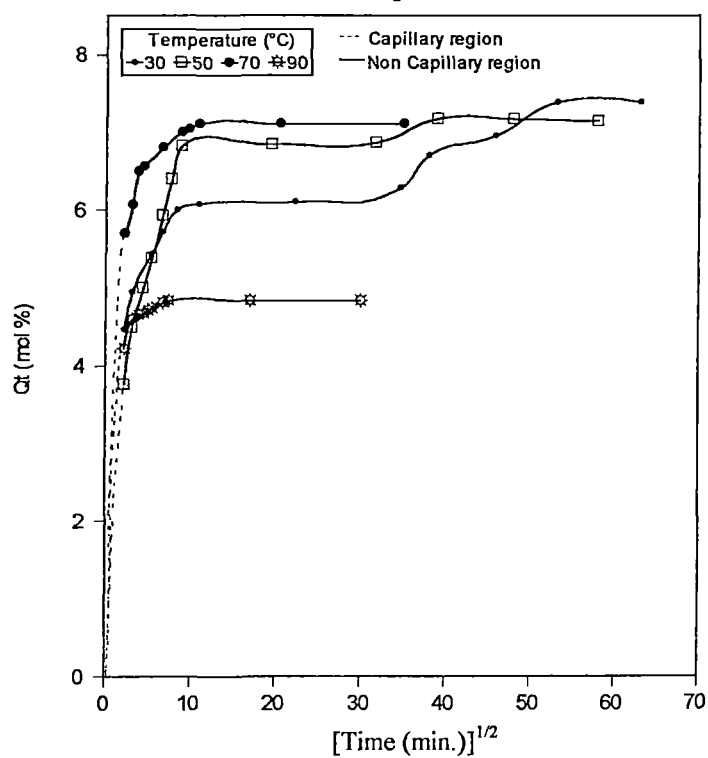


Figure 8.6 Sorption curves for mineral water/oil palm mesocarp fibre at different temperatures.

Table 8.1 Values of Q_{∞} for the Different Systems at Different Temperatures

Fibre	Solvent	Temperature °C	Q_{∞} mole %
OPEFB fibre	Distilled water	30	13.37
		50	11.17
		70	10.15
		90	8.71
	Mineral water	30	12.73
		50	11.24
		70	10.72
		90	9.09
	Salt water	30	13.33
		50	11.12
		70	10.84
		90	9.76
Mesocarp fibre	Distilled water	30	8.23
		50	7.40
		70	7.27
		90	5.38
	Mineral water	30	7.38
		50	7.17
		70	7.10
		90	5.38
	Salt water	30	7.16
		50	9.19
		70	7.05
		90	5.16

by leaching out of waxy materials and consequently the uptake decreases. Thermo dynamic explanation for this behaviour is given later in this article.

The diffusion of water in water-cellulose system is reported to be non-Fickian or anomalous by Newns and by Stamm.^{17, 18} It is also reported that a two stage absorption behaviour is observed in natural fibres. We can see a similar observation for both the oil palm fibres at lower temperatures especially at 30 and 50°C. The two stage behaviour is prominent for distilled water and mineral water

sorption. The initial stage completes rapidly while the second stage is a slow process. The second stage sorption is independent of the thickness of the sample to a great extent, suggesting the process is no longer diffusion controlled.¹⁹

The sol-gel theory suggested by Feughelman can be applied to explain the water absorption by natural fibres.^{10, 20} He had suggested that during sorption, the initial hydrogen bonds in the water accessible regions of the fibre were broken to form a sol like structure which slowly converted to a gel form with the reformation of interchain hydrogen bonds.

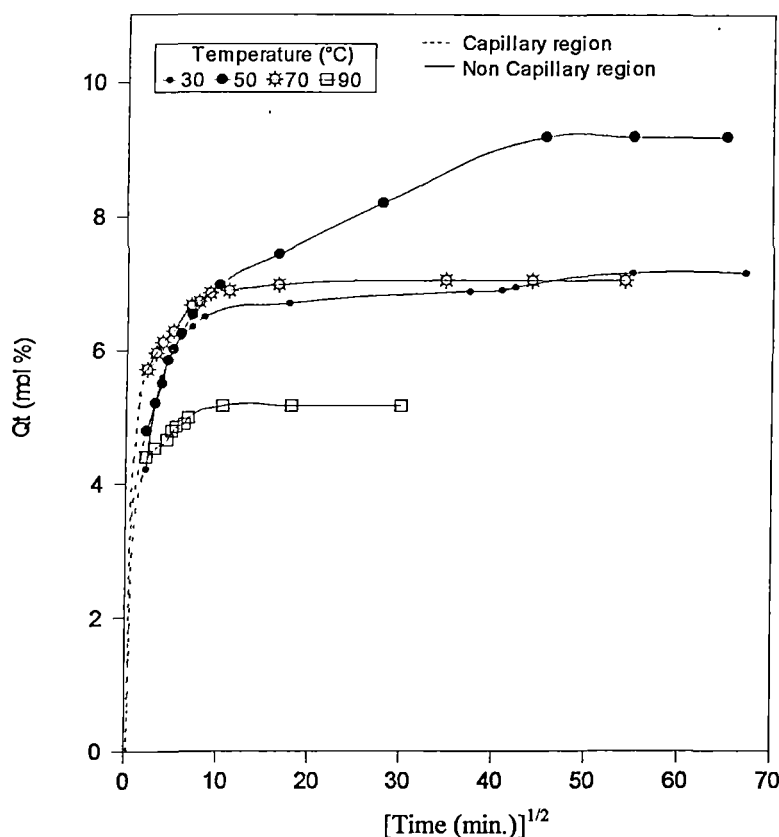


Figure 8.7 Sorption curves for salt water/oil palm mesocarp fibre at different temperatures.

8.2 EFFECT OF OPEFB FIBRE TREATMENT ON THE MECHANISM OF SORPTION

Figures 8.8, 8.9, 8.10 and 8.11 gives the sorption behaviour of treated OPEFB fibre in distilled water at 30, 50, 70 and 90°C respectively. Treatment

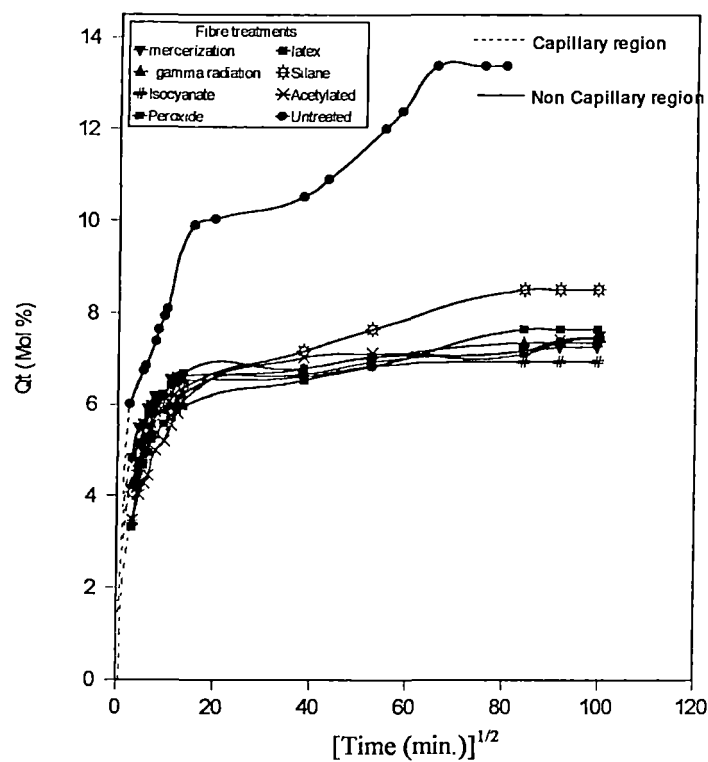


Figure 8.8 Sorption curves for distilled water/treated OPEFB fibre at 30°C.

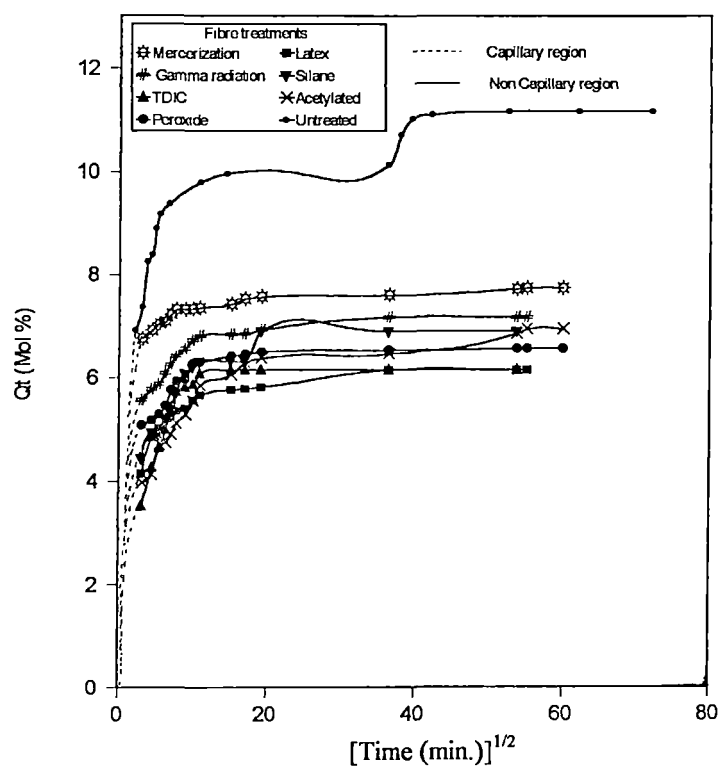


Figure 8.9 Sorption curves for distilled water/treated OPEFB fibre at 50°C.

considerably reduces the overall water uptake at all temperatures. The initial uptake due to the capillary action is also reduced. The equilibrium mol% uptake for the treated fibres in distilled water at different temperatures are given in Table 8.2. As the temperature increases generally the uptake decreases. However there is irregularities observed in different treated systems.

Table 8.2 Values of Q_{∞} for the Treated OPEFB Fibres in Distilled Water at Different Temperatures

Treatment	Temperature (°C)	Q_{∞} (Mol %)
Mercerization	30	7.26
	50	7.74
	70	6.91
	90	7.37
Latex	30	7.65
	50	6.15
	70	6.06
	90	5.89
γ irradiation	30	7.36
	50	7.17
	70	6.68
	90	7.37
Silane	30	8.51
	50	6.90
	70	7.14
	90	6.27
Isocyanate	30	6.94
	50	6.15
	70	6.61
	90	6.68
Acetylated	30	7.48
	50	6.94
	70	6.44
	90	6.59
Peroxide	30	7.44
	50	6.56
	70	6.76
	90	6.59
Untreated	30	13.37
	50	11.17
	70	10.15
	90	8.71

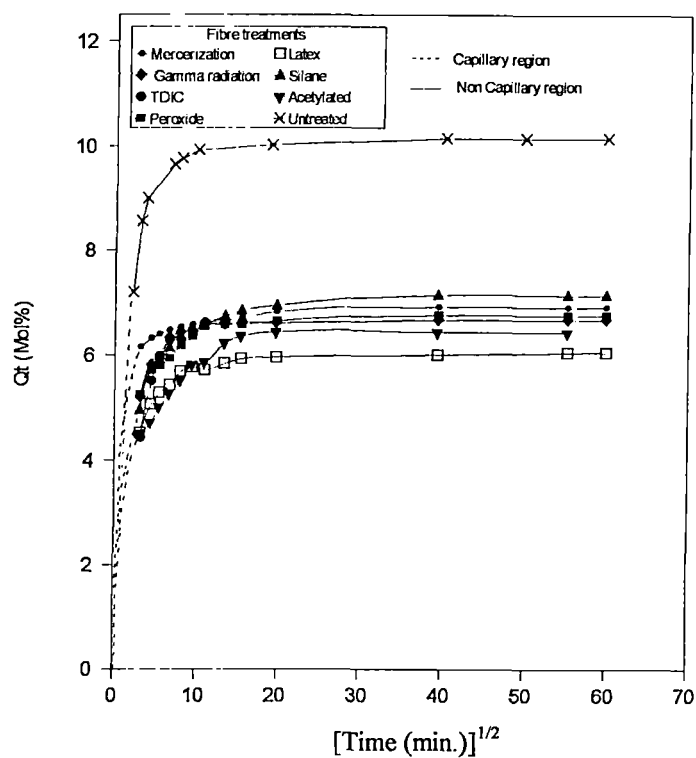


Figure 8.10 Sorption curves for distilled water/treated OPEFB fibre at 70°C.

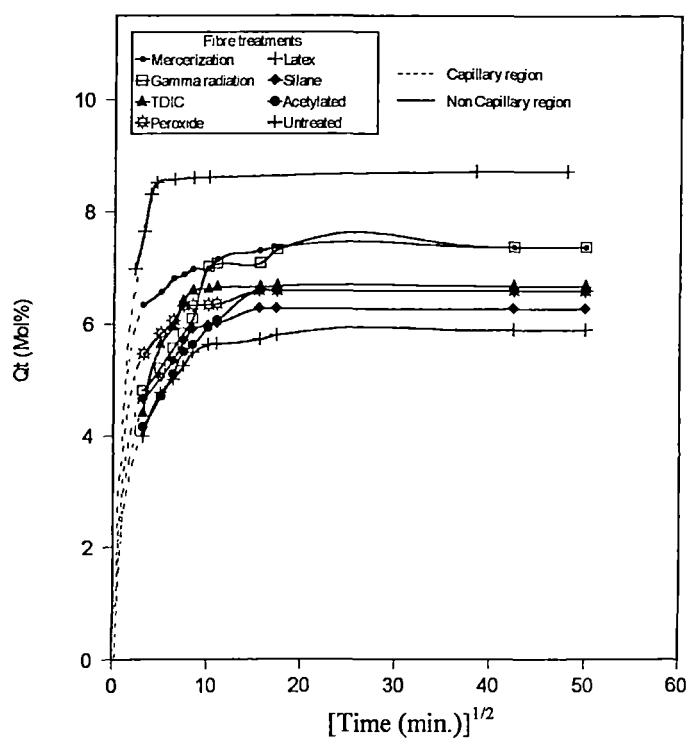


Figure 8.11 Sorption curves for distilled water/treated OPEFB fibre at 90°C.

The decrease in uptake value for treated fibres will be attributed to the physical and chemical changes occurred to the fibres upon different treatments. The scanning electron micrographs of the treated fibre surfaces reveal the physical and chemical changes occurred in the porous structure of the fibre (refer Chapter 3). The leaching out of the amorphous waxy cuticle layer upon mercerization results in reduced sorption. Decreased sorption at the capillary region is observed for the latex coated fibres due to the partial masking of the pores on the fibre surfaces by latex. Gamma ray irradiation partially eliminates the porous structure and causes microlevel disintegration of the fibre. Reduced sorption is observed due to decreased capillary action. Introduction of coupling agents and acetylation make the fibre hydrophobic and thus reduce the moisture absorption. The shrinkage of the micropores and collapse of the capillaries upon treatments will block the capillary absorption. The isocyanate treated fibre shows least water sorption due to its high hydrophobic nature. It is reported by Joly and coworkers that alkyl isocyanate treatment on cotton cellulose fibres leads to decreased water uptake.¹¹ The interstices between the groups of microfibrils of the fibre would be blocked by the linked agents which reduce the water accessibility.

The thermodynamics of sorption process is evaluated from the diffusion data. The activation energies for permeation and diffusion processes were calculated from the Arrhenius relationship¹⁹

$$X = X_0 e^{(-E_x/RT)} \quad (8.1)$$

where $X = P$ or D

$X_0 = P_0$ or D_0 which is a constant

$E_x =$ Activation energy.

The values of permeation activation energy E_p and diffusion activation energy E_D were calculated by linear regression analysis and is given in Table 8.3. The diffusion activation energy is higher than the permeation activation energy for both the fibres. OPEFB fibres have got higher values of E_p and E_D . But the values are negative for both the fibres in salt water.

Arrhenius plots of $\ln P$ versus $1/T$ for both the fibres are drawn (Figures 8.12 and 8.13). This explains the temperature dependence of permeation coefficient and diffusion coefficient. The heat absorption ΔH_s is also calculated (Table 8.3).

$$\Delta H_s = E_p - E_D \quad (8.2)$$

The activation energy for salt water permeation and diffusion are negative (Table 8.4). Presence of ions will have an effect on the permeation and diffusion process. Highest activation energy is observed for distilled water. Similar trend is observed for both the fibres.

Table 8.3 Values for Activation Energies for Water Absorption in Oil Palm Fibres

Fibre	Solvent	E_p (KJ/mol)	E_D (KJ/mol)	ΔH_s (KJ k ⁻¹ mol ⁻¹)
OPEFB	Distilled water	9.91	58.88	-48.97
	Mineral water	0.62	8.07	-7.46
	Salt water	-4.34	-18.59	14.25
Mesocarp	Distilled water	2.94	21.38	-18.44
	Mineral water	1.66	14.44	-12.78
	Salt water	-8.39	-39.12	30.73

Thermodynamic functions ΔS , ΔH and ΔG were calculated by linear regression analysis using Vant Hoff relation¹⁸ and is given in Table 8.4.

$$\ln K_s = \Delta S/R - \Delta H_s/RT \quad (8.3)$$

$$\Delta G = \Delta H - T\Delta S \quad (8.4)$$

$$\text{where } K_s = \frac{\text{No. of moles of solvent sorbed at equilibrium}}{\text{Mass of the fibre}}$$

ΔS = Entropy of sorption

ΔH_s = Enthalpy of sorption

ΔG = Free energy change

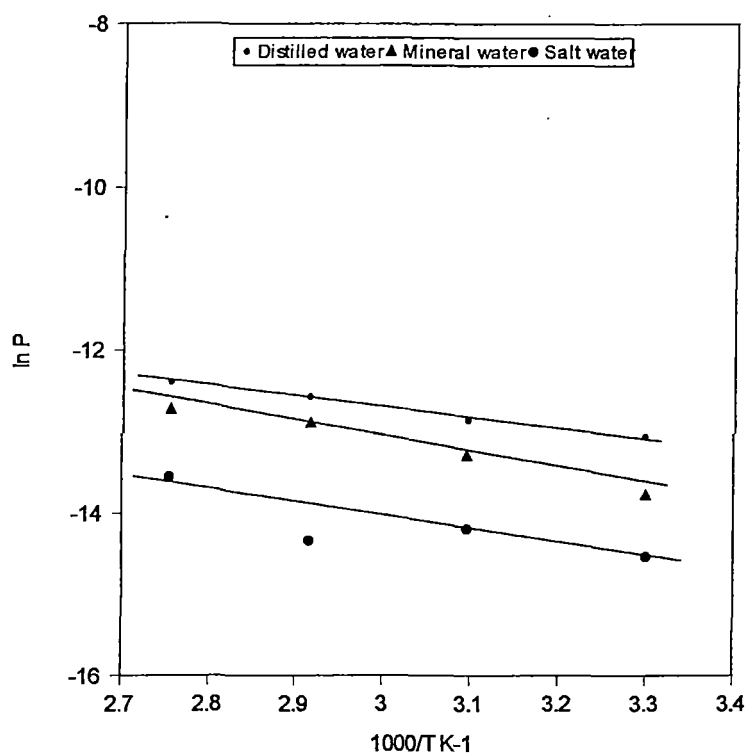


Figure 8.12 Arrhenius plots of $\ln P$ vs $1/T$ for water/OPEFB fibre.

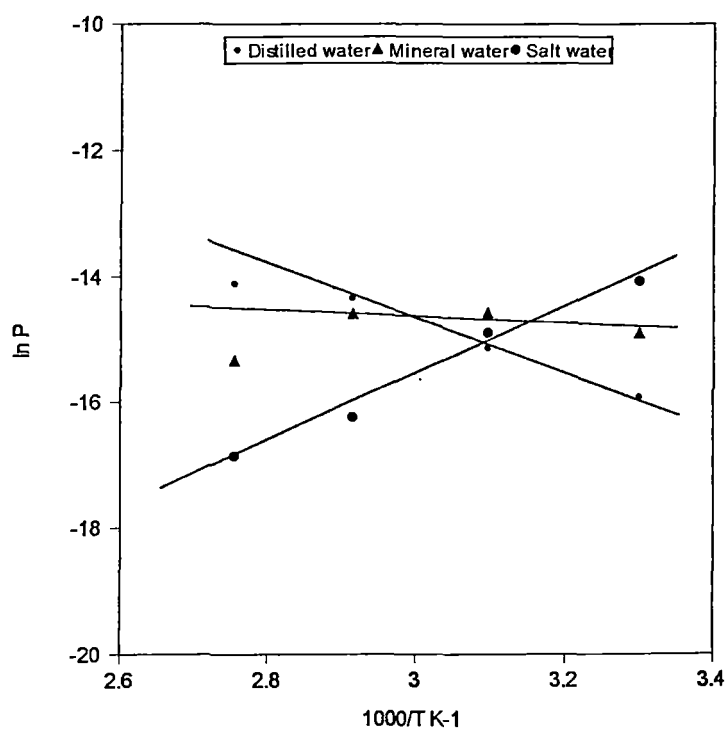


Figure 8.13 Arrhenius plots of $\ln P$ vs $1/T$ for water/oil palm mesocarp fibre.

The ΔH and ΔS values are negative for both the fibres showing that the process is exothermic. Hedges²¹ and many other researchers²²⁻²⁴ reported a large negative value of ΔH for natural fibres at zero regain and a rapid increase in ΔH with increasing regain. It is also reported that corresponding entropy of sorption is generally negative following the increase in ΔH with regain. The ΔG values are found to be positive for all the systems.

Table 8.4 Thermodynamic Functions ΔH , ΔS and ΔG for Water Absorption in Oil Palm Fibres.

Fibre	Solvent	ΔH (KJ/mol)	ΔS (KJ/mol)	ΔG (KJ/Mol)
OPEFB	Distilled water	-6.32	-37.62	5.08
	Mineral water	-4.81	-32.95	5.18
	Salt water	-4.43	-31.56	5.14
Mesocarp	Distilled water	-5.79	-39.57	6.21
	Mineral water	-5.65	-39.72	6.39
	Salt water	-5.37	-38.31	6.24

8.3 TENSILOMETRY

Major tensile properties of both the fibres in the swollen stage and in the desorbed stage are given in Table 8.5. Large fibre to fibre variations in tensile properties are observed for both the fibres. Therefore an average value of each property is reported. The tensile strength values decreased upon sorption in the case of both the fibres. The decrease in the tensile strength is most prominent in salt water sorbed fibre. Around 30% decrease is observed in this case. The tensile strength of the desorbed fibres also shows considerable decrease except in mesocarp fibre. In mesocarp fibres, the desorbed fibres almost retain their strength. However, a small decrease is observed in salt water and mineral water desorbed fibre. The percentage elongation at break of the fibres considerably increased in the swollen stage. Almost three times improvement is observed in the case of OPEFB fibre.

The elongation at break of the desorbed OPEFB fibre is greater than the original value. In the case of desorbed mesocarp fibre, the elongation values show a decrease as compared to the original values. Figures 8.14-8.17 show the stress-strain characteristics of OPEFB and mesocarp fibres, both in the swollen stage and in the desorbed stage. Major slope change is observed at lower elongations for the swollen and desorbed OPEFB fibres irrespective of the virgin fibre. Similar trend is observed in the case of swollen mesocarp fibres. But for desorbed mesocarp fibres the stress-strain characteristics is very similar to that of virgin fibre. Water sorption reduces the crystallinity of the fibres. The stress-strain behaviour of the fibres show a brittle to tough change on sorption. Decreased crystallinity makes the fibre more extensible.

Table 8.5 Tensile Properties of Untreated, Swollen and Desorbed Oil Palm Fibres.

Fibre	Tensile strength (MPa)	Elongation at break (%)	Young's Modulus (MPa)
Virgin fibre (OPEFB fibre)	248	14	6700
<i>Distilled water</i>			
Swollen	224	40	2200
Desorbed	217	32	1800
<i>Mineral water</i>			
Swollen	156	37	2200
Desorbed	226	29	2800
<i>Salt water</i>			
Swollen	152	28	1200
Desorbed	138	15	800
Virgin fibre (Oil palm mesocarp fibre)	80	17	474
<i>Distilled water</i>			
Swollen	64	20	516
Desorbed	80	10	3030
<i>Mineral water</i>			
Swollen	64	26	774
Desorbed	78	9	1392
<i>Salt water</i>			
Swollen	50	20	387
Desorbed	75	11	2048

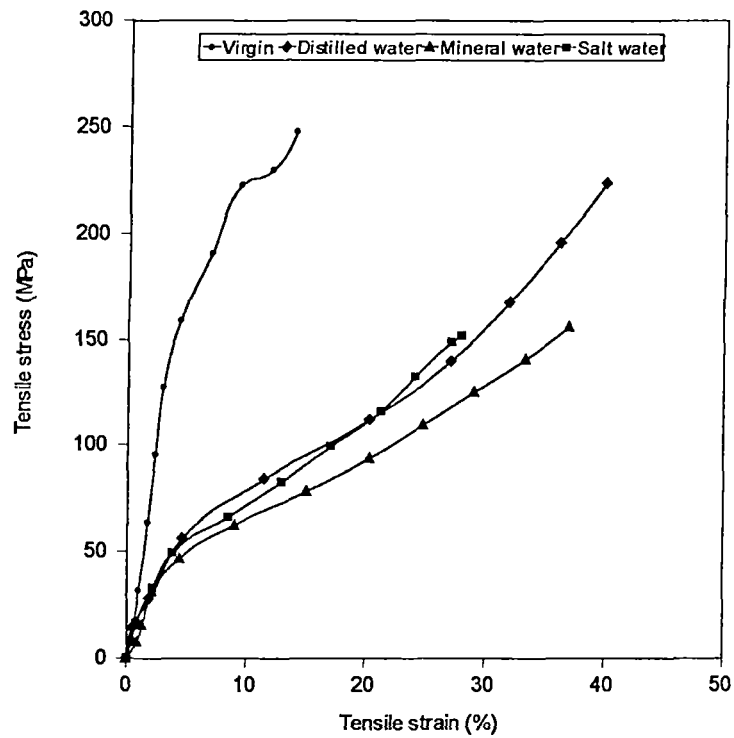


Figure 8.14 Stress-strain behaviour of OPEFB fibre in swollen stage.

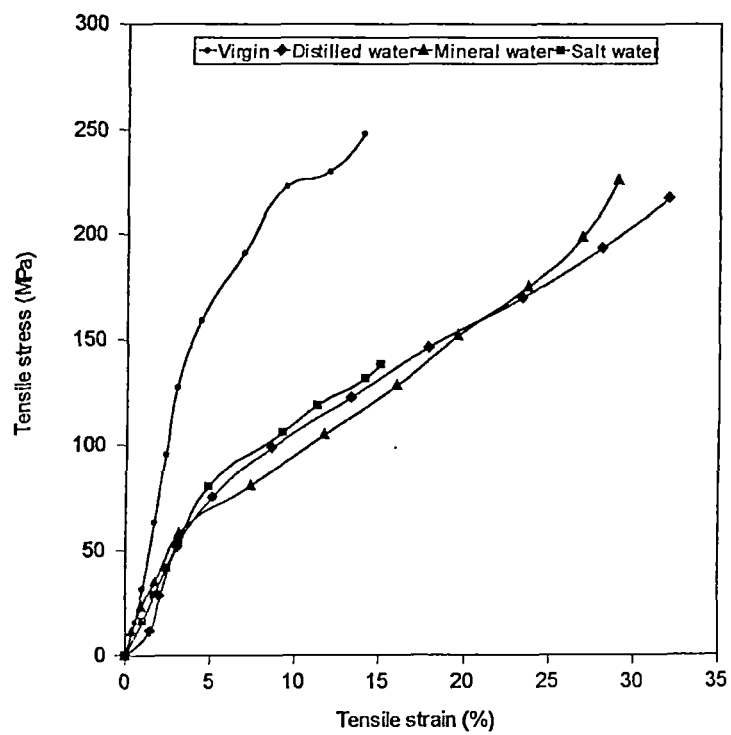


Figure 8.15 Stress-strain behaviour of OPEFB fibre in desorbed stage.

Modulus of the fibres shows considerable variation upon sorption. Modulus at 5% elongation of OPEFB fibres decreases upon sorption and desorption. But in the case of mesocarp fibre the values show enhancement upon desorption. Mannan and Talukder¹⁵ investigated on the stress-strain behaviour and other tensile properties of jute fibres. They have obtained a two stage elastic elongation due to the amorphous and crystalline phase of the fibres. Mechanical performance of the fibres depends on the chemical structure, cellulose content and microfibrillar angle. Decrease in the microfibrillar angle and increase in cellulose content enhance the mechanical properties of the fibre. Lignin and hemicellulose play a cementing role in the three dimensional network of the fibre structure. The amorphous phase of the fibres accounts for the high elongation of the fibres. Upon sorption water molecule enters into the spaces between the cellulose fibrils and microfibrils. Microporous nature of the oil palm fibres helps the retention of moisture on to the fibres. Presence of water molecule destroys the lignin cellulose network thereby decreasing the strength properties. The amorphous phase becomes more active in the swollen stage which accounts for the high elongation behaviour.

Figures 3.22 and 3.29 (refer Chapter 3) are the scanning electron micrographs of tensile fracture surface of OPEFB fibre and mesocarp fibre. The structural failure of the fibres upon the application of stress is clear from the micrographs. The fractured surface shows irregularities in its morphology. As the applied stress is increased the weak primary cell wall collapses and decohesion of cells occurs which leads to the failure of the fibre.

8.4 EFFECT OF FIBRE TREATMENT ON THE TENSILE PROPERTIES OF THE OPEFB FIBRE ON SORPTION

Tensile properties of the OPEFB fibre in the unswollen, swollen and deswollen stage are given in Table 8.6. Treatment reduces the strength of the fibres except for silane treatment. Treatments lead to the breakage of the bound structure and disintegration of the noncellulosic materials. This will reduce the strength of the

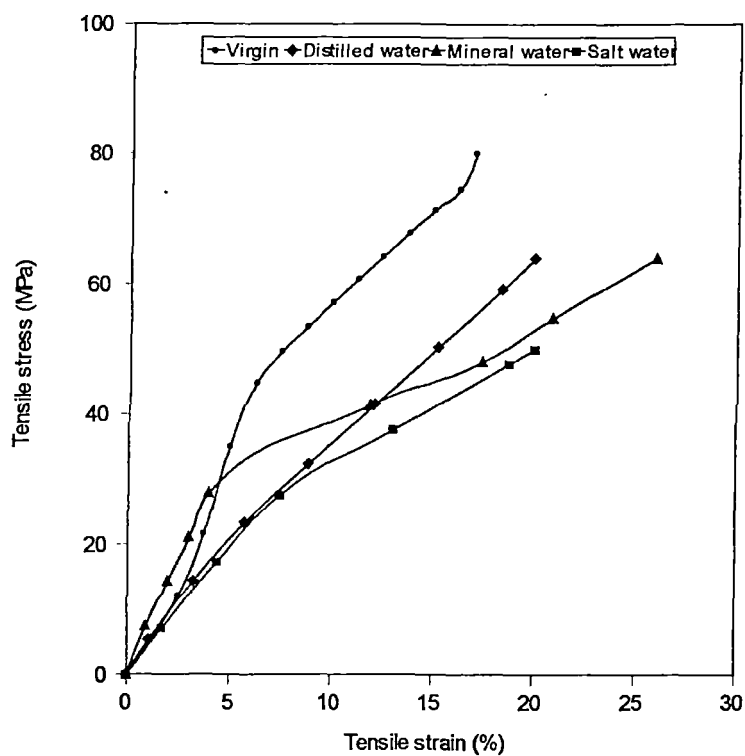


Figure 8.16 Stress-strain behaviour of oil palm mesocarp fibre in swollen stage.

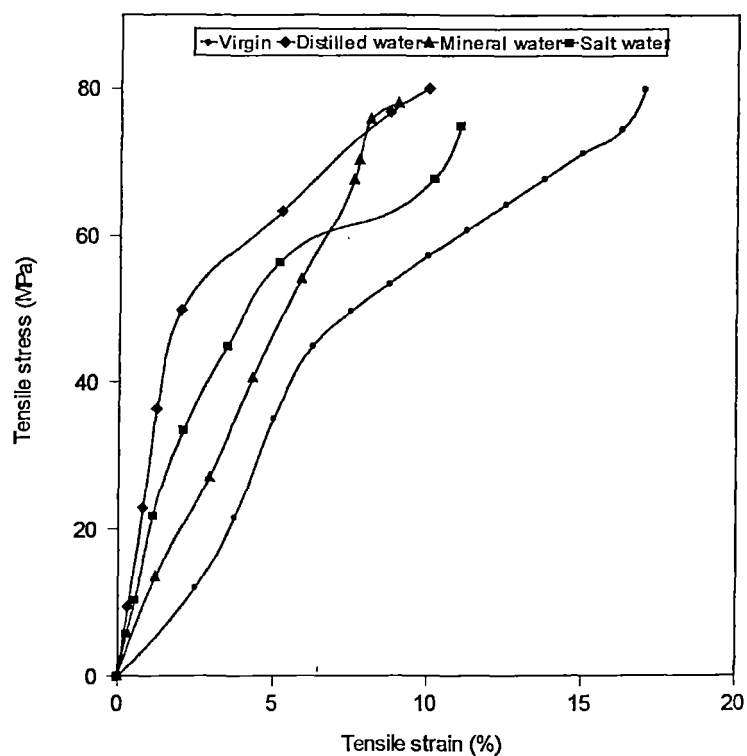


Figure 8.17 Stress-strain behaviour of oil palm mesocarp fibre in desored stage.

fibres. The elongation properties show sharp increase upon modifications except for silane treatment. Young's modulus of the fibre shows enhancement upon mercerization and silane treatment. This may be attributed to the modifications occurred at the cellulose region of the fibres. In swollen stage the strength and modulus were found to decline. Young's modulus of the treated fibres except silane treatment reduced to a lower value on sorption. Amorphous layer of the fibre becomes more active in presence of water. As expected higher elongation is observed in swollen stage.

The tensile stress-strain behaviour of the treated OPEFB fibre in the unswollen and in swollen stage are shown in Figures 3.21 (refer Chapter 3) and 8.18 respectively. The silane treated fibre can withstand higher stress than the untreated fibre. The fibre became more elastic upon treatments. This is evident from the slope change of the stress-strain curves after an initial linear sorption. Untreated, silane treated and mercerized fibres exhibit brittle behaviour which is due to its crystalline nature. The crystallinity of the fibre is due to the increased molecular interactions due to the above treatments.

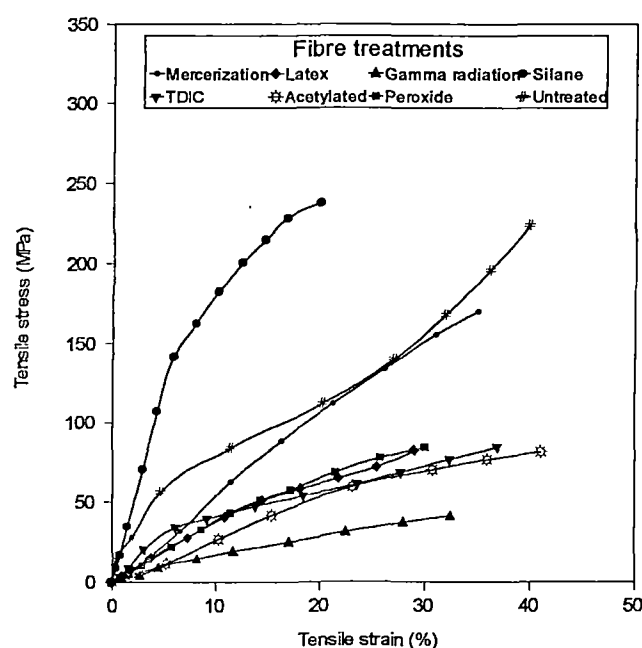


Figure 8.18 Stress-strain behaviour of treated OPEFB fibre in the swollen stage.

Table 8.6 Tensile Properties of the Treated OPEFB Fibre

Treatment	Fibre	Tensile Strength (MPa)	Elongation at Break (%)	Young's Modulus (MPa)
Untreated	Unswollen	248	14	6700
	Swollen	224	40	2200
Mercerization	Unswollen	224	16	5000
	Swollen	170	35	265
Latex	Unswollen	98	23	1850
	Swollen	82	29	455
γ irradiation	Unswollen	88	25	1600
	Swollen	41	33	190
Silane	Unswollen	273	14	5250
	Swollen	238	20	2500
Isocyanate	Unswollen	160	22	2000
	Swollen	84	37	341
Acetylated	Unswollen	143	28	2000
	Swollen	81	41	341
Peroxide	Unswollen	133	24	1100
	Swollen	84	30	190

Crystallinity of the fibre is dependent on the structural regularity, cellular arrangement, secondary interactions within the fibre etc. Treatments like latex coating leads to physical interaction through the micropores present on the fibre surface. The elongation of the fibre increased upon treatments like isocyanate, peroxide, acetylation, latex coating and gamma irradiation in the unswollen stage. In the swollen stage, all treated fibres except silane treatment exhibits a linear enhancement in stress without significant slope change. The exceptional behaviour of the silane treated fibre will be due to the decreased water absorption. The elongation at break of the fibres considerably increased upon sorption. Fibre surface modification leads to major changes in the fibrillar structure and removal of amorphous components. This affects the slope changes in the stress-strain

curve and fracture pattern of the fibres. The elongation at break is increased due to the plasticisation action of the water molecules.

REFERENCES

1. R. Selzer and K. Friedrigh, *J. Mat. Sci.*, **30**, 334 (1995)
2. T. M. Aminabhavi & P. E. Cassidy, *J. Polym. Mater.*, **2**, 186 (1985)
3. C. H. Shen and G. S. Springer, *J. Comp. Mater.*, **11**, 2 (1977)
4. A. C. Loos and G. S. Springer, *J. Comp. Mater.*, **13**, 131 (1979)
5. G. Mensitieri, A. Apicella, J. M. Kenny and L. Nicolais, *J. Appl. Polym. Sci.*, **37**, 381 (1989)
6. R. Schiver, P. Thepin and G. Torres, *J. Mat. Sci.*, **27**, 3424 (1992)
7. T. Marzi, U. Schroder, M. Heb and R. Kosfeld, *Mat. Res. Soc. Symp. Proc.*, Vol. **170**, 123 (1990)
8. S. Sapieha, M. Caron and H. P. Schreiber, *J. Appl. Polym. Sci.*, **32**, 5661 (1986)
9. M. Feughelman and P. Nordan, *J. Appl. Polym. Sci.*, **6**, 670 (1962)
10. M. Feughelman, *J. Appl. Polym. Sci.*, **2**, 189 (1959)
11. C. Joly, R. Gauthier and M. Escoubes, *J. Appl. Polym. Sci.*, **61**, 57 (1996)
12. L. Valentine, *J. Polym. Sci.*, **27**, 313 (1958)
13. R. Jeffries, *J. Text. Inst.*, **51**, T 339, T 399, T 441 (1960)
14. A. R. Urquhart, In *Moisture in Textiles*, J. W. S. Hearle and R. H. Peters (eds.), p.14, *Butter worths*, London (1960)
15. Kh. M. Mannan and M. A. I. Talukder, *Polymer*, **38**, 2493 (1997)
16. E.W. Washburn, *Phys. Rev.*, **17**, 273 (1921)
17. A. C. Newns, *J. Polym. Sci.*, **41**, 425 (1959)
18. A. J. Stamm, *J. Phys. Chem.*, Wash. 60, **76**, 83 (1956)
19. J. Crank and G. S. Park, *Diffusion in Polymers*, *Academic press*, London (1968)
20. M. Feughelman, *Text. Res. J.*, **29**, 967 (1959)
21. J. J. Hedges, *Trans. Faraday Soc.*, **22**, 178 (1926)
22. A. D. McLaren and J. W. Rowen, *J. Polym. Sci.*, **7**, 289 (1951)
23. J. B. Taylor, *J. Text. Inst.*, **43**, T 157 (1952)
24. F. A. Bettleheim and S. H. Ehrlich, *J. Phys. Chem. Wash.*, **67**, 1948 (1963)

PART II WATER SORPTION IN OIL PALM FIBRE REINFORCED PHENOL FORMALDEHYDE COMPOSITES

Water sorption in polymer composites receives considerable attention owing to its theoretical and practical significance, as they are important for many applications such as wastewater treatment, packaging, and building industry. Water sorption have effects on the physical properties of the composites and can affect the matrix structure and the fibre-matrix interface resulting in changes of bulk properties such as dimensional stability, mechanical and electrical properties. The important factors that affect water sorption of composites are the hydrophilicity of the individual components and the structural arrangement of the fibres within the matrix.

Natural fibres being lignocellulosic are highly hydrophilic in nature and are permeable to water. Incorporation of natural fibres into polymeric matrices thus generally increases the water sorption ability. Aditya and Sinha reported that moisture diffusivities of epoxy- jute composites were observed to be eight times as high as that of equivalent epoxy-glass laminates.¹ Oil palm fibre is lignocellulosic having 65% cellulose and 19% lignin content. The fibre is highly hydrophilic due to its polarity owing to the free hydroxyl groups from cellulose and lignin. These hydroxyl groups can hold water molecules by hydrogen bonding. Cellulose is a hydrophilic glucan polymer consisting of linear chain of 1, 4- β anhydro glucose units. The hydroxyl groups on crystalline regions can form hydrogen bonds between parallel chains thereby reducing the water sorption. The mechanism of absorption in fibre incorporated composite material can be illustrated with the help of a schematic model (Fig 8.19). Water can enter through the interface and can enter directly through the porous structure of the fibres as seen in the figure. The cross sectional area of the composite becomes the main absorption face. Each fibre is found to be surrounded by the PF resin as they can penetrate through individual fibres. Three dimensionally crosslinked thermoset matrix have practically no sorption. The water penetration and diffusion are mainly through the fibre-matrix

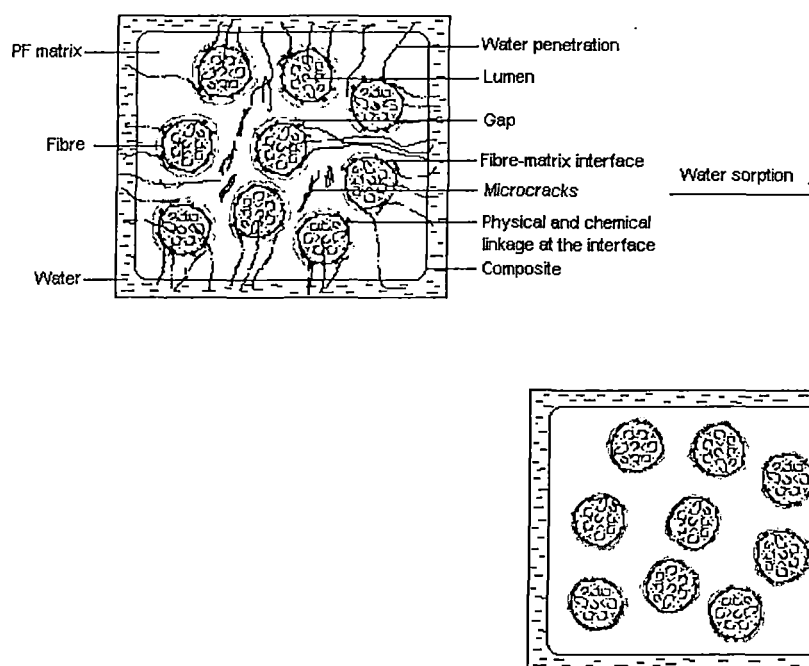


Figure 8.19 Schematic representation of water sorption mechanism at cross-section of oil palm fibre reinforced PF composite

interfacial region and cross sectional portions of the fibre by capillary mechanism. This mechanism involves flow of water molecules along the fibre-matrix interface, followed by diffusion from the interface into the matrix and fibres.² Extent of fibre-matrix adhesion is an important factor in determining the sorption behaviour of the composite. The cross sectional structure of the oil palm fibre is evident from the scanning electron micrographs of the fracture surfaces of the embedded fibres in PF matrix (Fig. 8.20). It shows a lacuna like portion in the middle surrounded by porous tubular structures. This can be a major access to the penetrating water. Karmaker et al.³ reported that in jute fibre reinforced polypropylene composites, a gap surrounding the fibre results from the thermal shrinkage of the matrix. In the case of thermoset matrix this thermal shrinkage during curing is comparatively high and result in decohesion between oil palm fibre and PF matrix resin. This is evident from the scanning electron micrograph of the cross section of an embedded

oil palm fibre in PF matrix (Fig. 8.21). Due to the high hydrophilic nature of phenolic resin and oil palm fibre, higher compatibility is achieved at this interfacial region. Thus the gap width is comparatively lower in phenolic composites. This gap is pictorised in the schematic model (Figure 8.19). The mechanism of water sorption is pictorised in the model. Water sorption by the fibres results in an increase of the fibre diameter and fills the gap surrounding the fibres. This results in a better stress transfer at the interface and thus the interfacial properties of the composite enhanced at swollen stage. This is discussed later in this chapter.

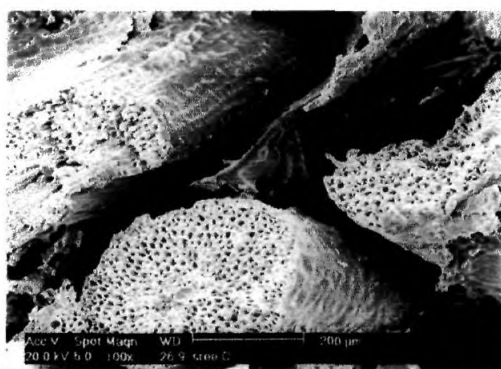


Figure 8.20 SEM of fractured oil palm fibre embedded in PF matrix (x100)

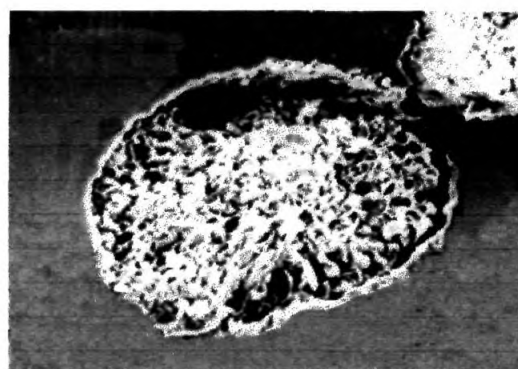


Figure 8.21 SEM of cross section of an embedded oil palm fibre in PF matrix (x200)

Moisture is sorbed in the polymer composite mainly by the dissolution of water in the polymer network, moisture sorption onto the free volume if any present in the glassy structure and by the hydrogen bonding between hydrophilic groups of water and the components of the composite. Microcracks can also pave way to moisture transport involving flow and storage of water within the cracks. The present article summarises the water sorption behaviour of untreated and treated oil palm fibre reinforced PF composites and oil palm fibre/glass hybrid PF composites. The effects of fibre loading, fibre treatment and relative volume fractions of fibres in hybrid composites on the sorption kinetics are highlighted in this study. The mole percent uptake of water by the composites at four different temperatures, ie. 30, 50, 70 and 90°C were analysed. The kinetic parameters of water diffusion

were determined in order to understand the mechanism of sorption. The values of diffusion coefficient, sorption coefficient and permeability coefficient were also calculated. Activation energy values and thermodynamics of water sorption were studied. The concentration dependency of the diffusion coefficient at room temperature was analysed. Finally the mechanical performance of the swollen composites were compared with that of the normal composite. The effects of water sorption on the tensile, flexural and impact performance of the composites were investigated. Scanning electron micrographs of the fractured portions were taken to study the failure mechanism.

8.5 WATER UPTAKE

Water absorption in a fibrous composite is dependent on temperature, fibre loading, orientation of fibres, permeability of the fibre, surface protection, area of the exposed surfaces, diffusivity etc. Mole percent uptake of the untreated, treated and hybrid composites as a function of immersion time at different temperatures is given in Figures 8.22-8.33. The variations in water uptake of the untreated oil palm fibre/PF composites as a function of fibre content at 30°C are evident from Figure 8.22. Upon reinforcing PF resin with oil palm fibre, a large increase in sorption (10wt.%) takes place and thereafter it decreases. Lowest sorption is observed for composite having 40wt.% fibre loading. The value is lower than that of PF gum sample. Beyond 40wt.% fibre loading the sorption again increased. It is already reported that composite having 40wt.% fibre loading exhibits maximum mechanical properties.⁴ Similar results are observed in the case of epoxy-glass composite laminates.⁵ But at longer durations cross over takes place and the water content of the laminate becomes higher than that of the pure resin system. It is also reported that in the case of glass-polyester composites, the plain resin shows lower water sorption than the reinforced resin upto the saturation level.⁶ The decreased water sorption and the good mechanical performance at 40 wt.% fibre loading is due to the increased fibre-matrix adhesion. The hydrophilic oil palm

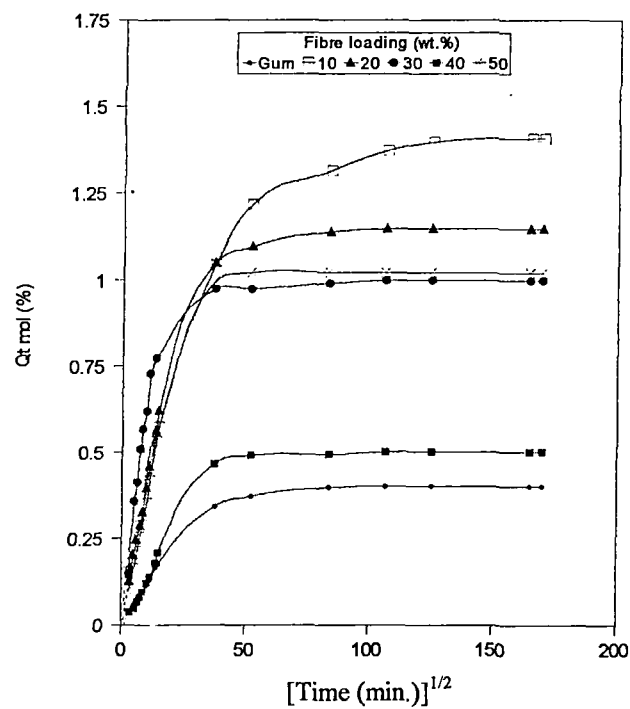


Figure 8.22 Sorption curves showing the mol percent uptake of oil palm fibre reinforced PF composites having different fibre loading at 30°C.

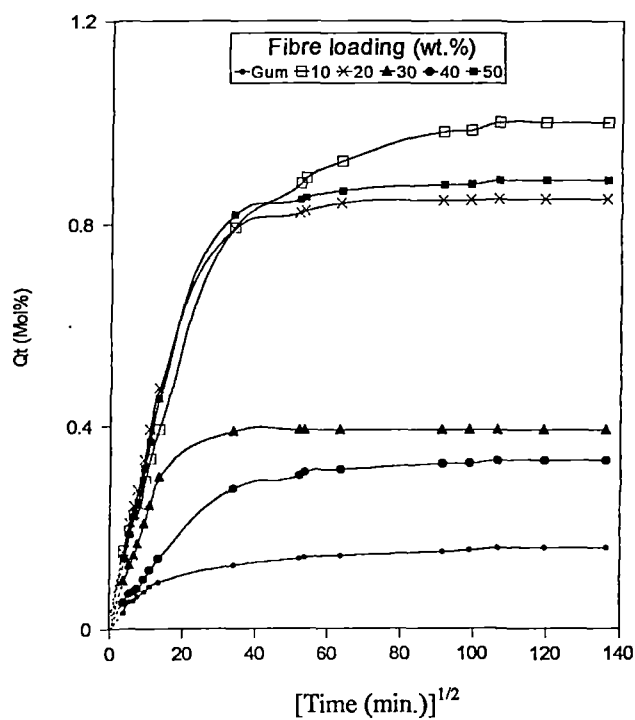


Figure 8.23 Sorption curves showing the mol percent uptake of oil palm fibre reinforced PF composites having different fibre loading at 50°C.

Table 8.7 Values of Q_{∞} for Oil Palm Fibre/PF Composites having Different Fibre Loading at Different Temperatures

Composite fibre loading (wt.%)	Temperature ($^{\circ}\text{C}$)	Q_{∞} mole(%)
Gum	30	0.40
	50	0.16
	70	0.20
	90	0.18
10	30	1.41
	50	1.00
	70	1.35
	90	1.21
20	30	1.14
	50	0.85
	70	1.07
	90	1.13
30	30	1.00
	50	0.39
	70	0.75
	90	0.59
40	30	0.50
	50	0.33
	70	0.42
	90	0.47
50	30	1.02
	50	0.89
	70	0.98
	90	1.21

fibre and PF resole resin leads to strong chemical interaction at fibre-matrix interface. Effect of temperature on sorption can be understood from the respective sorption curves in Figures 8.23-8.25. At all temperatures the neat PF gum sample exhibits lower water uptake. Water sorption is comparatively maximum in composites having 10 and 50wt.% fibre loading at all temperatures. On increasing the temperature the extent of sorption is considerably reduced. This is evident from the Q_{∞} values of the composites having various fibre contents at different temperatures (Table 8.7). Lower sorption is observed at 50°C . The value shows increase upon increasing the temperature. However the value shows its maximum at 30°C except in the case of 40wt.% fibre loaded composite in which case

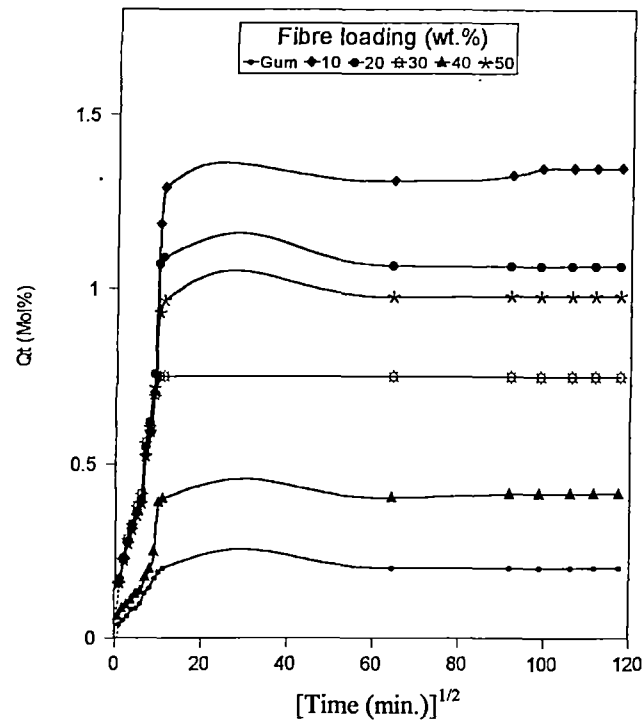


Figure 8.24 Sorption curves showing the mol percent uptake of oil palm fibre reinforced PF composites having different fibre loading at 70°C.

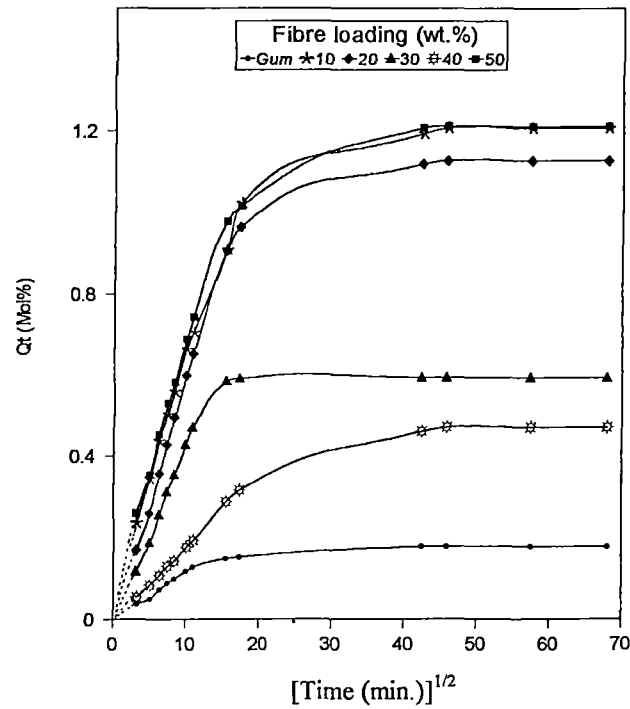


Figure 8.25 Sorption curves showing the mol percent uptake of oil palm fibre reinforced PF composites having different fibre loading at 90°C.

maximum sorption is observed at 90°C. The lowest sorption in this case is observed at 50°C. It was found that in ultrahigh modulus polyethylene fibre reinforced epoxy resin composites, the increase of temperature, enhances the rate and extent of sorption of water by the epoxy resin.² This is attributed to higher microcavitation expected to occur at elevated temperatures since water solubility is a decreasing function of temperature. They also found that the filler volume fraction has a negative contribution to the extent of water sorption.

Effect of fibre modifications on the water sorption characteristics of the composites is clear from the sorption curves in Figures 8.26-8.29. Most of the treatments increase water sorption of the oil palm fibre/PF composites. However alkali treatment decreases the water sorption. Normally the free hydroxyl groups of cellulose and lignin become chemically bonded in treated fibres thereby the hydrophilic character of the fibre is reduced. This will decrease the moisture uptake of the fibres. In the case of oil palm fibres, all these fibre surface modifications resulted in considerable decrease in water uptake. But in the case of composites a reverse trend observed. As explained in Figure 8.19, water sorption is not only dependent on the fibre and matrix structure but also on the fibre-matrix interface. The more hydrophobic is the fibre, the less is the extent of fibre-matrix interaction. This will lead to a substantial decrease in the interaction between fibre and matrix, which facilitates the sorption process. But in the case of alkali treatment, the amorphous waxy cuticle layer of the fibre, which holds water molecules is removed. Moreover, the inactive hydroxyl groups become active by alkali treatment and a strong chemical interaction between the fibre and matrix is possible. This will reduce the moisture sorption and is evident from the sorption curves. We have already found that latex coating makes the fibre most hydrophobic and this will reduce the interfacial adhesion.⁷ This latex treated composite exhibits maximum water sorption. Other treatments such as silane, acrylonitrile etc. also exhibits higher sorption. The decreased fibre-matrix adhesion in silane treated composite is evident from the tensile and impact fracture

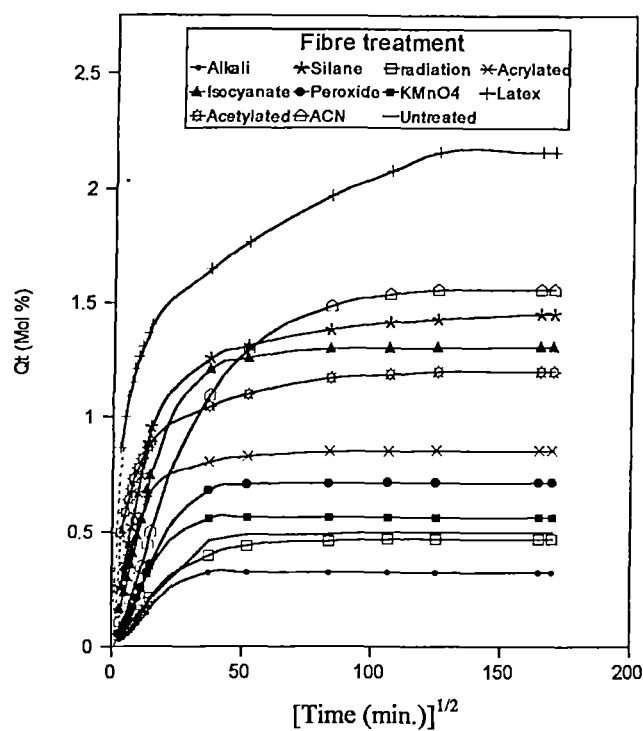


Figure 8.26 Sorption curves showing the mol percent uptake of treated oil palm fibre reinforced PF composites having 40wt.% fibre loading at 30°C.

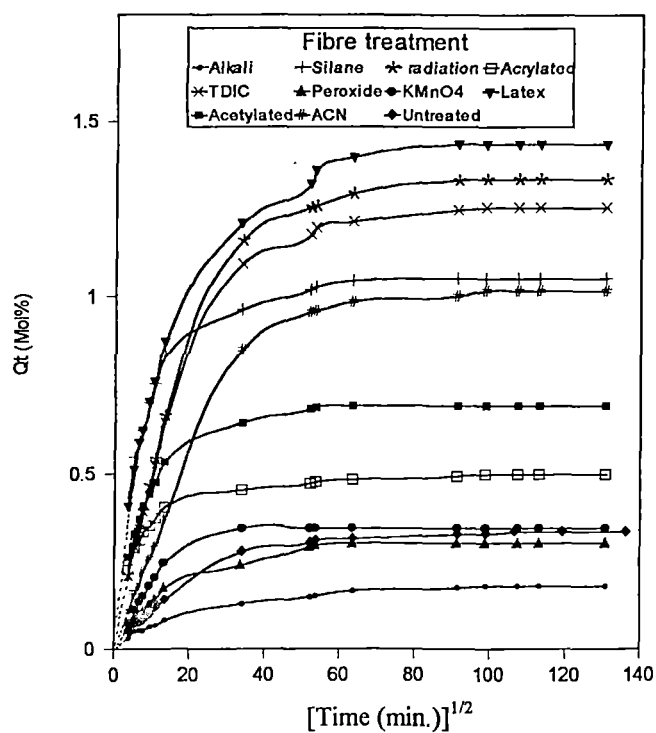


Figure 8.27 Sorption curves showing the mol percent uptake of treated oil palm fibre reinforced PF composites having 40wt.% fibre loading at 50°C.

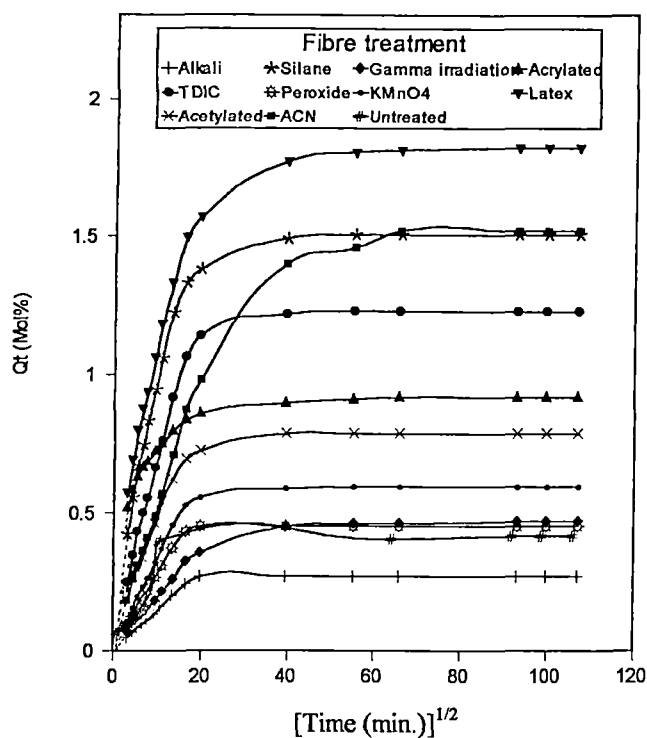


Figure 8.28 Sorption curves showing the mol percent uptake of treated oil palm fibre reinforced PF composites having 40wt.% fibre loading at 70°C.

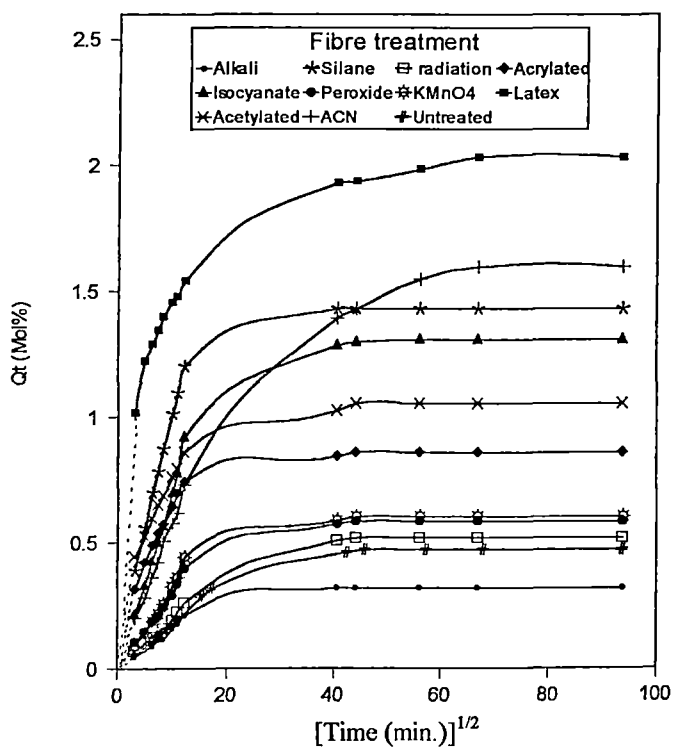


Figure 8.29 Sorption curves showing the mol percent uptake of treated oil palm fibre reinforced PF composites having 40wt.% fibre loading at 90°C.

of the silane treated composite (Figure 4.9 and 4.17). The weak interface could lead to the formation of void structures within the composites, which facilitate the water sorption. It is reported by Mishra and Naik⁸ that the absorption of water increases with increase in time in hemp, banana and agave fibre/polystyrene composites and on esterification with maleic anhydride, all these composites showed decrease in water sorption. This is due to the decrease in the number of free hydroxyl groups upon reaction with MA. The absorption of water is due to the capillary phenomenon but the presence of hydroxyl groups enhances the absorption of water by forming hydrogen bonding.

The Q_{∞} values of the treated composites at different temperatures are given in Table 8.8. As the temperature is increased from 30 to 90°C the water uptake first decreases and then increases. In most cases maximum sorption is observed at 30°C. This shows that temperature has a strong effect on the fibre-matrix interaction. At higher temperature the adhesive bonding is deteriorated. The temperature affects the penetration rate of the water to the interface. Bellenger et al.⁹ observed that in styrene crosslinked polyesters, the water equilibrium concentration is an increasing function of temperature whereas in epoxies it is practically constant with temperature. With increase of temperature, as a result of the expansion the volume fraction accessible to water molecules is increased and enhances the water uptake.

Changes in the water sorption characteristics of oil palm fibre/PF composites upon hybridisation with glass fibre at different temperatures were studied. Sorption curves of hybrid composites having different relative volume fractions of oil palm fibre at 30, 50, 70 and 90°C are given in Figures 8.30-8.33 respectively. From the sorption curves it is evident that a rapid initial uptake occurs in hybrid composites unlike in unhybridised composites. This is most predominant at higher temperatures. The unhybridised glass/PF and oil palm/PF composites show much less absorption at all temperatures than the hybrid composites.

Table 8.8 Values of Q_{∞} for Treated Oil Palm Fibre/PF Composites having 40wt.% Fibre Loading at Different Temperatures.

Treatment	Temperature ($^{\circ}\text{C}$)	Q_{∞} mole (%)
Untreated	30	0.50
	50	0.33
	70	0.42
	90	0.47
Alkali	30	0.32
	50	0.18
	70	0.28
	90	0.32
Silane	30	1.45
	50	1.05
	70	1.51
	90	1.43
γ radiation	30	0.47
	50	1.33
	70	0.47
	90	0.52
Acetylated	30	0.85
	50	0.50
	70	0.92
	90	0.86
Isocyanate	30	1.31
	50	1.25
	70	1.23
	90	1.31
Peroxide	30	0.72
	50	0.30
	70	0.45
	90	0.58
KMnO ₄	30	0.56
	50	0.34
	70	0.59
	90	0.60
Latex	30	2.16
	50	1.43
	70	1.82
	90	2.03
Acetylated	30	1.20
	50	0.69
	70	0.79
	90	1.05
ACN	30	1.55
	50	1.02
	70	1.52
	90	1.60

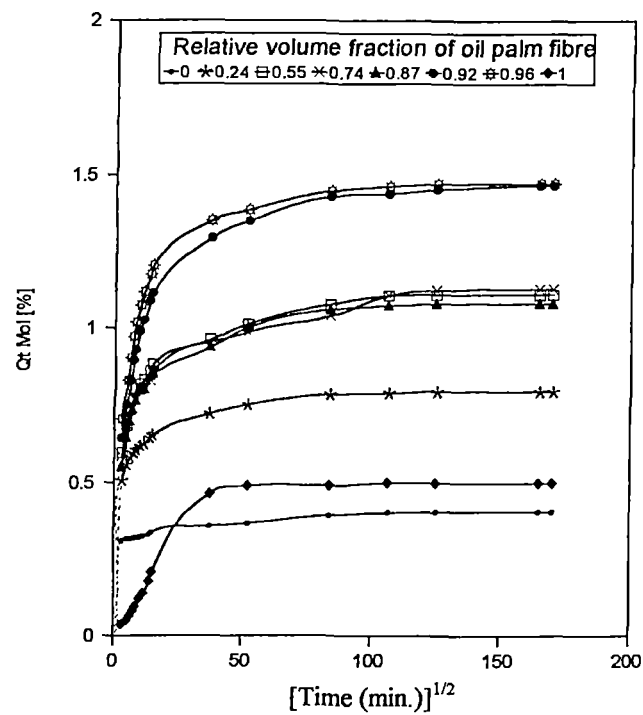


Figure 8.30 Sorption curves showing the mol percent uptake of oil palm fibre/glass hybrid PF composites having different relative volume fractions of oil palm fibre and glass at 30°C.

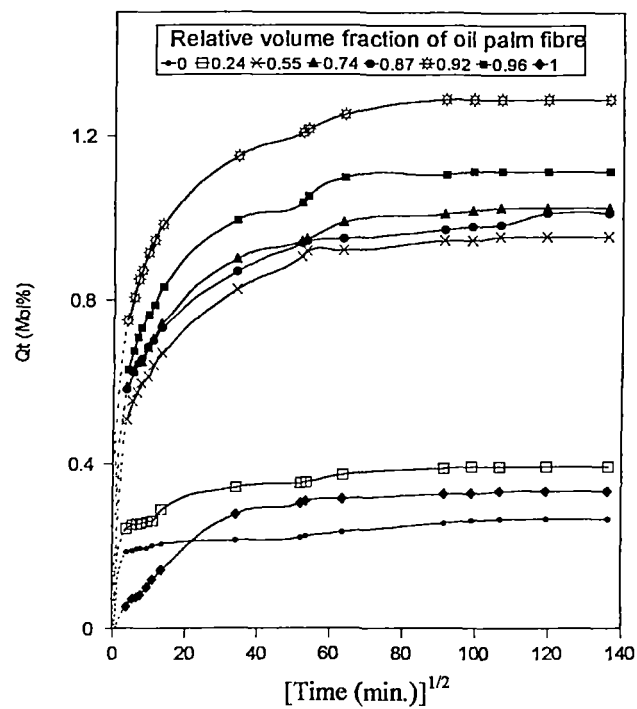


Figure 8.31 Sorption curves showing the mol percent uptake of oil palm fibre/glass hybrid PF composites having different relative volume fractions of oil palm fibre and glass at 50°C.

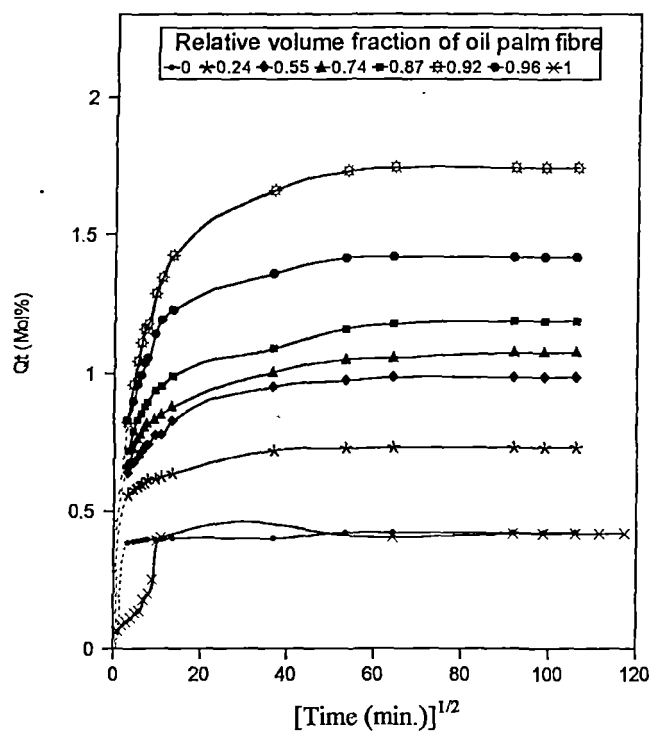


Figure 8.32 Sorption curves showing the mol percent uptake of oil palm fibre/glass hybrid PF composites having different relative volume fractions of oil palm fibre and glass at 70°C.

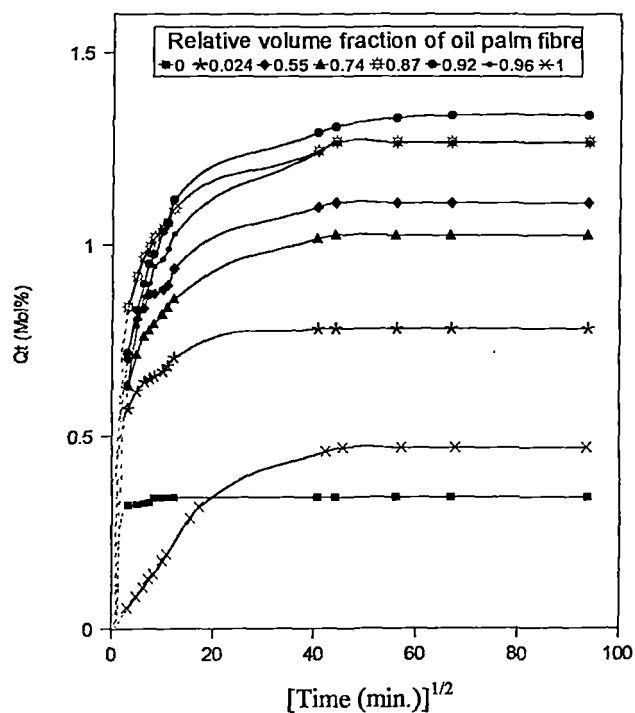


Figure 8.33 Sorption curves showing the mol percent uptake of oil palm fibre/glass hybrid PF composites having different relative volume fractions of oil palm fibre and glass at 90°C.

As the relative volume fraction of oil palm fibres is increased, the water absorption linearly increases. At 30°C, the hybrid composite having a relative volume fraction of oil palm fibre, 0.96 shows highest sorption while at higher temperature the highest sorption is observed for the hybrid composite having relative volume fraction of oil palm fibre, 0.92. The increased sorption of the hybrid composites can be attributed to the poor compatibility between glass fibre and oil palm fibre. At higher volume fractions of oil palm fibres, the microlevel processing of composites becomes difficult and may lead to the fibre layering out which creates micro voids and cracks within the composites. This will facilitate the water sorption. This is evident from the scanning electron micrograph of tensile fracture of hybrid composite (Fig. 5.10, refer Chapter 5). Antoon and Koenig reported that water can chemically degrade glass fibres and roughen the surface of the fibres.¹⁰

The equilibrium sorption values, Q_{∞} of hybrid composites is given in Table 8.9. It is observed that at 30 and 70°C the sorption for oil palm/PF and glass/PF composites are equal. Eventhough oil palm fibre is highly hydrophilic the composite based on this exhibits low water sorption. This is due to the higher compatibility between the hydrophilic fibre and matrix resin. There will not be any inhomogenety or unreacted species within the composite, presence of which may enhance the water sorption. At 50 and 90°C glass/PF composites show comparatively lower sorption. For all hybrid composites lowest sorption is observed at 50°C.

8.6 KINETICS OF WATER SORPTION

In order to study the mechanism of water sorption the kinetic parameters n and k , diffusion coefficient, sorption coefficient and permeability coefficient of water sorption in different systems were analysed from the following relationships.

$$\log (Q_t/Q_{\infty}) = \log k + n \log t \quad (8.5)$$

Table 8.9 Values of Q_{∞} for Oil Palm Fibre/Glass Hybrid PF Composites having 40wt.% Fibre Loading with Various Relative Volume Fractions of Oil Palm Fibre at Different Temperatures.

Relative V.F of oil palm fibre	Temperature ($^{\circ}\text{C}$)	Q_{∞} mole(%)
0	30	0.41
	50	0.26
	70	0.42
	90	0.34
0.24	30	0.80
	50	0.39
	70	0.73
	90	0.78
0.55	30	1.11
	50	0.95
	70	0.99
	90	1.11
0.74	30	1.13
	50	1.02
	70	1.08
	90	1.03
0.87	30	1.08
	50	1.01
	70	1.19
	90	1.27
0.92	30	1.47
	50	1.29
	70	1.74
	90	1.34
0.96	30	1.47
	50	1.11
	70	1.42
	90	1.27
1	30	0.50
	50	0.33
	70	0.42
	90	0.47

where Q_t is the mole percent increase in uptake at time t , Q_{∞} is the mole percent increase in uptake at equilibrium, t is the time and k is a constant characteristic of the polymer, which indicates the interaction between polymer and water. The values of n and k are determined by linear regression analysis.

The value of diffusion coefficient D was calculated from the relationship:

$$D = \pi (h\theta / 4Q_{\infty})^2 \quad (8.6)$$

where θ is the slope of the initial linear portion of the sorption curves and h is the initial thickness of the samples.

The sorption coefficient has been calculated using the equation

$$S = \frac{M_{\alpha}}{M_p} \quad (8.7)$$

where M_{∞} is the mass of water taken up at equilibrium and M_p is the initial mass of the polymer.

The permeability coefficient can be expressed as

$$P = DS \quad (8.8)$$

Table 8.10 shows values of n and k for water sorption in oil palm fibre/PF composites having different fibre loadings at different temperatures. The value of n is equal to 0.5 for a Fickian diffusion mechanism. At all fibre loading the value is very close to 0.5, i.e. the amount of water sorption increases linearly with the square root of time and then gradually approaches the equilibrium plateau. This means that water sorption is diffusion controlled and the same mechanism was reported for reinforced epoxies.¹¹ A slight deviation from Fickian behaviour was observed at 50°C in all cases. The diffusion coefficient, sorption coefficient and permeability coefficient of the unhybridised composites having different fibre loading is given in Table 8.11. The diffusion coefficient is found to be increased with increase in fibre content at lower temperatures. This is due to the inherent hydrophilic nature of the fibres. The diffusion coefficient increases with increase in temperature except in the case of 40wt.% fibre loaded composite. At higher temperature the diffusion coefficient varies irregularly with fibre content. The diffusion coefficient characterizes the ability of water molecule to diffuse through the polymer. The sorption coefficient is found to be higher at lower fibre loading and is related to the equilibrium sorption of the water. As the temperature

increases the sorption coefficient decreases at lower fibre loading. The permeability coefficient, a function of sorption and diffusion, shows sharp increase with increase in temperature. Maximum value of permeability coefficient is observed for composite having 30wt.% fibre loading (Table 8.11).

Table 8.10 Values of n and k For Oil Palm Fibre/PF Composites having Different Fibre Loading at Different Temperatures.

Composite Fibre loading (wt.%)	Temperature (°C)	n	k (g/g min ²)
Gum	30	0.450	0.035
	50	0.451	0.063
	70	0.508	0.058
	90	0.502	0.064
10	30	0.519	0.022
	50	0.332	0.063
	70	0.461	0.044
	90	0.447	0.069
20	30	0.485	0.036
	50	0.450	0.054
	70	0.506	0.046
	90	0.555	0.041
30	30	0.621	0.040
	50	0.430	0.075
	70	0.539	0.061
	90	0.575	0.052
40	30	0.482	0.023
	50	0.335	0.064
	70	0.418	0.057
	90	0.497	0.037
50	30	0.382	0.061
	50	0.445	0.047
	70	0.494	0.051
	90	0.423	0.079

Water sorption behaviour of treated composites is different from that of untreated composites. Sorption mechanism of the composites deviated from Fickian behaviour on treatments like silane, acrylation, latex coating and

Table 8.11 Values of Diffusion Coefficient, Sorption Coefficient and Permeability Coefficient at Different Temperatures for Oil Palm Fibre/PF Composites having Different Fibre Loading.

Composite fibre loading (wt.%)	Temperature ($^{\circ}\text{C}$)	$D \times 10^5$ (cm^2S^{-1})	S (g/g)	$P \times 10^6$ (cm^2S^{-1})
Gum	30	02.10	0.072	01.50
	50	01.50	0.029	00.43
	70	15.00	0.036	05.42
	90	16.80	0.032	05.39
10	30	01.35	0.253	03.40
	50	01.12	0.180	02.02
	70	02.81	0.239	06.70
	90	05.94	0.217	12.90
20	30	02.4	0.206	04.95
	50	02.83	0.153	04.33
	70	04.90	0.192	09.40
	90	06.34	0.203	12.90
30	30	10.40	0.178	18.50
	50	05.61	0.071	03.96
	70	12.80	0.135	17.30
	90	12.90	0.107	13.80
40	30	01.05	0.090	00.45
	50	07.35	0.060	04.40
	70	04.15	0.075	03.10
	90	03.55	0.086	03.05
50	30	01.95	0.184	03.58
	50	01.88	0.160	03.00
	70	04.51	0.177	07.96
	90	05.01	0.218	10.90

acetylation. Value of k shows irregular trend with temperature (Table 8.12). Diffusion coefficient in treated composites show higher value compared to untreated composites (Table 8.13). In most cases the diffusion coefficient increases with temperature. Higher sorption coefficient values are observed for latex treated composite than untreated composite. Silane treatment, isocyanate treatment and acrylation reaction raise the permeability coefficient to a higher value than untreated composite. Increase in temperature increases the permeability coefficient to a certain extent (Table 8.13).

Effects of hybridisation of oil palm fibre with glass on the kinetic parameters were analysed and are given in Tables 8.14 and 8.15. The diffusion mechanism shows non-Fickian behaviour as is evident from the value of n in hybrid composites. Higher k values are observed for hybrid composites. The value increases with increase in temperature. The diffusion coefficient decreases as the volume fraction of glass in the hybrid composite is increased. This is due to the lower hydrophilicity of glass than oil palm fibres. Sorption coefficient shows irregular trend with increases in temperature. Permeability coefficient shows its highest value at 0.96 volume fraction of oil palm fibre in hybrid composites (Table 8.15).

8.7 THERMODYNAMICS OF WATER SORPTION

The temperature dependence of permeation and diffusion coefficient can be used to calculate the energy of activation for the process from the Arrhenius relationship

$$X = X_0 \exp(-E_x/RT) \quad (8.9)$$

where X is the transport coefficient, X_0 is a constant, E_x is the activation energy, R the universal gas constant and T the absolute temperature. The Arrhenius plots of $\ln P$ and $\ln D$ versus $1/T$ are shown in Figures 8.34 and 8.35 respectively. From the slope of the curves, the activation energy of permeation E_p and that of diffusion E_D were calculated by linear regression analysis.

The heat of sorption ΔH_s , is given by

$$\Delta H_s = E_p - E_D \quad (8.10)$$

The values of E_p , E_D and ΔH_s for untreated, treated and hybrid composites are given in Table 8.16. There is no systematic trend observed with increase in fibre loading and on treatments. However at higher volume fraction of oil palm fibres, the activation energy of permeation becomes higher than that of diffusion in hybrid composites.

Table 8.12 Values of n and k for Treated Oil Palm Fibre/PF having 40wt.% Fibre Loading at Different Temperatures

Treatment	Temperature °C	n	k (g/g min ²)
Alkali	30	0.507	0.027
	50	0.357	0.073
	70	0.558	0.046
	90	0.488	0.047
Silane	30	0.419	0.067
	50	0.261	0.207
	70	0.380	0.119
	90	0.416	0.104
γ radiation	30	0.453	0.035
	50	0.444	0.048
	70	0.455	0.053
	90	0.445	0.047
Acrylated	30	0.319	0.137
	50	0.245	0.242
	70	0.160	0.394
	90	0.312	0.178
Isocyanate	30	0.475	0.041
	50	0.439	0.052
	70	0.455	0.072
	90	0.497	0.052
Peroxide	30	0.579	0.020
	50	0.459	0.055
	70	0.507	0.063
	90	0.416	0.069
KMnO ₄	30	0.575	0.026
	50	0.498	0.057
	70	0.512	0.056
	90	0.536	0.043
Latex	30	0.172	0.268
	50	0.304	0.126
	70	0.278	0.167
	90	0.161	0.351
Acetylated	30	0.198	0.260
	50	0.298	0.171
	70	0.307	0.136
	90	0.229	0.245
ACN	30	0.446	0.022
	50	0.487	0.029
	70	0.454	0.043
	90	0.464	0.042

Table 8.13 Values of Diffusion Coefficient, Sorption Coefficient and Permeability Coefficient at Different Temperatures for Treated Oil Palm Fibre/PF Composites having 40 wt.% Fibre Loading.

Treatment	Temperature °C	$D \times 10^5$ (cm^2S^{-1})	S g/g	$P \times 10^6$ (cm^2S^{-1})
Untreated	30	01.05	0.090	00.45
	50	07.35	0.060	04.40
	70	04.15	0.075	03.10
	90	03.55	0.086	03.05
Alkali	30	01.69	0.058	00.98
	50	01.48	0.032	00.47
	70	04.81	0.050	02.40
	90	03.81	0.057	02.19
Silane	30	03.83	0.261	09.99
	50	05.54	0.189	10.50
	70	07.95	0.271	21.50
	90	11.40	0.258	29.40
γ radiation	30	02.17	0.085	01.83
	50	03.78	0.240	09.06
	70	04.37	0.084	03.69
	90	03.44	0.093	03.20
Acrylated	30	02.83	0.154	04.35
	50	07.45	0.089	06.66
	70	05.78	0.165	09.54
	90	12.00	0.155	18.60
Isocyanate	30	03.26	0.235	07.66
	50	03.66	0.225	08.24
	70	08.98	0.221	19.90
	90	06.56	0.235	15.40
Peroxide	30	02.18	0.129	02.81
	50	04.55	0.054	02.46
	70	09.30	0.081	07.56
	90	04.51	0.105	04.74
KMnO ₄	30	03.53	0.102	03.58
	50	06.45	0.062	03.99
	70	06.91	0.107	07.39
	90	05.79	0.108	03.93
Latex	30	01.98	0.389	07.70
	50	03.06	0.258	07.89
	70	04.37	0.328	14.30
	90	02.95	0.365	10.80
Acetylated	30	02.68	0.216	05.78
	50	04.61	0.125	05.74
	70	03.73	0.142	05.29
	90	03.61	0.190	06.84
ACN	30	01.22	0.280	03.41
	50	02.66	0.183	04.87
	70	04.01	0.274	11.00
	90	04.90	0.287	14.10

Table 8.14 Values of n and k for Oil Palm Fibre/Glass Hybrid PF Composites having 40 wt.% Fibre Loading with Various Relative Volume Fractions of Oil Palm Fibre at Different Temperatures.

Relative V.F of oil palm fibre.	Temperature °C	n	k (g/g min ²)
0	30	0.015	0.743
	50	0.032	0.636
	70	0.016	0.879
	90	0.024	0.882
0.24	30	0.091	0.519
	50	0.039	0.553
	70	0.048	0.682
	90	0.073	0.623
0.55	30	0.153	0.377
	50	0.107	0.401
	70	0.087	0.528
	90	0.113	0.497
0.74	30	0.139	0.376
	50	0.080	0.465
	70	0.115	0.478
	90	0.116	0.478
0.87	30	0.170	0.345
	50	0.090	0.453
	70	0.125	0.455
	90	0.100	0.528
0.92	30	0.193	0.280
	50	0.110	0.432
	70	0.213	0.290
	90	0.159	0.375
0.96	30	0.188	0.310
	50	0.108	0.422
	70	0.137	0.424
	90	0.210	0.311
1	30	0.482	0.023
	50	0.335	0.064
	70	0.418	0.057
	90	0.497	0.037

The activation energy of permeation lies in the range 45.43 to –6.74 kJmol⁻¹ and that for diffusion lies between 48.46 and –6.57 kJmol⁻¹.

The enthalpy and entropy of sorption have been calculated from van't Hoff relation:

Table 8.15 Values of Diffusion Coefficient, Sorption Coefficient and Permeability Coefficient at Different Temperatures for Oil Palm Fibre/Glass Hybrid PF composites having 40wt.% Fibre Loading with Various Relative Volume Fractions of Oil Palm Fibre.

Relate V.F of oil palm fibre	Temperature °C	D x 10 ⁵ (cm ² S ⁻¹)	S g/g	P x 10 ⁶ (cm ² S ⁻¹)
0	30	0.03	0.073	00.02
	50	0.10	0.048	00.05
	70	0.06	0.076	00.05
	90	0.24	0.061	00.15
0.24	30	1.23	0.143	01.76
	50	0.11	0.071	00.08
	70	0.57	0.132	00.75
	90	0.89	0.141	01.25
0.55	30	2.62	0.200	05.23
	50	0.68	0.172	01.22
	70	1.03	0.177	01.83
	90	1.51	0.200	03.01
0.74	30	2.15	0.203	04.36
	50	0.71	0.184	01.31
	70	2.18	0.194	04.22
	90	1.96	0.185	03.62
0.87	30	3.93	0.194	07.64
	50	0.95	0.182	01.72
	70	3.19	0.214	06.82
	90	2.09	0.228	04.76
0.92	30	4.49	0.264	11.80
	50	2.12	0.232	04.91
	70	7.79	0.314	24.40
	90	4.33	0.240	10.40
0.96	30	5.26	0.265	13.90
	50	1.53	0.200	03.06
	70	4.56	0.255	11.60
	90	5.28	0.228	12.00
1	30	01.05	0.090	00.45
	50	07.35	0.060	04.40
	70	04.15	0.075	03.10
	90	03.55	0.086	03.05

$$\ln K_s = \Delta s/R - \Delta H_s/RT \quad (8.11)$$

where $K_s = \frac{\text{No. of moles of solvent sorbed at equilibrium}}{\text{Mass of the polymer}}$

The ΔS and ΔH values are given in Table 8.17. The ΔS is found to be negative in all cases. In composites having 20, 40 and 50wt.% fibre loading and in hybrid composites having 0.24 and 0.87 volume fraction of oil palm fibre, the ΔH is found to be positive. Alkali, silane, acrylation, permanganate and acrylonitrile treatment lead to composite having positive enthalpy value. The free energy ΔG can be calculated from the relation

$$\Delta G = \Delta H - T\Delta S \quad (8.12)$$

In all cases the ΔG value is found to be positive (Table 8.17)

8.8 CONCENTRATION DEPENDENCE OF DIFFUSION COEFFICIENT

The diffusion coefficient is found to be dependent on the concentration of the sorbed water. Figure 8.36 shows the concentration dependency of diffusion coefficient in oil palm fibre/PF composites having different fibre loading. Upto the concentration range of sorbed water, 30-40 wt.% the diffusion coefficient increases and thereafter decreases. The diffusion coefficient of composite having 30wt.% fibre loading shows a constant value in the concentration region, 50-65wt.% of the sorbed water. The maximum diffusion coefficient is observed for composite having 30wt.% fibre loading and a sharp decrease with increase in concentration of sorbed water is observed in this case. Effect of concentration of the sorbed water on the diffusion coefficient of hybrid composites and treated composites are shown in Figure 8.37 & 8.38. In isocyanate treated composites an increasing trend is observed upto 60wt.% sorbed water. In acrylonitrile grafted composites the value declined beyond 20wt.% concentration. In acrylated, permanganate treated, acetylated and latex treated composites, the diffusion coefficient increased upto 45wt.% concentration. In silane treated, peroxide treated, alkali treated and gamma irradiated composites, the diffusion coefficient values decline around 35wt.% concentration of the sorbed water. The relationship between solvent concentration and diffusion coefficient was discussed by Kokes et al.¹²

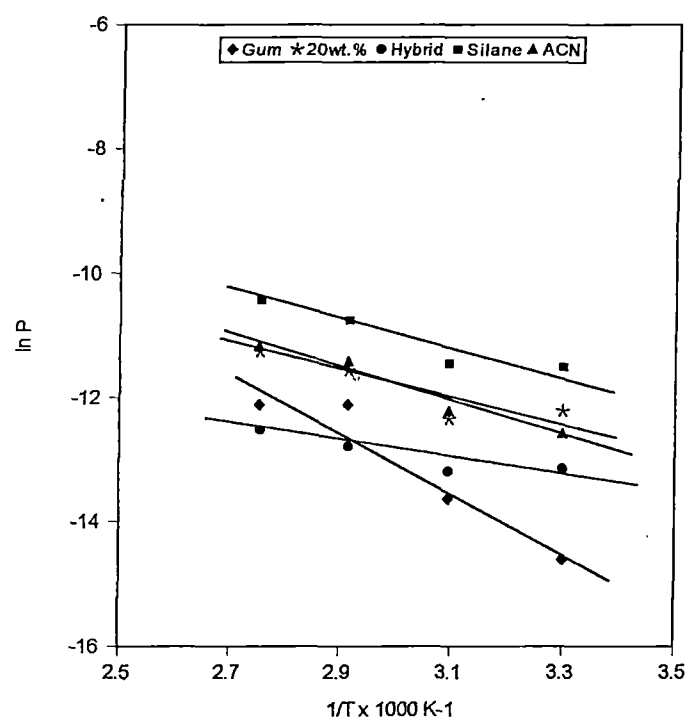


Figure 8.34 Arrhenius plots of $\ln P$ versus $1/T$

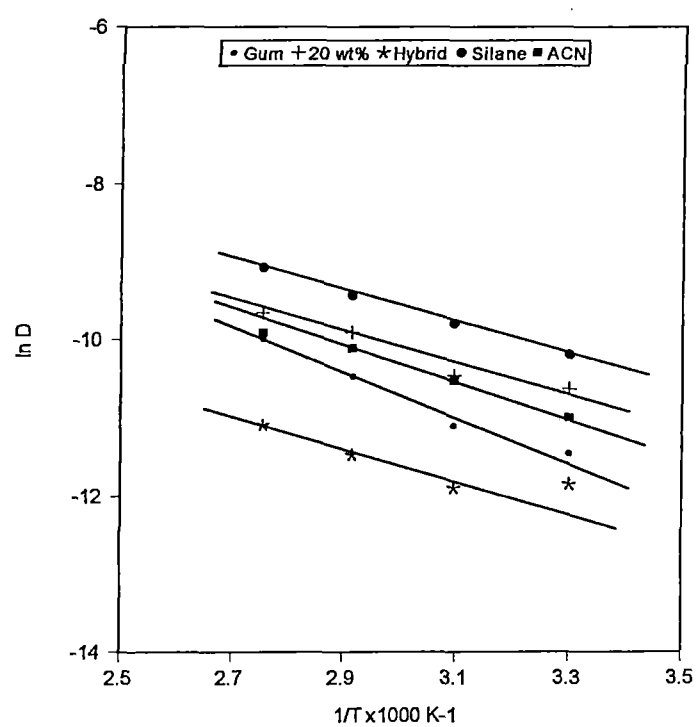


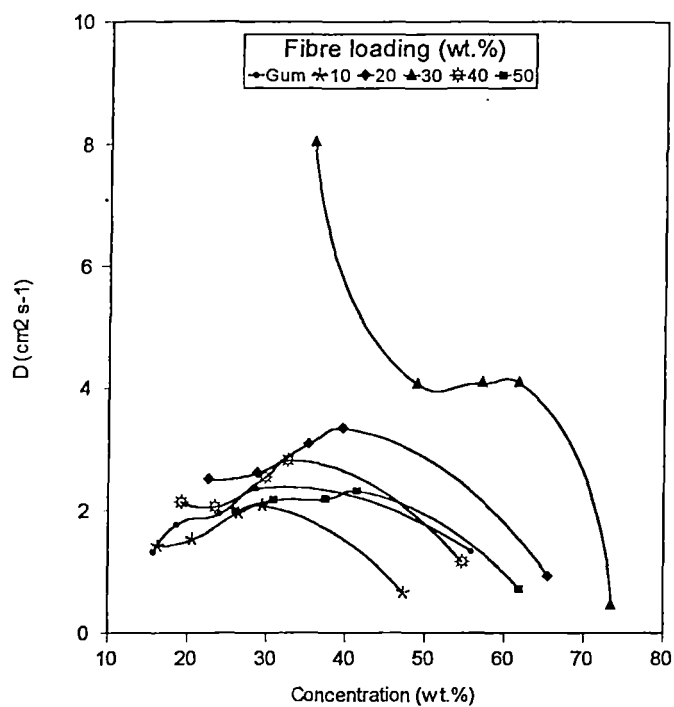
Figure 8.35 Arrhenius plots of $\ln D$ versus $1/T$

Table 8.16 Values of Activation Energy For Untreated Oil Palm Fibre/PF Composites having Different Fibre Loading, Oil Palm Fibre/Glass Hybrid PF Composites having Various Relative Volume Fractions of Oil Palm Fibre and Treated Oil Palm Fibre/PF Composites. [Total Fibre Loading = 40wt.%]

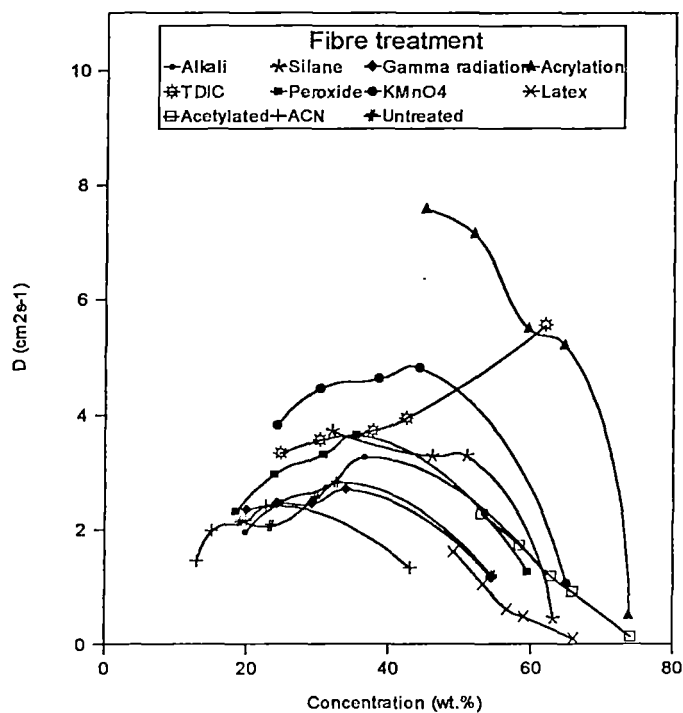
Composite Oil palm fibre loading (wt.%)	E_p (kJmol ⁻¹)	E_D (kJmol ⁻¹)	ΔH_s (kJmol ⁻¹)
Gum	45.43	48.46	-3.03
10	23.19	23.89	-0.7
20	16.42	15.71	0.71
30	02.01	6.29	-4.28
40	08.73	5.30	3.43
50	19.34	11.08	8.26
Relate V.F of oil palm fibre in hybrid composites			
0	24.74	26.03	-1.29
0.24	02.57	1.48	1.09
0.55	-06.74	-6.57	-0.17
0.74	02.12	3.33	-1.21
0.87	00.98	3.82	-2.84
0.92	05.59	5.25	0.34
0.96	03.16	2.55	0.61
1	08.73	5.30	3.43
Treatment (Fibre loading 40wt.%)			
Untreated	08.73	5.30	3.43
Alkali	17.92	16.48	1.44
Silane	17.83	16.54	1.29
γ radiation	42.61	07.36	35.25
Acrylated	24.8	18.65	6.15
Isocyanate	13.78	13.87	-0.09
Peroxide	12.40	13.51	-1.11
KMnO ₄	04.40	07.44	-3.04
Latex	07.35	02.65	4.7
Acetylated	01.81	03.42	-1.61
ACN	23.14	21.18	1.96

Table 8.17 Thermodynamic Functions For Untreated Oil Palm Fibre/PF Composites having Different Fibre Loading, Oil Palm Fibre/Glass Hybrid PF composites having Various Relative Volume Fractions of Oil Palm Fibre and Treated Oil Palm Fibre/PF Composites. (Total Fibre Loading = 40wt.%)

Composite Oil palm fibre loading (wt.%)	ΔH (kJmol ⁻¹)	$-\Delta S$ (JK ⁻¹ mol ⁻¹)	$+\Delta G$ (kJmol ⁻¹)
Gum	-13.21	+89.62	13.76
10	-00.97	+39.53	11.00
20	01.27	+34.26	11.66
30	-02.77	+50.23	12.44
40	04.04	+33.77	14.25
50	02.89	+29.35	11.77
Relative V.F of oil palm fibre in hybrid composites			
0	-02.65	+55.02	14.02
0.24	02.08	+35.50	12.84
0.55	-00.11	+38.18	11.40
0.74	-00.91	+40.61	11.39
0.87	03.09	+27.79	11.51
0.92	-00.62	37.05	10.61
0.96	-00.96	38.83	10.81
1	04.04	33.77	14.25
Treatment (Fibre loading 40wt.%)			
Untreated	04.04	33.77	14.25
Alkali	01.59	44.25	15.0
Silane	01.31	31.84	10.96
γ radiation	-03.77	53.34	12.39
Acrylated	02.35	33.24	12.42
Isocyanate	-00.41	37.41	10.92
Peroxide	-00.44	45.31	13.29
KMnO ₄	02.74	35.65	13.54
Latex	-00.54	34.88	10.03
Acetylated	-01.11	42.20	11.68
ACN	01.56	30.74	10.87



8.36 Concentration dependence of the diffusion coefficient for oil palm fibre/PF composites having different fibre loading at 30°C.



8.37 Concentration dependence of the diffusion coefficient for treated oil palm fibre/PF composites having 40wt.% fibre loading at 30°C.

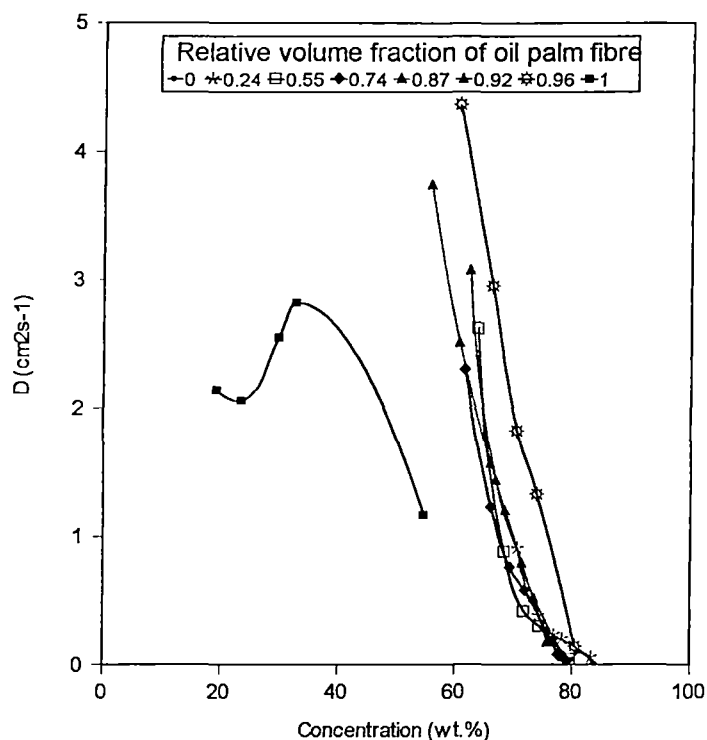


Figure 8.38 Concentration dependence of the diffusion coefficient for oil palm fibre/glass fibre hybrid PF composites having different relative volume fractions of oil palm fibres at 30°C.

Conflicting reports are there in literature about the concentration dependence of the water diffusion coefficient in polymers. It was reported by Hsu et al.¹³ that interpolymer hydrogen bonding decreases the diffusion coefficient of water clusters in PMMA and the diffusion coefficient decreases with increasing concentration of the diffusant. In hybrid composites, the initial water uptake is higher than unhybridised composites. Hence the evaluation of diffusion coefficients at lower concentration is difficult. However for the entire hybrid composites and glass/PF composite the diffusion coefficient decrease sharply beyond 55wt.% of sorbed water concentration (Figure 8.38).

8.9 EFFECT OF WATER SORPTION ON THE MECHANICAL PROPERTIES OF THE COMPOSITES

8.9.1 Tensile Properties

Water molecules can diffuse into the polymer matrix and can alter the fibre-matrix adhesive strength. Tensile properties of the composites before and after water sorption are given in Table 8.18. Silane and latex treated composites show higher extensibility upon water sorption. The tensile strength values of composite increased upon water sorption except in untreated and gamma irradiated composites in which cases the values remain almost constant. Water sorption results in swelling of the reinforced fibres and can produce some radial pressure at the fibre-matrix interface.³ This can enhance the tensile strength of the composites. Chua and Piggott¹⁴ have worked on the effect of water on interface pressure on the mechanical properties of glass/polyester interphase. The pressure

Table 8.18 Tensile Properties of the Composites having 40wt.% Fibre Loading Before and Water Sorption

Composite	Before water sorption			After water sorption		
	Tensile strength (MPa)	Elongation at break (%)	Tensile modulus (MPa)	Tensile strength (MPa)	Elongation at break (%)	Tensile modulus (MPa)
Untreated	37	4	1150	36	4	1068
Hybrid	30	4	1600	54	4	1727
Alkali	35	3	1300	39	5	1932
Silane	15	8	700	25	12	773
γ irradiated	21	3	825	17	7	591
Acrylated	18	9	600	19	8	830
Isocyanate	20	8	700	29	7	955
Peroxide	37	5	1050	37	8	1318
KMnO ₄	40	4	1200	46	4	1523
Latex	13	9	550	14	15	364
Acetylated	19	6	800	21	7	727
ACN	26	4	800	35	5	830

was governed by the thermal and chemical shrinkages, water dilation of the polymer etc. Tensile fracture behaviour of the composites before and after water sorption can be understood from the respective scanning electron micrographs (Figure 4.5, 4.8; refer Chapter 4 and 8.39a & b). Pulled out fibres are seen in alkali treated composites before water sorption (Figure 4.5). The fibre-matrix debonding is reduced to some extent in water sorbed composite as is evident from the decreased fibre-matrix interaction (Figure 8.39a). In permanganate treated composite the fibre breakage pattern is changed upon water sorption. Brittle breakage is observed in water sorbed composite (Figures 4.8 and 8.39b). Tensile modulus of the composite also showed increase on water sorption. However untreated, latex treated and acetylated composites show small decrease in the modulus value upon water sorption. Modulus is a measure of the stiffness of the composite.

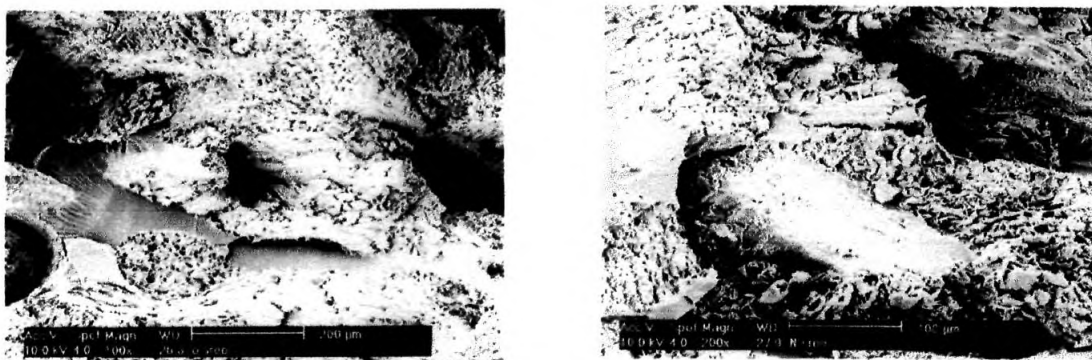


Figure 8.39 Scanning electron micrographs of tensile fracture of composites
(a) Alkali treated (Water sorbed) (b) Permanganate treated (Water sorbed)

8.9.2 Flexural Properties

Water absorption does not make much effect on silane, acrylated, isocyanate treated, acetylated and latex treated composites. Latex coating imparts hydrophobicity to the fibre surface. Water sorption can further lower the adhesive strength between latex coated fibre and matrix. This results in a lower value of

flexural strength. Flexural strength of the composites decreased upon water sorption except in the case of acrylated and hybrid composites (Table 8.19). The decrease can be attributed to the slippage of the sorbed fibre upon the application of compressive force. Glass fibre exhibits decreased water sorption. Presence of glass fibres can withstand slippage to a certain extent and enhances the flexural strength of the composites. The flexural strain increases on sorption except in the case of peroxide treated composite. Elongation of fibre increased considerably on water sorption. This high elongation of fibre on water sorption can withstand compressive force avoiding brittle failure of the composite and increases the flexural strain. However there is a considerable decrease in flexural modulus values in all unhybridised composites upon water sorption.

Table 8.19 Flexural Properties of the Composites having 40wt.% Fibre Loading Before and After Water Sorption.

Composite	Before water sorption			After water sorption		
	Flexural strength (MPa)	Flexural strain (%)	Flexural modulus at 1% strain (MPa)	Flexural strength (MPa)	Flexural strain (%)	Flexural modulus at 1% strain (MPa)
Untreated	49	6	3050	34	7	1284
Hybrid	56	2	3889	78	4	6149
Alkali	75	6	2950	61	6	2687
Silane	23	8	1200	16	8	776
γ irradiated	30	2	2200	22	9	1284
Acrylated	29	8	1800	30	8	1612
Isocyanate	32	9	1800	24	10	1284
Peroxide	54	7	3050	35	6	2299
KMnO ₄	55	3	3750	49	5	3224
Latex	16	8	700	11	8	448
Acetylated	36	7	1900	22	8	1015
ACN	52	5	2500	32	7	1731

The high modulus glass fibre in hybrid composites increases the flexural modulus of the composites on sorption. This may be due to the increased compatibility of the natural fibre, glass fibre and matrix on water sorption.

8.9.3 Impact Properties

Impact properties of the composites before and after water sorption are given in Table 8.20. An irregular trend is observed among treated composites. Impact strength of untreated, alkali treated, isocyanate treated, peroxide treated and acrylonitrile grafted composites enhanced on water sorption. In hybrid composites and in some treated composites (gamma irradiated, latex treated and acetylated composites) commendable decrease is observed. Decreased impact strength is due to the increased compatibility of the water sorbed hydrophilic fibres. Changes in the impact fracture mechanism on water sorption are evident from Figures 4.13 (refer Chapter 4) and 8.40a, b & c.

Table 8.20 Impact Properties of the Composites having 40wt.% Fibre Loading Before and After Water Sorption.

Composite	Impact strength (kJ/m ²) Before water sorption	Impact strength (kJ/m ²) After water sorption
Untreated	41	48
Hybrid	280	202
Alkali	48	50
Silane	165	160
γ irradiated	105	69
Acrylated	129	120
TDIC	155	162
Peroxide	56	200
KMnO ₄	53	45
Latex	190	102
Acetylated	181	120
ACN	59	63

In the untreated composite, fibre-matrix debonding is found to be one of the main failure criteria in the sorbed stage. Extra energy is needed to do the work of debonding and increases the impact strength of the composite. In latex treated composite, the elasticity of fibres withstand the brittle failure. More fibrillation is observed in water sorbed composite.

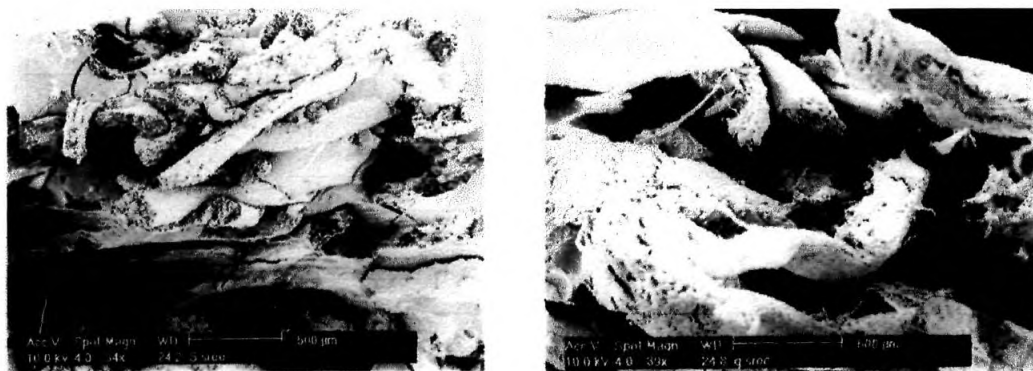


Figure 8.40 Scanning electron micrographs of impact fracture of composites
(a) Untreated (Water sorbed) (b) Latex treated (Before water sorption)

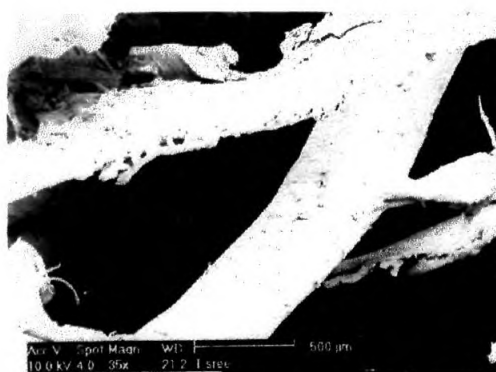


Figure 8.40 Scanning electron micrographs of impact fracture of composites
(c) Latex treated (Water sorbed)

REFERENCES

1. P. K. Aditya and P. K. Sinha, *Polym. Comp.*, **1**(5), 341 (1993)
2. A. G. Andreopoulos, P. A. Tarantili, *J. Appl. Polym. Sci.*, **70**, 747 (1998)
3. A. C. Karmaker, A. Hoffmann and G. Hinrichsen, *J. Appl. Polym. Sci.*, **54**, 1803 (1994)
4. M. S. Sreekala, S. Thomas and N. R. Neelakantan, *J. Polym. Eng.*, **16**, 265 (1997)
5. T. Marzi, U. Schroder, M. HeB, R. Kosfeld, *Mat. Res. Soc. Symp. Proc.*, Vol. **170**, 123 (1990)
6. T. Morii, H. Hamada, Z. Maekawa, T. Tanimoto, T. Hirano, K. Kiyosumi and T. Tsujii, *Comp. Sci. Techn.*, **50**, 373 (1994)
7. M. S. Sreekala, M. G. Kumaran and S. Thomas, *Appl. Comp. Mater.*, (In press)
8. S. Mishra, J. B. Naik, *J. Appl. Polym. Sci.*, **68**, 681 (1998)
9. V. Bellenger, B. Mortaigne and J. Verdu, *J. Appl. Polym. Sci.*, **41**, 1225 (1990)
10. M. K. Antoon and J. L. Koenig, *J. Polym. Sci. Part B Polym. Phys.*, **19**, 197 (1981)
11. J. J. Imaz, J. L. Rodriguez, A. Rubio and I. Mondragon, *J. Mater. Sci.*, **10**, 662 (1991)
12. R. J. Kokes and F. A. Long, *J. Am. Chem. Soc.*, **75**, 6142 (1953)
13. W. P. Hsu, R. J. Li, A. S. Myerson and T. K. Kwei, *Polymer*, **34**, 597 (1993)
14. P. S. Chua and M. R. Piggott, *J. Mater. Sci.*, **27**, 925 (1992)

CHAPTER 9

Environmental Effects in Oil Palm Fibre Reinforced Phenol Formaldehyde Composites: Studies on Thermal, Biological, Moisture and High Energy Radiation Effects

*Results of this study have been submitted for publication in the journal **Composites***

Abstract

Accelerated weathering studies of untreated and treated oil palm fibre reinforced phenol formaldehyde composites and oil palm/glass hybrid fibre reinforced phenol formaldehyde composites were conducted. Thermal, water, biological and γ radiation effects on the composite properties were analysed. Mechanical properties such as tensile, flexural and impact properties of thermal and water aged samples were investigated. The extent of biodegradation and γ irradiation effects was estimated from variations in tensile and impact properties. The tensile and impact fracture mechanism and changes in fibre-matrix adhesion were studied using scanning electron microscopic analysis. The changes in the tensile and flexural stress-strain characteristics as well as deformation behaviour of aged composites are well explained by respective stress-strain curves. Thermogravimetric analysis of the composites was done to determine thermal stability of the materials. Mechanical performance of the composites decreased upon thermal ageing. Marked decrease in these properties of the composites is observed upon radiation ageing. However water immersion leads to an increase in strength properties in some treated composites such as on acetylation, silane, acrylonitrile grafting, isocyanate, permanganate treatment, alkali treatment etc. It is found that oil palm fibre increases the biodegradability of the composites.

Response of polymer composites to environmental exposure must be known to utilise their full potential as a structural material. Polymers often undergo degradation rapidly in outdoor applications. The environmental degradation of polymeric materials includes thermal, mechanical, photochemical, radiation, biological, chemical degradation etc. Polymer degradation is mainly caused by chemical bond scission reactions in macromolecules.¹ Several studies have been reported on the thermal, photo, biological and outdoor weathering of polymer composites.²⁻⁶ It was found that long-term exposure of the composites to elevated conditions affect the mechanical properties. Recently Hancox reviewed the effects of temperature and environment on the performance of polymer matrix composites.⁷

Natural fibres are susceptible to moisture, temperature, high energy radiation and attack from bio organisms. Most of the natural fibres are stable upto 300°C. Hence incorporation of natural fibres into plastics changes their environmental stability. Phenolic resins are highly heat resistant and they find applications in aerospace as ablative heat shields for protection of space vehicles. Changes in the thermal degradation behaviour of natural fibre reinforced phenolic composites can be evaluated from thermogravimetric analysis. Incorporation of natural fibres accelerates the thermal degradation process.

Present work describes various ageing effects on the mechanical properties of oil palm fibre reinforced phenol formaldehyde composites. Thermal, water, boiling water, γ irradiation and biodegradation effects are investigated. Thermogravimetric analysis is used to study the degradation behaviour of the composites.

9.1 AGEING EFFECTS ON TENSILE PROPERTIES

The tensile stress-strain behaviour of unaged and aged composites are given in Figures 9.1-9.6. The unaged composite shows necking followed by catastrophic failure (Fig. 9.1). Alkali and permanganate treatments improve the fibre-matrix interaction leading to the brittle fracture of the composites for which the

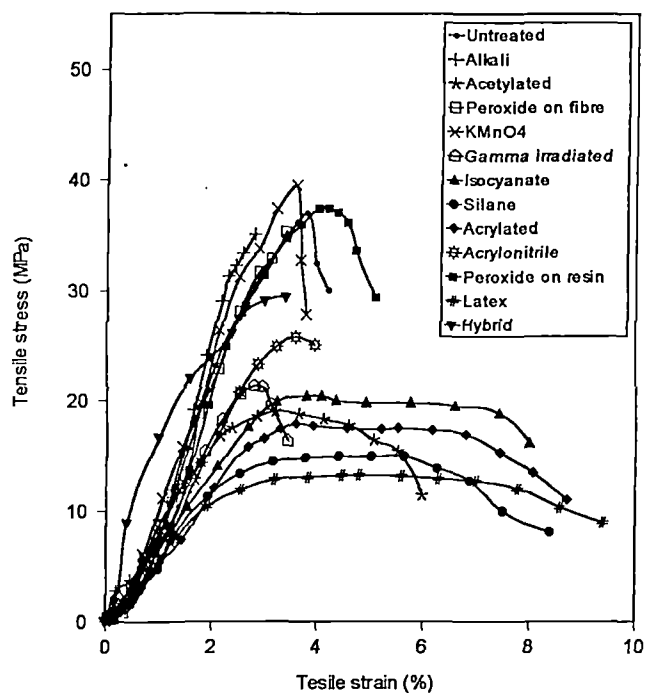


Figure 9.1 Tensile stress-strain characteristics of unaged composites.

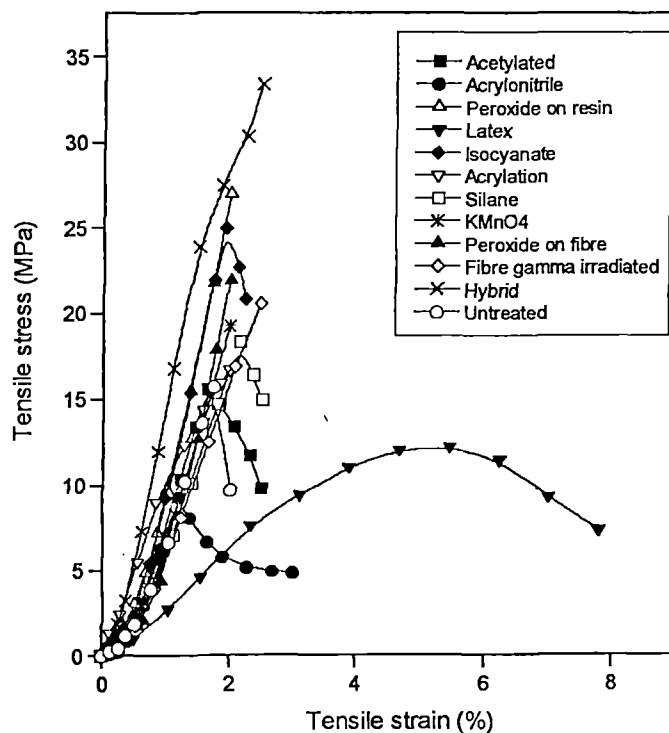


Figure 9.2 Tensile stress-strain characteristics of thermal aged composites.

stress-strain curves are evidence. Presence of oil palm fibre in hybrid composites makes the composite less brittle. Treatments such as peroxide on resin, acrylonitrile grafting and gamma irradiation cause necking effect. The stress-strain curves of unaged, isocyanate, acrylated, acetylated, silane and latex treated composites show major slope change at an early stage. These composites exhibit yielding and higher extensibility. A dramatic change in the stress-strain behaviour of the composites was observed upon thermal ageing (Fig. 9.2). Except latex treated composites all composites show sharp brittle failure. Crack propagation in a thermal aged composite is faster which leads to catastrophic failure of the system. Fibre breakage will also easier in a thermal aged composite. In latex treated composite, latex can form a protective coating on the fibre surface. Crack propagation can be hindered by the presence of elastic phase and leads to a higher elongation. On water immersion the necking effect becomes more prominent (Fig. 9.3). The decreased brittle nature is attributed to the plasticising effect of water in composites. Effect of boiling water ageing on the tensile stress-strain behaviour of the selected composites was given in Figure 9.4. Catastrophic failure occurred in untreated and in peroxide treated fibre composites. It is found that biological effects by the fungi affect the stress-strain behaviour of the composites. A prominent necking effect is observed in silane treated composite upon biodegradation (Fig. 9.5). The radiation effects on the stress-strain behaviour are evident from Figure 9.6. Gamma irradiated acrylated composite shows exceptionally high elongation. Hybrid composite shows higher brittle behaviour.

The effect of ageing on the tensile strength values of the composites is given in Table 9.1. Untreated and most of the other treated composites show changes in properties upon thermal ageing, biodegradation and radiation ageing. However, on water immersion the tensile strength retains and in most cases enhancement in strength value is observed. This is due to the swelling of the fibre on water immersion thereby decreasing the void size at the fibre-matrix interphase. This can exert a radial pressure leading to higher tensile strength values. Among water aged composites boiling water aged composites show comparatively lower values.

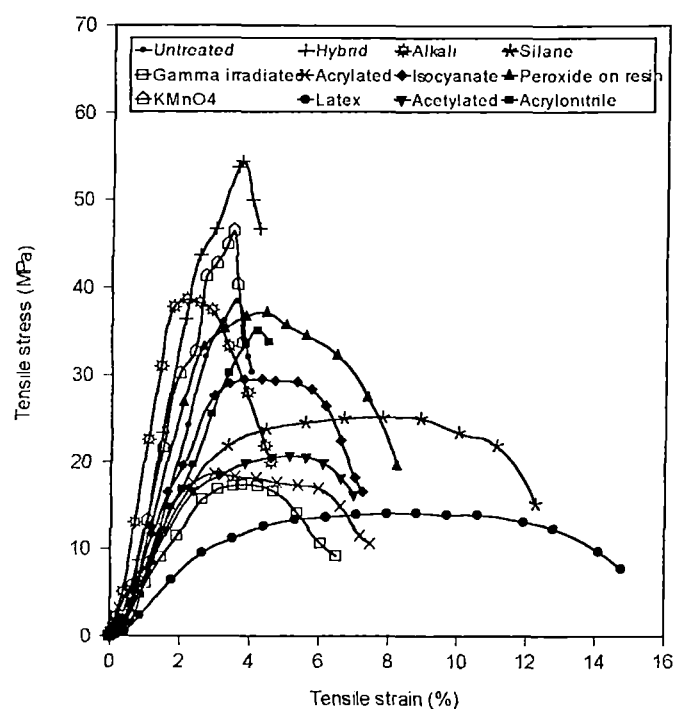


Figure 9.3 Tensile stress-strain characteristics of cold water aged composites.

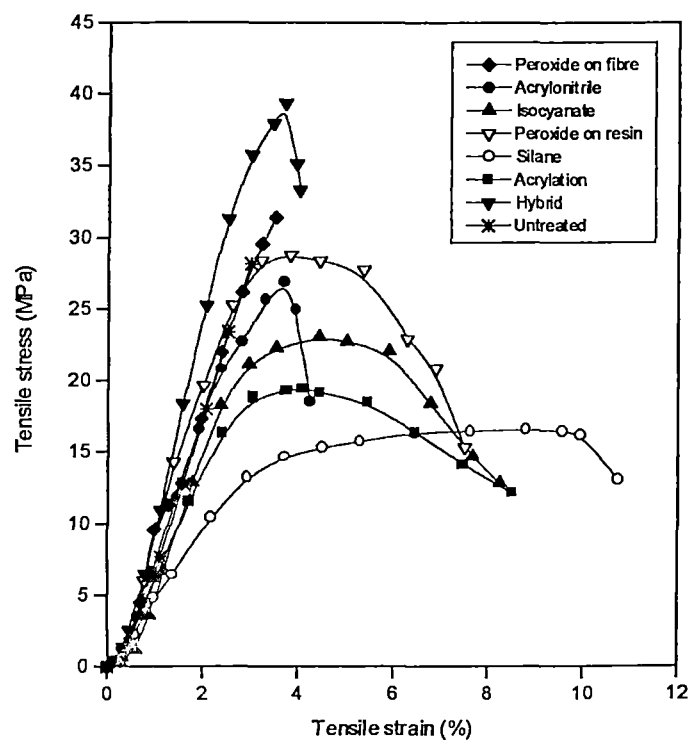


Figure 9.4 Tensile stress-strain characteristics of boiling water aged composites.

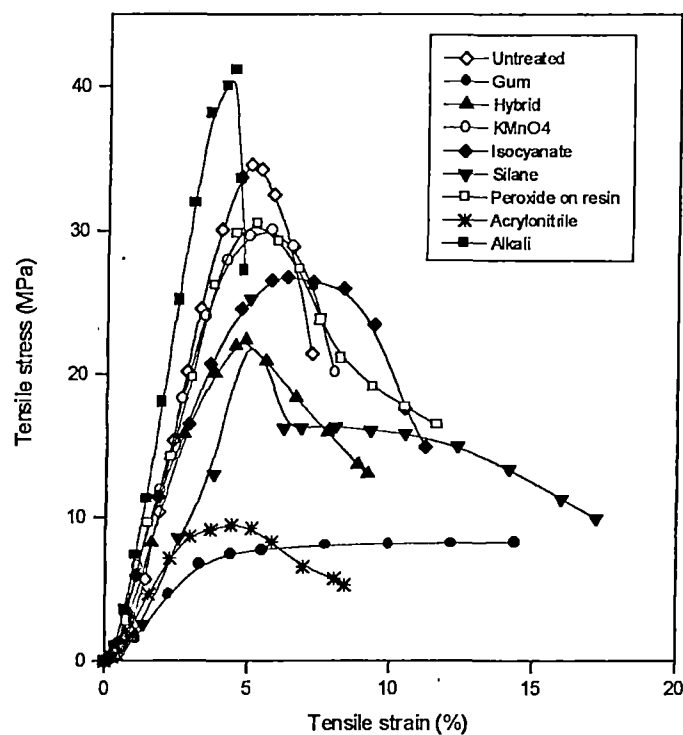


Figure 9.5 Tensile stress-strain characteristics of biodegraded composites.

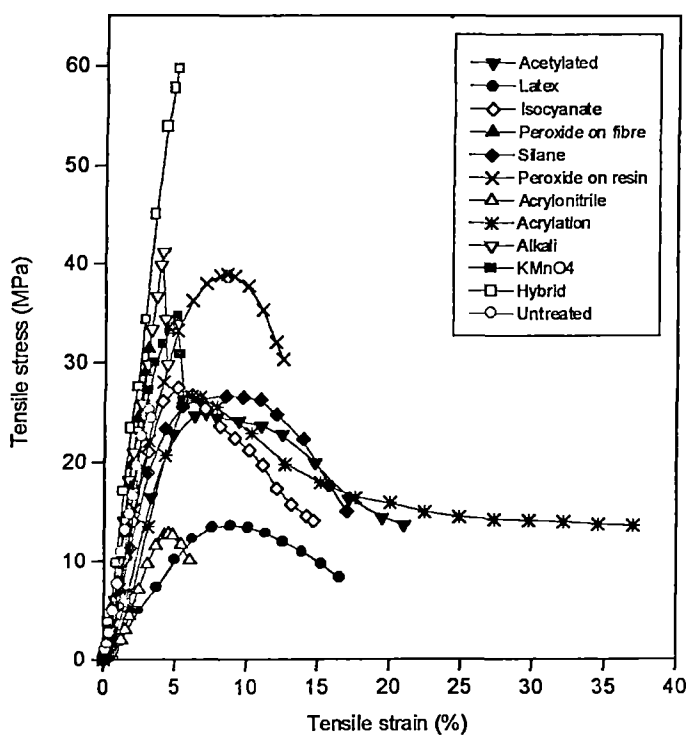


Figure 9.6 Tensile stress-strain characteristics of gamma irradiated composites.

Table 9.1 Tensile Strength Values (MPa) of Unaged and Aged Composites

Sample	Unaged	Thermal aged (100°C; 72hrs.)	Cold Water aged (2 weeks)	Boiling water aged (2hrs.)	Biodegradation (8 months)	Gamma irradiation				
						Dose (Mrad)				
						0.1	1	10	50	100
Untreated	37	16	38	28	35	28	25	20	5	6
Hybrid	30	33	54	39	22	39	60	45	40	33
Acetylated	19	16	21	----	----	22	19	24	14	11
Acrylonitrile	26	9	35	27	9	29	13	29	10	11
Peroxide on resin	37	27	37	29	31	27	39	32	26	18
Latex	13	12	14	----	----	16	14	18	13	11
Isocyanate	20	25	29	23	27	22	23	28	21	10
Acrylation	18	17	19	19	----	20	27	22	12	10
Silane	15	18	25	17	16	25	27	20	14	11
KMnO ₄	40	19	46	----	30	46	35	32	19	16
Mercerisation	35	----	39	----	41	40	41	34	31	30
Peroxide on fibre	35	22	----	31	----	33	31	33	30	12
Fibre irradiated γ	21	21	17	----	----	----	----	---	---	----

Similar enhancement in strength properties of various natural fibre reinforced polymer composites was reported.^{8, 9} The retention in tensile properties can be attributed to the plasticising effect of water and better fibre-matrix adhesion at lower water absorption stage. Thermal degradation occurred in composites except hybrid, isocyanate and silane treated composites. Glass fibre is stable above 900°C without any weight reduction. Major degradation in phenolics occurs at 500°C. Oil palm fibres were found to be stable upto 325°C. Upon thermal ageing, degradation in interface properties may occur from the decrease in fibre-matrix adhesion. Physical interaction between the fibre and matrix decreases owing to the shrinkage of the oil palm fibre in thermal environment. But fibre coatings like silane and

protective layers by glass etc. can eliminate this type of thermal deterioration in composites. Among the biodegraded composites, isocyanate, silane and alkali treated composites show enhanced tensile strength values. Presence of moisture can lead to more stable system by plasticising effect. Studies have been reported on the degradation behaviour in various thermosetting composites under thermal and chemical environments.^{10, 11} It was found that thermal degradation is a complex phenomenon that changes thermal and mechanical properties of the material in an irreversible form. A small dose of gamma irradiation on composite increases the tensile strength except in untreated and resin peroxide treated composites. However at higher doses of radiation, the strength decreased considerably. It is reported that gamma irradiation of polymers can result in chain scission, molecular weight changes, molecular rearrangements, free radical initiation etc.¹² The free radicals formed can enhance the crosslinking between the fibre and matrix thereby enhancing the strength. But at higher radiation doses, disintegration of fibre and matrix causes degradation in properties. Similar results have been reported in carbon fibre reinforced epoxy composites in which case the ultimate tensile strength keeps its value until the first influence and then falls to 60-70% at higher dose levels.¹³ Also, in graphite reinforced epoxy composite, the graphite fibre strength is not affected by radiation, but the tensile properties of the epoxies were adversely affected by the radiation.¹⁴ However in this system it is reported that the interfacial shear strength value increases with the radiation dose.

Variation in elongation at break of the composites upon various ageing is given in Table 9.2. The elongation of the composites decreased upon thermal ageing. In most cases the values show enhancement upon water ageing and biodegradation. The decreased elongation upon thermal ageing is due to the decreased elongation of the fibre on thermal degradation. It has already been found that the elongation at break of oil palm fibre considerably enhanced upon water immersion.¹⁵ The intrinsic elongation behaviour of the fibre on water ageing leads to composites with higher elongation. Gamma irradiation increases the elongation of the composites. Changes in the fibre-matrix interactions are responsible for the

enhancement in elongation of the composites. However in the case of thermoplastics such as polyethylene, a decrease in elongation at break is reported with absorbed dose of high energy ion irradiation.¹⁶

Table 9.2 Elongation at Break Values (%) of Unaged and Aged Composites.

Sample	Unaged	Thermal aged (100°C; 72hrs.)	Cold Water aged (2 weeks)	Boiling water aged (2hrs.)	Biodeg- radation (8 months)	Gamma irradiation				
						Dose (Mrad)				
						0.1	1	10	50	100
Untreated	4	2	4	3	7	8	5	5	26	21
Hybrid	4	3	4	4	9	12	5	6	6	7
Acetylated	6	3	7	----	----	11	15	11	5	25
Acrylonitrile	4	3	5	4	8	9	6	23	4	26
Peroxide on resin	5	2	8	8	12	11	13	5	5	10
Latex	9	8	15	----	----	18	17	11	4	9
Isocyanate	8	2	7	8	11	9	11	8	6	3
Acrylation	9	2	8	9	----	12	37	13	15	12
Silane	8	3	12	11	17	20	17	15	5	3
KMnO ₄	4	2	4	----	8	8	6	6	5	4
Mercurisation	3	----	5	----	5	4	4	4	4	3
Peroxide on resin	3	2	----	4	----	6	3	6	5	18
Fibre irradiated	3	3	7	----	----	---	---	----	---	----

The tensile moduli of the composites at 1% strain of the unaged and aged composites are compared in Table 9.3. Thermal ageing leads to enhanced modulus in acetylated, peroxide treated resin, isocyanate, acrylated and silane treated composites. Increased temperature leads to increase in cross linking which increases the modulus of the composites. The stiffness of the peroxide, isocyanate, acrylated, silane, permanganate and alkali treated composite increased upon water

ageing. Upon biodegradation decrease in modulus is observed in all systems. Modulus of the untreated composite enhanced upon gamma irradiation. Peroxide on fibre and alkali treated composite also showed enhanced modulus values upon gamma irradiation.

Table 9.3 Tensile Modulus Values (MPa) of Unaged and Aged Composites

Sample	Unaged	Thermal aged (100°C; 72hrs.)	Cold Water aged (2 weeks)	Boiling water aged (2hrs.)	Biodeg- radation (8 months)	Gamma irradiation 1Mrad
Untreated	746	600	688	702	286	873
Hybrid	1665	1438	1217	1010	412	1223
Acetylated	682	740	633	----	----	304
Acrylonitrile	810	670	605	758	259	164
Peroxide on resin	685	938	1022	996	552	528
Latex	575	262	299	----	----	136
Isocyanate	660	938	828	535	552	528
Acrylation	468	623	661	632	----	234
Silane	532	542	633	521	189	500
KMnO ₄	1045	646	1189	----	552	667
Mercerisation	853	----	2107	----	678	947
Fibre γ irradiated	746	530	578	----	----	----
Peroxide on fibre	858	565	----	954	----	947

9.1.1 Tensile Fracture Mechanism

Tensile fracture mechanism in aged condition is studied by scanning electron microscopy. Tensile fractograph of water aged alkali treated composites is given in Figure 9.7. Better fibre-matrix interaction is evidenced from the fracture surface.

Major failure occurred by fibre breakage. Effect of gamma radiation on the matrix failure is clear from the scanning electron micrograph of tensile fracture of PF gum sample (Fig. 9.8).

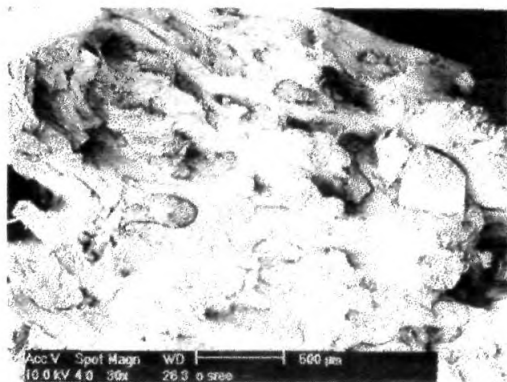


Figure 9.7 SEM of tensile fracture of cold water aged alkali treated oil palm fibre/PF composite.(X30)

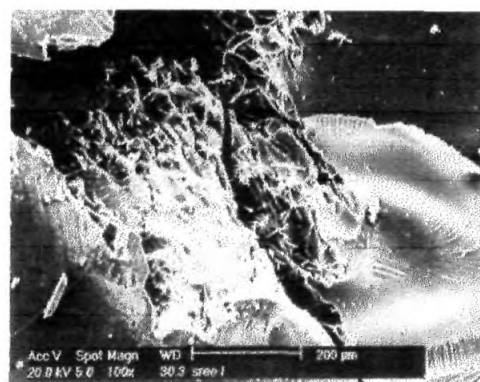


Figure 9.8 SEM of tensile fracture of gamma irradiated neat PF sample.(X100)

Multiple fracture arising from the disintegration of the sample by radiation is evident from the above figure. Tensile fracture of gamma irradiated alkali treated composite shows matrix cracking (Fig. 9.9). Brittle fibre failure is observed here. In gamma ray irradiated permanganate treated composite, fibrillation is observed(Fig. 9.10).

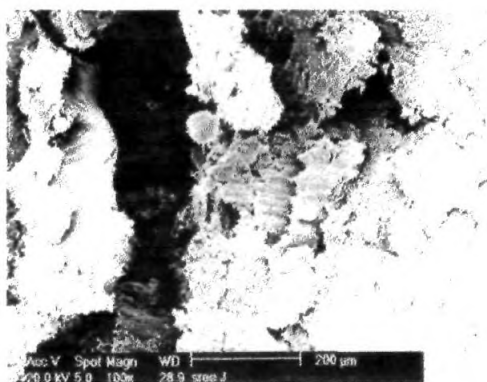


Figure 9.9 SEM of tensile fracture of gamma irradiated alkali treated oil palm fibre/PF composite.(x100)

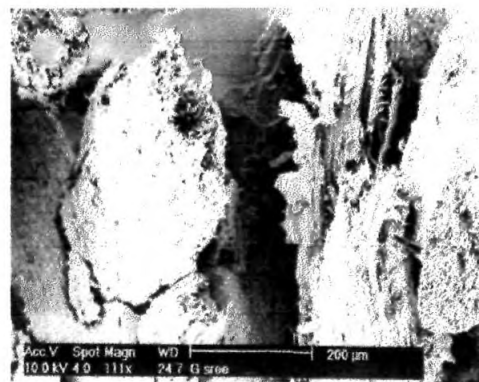


Figure 9.10 SEM of tensile fracture of gamma irradiated permanganate treated oil palm fibre/PF composite.(x111)

Fibre-matrix debonding and ductile failure of the fibre is seen. In hybrid composites, radiation causes disintegration. This is clear from the micrograph (Fig. 9.11). Glass fibre-matrix debonding becomes easier upon radiation ageing which is evident from the debonded paths found in the micrograph.

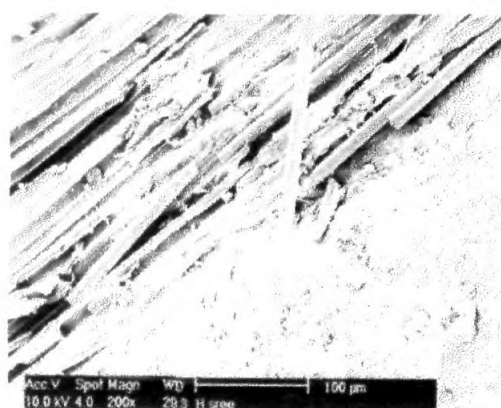


Figure 9.11 SEM of tensile fracture of gamma irradiated oil palm/glass hybrid fibre PF composite.(x200)

9.2 AGEING EFFECTS ON THE FLEXURAL PROPERTIES

The flexural stress-strain behaviour of unaged, thermal aged and water aged composites are given in Figures 9.12-9.15. Due to the presence of glass fibre, the hybrid composite undergoes catastrophic failure upon application of flexural force, which is a combination of tension and compression. Fibre exposed to gamma irradiation and permanganate treated composites failed at lower flexural strain in unaged condition (Fig. 9.12). On thermal ageing the failure strain decreased to a very low value. However in thermal aged composites, acetylated and gamma irradiated fibre reinforced composites withstand higher strain (Fig. 9.13). On water ageing the composite became more flexible due to the presence of water and therefore less brittle behaviour is observed (Fig. 9.14 & 9.15).

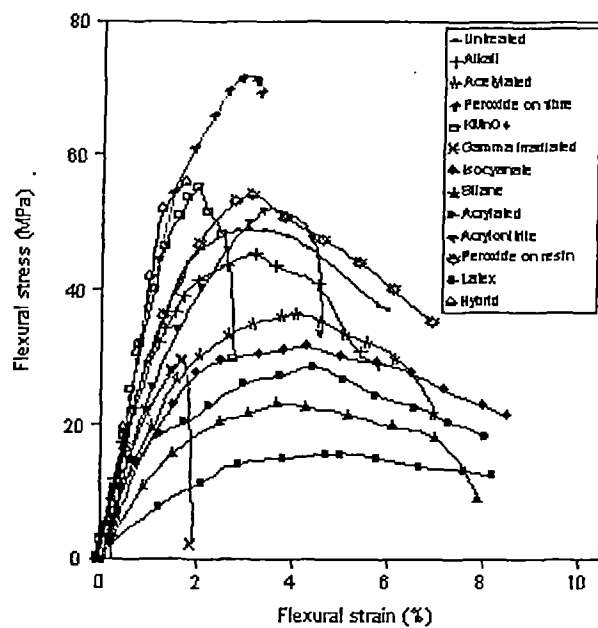


Figure 9.12 Flexural stress-strain characteristics of unaged composites.

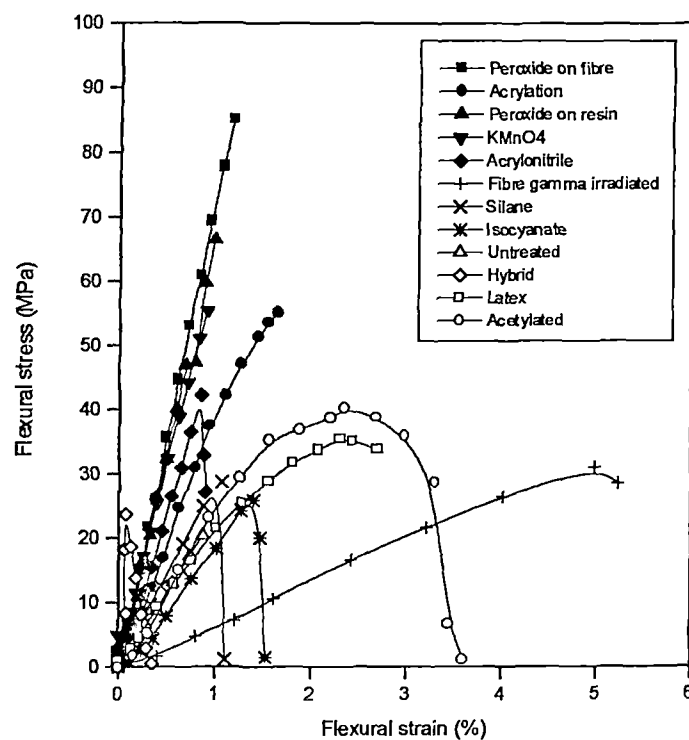


Figure 9.13 Flexural stress-strain characteristics of thermal aged composites.

Variation of flexural strength on thermal and water ageing are given in Table 9.4. Flexural strength of untreated composites decreased upon ageing. The flexural properties of peroxide, latex modified and acrylated fibre composites showed increase upon thermal ageing. However untreated and most of the treated composites show decreased flexural performance on water ageing. Flexural modulus shows similar trend (Table 9.5). In the case of hybrid composites cold water ageing increased the flexural properties. Water can act as a plasticizer at the fibre-matrix interface. The absorbed water affects the interlaminar properties of the composites and hence the compressive failure of the composites.

Table 9.4 Flexural Strength Values (MPa) of Unaged and Aged Composites

Sample	Unaged	Thermal aged (100°C; 72hrs.)	Cold Water aged (2 weeks)	Boiling water aged (2hrs.)
Untreated	49	20	33	23
Hybrid	----	23	78	65
Acetylated	36	40	22	26
Acrylonitrile	52	42	32	29
Peroxide on resin	54	67	35	40
Latex	16	35	11	11
Isocyanate	32	26	24	24
Acrylation	29	55	30	25
Silane	23	29	16	14
KMnO ₄	55	55	49	43
Mercerisation	75	----	61	----
Fibre γ irradiated	30	31	22	18
Peroxide on fibre	71	85	----	30

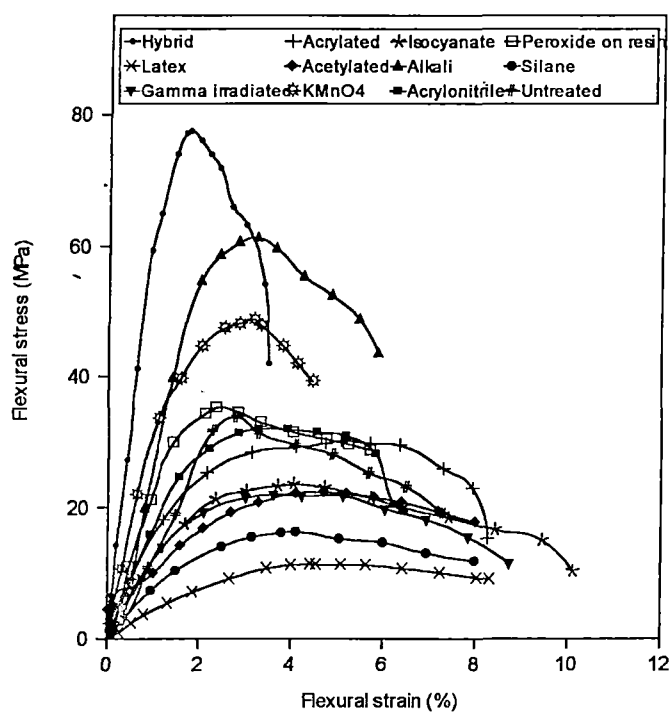


Figure 9.14 Flexural stress-strain characteristics of cold water aged composites.

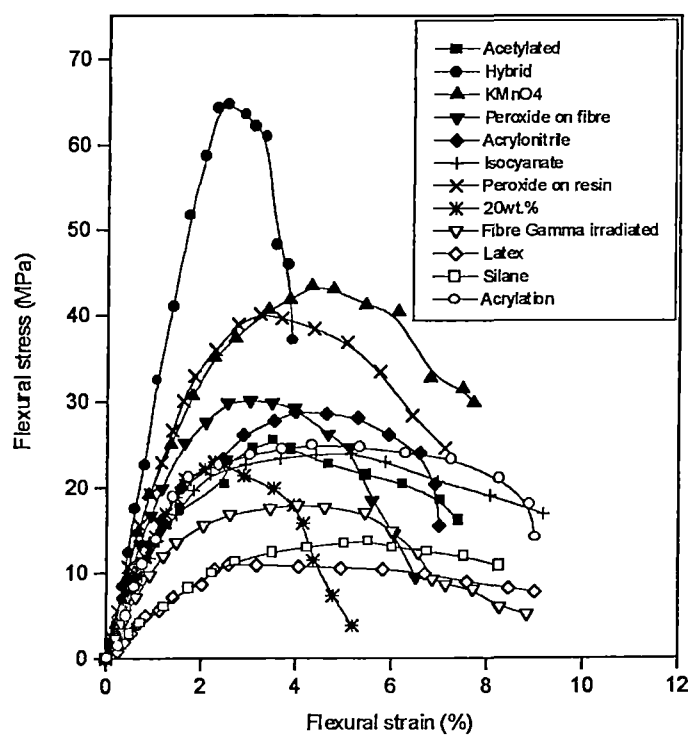


Figure 9.15 Flexural stress-strain characteristics of boiling water aged composites.

9.3 AGEING EFFECTS ON THE IMPACT PROPERTIES

Izod impact strength values of composites on various ageing are given in Table 9.6. Impact strength enhanced upon water ageing in untreated, acrylonitrile, peroxide and isocyanate treated composites. Composite impact strength degraded upon thermal, biodegradation and on gamma irradiation. The decrease is prominent at higher doses of radiation and on thermal ageing. Izod impact strength is a measure of the energy required to initiate and propagate a crack. Phenolics exhibit superior heat resistance compared to polyesters and epoxies. This is directly related to the structure and thermal degradation mechanism of phenolics.

Table 9.5 Flexural Modulus Values (MPa) of Unaged and Aged Composites.

Sample	Unaged	Thermal aged (100°C; 72hrs.)	Cold Water aged (2 weeks)	Boiling water aged (2hrs.)
Untreated	3596	2292	1184	1402
Hybrid	4194	----	7652	2740
Acetylated	2280	2180	1568	1522
Acrylonitrile	2578	----	2032	1562
Peroxide on resin	3656	6596	2648	2218
Latex	782	2292	490	620
Isocyanate	1860	1622	1568	1316
Acrylation	2100	3800	2032	1358
Silane	1260	2906	952	490
KMnO ₄	4136	6484	4034	2218
Mercerisation	3478	----	2724	----
Fibre γ irradiated	2578	504	1568	1098
Peroxide on fibre	3814	7156	----	1912

Several research studies have been reported in improving the low impact strength of the phenolics.^{17, 18} It is found that impact strength is strongly influenced by fibre/matrix interface and fibre length. Maximum energy can be dissipated by mechanical friction during the pull out process and by debonding of the fibres.¹⁸ The decline in the properties of the phenolic composite upon thermal ageing is due to the breakdown of the bonds at the fibre-matrix interface. The unnotched and notched izod impact performance of phenolic composites following thermal exposure was studied in detail by Kuzak et al.¹⁹ They observed that the impact performance of the S-glass (Strength-glass) reinforced phenolic composite declined when exposed to 300°C temperature.

Table 9.6 Impact Strength Values (kJ/m²) of Unaged and Aged Composites

Sample	Unaged	Thermal aged (100°C; 72hrs.)	Cold Water aged (2 weeks)	Boiling water aged (2hrs.)	Biodegradation (8 months)	Gamma irradiation				
						Dose (Mrad)				
						0.1	1	10	50	100
Untreated	41	16	48	59	17	7	18	6	3	2
Hybrid	280	106	202	115	52	53	47	34	14	25
Acetylated	181	46	119	135	53	46	53	40	7	3
Acrylonitrile	59	12	63	54	11	20	23	15	4	5
Peroxide on resin	56	21	199	152	28	38	27	18	4	2
Latex	190	65	102	105	35	31	47	23	12	2
Isocyanate	155	26	162	149	62	47	39	27	7	4
Acrylation	129	14	119	78	19	28	30	11	3	3
Silane	165	25	160	131	60	99	70	46	4	24
KMnO ₄	53	18	45	52	27	27	20	28	3	43
Fibre γ irradiated	105	21	69	64	28	---	---	----	---	----
Peroxide on fibre	44	22	----	53	17	17	16	7	4	4

They prepared a phenolic blend from resole and novolac and found to have best retention in impact properties on thermal exposure. The izod impact strength of all the composites declined to a very low value upon gamma irradiation. This is due to the bond scission and disintegration at the fibre-matrix interface.

9.3.1 Impact Fracture Mechanism

Scanning electron micrographs of the impact fracture surfaces were taken to study the fracture mechanism(Figs. 9.16 - 9.21). Pulled out fibre are seen in water aged, acetylated and latex treated composites (Figs. 9.16 and 9.17). Moderate retention in impact strength in these composites is observed. The exposed fibre indicates weak adhesion at the interface.



Figure 9.16 SEM of impact fracture of water aged, acetylated oil palm fibre/PF composite.(x19)

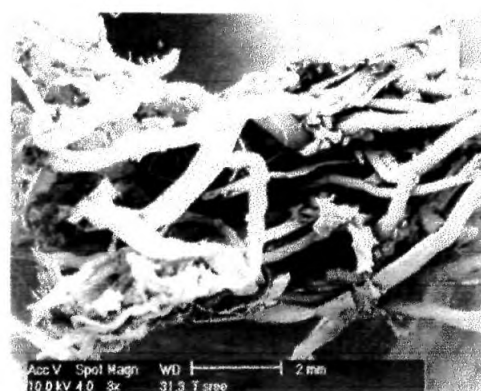


Figure 9.17 SEM of impact fracture of water aged, latex coated oil palm fibre/PF composite.(x8)

The impact fracture lines are clearly visible on failure surface of gamma irradiated neat PF sample (Fig. 9.18). The interfacial disintegration on gamma irradiation is evident from the fractograph of acetylated composite(Fig. 9.19). Fibrillation is also observed. Fibre failure due to the cracking and splitting of the fibres is visible in the failed surface of the gamma irradiated, latex coated composite (Fig. 9.20). The fibre strength is decreased considerably in silane treated composite upon gamma irradiation as is evident from the breaking pattern of the fibre (Fig. 9.21).

9.4 THERMAL STABILITY OF THE COMPOSITES

The degradation temperature of the composites was determined using thermogravimetric analysis and differential thermogravimetry. Figure 9.22 shows the TG and DTG curves of neat PF sample and composites, analysed from ambient

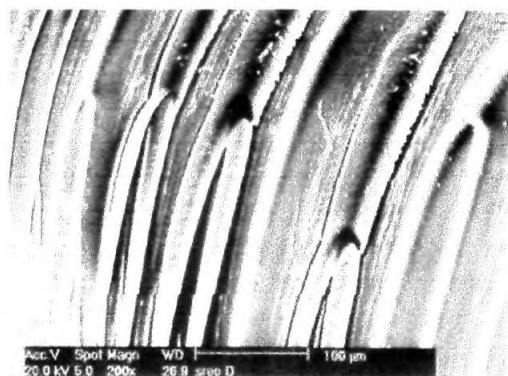


Figure 9.18 SEM of impact fracture of gamma irradiated, neat PF sample.(x200)

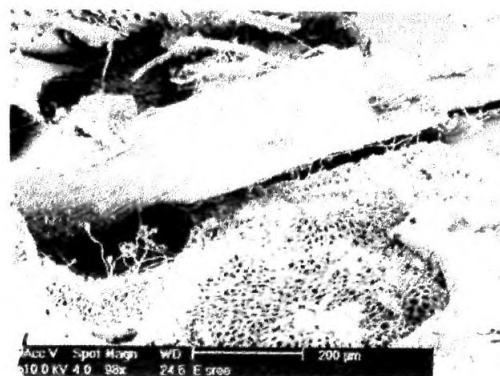


Figure 9.19 SEM of impact fracture of gamma irradiated, acetylated oil palm fibre/PF composite.(x98)

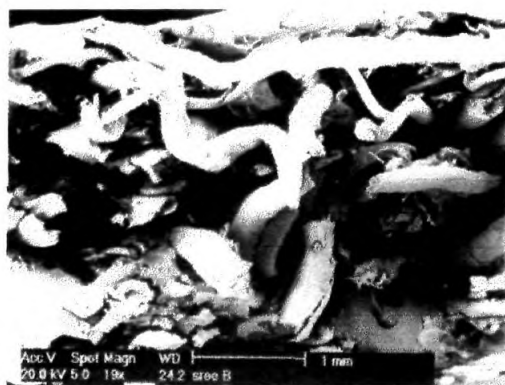


Figure 9.20 SEM of impact fracture of gamma irradiated, latex coated oil palm fibre/PF composite.(x19)



Figure 9.21 SEM of impact fracture of gamma irradiated, silane treated oil palm fibre/PF composite.(x49)

to 800°C. The major degradation of phenolic resin occurs around 550°C (Fig. 9.22a). Measurable weight loss occurs initially due to the escape of water molecules from the resin. Degradation processes originate from an initial bond

breaking reaction. This may be a prelude to a series of secondary chemical reactions leading to further bond scission, recombination or substitution reaction. Above 250°C cured phenolic resin decomposes.²⁰ Oxygen is present in the amorphous domains of all polymers, degradation by chain oxidation reactions involving oxygen is the most prevalent destructive process and is implicated in the degradation above 600°C.

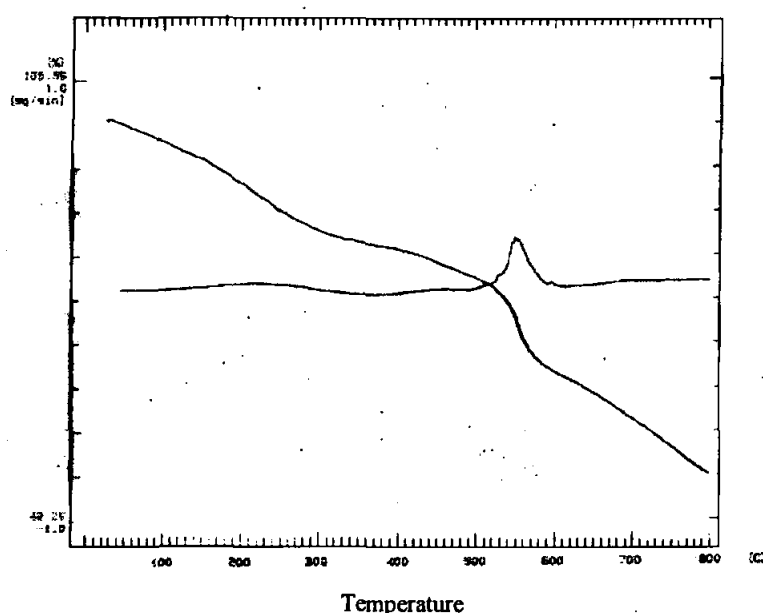


Figure 9.22a TGA and DTG curves of neat PF sample.

The DTG curve of the sample shows a sharp peak at 550°C. The glass reinforced PF composites show one major peak in its DTG curve at 580°C due to the degradation of the resin (Fig. 9.22b). Pektaş²¹ reported that E-glass fibres show no mass loss upto 900°C. The slight weight loss at about 430°C is due to the breakdown of methylene linkages in the phenolic network. In oil palm fibre/PF composite, the major degradation occurs at 345°C followed by two minute peaks at 425°C and 575°C (Fig. 9.22c). It is found that oil palm fibres are stable upto 325°C. The thermogravimetric curves of untreated and treated oil palm fibres are given in Figure 3.19 and 3.20. Dehydration process occurs within the fibre and at

fibre-matrix interface, which accounts for the very initial weight loss in composite samples. As the temperature increases, the primary bonds weaken and less ordered region increases.

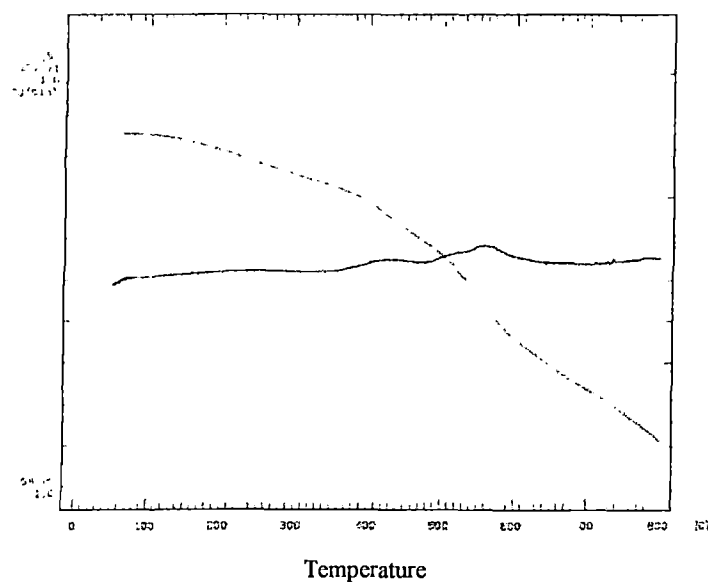


Figure 9.22b TG and DTG curves of glass fibre/PF composites.

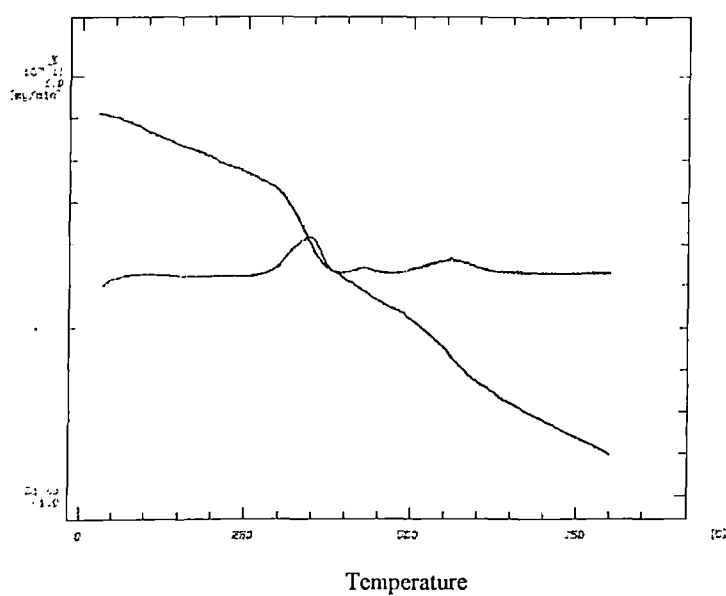


Figure 9.22c TG and DTG curves of oil palm fibre/PF composites.

Further increase in temperature destroys the cellular structure of the fibre which leads to the degradation of the fibre part. The thermal degradation of dehydrocellulose also takes place at this temperature (345°C). It is reported that maximum pyrolysis in PMMA grafted wood pulp occurs at 305-306°C.²² Studies have been reported on the effect of crystallinity, orientation and crosslinking on the pyrolytic behaviour of celluloses.^{23, 24} In a fibrous composite the fibre-matrix adhesion plays a key role in thermal stability.

Figure 9.22d shows the thermal behaviour of oil palm fibre/glass hybrid PF composite. A major weight loss is observed at about 200°C which can be attributed to the escape of adsorbed water on the fibres. This is followed by the major degradation due to the fibre at 350°C. The phenolic disintegration starts at 550°C. A shoulder peak is observed in between these two peaks. This is due to the chemical degradation at the interface. The treated fibre composites show variation in thermal stability. It was reported that 5-15% alkali treatment leads to an optimum thermal stability to coir fibres.²⁵

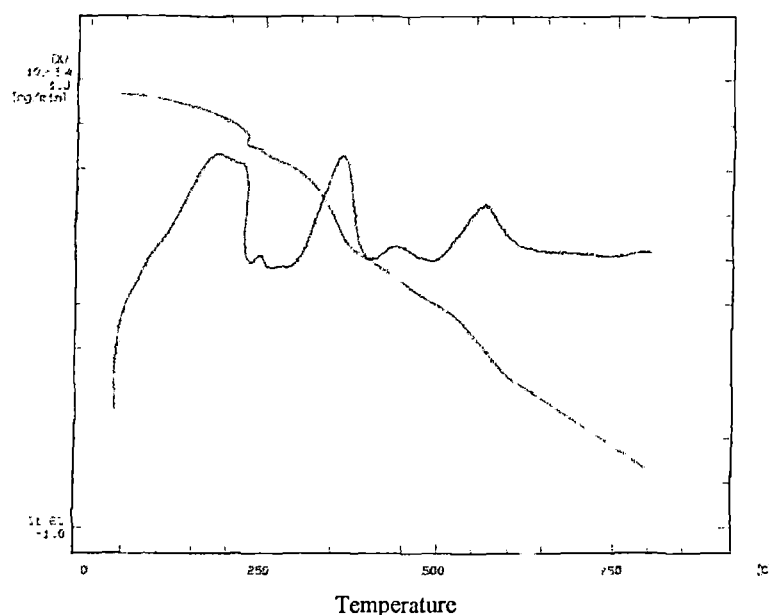


Figure 9.22d TG and DTG curves of oil palm/glass fibre hybrid PF composites.

Nishioka et al.²⁶ studied the thermal decomposition behaviour of miscible cellulose/synthetic polymer blends. They found a decrease in thermal stability of cellulose in the blends and were correlated to the miscibility effects.

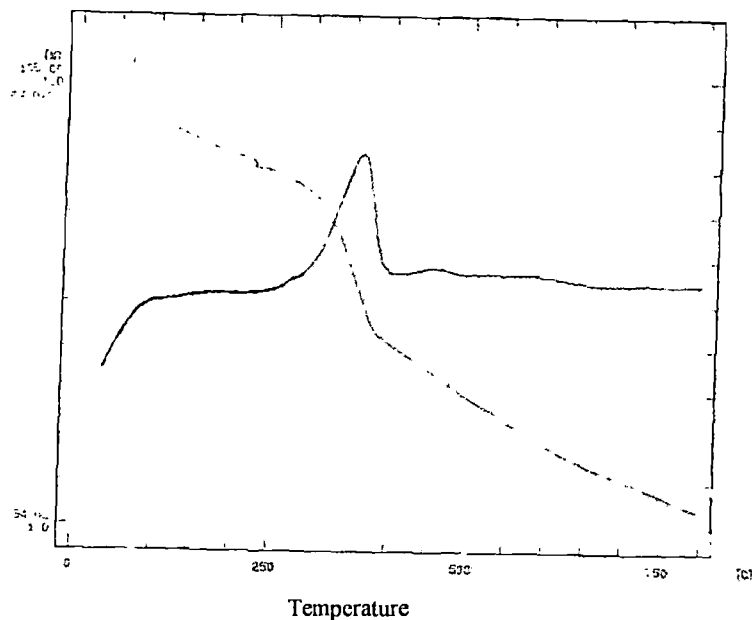


Figure 9.22e TG and DTG curves of silane treated oil palm fibre/PF composites.

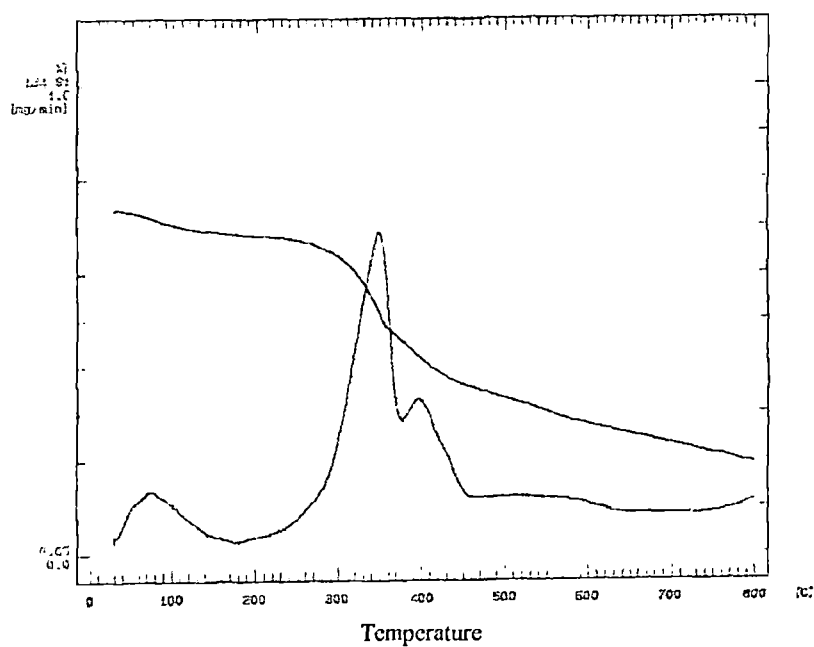


Figure 9.22f TG and DTG curves of latex treated oil palm fibre/PF composites.

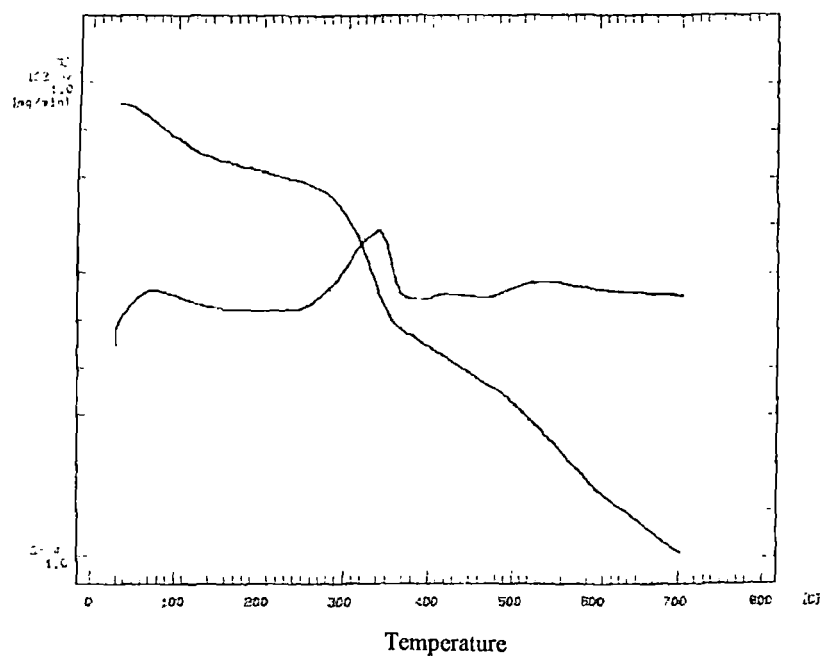


Figure 9.22g TG and DTG curves of isocyanate treated oil palm fibre/PF composites.

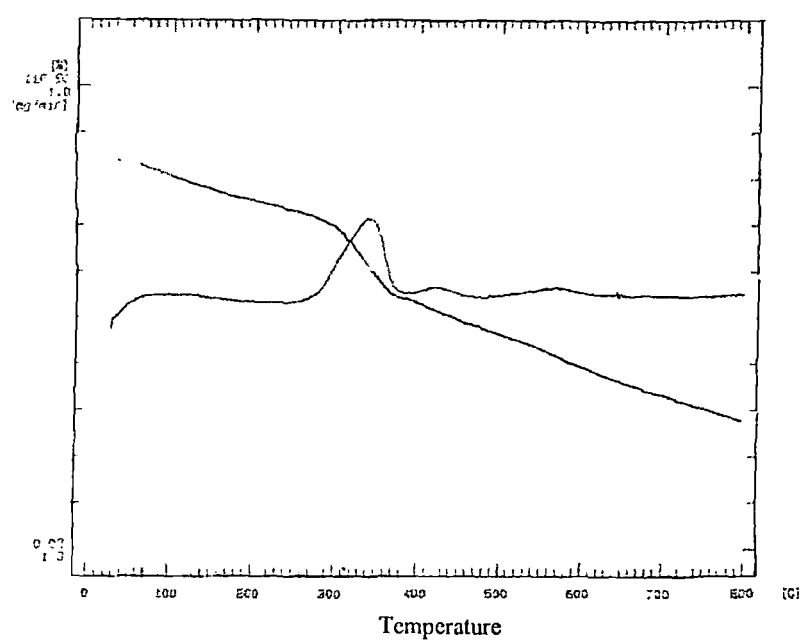


Figure 9.22h TG and DTG curves of KMnO_4 treated oil palm fibre/PF composites.

In the case of oil palm fibre/PF composites, most of the treatments decreased the degradation temperature (Fig. 9.22e, f, g, h, i & j). Only silane treatment gives higher initial degradation temperature (Fig. 9.22e). Silane treated fibres show higher stability (Fig. 3.19). However the total degradation occurred is lower for the untreated system. The decreased thermal stability of the treated composite can be attributed to the decreased fibre-matrix bonding and the decreased stability of the treated fibres (Fig. 3.19 and 3.20). In latex treated composite a shoulder peak is observed at 398°C which corresponds to the degradation of the rubber phase present (Fig. 9.22f). Major degradation occurs at 345°C. In alkali, permanganate and isocyanate treated composites, the degradation peak in the DTG curve observed at 340°C (Fig. 9.22g, h & i). The peak shifted to lower temperature (338°C) in acetylated composite (Fig. 9.22j). The weight loss occurred in various composites at selected temperature are given in Table 9.7.

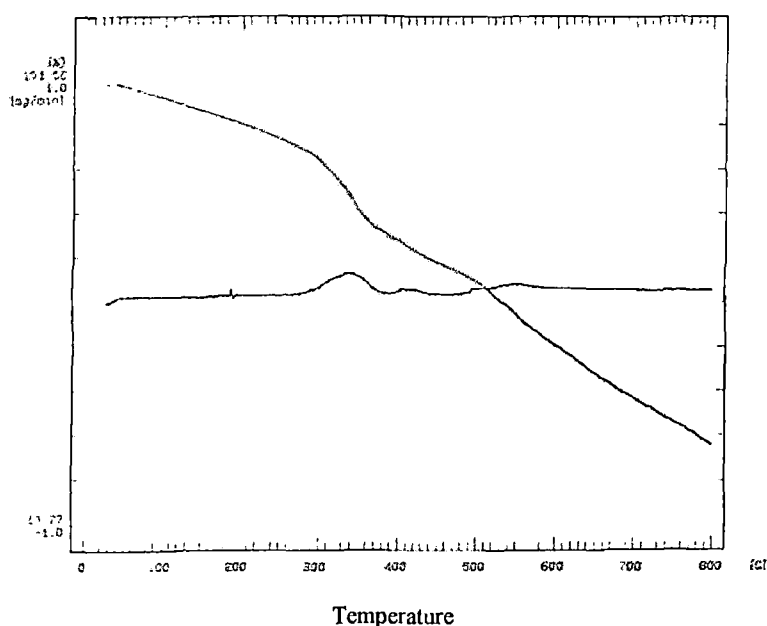


Figure 9.22i TG and DTG curves of mercerised oil palm fibre/PF composites.

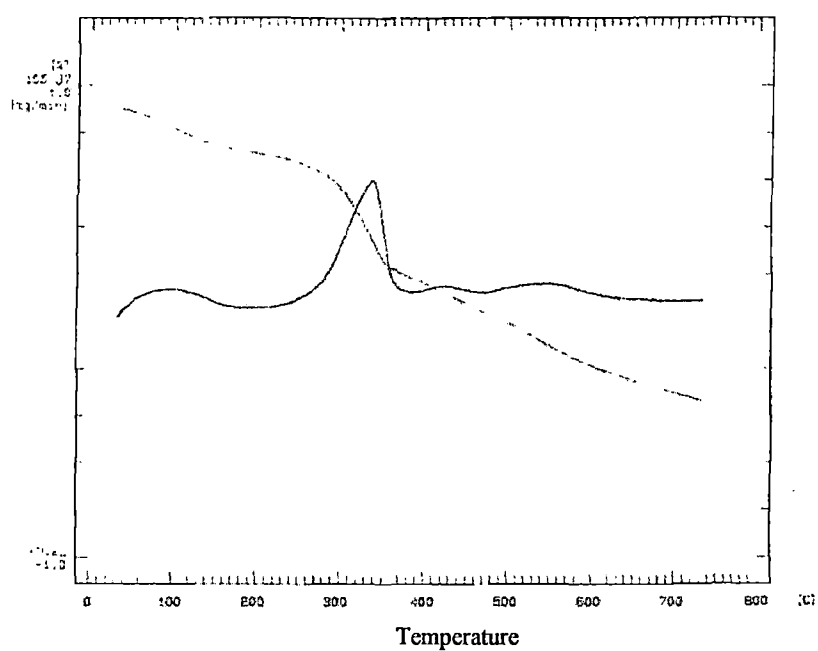


Figure 9.22j TG and DTG curves of acetylated oil palm fibre/PF composites.

Table 9.7 Weight Losses of Composites at Different Temperature

Sample	Weight loss (%)			
	100°C	300°C	500°C	700°C
Neat PF	4	15	23	44
Glass/PF	0.2	6	17	34
Oil palm/PF	2	15	37	54
Oil palm/ glass hybrid PF	3	15	34	51
Acetylated oil palm/PF	5	19	47	61
Latex coated oil palm/PF	5	15	55	68
Isocyanate treated oil palm/PF	6	20	50	74
Silane treated oil palm/PF	4	23	45	58
KMnO ₄ treated oil palm/PF	3	18	44	60
Mercerised oil palm/PF	3	16	38	61

The decreased hydrophilicity of the fibre upon treatments will lead to weak chemical bonding at the fibre-matrix interface. This will facilitate the thermal degradation at an early time leading to higher weight loss. At 100°C, glass/PF composite shows negligible weight loss. Compared to the hybrid and other treated composites, oil palm fibre/PF composite exhibits better thermal stability particularly at lower temperatures. The total degradation can be minimised by hybridisation of oil palm fibre with glass.

REFERENCES

1. W. Schnabel (Ed.), *Polymer degradation, Principles and Practical applications*, Macmillan Publishing Co. Inc., New York (1981)
2. L. Barral, J. Cano, J. Lopez, P. Nogueira and C. Ramirez, *J. Appl. Polym. Sci.*, **63**, 1841 (1997)
3. T. C. Uzomah and G. C. Unuoha, *J. Appl. Polym. Sci.*, **69**, 2533 (1998)
4. H. Lin, D. E. Day and J. O. Stoffer, *Polym. Comp.*, **14**, 402 (1993)
5. T. Nakashima and M. Matsuo, *J. Macromol. Sci.-Phys.*, **B 35(3&4)**, 659 (1996)
6. H. Parvatareddy, J. Z. Wang, D. A. Dillard, T. C. Ward and M. E. Rogalski, *Comp. Sci. Technol.*, **53**, 399 (1995)
7. N. L. Hancox, *Plast. Rubb. Comp. Process. Appln.*, **27**, 97 (1998)
8. J. George, S. S. Bhagawan and S. Thomas, *Comp. Sci. Technol.*, **58**, 1471 (1998)
9. K. Joseph and S. Thomas, *Comp. Sci. Technol.*, **53**, 99 (1995)
10. S. P. Sonawala and R. J. Spontak, *J. Mater. Sci.*, **31**, 4745 (1996)
11. *Ibid*, **31**, 4757 (1996)
12. L. Dong, D. J. T. Hill, J. H. O'Donnell, P. J. Pomery and K. Hatada, *J. Appl. Polym. Sci.*, **59**, 589 (1996)
13. S. M. SpieBberger, K. Humer, E. K. Tschegg, H. W. Weber, K. Noma and Y. Iwasaki, *Cryogenics*, **37**, 135 (1997)

14. A. N. Netravali and A. Manji, *Polym. Comp.*, **12**, 153 (1991)
15. M. S. Sreekala, M. G. Kumaran and S. Thomas, Water sorption kinetics in oil palm fibres. (Submitted to *Eur. Polym. J.*)
16. H. Kudoh, T. Sasuga, T. Seguchi and Y. Katsumura, *Polymer*, **37**, 3737 (1996)
17. J. T. Carter, *Plast. Rubb. Comp. Proc. Appln.*, **16**, 157 (1991)
18. A. Matsumoto, K. Hasegawa, A. Fukuda and K. Otsuki, *J. Appl. Polym. Sci.*, **44**, 1547 (1992)
19. S. G. Kuzak, J. A. Hiltz and P. A. Waitkus, *J. Appl. Polym. Sci.*, **67**, 349 (1998)
20. H. F. Mark (Ed.), *Encyclopedia of Polymer Science and Engineering*, John Wiley and Sons, New York, **Vol. 4** (1985)
21. I. Pektas, *J. Appl. Polym. Sci.*, **68**, 1337 (1998)
22. L. Kessira and A. Richard, *J. Appl. Polym. Sci.*, **49**, 1603 (1993)
23. A. Basch and M. Lewin, *J. Polym. Sci. Polym. Chem. Ed.*, **12**, 2053 (1974)
24. H. Rodrig, A. Basch and M. Lewin, *J. Polym. Sci. Polym. Chem. Ed.*, **13**, 1921 (1975)
25. D. N. Mahato, B. K. Mathur and S. Bhattacharjee, *Ind. J. Fib. Text. Res.*, **20**, 202 (1995)
26. N. Nishioka, S. Hamabe, T. Mukrakami and T. Kitayawa, *J. Appl. Polym. Sci.*, **69**, 2133 (1998)

CHAPTER 10

Electrical Properties of Oil Palm Fibre/Phenol Formaldehyde Composites : Effect of Fibre Loading, Fibre Surface Modifications and Hybridisation of Oil Palm Fibre with Glass

*Results of this study have been submitted for publication in **Journal of Reinforced Plastics and Composites***

Abstract

The electrical properties of oil palm fibre/phenol formaldehyde composites have been studied with special reference to the effect of fibre loading, fibre content and hybridisation of oil palm fibre with glass. The electrical properties were studied in the frequency range, 10KHz to 10MHz. The volume resistivity of PF resin is increased with oil palm fibre loading. Fibre surface modifications such as silane, isocyanate, acetylation, acrylation, acrylonitrile grafting and latex treatment increase the resistivity of the composites. On hybridisation of oil palm fibre with glass, the resistivity was found to decrease with increase of glass fibre content. The dielectric constant of PF decreases considerably upon oil palm fibre reinforcement. The value again decreases upon isocyanate treatment. However the incorporation of glass fibre increases the dielectric constant of the composites. Loss factor and dissipation factor show almost similar trend as in the case of dielectric constant.

Now-a-days fibre reinforced thermoset composites have been increasingly used in the manufacture of enclosures for electronic equipments. This is mainly due to its electrical insulating properties, mechanical performance, environmental stability and ease of fabrication. Most of the polymeric materials in their pure state are excellent electrical insulators. Phenol formaldehyde already proved its applications in electronic industry. Incorporation of fillers and reinforcement changes the electrical properties of polymers. The shape of the filler particles, dispersion, orientation of the particles etc. affect the electrical properties of a composite. It is reported that anisotropy of electrical conductivity is observed in carbon black, carbon fibre, steel fibre and aluminium flake filled polyethylene composites.¹ However isotropy of electrical conductivity is observed in randomly oriented composites.

Generally the introduction of conductive fillers to matrix resin is found to develop conductivity to the final composite product.²⁻⁴ In these cases, carbon fibre, carbon black powder and glass fibre were used to improve the conductivity of the polymers such as high density polyethylene (HDPE)/poly methyl methacrylate (PMMA) blends, ethylene/ethyl acrylate copolymers and epoxy resin. In HDPE/PMMA blends, a percolation threshold was observed at 1.25phr carbon fibre content, which is much lower than those of the individual polymers when reinforced with the carbon fibre.² The filler content and the electrical conductivity of the composites are interconnected since the conductivity of the composites implies some sudden changes in the dispersion state of the conductive particles. The cross over from a non-conducting stage to a conducting stage occurs at critical filler content that is called the percolation threshold. A theoretical study of percolation phenomena was reported by Kortschot et al.⁵ They compared the theoretical predictions with the experimental data and provided some practical suggestions for maximising the efficiency of conductive fillers. The percolation threshold is dependent upon the type of filler, polymer, dispersion state of the filler and the morphology of the matrix. It is reported that processing techniques as well as processing conditions influence the electrical property of the end product.⁶⁻⁹ They

have found that an increase of mould time, mould temperature and mould pressure increases the conductivity of the composites.

Incorporation of lignocellulosic fibres into polymers changes the electrical behaviour of the polymer. Normally lignocellulosic natural fibres and wood act as insulators. Bhadani et al.¹⁰ succeeded in converting insulating natural fibres such as cotton, silk and wool to moderately conducting by subjecting them to electrical treatment in the polymerising solution of pyrrole and thiophene. The electrical property of natural fibre mainly depend upon the amorphous and crystalline components of the fibre, polarity, dipole interactions etc. Recently electrical property studies of sisal fibre-low density polyethylene (LDPE), coir fibre-LDPE and pineapple fibre-LDPE were reported from this laboratory.^{11, 12, 13} The dielectric constants of sisal-LDPE, coir-LDPE and pineapple fibre-LDPE were found to increase with increase in fibre loading. In the present work we report on the effect of fibre loading, fibre treatment and hybridisation with glass on the electrical properties of oil palm fibre/PF composites. The volume resistivity, dielectric constant, loss factor and dissipation factor of the composites have been evaluated.

10.1 VOLUME RESISTIVITY

10.1.1 Effect of Fibre Loading

The volume resistivity of the composites is a very important property which indicates their suitability as insulating materials for specific applications. Changes in the volume resistivity of PF resin on oil palm fibre reinforcement are given in Figure 10.1. Incorporation of the fibre marginally increases the resistivity of the resin. At lower frequency 20wt.% fibre loading shows maximum resistance, but at higher frequency 40wt.% fibre loading exhibits maximum resistivity. It is already proved by earlier studies that natural fibres have got excellent electrical resistance.¹⁴ They can be used as a replacement for wood in electrical applications. Increased resistivity of the composite is attributed to the high resistivity of the fibres.

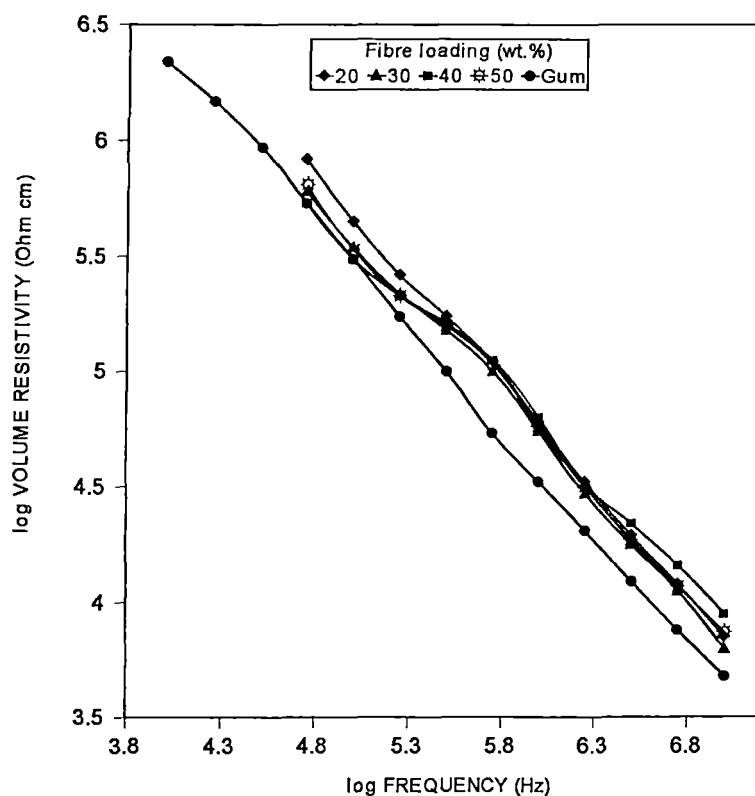


Figure 10.1 Variation of volume resistivity of oil palm fibre/PF composites with frequency at different fibre loading.

The resistivity of lignocellulosic fibres is dependent upon the moisture content, crystallinity and amorphous component present, presence of impurities, chemical composition, cellular structure, microfibrillar angle etc. The shape of the reinforcement determines the interparticle contact which affects the conductivity of the system. Elongated shapes such as fibres and flakes are much more efficient in enhancing electrical conductivity.¹⁵ As the moisture content increases the resistivity of the fibre falls. It is also reported by Kulkarni et al.¹⁴ that defects occurring to fibres during processing will also increase its resistivity. In oil palm fibre/PF composite the resistivity values lie in between that of neat PF and lignocellulosic fibres. With the increase in amorphous material the resistivity is found to increase. Electrical resistivity of short fibre composites is highly sensitive to the presence of voids, fibre orientation and microstructure. Since the oil palm fibre/PF composite is randomly oriented it shows isotropy in electrical properties. As the frequency increases the resistivity shows linear decrease (Fig. 10.1). This is due to the change

in interfacial polarisation arising due to the heterogeneity of the system. Effect of fibre loading on the volume resistivity at different frequencies is clear from Figure 10.2. It is seen that the increase in electrical resistivity with fibre loading is only marginal.

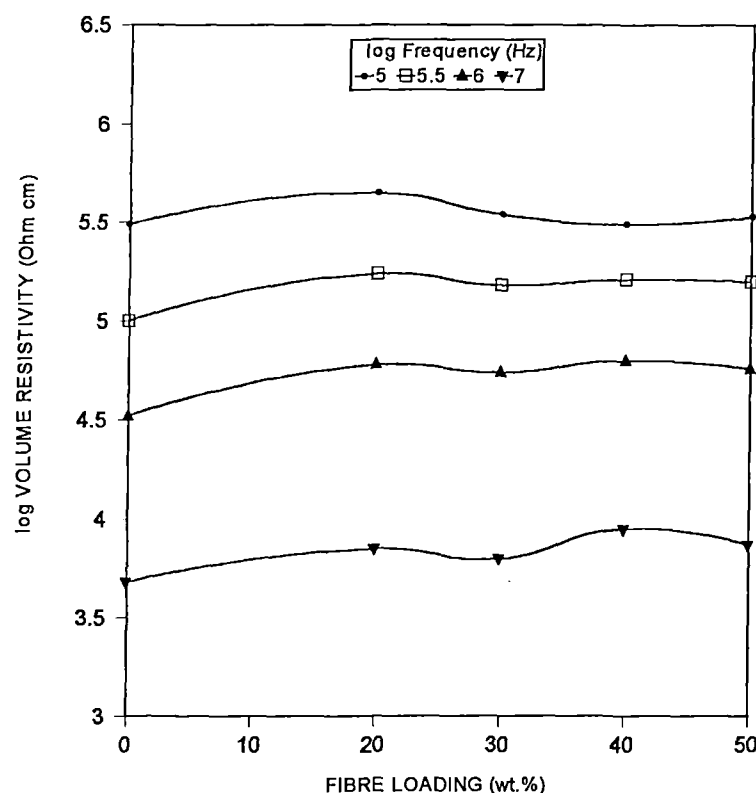


Figure 10.2 Variation of volume resistivity of oil palm fibre/PF composites with fibre loading at specified frequencies.

10.1.2 Effect of Fibre Treatment

Oil palm fibre surface modifications with silane, isocyanate, acetylation, acrylation, acrylonitrile grafting and latex lead to composites having higher electrical resistivity at all frequencies (Fig. 10.3). However in alkali and permanganate treated composites, a decrease in resistivity is observed. The difference in resistivity of the treated composites from the untreated one is attributed to the physical and chemical modifications happened to the fibre as discussed earlier in this paper. A decrease in

amorphous component is observed upon alkali and permanganate treatment by bleaching out of the waxy materials thereby increasing the crystalline component. This will decrease resistivity because current flow is mainly associated with the crystalline region of polymers. As in untreated composites, linear decrease in resistivity is observed with increase in frequency.

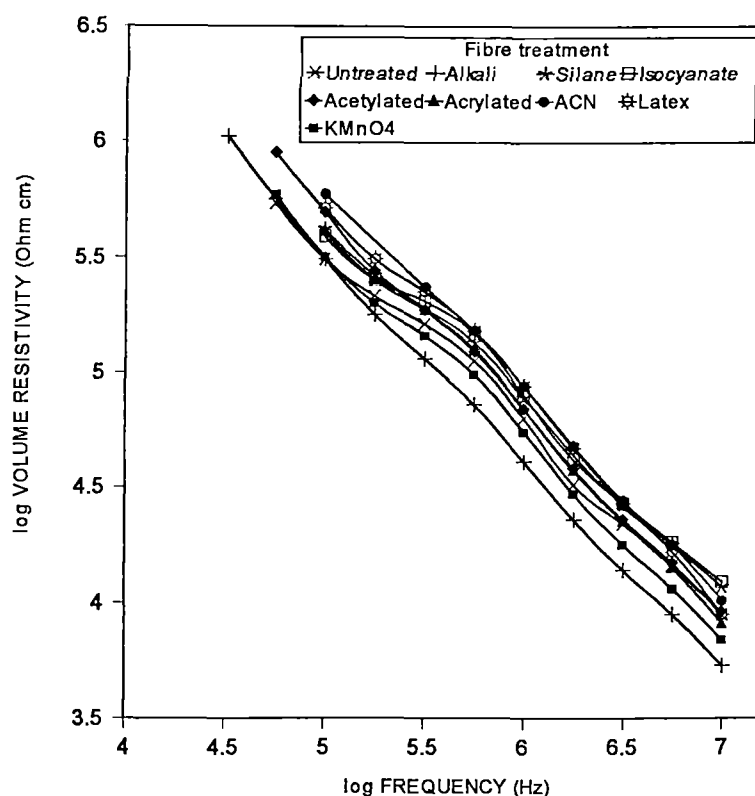


Figure 10.3 Variation of volume resistivity of treated oil palm fibre/PF composites with frequency.

Figure 10.4 shows the resistivity values of treated composites at different frequencies. At all frequencies alkali treated composite showed lowest resistivity. The alkali treatment makes the fibre surface more rough and leads to better compatibility with the matrix PF and may induce ionic conduction in the composite. Usually in polymers, ionic conduction takes place from ions derived from fragments of polymerisation catalyst, degradation and dissociation products of the polymer itself and absorbed water.¹⁵

10.1.3 Effect of Hybridisation

In oil palm fibre/glass hybrid PF composites, the resistivity increased with increase in oil palm fibre volume fraction (Fig. 10.5). The resistivity of unhybridised composite lies in the hybrid resistivity region. At high oil palm fibre loading, the compatibility between glass and oil palm fibre decreases and this will result in the increase of resistivity. Figure 10.6 shows the volume resistivity of hybrid composites with relative volume fractions of oil palm fibre at different frequencies. By replacing small amount of oil palm fibre with glass fibre in oil palm fibre/PF composite results in hybrid composite having higher electrical resistivity. In all the above discussed cases, no percolation threshold is observed which is indicated by insulator-conductor transition.

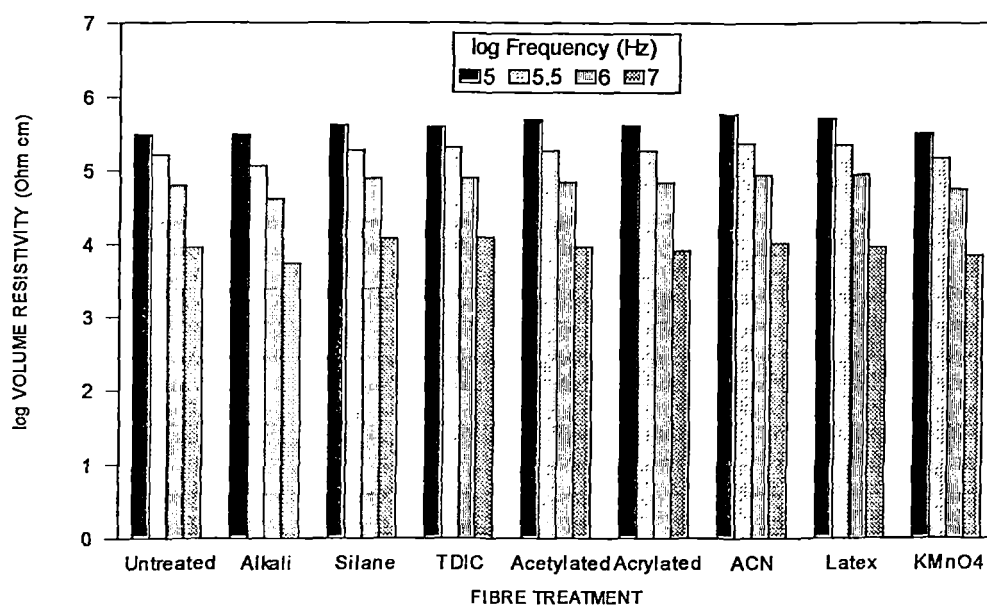


Figure 10.4 Volume resistivity of treated oil palm fibre/PF composites at specified frequencies.

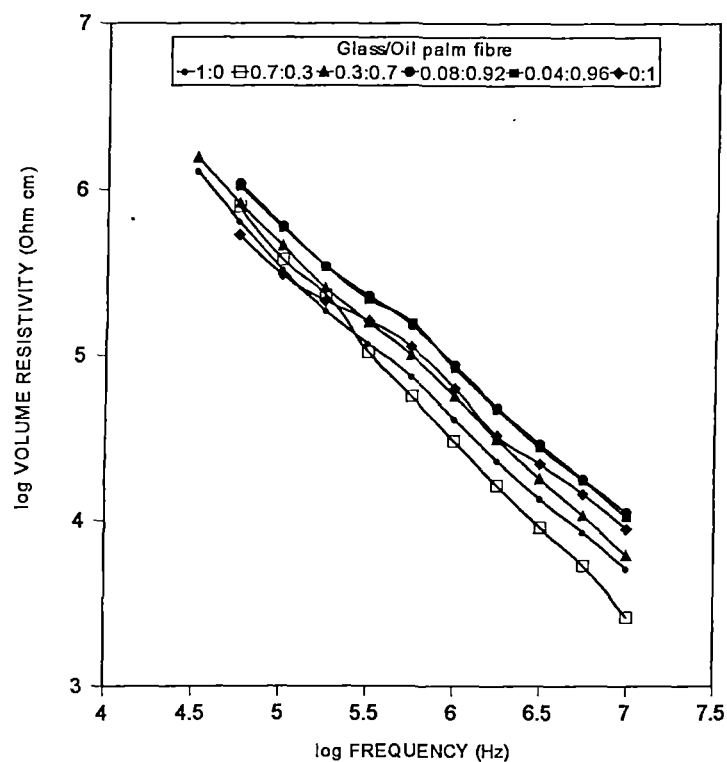


Figure 10.5 Variation of volume resistivity of oil palm fibre/PF hybrid composites with frequency at different relative volume fractions of glass and oil palm fibre.

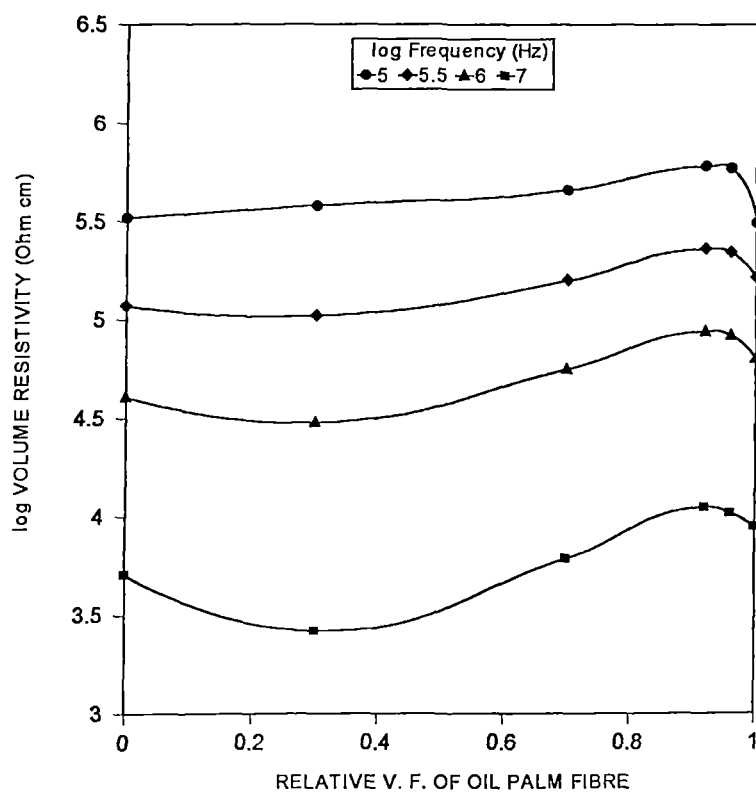


Figure 10.6 Volume resistivity of hybrid composites at specified frequencies.

10.2 DIELECTRIC CONSTANT

10.2.1 Effect of Fibre Loading

The dielectric constant of a composite material is mainly dependent on the dipole interactions present and orientation effects. It is reported that the dielectric constant of non polar polymers lies in the region 1.8-2.5.¹⁶ The ϵ' values for neat PF and oil palm fibre/PF composites are higher than this (Fig. 10.7). The dielectric study of cellulose fibres was carried out by Pai et al.¹⁷ They have got a reasonably high value of ϵ' for natural fibres like jute, hemp and ramie. The differences in ϵ' within the natural fibres is due to the difference in the amorphous and crystalline components in the fibres. The dielectric constant of neat PF is found to be greater than that of lignocellulosic fibres. The incorporation of these fibres in PF resin is found to decrease the dielectric constant (Fig. 10.7).

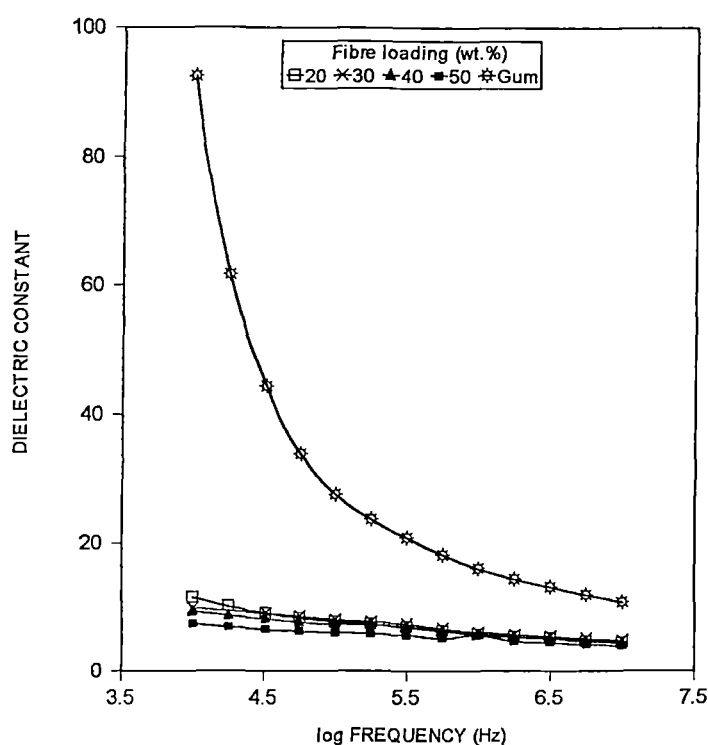


Figure 10.7 Variation of ϵ' of untreated oil palm fibre/PF composites with frequency.
Fibre loading: 40wt.%

At lower frequencies the gum sample exhibits exceptionally high value of ϵ' . The intrinsic ϵ' of a homogeneous solid will be very high. Interfacial polarisation as a result of heterogeneity contributes to the dielectric constant at lower frequencies. Structural defects usually occur during the curing process of highly brittle PF resin. Resin shrinkage during curing is highest for PF among thermosets, which also leads to defects in the physical structure of the cured resin. Presence of voids in polymeric materials causes internal discharges in an applied field. The dielectric constant of the gas filling a void is generally less than that of the polymer.¹⁵

The decreased ϵ' by the incorporation of oil palm fibre will be due to the comparatively low dielectric value of the fibres. As the fibre loading is increased, the value gradually decreased. The chemical and physical properties of oil palm fibre and their compatibility with PF resin were reported elsewhere.^{18, 19} Oil palm fibre exhibits polarity owing to the polar hydroxyl groups from cellulose and lignin. There is good compatibility between hydrophilic PF resin and hydrophilic fibres. This is evident from the scanning electron micrograph of tensile fractured portion of the untreated composite (Fig. 4.4; refer Chapter 4). Fibre breakage is seen. The efficient physical and chemical bonding in the composite minimises the orientation polarisation which decreases the ϵ' . The ϵ' obtained for oil palm fibre/PF composites is comparable to that of pineapple leaf fibre/LDPE, sisal/LDPE and coir/LDPE composites which is reported elsewhere.^{11, 12} Figure 10.8 shows the variation of ϵ' with fibre loading at different frequencies. The value is almost constant with increase in fibre loading. A sharp drop in the ϵ' value of gum sample occurred with fibre incorporation.

10.2.2 Effect of Treatments

Treated composites show higher ϵ' than untreated composite (Figure 10.9). Modifications bring out major physical and chemical changes in the fibre as discussed earlier. Upon treatments with alkali, silane, acrylation, acetylation and permanganate introduces polarisability in the fibre.

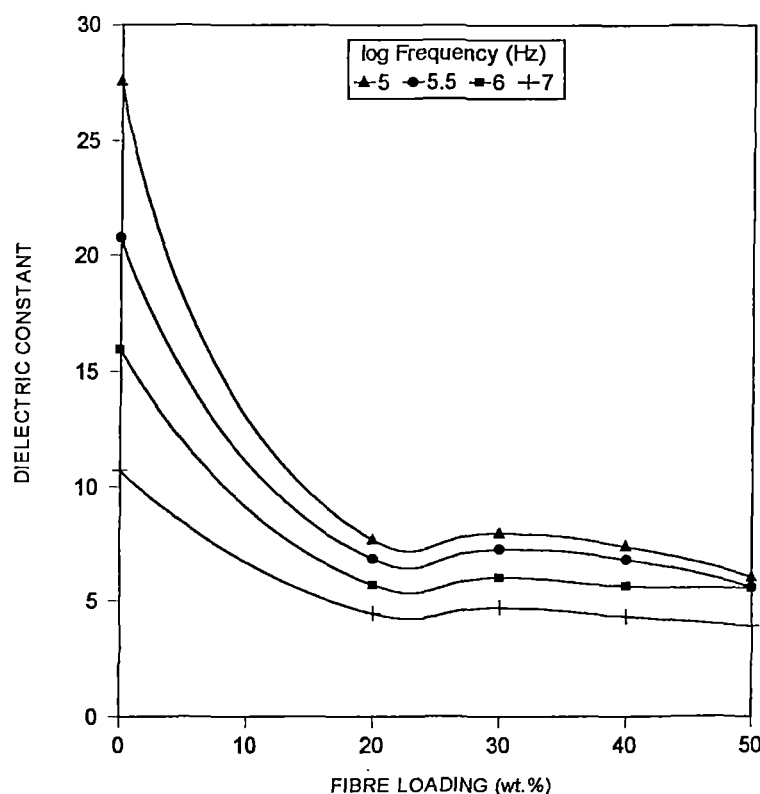


Figure 10.8 Variation of ϵ' of untreated oil palm fibre/PF composites with fibre loading at specified frequencies.

Treatments like alkali and acrylation make the fibre more hydrophilic and become more compatible with the matrix while treatments like latex coating makes the fibre hydrophobic and hence results in a weak bonding with the matrix. This will affect the electronic, atomic and orientation polarisations and thus the ϵ' . Moisture content enhances the polarisation. Moisture uptake of the fibre is decreased by the treatments like latex coating and isocyanate treatment. This decreases the dielectric constant. Variation of the ϵ' of various treated composites at different frequencies are given in Figure 10.10. Alkali treated composite shows highest value at all frequencies. Alkali treatment increases the polarity of the fibre by the intermolecular and intramolecular hydrogen bonding through hydroxyl groups of the fibre. This will enhance the fibre-matrix adhesion and at the same time can enhance the polarisability. This contributes to the higher ϵ' value.

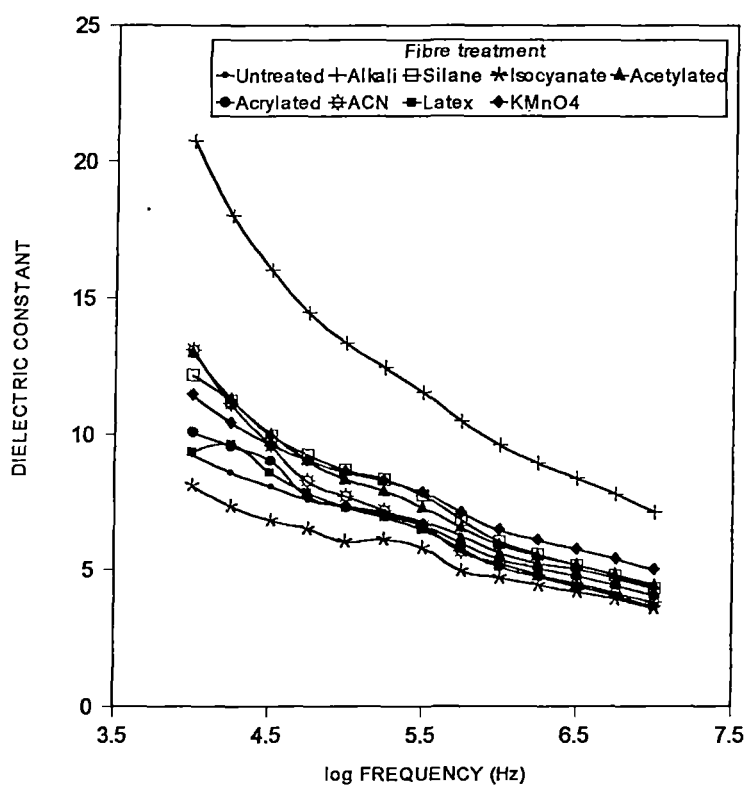


Figure 10.9 Variation of ϵ' of treated oil palm fibre/PF composites with frequency. Fibre loading: 40wt.%

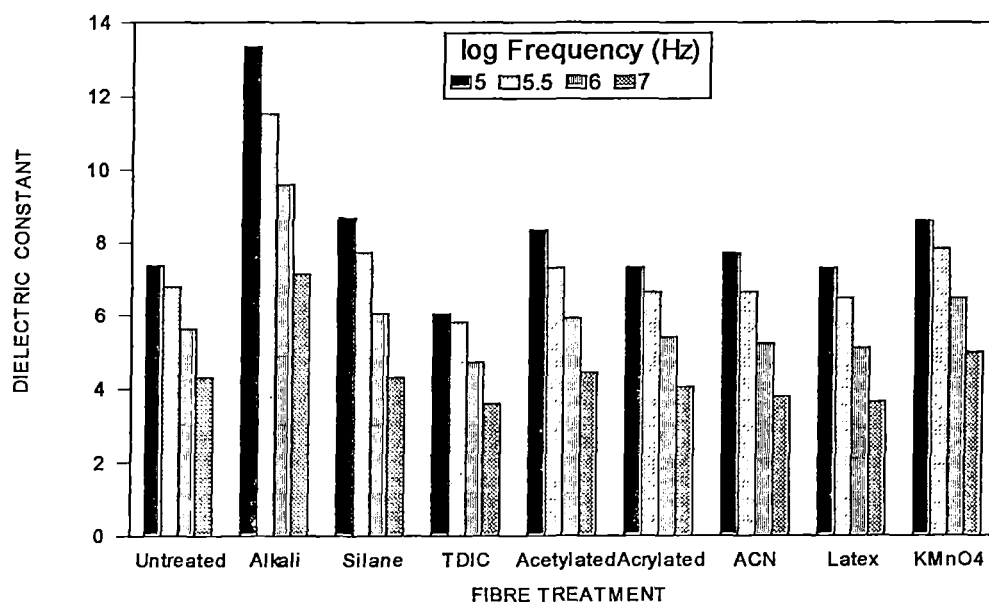


Figure 10.10 Variation of ϵ' of treated oil palm fibre/PF composites with fibre loading at specified frequencies.

10.2.3 Effect of Hybridisation

Figure 10.11 gives the dielectric constant values of hybrid composites. The unhybridised oil palm fibre/PF composite shows least ϵ' . The glass/PF composite also exhibits low value compared to hybrid composites at lower frequencies. Highest ϵ' observed for hybrid composite having 0.7 relative volume fraction (V.F) oil palm fibre. Further increase in volume fraction of oil palm fibre decreases the value. Highest glass fibre concentration also reduces the value. This can be attributed to the compatibility in hybrid fibre composites. There exists a weak compatibility between oil palm and glass fibre layers. The decreased compatibility between glass and oil palm fibre results in an increased heterogeneity of the system. This enhances the interfacial polarisation. But at higher oil palm fibre or glass fibre loaded composites, the compatibility enhances and the ϵ' is decreased. This is further clarified in Figure 10.12.

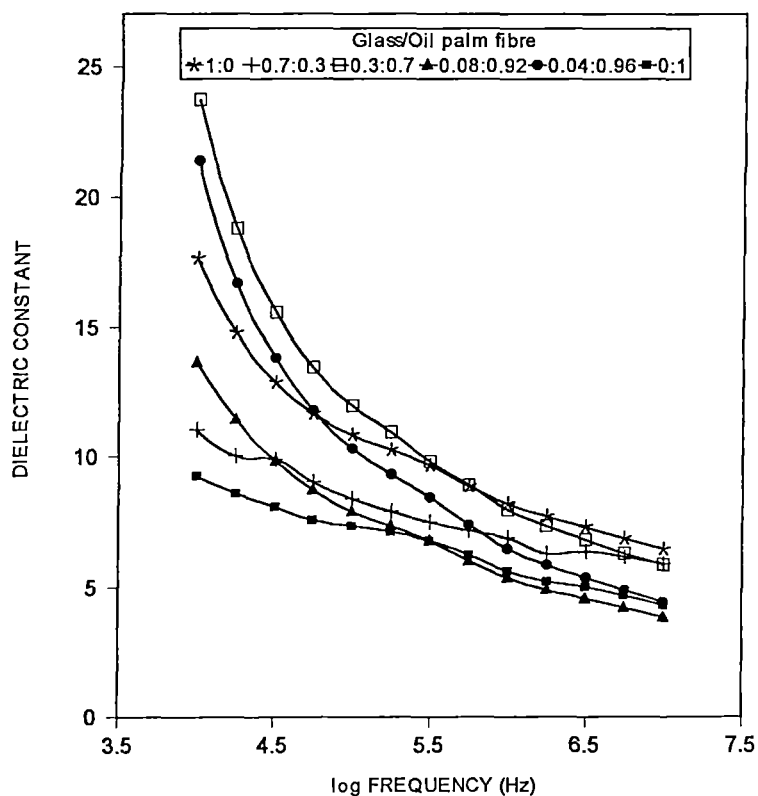


Figure 10.11 Variation of ϵ' of oil palm fibre/glass hybrid PF composites with frequency at different relative volume fractions of glass and oil palm fibre.
Fibre loading: 40wt.%

10.3 LOSS FACTOR AND DISSIPATION FACTOR

10.3.1 Effect of Fibre Loading

Variation of dielectric loss factor and dissipation factor of oil palm fibre/PF composites with frequency is represented in Figures 10.13 and 10.14. The neat PF sample exhibits highest loss factor and dissipation factor. Upon the incorporation of oil palm fibre, both $\tan\delta$ and ϵ'' value decreased considerably and similar trend is observed in both the cases. In the $\tan\delta$ curve, a relaxation peak is observed at a frequency of $10^{5.7}$ Hz in both gum and composites (Fig. 10.14). This indicates that the fibrous reinforcement does not affect the dielectric relaxation. The dissipation factor is a measure of the energy lost during the reversal of electrical polarisation. The decreased value of loss factor and $\tan\delta$ on fibrous reinforcement can be explained on the basis of higher fibre-matrix compatibility as discussed earlier.

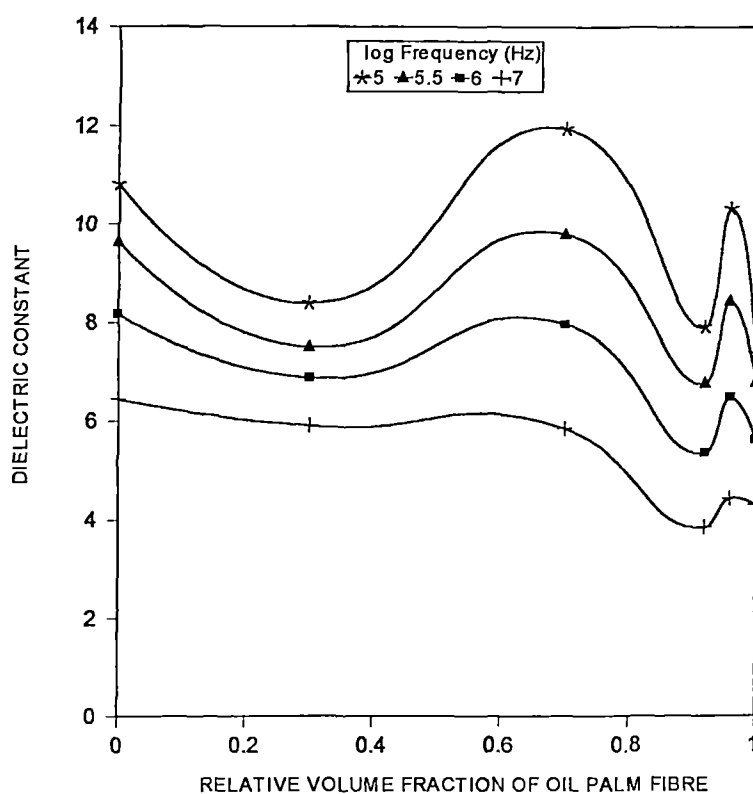


Figure 10.12 Variation of ϵ' of oil palm fibre/glass hybrid PF composites with relative volume fractions of glass and oil palm fibre at specified frequencies.
Fibre loading: 40wt.%

Electrical properties of ramie fibres were studied in detail by Sao et al.²⁰ They reported that the $\tan\delta$ curve of ramie fibres show no specific relaxation. Expecting this behaviour to all lignocellulosic fibres, it can be concluded that the dielectric relaxation in composites is mainly due to the PF. Figures 10.15 and 10.16 depict the changes in ϵ'' and $\tan\delta$ with fibre loading at different frequencies. The ϵ'' decreases by the incorporation of fibre followed by a levelling off. But $\tan\delta$ decreases linearly with fibre loading at lower frequencies. At higher frequencies, an increase is observed at 40wt.% fibre loading.

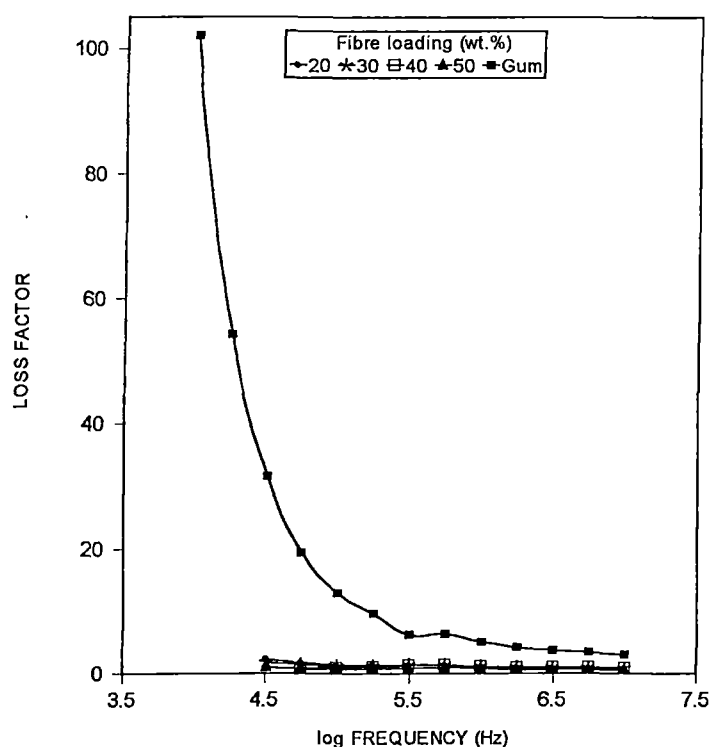


Figure 10.13 Variation of ϵ'' of untreated oil palm fibre/PF composites with frequency.

10.3.2 Effect of Fibre Treatment

Figure 10.17 and 10.18 shows the ϵ'' and $\tan\delta$ values of treated oil palm fibre/PF composites. All treatments except isocyanate show higher values of ϵ'' and $\tan\delta$ compared to untreated composites. Relaxation peak is observed in all cases at $10^{5.7}$ frequency. The increased values may be due to the increased polarisation on treatments.

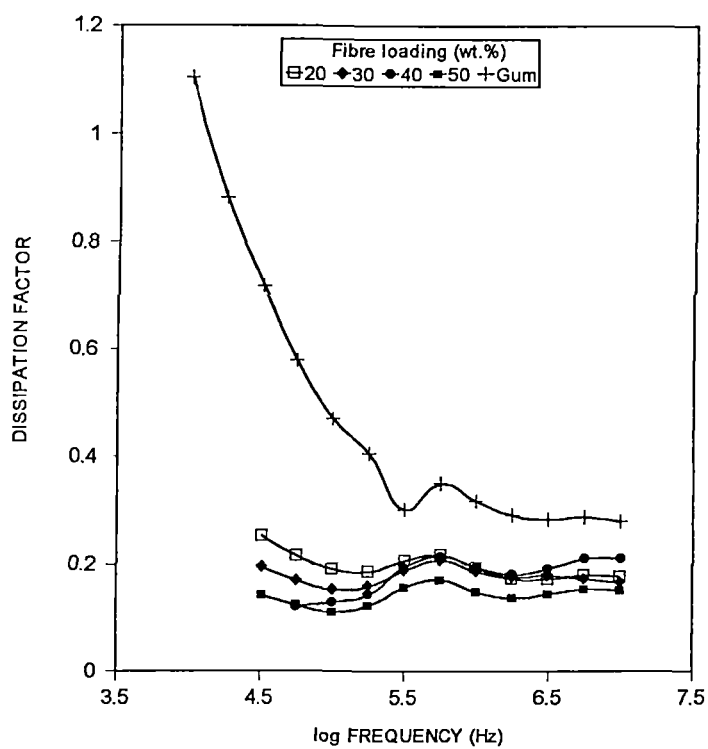


Figure 10.14 Variation of $\tan\delta$ of untreated oil palm fibre/PF composites with frequency.

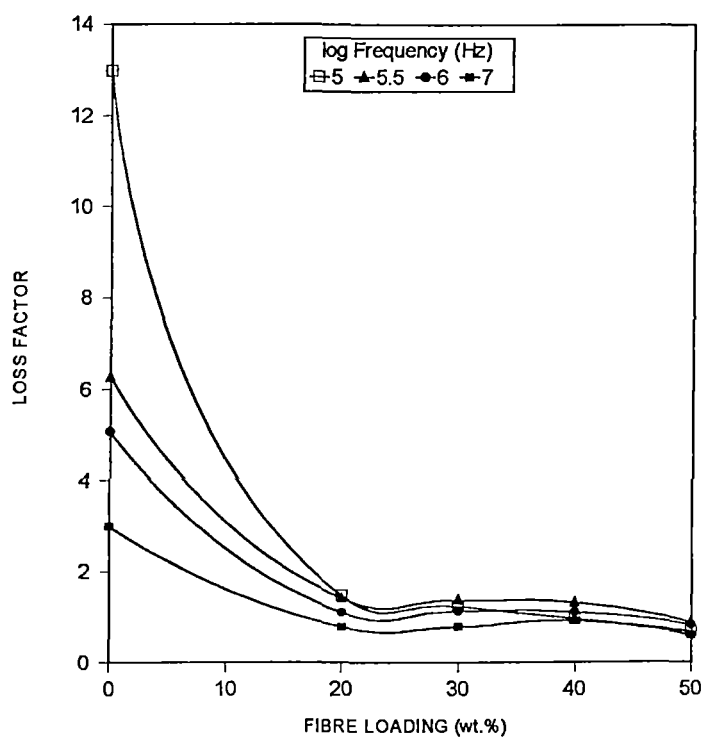


Figure 10.15 Variation of ϵ'' of untreated oil palm fibre/PF composites with fibre loading at specified frequencies.

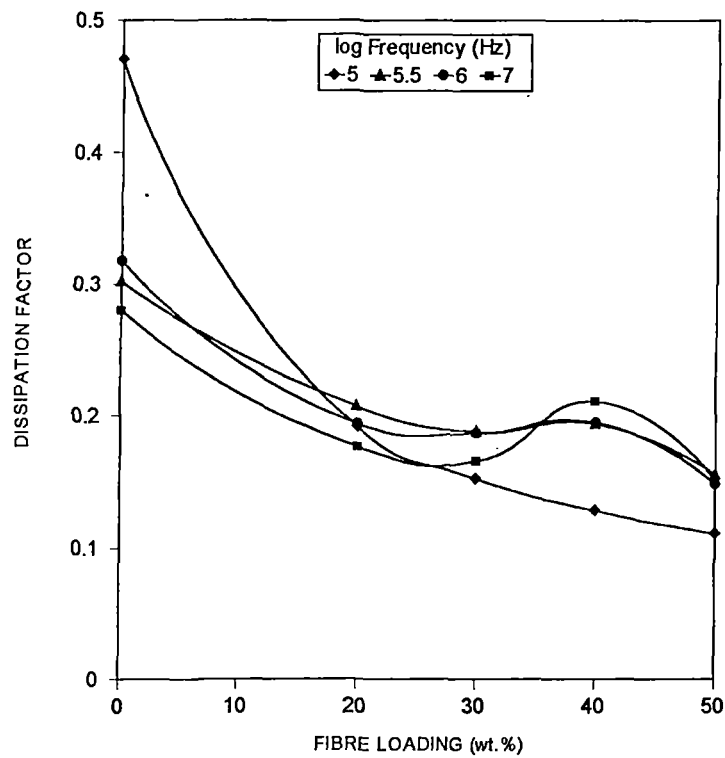


Figure 10.16 Variation of $\tan\delta$ of untreated oil palm fibre/PF composites with fibre loading at specified frequencies.

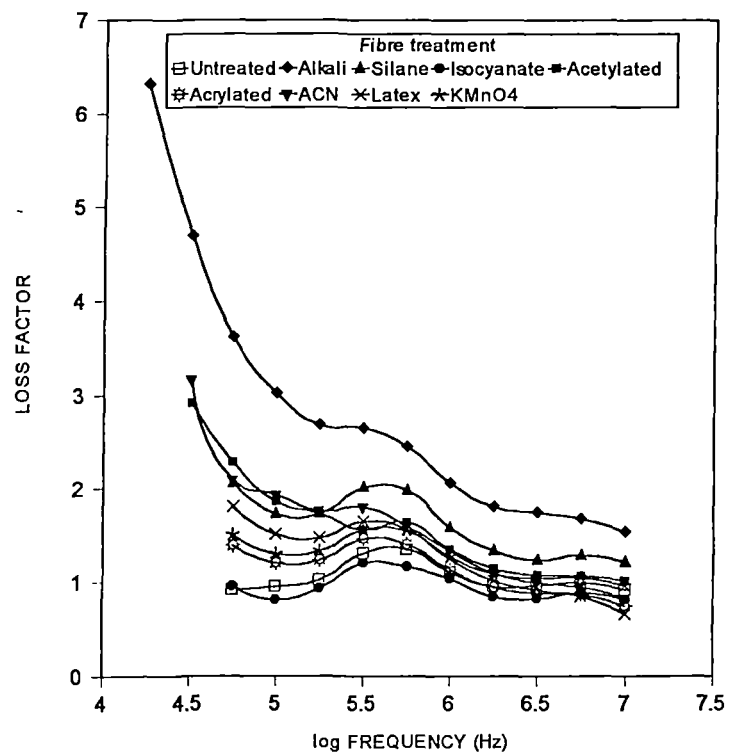


Figure 10.17 Variation of ϵ'' of treated oil palm fibre/PF composites with frequency. Fibre loading: 40wt.%

The polarity enhancement is highest on alkali treatment. The ϵ'' and $\tan\delta$ value of treated composites at different frequencies is shown in Figures 10.19 and 10.20. Alkali treatment shows the highest ϵ'' at all frequencies. Isocyanate treatment decreases the ϵ'' and $\tan\delta$ value at lower frequencies. Silane treated composite exhibits highest $\tan\delta$ at higher frequencies.

10.3.3 Effect of Hybridisation

The hybridisation of oil palm fibre with glass shows a similar trend as in the case of dielectric constant (Fig. 10.21). The unhybridised composites show comparatively lower values for ϵ'' and $\tan\delta$ (Fig. 10.22). Hybrid composite having 0.7 relative V.F of oil palm fibre show highest value of ϵ'' . Hybrid composite having highest oil palm fibre content exhibits maximum dissipation factor. The enhancement in values is due to the extent of bonding between fibre and matrix as discussed earlier. With the increase in frequency the ϵ'' and $\tan\delta$ decrease.

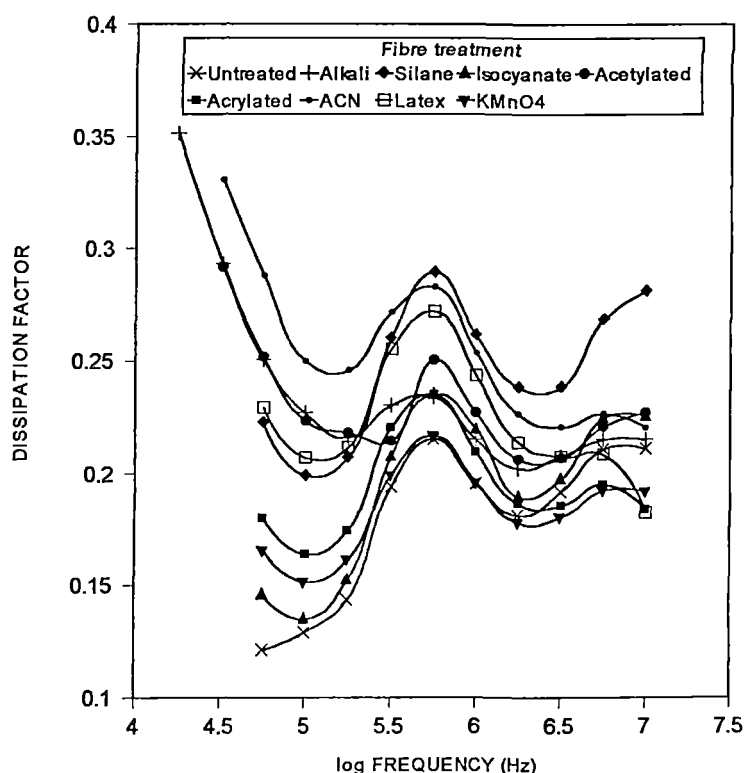


Figure 10.18 Variation of $\tan\delta$ of treated oil palm fibre/PF composites with frequency. Fibre loading: 40wt.%

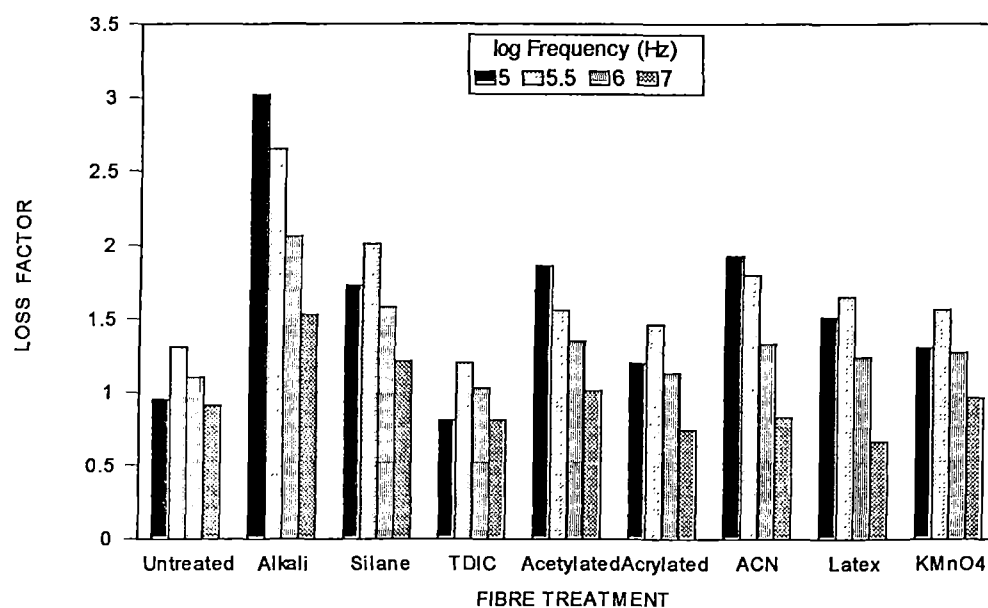


Figure 10.19 Loss factor values of treated composites at specified frequencies.

Similar trend is observed in the variation of ϵ'' with relative V.F of oil palm fibre at all frequencies (Fig. 10.23). A lower value of ϵ'' is observed at 0.92 relative V.F of oil palm fibre. At this composition a lower value of $\tan\delta$ is also observed at lower frequencies (Fig. 10.24).

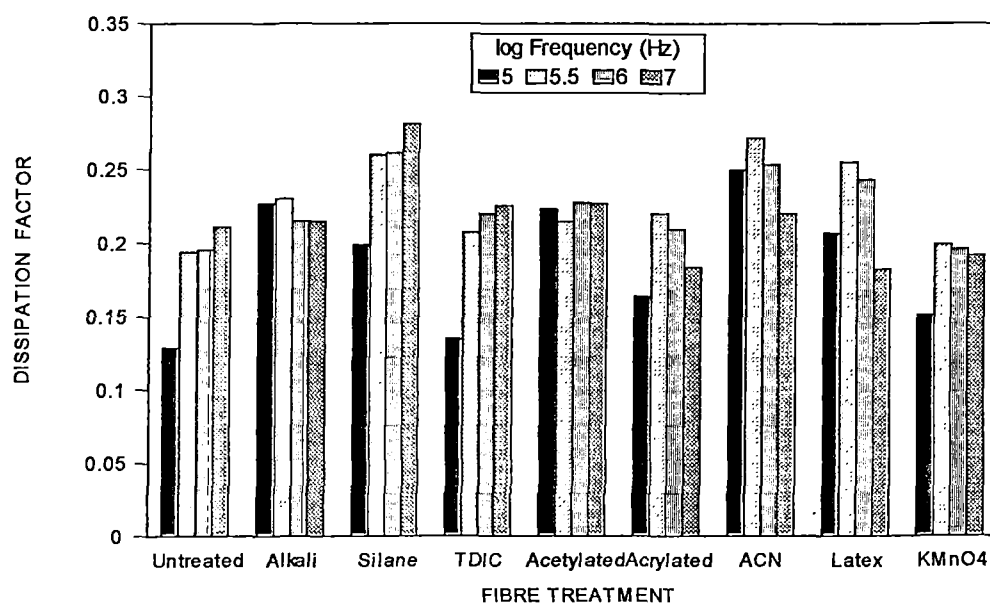


Figure 10.20 $\tan\delta$ values of treated composites at specified frequencies.

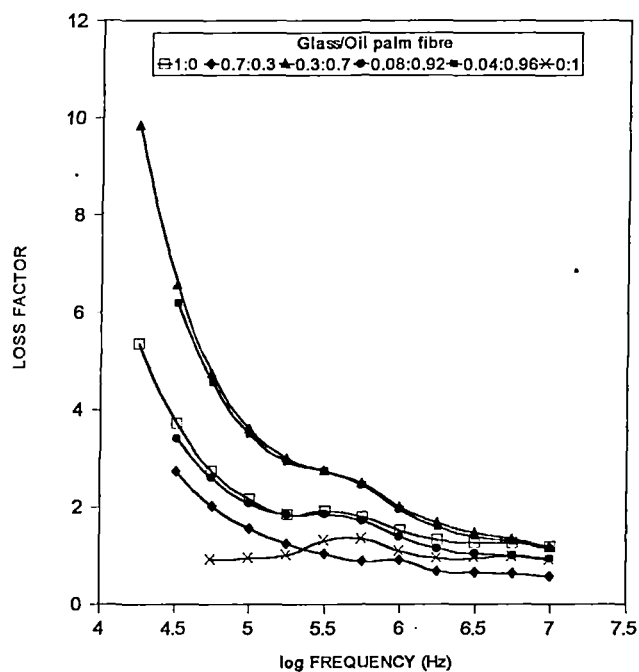


Figure 10.21 Variation of ϵ'' of oil palm fibre/glass hybrid PF composites with frequency at different relative volume fractions of glass and oil palm fibre.
Fibre loading: 40wt. %

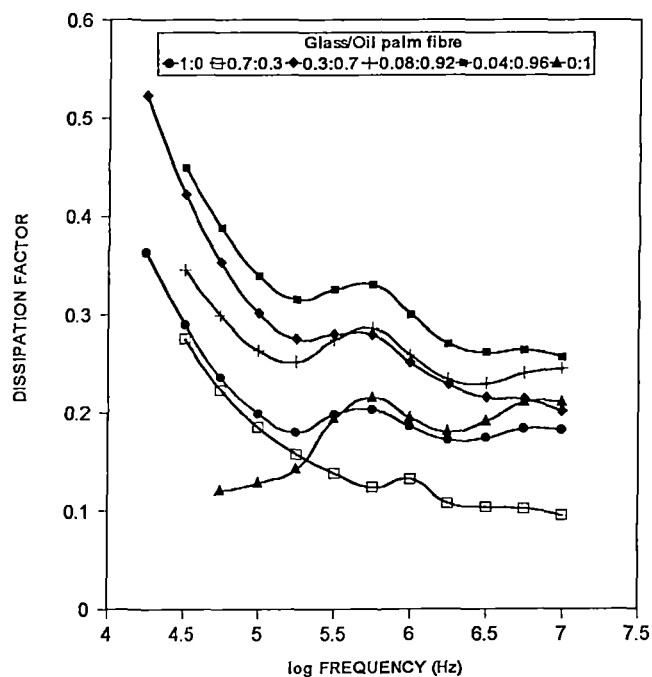


Figure 10.22 Variation of $\tan \delta$ of oil palm fibre/glass hybrid PF composites with frequency at different relative volume fractions of glass and oil palm fibre.
Fibre loading: 40wt. %

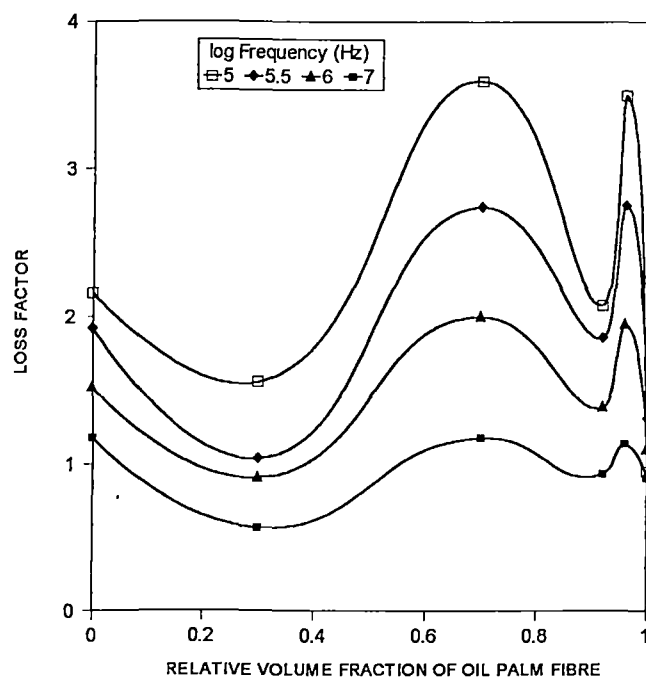


Figure 10.23 Variation of ϵ'' of oil palm fibre/glass hybrid PF composites with relative volume fractions of glass and oil palm fibre at specified frequencies.
Fibre loading: 40wt.%

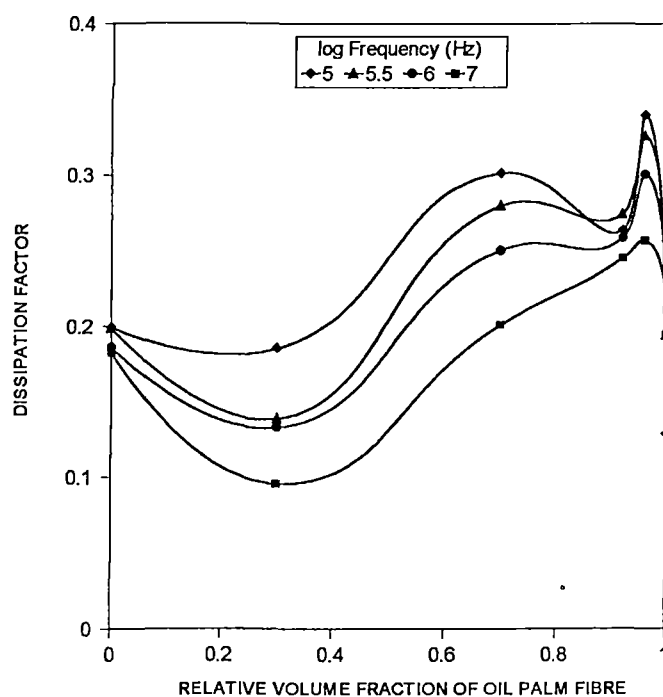


Figure 10.24 Variation of $\tan\delta$ of oil palm fibre/glass hybrid PF composites with relative volume fractions of glass and oil palm fibre at specified frequencies.
Fibre loading: 40wt.%

REFERENCES

1. J. Martinsson and J. L. White, *Polym. Comp.*, **7**, 302 (1986)
2. C. Zhang, X. Yi; H. Yui, S. Asai and M. Sumita, *J. Appl. Polym. Sci.*, **69**, 1813 (1998)
3. H. Tang, X. Chen and Y. Luo, *Eur. Polym. J.*, **32**, 963 (1996)
4. M. Kupke, H. P. Wentzel and K. Schulte, *Materials Research Innovations*, **2**, 164 (1998)
5. M. T. Kortschot and R. T. Woodhams, *Polym. Comp.*, **9**, 60 (1988)
6. B. L. Lee, *Polym. Eng. Sci.*, **32**, 36 (1992)
7. M. Sumita, H. Abe, H. Kayaki and K. Miyasaka, *J. Macromol. Sci. Phys. B*, **25**, 171 (1986)
8. C. M. Thomson and J. S. Allen, *Rubb. Chem. Technol.*, **67**, 107 (1994)
9. B. G. Soares, K. M. N. Gamboa, A. J. B. Ferreira, E. Ueti and S. S. Camargo, *J. Appl. Polym. Sci.*, **69**, 825 (1998)
10. S. N. Bhadani, S. K. Sen Gupta and M. K. Gupta, *Ind. J. Fib. Text. Res.*, **18**, 46 (1993)
11. A. Paul and S. Thomas, *J. Appl. Polym. Sci.*, **63**, 247 (1997)
12. A. Paul and S. Thomas, *Comp. Sci. Technol.*, **57**, 67 (1997)
13. G. Jayamol, S. S. Bhagawan and S. Thomas, *J. Polym. Eng.*, **17**, 383 (1997)
14. A. G. Kulkarni, K. G. Satyanarayana and P. K. Rohatgi, *J. Mater. Sci. Letts.*, **16**, 1719 (1981)
15. A. R. Blythe (Ed.), Electrical properties of polymers, *Cambridge University Press*, Cambridge, London (1979)
16. H. F. Mark (Ed.), Encyclopedia of polymer science and engineering, Vol. **5**, *John Wiley and Sons*, New York (1985)
17. B. C. Pai, A. G. Kulkarni, T. A. Bhasker and N. Balasubramanian, *J. Mater. Sci. Letts.*, **15**, 1856 (1980)
18. M. S. Sreekala, M. G. Kumaran and S. Thomas, *J. Appl. Polym. Sci.*, **66**, 821 (1997)
19. M. S. Sreekala, S. Thomas and N. R. Neelakantan, *J. Polym. Eng.*, **16**, 265 (1997)
20. K. P. Sao, B. K. Samantaray and S. Bhattacharjee, *J. Mater. Sci. Letts.*, **9**, 466 (1990)

CHAPTER 11

Theoretical Modelling of Tensile Properties of Oil Palm Fibre/PF and Oil Palm Fibre/Glass Hybrid PF Composites

*Results of this study have been submitted for publication in **Journal of Materials Science***

Abstract

Various theoretical models were used to predict the tensile strength and young's modulus of untreated and treated oil palm fibre/PF composites and oil palm fibre/glass hybrid PF composites. The theoretical predictions were compared with experimental results. The models selected were parallel, series, Hirsch, modified Bowyer and Bader's and modified rule of mixtures. Modified rule of mixtures show good agreement with the experimental tensile properties. Hirsch's model also predicts the strength of the composites, which is close to the experimental values. All models except rule of mixtures are based on the assumption that there is perfect fibre-matrix interaction and the fibre is perfectly cylindrical having smooth surface characteristics. Hence deviation from the experimental value was observed in the case of real composites where the above mentioned factors are not fully obeyed.

Prediction of strength in reinforced polymers is a complex problem. A number of theories have been developed and reported in literature to describe the properties of composite materials. Historically, the composite strength prediction began with the work of Cox¹ in 1952. This treatment served as the basis of later development - what is now called the shear lag analysis. Detailed analysis by Dow² and Rosen³ produced the same basic result with a slightly different formulation of the constant. Kelly⁴ has derived a multifibre shear lag expression, which predicts that 95% of the strength obtainable with continuous fibres will be obtained with discontinuous ones. Outwater⁵ has developed a mechanical friction theory for stress transfer to discontinuous fibres. Lees⁶ attempted to modify the shear lag approach of Kelly by accounting for fibre lengths both above and below the critical transfer length, as well as the shrinkage stress generated during cooling of the fabricated composites. Except for very low volume fraction of fibres, agreement with experimental results was poor. The main limitation of Lees equation was that the shear lag analysis namely stress concentrations were not considered.

Schultrich et al.⁷ developed a theory to predict the stress-strain behaviour of short fiber composites. They accounted for fibre-fibre interactions but no comparison with experiment was provided. Other noteworthy contributions to composite strength prediction were given by Piggott.⁸ Piggott modified Cox's theory by introducing a new theory that combines plastic deformation at the fibre ends with elastic deformation towards the centre of the fibre during tensile loading. Robinson and Robinson⁹ reviewed fundamental theory for discontinuous fibre reinforcement in plastics. The theory given provides an adequate description of fibre reinforcement predictions for the critical fibre length in model composites based on glass fibres embedded in a range of matrices with different volume fractions. Curtin et al.¹⁰⁻¹² proposed models to predict the strengths of various polymer matrix composites reinforced with graphite fibres and found good agreement between experiment and theory. Various parameters such as inherent strength properties of matrix, filler, fibre-matrix interactions etc. were taken into account. Factors such as fibre orientation, fibre length and fibre dispersion can also

influence the properties and hence must be taken into account while predicting the properties. Various models, which could be applied for composites having rigid inclusions in rigid matrix, were tried to predict the tensile properties of oil palm fibre/PF composites. Of these, the following theories could be used to predict the strength of the composites.

1 Parallel model

According to this model, the tensile strength T_c and Young's modulus M_c are given by the following equations.

$$T_c = T_f V_f + T_m V_m \quad (11.1)$$

$$M_c = M_f V_f + M_m V_m \quad (11.2)$$

where T_c , T_m and T_f are the tensile strength of the composite, matrix and fibre respectively. M_c , M_m and M_f are the Young's moduli of the composite, matrix and fibre respectively.

2 Series model

According to this model, the tensile strength is given by,

$$T_c = \frac{T_m T_f}{T_m V_f + T_f V_m} \quad (11.3)$$

$$M_c = \frac{M_m M_f}{M_m V_f + M_f V_m} \quad (11.4)$$

3 Hirsch's model

This is a combination of parallel and series models.¹³ According to this model, the strength and modulus are given by the following equations.

$$T_c = x(T_m V_m + T_f V_f) + (1 - x) \frac{T_f T_m}{T_m V_f + T_f V_m} \quad (11.5)$$

$$M_c = x(M_m V_m + M_f V_f) + (1 - x) \frac{M_f M_m}{M_m V_f + M_f V_m} \quad (11.6)$$

where x varies between 0 and 1 which determine the stress-transfer between fibre and matrix.

4 Modified Bowyer and Bader's model

According to this model the strength of the composite is the sum of the contributions from subcritical and supercritical fibres and that from the matrix.

The tensile strength is given by the following equation.

$$T_c = T_f K_1 K_2 V_f + T_m V_m \quad (11.7)$$

where K_1 is the fibre orientation factor and K_2 is the fibre length factor. K_1 changes according to the changes in fibre orientation. For aligned short fibre composites K_1 is reported to be 1.¹⁴ For composites having fibres arranged in random fashion, the K_1 is reported to be 0.2. The value of K_2 can be calculated as follows.

For fibres with length $l > l_c$

$$K_2 = 1 - \frac{l_c}{2l} \quad (11.8)$$

For fibres with length $l < l_c$

$$K_2 = \frac{l}{2l_c} \quad (11.9)$$

where l is the length of the fibre and l_c is the critical fibre length. Young's modulus also can be calculated in a similar way and is given by the following equation.

$$M_c = M_f K_1 K_2 V_f + M_m V_m \quad (11.10)$$

5 Modified rule of mixtures

Rule of mixtures (ROM) gives a simple and effective way of predicting the properties of fibre reinforced composites, but it fails to predict accurately the

strength of a fibre reinforced composite.¹⁵⁻¹⁷ Rule of mixtures is based on the assumption that fibres in the composite are uniformly dispersed and a perfect interaction exists between the fibre and the matrix. But in a real composite, non-homogeneity of fibre dispersion and misalignment of fibre orientation may happen during the various processing steps. Thus the ultimate strength of a composite is affected not only by the fibre and matrix fractions but also the microgeometry of the composite components. Lee and Hwang¹⁸ modified the rule of mixtures by considering the factors influencing strength degradation. The modified rule of mixtures can be given as follows:¹⁸

$$\sigma_{cu} = \sigma'_m(1 - V_f) + \sigma_{fu}V_{fe} \quad (11.11)$$

where σ_{cu} is the ultimate strength of the composites, σ'_m is the matrix strength at the failure strain of the fibre, σ_{fu} is the ultimate strength of the fibre, V_f is the fibre volume fraction and V_{fe} is the effective fibre volume fraction. The effective volume fraction is given in terms of the fibre volume fraction and the ratio of real contribution as given below.

$$V_{fe} = V_f(1 - P) \quad (11.12)$$

where P is the degradation parameter for the effective fibre volume fraction, which varies in the range 0 to 1. P can be calculated from the microgeometry of the composite components and depends only on the fibre volume fraction and processing technique. The following equation is obtained from the rule of mixtures with the modification.

$$\frac{\Delta\sigma_{cu}}{\sigma_{fu}} = V_f P \quad (11.13)$$

where $\Delta\sigma_{cu}$ is the difference between the experimentally measured strength and the strength predicted by the rule of mixtures.

These models were used to calculate the tensile strength and young's modulus of untreated and treated oil palm fibre reinforced PF composites and the hybrid reinforcing effect of oil palm fibre and glass fibre in PF resin.

The law of additive rule of hybrid mixtures¹⁹ was used to calculate the hybrid effect. The rule is given by;

$$X_H = X_1V_1 + X_2V_2 \quad (11.14)$$

where X_H is characteristic property of hybrid composite. X_1 and X_2 are characteristic properties of individual composites. V_1 and V_2 are the volume fractions of the reinforcements in hybrid composites. All these models except modified ROM is based on the assumption that there exists perfect fibre-matrix interface and uniform fibre dispersion within the matrix. The possibility of formation of microvoids during the preparation of composites is not accounted for. Also, it is assumed that the fibres are perfectly cylindrical in shape. But in the actual composite this does not hold good and is reflected in the deviation of the experimental values from the theoretical predicted results.

11.1 THEORETICAL PREDICTION OF TENSILE PROPERTIES OF COMPOSITES

Figures 11.1 and 11.2 compare the theoretically predicted tensile strength and Young's modulus values by various models at different fibre loading respectively. Modified rule of mixtures predicts the tensile strength and Young's modulus of the composites, which is in good agreement with the experimental data. The modified rule of mixtures accounts for the degradation of the fibre and matrix materials, structural defects and non-uniformity if any occur in the composites which enables to predict the strength exactly. The values predicted by Hirsch's model are very close to the experimental values. Series and modified Bowyer and Bader's models give lower values than experimental strength values. Parallel model is found to be in least correlation with the experimental values. It is observed that all the predicted strength values except by modified ROM show increase with increase in fibre loading. Experimentally, the tensile strength and Young's modulus of the

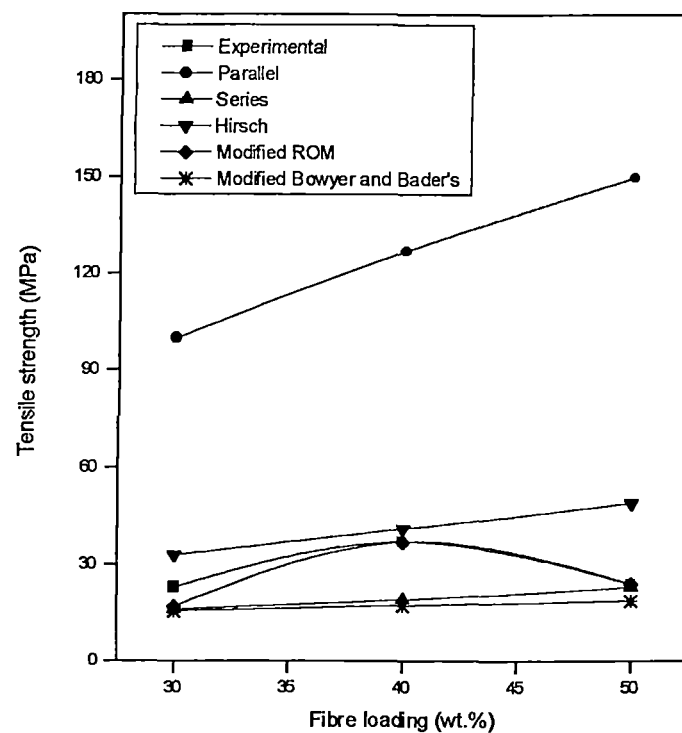


Figure 11.1 Variation of experimental and theoretical tensile strength values of oil palm fibre/PF composites as a function of fibre loading.

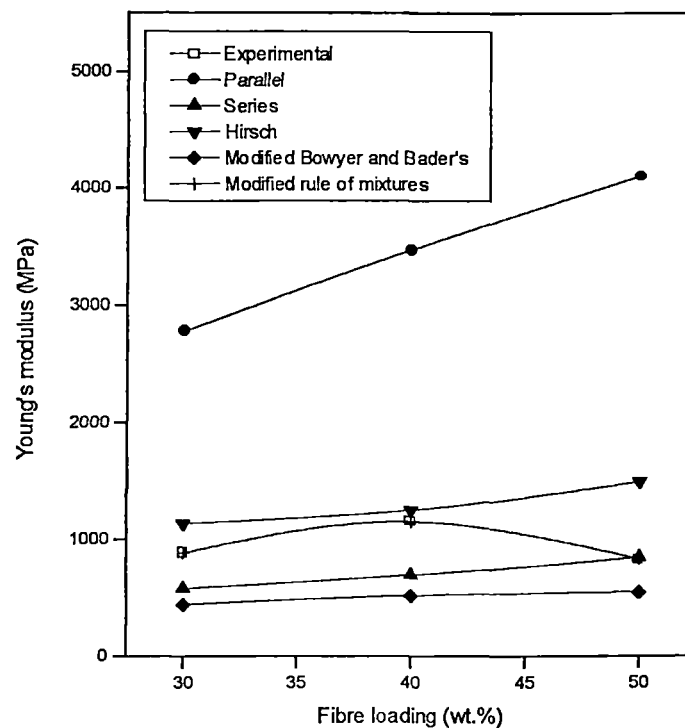


Figure 11.2 Variation of experimental and theoretical Young's modulus values of oil palm fibre/PF composites as a function of fibre loading.

composites were found to decrease above 40wt.% fibre loading. Large deviation of the predicted values from experimental result at higher fibre loading can be attributed to the structural defects occurred during processing. At higher fibre loading, the processing becomes difficult and fibre agglomeration or phase separation may occur during processing. This increases the fibre to fibre contact, which results in decreased fibre-matrix adhesion and in decreased strength properties. Except in the case of modified ROM, all the other models do not taken into account the above mentioned factors.

The tensile strength and Young's modulus of the composites with various fibre lengths were predicted by modified Bowyer and Bader's model (Figure 11.3 and 11.4). The predicted values are lower than that of experimental values. In a randomly oriented fibre reinforced polymer composite, the effective fibre length varies according to the processing characteristics. The theoretical curve shows same trend as that of the experimental curve in both the cases.

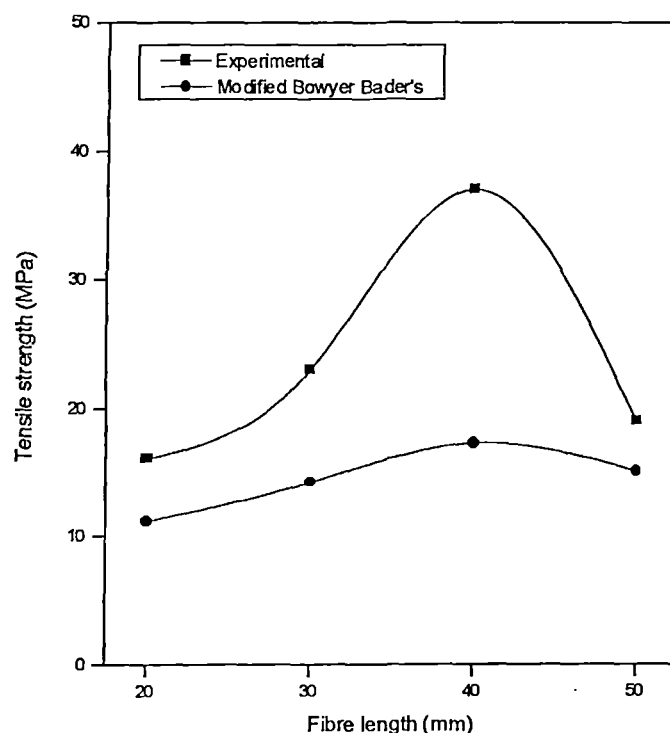


Figure 11.3 Variation of experimental and theoretical tensile strength values of oil palm fibre/PF composites as a function of fibre length.

However higher value is observed at 40mm fibre length, which was found to be the critical length of the composite. Theoretical prediction also gave highest value of tensile strength of the composite for 40mm fibre length. Kalaprasad et al.²⁰ reported the tensile strength and Young's modulus prediction of sisal fibre reinforced low-density polyethylene composites using the modified Bowyer and Bader's model. They observed a linear increase in the properties with increase in fibre length irrespective of the experimental results. The exceptionally high strength value at 40mm fibre length is due to the uniform dispersion and perfect fibre-matrix interaction at the critical length.

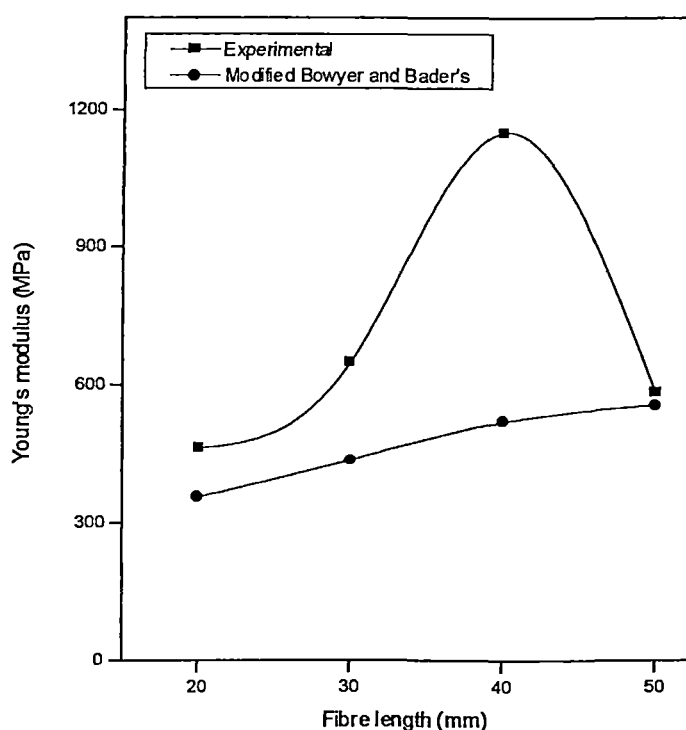


Figure 11.4 Variation of experimental and theoretical Young's modulus values of oil palm fibre/PF composites as a function of fibre length.

Tensile properties of the treated composites were also predicted by various models. Figure 11.5 and 11.6 give a comparison of the experimental and theoretical tensile strength and tensile modulus value of untreated and treated composites. Experimentally the strength of the composite decreased upon the incorporation of

many of the treated fibres due to decreased fibre-matrix adhesion arising from the increased hydrophobicity of the fibre. However, permanganate and alkali treatment marginally increase the properties. Modified rule of mixtures and modified

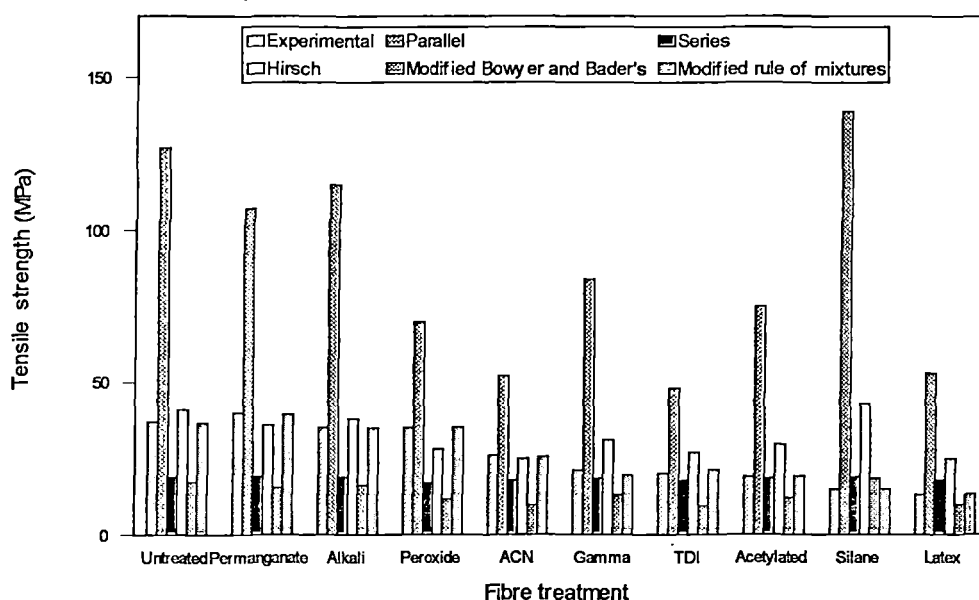


Figure 11.5 Variation of experimental and theoretical tensile strength values of treated oil palm fibre/PF composites having 40mm fibre length and 40wt.% fibre loading.

Bowyer and Bader's model predict the values of the treated composites which is in good agreement with the experimental results. Parallel, series and Hirsch's models show deviation from the experimental values of the treated composites (Figure 11.5 and 11.6). These models are not reckoned with the topological characteristics of the fibre. They are based on the assumption that the fibre surface is perfectly smooth. But in the real composites, the fibre surface topology changes were observed in various treated composites (refer Chapter 3). These variations affect the fibre-matrix interlocking. This affects the effective stress transfer through the interface. Because of these variations in the morphological properties, the strength predicted by these models agrees least with that of the experimental value.

Figures 11.7 and 11.8 compare the experimental tensile properties of the hybrid composites with theoretically predicted values. All the models show similar trend as that of the experimental curve. Except parallel model, all the other models

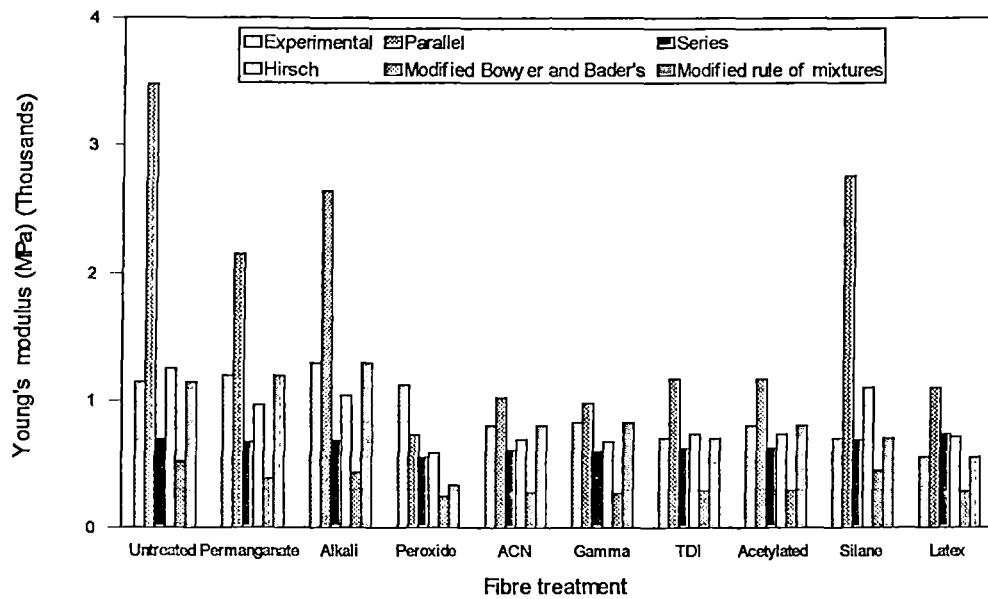


Figure 11.6 Variation of experimental and theoretical Young's modulus values of treated oil palm fibre/PF composites having 40mm fibre length and 40 wt.% fibre loading.

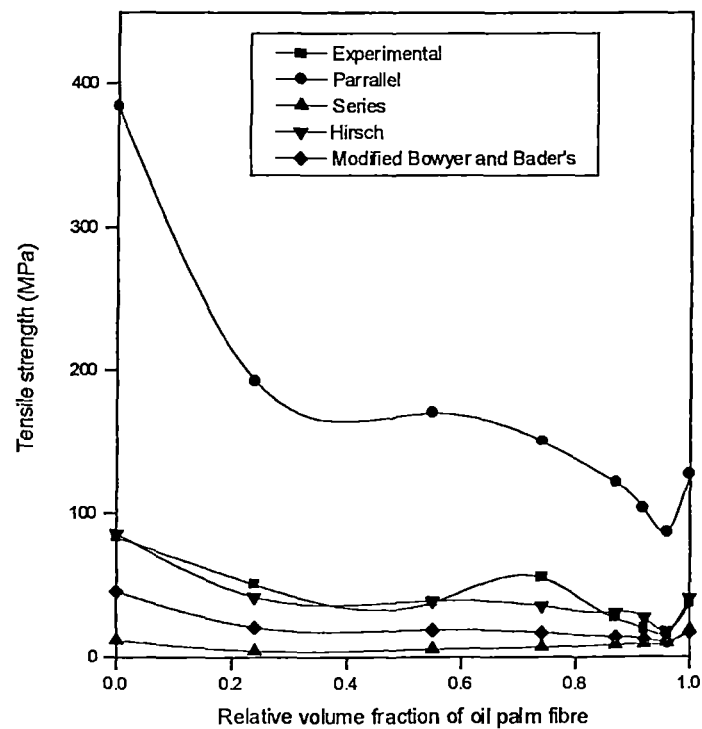


Figure 11.7 Variation of experimental and theoretical tensile strength values of oil palm fibre/glass hybrid PF composites with various relative volume fraction ratio of oil palm fibre and glass.

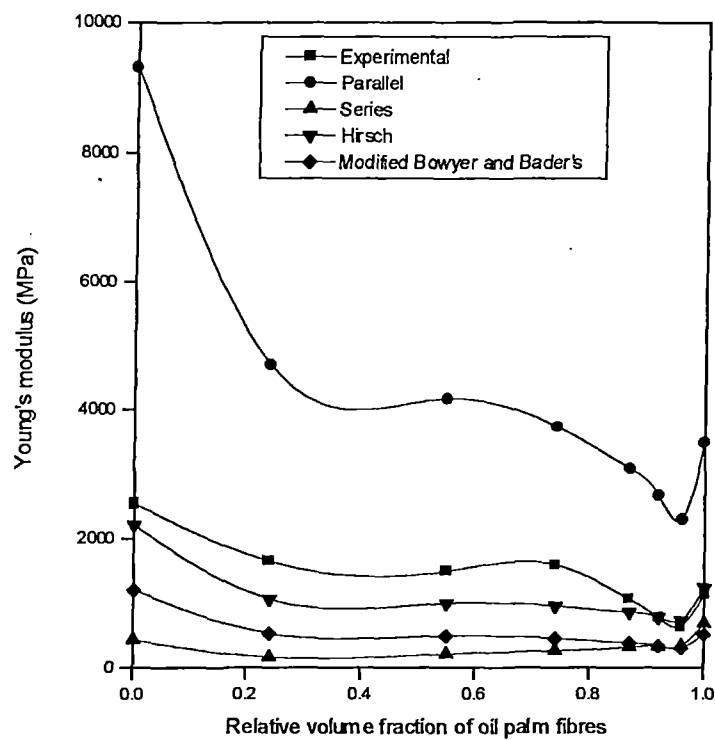


Figure 11.8 Variation of experimental and theoretical Young's modulus values of oil palm fibre/glass hybrid PF composites with various relative volume fraction ratio of oil palm fibre and glass.

predict lower values than experimental value. Theoretically perfect compatibility between individual fibres are expected. However due to the difference in the surface characteristics and other physical property changes, the compatibility between oil palm fibre and glass fibre decreased in the oil palm/glass hybrid fibre reinforced PF composites. Tensile strength and tensile modulus show negative hybrid effect at lower and higher OPEFB fibre volume fractions. Theoretical prediction expects complete intermingling of both the fibres within the matrix. In the present study fibre layers are maximally intermingled, even though there is layering out observed. This is evident from the tensile fractograph of hybrid composite (Fig. 5.10; refer Chapter 5). A hundred percent hybrid effect can not be achieved in sandwich type composites because full intermingling is not possible. This may be the reason for the negative hybrid effect.

REFERENCES

1. H. L. Cox, *Brit. J. Appl. Phys.*, **3**, 72 (1952)
2. N. F. Dow, *General Electric Report*, **R 635 D 61** (1963)
3. B. W. Rosen (Ed.), *Fiber Composite Materials*, *American Society for Metals*, Metals Park, Ohio (1965)
4. A. Kelly, *Strong Solids*, *Clarendon Press*, Oxford (1966)
5. J. O. Outwater, *J. Mod. Plast.*, **33**, 156 (1956)
6. J. K. Lees, *Polym. Eng. Sci.*, **8**, 195 (1968)
7. B. Schultrich, W. Pompe, H. J. Weiss, *Fib. Sci. Technol.*, **11**, 1 (1978)
8. M. R. Piggott, *J. Mater. Sci.*, **16**, 2837 (1981)
9. I. M. Robinson and J. M. Robinson, *J. Mater. Sci.*, **29**, 4663 (1994)
10. S. J. Zhou and W. A. Curtin, *Acta Met. Mat.*, **43**, 3093 (1995)
11. M. Ibnabdeljalil and W. A. Curtin, *Int. J. Sol. Str.*, **34**, 2649 (1997)
12. W. A. Curtin and N. Takeda, *J. Comp. Mater.*, **32**, 2060 (1998)
13. T. J. Hirsch, *J. Am. Con. Inst.*, **59**, 427 (1962)
14. P. T. Curtis, M. G. Bader and J. E. Bailey, *J. Mater. Sci.*, **13**, 377 (1978)
15. B. D. Agarwal and L. J. Broutman, *Analysis and Performance of Fibre Composites*, *John Wiley and Sons Inc.*, New York (1980)
16. K. K. Chawla, *Composite Materials, Science and Engineering*, *Springer-verlag*, New York (1987)
17. C. Zweben, H. T. Hahn and T. W. Chou, *Delaware Composite Design Encyclopedia*, *Technomic Publishing Co.*, USA, Vol. 1 (1989)
18. C. Lee and W. Hwang, *J. Mater. Sci. Lett.*, **17**, 1601 (1998)
19. G. Kretsis, *Composites*, **18**, 13 (1987)
20. G. Kalaprasad, K. Joseph, S. Thomas and C. Pavithran, *J. Mater. Sci.*, **32**, 4261 (1997)

Conclusions and Future Outlook

The present study reveals that oil palm fibres represent a potential reinforcement in resole type phenol formaldehyde resin. The main benefits of incorporating oil palm fibres in phenolics are decreased shrinkage, reduced thermal stress during curing, improved impact resistance, stiffness and lower costs. Hybridisation of oil palm fibre with glass was tried to make high performance composites.

Structure and properties of the two important oil palm fibres, OPEFB fibre and mesocarp fibres were analysed. Chemical composition of the fibres was determined. The major constituents of these fibres were found to be cellulose. Lignin content is comparatively low. The OPEFB fibre is more cellulosic than the mesocarp fibre. The oil palm mesocarp fibre contains higher percentage of ether soluble and caustic soda soluble matter. Chemical modification of fibres by alkali treatment, acetylation and silane treatment has been carried out. This is to improve the strength and therefore the reinforcing ability of these fibres. Morphological studies revealed that treatment modified the fibre surface. The fine structural changes of the fibres can be seen from the respective scanning electron micrographs. IR studies give evidence for the chemical modification occurred during treatments. Thermal stability and degradation characteristics of the fibres were investigated by thermogravimetry and differential thermal analysis. It is found that alkali and silane treatments increase the thermal stability of the fibres. Fibres are stable up to 300°C without any considerable weight loss.

The silane treated OPEFB fibre showed maximum tensile strength. Alkali treatment slightly decreases the tensile strength. The Young's modulus of the fibre showed enhancement upon silane and alkali treatments. The strength of the mesocarp fibre is less than that of OPEFB fibre. This is due to the high cellulose content of OPEFB fibre. Silane treatment increases the strength of the fibre while alkali treatment decreases. However, the stiffness of the fibre is increased by both alkali and silane treatments. The untreated mesocarp fibre shows very good elongation. Treatment reduces the elongation of the fibre. Microfibrillar angle and strength of the fibres were theoretically predicted. The theoretical strength of the OPEFB fibre was found to be close to the experimental value. However, in the case

of mesocarp fibre, there is great deviation from the theoretical strength. It is important to mention that the properties of oil palm fibres are comparable to other natural fibres and therefore they could be used as a potential reinforcing material for polymer matrices.

Oil palm fibres were incorporated as a reinforcement in phenol formaldehyde matrix. Mechanical performance of the matrix is greatly enhanced by the fibrous reinforcement. Chemical treatment of the fibre leads to composites having excellent impact properties. Oil palm fibre is highly hydrophilic due to the presence of hydroxyl groups from cellulose and lignin. Acetylation, isocyanate treatment, silane treatment, acrylation and acrylonitrile grafting lead to strong covalent bond formation thereby reducing the hydrophilicity of the fibre. The scanning electron microscopy and IR studies revealed the physical and chemical modifications occurred to the fibres. Tensile strength of the fibre declined upon various treatments. However, silane treatment and acrylation enhanced the strength. The brittleness of the fibres decreased upon chemical treatments. The Young's modulus and elongation at break of individual fibres increased upon chemical modifications. Optimum mechanical performance is observed for silane treated and acrylated fibre. Latex modification imparts elasticity to the fibres. The fibre elongation properties show sharp increase upon modifications.

Due to the hydrophilicity of PF resin and oil palm fibre, they are highly compatible. Incorporation of the treated fibres in PF matrix reduces the tensile strength of the composite except for permanganate treatment, which exhibit improved tensile strength. Fibre became more hydrophobic upon modifications that reduce the interaction with PF resin, which leads to a decline in interface properties. Extensibility of the composite considerably increased upon treatment. Maximum elongation is observed for latex coated composites. Tensile modulus of the composite shows enhancement upon mercerisation and permanganate treatment. Scanning electron microscopic studies revealed the tensile failure mechanism. Mercerisation, peroxide treatment, permanganate treatment and acrylonitrile grafting resulted in composites having better flexural properties. Decreased

hydrophilicity of the fibres upon chemical modifications resulted in composites having very high impact resistance. Latex coating, acetylation, silane and isocyanate treatments led to high impact composites. This is attributed to the relatively poor fibre-matrix adhesion resulting from the hydrophobicity of the modified fibres. This enables the samples to dissipate maximum energy by mechanical friction during failure process. Debonding of the fibres was facilitated upon various modifications and is evident from the scanning electron micrographs. Major failure processes occurred were found to be fibre-matrix debonding leading to fibre pullout and fibre breakage. Thus by reducing the hydrophilic nature of the oil palm fibre, high impact composites could be obtained from PF resin and oil palm fibre.

Mechanical properties of glass/PF and glass/OPEFB hybrid PF composites were studied. Glass effectively reinforces in PF resin and mechanical performance is maximum at 40wt.% loading. Different volume fractions of glass were added to OPEFB fibre/PF composites. Composite properties such as tensile and flexural behaviour showed considerable enhancement by the incorporation of small volume fractions of glass fibre. The tensile and flexural properties of glass/PF and glass/OPEFB hybrid PF composites were studied from the stress-strain curves. Presence of OPEFB fibre enhances the impact strength of the composites. Maximum value of the impact strength was observed for the hybrid composite containing 0.74 volume fraction of OPEFB fibre. The value is greater than glass reinforced PF composites. By replacing the brittle glass fibre by OPEFB fibre the toughness of the composite could be increased. The tensile and impact fracture mechanisms were evident from the respective scanning electron micrographs. On enhancing the glass fibre loading in glass/PF composites the void content increases and this can be understood from the decreased value of experimental density than the theoretically predicted value. Porosity of the composite decreased upon oil palm fibre reinforcement. Void formation associated with the fibre packing defects is minimised upon oil palm fibre addition. Hardness and density of the composite decrease as the volume fraction of OPEFB fibre increases. Phenol formaldehyde

gum sample exhibits maximum hardness. Glass fibre reinforcement decreases the hardness while increasing the density of the composite. Hybridisation of glass fibre with 0.74 volume fraction of OPEFB fibre resulted in composites having superior mechanical performance. Positive hybrid effect is observed in impact properties.

Stress relaxation behaviour of oil palm empty fruit bunch fibre and of the oil palm fibre reinforced phenol formaldehyde composites were studied in detail. Fibre surface modifications were carried out in order to improve the interface properties. Silane treatment, isocyanate treatment, latex coating, mercerisation, acetylation and radiation treatment were attempted to modify the interface. The effect of these treatments on the relaxation behaviour of the fibre was investigated. Latex coating decreases the rate of stress relaxation of the fibre considerably. Other modifications increase the rate of stress relaxation initially, however the relaxation rate is very low at long durations of time as compared to untreated fibre. Thermal aged and water sorbed oil palm fibres were subjected to stress relaxation experiments. Stress relaxation rate is decreased upon both thermal and water ageing of the fibre. Effect of strain level on the relaxation of the fibre was studied. Rate of relaxation is maximum at 10% strain level. Stress relaxation behaviour in oil palm fibre/PF composites was investigated by giving special emphasis to the effect of fibre loading, fibre treatment, physical ageing and strain level. Higher relaxation is observed for 30wt.% fibre loading. Alkali treated composite showed decreased relaxation than untreated composite. Latex coating and introduction of coupling agents increased the relaxation rate of composites. Latex coated composite exhibits maximum relaxation. This is attributed to the decreased fibre-matrix interaction between the less hydrophilic latex coated fibre and more hydrophilic phenolic resin. Water ageing increased the relaxation of the composites. The variation in the relaxation process of aged composites is due to the changes in the interface properties upon ageing. On application of lower strain, the relaxation was comparatively less and on further increase upto 2%, higher relaxation was observed. At very high strain levels the relaxation again decreased. This may be due to the extent of fibre breakage pattern at different strain levels. Interesting results are

obtained upon hybridisation of oil palm fibre with glass fibre. Very low stress relaxation is observed for the hybrid composites. Relaxation modulus of the fibre and the composite was also studied. To explain the long-term stress relaxation behaviour of the fibre and composites with respect to strain levels, a master curve is constructed by superimposing points at different strain levels by a horizontal shift along the logarithmic time axis.

Dynamic mechanical behaviour of the oil palm fibre reinforced PF composites and oil palm fibre/glass hybrid PF composites were investigated. Variations in dynamic modulus, loss modulus and mechanical damping parameter were analysed as a function of temperature and frequency. It is found that incorporation of oil palm fibre increases the modulus and damping characteristics of the neat sample. Irregular trend is observed with fibre length. Maximum damping is observed for 20 and 40mm fibre lengths. As the fibre content increases mechanical damping linearly increases. However maximum stiffness is observed for 30wt.% fibre loading. The loss modulus value decreases with fibre loading. Incorporation of oil palm fibre in PF resulted in decrease of glass transition temperature. Lower T_g values are obtained from E'' curve. Effect of fibre modification by mercerisation on the dynamic properties of the composites was analysed. Modification improves the interface properties. Highest value of $\tan\delta$ is observed for 24hrs mercerised composite. As the frequency increases, the $\tan\delta$ decreases. Latex treated composite exhibits highest damping behaviour. Glass transition shifts to higher temperature with increase in mercerisation time. Stiffness of the composite also increases with treatment. Dynamic modulus of the oil palm fibre/PF composites is increased by fibre treatments. Irregular trend in the variation of loss modulus is observed with treatment time. Acrylated and latex treated composites show lower loss modulus. Effect of hybridisation of oil palm fibre with glass fibre on the dynamic properties was analysed. Hybridisation increases the damping value. The damping increased with relative volume fraction of oil palm fibre. Glass transition temperature of the hybrid composite is lower than that of the unhybridised composite. The storage modulus and loss modulus decrease with

increase in relative oil palm fibre volume fraction in hybrid composites after relaxation. However maximum modulus was obtained for composite having 0.3 relative volume fraction of oil palm fibre. This is due to the better fibre dispersion in hybrid composites at lower loading of oil palm fibre. Gradual decrease in loss modulus of the hybrid composites was observed with increase in frequency.

Activation energy required for the major relaxation processes in different composites during dynamic loading were calculated from the Arrhenius relationship. Activation energy for relaxation at glass transition region for PF gum sample is comparatively low. The value increased upon oil palm fibre reinforcement. As the fibre content increased the activation energy decreased. Highest value is observed for the unhybridised composite having 30wt.% fibre loading and 40mm fibre length. Mercerisation for about 48hrs increases the activation energy due to the increased interfacial adhesion. Except mercerisation and permanganate treatments all other treatments decrease the activation energy for relaxation at glass transition region. Activation energy decreases upon incorporation of glass fibre in hybrid composites. Cole-Cole analysis reveals that the composites are not perfectly homogenous. The long term dynamic behaviour of the composites was predicted by master curve based on time-temperature superposition principle.

Water sorption behaviour of both oil palm empty fruit bunch fibre and oil palm mesocarp fibre has been investigated. Sorption behaviour of distilled water, mineral water and salt water at 30, 50, 70 and 90°C was evaluated. Salt water sorption is slightly different from that of distilled water and mineral water and can be understood from the sorption curves. This is due to the presence of ions in salt water. The OPEFB fibre showed higher sorption than oil palm mesocarp fibre. This may be due to higher number of micropores present on the OPEFB fibre surface than mesocarp fibre which facilitates the capillary action. Scanning electron microscopic studies reveal the porous structure of both the fibres. Both the fibres show a higher initial capillary uptake of water. A decrease in uptake with temperature is observed in all systems except for salt water/mesocarp fibre systems.

At lower temperature a two step behaviour is observed for distilled water and mineral water. The effect of OPEFB fibre treatment on the sorption behaviour in distilled water is studied at different temperatures. Treatment reduces the water uptake at all temperatures. The decrease is due to its physical and chemical changes occurred to the fibres upon various modifications. Hydrophilicity of the fibre decreased upon modifications and decreases water uptake. The thermodynamics of sorption were studied in detail. The ΔH and ΔS values are found to be negative for all the systems suggesting the sorption process exothermic. The mechanical performance of the fibres decreases upon water sorption and it regains on desorption. However modulus of the OPEFB fibre decreases on sorption and desorption. In mesocarp fibres modulus shows enhancement upon desorption. Treatment reduces the mechanical strength of the fibres. The elongation of the fibres considerably increased upon treatments except silane. Young's modulus shows enhancement upon mercerisation and silane treatment. In swollen stage the stiffness of the fibre is considerably reduced.

Water sorption characteristics of untreated and treated oil palm fibre reinforced PF composites and oil palm fibre/glass hybrid PF composites were studied. The effects of fibre loading, fibre treatment and relative volume fractions of fibres in hybrid composites on the kinetic and thermodynamic parameters of water sorption were analysed. Water sorption parameters of the composites at four different temperatures 30, 50, 70 and 90°C were investigated and compared. Among the untreated composites, highest sorption of water is found to be for systems containing 10 and 50wt.% fibre loaded composites at 30°C. Fibre surface treatment increases water absorption except in alkali treated composite. Most of the treatments make the fibre hydrophobic, which decrease the fibre-matrix adhesion and facilitate water sorption. The decreased fibre-matrix interface facilitates void formation and can enhance sorption. Latex treated composite exhibits maximum water sorption. In hybrid composites, as the relative volume fraction of oil palm fibres is increased, the water sorption linearly increases. It is found that the

unhybridised composites, glass/PF and oil palm fibre/PF exhibit less absorption than hybrid composites.

The kinetic parameters of water sorption, n , k , diffusion coefficient, sorption coefficient and permeability coefficient for different composites were calculated. Untreated composites at all fibre loading exhibit Fickian diffusion mechanism. Fibre surface treatment and hybridisation of oil palm fibre with glass deviate the mechanism from Fickian sorption. The diffusion coefficient is found to be increased with increase in the fibre content of the composites. Fibre modification also lead to high values of diffusion coefficient. In hybrid composites the diffusion coefficient values decrease as the volume fraction of glass is increased. Sorption coefficient is found to be higher at lower fibre loading. Latex treated composites have got higher sorption coefficient. Sorption coefficient in hybrid composites shows irregular trend with temperature. Permeability coefficient shows its highest value for 30wt.% fibre loaded composite. Treatments like silane, isocyanate and acrylation raise the value than untreated composite. Highest value of permeability coefficient in hybrid composites is observed for composite with highest volume fraction of oil palm fibre. Activation energies for the permeation and diffusion processes were calculated. The activation energy for permeation becomes higher than that of diffusion in hybrid composites at higher volume fractions of oil palm fibres. The entropy of sorption is found to be negative in all systems. The diffusion coefficient is found to be concentration dependent of the sorbed water. Upto 30-40wt.% sorbed water, the diffusion coefficient increases and thereafter decreases.

Variations in the tensile, flexural and impact properties on water sorption were analysed. In most cases tensile strength values increased upon water sorption. Scanning electron micrographs of tensile fracture surfaces revealed the changes in the fibre-matrix interaction and failure criteria of the composites before and after water sorption. Stiffness of the composites also increased upon water sorption. However flexural strength and flexural modulus were considerably decreased on

sorption. Impact strength values change irregularly among treated composites on water sorption.

Environmental effects on the mechanical properties of oil palm fibre reinforced PF composites have been investigated. Ageing effects were compared with those of glass/PF and oil palm/glass hybrid PF composites. Various fibre modifications were carried out and their effect on the ageing process was studied. Thermal ageing, cold water and boiling water ageing, biodegradation and gamma irradiation effects on the composite properties were analysed. Influence of ageing on the tensile, flexural and impact properties of the composites was investigated. The tensile and flexural stress-strain behaviours of the composites were affected by ageing. The tensile strength of the composites decreased upon thermal, biodegradation and gamma irradiation. However, water ageing did not decrease the properties of the composites and in some cases enhancement is observed. The extensibility of the composites decreased upon thermal ageing. However the value increased upon biodegradation, water ageing and gamma irradiation. Thermal and water ageing increased the tensile modulus of composites treated with silane, peroxide, isocyanate and acrylated samples. Biodegradation decreases the modulus values of all systems. Untreated, alkali and peroxide treated fibre composite show enhancement in tensile modulus values upon gamma irradiation. Various tensile failure processes were studied by scanning electron microscopy. The flexural properties of the composites decreases upon water ageing. Thermal ageing leads to higher flexural properties in composites treated with peroxide, latex and acrylic acid. Izod impact strength of the untreated, acrylonitrile, peroxide and isocyanate treated composites increased upon water ageing. Biodegradation, thermal ageing and gamma irradiation decreased the impact resistance of the composite. Scanning electron micrograph of the impact fracture surface revealed the failure mechanism. Finally the thermal stability of the composites was determined by TG and DTG analysis. The study showed that the untreated oil palm fibre/PF composite is thermally stable upto 350°C without any considerable weight loss. The thermal

stability can be improved by hybridising the oil palm fibre with small amount of glass fibre.

Electrical properties of oil palm fibre/PF composites and oil palm fibre/glass hybrid PF composites were studied with special reference to the effect of fibre loading, fibre treatment and hybrid fibre ratio. Volume resistivity, dielectric constant, loss factor and dissipation factor of the composites were analysed. Oil palm fibre reinforcement increased the volume resistivity of PF resin. Fibre treatments enhanced the resistivity of the composites. Hybridisation of oil palm fibre with small amount of glass fibre again increased the electrical resistivity of the composites. The changes in the resistivity values were attributed to the inherent electrical resistivity of lignocellulosic oil palm fibres and the interactions at the fibre-matrix interface. With the increase in frequency, the resistivity of the composites decreased linearly. The incorporation of oil palm fibre decreases the dielectric constant, loss factor and dissipation factor of PF resin. This may be due to the lower dielectric values of lignocellulosic fibres. Changes in the polarisability occurring in the composite determine the dielectric properties. Fibre treatments were found to have great influence in the dipole interaction at the fibre-matrix interface. Hybridisation of oil palm fibre with glass increases the dielectric constant, loss factor and dissipation factor. The changes were due to the decreased compatibility between oil palm and glass fibre layers in hybrid composite. The scanning electron microscopic studies gave insight into fibre-matrix interface.

Thus oil palm fibre reinforcement in phenolic resin results in cost effective and environment friendly composite materials. Hybridisation of glass and OPEFB fibre and their reinforcement in PF resin resulted in lightweight composites having good performance qualities. These composites may find applications as structural materials where higher strength and cost considerations are important. By suitable selection of the composition of the reinforcing fibres, high performance composites having better damping and modulus characteristics can be prepared. This composite will be a value-added substitute for conventional structural materials in engineering applications. Also they can be safely used for structural applications in

water environment without sacrificing the mechanical strength. They offer high electrical resistivity, which is the most desirable characteristic of an insulator to resist the leakage of electric current in electrical applications. The composite material prepared could be safely used for high impact applications in building and automotive industry. It will be a good candidate for wall panelling and interior room partitioning as a wood substitute in low cost housing. Oil palm fibre reinforced PF composites are lower in cost compared to particleboards from other natural fibre reinforced polymer composites. Their reinforcement costs are negligible. No complicated processing is needed in the preparation of these composites. This makes them less expensive. Since natural fibres are biodegradable compared to other synthetic fibres, natural fibre reinforced thermoset composites can find application in cars of the coming millennium. Low cost, low density, high strength, biodegradability and eco-friendliness make them outstanding among polymer composites.

Future Scope

In order to evaluate the versatile applicable potential of these composite materials, further investigation in this topic is needed to characterise the various aspects of reinforcement.

Flame Retardant Properties:- As the phenolics are highly heat resistant materials, the flame retardant properties of composites should be studied to assess the suitability of the composite material in thermal environments.

Bio-degradability:- Now-a-days, the non-degradable plastic pollution has emerged as a major issue world-wide. Here comes the importance of added biodegradability to composites. The synthetic matrix part in composites can be made more biodegradable by introducing starch onto the polymers. For high performance applications, these composite materials must have high strength coupled with low density and biodegradability.

Textile Composites:- To explore high strength materials, maximum reinforcing action of the fibres could be achieved. This will lead to the preparation of textile composites. Composites with tailor made properties could be achievable by hybrid textile composites.

Other Hybrid Composites:- Oil palm fibres can be hybridised with other natural fibres or with strain compatible synthetic fibres such as polyethylene fibres to achieve better properties. The reinforcing ability of these fibres in other polymer matrices—both thermoplastic and thermoset—has to be investigated. Based on the specific utility, the best composite can be chosen.

Appendices

CURRICULUM VITAE

1. **Name** : SREEKALA. M. S.
2. **Official Address** : Senior Research Fellow
School of Chemical Sciences
Mahatma Gandhi University
Priyadarshini Hills P.O
Kottayam, Kerala
India-686 560
Tel: 91-481-598015
Fax: 91-481-561190
91-481-561800
E-mail < mgu@md2.vsnl.net.in >
3. **Permanent Address for Communication** : Sreebhavan
South Pampady P. O.
Kottayam, Kerala
India – 686 521
Tel: 91- 481-505163
4. **Nationality** : Indian
5. **Completed Age & Date of Birth** : 29 years, May 20th 1970

6. **Education**

Degree	Name of University	Year of passing	Division
Ph. D (Chemistry)	Mahatma Gandhi University	(Thesis Submitted)	
M. Phil (Chemistry)	Mahatma Gandhi University	1995	‘A’ grade
M. Sc (Analytical Chemistry)	Mahatma Gandhi University	1992	First class

7. **Fellowships & Awards** : 1. **Best Paper Award** in National
Level Technical Symposium,
Elastofest ‘99’
2. CSIR Senior Research Fellowship
New Delhi

8. ***Number of publications in International Journals*** : Published : 6
Submitted : 9
9. ***Papers Published in National and International Conferences*** : 10
10. ***Research Interests*** : Fibre filled polymer composites,
Particulate filled polymer composites,
Ageing, Degradation and Diffusion.
11. ***Skills*** : TGA, DMTA, FTIR, UV, DSC, GPC,
SEM, Optical Microscopy, UTM, Rubber
and Plastic Processing and Testing
Machinery.
12. ***Teaching Experience*** : Lecturer in Chemistry, Vocational Higher
Secondary Education, Kerala, India (1993)
Lecturer in Chemistry, Institute of Human
Resources Development for Electronics,
Kerala, India (1992).
13. ***Membership of professional Bodies*** : 1. Member of Indian Science Congress
Association.
2. Member of Indian Society of Disordered
Materials.
3. Member of Mahatma Gandhi University
Chemical Society.

Publications in International Journals

- (1) M. S. Sreekala, Sabu Thomas and N. R. Neelakantan, "Utilization of short oil palm, empty fruit bunch fibre as a reinforcement in phenol formaldehyde resin: Studies on mechanical properties", *J. Polym. Eng.*, 16, 265 (1997).
- (2) M. S. Sreekala, M. G. Kumaran and Sabu Thomas, "Oil Palm Fibres: Morphology, Chemical composition, Surface modification and Mechanical properties", *J. Appl. Polym. Sci.*, 66, 821 (1997)
- (3) J. George, M. S. Sreekala, S. S. Bhagawan, N. R. Neelakantan and Sabu Thomas "Stress relaxation behaviour of pineapple fibre reinforced low density polyethylene composites", *J. Reinf. Plast. Comp.*, 17, 579 (1998)
- (4) M. S. Sreekala, M. G. Kumaran and Sabu Thomas, "Oil palm fibre reinforced phenol formaldehyde composites: Influence of fibre surface modifications on the mechanical performance", *Appl. Comp. Mater.* (In press)
- (5) R. Agrawal, N. S. Saxena, M. S. Sreekala & Sabu Thomas, "Effect of treatment on thermal conductivity and thermal diffusivity of oil palm fibre reinforced phenol formaldehyde composites", *J. Polym. Sci. Part B; Polym. Phys.* (In press)
- (6) J. George, M. S. Sreekala & Sabu Thomas, "Natural fibre reinforced plastic composites: Interface modification and characterisation". (*Macromol. Sci.-Review, In press*)
- (7) M. S. Sreekala, M. G. Kumaran and Sabu Thomas, "Water sorption characteristics of oil palm fibers". (*Submitted to 'Eur. Polym. J.'*)
- (8) M. S. Sreekala, J. George, M. G. Kumaran and Sabu Thomas, "Mechanical performance of oil palm empty fruit bunch fibre/glass hybrid PF composites". (*Submitted to 'Comp. Sci. Technol.'*)
- (9) M. S. Sreekala, M. G. Kumaran, Reethamma Joseph & Sabu Thomas, "Stress relaxation behaviour in oil palm fibre reinforced phenol formaldehyde composites". (*Submitted to 'Comp. Sci. Technol.'*)
- (10) M. S. Sreekala, M.G. Kumaran, & SabuThomas, "Stress relaxation behaviour in oil palm fibres". (*Submitted to 'J. Appl. Polym. Sci.'*)
- (11) M. S. Sreekala, M. G. Kumaran, G. Groeninckx & Sabu Thomas, "Dynamic mechanical relaxation properties of oil palm fibre/PF composites and oil palm fibre-glass hybrid PF composites". (*Submitted to 'Polym. Eng. Sci.'*)

- (12) M. S. Sreekala, M. G. Kumaran & Sabu Thomas, "Water sorption kinetics in oil palm fibre reinforced phenol formaldehyde composites: Influence of fibre loading, fibre treatment and hybridisation of oil palm fibre with glass". *(Submitted to 'Eur. Polym. J.')*
- (13) M. S. Sreekala, M. G. Kumaran & Sabu Thomas, "Electrical properties of oil palm fibre/phenol formaldehyde composites: Effect of fibre loading, fibre surface modifications and hybridisation of oil palm fibre with glass". *(Submitted to 'J. Reinf. Plast. Comp.')*
- (14) M. S. Sreekala, M. G. Kumaran & Sabu Thomas, "Environmental effects in oil palm fibre reinforced phenol formaldehyde composites: Studies on thermal, biological, moisture and high energy radiation effects". *(Submitted to 'Composites')*
- (15) M. S. Sreekala, M. G. Kumaran & Sabu Thomas, "Theoretical modelling of tensile properties of short oil palm fibre/PF composites". *(Submitted to 'J. Mater. Sci.')*

Papers Published/Presented in National and International Conferences

- (1) Effect of chemical modifications on the mechanical performance of oil palm fibre reinforced phenol formaldehyde composites, M. S. Sreekala, M. G. Kumaran and Sabu Thomas
9th Swadeshi science congress, November 5th – 7th 1999, Kollam, Kerala.
- (2) Mechanical performance of oil palm-glass hybrid fibre/PF composites : Improved interactions and hybrid effect, M. S. Sreekala and Sabu Thomas
The polymer processing society, Fifteenth annual meeting, The Netherlands
May 31-June 4, 1999
- (3) ***Best paper award:***
'Oil Palm fibre reinforced Phenol Formaldehyde composites for high impact applications: Influence of fibre surface modifications on the mechanical performance', M. S. Sreekala, M. G. Kumaran and Sabu Thomas
A National Level Technical Symposium 'ELASTOFEST '99', held at Madras Institute of Technology, Anna University, Chennai, April 7&8, 1999

- (4) Dynamic Mechanical Relaxation Properties of Oil Palm Fibre/Phenol Formaldehyde and Oil Palm-Glass Hybrid Fibre/Phenol Formaldehyde Composites, M. S. Sreekala, M. G. Kumaran and Sabu Thomas
National seminar on polymers for the new millennium, held at Chennai, March 25 & 26, 1999
- (5) Short Oil Palm Empty Fruit Bunch fibre as a reinforcement in PF resin: Studies on Mechanical Performance, M. S. Sreekala
Proceedings of the 86th Session of the Indian Science Congress held at Chennai, Jan. 3-7, 1999
- (6) Cost effective utilization of oil palm fibres as reinforcement in composite materials: Surface modifications and mechanical performance, M. S. Sreekala, M. G. Kumaran & Sabu Thomas.
International Conference on Polymers, 'POLYMERS 99', held at New Delhi, Jan. 1999, P.564
- (7) Impact properties and fractography of surface modified oil palm fibre reinforced phenol formaldehyde composites, M. S. Sreekala, M. G. Kumaran & Sabu Thomas.
National symposium on advances in polymer technology, APT '98, held at Cochin University of Science and Technology, Kochi, March 27-28, 1998, P.18
- (8) Cost effective composite materials from Oil Palm fibre and Phenol Formaldehyde resin, M. S. Sreekala, M. G. Kumaran & Sabu Thomas.
Proceedings of the IUPAC International symposium on Advances in Polymer Science and Technology, held at CLRI, Chennai, Jan 5-9, 1998, P.724
- (9) Short Oil Palm Empty Fruit Bunch fibre : A potential reinforcement in Phenol Formaldehyde resin, M. S. Sreekala.
Proceedings of the Xth Kerala Science Congress held at Kozhikode, Jan. 2-4, 1998, P.430
- (10) Mechanical properties of short oil palm empty fruit bunch fibre reinforced phenol formaldehyde composites, M. S. Sreekala, Sabu Thomas & N. R. Neelakantan.
Proceedings of the International Conference on Fibre Reinforced Structural Plastics in Civil Engineering, IIT Madras, Tata Mc Graw Hill Publishers, Dec. 18-20, 1995, P.53

UTILIZATION OF SHORT OIL PALM EMPTY FRUIT BUNCH FIBER (OPEFB) AS A REINFORCEMENT IN PHENOL-FORMALDEHYDE RESINS: STUDIES ON MECHANICAL PROPERTIES

M.S. Sreekala and Sabu Thomas*

*School of Chemical Sciences, Mahatma Gandhi University
Priyadarshini Hills P.O., Kottayam-686 560, Kerala, India*

N.R. Neelakantan

Indian Institute of Technology, Madras, India

ABSTRACT

The brittle thermosetting plastic, phenol-formaldehyde, was reinforced with oil palm empty fruit bunch fiber. Composites were prepared from resol type phenol-formaldehyde resin. Hand lay up technique followed by compression molding was used for composite preparation. Fiber lengths of 20, 30, 40 and 50 mm were used for composite fabrication. The effect of fiber length and fiber loading on the mechanical properties was studied. Tensile, flexural and impact properties of the composites were analyzed. The experimental results are compared with the theoretical predictions. Scanning electron micrographs of the fracture surfaces were taken to analyze the fiber-matrix adhesion, fiber pull-out and fiber surface topography. Finally, the properties of the composites were compared to those of other natural fiber filled PF composites.

*To whom all correspondence should be addressed.

INTRODUCTION

Natural fiber reinforced thermoset composites have received considerable attention, as they demonstrate good mechanical properties, dimensional stability and remarkable environmental and economical advantages. Natural fibers are characterized by non-toxicity, light weight, and high modulus. They are one of the major renewable resource materials in the tropics. The full commercial potential of natural fibers as a reinforcement in plastics has not been achieved due to lack of research and development of high technology applications. Satyanarayana *et al.* reviewed the potential of natural fibers as a resource for industrial materials /1,2/. Several studies have been reported on natural fiber reinforced thermoset composites especially in phenolic, epoxy and polyester matrices /3-12/.

The addition of cellulosic fillers in polymers would considerably reduce material costs while retaining the stiffness and weight efficiency. Woodhams *et al.* /13/ reported that wood pulp is a cost effective reinforcement in polypropylene in terms of bending stiffness. Raj *et al.* /14/ used wood fiber as a filler in polyethylene. They have reported increase in tensile strength of the composites upon the addition of fibers.

Oil palm (*Elaeis Guineensis*) originated in the tropical forests of West Africa. It has now become a major cash crop and is cultivated commercially in Malaysia, India, etc. Empty fruit bunch fiber is one of the fillers obtained from oil palm. It represents a very abundant, inexpensive, renewable resource. Many million tons of empty fruit bunch on dry weight basis are produced annually throughout the world. This is an industrial waste which is left unutilized after the removal of the oil seeds for oil extraction. This creates a good habitat for insects, pests and rodents, thereby causing severe environmental problems. To date no commercial utilization of this empty fruit bunch has been reported. Therefore the utilization of this fiber as a reinforcement in plastics has economical as well as ecological importance.

Among various natural fibers, OPEFB fiber shows excellent mechanical properties and becomes a cost effective replacement for synthetic fibers. The processing of this fiber is comparatively easier than that of other natural

fibers. It is processed by retting technique. OPEFB fiber can act as a better reinforcement in brittle plastics such as phenol-formaldehyde since it can improve the toughness of brittle plastics. The use of cellulosic materials as reinforcement in phenolics is well established and has resulted in composites having decreased shrinkage (buckling) and reduced thermal stress during curing /15/. Cox /16/ studied the shrinkage and buckling in three dimensional composites. Reinforcement using OPEFB fiber makes the composite light weight and inexpensive with desirable mechanical properties and performance characteristics. Wood based composite materials like particle boards, wafer boards, plywoods, etc., play an important role in structural engineering where cost considerations outweigh strength requirements. Recently, Thomas and coworkers have reported on the use of various natural cellulosic fibers (sisal, coir, pineapple, banana) in thermoplastics, thermosets and rubbers /17-23/. OPEFB fiber reinforced phenol formaldehyde composite will be a cost effective substitute for the conventional building materials. It may find application for the fabrication of speciality tiles, doors, windows, roofings, etc.

In this paper we report on the mechanical characteristics of the OPEFB fiber and its composites with PF resin. Mechanical properties such as tensile strength, tensile modulus, elongation at break, flexural strength, flexural modulus and impact properties were evaluated. The effects of fiber length and fiber loading on the properties have been analyzed.

EXPERIMENTAL

Oil palm empty fruit bunch was supplied by Oil Palm India Ltd., Kottayam, India. Phenolformaldehyde resin (resol type) was procured from West Coast Polymers Pvt. Ltd. Solid content of the resin is $50 \pm 1\%$. Caustic soda was the catalyst used during the manufacture.

Hand lay up technique followed by compression molding was adopted for the composite preparation. At first fiber was processed from the empty fruit bunch by the retting process. The pithy materials were removed, washed and

dried at 60°C. It was chopped into 20, 30, 40 and 50 mm lengths. Fiber mat was prepared by hand lay up method. This was then impregnated in liquid resin. The prepreg thus prepared was kept at room temperature till the resin became non-sticky. This pre-condensation time enhances the bonding between fiber and matrix. The precured mat was then hot cured at 100°C for about 30 min in a closed mold. After curing, the mold was allowed to cool in order to release the residual stress. The cured composites were trimmed and cut into the required size. Tensile property tests were carried out according to ASTM D638-76. A 3 point flexure test was used for flexural property analysis. The samples were cut with a dimension of 120 mm length, 12 mm breadth and 2.5 mm thickness.

The mechanical properties of the composites were investigated at room temperature using a Zwick 1461 Universal Testing Machine at a strain rate of 5 mm per minute for tensile and 4 mm per minute for flexural tests. Gauge lengths of 73 mm for tensile and 80 mm for flexural tests were used. Impact testing was done following the Charpy impact test method. The fracture surfaces of the composites and fiber surfaces were examined by scanning electron microscope (Philips Model PSEM-500).

RESULTS AND DISCUSSION

1. Properties in Tension

Tensile strength of the composites gives a measure of the ability of a material to withstand forces that tend to pull it apart and this determines to what extent the material stretches before breaking. Tensile modulus, an indication of the relative stiffness of a material, can be determined from the stress-strain diagram. Pukanszky /24/ investigated the mechanism of adhesion on the ultimate tensile properties of polymer composites and proposed a model for its description. Many scientists studied the effect of fiber/resin adhesion on the tensile properties of polymer composites /25-28/. The interface interaction depends on the aspect ratio, size of the interface,

strength of the interaction, filler anisotropy, orientation, aggregation, etc. Single fiber pullout tests and scanning electron microscopy can be used to characterize the fiber-matrix interface /29-32/.

1.1. Tensile behavior of OPEFB fiber

Table 1 shows tensile properties of OPEFB fiber and some important natural fibers /33/. Compared to other natural fibers OPEFB fiber shows very good elongation. Properties of lignocellulosic fibers depend on the cellulose content and microfibril angle. McLaughlin and Tait /34/ observed that there

Table 1
Mechanical properties of some important natural fibers.

Fiber	Strength (MN/m ²)	Elongation (%)	Toughness (MN/m ²)
Oil palm empty fruit bunch fiber	77	10	1250
Sisal	580	4.3	1250
Pineapple	640	2.4	970
Banana	540	3.0	816
Coir	140	25.0	3200

Source: Reference 33.

is increase in Young's modulus and tensile strength of cellulose based fibers with decreasing microfibril angle and increasing cellulose content. Stress-strain behavior of the fiber is shown in Figure 1. At the very beginning there is linearity and thereafter a curvature is observed. As the applied stress increases, the weak primary cell wall collapses and decohesion of cells occurs, resulting in the mechanical failure of the fiber. The fiber is composed of mainly cellulose and lignin. Lignin, "nature's glue", exists as a three dimensional network binding together the fibrils. The high elongation

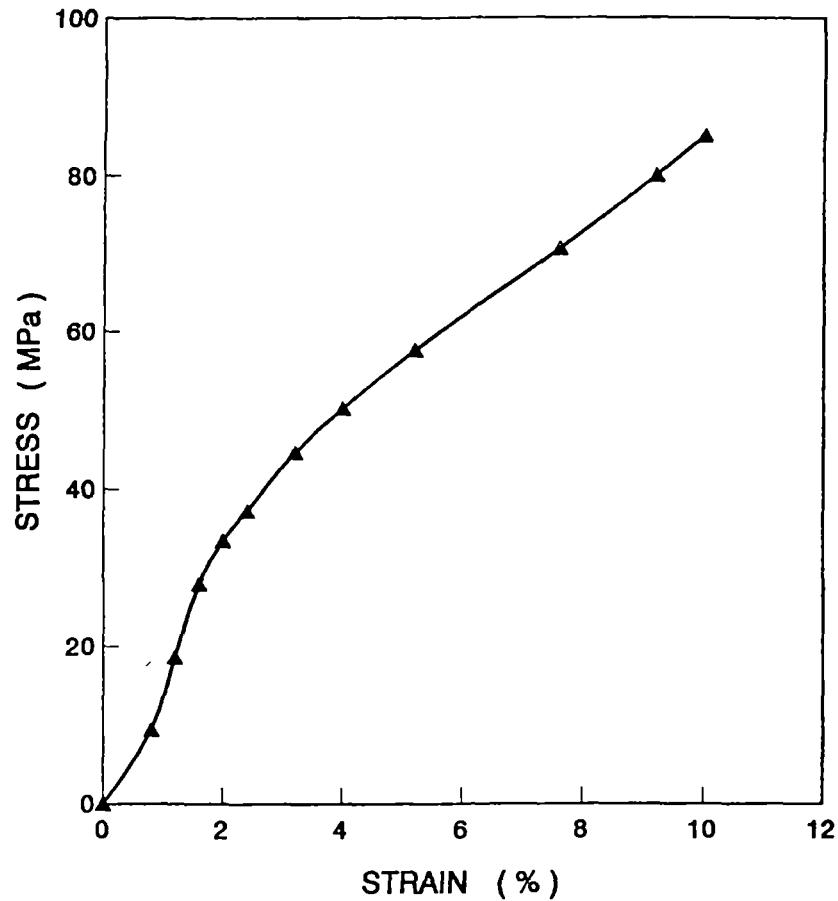


Fig. 1: Stress-strain characteristics of oil palm empty fruit bunch (OPEFB) fiber on application of tensile stress.

of the fiber observed may be due to this firmly bound chemical structure. The morphology of the fiber surface and cross section are as shown in Figure 2a and b respectively. The fiber shows micro pores on its surface. The porous surface would help to create strong mechanical interlocking at the interface. The fiber cross-section shows a lacuna like portion in the middle (Figure 2b).

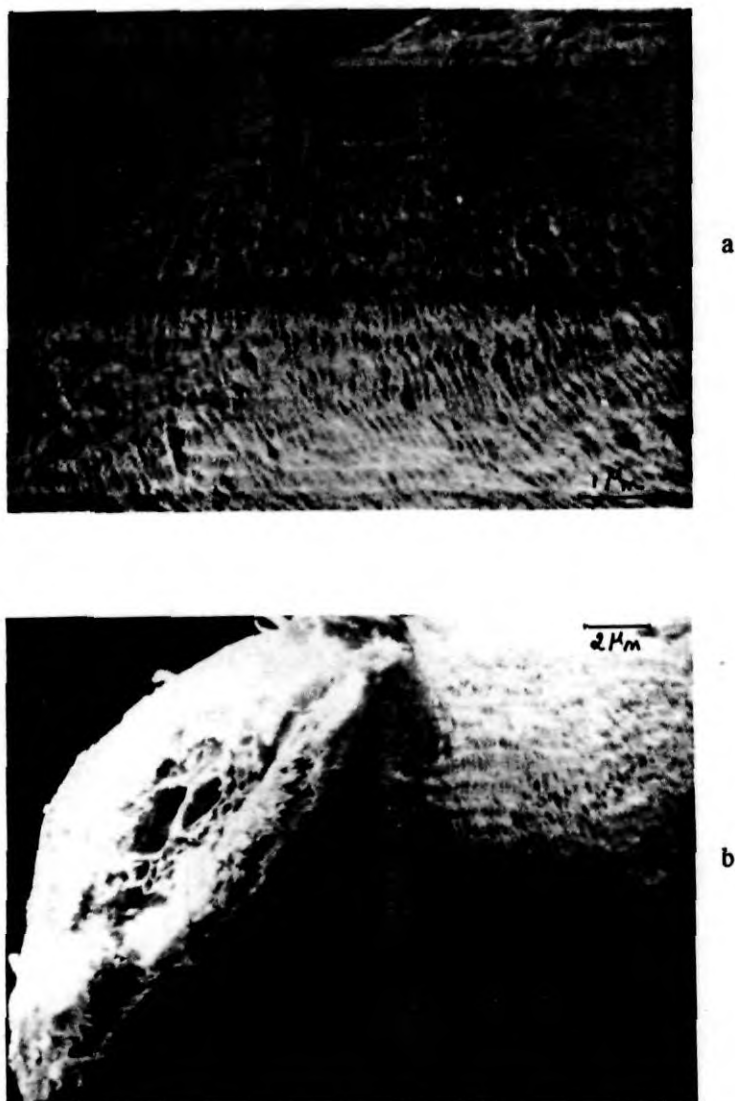


Fig. 2: Scanning electron micrographs of untreated OPEFB fiber: (a) fiber surface (x 400), (b) fiber surface showing cross section (x 200).

1.2. Tensile behavior of OPEFB fiber/PF composites**1.2.1. Effect of fiber length**

Stress-strain behavior of the composites for different fiber lengths on application of tensile stress is shown in Figure 3. The stress-strain curve of the neat sample shows a brittle nature. In the case of composites, at first there is a linear deformation and thereafter a nonlinear behavior is observed. This

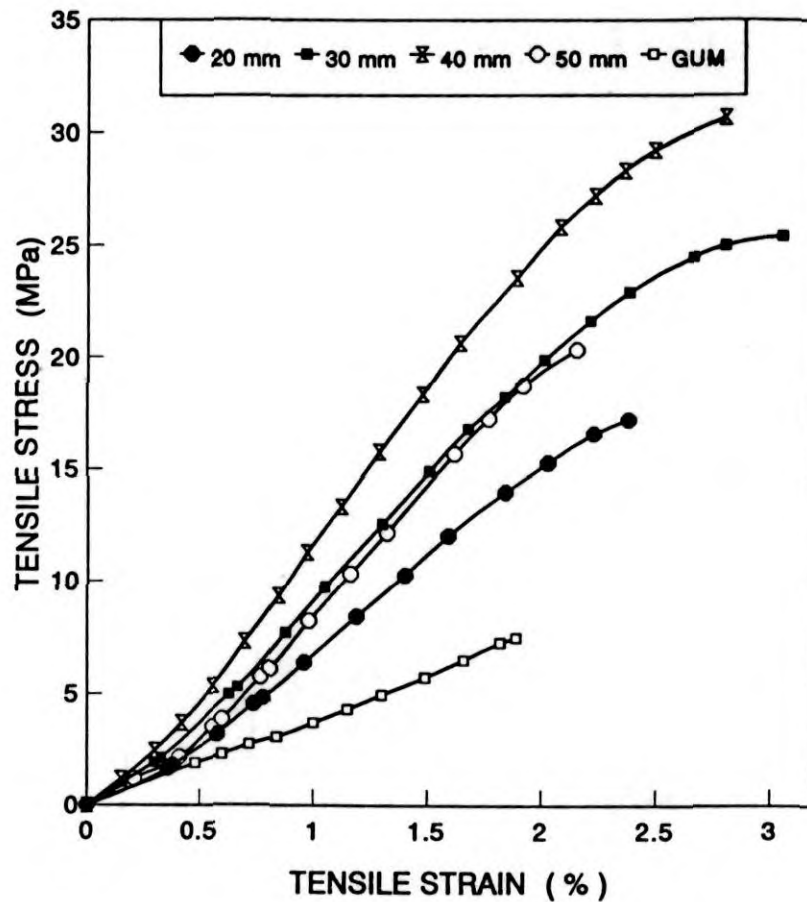


Fig. 3: Stress-strain characteristics of OPEFB fiber/PF composites on application of tensile stress under various fiber lengths. [Fiber loading 38 wt%.]

deviation from linearity accounts for the decreased brittleness of the composite. The effective Young's modulus and yield stress of the composites were found to increase with increase in fiber length up to 40 mm. The effect of fiber length on the tensile strength and tensile modulus is sketched in Figure 4. The tensile strength and the Young's modulus show maxima at a fiber length of 40 mm. As compared to neat PF sample an increase of 190%

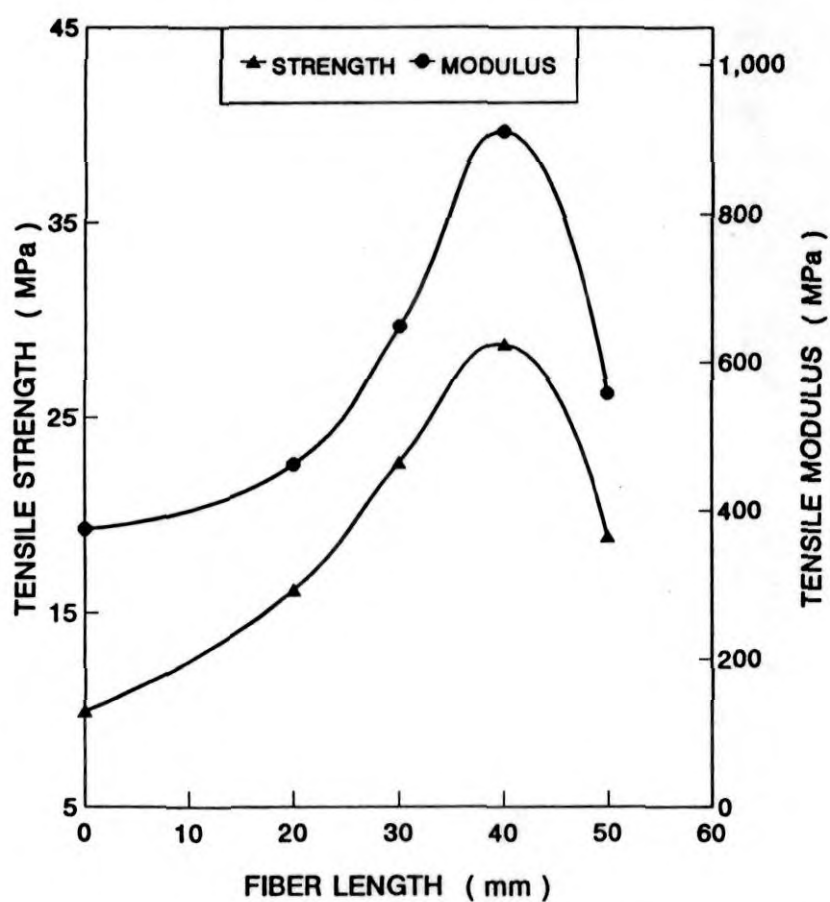


Fig. 4: Variation of tensile strength and tensile modulus of OPEFB fiber/PF composites with fiber length. [Fiber loading 38 wt%.]

in tensile strength and 140% in tensile modulus is observed for 40 mm fiber length. When the length of the fiber is far greater than diameter, the modulus of the composite approaches the limiting value. Thus at the critical fiber length the fiber is in its fully stressed condition in the matrix. At lengths higher than the critical fiber length, the effective stress transfer is not possible due to the entanglement. The concept of critical fiber length and effect of fiber length on the properties of short fiber reinforced polymer composites were reported earlier [35,36].

There is a dramatic increase in the percentage elongation of the phenol-formaldehyde resin by OPEFB fiber reinforcement. This may be due to the higher intrinsic elongation properties of the fiber. Change in percentage elongation at break with respect to fiber length is shown in Figure 5.

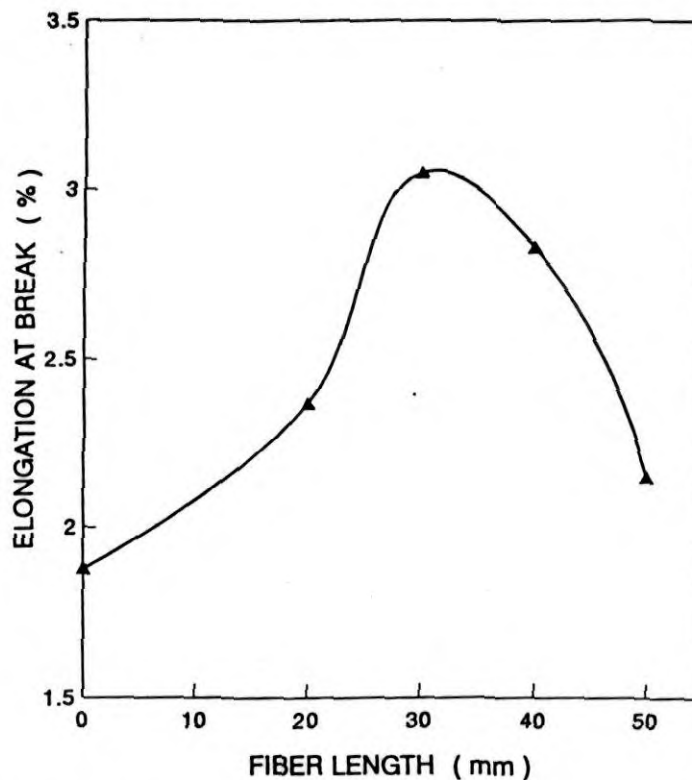


Fig. 5: Effect of fiber length on the percentage elongation at break of OPEFB fiber/PF composites. [Fiber loading 38 wt%.]

Maximum value of elongation at break is observed for composite prepared from 30 mm fiber length. The extent of deformation of fiber in a composite is dependent on fiber length because of the difference in stress distribution within the fiber. The fiber elongation may become fully effective only at 30 mm length. Above this length composite failure may occur due to other factors without full elongation of the fiber.

1.2.2. Effect of fiber loading

Stress-strain behavior of the composites for different fiber loadings on application of tensile stress is shown in Figure 6. The neat PF shows brittle

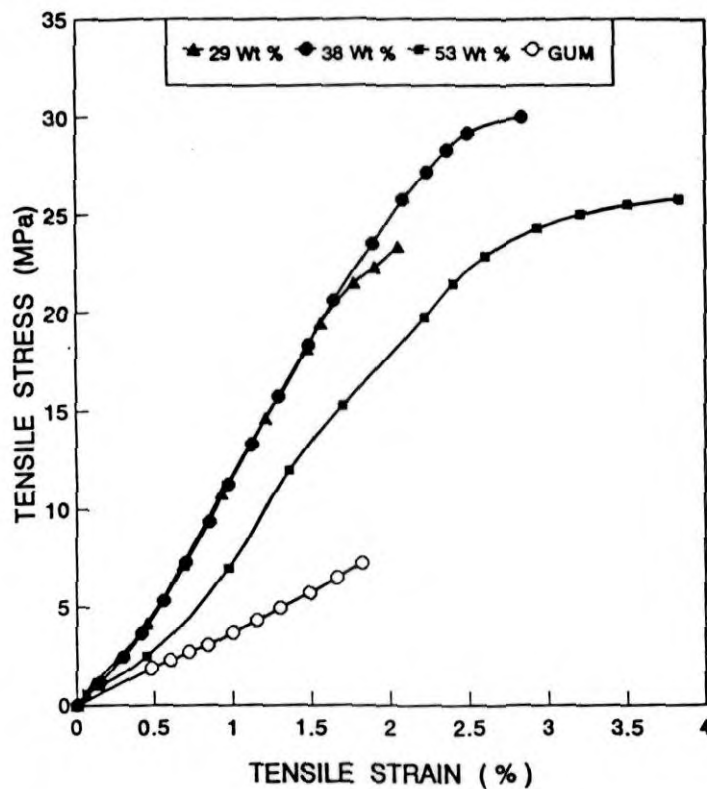


Fig. 6: Stress-strain characteristics of OPEFB fiber/PF composites on application of tensile stress under various fiber loadings. [Fiber length 40 mm.]

behavior. As the fiber content increases so does the toughness of the sample. The Young's modulus and yield stress of the composites show peak values at fiber loading 38 wt%. Chow /37/ studied the stress-strain behavior of polymer composites as a function of filler concentration, strain rate and temperature.

The dependence of tensile strength and tensile modulus on fiber loading is represented in Figure 7. Both tensile strength and modulus increase

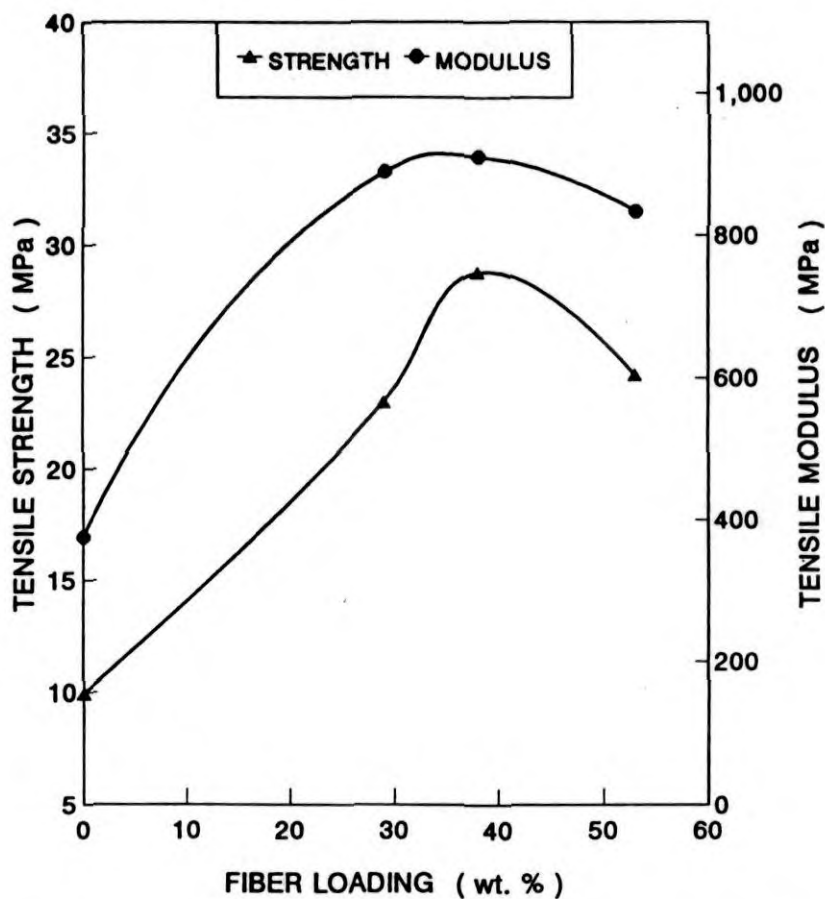


Fig. 7: Variation of tensile strength and tensile modulus of OPEFB fiber/PF composites with percentage of fiber by weight. [Fiber length 40 mm.]

linearly up to 38 wt% of fiber followed by a decrease at higher fiber loading. The decrease at higher fiber loading can be explained as follows: At higher fiber loading there is a chance of phase separation and agglomeration of fibers, thereby reducing the effective aspect ratio. Crack initiation and its propagation will be easier at higher loadings. Fiber-fiber contact increases at higher loadings, which decreases the fiber-matrix adhesion.

The effect of fiber loading on the percentage elongation at break is shown in Figure 8. Elongation at break increases with increase in fiber loading.

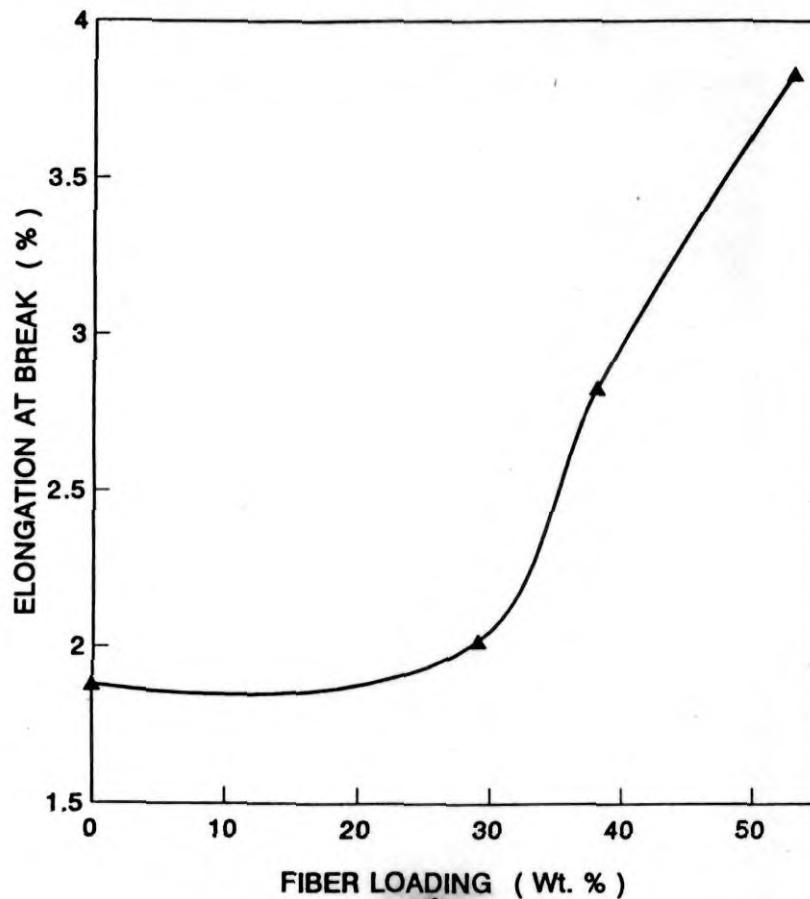


Fig. 8: Effect of fiber loading on the percentage elongation at break of OPEFB fiber/PF composites. [Fiber length 40 mm.]

1.2.3. Fractography of tensile fracture surfaces

Figure 9 shows the scanning electron micrograph of tensile fracture surface of the neat PF resin. Figures 10a and 10b give the fractographs of the tensile fracture surfaces of the composite having a fiber content of 38 wt% and fiber length of 40 mm. The fracture paths observed in different planes indicate the brittle nature of the neat PF resin (Figure 9). Many holes are visible on the



Fig. 9: Scanning electron micrograph of tensile fracture surface of neat phenol-formaldehyde sample (x 800).

tensile fracture surface of composite, resulting from fiber pullout (Figure 10). Fiber breakage is also observed. Figure 10a clearly explains the debonding of fiber from the matrix and matrix failure. Under high tensile stresses debonding occurs due to the bonding failure, and the debonded sites facilitate the crack growth. The fiber pullout and resin fractures can be visualized from the fracture surfaces. At fiber failure, stress at each of its broken ends becomes zero and maximum at the central portion of the fiber. Stress is concentrated in the matrix near the fiber ends. Initiation of a microcrack in the matrix is due to high stress concentration. Opening of the

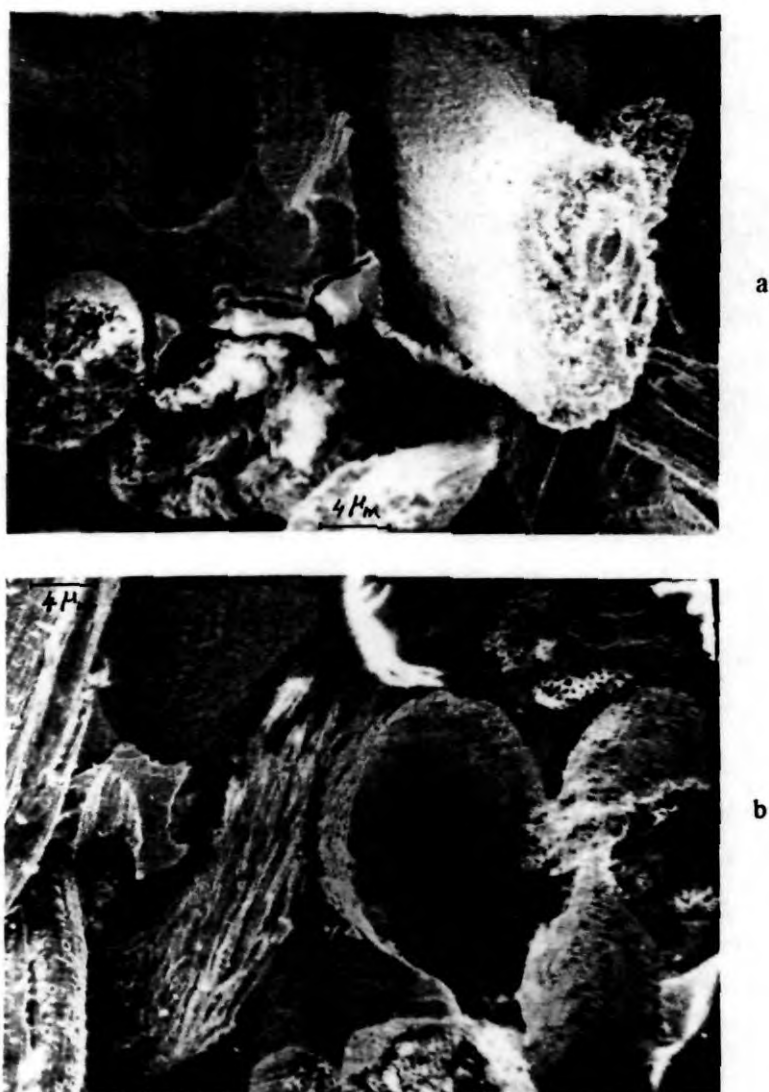


Fig. 10a, b: Scanning electron micrographs of tensile fracture surfaces of OPEFB fiber/PF composites (x 100).

matrix crack may cause broken fibers to pull out from the surrounding matrix. Gent *et al.* /38/ reported the possibilities of either pullout or resin cracking which can take place upon tensile failure. A splitting test method was proposed by Tschegg *et al.* /39/ to characterize the crack growth.

2. Properties in Flexure

Flexural strength is the ability of the material to withstand bending forces applied perpendicular to its longitudinal axis. The flexural modulus is a measure of the stiffness during the first or initial part of the bending process. Flexural stress is a combination of compression and tension. It can be said that interfacial adhesion is more effective in compression loading than tensile. The high values of flexural properties indicate the strong interfacial adhesion. On application of the flexural stress the composite did not break, proving the excellent physical and chemical interlocking between the fiber and matrix.

2.1. Effect of fiber length

The stress-strain behavior of OPEFB fiber reinforced PF composites for different fiber lengths on application of flexural stress is shown in Figure 11. The difference in stress-strain characteristics of the composites, on application of tensile and flexural stress, implies that the type of stress applied to a system plays an important role in nonlinear deformations. In the case of neat PF, the stress-strain curve is similar to that of brittle materials. Addition of fibers increases the ductility of the sample.

The variation of flexural strength and flexural modulus as a function of fiber length is sketched in Figure 12. Both flexural strength and flexural modulus show maxima at 40 mm fiber length followed by a decrease at higher fiber length.

2.2. Effect of fiber loading

The effect of fiber loading on the stress-strain characteristics of the composites on application of flexural stress is shown in Figure 13. The flexural stress-strain curve for the neat sample indicates low stiffness value and brittle nature. The yield stress for gum sample is very low compared to composites. The influence of fiber loading on the flexural strength and flexural modulus of the composites is given in Figure 14. Composites pre-

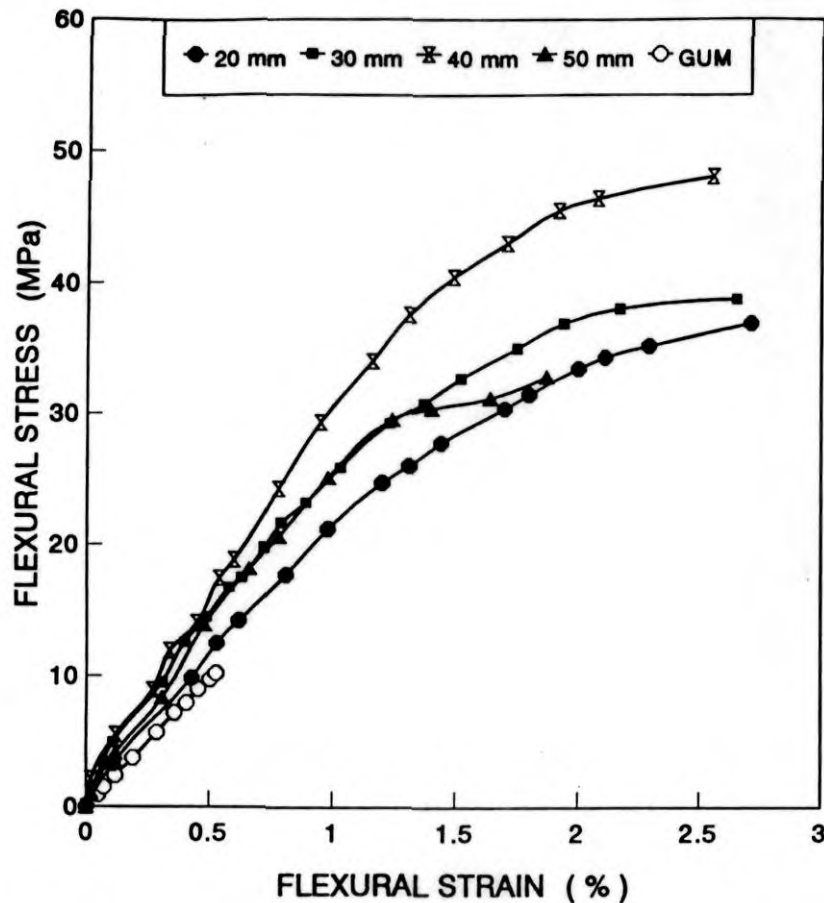


Fig. 11: Stress-strain characteristics of OPEFB fiber/PF composites on application of flexural stress under various fiber lengths. {Fiber loading 38 wt%.}

pared from fiber loading of 38 wt% exhibit maximum flexural strength and flexural modulus.

Owolabi *et al.* reported an enhancement of the tensile and flexural strength of phenol formaldehyde resin by coconut hair reinforcement /8/. The strength properties of particle boards made from OPEFB fiber and urea formaldehyde resin have been investigated by Yamani *et al.* /40/. They found that properties increase linearly with an increase in board density.

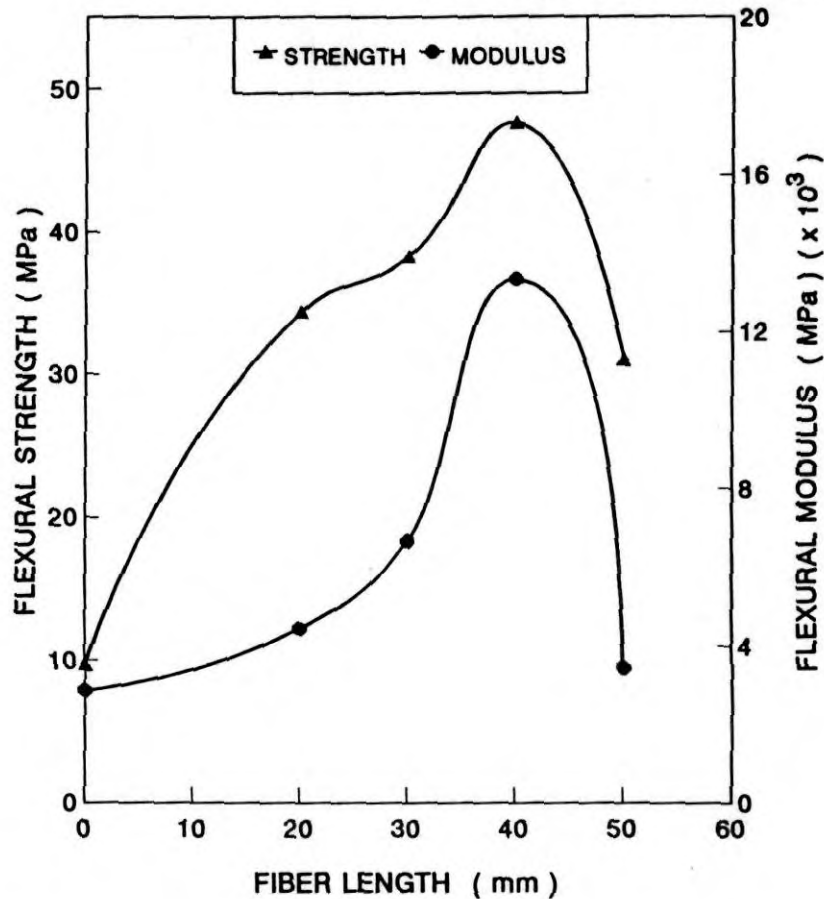


Fig. 12: Variation of flexural strength and flexural modulus of OPEFB fiber/PF composites with fiber length. [Fiber loading 38 wt%.]

3. Impact behavior

The fracture toughness of composite is perhaps its most characteristic property. It is manifested in impact tests. The toughness of a fiber composite is mainly dependent on the fiber stress-strain behavior. Fibers with excellent mechanical properties impart high work of fracture /9/. Impact behavior is a measure of the energy required to cause damage and the progress of failure within the composite. Cantwell *et al.* /41/ reviewed the impact resistance of

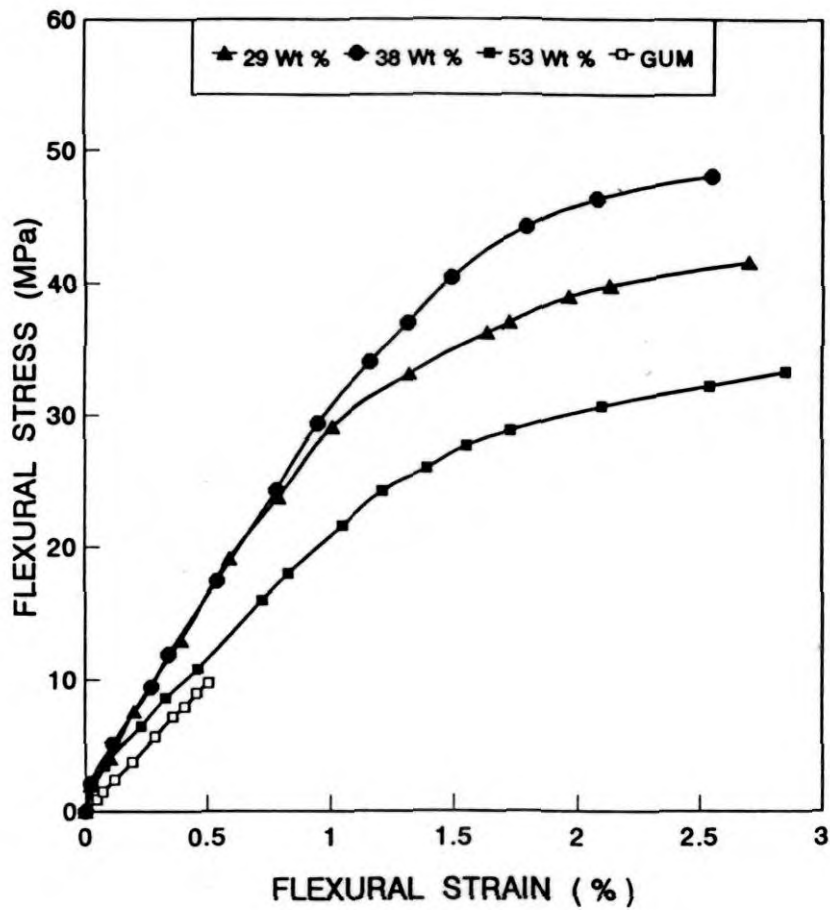


Fig. 13: Stress-strain characteristics of OPEFB fiber/PF composites on application of flexural stress under various fiber loadings. [Fiber length 40 mm.]

composite materials. Impact performance of carbon fiber reinforced epoxy composites was studied by Adams *et al.* /42/. The influence of the reinforcing fiber in determining impact response and its failure mechanisms were investigated by Curson *et al.* /43/.

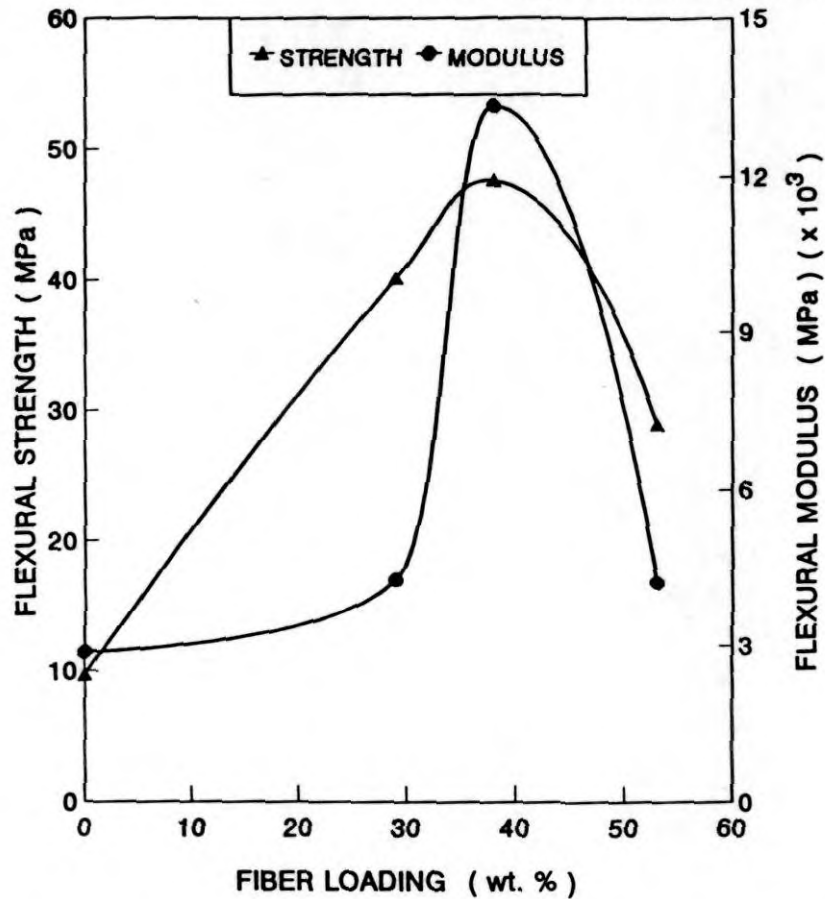


Fig. 14: Variation of flexural strength and flexural modulus of OPEFB fiber/PF composites with percentage of fiber by weight. [Fiber length 40 mm.]

3.1. Effect of fiber length

Figure 15 shows a linear increase in impact strength with fiber length keeping the fiber loading constant. This can be attributed to the weaker interfacial bond formed as the fiber length is increased to higher values. Since the interfacial bond is weak, debonding occurs and extra energy is needed to do the work of debonding. Greater force is required to propagate a

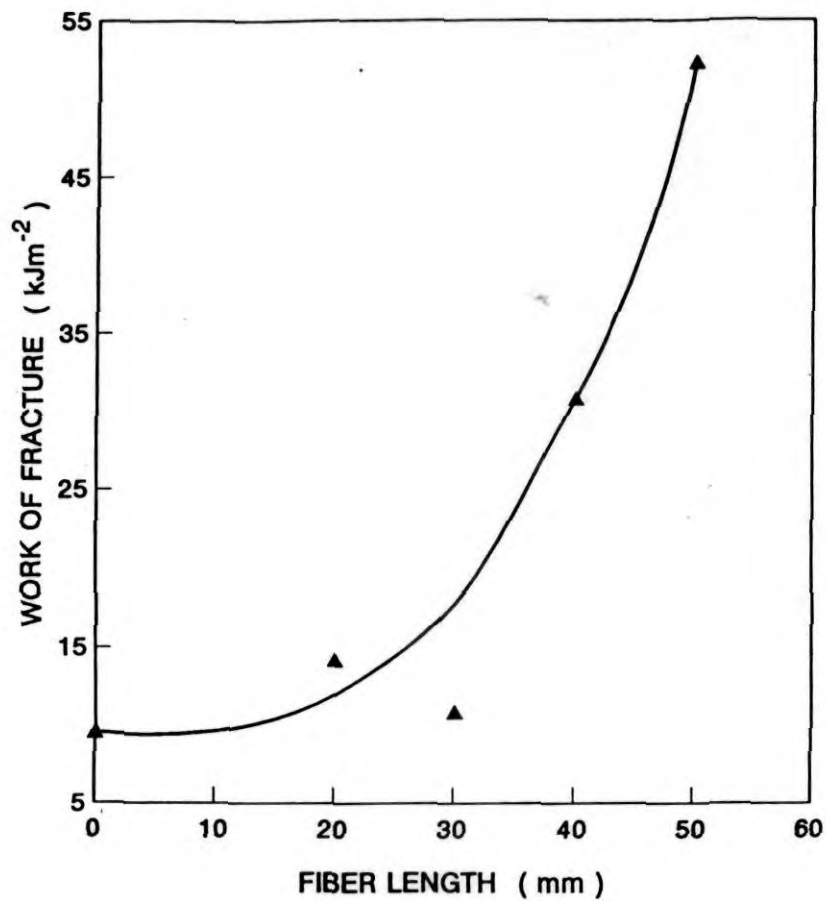


Fig. 15: Variation of work of fracture of OPEFB fiber/PF composites with fiber length. [Fiber loading 38 wt%.]

crack through the interface during impact. Upon impact loading, fiber fracture may occur and the broken ends of the fiber have to be pulled out as the fracture proceeds, which requires additional energy.

3.2. Fractography of impact fracture surfaces

Scanning electron micrographs of impact fracture surfaces of neat PF and that of composite sample are shown in Figures 16 and 17a, b, respectively.

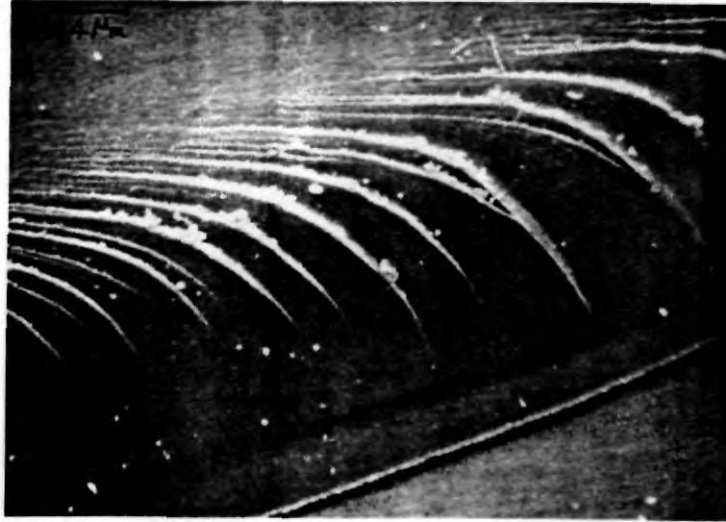


Fig. 16: Scanning electron micrographs of impact fracture surface of neat phenol-formaldehyde sample (x 100).

The brittle failure of the neat sample is evident from the fracture lines in different planes (Figure 16). The fracture surface of the composite sample shows fiber breakage and pullout (Figures 17a, b). The failure of the composite is mainly due to fiber breakage and matrix cracking. Figure 17a in fact gives typical fiber breakage and matrix failure. After fiber breakage, crack is propagated very fast, leading to complete failure of the composite. Matrix failure is comparable to that of the neat PF sample.

THEORETICAL MODELING

Modulus is a bulk property which depends primarily on geometry, particle size distribution and concentration of the filler. But tensile strength of a composite depends strongly on local polymer filler interactions as well as the above factors. The filler particle geometry has a significant influence on the strength of a filled polymer. Impact strength of the composite depends on the degree of fiber-matrix adhesion and is very complex. The microscale

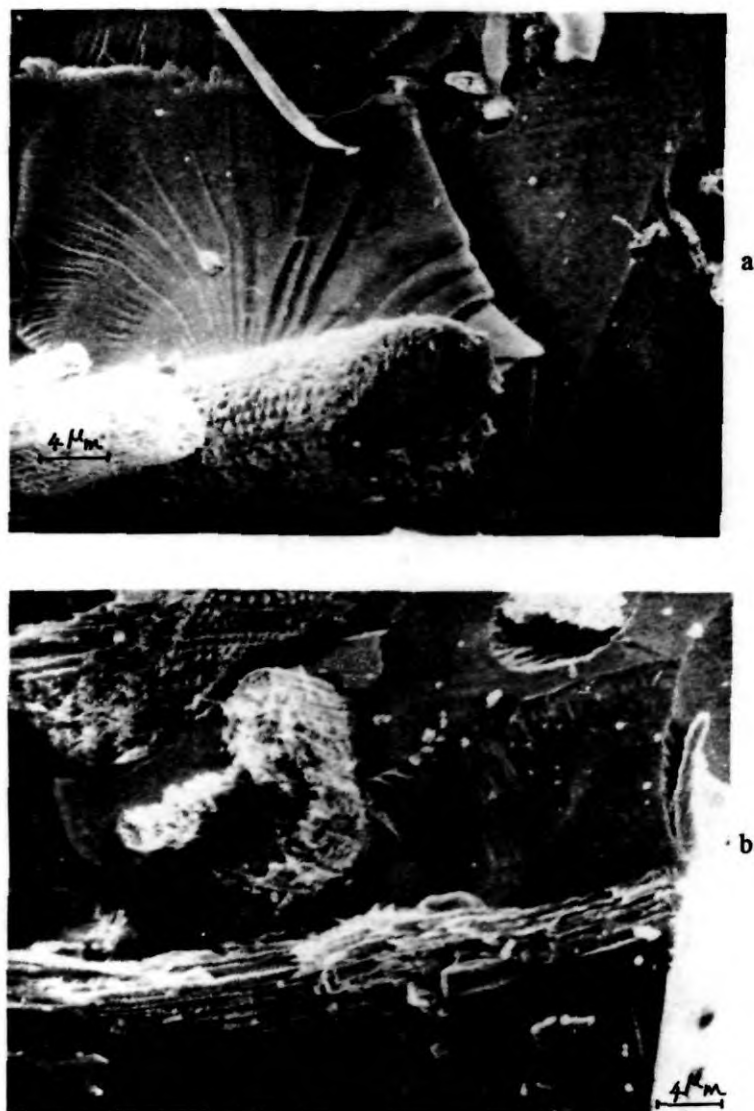


Fig. 17a, b: Scanning electron micrographs of impact fracture surfaces of OPEFB fiber/PF composites (x 100).

morphological changes in the matrix caused by the fiber affect the impact strength of composites. There are no viable theoretical relationships that can be used to predict the impact strength of composites.

The parallel model and Hirsch model are tried to predict tensile strength of the composites. Following are the equations used for calculating the tensile strength of the composites.

Parallel model

According to this model

$$T_c = T_f V_f + T_m V_m \quad (1)$$

where T_c = composite strength, T_f = fiber strength, T_m = matrix strength, V_f = volume fraction of fibers, V_m = volume fraction of matrix.

In this equation T_f is given by

$$T_f = \frac{l_c \tau}{r} \quad (2)$$

But $l = l_c$

where τ = interfacial shear strength, r = radius, l_c = critical fiber length.

$$\tau = \frac{l \sigma_f}{2 l_c} \quad (3)$$

where σ_f = fiber stress.

Hirsch model

This model is a combination of series and parallel models. According to this model

$$T_c = (T_m V_m + T_f V_f) + (1-x) \left[\frac{T_f T_m}{T_m V_f + T_f V_m} \right] \quad (4)$$

where x = a parameter which varies between 0 and 1.

The experimental and theoretical values of tensile strength of the composite as a function of fiber loading are given in Figure 18. The experimental values are very close to Hirsch model up to 38% fiber loading. The experimental values show a negative deviation at higher fiber loadings. This is due to the fact that the theoretical models imply an absolute matrix-

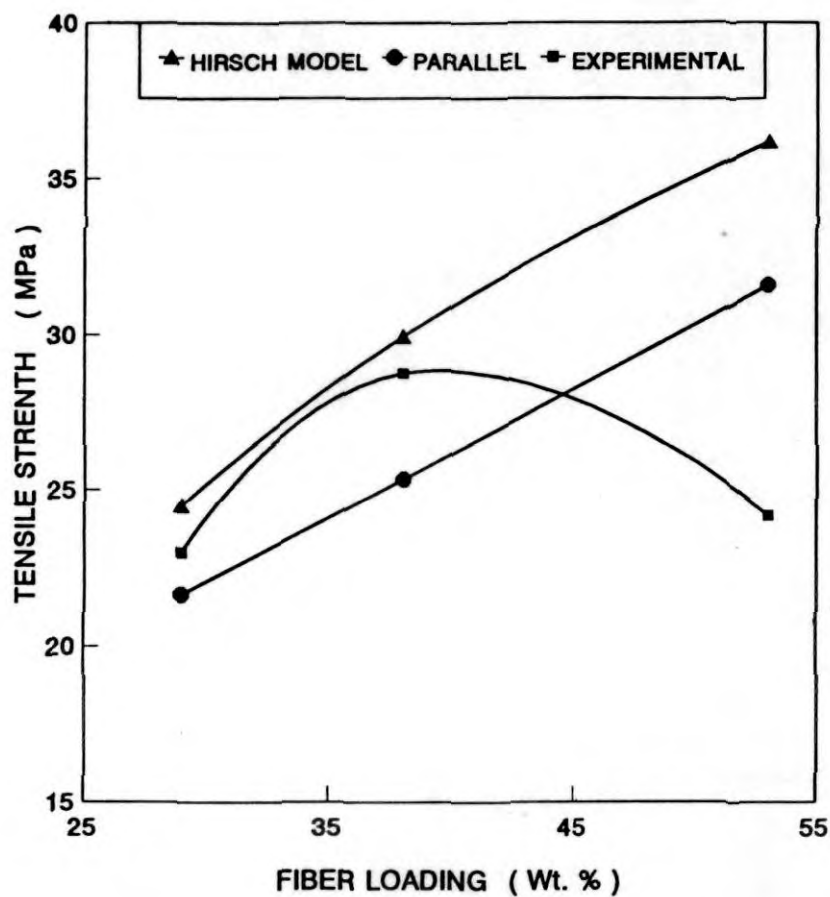


Fig. 18: Comparison of theoretically predicted strength values of composites with experimental values as a function of fiber loading.

to-filler adhesion and uniform filler distribution in the matrix. However, in the actual case the situation is very different. At low fiber loadings agglomeration does not practically affect the properties. But at higher fiber loadings agglomeration results which decreases the fiber-matrix interaction.

COMPARISON OF THE STRENGTH PROPERTIES OF SHORT OPEFB FIBER/PF COMPOSITES WITH OTHER SHORT NATURAL FIBER REINFORCED PHENOL-FORMALDEHYDE COMPOSITES

Table 2 gives the reported results on the mechanical property analysis of coir fiber reinforced phenol-formaldehyde composites and sisal fiber reinforced phenol-formaldehyde composites. The results show that the impact properties of OPEFB fiber/PF composites are excellent when compared with those of other natural fiber reinforced phenol-formaldehyde composites. Maximum impact strength in the reported work is 19.1 kJm^{-2} for coir fiber reinforcement and 10 kJm^{-2} for sisal fiber reinforcement while OPEFB fiber reinforcement gives a value of 52 kJm^{-2} . In the case of flexural strength, enhancement by OPEFB fiber reinforcement is close to that given by coir fiber reinforcement.

Table 2

Comparison of the strength properties of short OPEFB fiber/PF composites with other short natural fiber reinforced phenol-formaldehyde composites

Composite	Tensile strength (MPa)	Flexural strength (MPa)	Impact strength (kJ/m^2)
OPEFB fiber/PF	28.79	47.61	52.34
Sisal fiber/PF	42	66	10
Coconut fiber/PF	-	53	19.1

Source: References 8 and 44.

CONCLUSION

Utilization of oil palm empty fruit bunch fiber will eliminate the problem of waste disposal and will lead to a new composite product. The mechanical properties of OPEFB fiber were analyzed. It shows very good elongation properties. Tensile, flexural and impact properties of the OPEFB fiber/PF composites were investigated as a function of fiber length and fiber loading. All these mechanical properties showed improvement upon reinforcing with the fiber. The elongation, brittle nature and buckling characteristics of PF resin were considerably improved by incorporating the fiber.

Maximum tensile properties of the composites were observed for 40 mm fiber length and at 38% fiber loading. Flexural behavior also showed a similar trend. There is a possibility of fiber entanglement at higher fiber lengths which may be the reason for the decrease in properties beyond 40 mm fiber length. The impact properties showed linear enhancement with increase in fiber length up to 50 mm. However, for the best balance of mechanical properties, the optimum fiber length and fiber loading are considered to be 40 mm and 38%, respectively.

Scanning electron micrographs of fiber surface, tensile and impact fracture surfaces were taken to study the morphology and failure mechanism.

The experimental values were compared with those theoretically predicted. The Hirsch model closely agreed with the experimental results. At higher fiber loadings the experimental values showed a deviation from the Hirsch model, which may be due to the possible fiber agglomeration.

The mechanical properties of OPEFB fiber/PF composites and other natural fiber reinforced PF composites were compared. Comparison of impact properties with those of sisal and coir fiber reinforcement indicated that OPEFB fiber acts as an efficient reinforcement in PF resin.

Thus OPEFB fiber/PF composites will be a cost effective, value added substitute for the conventional building materials. They can replace the materials where cost considerations and visual performance are important.

Finally, it is important to mention that these composites can act as a better substitute for wood in the building industry.

ACKNOWLEDGEMENT

The authors are grateful to Oil Palm India Ltd. for supplying the oil palm fibers.

REFERENCES

1. K.G. Satyanarayana, A.G. Kulkarni and P.K. Rohatgi, *J. Scient. Ind. Res.*, **40**, 222 (1981).
2. K.G. Satyanarayana, A.G. Kulkarni and P.K. Rohatgi, *J. Scient. Ind. Res.*, **42**, 425 (1983).
3. I.M. Low, P. Schmidt and J. Lane, *J. Mater. Sci. Lett.*, **14**, 170 (1995).
4. E.C. McLaughlin, *J. Mater. Sci.*, **15**, 886 (1980).
5. M.K. Sridhar, G. Basavarappa, S.G. Kasturi and N. Balasubramanian, *Ind. J. Technol.*, **22**, 213 (1984).
6. A.R. Sanadi, S.V. Prasad and P.K. Rohatgi, *J. Mater. Sci.*, **21**, 4299 (1986).
7. G. Freischmidt, A.J. Michell, M.J. Lewis and N. Vanderhock, *Polym. International*, **24**, 113 (1991).
8. O. Owolabi, T. Czvikovszky and I. Kovacs, *J. Appl. Polym. Sci.*, **30**, 1827 (1985).
9. C. Pavithran, P.S. Mukherjee, M. Brahmakumar and A.D. Damodaran, *J. Mater. Sci. Lett.*, **6**, 882 (1987).
10. K.K. Chawla and H.C. Bastos, *Proc. 3rd Inter. Conf. Mech. Behav. Mater.*, Cambridge, **3**, 191 (1979).
11. P.J. Roe and M.P. Ansell, *J. Mater. Sci.*, **20**, 4015 (1985).
12. D.N. Bhattacharya, I.B. Chakravarthy and S.R. Sengupta, *J. Scient. Ind. Res.*, **20D**, 168 (1961).

13. R.T. Woodhams, G. Thomas and D.K. Rodgers, *Polym. Eng. Sci.*, **24** (15), 1166 (1984).
14. R.G. Raj, B.V. Kokta, G. Groleau and C. Daneault, *Plastics and Rubber Processing Applications*, **11**, 215 (1989).
15. P. Zadorecki and A.J. Michell, *Polym. Compos.*, **10**, 69 (1989).
16. B.N. Cox, *J. Comp. Mater.*, **28** (12), 1114 (1994).
17. V.G. Geethamma, R. Joseph and S. Thomas, *J. Appl. Polym. Sci.*, **55**, 583 (1995).
18. J. George, K. Joseph, S.S. Bhagawan and S. Thomas, *Mater. Lett.*, **18**, 163 (1993).
19. S. Varghese, B. Kuriakose, S. Thomas and A.T. Koshy, *Indian J. Nat. Rubber Res.*, **5**(1&2), 18 (1992).
20. S. Varghese, B. Kuriakose and S. Thomas, *J. Appl. Polym. Sci.*, **53**, 1051, (1995).
21. K. Joseph, S. Thomas and C. Pavithran, *Comp. Sci. Technol.*, **53**, 99 (1995).
22. K. Joseph, C. Pavithran and S. Thomas, *Mater. Lett.*, **15**, 224 (1992).
23. L. Uma Devi, M. Phil. Thesis, Mahatma Gandhi University, Kottayam, 1993.
24. B. Pukanszky, *Composites*, **21**, 3 (1990).
25. A.G. Evans, F.W. Zok and J. Davis, *Comp. Sci. Techn.*, **42**, 3 (1991).
26. J. Kalantar and L.T. Drzal, *J. Mater. Sci.*, **25**, 4186 (1990).
27. J.W. Teh and A. Rudin, *J. Polym. Sci. Part C, Polym. Lett.*, **28**, 363 (1990).
28. B. Tissington, G. Pollard and I.M. Ward, *J. Mater. Sci.*, **26**, 82 (1991).
29. E. Mader and K.H. Freitag, *Composites*, **21** (5), 397 (1990).
30. M.J. Pitkethly and J.B. Doble, *Composites*, **21** (5), 389 (1990).
31. C.Y. Cha, J.F. Fellers and A. Mathews, *Adv. Polym. Techn.*, **9** (3), 253 (1989).
32. Jian-Xin Li, *J. Appl. Polym. Sci.*, **53** (2), 225 (1994).
33. P.S. Mukherjee and K.G. Satyanarayana, *J. Mater. Sci.*, **21**, 4162 (1986).

34. E.C. McLaughlin and R.A. Tait, *J. Mater. Sci.*, **15**, 89 (1980).
35. L. Monette, M.P. Anderson and G.S. Grest, *Polym. Compos.*, **14** (2), 101 (1993).
36. S.A. Hitchen, S.L. Ogin, P.A. Smith and C. Soutis, *Composites*, **25** (6), 407 (1994).
37. T.S. Chow, *Polymer*, **32**, 29 (1991).
38. A.N. Gent and Chi Wang, *J. Mater. Sci.*, **28**, 2494 (1993).
39. E.K. Tschegg, K. Humer and H.W. Weber, *J. Mater. Sci.*, **28**, 2471 (1993).
40. S.A.K. Yamani, A.J. Ahmad, J. Kasim, N.M. Nasir and J. Harun, *Proc. of the Int. Symposium on Biocomposites and Blends based on Jute and Allied Fibers*, 1994; p. 135.
41. W.J. Cantwell and J. Morton, *Composites*, **22** (5), 347 (1991).
42. D.F. Adams and L.G. Adams, *J. Comp. Mater.*, **24**, 256 (1990).
43. A.D. Curson, D.C. Leach and D.R. Moore, *J. Thermoplast. Comp. Mater.*, **3**, 24 (1990).
44. K. Joseph, Ph.D. Thesis, Mahatma Gandhi University, Kottayam, 1992.

Oil Palm Fibers: Morphology, Chemical Composition, Surface Modification, and Mechanical Properties

M. S. SREEKALA,¹ M. G. KUMARAN,¹ SABU THOMAS²

¹ Rubber Research Institute of India, Kottayam-686 009, Kerala, India

² School of Chemical Sciences, Mahatma Gandhi University, Priyadarshini Hills P.O., Kottayam-686 560, Kerala, India

Received 3 October 1996; accepted 14 February 1997

ABSTRACT: Oil palm fiber is an important lignocellulosic raw material for the preparation of cost-effective and environment-friendly composite materials. The morphology and properties of these fibers have been analyzed. The properties of two important types of fibers, the oil palm empty fruit bunch fiber and the oil palm mesocarp fiber (fruit fiber) have been described. The surface topology of the fibers has been studied by scanning electron microscopy. Thermogravimetry and differential thermal analysis were used to determine the thermal stability of the fibers. Fiber surface modifications by alkali treatment, acetylation, and silane treatment were tried. The modified surfaces were characterized by infrared spectroscopy and scanning electron microscopy. The chemical constituents of the fibers were estimated according to ASTM standards. Mechanical performance of the fibers was also investigated. Microfibrillar angle of the fibers was theoretically predicted. The theoretical strength of the fibers was also calculated and compared with the experimental results. © 1997 John Wiley & Sons, Inc. *J Appl Polym Sci* 66: 821–835, 1997

Key words: oil palm fibers; surface modification; morphology; IR spectroscopy; thermal analysis; mechanical property

INTRODUCTION

Oil palm is one of the most economical and very-high-potential perennial oil crops. It belongs to the species *Elaeis guineensis* under the family *Palmacea*, and originated in the tropical forests of West Africa. Major industrial cultivation is in Southeast Asian countries such as Malaysia and Indonesia. Large-scale cultivation has come up in Latin America. In India, oil palm cultivation is coming up on a large-scale basis with a view to attaining self sufficiency in oil production.

Oil palm empty fruit bunch (OPEFB) fiber and oil palm mesocarp fiber are two important types of fibrous materials left in the palm-oil mill. Figure 1 shows the photographs of fruit bunch fiber and oil palm mesocarp fiber. OPEFB is obtained after the removal of oil seeds from fruit bunch for oil extraction. Photograph of an empty fruit bunch is shown in Figure 2. OPEFB fiber is extracted by the retting process of the empty fruit bunch. Average yield of OPEFB fiber is about 400 g per bunch. Mesocarp fibers are left as a waste material after the oil extraction. These fibers must be cleaned of oily and dirty materials. The only current uses of this highly cellulosic material are as boiler fuel and in the preparation of potassium fertilizers. When left on the plantation floor, these waste materials create great environmental problems. Therefore, economic utilization of these fibers will be beneficial. This requires

Correspondence to: S. Thomas.

Contract grant sponsor: Council of Scientific and Industrial Research, New Delhi, India.

Journal of Applied Polymer Science, Vol. 66, 821–835 (1997)
© 1997 John Wiley & Sons, Inc. CCC 0021-8995/97/050821-15

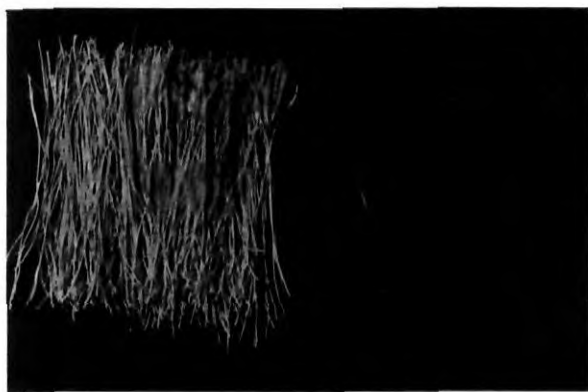


Figure 1 Photograph of (a) oil palm empty fruit bunch fiber and (b) oil palm mesocarp fiber.

extensive study of the chemical and physical characteristics of these fibers.

We have reported earlier about the possibilities of using OPEFB fiber as a potential reinforcement in phenol-formaldehyde resin.¹ The mechanical performance of phenol-formaldehyde resin is greatly improved by the incorporation of these fibers. The resultant composite product will be a cost-effective and value-added substitute for conventional building materials which can act as a better substitute for wood in building industry.

Many of the natural fibers—such as coir, banana, sisal, talipot, palmyrah, jute, pineapple leaf fiber, etc.—find applications as a resource for industrial materials.^{2,3} Properties of the natural fibers depend mainly on the nature of the plant, locality in which it is grown, age of the plant, and the extraction method used. For example, coir is a hard and tough multicellular fiber with a central portion called “lacuna.” On the other hand, banana fiber is weak and cylindrical in shape. Sisal is an important leaf fiber and is strong. Pineapple leaf fiber is soft and has high cellulose content. Investigations based on these fibers are still ongoing. Many studies have reported on the natural fiber based composite products.^{4–6} Oil palm fibers are hard and tough, and show similarity to coir fibers in cellular structure. To date, no systematic work has been undertaken to evaluate the morphology and physical properties of oil palm fibers.

The physical properties of other natural fibers have already been reported.^{7–15} Barkakaty⁷ reported on the structural aspects of sisal fibers. Martinez and colleagues⁸ studied the physical and mechanical properties of the lignocellulosic henequen fibers. Thermal stability and moisture

regain of wood fibers were studied by Rao and Gupta.⁹ They utilized a scanning electron microscope to study the morphological characteristics.

Chemical treatments of cellulosic materials usually change the physical and chemical structure of the fiber surface.¹⁰ Mukherjee and associates¹¹ reported the effect of ethylene diamine on the physicochemical properties of jute fibers. X-ray and infrared (IR) studies can be used to investigate the changes in the fine structure of fiber surface.¹² Effects of alkali, silane coupling agent, and acetylation have been tried on the oil palm fibers. It is reported that the alkali treatment on coir fiber enhances the thermal stability and maximum moisture retention.¹³ Prasad and coworkers¹⁴ reported that the use of alkali-treated coir fibers greatly improves the mechanical properties of coir-polyester composites. Chemical analysis of the oil palm fibers shows that the principal component is cellulose. The cellulose content plays an important role in the fiber's performance. The properties of the particle boards prepared from OPEFB fiber and urea formaldehyde resin have been reported earlier.¹⁵ Many studies have reported on the determination of fiber strength using various techniques.^{16–18}

In this article, we report on the chemical, physical, and morphological characteristics of the oil palm fibers. Surface modifications of the fibers by alkali treatment, silane treatment, and acetylation have been tried. Morphological analysis has been carried out with the help of IR and scanning electron microscopy (SEM) studies. Chemical constituents of the fibers were determined. Mechanical properties such as tensile strength, Young's modulus, and elongation at break were evaluated.



Figure 2 Photograph of an oil palm empty fruit bunch.

Table I Chemical Composition of Oil Palm Fibers and Some Important Natural Fibers

Fiber	Lignin (%)	Cellulose (%)	Hemicellulose (%)	Ash Content (%)
OPEFB fiber	19	65	—	2
Oil palm mesocarp fiber	11	60	—	3
Coir	40–45	32–43	0.15–0.25	—
Banana	5	63–64	19	—
Sisal	10–14	66–72	12	—
Pineapple leaf fiber	12.7	81.5	—	—

Source: ref. 1.

The deformation characteristics of the fibers were studied with the help of stress-strain curves. Thermogravimetric (TGA) and differential thermal analyses (DTA) were carried out to study the thermal stability of the fibers. Microfibrillar angle and strength of the fibers were theoretically calculated.

MATERIALS AND EXPERIMENTAL

The fibers were collected from Oil Palm India Ltd., Kottayam, India. The empty fruit bunch was subjected to retting. Fibers were then cleaned, washed, and dried.

Fiber Surface Modification

Alkali Treatment

Fibers were dipped in 5% sodium hydroxide solution for about 48 h. These were further washed with water containing a few drops of acetic acid. Finally, the fibers were washed again with fresh water and dried.

Silane Treatment

Fibers were dipped in 1% silane solution (triethoxy vinylsilane) in water-ethanol mixture (40 : 60) for about 3 h. The pH of the solution was maintained to 3.5–4. Fibers were washed and then dried.

Acetylation

Fibers were treated in glacial acetic acid for 1 h. This was further treated with acetic anhydride containing concentrated H_2SO_4 as catalyst for 5 min. Fibers were then washed with water and dried.

SEM Examination

The SEM photographs of fiber surfaces and cross sections of untreated and treated fibers were taken using a scanning electron microscope, Philips model PSEM-500.

IR Spectra

KBr disk method was followed in taking IR spectra. The instrument used was a Shimadzu IR-470 infrared spectrophotometer.

Table II Solubility of Oil Palm Fibers in Different Solvents

Chemical Constituent	Oil Palm Empty Fruit Bunch Fiber (%)	Oil Palm Mesocarp Fiber (Fruit Fiber) (%)
Alcohol-benzene solubility	12	12
Ether solubility	12	20
1% caustic soda solubility	20	27
Cold-water solubility	8	12
Hot-water solubility	10	12

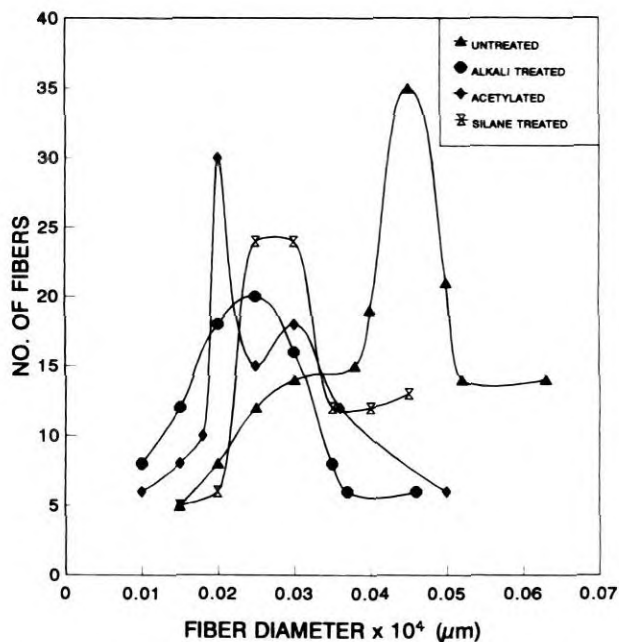


Figure 3 Distribution curve of fiber diameter of untreated and treated OPEFB fibers.

Thermal Analysis

Thermograms of untreated and treated fibers were taken in an inert atmosphere at a heating rate of 10°C/min. A Shimadzu DT-40 thermal analyzer was used for the study.

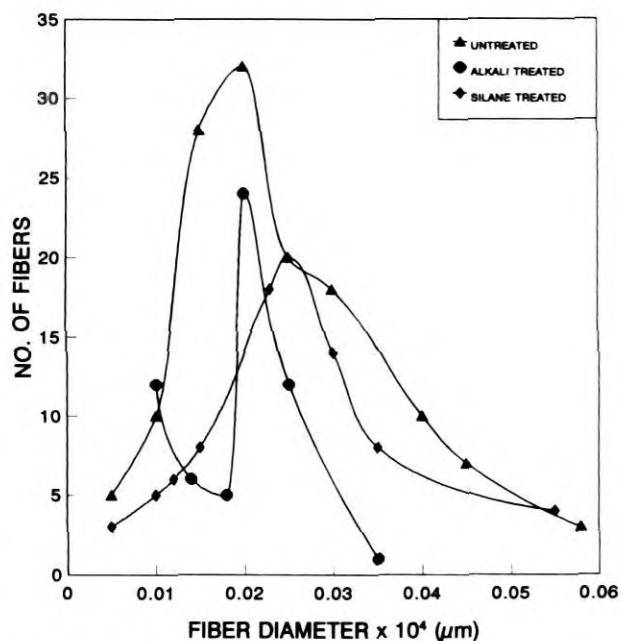
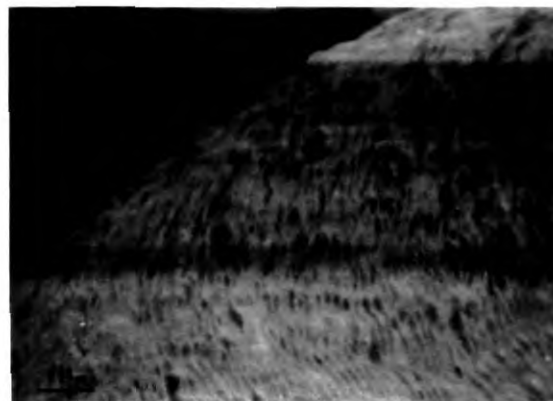
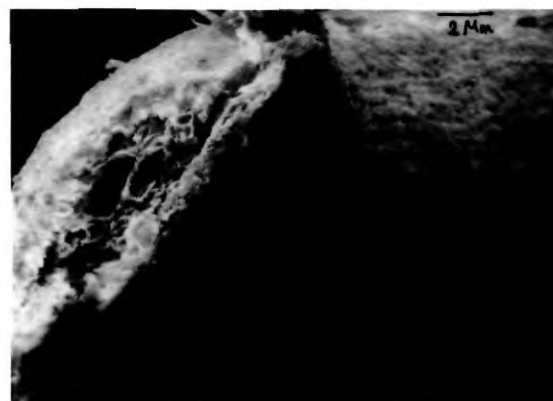


Figure 4 Distribution curve of fiber diameter of untreated and treated oil palm mesocarp fibers.



(a)



(b)

Figure 5 Scanning electron micrographs of untreated OPEFB fiber: (a) fiber surface ($\times 400$) and (b) cross section ($\times 200$).

Chemical Estimation

Chemical compositions of fibers were estimated according to the following ASTM procedures: lig-

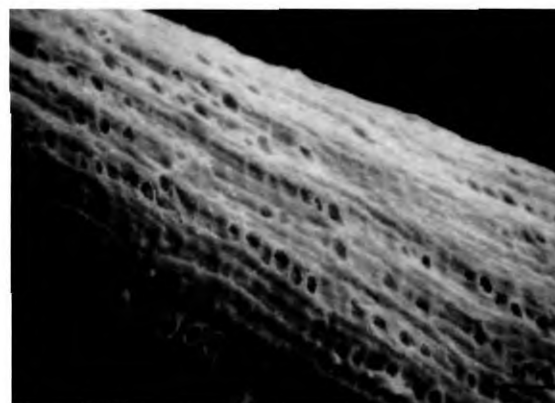


Figure 6 Scanning electron micrograph of alkali-treated OPEFB fiber surface ($\times 400$).

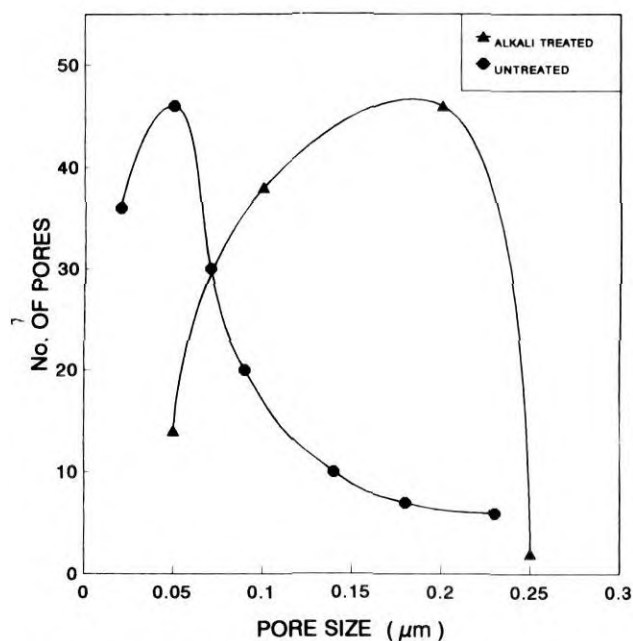


Figure 7 Distribution curve of pore size of the untreated and alkali-treated OPEFB fiber surface.

nin—ASTM D1106; holocellulose—ASTM D1104; ash content—ASTM D1102; alcohol–benzene solubility—ASTM D1107; ether solubility—ASTM D1108; 1% caustic soda solubility—ASTM D1109; and water solubility—ASTM D1110.

Mechanical Property Tests

Strength of the oil palm fibers was determined using a FIE TNE-500 electronic tensile testing machine. The fibers were mounted in a fixture made of paperboard with a central window and

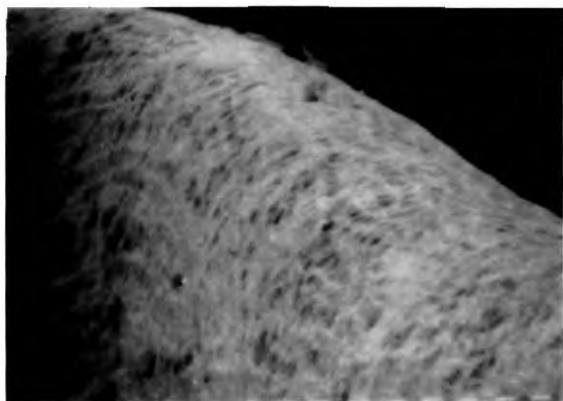


Figure 8 Scanning electron micrograph of silane-treated OPEFB fiber surface (×400).

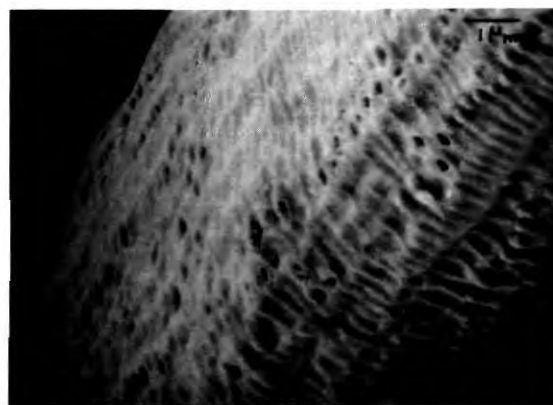


Figure 9 Scanning electron micrograph of acetylated OPEFB fiber surface (×400).

pulled at a strain rate of 20 mm/min. The gauge length was 50 mm and 20 mm in the case of OPEFB fiber and oil palm mesocarp fiber, respectively. Strength, Young's modulus, and elongation at break were evaluated.

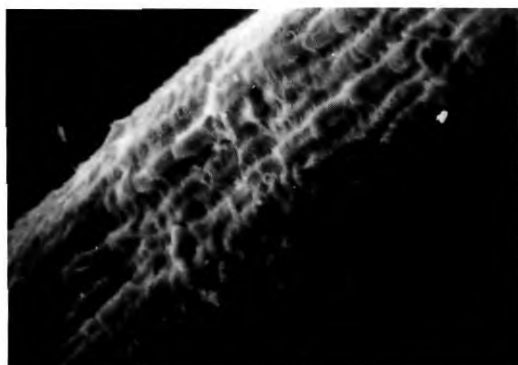
RESULTS AND DISCUSSION

Chemical Analysis

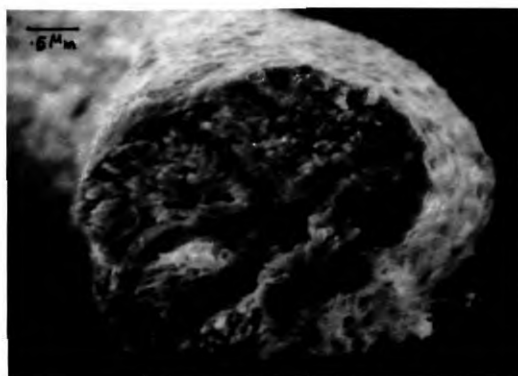
Table I shows the various chemical components present in the OPEFB fiber and oil palm mesocarp fiber. The OPEFB fiber contains a higher percentage of cellulose. Lignin content is comparatively low. The total cellulose content (holocellulose) of the fiber was found to be 65%. The fiber was found to have a very low ash content. All these factors contribute to better performance of the fiber as a reinforcement in polymers. The fiber is hygroscopic and its moisture content was found to be 12%. Cellulose and lignin content of mesocarp fiber is less than that of OPEFB fiber.

Table I compares the results with those of some other important natural fibers. Compared with coir fibers, OPEFB fiber is highly cellulosic. Coir has a higher percentage of lignin than OPEFB fiber. However, the cellulose content of OPEFB fiber is slightly less than that of banana and sisal fibers, and much less than that of pineapple leaf fiber. The lignin contents of banana, sisal, and pineapple leaf fibers are less than that of OPEFB fiber.

Solubility of the fibers in different solvents is given in Table II. Caustic soda solubility is higher when compared with other solvent solubility. The OPEFB fiber contains 10% water-soluble matter.



(a)



(b)

Figure 10 Scanning electron micrographs of untreated oil palm mesocarp fiber: (a) fiber surface ($\times 400$) and (b) cross section ($\times 800$).

Mesocarp fiber surface contains traces of oils, dissolves on treatment with NaOH solution, and shows a higher-percentage solubility in ether, caustic soda, cold water, and hot water than does OPEFB fiber. Moisture content of the mesocarp fiber was found to be 11%.

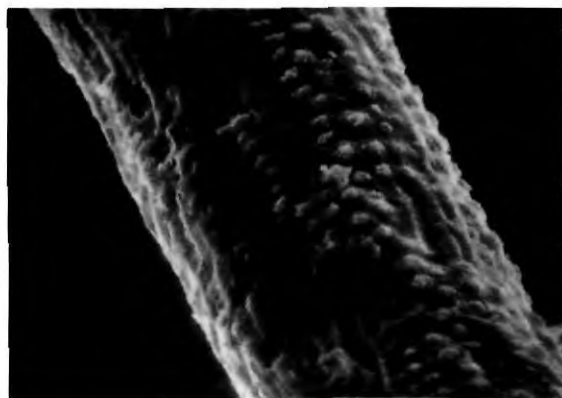


Figure 11 Scanning electron micrograph of alkali-treated oil palm mesocarp fiber surface ($\times 400$).

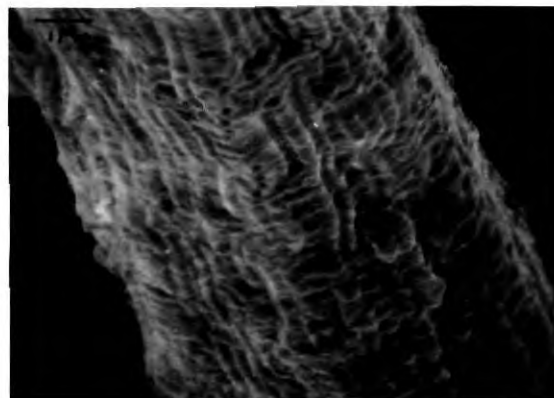
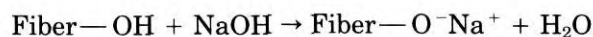


Figure 12 Scanning electron micrograph of silane-treated oil palm mesocarp fiber surface ($\times 400$).

Chemical Modifications

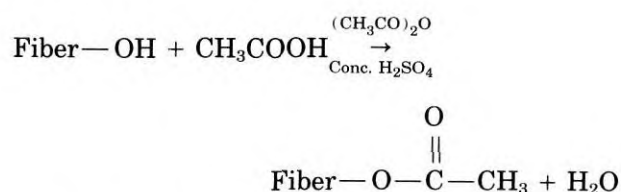
Fiber treatments such as alkali treatment, acetylation, and silane treatment were tried for OPEFB fiber. Mesocarp fiber was subjected to alkali and silane treatments. Possible mechanisms of the chemical modifications are given as follows.¹⁹

Alkali Treatment



NaOH treatment leads to the irreversible mercerization effect which increases the amount of amorphous cellulose at the expense of crystalline cellulose. Mercerization treatment improves the fiber surface adhesive characteristics by removing natural and artificial impurities, thereby producing a rough surface topography. The weight of the OPEFB fiber was decreased by 22% after the alkali treatment. For mesocarp fiber, the weight reduction observed was 25%.

Acetylation



The extent of acetylation is estimated by the titrimetric method. The number of O—acetyl groups in a certain amount of acetylated fiber is estimated by hydrolyzing with excess normal caustic soda; the unreacted alkali is then determined by titrating

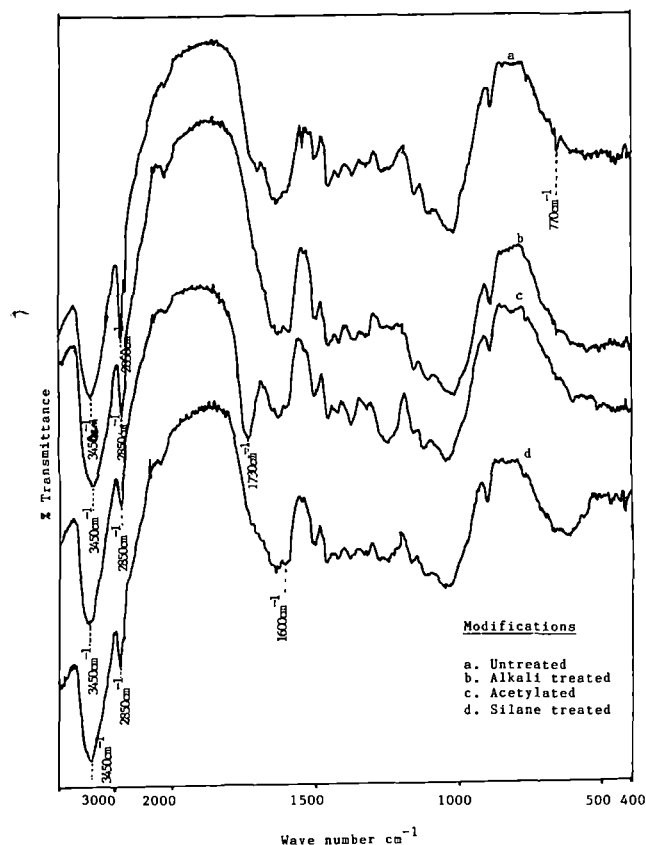
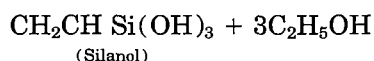
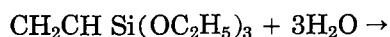
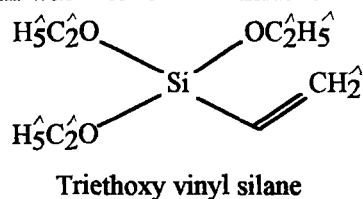


Figure 13 IR spectra of OPEFB fiber before and after treatments.

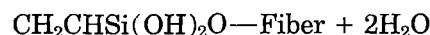
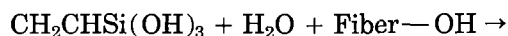
against normal oxalic acid. The number of O—acetyl groups in 0.5 g of acetylated OPEFB fiber was found to be 0.006. The reaction is expected to take place at the free OH groups available on cellulose molecules. There was no significant weight change of the fiber on acetylation. The fiber became more hydrophobic after the treatment.

Silane Treatment

The silane having the following chemical structure reacts with water to form a silanol and an alcohol.



Silane molecules are chemisorbed onto the fiber. The extent of silane chemisorption depends on the availability of free OH groups in the fiber. In presence of moisture, silanol reacts with cellulosic hydroxyl groups in the fiber, forming stable covalent bonds to the cell wall.



The weight of the OPEFB fiber decreased by 6% on silnylation. A 7% decrease was observed for mesocarp fibers. Hydrophobicity of the fibers increased on silnylation. The hydrophobic coupling agent forms a protective monolayer on the proton-bearing surfaces and thus removes the sites for moisture absorption.

These modifications are most effective in the surface regions. As the concentration and time of treatment increases, the treatment effect may

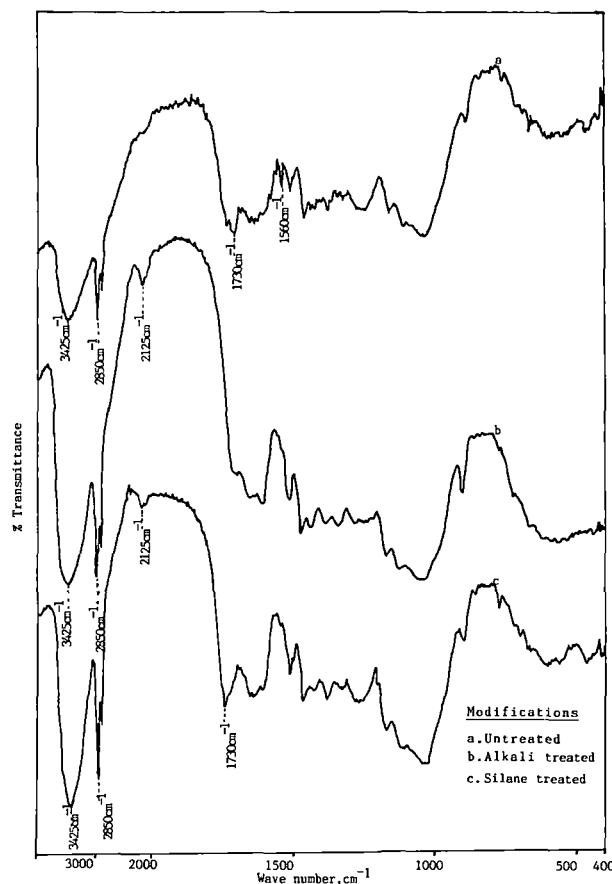


Figure 14 IR spectra of treated and untreated oil palm mesocarp fibers.

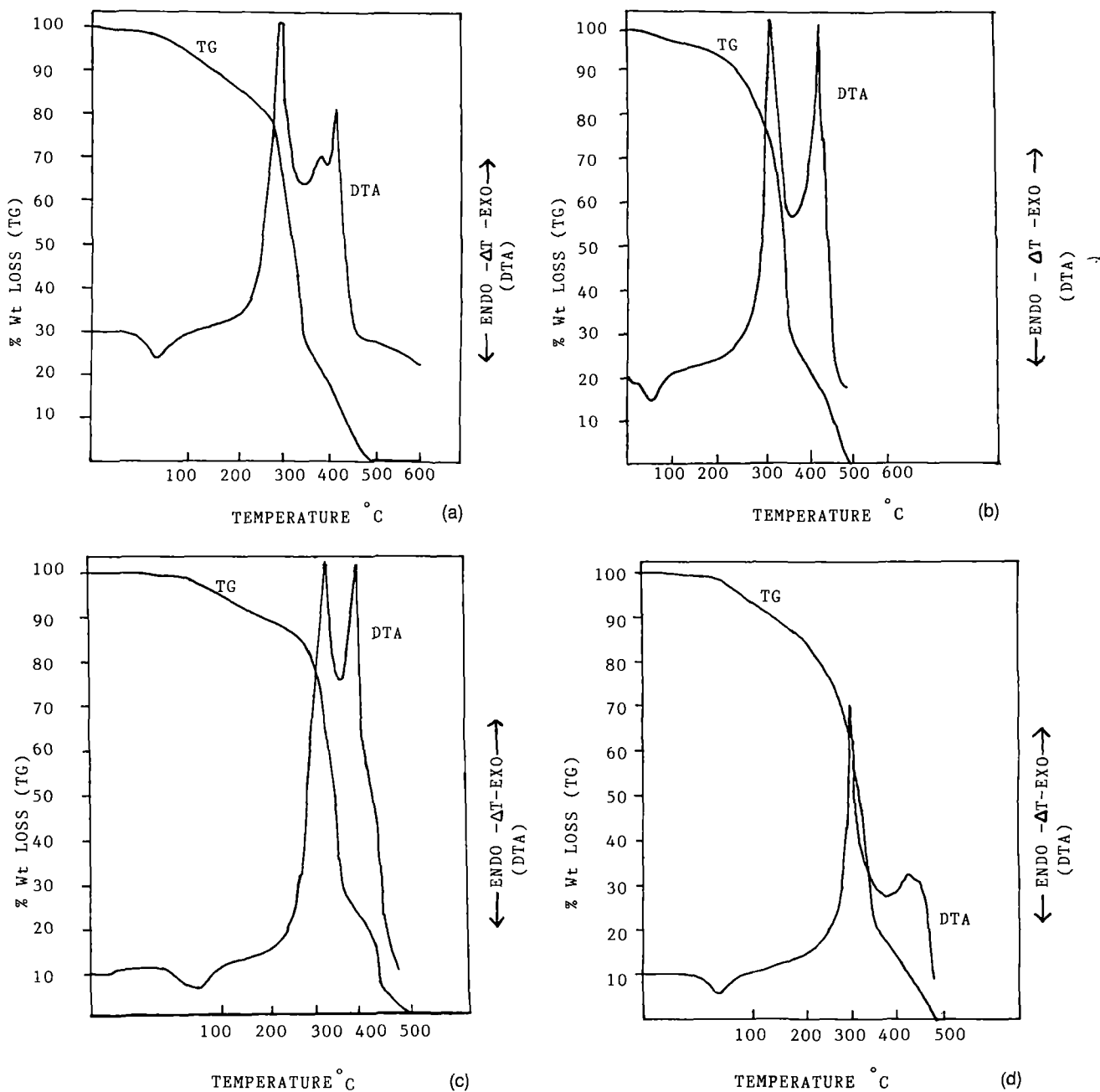


Figure 15 TGA and DTA curves of OPEFB fibers: (a) untreated, (b) alkali-treated, (c) silane-treated, and (d) acetylated.

penetrate into the fiber. However, there will be a saturation point beyond which no further reaction takes place.

Dimensional Changes on Treatments

The dimensional changes of the fibers after treatments can be seen from the distribution curves (Figs.

3 and 4). The diameters of about 100 fibers before and after treatments were measured and distribution curves plotted. Chemical treatment significantly reduces the fiber diameter in both the fibers.

SEM Studies

Figure 5 shows SEM photographs of the untreated OPEFB fiber surface and its cross section.

Table III Weight Losses of Untreated and Treated OPEFB Fibers at Various Temperatures

Untreated (°C)	Alkali-treated (°C)	Acetylated (°C)	Silane-treated (°C)	Weight Loss (%)
150	235	145	180	10
260	290	240	300	20
300	325	285	328	30
315	350	308	360	40
340	352	325	370	50
340	352	338	370	60
345	360	340	370	70
395	415	370	420	80
440	460	435	440	90
480	510	495	520	100

The photographs show minute pores on the surface of the fiber. The pores were found to have an average diameter of $0.07\ \mu\text{m}$. The cross section of the fiber shows a lacuna-like portion in the middle. The porous surface morphology is useful for better mechanical interlocking with the matrix resin for composite fabrication. The alkali-treated fiber surface is presented in Figure 6. The pores became more prominent upon alkali treatment. Average diameter of the pores was found to be $0.15\ \mu\text{m}$. The distribution of the pores of different size before and after alkali treatment can be understood from the distribution curve (Fig. 7). Pore size of about 100 micropores (selected at random) on the fiber surface were measured from SEM photographs and the distribution curve drawn.

Figures 8 and 9 give the micrographs of silane-treated and acetylated fiber surfaces, respectively. Acetylation clearly eliminates the waxy cuticle layer on the surface. This is evident from the micrographs.

Surface characteristics of the untreated oil palm mesocarp fiber are clear from Figure 10(a). The fiber surface is rough, exhibiting protruding portions and groove-like structures on its surface. The cross section of the fiber is not uniform [Fig. 10(b)]. The morphological changes of fiber upon alkali treatment and silane treatment are evident from the respective SEM photographs given in Figures 11 and 12. Alkali-treated fiber surface shows some protrusions (Fig. 11). This may be associated with the removal of the cuticle layer from the fiber surface. The fiber surface became clear on silane treatment (Fig. 12). Large number of micropores could be seen on the surface, having an average diameter of $0.2\ \mu\text{m}$.

IR Studies

IR spectra of the untreated and treated OPEFB fibers are given in Figure 13. It can be understood from the spectra that some chemical reactions occurred during the different treatments. Major changes are observed in the IR absorbance of alkali-treated, acetylated, and silane-treated samples. Peaks at 770 and $2850\ \text{cm}^{-1}$, corresponding to C—O stretching and C—H stretching vibrations, are present in the untreated fiber. On modification, these peaks diminish. Alkali treatment may reduce the hydrogen bonding in cellulosic hydroxyl groups, thereby increasing the OH concentration. This is evident from the increased intensity of the OH peak ($3450\ \text{cm}^{-1}$) in alkali-treated fiber. The alkali-soluble matter in the fiber is 20%. A peak at $1730\ \text{cm}^{-1}$ in acetylated fiber indicates the presence of an ester group. The peak at $1525\ \text{cm}^{-1}$ in the untreated fiber is shifted to $1600\ \text{cm}^{-1}$ upon silane treatment. This may be due to the C=C stretching.

On comparing the IR spectra of untreated OPEFB fiber and oil palm mesocarp fiber, it is seen that there is structural similarity between these fibers. Both of the spectra show intense peaks at 3450 and $2850\ \text{cm}^{-1}$ (O—H stretching and C—H stretching, respectively).

The fine structural changes of oil palm mesocarp fibers upon chemical modification can be understood from the IR spectra given in Figure 14. Major changes in the absorbance occur in the case of alkali treatment. The C=O stretching frequency of the carboxylic group ($1730\ \text{cm}^{-1}$) disappears upon alkali treatment. This may be due to the removal of the carboxylic group by alkali. Car-

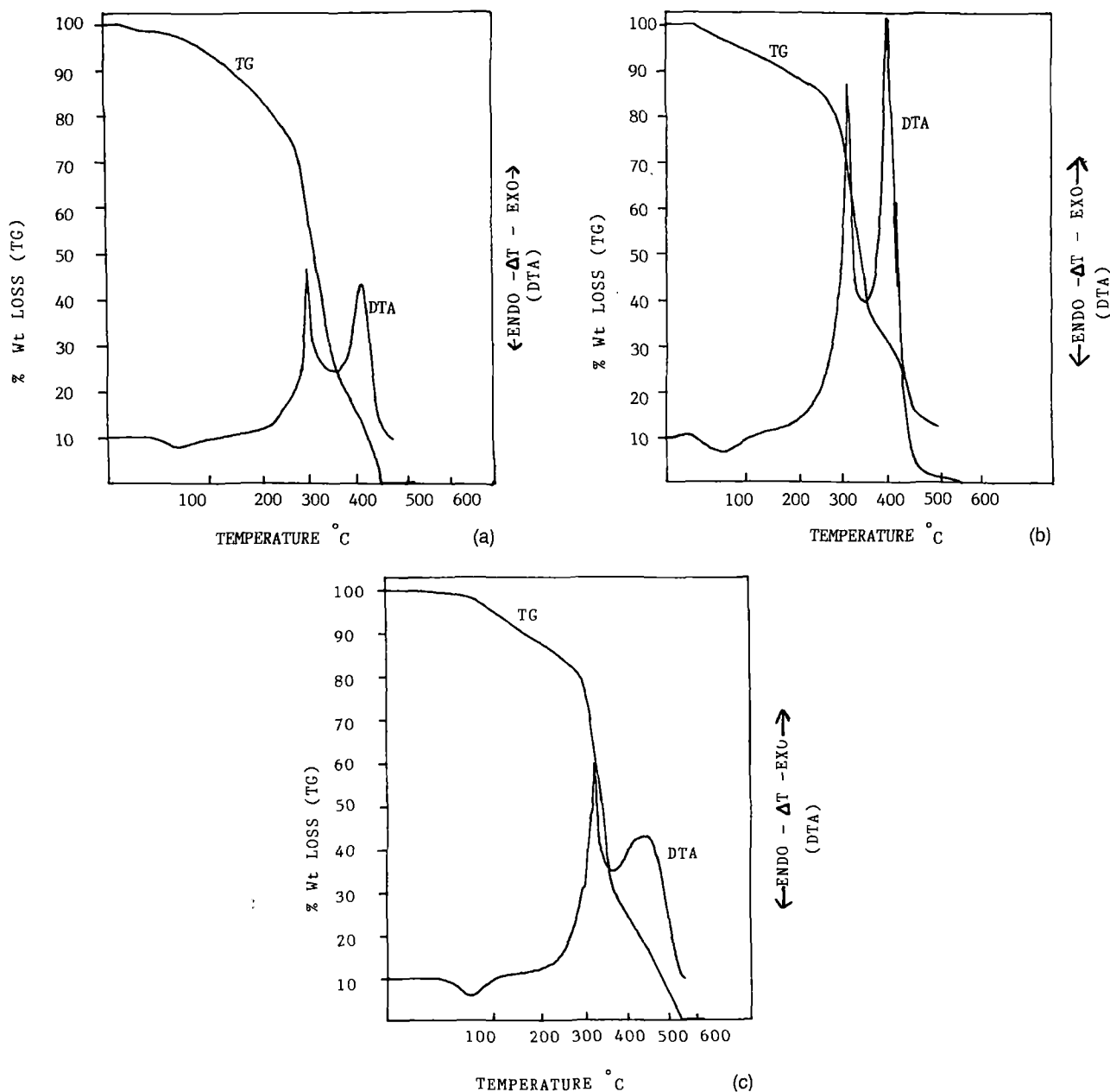


Figure 16 TGA and DTA curves of oil palm mesocarp fibers: (a) untreated, (b) alkali-treated, and (c) silane-treated.

boxylic groups may be present on the fiber surface from traces of fatty acids present. The intensity of the peak at 2125 cm^{-1} increases upon alkali and silane treatments. This may be due to the C—H stretching. Intensity of the hydroxy vibration absorption (3425 cm^{-1}) increased considerably upon alkali and silane treatments, as in the case of OPEFB fiber. Cellulosic hydroxyl groups may be involved in hydrogen bonding. There are chances for bonding with carboxylic groups of the

fatty acids present on the fiber. Presence of a peak at 1730 cm^{-1} in untreated fiber gives evidence for this. On treatments, these bonds may break. The peak at 1560 cm^{-1} (C=C stretching) disappeared upon alkali and silane treatments. This may be due to the treatments' removal of unsaturation present in the traces of oils. From these studies it is clear that several chemical reactions took place during treatments.

Sao and Jain²⁰ studied the mercerization effects

Table IV Weight Losses of Untreated and Treated Oil Palm Mesocarp Fibers at Various Temperatures

Untreated (°C)	Alkali-treated (°C)	Silane-treated (°C)	Weight Loss (%)
138	180	165	10
218	285	285	20
275	310	315	30
290	340	330	40
315	350	350	50
328	355	360	60
340	410	370	70
373	450	425	80
430	470	480	90
455	540	520	100

of aqueous NaOH on jute. Effect of weak alkalis such as sodium carbonate on jute fiber was reported by Sikdar and associates.²¹ The treatment cleaned the fiber surface and led to higher yarn productivity. The surface treatment of the fibers affects its mechanical properties.²² The incorporation of the treated fibers into plastics and rubber increases the usual strength of the composites.²³⁻²⁸

Thermal Studies

Figure 15 shows the thermal degradation pattern of untreated, alkali-treated, silane-treated, and acetylated OPEFB fibers. Below 100°C, a 5–8% weight loss was observed. This may be due to the dehydration of the fibers. Initial degradation temperature is higher for the alkali-treated fiber. This is evident from the DTA and TGA curves [Fig. 15(b)]. Major weight losses of the untreated and acetylated fibers take place at about 325°C. Alkali treatment raises this temperature to 350°C,

whereas silane treatment raises it to 365°C [Fig. 15(c)]. The DTA curve shows a major peak in this region, which may be due to the thermal depolymerization of hemicellulose and the cleavage of the glucosidic linkages of cellulose.²⁹ This is an exothermic process. At the first stage of degradation, the DTA curve shows an endothermic peak in all cases (Fig. 15). This peak may be due to the volatilization effect. Breakage of the decomposition products of the second stage (second peak) leads to the formation of charred residue. The third exothermic peak present in the DTA curve is due to this oxidation and burning of the high-molecular-weight residues. In acetylated fiber, the second peak is not prominent. Complete decomposition of all the samples takes place around 500°C. The percentage weight losses of untreated and treated fibers at various temperatures are given in Table III. From the table it can be understood that both alkali and silane treatment improve the thermal stability of the fibers.

Table V Mechanical Properties of Oil Palm Fibers

Fiber	Tensile Strength (MPa)	Young's Modulus (MPa)	Elongation at Break (%)
OPEFB			
Untreated	248	2,000	14
Alkali-treated	224	5,000	16
Silane-treated	273	5,250	14
Oil palm mesocarp fiber (fruit fiber)			
Untreated	80	500	17
Alkali-treated	64	740	6.5
Silane-treated	111	1,120	13.5

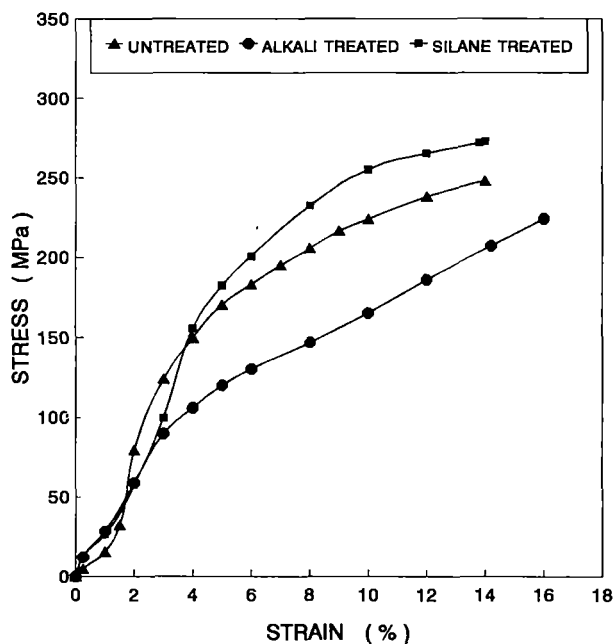


Figure 17 Stress-strain characteristics of untreated and treated OPEFB fibers.

Thermal stability of OPEFB fiber is higher than that of oil palm mesocarp fiber. Silane-treated OPEFB fiber is stable up to 365°C, whereas stability of the alkali-treated oil palm mesocarp fiber reaches 340°C. TGA and DTA scans of the untreated and treated mesocarp fibers are presented in Figure 16. The untreated fiber is stable up to 310°C. Alkali and silane treatment raises the stability of fiber to 340°C. Alkali treatment raises the initial degradation temperature (weight loss of 10%) to 180°C from 138°C. The initial weight loss may be due to the vaporization of water present in the sample. The DTA curve shows a corresponding endothermic peak in this region. Major degradation of untreated fibers

occurs at about 310°C; treatment raises this temperature to 340°C. Decomposition of cellulose may occur at this stage. A corresponding exothermic peak is observed in the DTA curve. The third exothermic peak in the DTA curve may be due to the formation of charred residue from the first degradation products. Broadening of the DTA peak is observed for the silane-treated sample. The gradual degradation and percentage weight losses of untreated and treated fibers can be understood from Table IV. From these results, it can be concluded that alkali treatment is more effective in improving the thermal stability.

It was reported by Mahato and colleagues¹³ that 5 to 15% of alkali-treated coir fibers showed maximum thermal stability. Varma and associates³⁰ also investigated the effect of alkali treatment of natural fibers on thermal stability. Shah and coworkers³¹ reported that sodium hydroxide treatment of lignocellulosic fibers leads to the formation of a lignin-cellulose complex which gives more stability to the fiber.

Mechanical Performance

The effects of various chemical treatments on mechanical properties of the OPEFB fiber were studied. The important mechanical properties of the fiber are given in Table V. The nature and texture of the fibers obtained from different plants may not be the same. The diameter of the fibers varies in the range from 0.015×10^4 to $0.05 \times 10^4 \mu\text{m}$. The density of these fibers lies in the range from 0.7 to 1.55 g/c³. All these factors will affect the properties of the fiber, therefore there is large variation in the observed properties. An average value of the properties is reported.

The untreated fiber shows 14% elongation. Elongation at break remains more or less same

Table VI Mechanical Properties of Some Important Natural Fibers

Fiber	Tensile Strength (MPa)	Elongation (%)	Toughness (MPa)
Sisal	580	4.3	1,250
Pineapple	640	2.4	970
Banana	540	3.0	816
Coir	140	25.0	3,200
OPEFB fiber	248	14	2,000
Oil palm mesocarp fiber	80	17	500

Source: ref. 32.

even after fiber treatment. This may be due to the firmly bound chemical structure of the fiber. Lignin binds the three-dimensional cellulose network as well as the fibrils. Figure 17 shows the stress-strain characteristics of the treated and untreated OPEFB fibers. At the very beginning (<1% elongation) there is linearity, and thereafter curvature is observed. As the applied stress increases, the weak primary cell wall collapses and decohesion of cells occurs, resulting in the mechanical failure of the fiber. The difference in stress-strain behavior of untreated and treated fibers is evident from Figure 17. Fiber modification by alkali treatment and silane treatment improves the overall mechanical performance of the fiber. Maximum tensile strength is given by silane-treated OPEFB fiber. The stiffness of the fiber is greatly improved upon modification. The properties of the fiber were compared with those of some important natural fibers (Table VI).³² The strength and stiffness of the OPEFB fiber is much higher than that of coir. Coir shows highest elongation among commonly used natural fibers. OPEFB fiber shows higher elongation than sisal, pineapple, and banana. The fiber is highly tough. However, the tensile strength of the fiber is less than that of sisal, pineapple, and banana fibers.

The strength and Young's modulus of the OPEFB fiber are greater than those of oil palm mesocarp fiber. But the mesocarp fiber shows a higher percentage of elongation. The mechanical performance of the mesocarp fiber is comparatively low with respect to other natural fibers (Table VI).

Properties of lignocellulosic fibers depend mainly on the cellulose content and microfibrillar angle. Various mechanical properties of oil palm mesocarp fibers are given in Table V. The density of the fiber was found to vary within the range from 0.6 to 1.18 g/c³. An average diameter of $0.02 \times 10^4 \mu\text{m}$ was observed for these fibers. In fact, the diameter even varied within a single fiber. The stress-strain characteristics of treated and untreated fibers are given in Figure 18. The modulus of the fiber increased upon modification by alkali and silane coupling agent. Silane treatment was found to be more effective. Silane-treated fiber showed maximum tensile strength. However, alkali treatment slightly decreased the tensile strength. The elongation at break was maximum for untreated fibers. The value showed decrease upon treatment. The firmly bound three-dimensional network of cellular arrangement may be partly destroyed upon treatment. Alkali treat-

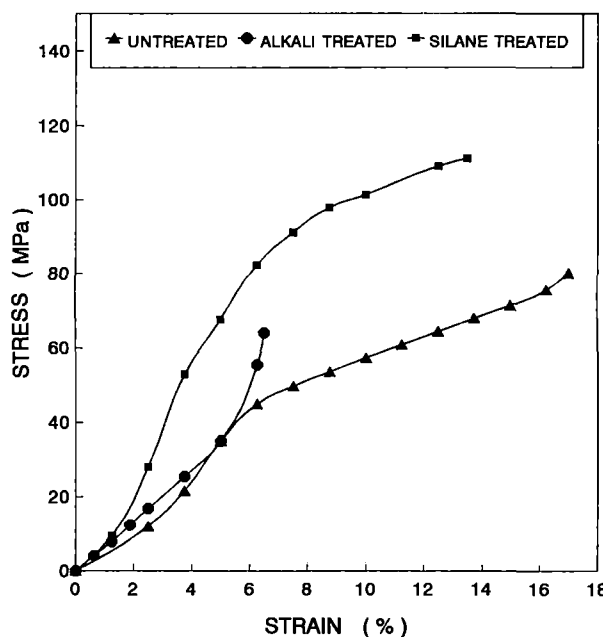


Figure 18 Stress-strain characteristics of untreated and treated oil palm mesocarp fibers.

ment reduced the tensile strength of the mesocarp fiber. This may be due to the bleaching of the oily and waxy materials from the fiber surface. Mesocarp fibers may contain traces of oil even after processing, since the oil is present in the flesh of the fruit. Silane treatment was found to be more effective in improving mechanical properties.

Theoretical Prediction of Microfibrillar Angle and Strength of the Fibers

Strength properties of the fibers are dependent mainly on the fibrillar structure, microfibrillar angle, and cellulose content. There is a correlation between percentage elongation ϵ and the microfibrillar angle θ as³³:

$$\epsilon = -2.78 + 7.28 \times 10^{-2}\theta + 7.7 \times 10^{-3}\theta^2 \quad (1)$$

Using this equation, the microfibrillar angle of OPEFB fiber is found to be 42°. There exists a relationship between the strength properties with microfibrillar angle and cellulose content.³³ This is given by

$$\sigma = -334.005 - 2.830\theta + 12.22W \quad (2)$$

where σ is the fiber strength, θ is the microfibrillar

angle, and W is the cellulose content. The strength of the fiber was calculated as 341 MPa; however, the experimental value was found to be 248 MPa.

The oil palm mesocarp fiber shows about 17% elongation at break. Using eq. (1), the microfibrillar angle of the fiber is calculated and found to be 46° . Using eq. (2), the strength of the fiber is predicted. The calculated strength of the fiber was 269 MPa, but the experimental value was very much lower than this. This may be due to the nature of cellular arrangement of the fiber and the effect of traces of oil present on the fiber surface.

CONCLUSIONS

Structure and properties of the two important oil palm fibers, OPEFB fiber and mesocarp fiber, were analyzed. Chemical compositions of the fibers were determined. The major constituents of these fibers were found to be cellulose. Lignin content is comparatively less. OPEFB fiber is more cellulosic than the mesocarp fiber. The oil palm mesocarp fiber contains a higher percentage of ether-soluble and caustic soda-soluble matter. Chemical modification of fibers by alkali treatment, acetylation, and silane treatment was carried out. This is to improve the strength and therefore the reinforcing ability of these fibers. Morphological studies revealed that treatment modified the fiber surface. The fine structural changes of the fibers can be seen from the respective scanning electron micrographs. IR studies give evidence for the chemical modifications that occurred during treatments. Thermal stability and degradation characteristics of the fibers were investigated by TGA and DTA. It was found that alkali and silane treatment increase the thermal stability of the fibers. Fibers are stable up to 300°C without any considerable weight loss.

The silane-treated OPEFB fiber showed maximum tensile strength. Alkali treatment slightly decreased the tensile strength. The Young's modulus of the fiber showed enhancement upon silane and alkali treatments. The strength of the mesocarp fiber is less than that of OPEFB fiber, because of the high cellulose content of OPEFB fiber. Silane treatment increased the strength of the fiber while alkali treatment decreased it. However, the stiffness of the fiber was increased by both alkali and silane treatments. The untreated meso-

carp fiber showed very good elongation. Treatment reduced the elongation of the fiber.

Microfibrillar angle and strength of the fibers were theoretically predicted. The theoretical strength of the OPEFB fiber was found to be closer to the experimental value. However, in the case of mesocarp fiber, there was great deviation. Finally, it is important to mention that the properties of oil palm fibers are comparable to other natural fibers and therefore they could be successfully used as a potential reinforcing material for polymer matrices. Several studies are progressing in this direction at this laboratory.

One of the authors (M.S.S.) is thankful to the Council of Scientific and Industrial Research, New Delhi, for granting the Senior Research Fellowship. The authors thank Oil Palm India Ltd., Kottayam, India, for supplying the oil palm fibers; and Ms. Snoopy George of the School of Chemical Sciences, Mahatma Gandhi University, Kottayam, India, for helping with the mechanical measurements.

REFERENCES

1. M. S. Sreekala, S. Thomas, and N. R. Neelakantan, *J. Polym. Eng.*, **16**, 265 (1977).
2. K. G. Satyanarayana, A. G. Kulkarni, and P. K. Rohatgi, *J. Sci. Ind. Res.*, **40**, 222 (1981).
3. K. G. Satyanarayana, A. G. Kulkarni, and P. K. Rohatgi, *J. Sci. Ind. Res.*, **42**, 425 (1983).
4. A. N. Shah and S. C. Lakkad, *Fiber Sci. Technol.*, **15**, 41 (1981).
5. C. Pavithran, P. S. Mukherjee, M. Brahmakumar, and A. D. Damodaran, *J. Mater. Sci. Lett.*, **6**, 882 (1987).
6. D. Maldas and B. V. Kokta, *Polym. Plast. Technol. Eng.*, **29**, 419 (1990).
7. B. C. Barkakaty, *J. Appl. Polym. Sci.*, **20**, 2921 (1976).
8. M. N. C. Martinez, P. J. Herrera-Franco, P. I. Gonzalez-Chi, and M. Aguilar-Vega, *J. Appl. Polym. Sci.*, **43**, 749 (1991).
9. D. R. Rao and V. B. Gupta, *Ind. J. Fiber Tex. Res.*, **17**, 1 (1992).
10. C. David, R. Fornasier, W. Lejong, and N. Vanlautem, *J. Appl. Polym. Sci.*, **36**, 29 (1988).
11. A. C. Mukherjee, S. K. Bandyopadhyay, A. K. Mukhopadhyay, and U. Mukhopadhyay, *Ind. J. Fiber Tex. Res.*, **17**, 80 (1992).
12. D. M. Brewis, J. Comyn, J. R. Fowler, D. Briggs, and V. A. Gibson, *Fiber Sci. Technol.*, **12**, 41 (1979).
13. D. N. Mahato, B. K. Mathur, and S. Bhattacharjee, *Ind. J. Fiber Tex. Res.*, **20**, 202 (1995).
14. S. V. Prasad, C. Pavithran, and P. K. Rohatgi, *J. Mater. Sci.*, **18**, 1443 (1983).

15. S. A. K. Yamini, A. J. Ahmad, J. Kasim, N. M. Nasir, and J. Harun, *Proc. Int. Symp. Biocomposites and Blends Based on Jute and Allied Fibers*, New Delhi, 1994, p. 135.
16. W. A. Curtin, *Polym. Comp.*, **15**, 474 (1994).
17. M. R. Nedele and M. R. Wisnom, *Comp. Sci. Technol.*, **51**, 517 (1994).
18. P. K. Jarvela, *Fiber Sci. Technol.*, **20**, 83 (1984).
19. E. T. N. Bisanda and M. P. Ansell, *Comp. Sci. Technol.*, **41**, 165 (1991).
20. K. P. Sao and A. K. Jain, *Ind. J. Fiber Tex. Res.*, **20**, 185 (1995).
21. B. Sikdar, A. K. Mukhopadhyay, and B. C. Mitra, *Ind. J. Fiber Tex. Res.*, **18**, 139 (1993).
22. O. P. Bahl, R. B. Mathur, and J. L. Dhami, *Polym. Eng. Sci.*, **24**, 455 (1984).
23. N. Chand, *J. Mater. Sci. Lett.*, **11**, 1051 (1992).
24. R. G. Raj, B. V. Kokta, G. Grouleau, and C. Deneault, *Polym. Plast. Technol. Eng.*, **29**, 339 (1990).
25. J. George, S. S. Bhagawan, N. Prabhakaran, and S. Thomas, *J. Appl. Polym. Sci.*, **57**, 843 (1995).
26. K. Joseph, S. Thomas, and C. Pavithran, *Comp. Sci. Technol.*, **53**, 99 (1995).
27. V. G. Geethamma, R. Joseph, and S. Thomas, *J. Appl. Polym. Sci.*, **55**, 583 (1995).
28. S. Varghese, B. Kuriakose, and S. Thomas, *J. Appl. Polym. Sci.*, **53**, 1051 (1994).
29. K. C. Manikandan Nair, S. M. Diwan, and S. Thomas, *J. Appl. Polym. Sci.*, **60**, 1483 (1996).
30. D. S. Varma, M. Varma, and I. K. Varma, *Thermochim. Acta*, **108**, 199 (1986).
31. S. C. Shah, P. K. Ray, S. N. Pandey, and K. Goswami, *J. Polym. Sci.*, **42**, 2767 (1991).
32. P. S. Mukherjee and K. G. Satyanarayana, *J. Mater. Sci.*, **21**, 4162 (1986).
33. K. G. Satyanarayana, C. K. S. Pillai, K. Sukumaran, S. G. K. Pillai, P. K. Rohatgi, and K. Vijayan, *J. Mater. Sci.*, **17**, 2453 (1982).

